GENOMIC BASIS OF ANTIBIOTIC RESISTANCE AND VIRULENCE IN ACINETOBACTER

EDITED BY: Santiago Castillo Ramírez, Benjamin Andrew Evans and Ayush Kumar
PUBLISHED IN: Frontiers in Microbiology

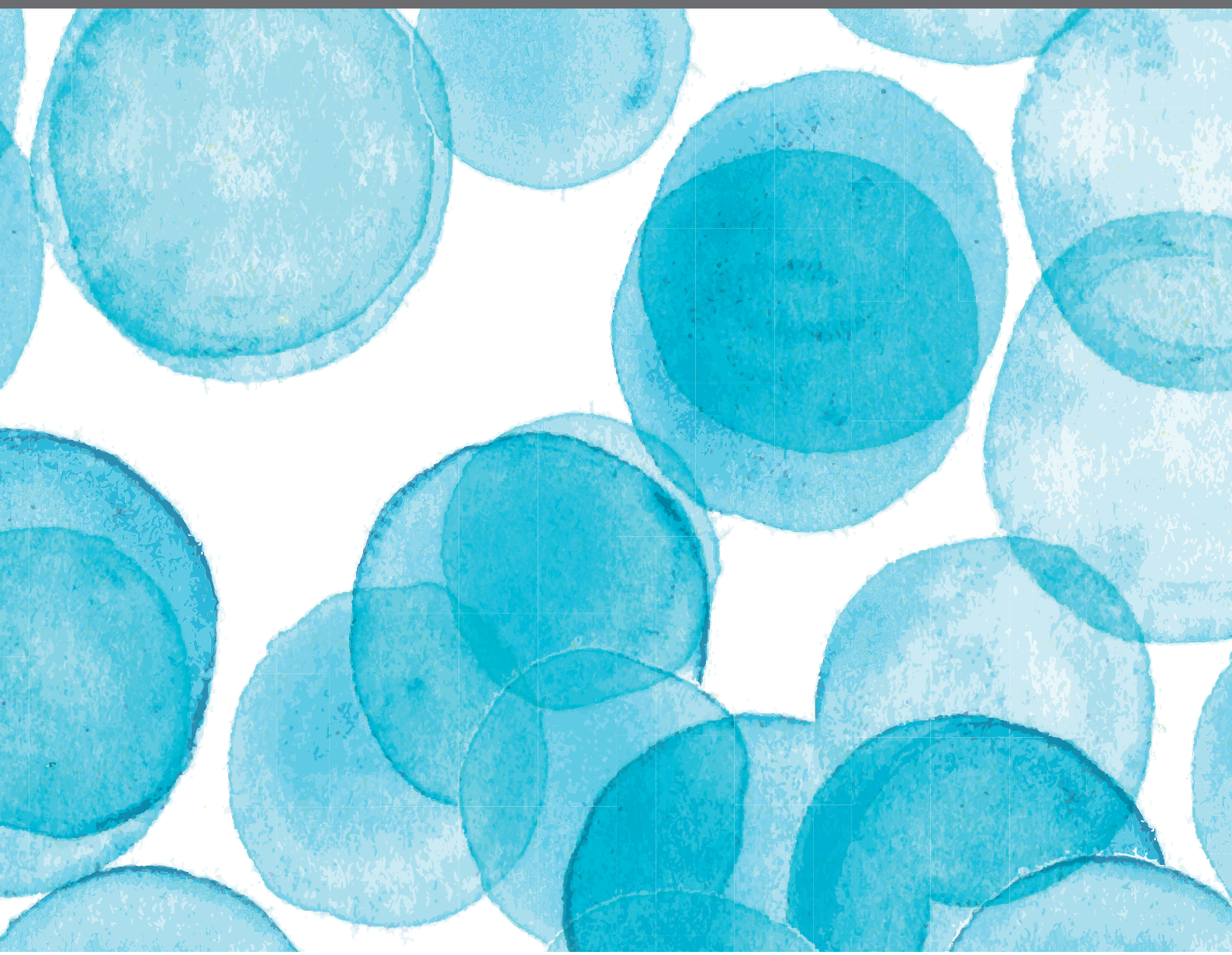

frontiers Research Topics

frontiers

ISSN 1664-8714
ISBN 978-2-88966-824-3
DOI 10.3389/978-2-88966-824-3

About Frontiers

Frontiers is more than just an open-access publisher of scholarly articles: it is a pioneering approach to the world of academia, radically improving the way scholarly research is managed. The grand vision of Frontiers is a world where all people have an equal opportunity to seek, share and generate knowledge. Frontiers provides immediate and permanent online open access to all its publications, but this alone is not enough to realize our grand goals.

Frontiers Journal Series

The Frontiers Journal Series is a multi-tier and interdisciplinary set of open-access, online journals, promising a paradigm shift from the current review, selection and dissemination processes in academic publishing. All Frontiers journals are driven by researchers for researchers; therefore, they constitute a service to the scholarly community. At the same time, the Frontiers Journal Series operates on a revolutionary invention, the tiered publishing system, initially addressing specific communities of scholars, and gradually climbing up to broader public understanding, thus serving the interests of the lay society, too.

Dedication to Quality

Each Frontiers article is a landmark of the highest quality, thanks to genuinely collaborative interactions between authors and review editors, who include some of the world's best academicians. Research must be certified by peers before entering a stream of knowledge that may eventually reach the public - and shape society; therefore, Frontiers only applies the most rigorous and unbiased reviews.
Frontiers revolutionizes research publishing by freely delivering the most outstanding research, evaluated with no bias from both the academic and social point of view. By applying the most advanced information technologies, Frontiers is catapulting scholarly publishing into a new generation.

What are Frontiers Research Topics?

Frontiers Research Topics are very popular trademarks of the Frontiers Journals Series: they are collections of at least ten articles, all centered on a particular subject. With their unique mix of varied contributions from Original Research to Review Articles, Frontiers Research Topics unify the most influential researchers, the latest key findings and historical advances in a hot research area! Find out more on how to host your own Frontiers Research Topic or contribute to one as an author by contacting the Frontiers Editorial Office: frontiersin.org/about/contact

GENOMIC BASIS OF ANTIBIOTIC RESISTANCE AND VIRULENCE IN ACINETOBACTER

Topic Editors:
Santiago Castillo Ramírez, National Autonomous University of Mexico, Mexico
Benjamin Andrew Evans, University of East Anglia, United Kingdom
Ayush Kumar, University of Manitoba, Canada

Citation: Ramírez, S. C., Evans, B. A., Kumar, A., eds. (2021). Genomic Basis of Antibiotic Resistance and Virulence in Acinetobacter. Lausanne: Frontiers Media SA. doi: 10.3389/978-2-88966-824-3

Table of Contents

frontiers in Microbiology

EDITORIAL
published: 30 March 2021
doi: 10.3389/fmicb.2021.670975

Editorial: Genomic Basis of Antibiotic Resistance and Virulence in *Acinetobacter*

Benjamin A. Evans[1], *Ayush Kumar*[2] *and Santiago Castillo-Ramírez*[3]*

[1] Norwich Medical School, University of East Anglia, Norwich, United Kingdom, [2] Department of Microbiology, University of Manitoba, Winnipeg, MB, Canada, [3] Centro de Ciencias Genómicas, Universidad Nacional Autónoma de Mexico, Cuernavaca, Mexico

Keywords: ***Acinetobacter*** **species, comparative genomics, antibiotic resistance, virulence, molecular epidemiology**

Editorial on the Research Topic

Genomic Basis of Antibiotic Resistance and Virulence in *Acinetobacter*

Genome sequencing has drastically changed our understanding of the biology of many bacteria. In this respect, species from the genus *Acinetobacter* are no exception. The main goal of this Research Topic was to broaden the knowledge about antibiotic resistance and virulence for *Acinetobacter* species from a genomic point of view. This Research Topic encompasses articles adding to the biology of the genus *Acinetobacter* in three major themes: Mobiles Genetic Elements (MGE), Antibiotic Resistance, and Epidemiology and Pathogenesis.

MGEs are one of the hallmarks of the accessory genome in many bacterial species. Furthermore, they are key elements for Horizontal Gene Transfer (HGT) and known spreaders of antibiotic resistance genes (ARGs). In their contribution Leal et al. analyzed 46 *Acinetobacter* spp. isolates (all but one *A. baumannii*) from 5 hospitals in Recife, Brazil. They showed that different lineages defined by multilocus sequence typing (MLST) sequence types (STs) are spreading in hospitals in Recife. Notably, ARGs were clearly associated with different MGEs. The authors concluded that polyclonal dissemination is peppered with exchange of MGEs containing ARGs. MGEs can also be a source of genome rearrangements; in this regard, Castro-Jamies et al. showed that this is the case for the understudied *A. haemolyticus*. Analyzing 47 genomes (including 30 Mexican isolates sequenced by them), they demonstrated that this species has an open pangenome and that hypervariable regions have an array of diverse MGEs. Notably, even isolates belonging to the same clade can have large differences in gene content. Thus, it is fair to say that *A. haemolyticus* has a very dynamic genome. Plasmids are one of the most well-known mechanisms for disseminating ARGs. To gain a better understanding of plasmid evolution in *A. baumannii*, Salgado-Camargo et al. conducted an *in silico* analysis of 173 *A. baumannii* plasmids covering 47 STs and 17 countries. They found that some plasmids might have the capacity to replicate in other bacterial genera, while other groups of plasmids seem to be confined to the genus *Acinetobacter*. Moreover, some plasmids are extensively distributed in the species, notwithstanding the apparent absence of the mobilization mechanisms. They also noted that around 35% of the plasmids have ARGs and that transposons are important elements concerning gene flow between plasmids. For their part, Mindlin et al. characterized 44 plasmids from 5 permafrost *A. lwoffii* isolates to understand the diversity of plasmids in this *Acinetobacter* species. They found that a small number of plasmids are distributed in clinical settings and the environment. Remarkably, plasmids from the permafrost isolates are closely related to plasmids from clinical isolates and some of them carry ARGs in the accessory region. The authors inferred that clinical plasmids originated from the plasmids present in the permafrost. The icing on

OPEN ACCESS

Edited by:
Daniel Yero, Autonomous University of Barcelona, Spain

Reviewed by:
Jesús Navas, University of Cantabria, Spain

***Correspondence:**
Santiago Castillo-Ramírez
iago@ccg.unam.mx

Specialty section:
This article was submitted to Evolutionary and Genomic Microbiology, a section of the journal Frontiers in Microbiology

Received: *22 February 2021*
Accepted: *08 March 2021*
Published: *30 March 2021*

Citation:
Evans BA, Kumar A and Castillo-Ramírez S (2021) Editorial: Genomic Basis of Antibiotic Resistance and Virulence in Acinetobacter. Front. Microbiol. 12:670975. doi: 10.3389/fmicb.2021.670975

the cake is the study by Ghaly et al. They studied 21 multidrug resistance mega-plasmids (present in 11 *Acinetobacter* spp.) sampled from diverse locales across the world. They demonstrated that plasmids sampled within the same region are often distantly related in terms of the core-genome; however, they are much more similar concerning the accessory genome. Importantly, they also determined that plasmids from different geographic areas are enriched in region-specific functional capacities. Importantly, these plasmids encode 221 ARGs conferring resistance against 13 drug classes. The authors concluded that mega-plasmids are spreaders of ARGs. Collectively, the above studies clearly show that MGEs in *Acinetobacter* have a very important role in spreading multidrug resistance phenotypes. Beyond that, these and others studies suggest that MGEs in *Acinetobacter* species significantly contribute to the acquisitions of genes required for functions under different living conditions.

Acinetobacter baumannii displays an impressive capability to resist the action of antibiotics. It uses a combination of intrinsic and acquired mechanisms to gain antibiotic resistance. In this issue half a dozen manuscripts describe some of these resistance mechanisms. Efflux of antibiotics, mediated by RND efflux pumps, is an important means of intrinsic resistance in Gram-negative bacteria. Antibiotic resistant *A. baumannii* isolates are reported globally and this is highlighted in the collection of manuscripts in this issue. Roy et al. describe a 7-year study from India where antibiotic resistance mechanisms were evaluated in neonatal septicaemia *A. baumannii* isolates. Worryingly, they found more than 90% of the isolates were resistant to fluoroquinolones (FQ). This resistance was associated primarily with mutations in the target genes, as more than 90% of the FQ resistant isolates carried mutations in *gyrA* and *parC*. They found widespread overexpression of efflux pumps, in particular that of AdeABC. This concerning finding highlights the prevalence of FQ resistance in *A. baumannii* and also underscores the fact that multiple resistance mechanisms in combination contribute to the reduced susceptibility of *A. baumannii*. Three additional manuscripts describe mobile resistance elements in *A. baumannii*. These studies come from three different continents highlighting the global spread of *A. baumannii*. Cerezales et al. studied the mobile genetic elements in three multidrug resistant (MDR) isolates of *A. baumannii* from Bolivia. Large and diverse numbers of transposons, plasmids and resistance islands were discovered in these isolates. Alarmingly, some of these elements conferred resistance to carbapenems, antibiotics of last resort for the treatment of MDR *A. baumannii*. Ayibieke et al. report carbapenem resistant *Acinetobacter* spp. from Ghana. This study is significant since there is limited data on carbapenem resistant *Acinetobacter* from sub-Saharan Africa. The study highlights the importance of surveillance to better understand the antibiotic resistance patterns in *Acinetobacter* from hospital settings. Xanthopoulou et al. report an *A. baumannii* isolate from northern Spain that harbors $bla_{\mathrm{NDM-6}}$. A number of variants of $bla_{\mathrm{NDM-6}}$ have been reported in various pathogens including *A. baumannii*. Critically, the $bla_{\mathrm{NDM-6}}$-carrying isolates reported in this study came from a patient who traveled to northern Spain following a medical procedure carried out in Northwest Africa. This leads to the possibility that $bla_{\mathrm{NDM-6}}$-harboring *A. baumannii* are perhaps present beyond northern Spain. While the majority of studies on *Acinetobacter* spp. focus on *A. baumannii,* there is increasing appreciation of the fact that non-*A. baumannii* isolates can be quite significant in clinical settings. Two other studies in this issue touch upon the growing clinical relevance of non-*A. baumannii* isolates. Zhang et al. describe an isolate of *A. pittii* isolated from Zhejiang Province in China. This isolate carried $bla_{\mathrm{OXA-499}}$, $bla_{\mathrm{OXA-826}}$, and $bla_{\mathrm{ADC-221}}$ genes, but is susceptible to imipenem and intermediately susceptible to meropenem. They were able to isolate an imipenem-resistant mutant of this isolate under selective pressure. This allowed them to characterize the mutations in $bla_{\mathrm{OXA-499}}$ that confer resistance to carbapenems, thus showing the potential of *A. pittii* isolates to develop carbapenem resistance if they carry a $bla_{\mathrm{OXA-499}}$ gene. In a different paper, Lee et al. show that overexpression of AdeABC in clinical isolates of *A. nosocomialis* is correlated with reduced susceptibilities to tetracyclines tigecycline, omadacycline, and eravacycline. This study further highlights the importance of efflux pumps in reduced susceptibility of bacteria such as *A. nosocomialis* to novel antibiotics.

One of the key components that contributes to the success of *A. baumannii* as an antibiotic-resistant pathogen is its complement of outer membrane proteins. In their mini-review, Uppalapati et al. discuss the latest research on the roles of the outer membrane proteins OmpA, CarO, and OprD as virulence factors and in altering membrane permeability in *A. baumannii*. They conclude that the evidence to date suggests a major role for outer membrane proteins in host interaction, infection, and surviving antibiotic exposure, but that significant gaps in our knowledge remain. In addition to the outer membrane, the capsule of *A. baumannii* is thought to be important for infection. To investigate this, Loraine et al. examined nearly 200 clinical isolates from three hospitals in Thailand. While isolates belonging to International Clone (IC) 2 predominated, a large number of isolates from very diverse STs were identified. Intriguingly, they found a correlation between the thickness of capsule being produced and serum resistance but were not able to determine the reason for the differences in capsule production between strains. This highlights the potential role of the capsule in infections with *A. baumannii* but shows that there is still much to learn about capsule variability, production, and function. Understanding the variation between the major clonal lineages of *A. baumannii*, and the implications of this, are a major goal of current research. To this end, Mancilla-Rojano et al. carried out a study of *Acinetobacter* isolates collected between 2015 and 2017 from a children's hospital in Mexico. A high proportion of the isolates were either MDR (44%) or extensively drug resistant (11%) and were spread across a diverse range of 27 different STs. Interestingly, they report nine instances of more than one ST causing infection in the same patient. Clonal complex (CC) 79 was the most prevalent (27% of isolates), which belongs to IC5. It has recently become apparent that the major epidemic lineages in Latin America are not IC1 and IC2, but are IC4, IC5, and IC7. There are very few detailed studies focussing on these strains, and therefore the study by Nodari et al.

looked to address this. They studied carbapenem resistant *A. baumannii* isolates from five different Brazilian hospitals, and found isolates belonged to either IC4 or IC5. All isolates were MDR including high levels of resistance to polymyxins (72%) and carried genes for the carbapenemases OXA-23 or OXA-72. These studies highlight the importance of International clones other than IC1 and IC2 in Latin America, which is an area that deserves far more attention. The global prevalence of carbapenem-resistant clonal lineages has made strategies to combat these a priority. This was the goal of Chen et al. who show the value of a long-term study on the impact of a comprehensive intervention designed to reduce the burden of *A. baumannii* in hospitals. The intervention was successful in reducing overall resistance rates, and the frequency and duration of outbreaks. However, levels of resistance in the imipenem-resistant isolates did not decrease, except for tigecycline. The prevalent OXA-58 carbapenemase-encoding isolates disappeared following the intervention and were replaced with isolates encoding OXA-23. While it is encouraging that such intervention strategies can be effective, their impact upon the population structure of *A. baumannii* and associated resistance and virulence phenotypes is still not clear.

The advent of affordable genomics has greatly increased our understanding of the factors influencing antibiotic resistance and virulence in *Acinetobacter* but significant gaps in our knowledge still remain. Large-scale genomic studies, in particular with unbiased isolate selection and including currently under-represented areas of the word, will reveal the true variation within species in the genus. By combining genomics with high-quality clinical and epidemiological data, and laboratory-based assays, we will achieve a far greater understanding of the link between genotype and phenotype in these species, shedding light on the factors that have resulted in *Acinetobacter* being amongst the most feared nosocomial pathogens.

AUTHOR CONTRIBUTIONS

BE, AK, and SC-R drafted and edited the manuscript. All authors approved the final version.

Conflict of Interest: The authors declare that the research was conducted in the absence of any commercial or financial relationships that could be construed as a potential conflict of interest.

frontiers in Microbiology

ORIGINAL RESEARCH
published: 06 April 2020
doi: 10.3389/fmicb.2020.00548

Genomic and Phenotypic Analyses of *Acinetobacter baumannii* Isolates From Three Tertiary Care Hospitals in Thailand

*Jessica Loraine[1†], Eva Heinz[2,3†], Rosesathorn Soontarach[4†], Grace A. Blackwell[3,5], Richard A. Stabler[6], Supayang P. Voravuthikunchai[4], Potjanee Srimanote[7], Pattarachai Kiratisin[8], Nicholas R. Thomson[3,6] and Peter W. Taylor[1]**

[1] School of Pharmacy, University College London, London, United Kingdom, [2] Liverpool School of Tropical Medicine, Liverpool, United Kingdom, [3] Wellcome Sanger Institute, Hinxton, Cambridge, United Kingdom, [4] Faculty of Science, Prince of Songkla University, Songkhla, Thailand, [5] European Bioinformatics Institute, European Molecular Biology Laboratory, Hinxton, Cambridge, United Kingdom, [6] London School of Hygiene and Tropical Medicine, London, United Kingdom, [7] Faculty of Allied Health Sciences, Thammasat University, Pathumtanee, Thailand, [8] Faculty of Medicine Siriraj Hospital, Mahidol University, Bangkok, Thailand

Antibiotic resistant strains of *Acinetobacter baumannii* are responsible for a large and increasing burden of nosocomial infections in Thailand and other countries of Southeast Asia. New approaches to their control and treatment are urgently needed and an attractive strategy is to remove the bacterial polysaccharide capsule, and thus the protection from the host's immune system. To examine phylogenetic relationships, distribution of capsule chemotypes, acquired antibiotic resistance determinants, susceptibility to complement and other traits associated with systemic infection, we sequenced 191 isolates from three tertiary referral hospitals in Thailand and used phenotypic assays to characterize key aspects of infectivity. Several distinct lineages were circulating in three hospitals and the majority belonged to global clonal group 2 (GC2). Very high levels of resistance to carbapenems and other front-line antibiotics were found, as were a number of widespread plasmid replicons. A high diversity of capsule genotypes was encountered, with only three of these (KL6, KL10, and KL47) showing more than 10% frequency. Almost 90% of GC2 isolates belonged to the most common capsule genotypes and were fully resistant to the bactericidal action of human serum complement, most likely protected by their polysaccharide capsule, which represents a key determinant of virulence for systemic infection. Our study further highlights the importance to develop therapeutic strategies to remove the polysaccharide capsule from extensively drug-resistant *A. baumanii* during the course of systemic infection.

Keywords: *Acinetobacter baumannii*, antibiotic resistance, phylogenomics, surface structures, complement, global clone 2

OPEN ACCESS

Edited by:
Benjamin Andrew Evans, University of East Anglia, United Kingdom

Reviewed by:
Nabil Karah, Umeå University, Sweden
Johanna J. Kenyon, Queensland University of Technology, Australia
Raffaele Zarrilli, University of Naples Federico II, Italy

***Correspondence:**
Peter W. Taylor
peter.taylor@ucl.ac.uk

† These authors have contributed equally to this work

Specialty section:
This article was submitted to Antimicrobials, Resistance and Chemotherapy, a section of the journal Frontiers in Microbiology

Received: *26 November 2019*
Accepted: *13 March 2020*
Published: *06 April 2020*

Citation:
Loraine J, Heinz E, Soontarach R, Blackwell GA, Stabler RA, Voravuthikunchai SP, Srimanote P, Kiratisin P, Thomson NR and Taylor PW (2020) Genomic and Phenotypic Analyses of Acinetobacter baumannii Isolates From Three Tertiary Care Hospitals in Thailand. Front. Microbiol. 11:548. doi: 10.3389/fmicb.2020.00548

INTRODUCTION

A. baumannii is an opportunistic pathogen that can cause potentially lethal nosocomial infections (Howard et al., 2012). These are frequently a result of trauma, surgery, catheterization or endotracheal intubation (Chopra et al., 2014), and *A. baumannii* can escape the local immune reaction by evading neutrophils, macrophages and complement (C') (Russo et al., 2008; García-Patiño et al., 2017). This immune escape therefore necessitates the use of antimicrobials, and the key determinant of clinical outcome of *A. baumannii* infection is treatment failure due to the high number of antibiotic resistant strains (Wong et al., 2017).

Multidrug resistant (MDR) strains of *A. baumannii* have spread rapidly over recent decades (Zarrilli et al., 2013; Hamidian and Nigro, 2019). The high prevalence of strains resistant to nearly all antibiotics, especially well-tolerated cephalosporins and carbapenems, has led to the revival of drugs considered to be of last resort such as polymyxins (Falagas and Kasiakou, 2005; Sahbudak Bal et al., 2018) for systemic administration. However, resistance to colistin is now more prevalent and polymyxins are now used less widely due to serious side effects associated with these agents (Sahbudak Bal et al., 2018). As a consequence, the World Health Organization has identified carbapenem-resistant *A. baumannii* (CRAB) as the greatest bacterial threat to global human health and the top priority pathogen for development of new antibiotics (Tacconelli et al., 2018).

Recent surveillance data indicates that *A. baumannii* causes under 2% of healthcare associated infections in the United States (Sievert et al., 2013; Bulens et al., 2018) but prevalence is much higher in Southern and South Eastern Asia, where it is frequently the major nosocomial infectious agent (Suwantarat and Carroll, 2016). The burden of *A. baumannii* infection is particularly severe in Thailand, with isolates accounting for 15–16% of hospital-acquired bacteremia cases and displaying very high levels (70–88%) of carbapenem resistance, and mortality rates in excess of 60% due to MDR *A. baumannii* bacteremia (Chaisathaphol and Chayakulkeeree, 2014; Hongsuwan et al., 2014; Suwantarat and Carroll, 2016; Hsu et al., 2017; Sirijatuphat et al., 2018). Presence of the over-expressed carbapenemase $bla_{\mathrm{OXA-23}}$, or $bla_{\mathrm{OXA-51}}$ in combination with IS elements, account for most of the CRAB phenotypes (Figueiredo et al., 2009; Teo et al., 2015; Wong et al., 2017). Molecular typing identified three European clones; two have spread globally and are now identified as GC1 and GC2 (Higgins et al., 2010; Hamidian and Nigro, 2019) and the majority of isolates from Asia belong to global clone 2 (GC2) (Kim et al., 2013; Kamolvit et al., 2015).

The large majority of *A. baumannii* strains produce a substantial capsular polysaccharide that protects them from external threats (Kenyon and Hall, 2013), and an attractive treatment option is enzymatic removal of the protective capsules (Mushtaq et al., 2004; Lin et al., 2014; Negus et al., 2015); capsule-free mutants were highly susceptible to C'-mediated attack (Lees-Miller et al., 2013), in marked contrast to their encapsulated parent strains. A major advantage of this approach is that it circumvents the accumulation of antibiotic resistance determinants, but has the potential disadvantage that variation of the capsular polysaccharide may limit the utility of individual depolymerases as found in bacteriophages or other organisms, which typically hydrolyze only one or a limited number of capsular types (Oliveira et al., 2017; Hernandez-Morales et al., 2018; Lin et al., 2018; Singh et al., 2018).

We report a detailed characterization of 191 recent isolates from three major hospitals in Thailand using whole-genome sequencing and functional assays, with particular reference to their surface properties and antibiotic resistance profiles. We also sought to identify factors that contribute to the capacity of GC2 isolates to cause infection through increased virulence (Zarrilli et al., 2013), using genomic data and bioassays, in relation to the role of the capsule in the determination of resistance to C'-mediated attack.

MATERIALS AND METHODS

Bacterial Isolates

A total of 191 *A. baumannii* isolates were cultured from wound pus, sputum, urine, blood, and excised tissue at the clinical microbiology laboratories of three tertiary referral hospitals in Thailand (**Figure 1A**). Bacteria were initially identified by routine biochemical tests implemented for identification of Gram-negative bacteria. Species were further confirmed by whole-genome sequencing and sequence typing as below. The hospitals were Thammasat University Hospital, Pathum Thani Province (47 isolates; April 2016), Siriraj Hospital, Bangkok (84 consecutive isolates; April 2016) and Songklanagarind Hospital, Hat Yai, Songkhla Province (60 isolates; August 2016). Siriraj is the largest hospital in Thailand with 2,300 beds, 1,000,000 outpatients per annum and 80,000 inpatients per annum; equivalent figures for Songklanagarind are 846, 1,019,375, and 40,936 and for Thammasat 601, 384,088, and 40,745 (data from 2017). Details of these isolates are given in **Supplementary Table S1**. Susceptibilities to clinically relevant antibiotics were determined using the Vitek 2 system (Bosshard et al., 2006).

Genome Sequencing, Assembly, and Annotation

Genomic DNA was extracted and sequenced using Illumina-B HiSeq X paired-end sequencing. Annotated assemblies were produced according to (Page et al., 2016a). Sequence reads were assembled *de novo* with Velvet v1.2 (Zerbino and Birney, 2008) and VelvetOptimiser v2.2.5 (Gladman and Seemann, 2008). Reads were annotated using PROKKA v1.11 (Seemann, 2014). The stand-alone scaffolder SSPACE (Boetzer et al., 2011) was used to refine contig assembly; sequence gaps were filled using GapFiller (Boetzer and Pirovano, 2012). Genomes with greater than 5% contamination levels as determined by Kraken (Wood and Salzberg, 2014), fully assembled genomes of less than 4.5 Mpb or comprising 500 or more contigs were removed. Putative genomes with less than 60% sequence similarity with the reference genome were assessed with CheckM (Parks et al., 2015) for genome completeness and contamination; isolates with

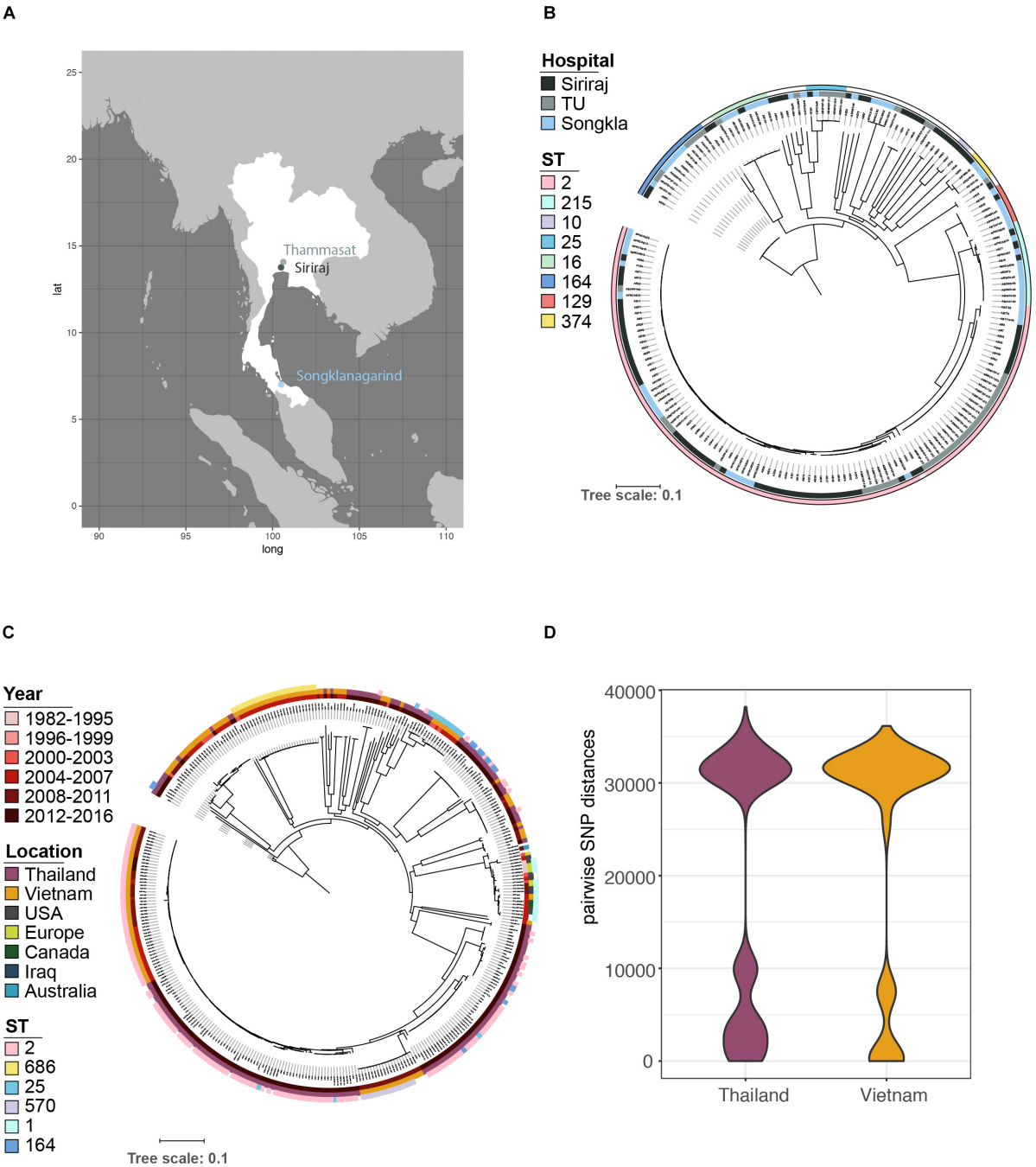

FIGURE 1 | The population structure of *A. baumannii* isolated from a variety of infections in April 2016 at three major Thai hospitals. **(A)** Samples were obtained from geographically distinct regions of the country. **(B)** Core gene phylogeny showed that the bacterial populations were circulating amongst the three hospitals; no single lineage dominated at any one location. **(C)** Our data in context with the global population structure based on published data. **(D)** A more detailed comparison of the data structure of pairwise SNP distances shows a similar distribution between our samples and a recent study from one hospital in Vietnam (Schultz et al., 2016), with a similarly high prevalence of ST2 **(C)**, but also a considerable number of more distantly related isolates from other regions.

greater than 3% contamination levels were excluded from the study. SNPs were called against the *A. baumannii* reference genome to identify heterozygous SNPs, and isolates with more than 2% were removed from further analysis (Page et al., 2016a), resulting in the 191 genomes analyzed in this study. As we could also observe several *gdhB* duplicate sequences, a known problem of the Oxford MLST scheme (Bartual et al., 2005; Gaiarsa et al., 2019), sequence types were assigned and are reported only based on the Pasteur scheme (Diancourt et al., 2010; Page et al., 2016). Novel sequence types were assigned for non-typeable isolates

through the PubMLST (**Supplementary Table S1**), three isolates could not be assigned as the assemblies were missing one allele.

Phylogenetic Analyses

The pan genome for the global and Thai isolate analyses was determined with Roary (Page et al., 2015) using a Protein BLAST identity of 95% and a core definition of 99%. SNPs were extracted from the core gene alignment using SNP sites (Page et al., 2016b) and the output used to run RAxML v8.2.8 (Stamatakis, 2014) to calculate the phylogenetic tree with 100 bootstraps under the GTR time-reversible model. The resulting alignment for the global dataset was also used to determine pairwise SNP distances with the dist.gene function from the ape package in R (Paradis et al., 2004). To place our isolates in a broader context, we compared them with recently published sequence data of *A. baumannii* causing ventilator-associated pneumonia in the intensive care unit of a Vietnamese hospital, in addition to data from several other published studies (**Supplementary Table S2**).

Antibiotic Resistance and Traits Associated With Infection

Antibiotic resistance genes were detected with the curated version of the ARG-ANNOT database available at the SRST2 site (Gupta et al., 2014; Inouye et al., 2014), *rpoB* SNP mutations were assessed comparing the sequences against described resistance mutations (Giannouli et al., 2012; Pérez-Varela et al., 2017), and virulence factors with VFDB (Chen et al., 2016), using the read-based search program ARIBA (Hunt et al., 2017). Plasmid replicons were detected with a custom database composed of 30 genes involved in plasmid replication, stabilization and mobilization from *Acinetobacter* plasmids (Bertini et al., 2010; Salto et al., 2018); some additional plasmids (Gao et al., 2011; Hamidian et al., 2012, 2016; Zhang et al., 2013; Jones et al., 2014; Blackwell and Hall, 2017; Hamidian et al., 2017) were also included (full database **Supplementary Dataset S1**); and analyses were undertaken using ARIBA software v2.12.1 (Hunt et al., 2017). To account for potential variation in surface proteins or other virulence factors, a custom-made collection of *A. baumannii* virulence factors (**Supplementary Table S6**) was searched against our isolates using phmmer (Eddy, 2011; Eijkelkamp et al., 2011, 2014; Harding et al., 2013; Scott et al., 2014; Weber et al., 2015; Lee et al., 2017). Representations of trees and metadata were performed using iTOL (Letunic and Bork, 2016) and the ggplot2 and ggtree packages in R (Wickham, 2009; Yu et al., 2018). KL and OCL genotypes of our isolates were identified using the capsule identification program kaptive, based on a curated *A. baumannii* specific database (Wyres et al., 2019; **Supplementary Table S1**).

C' Susceptibility

Commercial (MP Biomedicals, United Kingdom) pooled human serum was stored and used to determine susceptibility to C', essentially as previously described (Loraine et al., 2018). Early mid-logarithmic-phase Luria-Bertani (LB) broth cultures of *A. baumannii* were washed three times with 200 μl of gelatin-veronal-buffered saline containing Mg^{2+} and Ca^{2+} (GVB^{++}; pH 7.35) and suspended in 400 μl of GVB^{++}. The suspensions (200?μl) were mixed with 390 μl of pre-warmed (37°C) normal human serum to give a final concentration of ∼1 × 10^6 CFU, the mixtures incubated at 37°C for 3 h and bacteria quantified by serial dilution and overnight incubation on LB agar (see **Supplementary Table S3** for all raw data). The 45 GC2 isolates were exposed to 66% normal human serum and enumerated bacterial survivors over a 3 h incubation period (Malke, 1986). Isolates were assigned to one of three categories: resistant (R), showing no (or only transient) reduction in viable count during the incubation period; delayed susceptible (DS), displaying significant (∼90%) survival after 1 h and low survival (<10%) after 3 h incubation; the inocula of rapidly susceptible (S) isolates were reduced to below 10% after 1 h incubation. All experiments were performed in duplicate and results expressed as percent survival over this time period. Pre-warmed, heat-inactivated human serum (56°C, 30 min) served as control. All raw data is given in **Supplementary Table S3**.

Capsule Measurements

The size of the capsule for each isolate was determined by negative staining with India ink, microscopic imaging and calculation of the area occupied by the capsule using CellProfiler image analysis software (v3.1.9; Lamprecht et al., 2007). One bacterial colony was resuspended in PBS and mixed in a 1:1 ratio with India Ink stain (BD India Ink Reagent Dropper) and applied to a microscope slide with a coverslip. Microscopic imaging with a Zeiss Axiostar plus transmitted light microscope fitted with an Olympus SC30 digital camera and using a 100× oil immersion lens and embedded scale bar. All raw data is given in **Supplementary Table S4**.

Motility

Swarming and twitching motility were assayed by the subsurface agar method (Clemmer et al., 2011) using LB broth containing either 0.4 or 0.8% agar. Briefly, freshly grown cultures of *A. baumannii* were stabbed to enable spread of bacteria on the surface of 0.4% agar plates for swarming motility and the interphase between the bottom of the Petri dish and the 0.8% agar layer for twitching motility. The plates were incubated at 37°C for 48 h: positive swarming motility was defined as a zone greater than 10 mm around the site of inoculation. For twitching motility at the interstitial surface between the agar and the petri dish, the agar was discarded, and bacteria visualized by staining stained with 0.2% crystal violet. Positive twitchers were defined as those cultures that showed a zone diameter greater than 5 mm. Assays were performed a minimum of three times for each isolate. All raw data is provided in **Supplementary Table S5**.

RESULTS

Major Lineages Are Circulating in the Region

Phylogenetic analysis identified several lineages circulating in all the three hospitals (**Figures 1A,B**). The majority of isolates

belong to GC2 ($n = 106/191$), represented exclusively by sequence type 2 (ST2) of the Pasteur scheme. No isolates belonging to GC1 were identified, a key clonal group in the evolution of multi-drug resistance in *A. baumannii* (Holt et al., 2016). Non-GC2 isolates belonged to ST164 ($n = 14$; 7.3%), ST215 ($n = 13$; 6.8%), ST16 ($n = 9$; 4.7%), ST25 ($n = 6$; 3.1%), ST129 ($n = 6$; 3.1%), ST374 ($n = 4$; 2.1%), and ST10 ($n = 2$; 1.0%); three isolates could not be sequence-typed, most likely due to low-quality genomes, and thus missing one of the MLST alleles. The high prevalence of GC2 and lack of GC1 of our dataset from 2016 closely resembles the population structure from the Vietnamese hospital outbreak (Schultz et al., 2016) over the period 2009-12 (**Figure 1C**); both datasets include a considerable number of deep branching lineages. These similarities in population structure are also mirrored when comparing the distribution of pairwise single-nucleotide polymorphisms (SNPs) between the datasets from Vietnam and Thailand (**Figure 1D**).

Antimicrobial Resistance

Phenotypic resistance profiles for 115 of the strains confirmed the very high levels of antibiotic resistance encountered with clinical isolates of *A. baumannii*, especially against β-lactam agents (e.g., ceftriaxone: 115/115, 100%), including carbapenems (**Figure 2A**; 98/115, 85.2%), but also against other major antibiotic classes: fluoroquinolones [98/115, 85.2% resistant/intermediate (R/I)], aminoglycosides (79/115, 68.7% R/I) and trimethoprim (76/115, 66.1% R/I), and multidrug resistance was, as expected, associated with a high number of acquired resistance genes (**Figures 2A,C** and **Supplementary Figures S1, S2**) indicating either gain through larger elements carrying several genes as previously described as a key driver for *A. baumannii* resistance (Bonomo and Szabo, 2006; Post and Hall, 2009). $bla_{\mathrm{OXA-23}}$, the most prominent carbapenem resistance gene, is present in 85.2% of imipenem resistant strains (**Figure 2C**). Few isolates carried the $bla_{\mathrm{NDM-1}}$ gene and a low number of acquired *ampC* genes were detected (**Figure 2C** and **Supplementary Figure S2**). We also note the presence of the *arr* gene, as well as *rpoB* mutations, conferring rifampicin resistance, one of the last line antimicrobials used against CRAB (Thapa et al., 2009; Durante-Mangoni et al., 2014).

Mobile Elements

All but ten isolates contained at least one of the plasmid replicons (**Supplementary Dataset S1**) and 121 contained two to maximal five (**Figure 2B**). The three plasmid replicons detected at highest frequency were RepAci1, RepAci6, and RepApAB49. Each of these plasmid types were found across a number of STs, although RepAci1 plasmids were present in almost all the ST2 isolates (102/106) and RepApAB49 was found in 12/14 ST164 isolates. Recently, a RepAci1 plasmid was shown to be mobilized by a co-residing conjugative RepAci6 plasmid (Blackwell and Hall, 2019), and these two replicons co-occur in the genomes of 56 isolates; RepAci6 only was detected in one isolate, and RepAci1 only in 46. RepAci6 plasmids were the most common self-transmissible plasmids detected. Plasmid replicons detected frequently included those matching pRAY*, which is often associated with the *aadB* gene (Hamidian et al., 2012), RepAci3, p3ABAYE, pABTJ2, and RepAci9. RepMAci9 was detected in all thirteen ST215 isolates. Seven plasmid types were present in low frequency (**Figure 2B**) and an additional fifteen plasmid sequences were not detected in the Thai collection (**Supplementary Dataset S1**).

Genes Associated With Capsules and Outer Core

A. baumannii does not contain genes involved in lipopolysaccharide (LPS) O-antigen ligase activity (Kenyon and Hall, 2013; Weber et al., 2015), synthesizing instead a lipooligosaccharide (LOS) consisting of an outer core oligosaccharide (OCL) linked to Lipid A (Kenyon and Hall, 2013; Kenyon et al., 2014a); at least twelve distinct OCL structures have been inferred from genomic data (Kenyon et al., 2014b). We mapped all Thai isolates against an *A. baumannii* specific databases for capsular and LOS loci (KL and OCL, resp.; **Supplementary Figure S3**; Wyres et al., 2019). In similar fashion to the Vietnam study (Schultz et al., 2016), we noted a high diversity of KL within both GC2 and non-GC2 isolates. KL6 (15.2%), KL10 (15.7%), KL47 (11.0%), KL2 (8.4%), KL52 (7.9%), KL3 (7.3%), KL49 (6.3%), KL24 (5.8%), KL14 (3.1%), and KL28 (2.1%) were frequently encountered and KL32, KL63, KL57, KL8, KL108, KL19, KL113, KL116, KL60, KL43, KL37, KL9, KL125, and KL7 were represented in 2% or fewer isolates. KL could not be determined in 15 isolates (7.9%). KL2 and KL49 were found at least twice in the Vietnam isolates although we did not detect KL58, strongly represented in Schultz et al. (2016). Eight distinct capsule loci in our GC2 isolates were detected in isolates from all three hospitals during April 2016 and provide a challenge for novel therapies targeting bacterial cell surfaces. Furthermore, seven distinct LOS loci were detected amongst the Thai isolates (**Supplementary Figure S3** and **Supplementary Table S1**). The majority of GC2 isolates carried genes for OCL1 biosynthesis (91 isolates, 85.8% of all GC2 isolates, 61.8% total), whilst the other types, OCL2 (6.8%), OCL3 (4.2%), OCL4 (1.6%), OCL5 (15.7%), OCL6 (4.7%), and OCL7 (5.2%) were also widely distributed amongst our isolates; there was, however, no clear association between K- and LOS-types (**Figure 3**).

Linking Virulence-Associated Phenotype, Site of Isolation, and Genotype in GC2

We examined 45 GC2 isolates belonging to the major capsule types identified in the Thai collection: KL10 (eight isolates), KL2 (4), KL3 (2), KL47 (2), KL49 (5), KL52 (2), and KL6 (22). Although *A. baumannii* strains lack flagella, the species displays type IV-mediated twitching motility that facilitates spreading on abiotic surfaces (Vijayakumar et al., 2016), and it has been linked to the capacity of strains to cause systemic infection (Harding et al., 2018). Only six of our 45 GC2 isolates were derived from blood samples but all displayed twitching motility (**Table 1**, **Supplementary Table S5**, and **Figure 3A**). In contrast, none of six tissue isolates and only a minority of sputum isolates (10/33) were motile in this fashion. The capacity to swarm on semi-solid agar (surface-associated motility; Harding et al., 2018) can also be linked to a more virulent phenotype (Eijkelkamp et al., 2011;

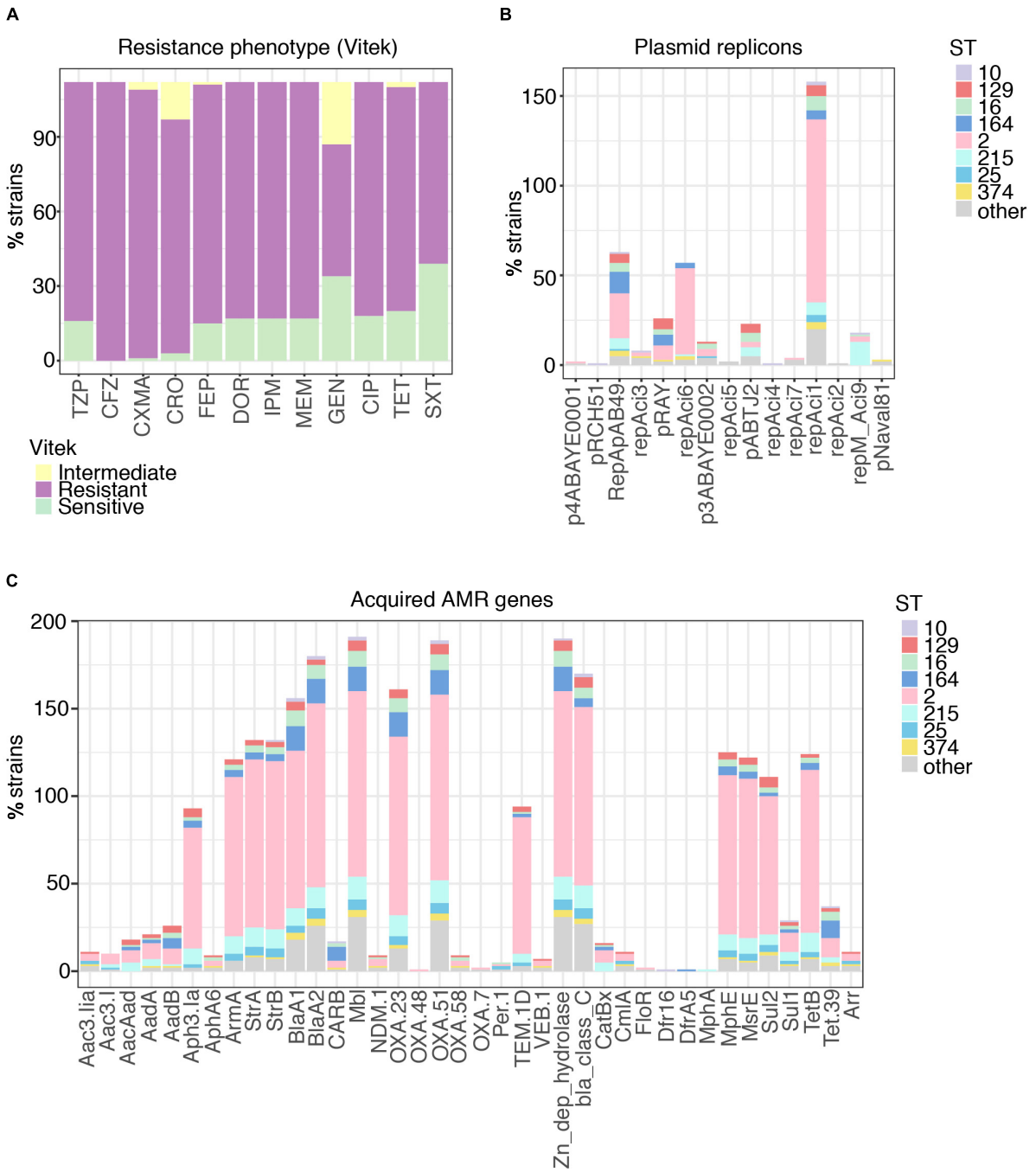

FIGURE 2 | Phenotypic resistance of *A. baumannii* at high levels for all antimicrobial classes. **(A)** Resistance phenotypes measured on site at time of isolation clearly demonstrate the highly problematic levels of resistance in *A. baumannii*, with > 70% non-sensitive against all tested classes. TZP, piperacillin-tazobactam; CFZ, cefazolin; CXMA, cefuroxime axetil; CRO, ceftriaxone; FEP, cefepime; DOR, doripenem; IPM, imipenem; MEM, meropenem; GEN, gentamicin; CIP, ciprofloxacin; TET, tetracycline; SXT, trimethoprim-sulfamethoxazole. **(B)** Distribution of plasmids carried by *A. baumannii* in relation to sequence type (ST). **(C)** Distribution of acquired antimicrobial resistance genes carried by *A. baumannii* in relation to sequence type (ST).

Tipton and Rather, 2017). 24/45 of the Thai GC2 isolates displayed surface-associated (swarming) motility; 6/6 of these were from tissue samples and 18/33 from sputum (**Table 1** and **Figure 3A**). Three isolates from sputum exhibited both forms of motility.

Many loci that have been linked to the capacity of *A. baumannii* to colonize, invade and disseminate within the host, such those encoding adhesins, capsules, quorum sensors, iron sequestering systems and other nutrient scavengers (Harding et al., 2018), are essential or advantageous for survival

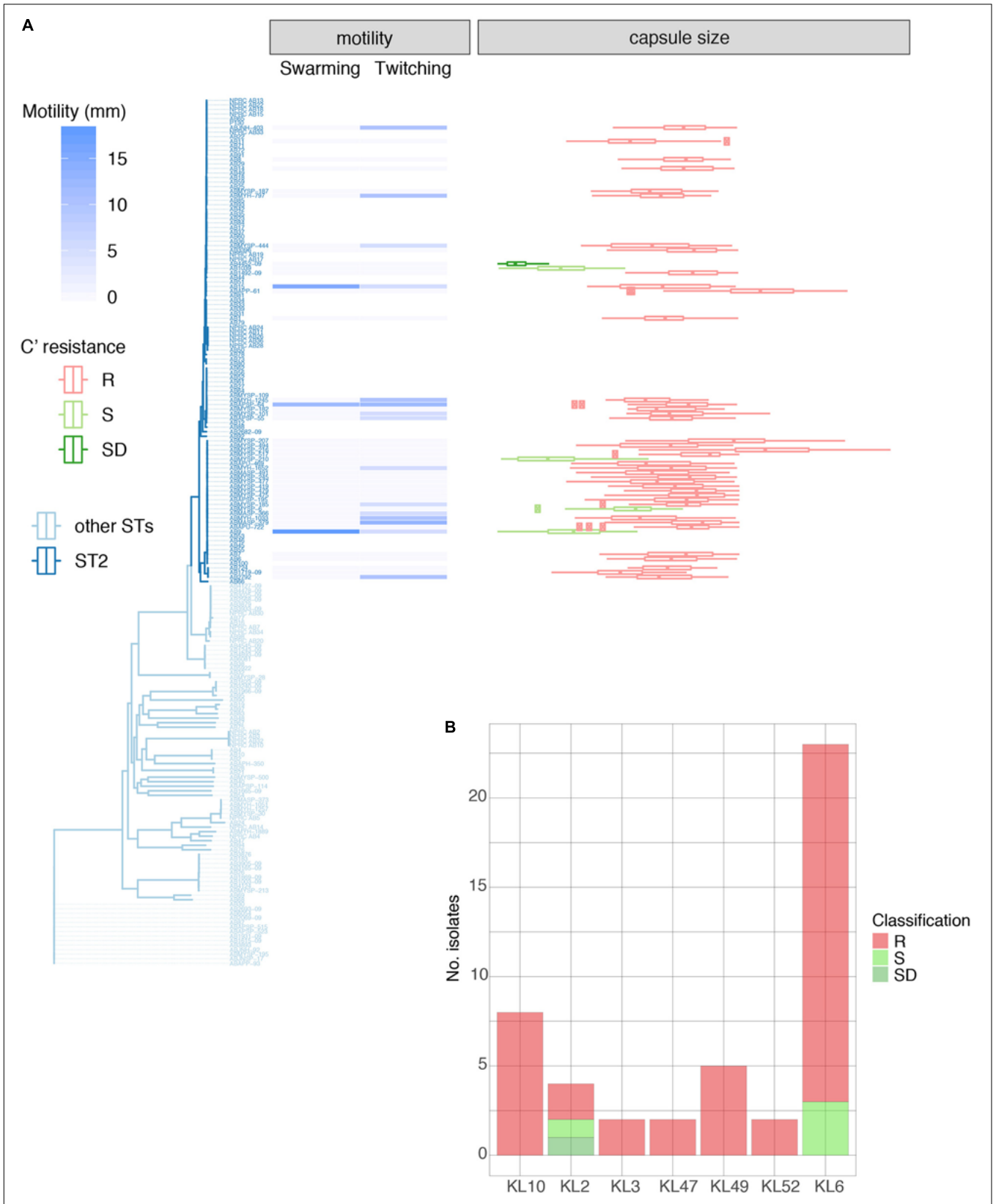

FIGURE 3 | Properties of 46 GC2 *A. baumannii* Thai isolates belonging to the common capsule genotypes encountered in this study. **(A)** Motility measurements, capsule size, and C' susceptibility in phylogenetic context. **(B)** C' resistance profiles stratified by capsule type.

TABLE 1 | Properties of GC2 *A. baumannii* clinical isolates.

Thai strain ID	Hospital	KL	OCL	ST	Sample source	Motility (mm)		C' Susceptibility[b]
						Swarming[c]	Twitching[d]	
ABMYSP-109	Thamm[a]	KL10	OCL1	2	Sputum	≤10	15	R
ABMYH-1245	Thamm	KL10	OCL1	2	Blood	≤10	10	R
ABAPSP-55	Thamm	KL10	OCL1	2	Sputum	≤10	5	R
ABAPSP-64	Thamm	KL10	OCL1	2	Sputum	12	12	R
ABMYSP-101	Thamm	KL10	OCL1	2	Sputum	≤10	5	R
ABMYSP-182	Thamm	KL10	OCL1	2	Sputum	14	<5	R
ABMYSP-187	Thamm	KL10	OCL1	2	Sputum	14	<5	R
ABMYH-797	Thamm	KL10	OCL1	2	Blood	≤10	10	R
AB1039	Songkla	KL2	OCL1	2	Sputum	19	<5	S
AB1492-09	Songkla	KL2	OCL1	2	Sputum	16	<5	R
AB3396	Songkla	KL2	OCL1	2	Tissue	15	<5	R
AB4452-09	Songkla	KL2	OCL1	2	Sputum	≤10	<5	DS
AB11	Siriraj	KL3	OCL1	2	Sputum	≤10	<5	R
ABJNH-403	Thamm	KL3	OCL1	2	Blood	≤10	10	R
AB15	Siriraj	KL47	OCL1	2	Sputum	15	5	R
ABAPP-61	Thamm	KL47	OCL1	2	Tissue	15	<5	R
AB8	Siriraj	KL49	OCL1	2	Sputum	15	<5	R
AB14	Siriraj	KL49	OCL1	2	Sputum	17	<5	R
AB724	Songkla	KL49	OCL1	2	Sputum	14	<5	R
AB1719-09	Songkla	KL49	OCL1	2	Tissue	15	<5	R
AB2792	Songkla	KL49	OCL1	2	Blood	≤10	10	R
AB1	Siriraj	KL52	OCL1	2	Tissue	14	<5	R
ABMYSP-444	Thamm	KL52	OCL1	2	Sputum	≤10	5	R
AB6	Siriraj	KL6	OCL1	2	Sputum	18	<5	R
AB7	Siriraj	KL6	OCL1	2	Sputum	17	<5	R
AB9	Siriraj	KL6	OCL1	2	Sputum	18	5	S
ABMYSP-185	Thamm	KL6	OCL1	2	Sputum	≤10	5	R
ABMYSP-216	Thamm	KL6	OCL1	2	Sputum	16	<5	R
ABMYH-1652	Thamm	KL6	OCL1	2	Blood	≤10	5	R
ABMYSP-475	Thamm	KL6	OCL1	2	Sputum	18	<5	R
ABMYSP-477	Thamm	KL6	OCL1	2	Sputum	15	<5	R
ABMYSP-479	Thamm	KL6	OCL1	2	Sputum	15	<5	R
ABMYSP-517	Thamm	KL6	OCL1	2	Sputum	≤10	<5	R
ABMASP-366	Thamm	KL6	OCL1	2	Sputum	≤10	5	R
ABMASP-379	Thamm	KL6	OCL1	2	Sputum	≤10	13	R
ABMASP-491	Thamm	KL6	OCL1	2	Sputum	≤10	<5	R
ABAPSP-195	Thamm	KL6	OCL1	2	Sputum	≤10	<5	R
ABAPU-469	Thamm	KL6	OCL1	2	Tissue	11	<5	R
ABAPU-722	Thamm	KL6	OCL1	2	Tissue	16	<5	R
ABMYSP-494	Thamm	KL6	OCL1	2	Sputum	16	<5	R
ABMYSP-6	Thamm	KL6	OCL1	2	Sputum	16	<5	S
ABMYSP-207	Thamm	KL6	OCL1	2	Sputum	≤10	<5	R
ABMYSP-210	Thamm	KL6	OCL1	2	Sputum	≤10	<5	S
ABMYSP-245	Thamm	KL6	OCL1	2	Sputum	≤10	<5	R
ABMYH-1033	Thamm	KL6	OCL1	2	Blood	≤10	10	R

[a] *Thamm: Thammasat Hospital; Songkla: Songklaragarind Hospital; Siriraj: Siriraj Hospital.* [b] *Complement reactivity: R, Resistant; DS, Delayed susceptible; S, Rapidly susceptible.* [c] *Values less than 10 mm are considered negative (Vijayakumar et al., 2016).* [d] *Values less than 5 mm are considered negative (Vijayakumar et al., 2016).*

in its natural habitat, predominantly soil and water (Baumann et al., 1968). The distribution of genes based on a publicly available virulence factor database is shown in **Supplementary Figure S4**, but whilst there are clear differences, no trend (for example increased prevalence in GC2) could be observed. As expected, siderophores, adhesins involved in biofilm formation and maintenance, and a variety of genes determining capsule biosynthesis are widely distributed among the isolates.

GC2 Capsule Size Correlates With Survival in Human Serum

A large proportion (40/45, 88.9%) were refractory to C'-mediated killing; of the remainder, only four were categorized as S (**Table 1**). All KL10, KL3, KL47, KL49, and KL52 isolates belonged to the R group, with only KL2 (2/4) and KL6 (3/23) capsule types displaying any degree of C' susceptibility (**Figures 3A,B**). All 45 GC2 isolates examined were encapsulated. The C' susceptible isolates elaborated significantly smaller capsules than R *A. baumannii* (R, mean 1.62 mm^2; DS, 0.31 mm^2; S, 0.81 mm^2); all capsule locus predictions however showed a perfect or almost perfect match, emphasizing that the capsule biosynthesis locus is likely intact (**Figure 3A**). Capsules containing sialic acids protect Gram-negative bacteria from C' attack (Rautemaa and Meri, 1999), and *N*-acetylneuramininc acid and related non-ulosonic and sialic acid structures have recently been found as repeat-unit constituents or as modifications of capsule structures in hypermucoviscous *K. pneumoniae* (Lin et al., 2014) and *A. baumannii* (Vinogradov et al., 2014; Kenyon et al., 2015; Singh et al., 2018), and associated with increased infectivity. Biosynthesis of sialic acids begins with the conversion of UDP-*N*-acetylglucosamine to UDP and *N*-acetylmannosamine by the hydrolyzing 2-epimerase NeuC; a homolog of this enzyme has been described for *A. baumannii* and its crystal structure determined (Ko et al., 2018). In our set of genomes, the *neuC* homolog (A0A154EJU5_ACIBA) was found only in the genomes of the five C' resistant isolates carrying genes for biosynthesis of the K49 capsular polysaccharide and is indeed a component of the KL49 locus and should thus correctly be annotated as *lgaC*; the repeat unit of the K49 capsular polysaccharide is composed of α-L-fucosamine, α-D-glucosamine and the non-ulosonic acid α-8-epi-legionaminic acid (Vinogradov et al., 2014).

OmpA, one of most abundant porins, is also known to bind factor H in human serum (Kim et al., 2009), and implicated to prevent C' mediated killing; it is however present in all our GC2 strains (**Supplementary Figure S4**). A more detailed analysis of putative factors explaining the phenotypes (type IV pili, surface proteins, secretion systems, biofilm formation (Weber et al., 2015; Lee et al., 2017; **Supplementary Table S6**) of the 47 GC2 isolates showed no differences that correlated with any of the phenotypes tested. We also included sequence analyses of PilA, which has been shown to influence twitching motility (Ronish et al., 2019), however, the sequences from all phenotyped isolates were identical.

DISCUSSION

Multi-drug resistant *A. baumannii* infections are rapidly increasing and require the use of last-line treatments such as colistin. An additional challenge further narrowing the spectrum of available options for highly resistant *A. baumannii* infections is that last-line treatments available often overlap with other highly problematic infections. One example is the use of rifampicin in combination with colistin against CRAB, which is also one of the last options to treat the increasing number of multi-drug resistant tuberculosis (MDR TB) cases, and use of rifampicin is therefore restricted in use against organisms other than MDR TB (Thapa et al., 2009; Durante-Mangoni et al., 2014; Leite et al., 2016; Seijger et al., 2019). There is therefore a growing interest in the potential of non-antibiotic therapeutic approaches including bacteriophage-derived capsule depolymerases as treatment alternative to antimicrobial chemotherapy (Waldor et al., 2005; García-Quintanilla et al., 2013; Seijger et al., 2019).

We present the analysis of a set of 191 *A. baumannii* clinical isolates from three major hospitals in Thailand with very high levels of drug resistance. The population structure is biased toward the major clone GC2, as has been observed in other studies in geographic proximity (Schultz et al., 2016). However, the inter-mixed origins of closely related isolates from all three hospitals clearly indicates that both GC2 as well as less dominant sequence types are circulating in the region, and are frequently (re)introduced into hospitals, as opposed to a clonal outbreak within one hospital. In addition to the phylogenetic diversity (almost 50% non-GC2 isolates) and the even spread across the three hospitals, we show that there is a high degree of strain-to-strain capsule variability, and development of depolymerase therapeutics will need to account for the challenge of a wide range of capsule types. Nevertheless, a recent study has demonstrated the potential of capsule depolymerase against *A. baumannii* in a *Galleria mellonella* (wax moth) larvae infection model and protection of both normal and immunocompromised mice from lethal peritoneal sepsis (Liu et al., 2019a).

The enzyme also sensitized the C'-resistant isolate to serum (Liu et al., 2019b), which is highly relevant as the large majority of our GC2 isolates (40/45) were C' resistant, in similar proportion to other recent studies (Sanchez-Larrayoz et al., 2017; Skerniškytė et al., 2019). LPS O-side chains prevent assembly of the C5b-9 complex by steric hindrance; *A. baumannii* however does not decorate its LOS with O-side chains but is able to modify the lipid A moiety of LOS by acylation, resulting in increased survival in blood (Bartholomew et al., 2019), which could prevent C5b-9 intercalation into the bilayer. Alternatively, there is some evidence that *A. baumannii* may prevent C' activation: resistant clinical isolates bound fH, a key inhibitor of the alternative C' pathway (Kim et al., 2009), preventing C5b-9 generation. King et al. (2009) found that clinical isolates did not bind fH but circumvented C3b deposition, again preventing C5b-9-mediated bacterial killing. Cell surface-located sialic acids are potent recruiters of fH and we therefore examined Thai GC2 isolates for evidence of *neuC*-dependent sialyl biosynthesis. The *neuC* homolog is part of the KL49 locus, however, non-ulosonic acid sugars are also found in the K2 and K6 types (Kenyon and Hall, 2013), which have C' sensitive as well as resistant phenotypes.

Current evidence indicates that C' killing of susceptible *A. baumannii* proceeds predominantly through the activation of the alternative pathway (Kim et al., 2009; Jacobs et al., 2010; Sanchez-Larrayoz et al., 2017). The lack of classical pathway killing may be due to the absence of C'-activating IgG or IgM directed against *A. baumannii* surface structures in normal human serum, suggesting that the predominant means to avoid bactericidal effects is prevention or subversion of activation of the

alternative pathway. It is likely that the polysaccharide capsule is the predominant macromolecule facilitating C' resistance (Harding et al., 2018) and the four fully C' susceptible isolates in the current study elaborated less capsule than the resistant group. Capsule depolymerases as an alternative means of resolving *A. baumannii* systemic infections would thus be worth exploring but may be limited by the wide diversity of capsule types likely to be encountered in current clinical isolates.

Whilst the current focus is placed on GC2, it is important to point out that GC1 and GC2 seem to follow different strategies for interacting with the immune system and hospital environment. Whilst we report low motility and high C' resistance for GC2 and the associated genetic background, GC1 seems to follow a very different route, with high motility profiles and different adherence profiles than GC2 (Skerniškytė et al., 2019). It is thus crucial to increase active surveillance of *A. baumannii* epidemiology, as different high-risk lineages may need different approaches to reduce their burden in the clinic.

DATA AVAILABILITY STATEMENT

The datasets generated for this study can be found in the European Nucleotide Archive ERS1930151–ERS1930323.

AUTHOR CONTRIBUTIONS

PT, NT, and RAS conceived the study. JL, EH, GB, and PT designed experimental procedures. JL, EH, RS, and GB performed the experiments, analyzed and curated the data. SV, PS, and PK assembled the bacterial collection. PT and EH wrote the manuscript.

FUNDING

This study was funded by the Newton Fund through Medical Research Council award MR/N012542/1. Assembly of the *A. baumannii* clinical isolate collection was enabled by National Science and Technology Development Agency award FDA-CO-2559-1448-TH. RS was supported by the Thailand Research Fund through the Royal Golden Jubilee PhD Programme (Grant No. PHD/0106/2559) funded by the Newton Fund delivered by the British Council Thailand. The funders played no role in the study or in the preparation of this article or in the decision to publish.

ACKNOWLEDGMENTS

The National Institute for Health Research University College London Hospitals Biomedical Research Centre provided infrastructural support. We acknowledge expert informatics support from the Pathogen Informatics team at the Wellcome Sanger Institute and thank Elisa Gonzalez de Herrero Martinez for assistance with DNA preparation.

SUPPLEMENTARY MATERIAL

The Supplementary Material for this article can be found online at: https://www.frontiersin.org/articles/10.3389/fmicb.2020.00548/full#supplementary-material

FIGURE S1 | Resistance genes and phenotypic resistance. The strains were grouped according to the number of agents in the Vitek screen the respective strains were resistant to, along the x-axis. The y-axis shows the number of strains in the relevant class, the color of the bars shows resistance (dark purple), intermediate (yellow), or sensitive (green) against the respective antimicrobial of the subplot. This shows that almost all strains are resistant against 12 reagents, sensitivity of the highly-resistant ones on the far end of the x-scale is only occasionally in sulfonamides or tetracycline, but all are fully resistant against the β-lactam class.

FIGURE S2 | Presence of genes encoding antibiotic resistance in Thai *A. baumannii* isolates. The guidance tree is shown in **Figure 3A**. Bla, β-lactamases; AGly, aminoglycosides; MLS, macrolides; Phe, chloramphenicol; Rif, rifampin; Sul, sulfonamides; Tet, tetracycline; Tmt, trimethoprim. AMR genes were sourced from the curated version of the ARG-ANNOT database available at the SRST2 site. Isolates from Thammasat University Hospital, Siriraj Hospital, and Songklanagarind Hospital are designated TU, Siriraj, and Songkla, respectively. Sequence types are shown, as indicated in the legend. Chromosomal mutations for RpoB are also shown, we could detect potential resistance-conferring changes (Giannouli et al., 2012; Pérez-Varela et al., 2017) D525N, H535Q, and S540F.

FIGURE S3 | Cell surface polysaccharide diversity of *A. baumannii* Thai isolates. Capsular (KL) and outer core loci (OCL) *in silico* typing of Thai isolates. *A. baumannii* shows considerable variation in K-type and a more conserved distribution of OCL-types.

FIGURE S4 | Virulence genes associated with Thai *A. baumannii* isolates. The guidance tree is shown in **Figure 3A**. Antibiotic resistance genes were detected with the curated version of the ARG-ANNOT database available at the SRST2 site using ARIBA. Isolates from Thammasat University Hospital, Siriraj Hospital, and Songklanagarind Hospital are designated TU, Siriraj, and Songkla, respectively. Sequence types are shown, as indicated in the legend.

TABLES S1–S6 | Properties of *A. baumannii* isolates.

DATASET S1 | The custom-made plasmid replicon collection used to assign plasmid types to *A. baumannii*.

REFERENCES

Bartholomew, T. L., Kidd, T. J., Sá Pessoa, J., Conde, Álvarez, R., and Bengoechea, J. A. (2019). 2-Hydroxylation of *Acinetobacter baumannii* Lipid A Contributes to Virulence. *Infect. Immun.* 87:e00066-19.. doi: 10.1128/IAI.00066-19

Bartual, S. G., Seifert, H., Hippler, C., Luzon, M. A. D., Wisplinghoff, H., and Rodríguez-Valera, F. (2005). Development of a multilocus sequence typing scheme for characterization of clinical isolates of *Acinetobacter baumannii*. *J. Clin. Microbiol.* 43, 4382–4390. doi: 10.1128/JCM.43.9.4382-4390.2005

Baumann, P., Doudoroff, M., and Stanier, R. Y. (1968). A study of the *Moraxella* group. II. Oxidative-negative species (genus *Acinetobacter*). *J. Bacteriol.* 95, 1520–1541. doi: 10.1128/jb.95.5.1520-1541.1968

Bertini, A., Poirel, L., Mugnier, P. D., Villa, L., Nordmann, P., and Carattoli, A. (2010). Characterization and PCR-based replicon typing of resistance plasmids in *Acinetobacter baumannii*. *Antimicrob. Agents Chemother.* 54, 4168–4177. doi: 10.1128/AAC.00542-10

Blackwell, G. A., and Hall, R. M. (2017). The *tet39* Determinant and the *msrE-mphE* Genes in *Acinetobacter* plasmids are each part of discrete modules flanked by inversely oriented pdif (XerC-XerD) sites. *Antimicrob. Agents Chemother.* 61:e00780-17. doi: 10.1128/AAC.00780-17

Blackwell, G. A., and Hall, R. M. (2019). Mobilisation of a small *Acinetobacter* plasmid carrying an *oriT* transfer origin by conjugative RepAci6 plasmids. *Plasmid* 103, 36–44. doi: 10.1016/j.plasmid.2019.04.002

Boetzer, M., Henkel, C. V., Jansen, H. J., Butler, D., and Pirovano, W. (2011). Scaffolding pre-assembled contigs using SSPACE. *Bioinformatics* 27, 578–579. doi: 10.1093/bioinformatics/btq683

Boetzer, M., and Pirovano, W. (2012). Toward almost closed genomes with GapFiller. *Genome Biol.* 13:R56. doi: 10.1186/gb-2012-13-6-r56

Bonomo, R. A., and Szabo, D. (2006). Mechanisms of multidrug resistance in *Acinetobacter* species and *Pseudomonas aeruginosa*. *Clin. Infect. Dis.* 43(Suppl. 2), S49–S56. doi: 10.1086/504477

Bosshard, P. P., Zbinden, R., Abels, S., Böddinghaus, B., Altwegg, M., and Böttger, E. C. (2006). 16S rRNA gene sequencing versus the API 20 NE system and the VITEK 2 ID-GNB card for identification of nonfermenting Gram-negative bacteria in the clinical laboratory. *J. Clin. Microbiol.* 44, 1359–1366. doi: 10.1128/JCM.44.4.1359-1366.2006

Bulens, S. N., Yi, S. H., Walters, M. S., Jacob, J. T., Bower, C., Reno, J., et al. (2018). Carbapenem-Nonsusceptible *Acinetobacter baumannii*, 8 US Metropolitan Areas, 2012-2015. *Emerging Infect. Dis.* 24, 727–734. doi: 10.3201/eid2404.171461

Chaisathaphol, T., and Chayakulkeeree, M. (2014). Epidemiology of infections caused by multidrug-resistant gram-negative bacteria in adult hospitalized patients at Siriraj Hospital. *J. Med. Assoc. Thai.* 97(Suppl. 3), S35–S45.

Chen, L., Zheng, D., Liu, B., Yang, J., and Jin, Q. (2016). VFDB 2016: hierarchical and refined dataset for big data analysis–10 years on. *Nucleic Acids Res.* 44, D694–D697. doi: 10.1093/nar/gkv1239

Chopra, T., Marchaim, D., Johnson, P. C., Awali, R. A., Doshi, H., Chalana, I., et al. (2014). Risk factors and outcomes for patients with bloodstream infection due to *Acinetobacter baumannii-calcoaceticus* complex. *Antimicrob. Agents Chemother.* 58, 4630–4635. doi: 10.1128/AAC.02441-14

Clemmer, K. M., Bonomo, R. A., and Rather, P. N. (2011). Genetic analysis of surface motility in *Acinetobacter baumannii*. *Microbiology* 157, 2534–2544. doi: 10.1099/mic.0.049791-0

Diancourt, L., Passet, V., Nemec, A., Dijkshoorn, L., and Brisse, S. (2010). The Population Structure of *Acinetobacter baumannii*: expanding multiresistant clones from an ancestral susceptible genetic pool. *PLoS One* 5:e10034. doi: 10.1371/journal.pone.0010034

Durante-Mangoni, E., Utili, R., and Zarrilli, R. (2014). Combination therapy in severe *Acinetobacter baumannii* infections: an update on the evidence to date. *Future Microbiol.* 9, 773–789. doi: 10.2217/fmb.14.34

Eddy, S. R. (2011). Accelerated Profile HMM Searches. *PLoS Comput. Biol.* 7:e1002195. doi: 10.1371/journal.pcbi.1002195

Eijkelkamp, B. A., Stroeher, U. H., Hassan, K. A., Papadimitrious, M. S., Paulsen, I. T., and Brown, M. H. (2011). Adherence and motility characteristics of clinical *Acinetobacter baumannii* isolates. *FEMS Microbiol. Lett.* 323, 44–51. doi: 10.1111/j.1574-6968.2011.02362.x

Eijkelkamp, B. A., Stroeher, U. H., Hassan, K. A., Paulsen, I. T., and Brown, M. H. (2014). Comparative analysis of surface-exposed virulence factors of *Acinetobacter baumannii*. *BMC Genomics* 15:1020. doi: 10.1186/1471-2164-15-1020

Falagas, M. E., and Kasiakou, S. K. (2005). Colistin: the revival of polymyxins for the management of multidrug-resistant gram-negative bacterial infections. *Clin. Infect. Dis.* 40, 1333–1341. doi: 10.1086/429323

Figueiredo, S., Poirel, L., Papa, A., Koulourida, V., and Nordmann, P. (2009). Overexpression of the naturally occurring blaOXA-51 Gene in *Acinetobacter baumannii* mediated by novel insertiON SEQuence ISAba9. *Antimicrobial. Agents Chemother.* 53, 4045–4047. doi: 10.1128/AAC.00292-09

Gaiarsa, S., Batisti Biffignandi, G., Esposito, E. P., Castelli, M., Jolley, K. A., Brisse, S., et al. (2019). Comparative analysis of the two *Acinetobacter baumannii* multilocus sequence typing (MLST) schemes. *Front. Microbiol.* 10:930. doi: 10.3389/fmicb.2019.00930

Gao, F., Wang, Y., Liu, Y.-J., Wu, X.-M., Lv, X., Gan, Y.-R., et al. (2011). Genome sequence of *Acinetobacter baumannii* MDR-TJ. *J. Bacteriol.* 193, 2365–2366. doi: 10.1128/JB.00226-11

García-Patiño, M. G., García-Contreras, R., and Licona-Limón, P. (2017). The Immune Response against *Acinetobacter baumannii*, an Emerging Pathogen in Nosocomial Infections. *Front. Immunol.* 8:441. doi: 10.3389/fimmu.2017.00441

García-Quintanilla, M., Pulido, M. R., López-Rojas, R., Pachón, J., and McConnell, M. J. (2013). Emerging therapies for multidrug resistant *Acinetobacter baumannii*. *Trends Microbiol.* 21, 157–163. doi: 10.1016/j.tim.2012.12.002

Giannouli, M., Di Popolo, A., Durante-Mangoni, E., Bernardo, M., Cuccurullo, S., Amato, G., et al. (2012). Molecular epidemiology and mechanisms of rifampicin resistance in *Acinetobacter baumannii* isolates from Italy. *Int. J. Antimicrob. Agents* 39, 58–63. doi: 10.1016/j.ijantimicag.2011.09.016

Gladman, S., and Seemann, T. (2008). *Velvet Optimiser*. Available online at: https://github.com/tseemann/VelvetOptimiser (accessed January, 2019).

Gupta, S. K., Padmanabhan, B. R., Diene, S. M., Lopez-Rojas, R., Kempf, M., Landraud, L., et al. (2014). ARG-ANNOT, a new bioinformatic tool to discover antibiotic resistance genes in bacterial genomes. *Antimicrob. Agents Chemother.* 58, 212–220. doi: 10.1128/AAC.01310-13

Hamidian, M., Ambrose, S. J., and Hall, R. M. (2016). A large conjugative *Acinetobacter baumannii* plasmid carrying the *sul2* sulphonamide and *strAB* streptomycin resistance genes. *Plasmid* 8, 43–50. doi: 10.1016/j.plasmid.2016.09.001

Hamidian, M., Nigro, S. J., and Hall, R. M. (2012). Variants of the gentamicin and tobramycin resistance plasmid pRAY are widely distributed in *Acinetobacter*. *J. Antimicrob. Chemother.* 67, 2833–2836. doi: 10.1093/jac/dks318

Hamidian, M., Nigro, S. J., Hartstein, R. M., and Hall, R. M. (2017). RCH51, a multiply antibiotic-resistant *Acinetobacter baumannii* ST103IP isolate, carries resistance genes in three plasmids, including a novel potentially conjugative plasmid carrying *oxa235* in transposon Tn6252. *J. Antimicrob. Chemother.* 72, 1907–1910. doi: 10.1093/jac/dkx069

Hamidian, M., and Nigro, S. J. (2019). Emergence, molecular mechanisms and global spread of carbapenem-resistant *Acinetobacter baumannii*. *Microb. Genom.* 5:e000242. doi: 10.1099/mgen.0.000306

Harding, C. M., Hennon, S. W., and Feldman, M. F. (2018). Uncovering the mechanisms of *Acinetobacter baumannii* virulence. *Nat. Rev. Microbiol.* 16, 91–102. doi: 10.1038/nrmicro.2017.148

Harding, C. M., Tracy, E. N., Carruthers, M. D., Rather, P. N., Actis, L. A., and Munson, R. S. (2013). *Acinetobacter baumannii* strain M2 produces type IV pili which play a role in natural transformation and twitching motility but not surface-associated motility. *mBio* 4:e0360-13. doi: 10.1128/mBio.00360-13

Hernandez-Morales, A. C., Lessor, L. L., Wood, T. L., Migl, D., Mijalis, E. M., Cahill, J., et al. (2018). Genomic and biochemical characterization of *Acinetobacter* podophage petty reveals a novel lysis mechanism and tail-associated depolymerase. *Activity. J. Virol.* 92, e1064-17. doi: 10.1128/JVI.01064-17

Higgins, P. G., Dammhayn, C., Hackel, M., and Seifert, H. (2010). Global spread of carbapenem-resistant *Acinetobacter baumannii*. *J. Antimicrob. Chemother.* 65, 233–238. doi: 10.1093/jac/dkp428

Holt, K., Kenyon, J. J., Hamidian, M., Schultz, M. B., Pickard, D. J., Dougan, G., et al. (2016). Five decades of genome evolution in the globally distributed, extensively antibiotic-resistant *Acinetobacter baumannii* global clone 1. *Microb. Genom.* 2:e000052. doi: 10.1099/mgen.0.000052

Hongsuwan, M., Srisamang, P., Kanoksil, M., Luangasanatip, N., Jatapai, A., Day, N. P., et al. (2014). Increasing incidence of hospital-acquired and healthcare-associated bacteremia in northeast Thailand: a multicenter surveillance study. *PLoS One* 9:e109324. doi: 10.1371/journal.pone.0109324

Howard, A., O'Donoghue, M., Feeney, A., and Sleator, R. D. (2012). *Acinetobacter baumannii*: an emerging opportunistic pathogen. *Virulence* 3, 243–250. doi: 10.4161/viru.19700

Hsu, L.-Y., Apisarnthanarak, A., Khan, E., Suwantarat, N., Ghafur, A., and Tambyah, P. A. (2017). Carbapenem-Resistant *Acinetobacter baumannii* and *Enterobacteriaceae* in South and Southeast Asia. *Clin. Microbiol. Rev.* 30, 1–22. doi: 10.1128/CMR.00042-16

Hunt, M., Mather, A. E., Sánchez-Busó, L., Page, A. J., Parkhill, J., Keane, J. A., et al. (2017). ARIBA: rapid antimicrobial resistance genotyping directly from sequencing reads. *Microb. Genom.* 3:e000131. doi: 10.1099/mgen.0.000131

Inouye, M., Dashnow, H., Raven, L.-A., Schultz, M. B., Pope, B. J., Tomita, T., et al. (2014). SRST2: rapid genomic surveillance for public health and hospital microbiology labs. *Genome Med.* 6:90. doi: 10.1186/s13073-014-0090-6

Jacobs, A. C., Hood, I., Boyd, K. L., Olson, P. D., Morrison, J. M., Carson, S., et al. (2010). Inactivation of phospholipase D diminishes *Acinetobacter baumannii* pathogenesis. *Infect. Immun.* 78, 1952–1962. doi: 10.1128/IAI.00889-09

Jones, L. S., Toleman, M. A., Weeks, J. L., Howe, R. A., Walsh, T. R., and Kumarasamy, K. K. (2014). Plasmid carriage of *bla* NDM-1 in clinical *Acinetobacter baumannii* isolates from India. *Antimicrob. Agents Chemother.* 58, 4211–4213. doi: 10.1128/AAC.02500-14

Kamolvit, W., Sidjabat, H. E., and Paterson, D. L. (2015). Molecular epidemiology and mechanisms of carbapenem resistance of *Acinetobacter* spp. *in Asia and Oceania. Microb. Drug Resist.* 21, 424–434. doi: 10.1089/mdr.2014.0234

Kenyon, J. J., and Hall, R. M. (2013). Variation in the complex carbohydrate biosynthesis loci of *Acinetobacter baumannii* genomes. *PLoS One* 8:e62160. doi: 10.1371/journal.pone.0062160

Kenyon, J. J., Holt, K. E., Pickard, D., Dougan, G., and Hall, R. M. (2014a). Insertions in the OCL1 locus of *Acinetobacter baumannii* lead to shortened lipooligosaccharides. *Res. Microbiol.* 165, 472–475. doi: 10.1016/j.resmic.2014.05.034

Kenyon, J. J., Nigro, S. J., and Hall, R. M. (2014b). Variation in the OC locus of *Acinetobacter baumannii* genomes predicts extensive structural diversity in the lipooligosaccharide. *PLoS One* 9:e107833. doi: 10.1371/journal.pone.0107833

Kenyon, J. J., Marzaioli, A. M., Hall, R. M., and De Castro, C. (2015). Structure of the K12 capsule containing 5,7-di-N-acetylacinetaminic acid from *Acinetobacter baumannii* isolate D36. *Glycobiology* 25, 881–887. doi: 10.1093/glycob/cwv028

Kim, D. H., Choi, J.-Y., Kim, H. W., Kim, S. H., Chung, D. R., Peck, K. R., et al. (2013). Spread of carbapenem-resistant *Acinetobacter baumannii* global clone 2 in Asia and AbaR-type resistance islands. *Antimicrob. Agents Chemother.* 57, 5239–5246. doi: 10.1128/AAC.00633-13

Kim, S. W., Choi, C. H., Moon, D. C., Jin, J. S., Lee, J. H., Shin, J.-H., et al. (2009). Serum resistance of *Acinetobacter baumannii* through the binding of factor H to outer membrane proteins. *FEMS Microbiol. Lett.* 301, 224–231. doi: 10.1111/j.1574-6968.2009.01820.x

King, L. B., Swiatlo, E., Swiatlo, A., and McDaniel, L. S. (2009). Serum resistance and biofilm formation in clinical isolates of *Acinetobacter baumannii*. *FEMS Immunol. Med. Microbiol.* 55, 414–421. doi: 10.1111/j.1574-695X.2009.00538.x

Ko, T.-P., Lai, S.-J., Hsieh, T.-J., Yang, C.-S., and Chen, Y. (2018). The tetrameric structure of sialic acid-synthesizing UDP-GlcNAc 2-epimerase from *Acinetobacter baumannii*: a comparative study with human GNE. *J. Biol. Chem.* 293, 10119–10127. doi: 10.1074/jbc.RA118.001971

Lamprecht, M. R., Sabatini, D. M., and Carpenter, A. E. (2007). CellProfiler: free, versatile software for automated biological image analysis. *BioTechniques* 42, 71–75. doi: 10.2144/000112257

Lee, C.-R., Lee, J. H., Park, M., Park, K. S., Bae, I. K., Kim, Y. B., et al. (2017). Biology of *Acinetobacter baumannii*: pathogenesis, antibiotic resistance mechanisms, and prospective treatment options. *Front Cell Infect Microbiol* 7:55. doi: 10.3389/fcimb.2017.00055

Lees-Miller, R. G., Iwashkiw, J. A., Scott, N. E., Seper, A., Vinogradov, E., Schild, S., et al. (2013). A common pathway for O-linked protein-glycosylation and synthesis of capsule in *Acinetobacter baumannii*. *Mol. Microbiol.* 89, 816–830. doi: 10.1111/mmi.12300

Leite, G. C., Oliveira, M. S., Perdigão-Neto, L. V., Rocha, C. K. D., Guimarães, T., Rizek, C., et al. (2016). Antimicrobial combinations against pan-resistant *Acinetobacter baumannii* isolates with different resistance mechanisms. *PLoS One* 11:e0151270. doi: 10.1371/journal.pone.0151270

Letunic, I., and Bork, P. (2016). Interactive tree of life (iTOL) v3: an online tool for the display and annotation of phylogenetic and other trees. *Nucleic Acids Res.* 44, W242–W245. doi: 10.1093/nar/gkw290

Lin, H., Paff, M. L., Molineux, I. J., and Bull, J. J. (2018). Antibiotic therapy using phage depolymerases: robustness across a range of conditions. *Viruses* 10:E622. doi: 10.3390/v10110622

Lin, T.-L., Hsieh, P.-F., Huang, Y.-T., Lee, W.-C., Tsai, Y.-T., Su, P.-A., et al. (2014). Isolation of a bacteriophage and its depolymerase specific for K1 capsule of *Klebsiella pneumoniae*: implication in typing and treatment. *J. Infect. Dis.* 210, 1734–1744. doi: 10.1093/infdis/jiu332

Liu, Y., Leung, S. S. Y., Guo, Y., Zhao, L., Jiang, N., Mi, L., et al. (2019a). The capsule depolymerase Dpo48 Rescues *Galleria mellonella* and mice from *Acinetobacter baumannii* Systemic Infections. *Front. Microbiol.* 10:545. doi: 10.3389/fmicb.2019.00545

Liu, Y., Mi, Z., Mi, L., Huang, Y., Li, P., Liu, H., et al. (2019b). Identification and characterization of capsule depolymerase Dpo48 from *Acinetobacter baumannii* phage IME200. *PeerJ* 7:e6173. doi: 10.7717/peerj.6173

Loraine, J., Heinz, E., De Sousa Almeida, J., Milevskyy, O., Voravuthikunchai, S. P., Srimanote, P., et al. (2018). Complement susceptibility in relation to genome sequence of recent *Klebsiella pneumoniae* isolates from thai hospitals. *mSphere* 3:e0537-18. doi: 10.1128/mSphere.00537-18

Malke, H. (1986). M. Sussman (Editor). The Virulence of Escherichia coli — Reviews and Methods. XV + 473 S., 45 Abb., 3S Tab. London-Orlando-San Diego-New. York-Toronto-Montreal Sydney-Tokyo 1985. Academic Press. $ 75.00. ISBN: 0-12-677520-6. *J Basic Microbiol.* 26, 127–128. doi: 10.1002/jobm.3620260219

Mushtaq, N., Redpath, M. B., Luzio, J. P., and Taylor, P. W. (2004). Prevention and cure of systemic *Escherichia coli* K1 infection by modification of the bacterial phenotype. *Antimicrob. Agents Chemother.* 48, 1503–1508. doi: 10.1128/aac.48.5.1503-1508.2004

Negus, D., Vipond, J., Hatch, G. J., Rayner, E. L., and Taylor, P. W. (2015). Parenteral administration of capsule depolymerase EnvD prevents lethal inhalation anthrax infection. *Antimicrob. Agents Chemother.* 59, 7687–7692. doi: 10.1128/AAC.01547-15

Oliveira, H., Costa, A. R., Konstantinides, N., Ferreira, A., Akturk, E., Sillankorva, S., et al. (2017). Ability of phages to infect *Acinetobacter calcoaceticus-Acinetobacter baumannii* complex species through acquisition of different pectate lyase depolymerase domains: specific genomic pattern variation of phages. *Environ. Microbiol.* 19, 5060–5077. doi: 10.1111/1462-2920.13970

Page, A. J., Cummins, C. A., Hunt, M., Wong, V. K., Reuter, S., Holden, M. T. G., et al. (2015). Roary: rapid large-scale prokaryote pan genome analysis. *Bioinformatics* 31, 3691–3693. doi: 10.1093/bioinformatics/btv421

Page, A. J., De Silva, N., Hunt, M., Quail, M. A., Parkhill, J., Harris, S. R., et al. (2016a). Robust high-throughput prokaryote de novo assembly and improvement pipeline for Illumina data. *Microb. Genom.* 2:e000083. doi: 10.1099/mgen.0.000083

Page, A. J., Taylor, B., Delaney, A. J., Soares, J., Seemann, T., Keane, J. A., et al. (2016b). SNP-sites: rapid efficient extraction of SNPs from multi-FASTA alignments. *Microb. Genom.* 2:e000056. doi: 10.1099/mgen.0.000056

Page, J. A., Taylor, B., and Keane, J. A. (2016). Multilocus sequence typing by blast from de novo assemblies against PubMLST. *JOSS* 1:118. doi: 10.21105/joss.00118

Paradis, E., Claude, J., and Strimmer, K. (2004). APE: analyses of phylogenetics and evolution in R language. *Bioinformatics* 20, 289–290. doi: 10.1093/bioinformatics/btg412

Parks, D. H., Imelfort, M., Skennerton, C. T., Hugenholtz, P., and Tyson, G. W. (2015). CheckM: assessing the quality of microbial genomes recovered from isolates, single cells, and metagenomes. *Genome Res.* 25, 1043–1055. doi: 10.1101/gr.186072.114

Pérez-Varela, M., Corral, J., Vallejo, J. A., Rumbo-Feal, S., Bou, G., Aranda, J., et al. (2017). Mutations in the β-Subunit of the RNA polymerase impair the surface-associated motility and virulence of *Acinetobacter baumannii*. *Infect. Immun.* 85:e0327-17. doi: 10.1128/IAI.00327-17

Post, V., and Hall, R. M. (2009). AbaR5, a large multiple-antibiotic resistance region found in *Acinetobacter baumannii*. *Antimicrob. Agents Chemother.* 53, 2667–2671. doi: 10.1128/AAC.01407-08

Rautemaa, R., and Meri, S. (1999). Complement-resistance mechanisms of bacteria. *Microbes Infect.* 1, 785–794. doi: 10.1016/s1286-4579(99)80081-1

Ronish, L. A., Lillehoj, E., Fields, J. K., Sundberg, E. J., and Piepenbrink, K. H. (2019). The structure of PilA from *Acinetobacter baumannii* AB5075 suggests a mechanism for functional specialization in *Acinetobacter* type IV pili. *J. Biol. Chem.* 294, 218–230. doi: 10.1074/jbc.RA118.005814

Russo, T. A., Beanan, J. M., Olson, R., MacDonald, U., Luke, N. R., Gill, S. R., et al. (2008). Rat pneumonia and soft-tissue infection models for the study of *Acinetobacter baumannii* biology. *Infect. Immun.* 76, 3577–3586. doi: 10.1128/IAI.00269-08

Sahbudak Bal, Z., Kamit Can, F., Yazici, P., Berna Anil, A., Duyu, M., Yilmaz Ciftdogan, D., et al. (2018). The evaluation of safety and efficacy of colistin use in pediatric intensive care unit: results from two reference hospitals and review of literature. *J. Infect. Chemother.* 24, 370–375. doi: 10.1016/j.jiac.2017.12.017

Salto, I. P., Torres Tejerizo, G., Wibberg, D., Pühler, A., Schlüter, A., and Pistorio, M. (2018). Comparative genomic analysis of *Acinetobacter* spp. plasmids originating from clinical settings and environmental habitats. *Sci. Rep.* 8:7783. doi: 10.1038/s41598-018-26180-3

Sanchez-Larrayoz, A. F., Elhosseiny, N. M., Chevrette, M. G., Fu, Y., Giunta, P., Spallanzani, R. G., et al. (2017). Complexity of Complement Resistance Factors Expressed by *Acinetobacter baumannii* needed for survival in human serum. *J. Immunol.* 199, 2803–2814. doi: 10.4049/jimmunol.1700877

Schultz, M. B., Pham Thanh, D., Tran, Do Hoan, N., Wick, R. R., Ingle, D. J., et al. (2016). Repeated local emergence of carbapenem-resistant *Acinetobacter baumannii* in a single hospital ward. *Microb. Genom.* 2:e000050. doi: 10.1099/mgen.0.000050

Scott, N. E., Kinsella, R. L., Edwards, A. V. G., Larsen, M. R., Dutta, S., Saba, J., et al. (2014). Diversity within the *O* -linked protein glycosylation systems of *Acinetobacter* Species. *Mol Cell Proteomics* 13, 2354–2370. doi: 10.1074/mcp.M114.038315

Seemann, T., and Gladman, S. (2014). Prokka: rapid prokaryotic genome annotation. *Bioinformatics* 30, 2068–2069. doi: 10.1093/bioinformatics/btu153

Seijger, C., Hoefsloot, W., Bergsma-de Guchteneire, I., Te Brake, L., van Ingen, J., Kuipers, S., et al. (2019). High-dose rifampicin in tuberculosis: experiences from a Dutch tuberculosis centre. *PLoS One* 14:e0213718. doi: 10.1371/journal.pone.0213718

Sievert, D. M., Ricks, P., Edwards, J. R., Schneider, A., Patel, J., Srinivasan, A., et al. (2013). Antimicrobial-resistant pathogens associated with healthcare-associated infections: summary of data reported to the national healthcare safety network at the centers for disease control and prevention, 2009-2010. *Infect. Control Hosp. Epidemiol.* 34, 1–14. doi: 10.1086/668770

Singh, J. K., Adams, F. G., and Brown, M. H. (2018). Diversity and function of capsular polysaccharide in *Acinetobacter baumannii*. *Front. Microbiol.* 9:3301. doi: 10.3389/fmicb.2018.03301

Sirijatuphat, R., Sripanidkulchai, K., Boonyasiri, A., Rattanaumpawan, P., Supapueng, O., Kiratisin, P., et al. (2018). Implementation of global antimicrobial resistance surveillance system (GLASS) in patients with bacteremia. *PLoS One* 13:e0190132. doi: 10.1371/journal.pone.0190132

Skerniškytė, J., Krasauskas, R., Péchoux, C., Kulakauskas, S., Armalytė, J., and Sužiedėlienė, E. (2019). Surface-related features and virulence among *Acinetobacter baumannii* Clinical isolates belonging to international clones I and II. *Front. Microbiol.* 9:3116. doi: 10.3389/fmicb.2018.03116

Stamatakis, A. (2014). RAxML version 8: a tool for phylogenetic analysis and post-analysis of large phylogenies. *Bioinformatics* 30, 1312–1313. doi: 10.1093/bioinformatics/btu033

Suwantarat, N., and Carroll, K. C. (2016). Epidemiology and molecular characterization of multidrug-resistant Gram-negative bacteria in Southeast Asia. *Antimicrob. Resist Infect. Control* 5, 15. doi: 10.1186/s13756-016-0115-6

Tacconelli, E., Carrara, E., Savoldi, A., Harbarth, S., Mendelson, M., Monnet, D. L., et al. (2018). Discovery, research, and development of new antibiotics: the WHO priority list of antibiotic-resistant bacteria and tuberculosis. *Lancet Infect. Dis.* 18, 318–327. doi: 10.1016/S1473-3099(17)30753-3

Teo, J., Lim, T.-P., Hsu, L.-Y., Tan, T.-Y., Sasikala, S., Hon, P.-Y., et al. (2015). Extensively drug-resistant *Acinetobacter baumannii* in a Thai hospital: a molecular epidemiologic analysis and identification of bactericidal Polymyxin B-based combinations. *Antimicrob. Resist Infect. Control* 4, 2. doi: 10.1186/s13756-015-0043-x

Thapa, B., Tribuddharat, C., Rugdeekha, S., Techachaiwiwat, W., Srifuengfung, S., and Dhiraputra, C. (2009). Rifampin resistance in carbapenem-resistant *Acinetobacter baumannii* in Siriraj Hospital, Thailand. *Nepal. Med. Coll J.* 11, 232–237.

Tipton, K. A., and Rather, P. N. (2017). An ompR-envZ two-component system ortholog regulates phase variation, osmotic tolerance, motility, and virulence in *Acinetobacter baumannii* strain AB5075. *J. Bacteriol.* 199:e0705-16. doi: 10.1128/JB.00705-16

Vijayakumar, S., Rajenderan, S., Laishram, S., Anandan, S., Balaji, V., and Biswas, I. (2016). Biofilm formation and motility depend on the nature of the *Acinetobacter baumannii* Clinical Isolates. *Front. Public Health* 4:105. doi: 10.3389/fpubh.2016.00105

Vinogradov, E., Maclean, L., Xu, H. H., and Chen, W. (2014). The structure of the polysaccharide isolated from *Acinetobacter baumannii* strain LAC-4. *Carbohydr. Res.* 390, 42–45. doi: 10.1016/j.carres.2014.03.001

Waldor, M. K., Friedman, D. I., and Adhya, S. L. (eds) (2005). *Phages: Their role in Bacterial Pathogenesis and Biotechnology*. Washington, D.C: ASM Press.

Weber, B. S., Harding, C. M., and Feldman, M. F. (2015). Pathogenic *Acinetobacter*: from the Cell Surface to Infinity and Beyond. *J. Bacteriol.* 198, 880–887. doi: 10.1128/JB.00906-15

Wickham, H. (2009). *Ggplot2: Elegant Graphics for Data Analysis*. New York, NY: Springer.

Wong, D., Nielsen, T. B., Bonomo, R. A., Pantapalangkoor, P., Luna, B., and Spellberg, B. (2017). Clinical and pathophysiological overview of *Acinetobacter* infections: a century of challenges. *Clin. Microbiol. Rev.* 30, 409–447. doi: 10.1128/CMR.00058-16

Wood, D. E., and Salzberg, S. L. (2014). Kraken: ultrafast metagenomic sequence classification using exact alignments. *Genome Biol.* 15:R46. doi: 10.1186/gb-2014-15-3-r46

Wyres, K. L., Cahill, S. M., Holt, K. E., Hall, R. M., and Kenyon, J. J. (2019). Identification of *Acinetobacter baumannii* loci for capsular polysaccharide (KL) and lipooligosaccharide outer core (OCL) synthesis in genome assemblies using curated reference databases compatible with Kaptive. *Microbiology* [Epub ahead of print],

Yu, G., Lam, T. T.-Y., Zhu, H., and Guan, Y. (2018). Two methods for mapping and visualizing associated data on phylogeny using ggtree. *Mol. Biol. Evol.* 35, 3041–3043. doi: 10.1093/molbev/msy194

Zarrilli, R., Pournaras, S., Giannouli, M., and Tsakris, A. (2013). Global evolution of multidrug-resistant *Acinetobacter baumannii* clonal lineages. *Int. J. Antimicrob. Agents* 41, 11–19. doi: 10.1016/j.ijantimicag.2012.09.008

Zerbino, D. R., and Birney, E. (2008). Velvet: algorithms for de novo short read assembly using de Bruijn graphs. *Genome Res.* 18, 821–829. doi: 10.1101/gr.074492.107

Zhang, W.-J., Lu, Z., Schwarz, S., Zhang, R.-M., Wang, X.-M., Si, W., et al. (2013). Complete sequence of the *bla*(NDM-1)-carrying plasmid pNDM-AB from *Acinetobacter baumannii* of food animal origin. *J. Antimicrob. Chemother.* 68, 1681–1682. doi: 10.1093/jac/dkt066

Conflict of Interest: The authors declare that the research was conducted in the absence of any commercial or financial relationships that could be construed as a potential conflict of interest.

frontiers in Microbiology

ORIGINAL RESEARCH
published: 13 May 2020
doi: 10.3389/fmicb.2020.00919

Mobile Genetic Elements Harboring Antibiotic Resistance Determinants in *Acinetobacter baumannii* Isolates From Bolivia

Mónica Cerezales[1†], Kyriaki Xanthopoulou[2,3†], Julia Wille[2,3], Oleg Krut[4], Harald Seifert[2,3], Lucía Gallego[1] and Paul G. Higgins[2,3]*

[1] Faculty of Medicine and Nursing, Department of Immunology, Microbiology, and Parasitology, University of the Basque Country UPV/EHU, Leioa, Spain, [2] Institute for Medical Microbiology, Immunology and Hygiene, University of Cologne, Cologne, Germany, [3] German Centre for Infection Research (DZIF), Partner Site Bonn-Cologne, Cologne, Germany, [4] Paul-Ehrlich-Institute, Federal Institute for Vaccines and Biomedicine, Langen, Germany

OPEN ACCESS

Edited by:
Benjamin Andrew Evans, University of East Anglia, United Kingdom

Reviewed by:
Nabil Karah, Umeå University, Sweden
Andres Felipe Opazo-Capurro, University of Concepcion, Chile

***Correspondence:**
Mónica Cerezales
mcerezales001@ikasle.ehu.eus; monicacerezalesg@gmail.com

† These authors have contributed equally to this work

Specialty section:
This article was submitted to Antimicrobials, Resistance and Chemotherapy, a section of the journal Frontiers in Microbiology

Received: *15 January 2020*
Accepted: *17 April 2020*
Published: *13 May 2020*

Citation:
Cerezales M, Xanthopoulou K, Wille J, Krut O, Seifert H, Gallego L and Higgins PG (2020) Mobile Genetic Elements Harboring Antibiotic Resistance Determinants in Acinetobacter baumannii Isolates From Bolivia. Front. Microbiol. 11:919. doi: 10.3389/fmicb.2020.00919

Using a combination of short- and long-read DNA sequencing, we have investigated the location of antibiotic resistance genes and characterized mobile genetic elements (MGEs) in three clinical multi-drug resistant *Acinetobacter baumannii*. The isolates, collected in Bolivia, clustered separately with three different international clonal lineages. We found a diverse array of transposons, plasmids and resistance islands related to different insertion sequence (IS) elements, which were located in both the chromosome and in plasmids, which conferred resistance to multiple antimicrobials, including carbapenems. Carbapenem resistance might be caused by a *Tn2008* carrying the bla_{OXA-23} gene. Some plasmids were shared between the isolates. Larger plasmids were less conserved than smaller ones and they shared some homologous regions, while others were more diverse, suggesting that these big plasmids are more plastic than the smaller ones. The genetic basis of antimicrobial resistance in Bolivia has not been deeply studied until now, and the mobilome of these *A. baumannii* isolates, combined with their multi-drug resistant phenotype, mirror the transfer and prevalence of MGEs contributing to the spread of antibiotic resistance worldwide and require special attention. These findings could be useful to understand the antimicrobial resistance genetics of *A. baumannii* in Bolivia and the difficulty in tackling these infections.

Keywords: *A. baumannii*, plasmids, mobile genetic elements, antimicrobial resistance, carbapenemase

INTRODUCTION

Acinetobacter baumannii is a non-fermenting Gram-negative bacilli and it is the second most common species after *Pseudomonas aeruginosa* in this group causing bacterial infections (Gonzalez-Villoria and Valverde-Garduno, 2016). While *A. baumannii* has been isolated from the wider environment such as water, soil, and animals, most studied isolates come from clinical samples, where *A. baumannii* has become a serious health problem, particularly in the intensive care unit, where it can cause serious and prolonged outbreaks (Gonzalez-Villoria and Valverde-Garduno, 2016). *A. baumannii* is often multidrug resistant (Peleg et al., 2008; Gonzalez-Villoria and Valverde-Garduno, 2016) making antimicrobial therapy of *A. baumannii* infections difficult.

In some cases, with the advent of resistance to last line antibiotics such as colistin, there are few therapeutic options left (Higgins et al., 2010; Manchanda et al., 2010; Göttig et al., 2014; Cayô et al., 2016).

Acinetobacter baumannii is known to have a great genome plasticity, which is the capacity to acquire and disseminate genes, especially those related to antimicrobial resistance which are commonly associated with insertion sequence (IS) elements in transposons and plasmids; this dynamism in the genome of *A. baumannii* contributed to the rapid evolution of drug resistance (Adams et al., 2010) as has been demonstrated for IS*Aba1* mobilizing antimicrobial resistance genes (Mugnier et al., 2009). These processes are achieved thanks to mobile genetic elements (MGEs) harboring resistance genes. The simplest MGEs are ISs, that can also form transposons (Tn), and there are more complex structures such as integrons, resistance islands (RI), and plasmids. Antimicrobial resistance genes are often integrated into resistance cassettes related to translocation elements, causing cumulative resistance to multiple drugs (Roca et al., 2012).

A diverse range of MGEs have been described in *A. baumannii,* for example transposons such as *Tn2008, Tn2008B*, *Tn2006*, *Tn2009*, or *Tn2007*, which represent different transposon configurations carrying the bla_{OXA-23} gene together with IS*Aba1* or IS*Aba4,* and additional genes (Nigro and Hall, 2016). Great variability in antimicrobial resistance platforms, including MGEs, have been recorded even within the same international clone (IC), illustrating their contribution to the evolution of drug resistance (Adams et al., 2010). Plasmids in *Acinetobacter* spp. are unique and unrelated to those from other genera, although they often share the same resistance determinants, such as *strA, strB*, *tet(B)* or *sul2*. In *A. baumannii*, a diverse array of plasmids have been found, ranging in size from 2 Kb to more than 150 Kb. The larger plasmids normally encode for more than one resistance gene, but up to now little is known about these plasmids (Carattoli, 2013; Hamidian et al., 2016).

The aim of this study was to characterize the MGEs such as plasmids and RI of three different *A. baumannii* clinical isolates, representing different clonal lineages.

MATERIALS AND METHODS

Bacterial Isolates

Three *A. baumannii* isolates recovered from two hospitals in Cochabamba, Bolivia, in September 2015, January 2016, and October 2016 (**Table 1**) representing three different ICs (IC4, IC5. and IC7) were selected for this study. We previously reported their carbapenem resistance mechanisms and molecular epidemiology (Cerezales et al., 2019).

Antimicrobial Susceptibility Testing

In addition to previously reported carbapenem susceptibility testing results, in the present study we investigated the following antimicrobials by agar dilution: amikacin, azithromycin, chloramphenicol, trimethoprim-sulfamethoxazole, erythromycin, levofloxacin, minocycline, kanamycin, and tetracycline.

TABLE 1 | *Acinetobacter baumannii* isolates data.

Isolate	Molecular epidemiology					MIC (mg/L) for various antimicrobials												
	STs Ox/Pas	IC	$bla_{OXA-51-like}$	Sample origin	GenBank accession number	AMK	AZI*	CHL	CIP	SXT*	CST	ERY*	GEN	IPM	KAN*	LVX	MEM	MIN*	TET*	TGC*
MC1	1518/991	IC7	bla_{OXA-64}	Catheter	NZ_QXPV00000000.1	>128 R	64	>128 R	>128 R	128	1 S	64	32 R	32 R	>256	32 R	64 R	64	>128	16
MC23	1520/79	IC5	bla_{OXA-65}	Urine	NZ_QXPJ00000000.1	>128 R	64	>128 R	128 R	128	1 S	64	>128 R	1 S	>256	32 R	2 S	1	16	4
MC75	236/15	IC4	bla_{OXA-51}	Ulcer	NZ_QXOL00000000.1	>128 R	32	128 R	>128 R	128	1 S	32	>128 R	32 R	>256	8 R	64 R	0,5	16	2

*AMK, amikacin; AZI, azithromycin; CHL, chloramphenicol; CIP, ciprofloxacin; SXT, trimethoprim-sulfamethoxazole; CST, colistin; ERY, erythromycin; GEN, gentamicin; IPM, imipenem; KAN, kanamycin; LVX, levofloxacin; MEM, meropenem; MIN, minocycline; TET, tetracycline; TGC, tigecycline. *No EUCAST breakpoints are available for these antimicrobials.*

TABLE 2 | Plasmid content, size, location resistance genes as determined by WGS, and accession numbers.

Isolate	Plasmids	Accession number	Size	Location of resistance genes	
				Plasmid	Chromosome
MC1	pMC1.1	MK531536	184 Kb	*strA* *strB* *aac(3)-IIa* *aac(6′)-Ian* *tet(B)* *sul2*	bla_{OXA-23}
	pMC1.2	MK531537	8.7 Kb		
MC23	pMC23.1	MK531538	67 Kb		*strA* *strB* *sul2* *floR* *aadA1* *sat2* *dfrA1*
	pMC23.2	MK531537	8.7 Kb		
	pMC23.3	MK531539	6 Kb	*aadB*	
MC75	pMC75.1	MK531540	149 Kb	*strA* *strB* *sul2*	bla_{OXA-23} *aphA6*
	pMC75.2	MK531541	13.9 Kb	bla_{TEM-1} *aac(3)-IIa*	

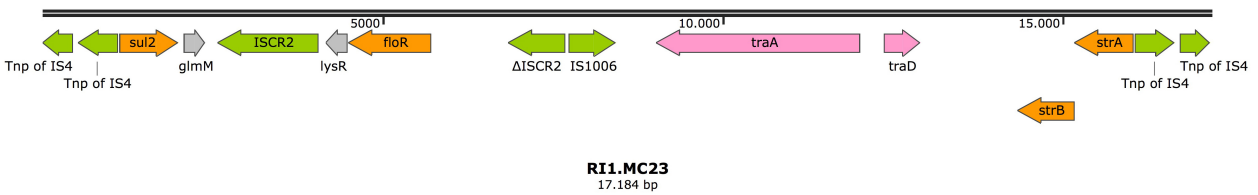

FIGURE 1 | Resistance island RI1.MC23 in isolate MC23. Arrows represent predicted ORFs and the direction of the arrow represents the direction of transcription. Resistance genes are shown by orange arrows and transposon-related genes, recombinases, and insertion sequences are indicated by green arrows. Genes involved in plasmid mobility are shown in pink. Other genes are indicated by gray arrows. Hypothetical proteins are not shown.

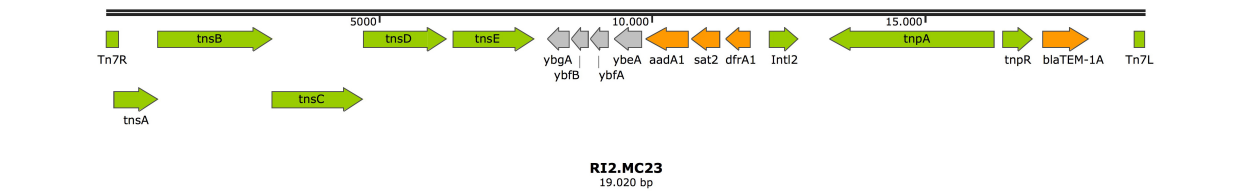

FIGURE 2 | Resistance island RI2.MC23 in isolate MC23. Arrows represent predicted ORFs and the direction of the arrow represents the direction of transcription. Resistance genes are shown by orange arrows and transposon-related genes, recombinases, and insertion sequences are indicated by green arrows. Other genes are indicated by gray arrows. Hypothetical proteins are not shown.

MICs were interpreted using the European Committee on Antimicrobial Susceptibility Testing (EUCAST) breakpoints[1].

MinION Long-Read Sequencing and Assembly

The Oxford Nanopore Technologies (Oxford, United Kingdom) MinION sequencer was used to obtain long reads to span repetitive elements and close genomes and plasmids. DNA extraction was performed using the Genomic-tip 100/G kit (Qiagen, Hilden, Germany). Library preparation was carried out according to manufacturer's indications using a combination of Native Barcoding Kit 1D and Ligation Sequencing Kit 1D; EXP-NBD103 and SQK-LSK108 (Oxford Nanopore Technologies, Oxford, United Kingdom), respectively.

The tool Albacore (Oxford Nanopore Technologies, Oxford, United Kingdom) was used for demultiplexing the reads which were later used to perform the Canu assembly (Koren et al., 2017). A hybrid assembly combining previous MiSeq short reads with MinION-generated long reads was performed using a hybridSpades (Antipov et al., 2016).

[1]http://www.eucast.org/clinical_breakpoints/

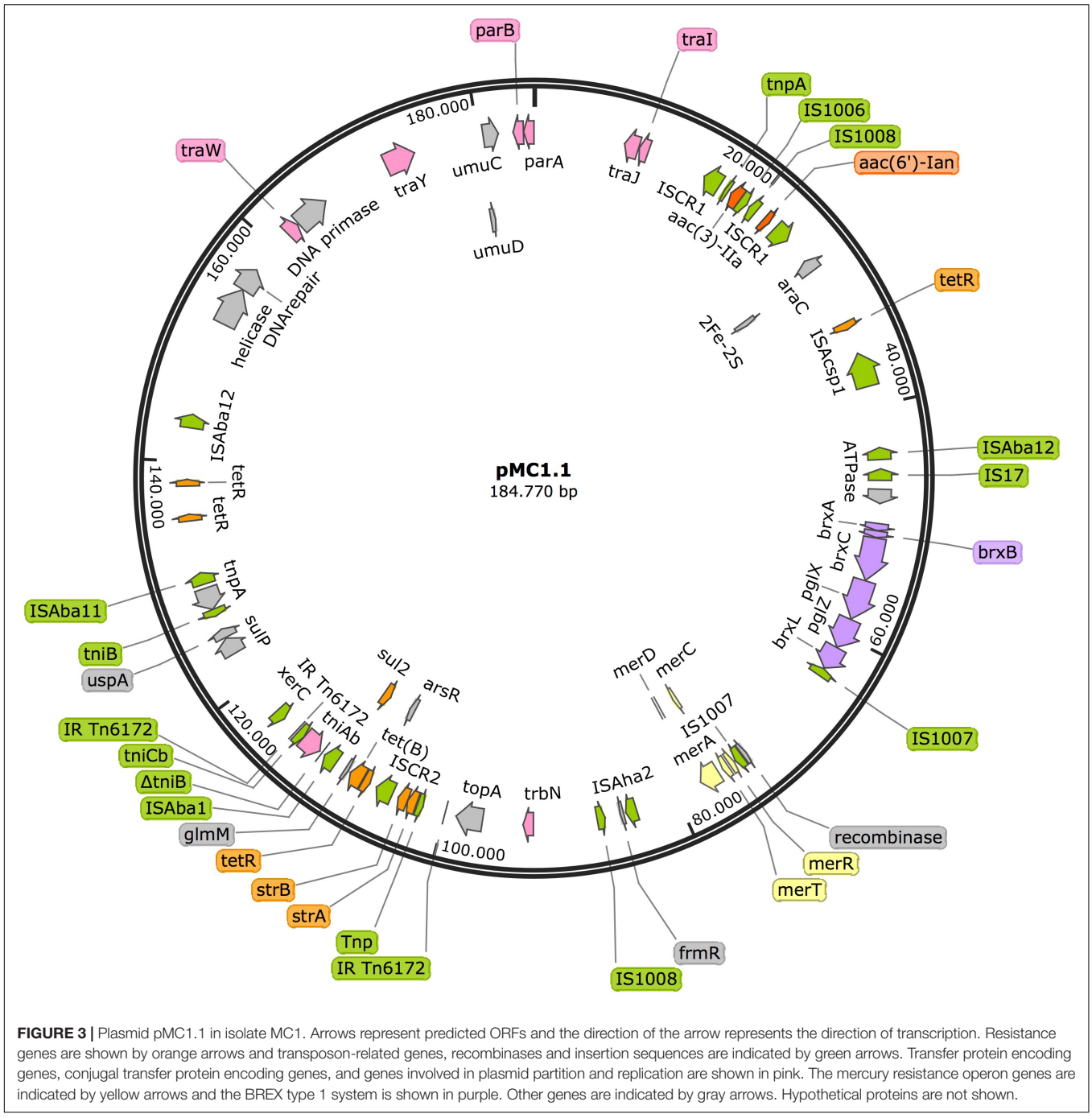

FIGURE 3 | Plasmid pMC1.1 in isolate MC1. Arrows represent predicted ORFs and the direction of the arrow represents the direction of transcription. Resistance genes are shown by orange arrows and transposon-related genes, recombinases and insertion sequences are indicated by green arrows. Transfer protein encoding genes, conjugal transfer protein encoding genes, and genes involved in plasmid partition and replication are shown in pink. The mercury resistance operon genes are indicated by yellow arrows and the BREX type 1 system is shown in purple. Other genes are indicated by gray arrows. Hypothetical proteins are not shown.

Plasmid Annotation and Visualization

ORFfinder (NCBI)[2] was used to predict the open reading frames (ORF) of the plasmids. A second functional annotation of the genomes was performed using the online tool Rapid Annotation Subsystem Technology (RAST)[3] (Genomics et al., 2008). Subsequently, the tool SnapGene Viewer (GSL Biotech)[4] was used to obtain a circular diagram of the plasmids. Graphic comparisons between similar plasmids, pMC1.1 and pA297-3, as well as pMC23.1 and pAC30c, were carried out with the tool Kablammo (Wintersinger and Wasmuth, 2015).

Conjugation Experiments

Broth mate conjugation experiments were performed to determine the location of antimicrobial resistance genes using the sodium azide-resistant *Escherichia coli* J53 and the rifampicin-resistant *A. baumannii* BM4547 as recipient

[2]https://www.ncbi.nlm.nih.gov/orffinder/

[3]https://rast.nmpdr.org/

[4]https://www.snapgene.com

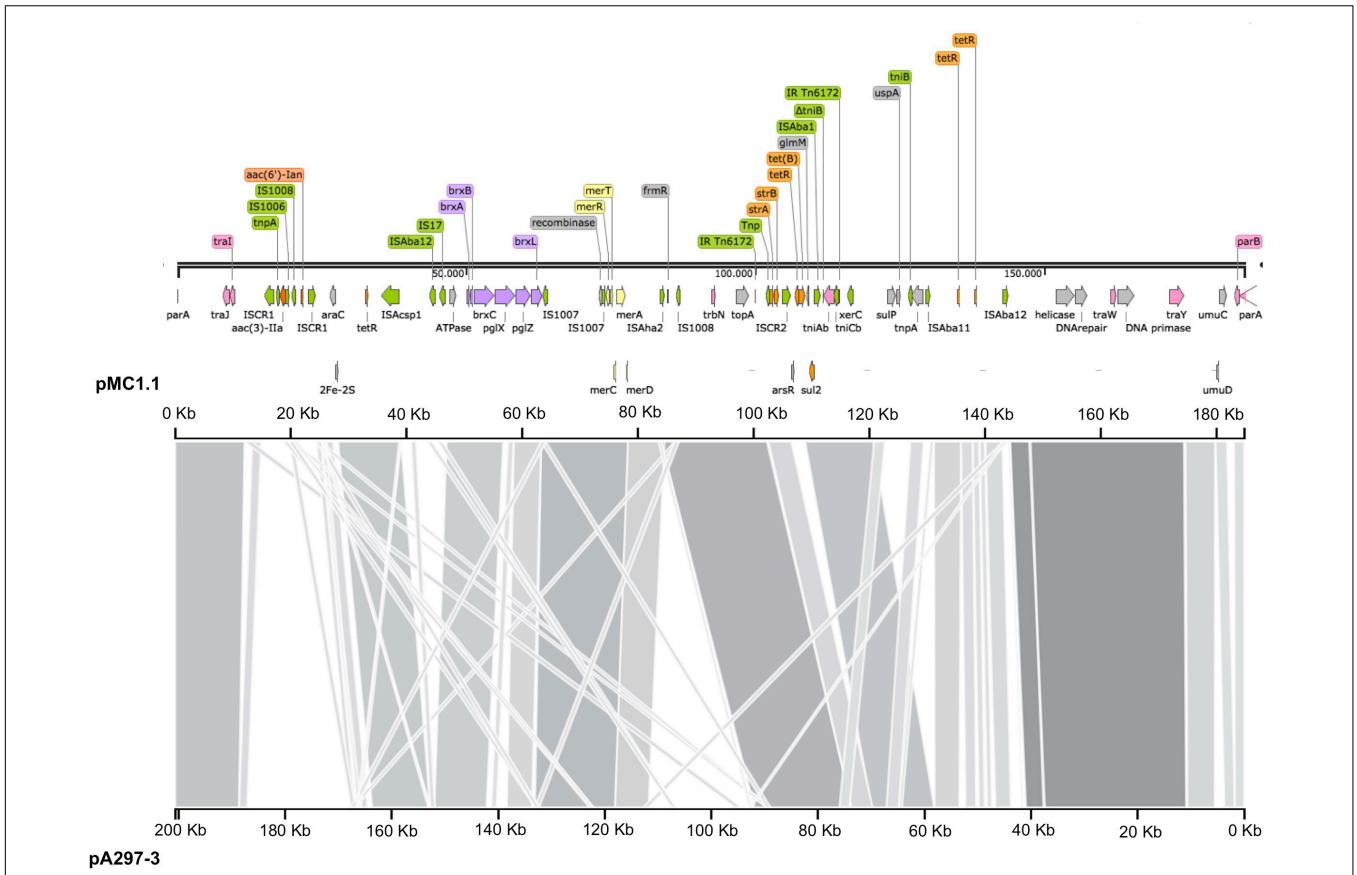

FIGURE 4 | Comparison of plasmids pMC1.1 and pA297-3. The top axis represents the pMC1.1, the bottom axis represents pA297-3. Gray shaded regions show the homologous regions between the two plasmids.

strains. Selection of *E. coli* J53 transconjugants was performed using sodium azide (200 mg/L) combined either with amikacin (30 mg/L), streptomycin (30 mg/L), kanamycin (30 mg/L), gentamicin (30 mg/L), or ticarcillin (100 mg/L), and selection for *A. baumannii* BM4547 was performed using rifampicin (60 mg/L) combined with gentamicin (30 mg/L) or ticarcillin (100 mg/L. Transconjugants were selected with the antimicrobials to select for the plasmids encoding their respective resistance genes. Strain MC1 was resistant to rifampicin, therefore conjugation with *A. baumannii* BM4547 could not be performed. The transconjugants were tested by PCR for the bla_{TEM} gene.

RESULTS AND DISCUSSION

MC1 and MC75 were previously tested as carbapenem-resistant and carried the carbapenemase encoding $bla_{\mathrm{OXA-23-like}}$ gene (Cerezales et al., 2019). Further testing revealed that MC1 and MC75 were also resistant to amikacin, chloramphenicol, ciprofloxacin, gentamicin, and levofloxacin. MC23 was resistant to amikacin, chloramphenicol, ciprofloxacin, gentamicin, and levofloxacin but was susceptible to carbapenems. All three isolates were susceptible to colistin (**Table 1**).

The $bla_{\mathrm{OXA-23}}$ encoding gene was located on the chromosome in a *Tn2008* vehicle in the isolates MC1 and MC75 (**Table 2**). In *A. baumannii*, the $bla_{\mathrm{OXA-23-like}}$ gene is associated with IS*Aba1*, which contributes to its overexpression as well as its mobilization (Nigro and Hall, 2016). *Tn2008* has previously been described in Bolivian *A. baumannii* isolates and this mirrors the spread of this structure among different ICs leading to a carbapenem-resistant phenotype (Nigro and Hall, 2016; Sennati et al., 2016; Chen et al., 2017; Ewers et al., 2017; Cerezales et al., 2018).

Resistance Islands

In the isolate MC23, the gene *strA* was located on a resistance island in the chromosome (RI1.MC23) (accession number MK531542), together with other antimicrobial resistance genes such as *sul2, floR*, and *strB*. Diverse IS elements were found, with the resistance island bracketed by two copies of a transposase from the IS4 family in reverse orientation (**Figure 1**). Two genes involved in conjugation were also present in this structure, suggesting a plasmid origin.

In addition, a second chromosomal resistance island was also found in this isolate (RI2.MC23) (accession number MK531543), that carried a typical structure from class 2 integrons,

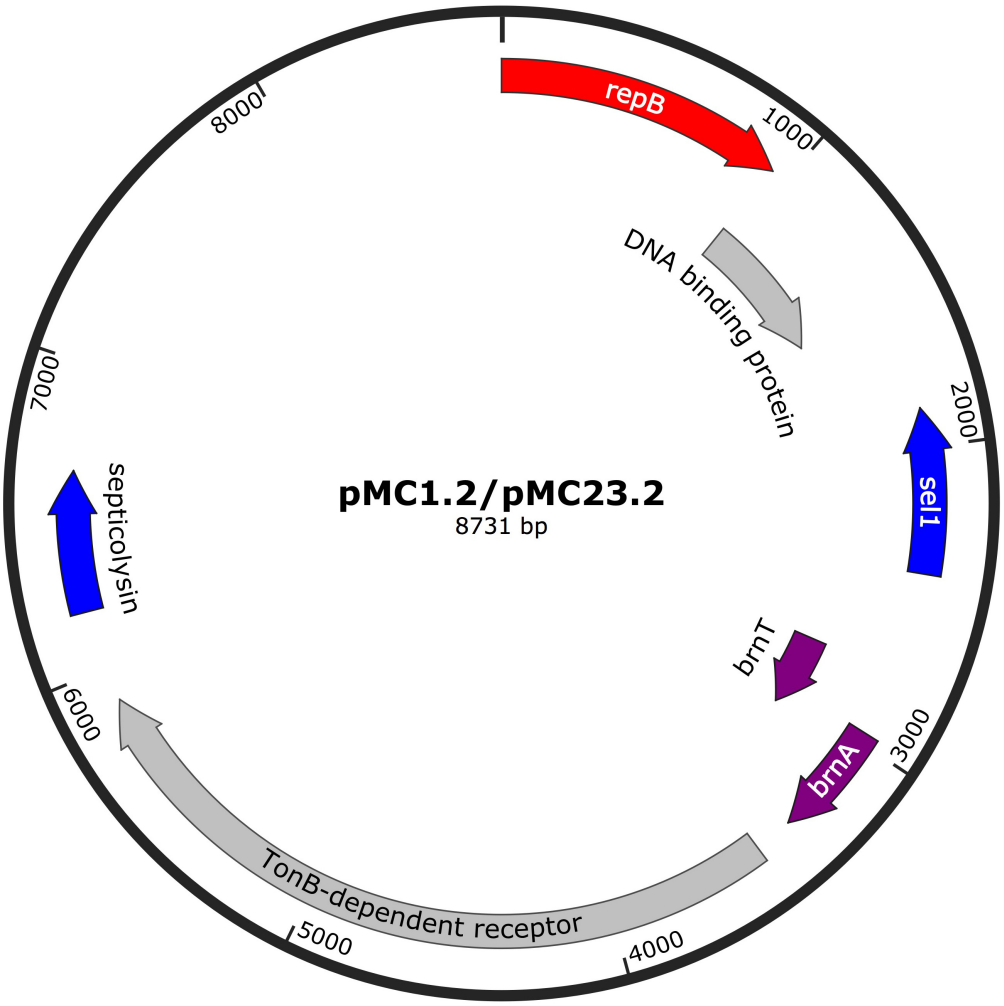

FIGURE 5 | Plasmids pMC1.2 and pMC23.2 in isolates MC1 and MC23, respectively. Arrows represent predicted ORFs and the direction of the arrow represents the direction of transcription. Red arrow is used for the replicon. The toxin-antitoxin system is indicated by violet arrows and blue arrows represent virulence genes. Other genes are shown in gray.

dfrA-sat2-aadA1-ybeA-ybfAybfB-ybgA, located between the Tn7 transposition module *tns*ABCDE and a non-functional Intl2 integrase. Additionally, a Tn3 transposon was found inserted in the Tn7 transposon, carrying three genes, *tnpA*, encoding for a Tn3 transposase; *tnpR* encoding a Tn3 resolvase; and the antimicrobial resistance gene $bla_{\mathrm{TEM-1A}}$ (**Figure 2**).

The gene encoding Apha6 was found on the chromosome of MC75 bracketed by two IS*Aba125* that is a composite transposon known as Tn*aphA6* (Matos et al., 2019).

Plasmids

pMC1.1

Annotation of pMC1.1 (accession number MK531536), 39% GC content, revealed many different IS elements such as IS*1006*, IS*1007*, IS*1008*, IS*Acsp1,* IS91 family, IS*Aha2*, IS*Aba11*, IS*Aba12,* and IS*17*. This plasmid carried a mercuric resistance operon, similar to an already described mercuric Tn in a 200 Kb plasmid (pA297-3) from an IC1 *A. baumannii* isolate, but it lacks the *merP* open reading frame (Hamidian et al., 2016). Different antimicrobial resistance determinants such as *strA, strB*, *aac(3)-IIa,* and *aac(6′)-Ian,* conferring resistance to aminoglycosides, *sul2* conferring resistance to sulphonamides, and *tet(B)* conferring resistance to tetracycline were also present. The region of the plasmid carrying *strA, strB, and sul2* shared high homology with *Tn6172,* located in pA297-3 as well (**Figure 3**), however, in pMC1.1 *arsR, tetR,* and *tet(B)* genes were also located within *Tn6172* with an IS*CR2* transposable element (IS91 family). This IS*CR* element has been described associated with different antimicrobial resistance genes in *A. baumannii*, especially with *sul2*, contributing to their mobilization thanks to a rolling circle transposition mechanism (Toleman et al., 2006), and was similar to other plasmids from Argentina (Vilacoba et al., 2013) and to plasmids found in an ST25 isolate from Australia (Hamidian and Hall, 2016). However, the location of *tetR-tetB* genes was different; they were located between *glmM* and *arsR*, suggesting a possible later insertion of these genes in

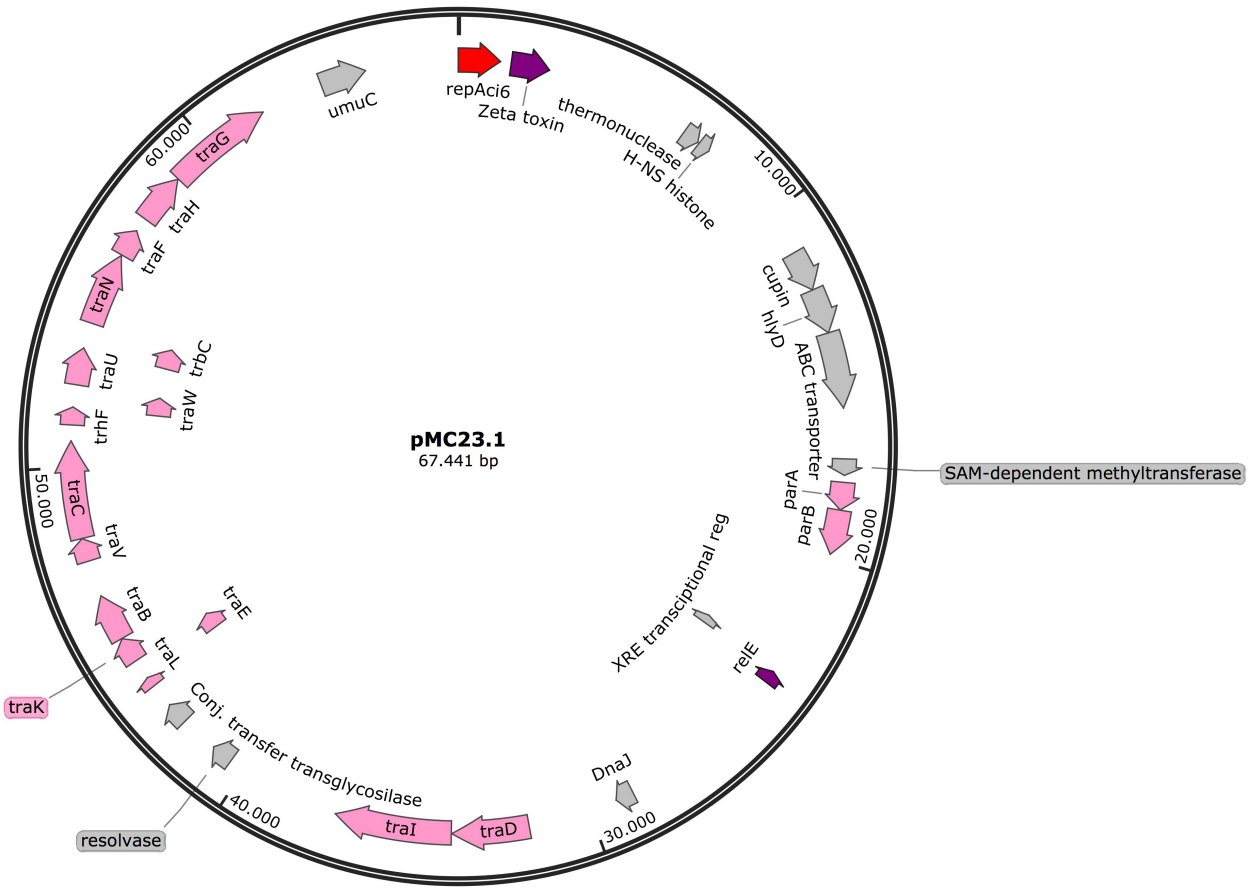

FIGURE 6 | Plasmid pMC23.1 in isolate MC23. Arrows represent predicted ORFs and the direction of the arrow represents the direction of transcription. Red arrow is used for the replicon. The toxins are indicated by violet arrows represent virulence genes. Transfer protein encoding genes, conjugal transfer protein encoding genes, and genes involved in plasmid partition and replication are shown in pink. Other genes are shown in gray. Hypothetical proteins are not shown.

different positions within the transposon (Vilacoba et al., 2013). In addition, the same inverted repeats (IR) generated by the insertion of the transposon were also found in pMC1.1 which together with the similar backbone with pA297-3 (**Figure 4**) suggest they share a common origin. The genes *aac(3)-IIa* and *aac(6′)-Ian* were associated with IS6 family IS and bracketed by two IS*CR1* in inverted orientation. IS*CR1* belongs to the IS91 family and has been described related to class 1 integrons and antimicrobial resistance genes in diverse Gram-negative species such as *Klebsiella pneumoniae*, *P. aeruginosa*, and *Citrobacter freundii* (Toleman et al., 2006). Different transfer genes (*tra*) were also found in this plasmid, as well as genes involved in plasmid partition and replication (*parB/repB* and *xerC*) that are related to segregational stability of plasmids. This plasmid also encoded a system called BREX type 1 (bacteriophage exclusion) which has been described to be involved in phage resistance (Goldfarb et al., 2015).

pMC1.2/pMC23.2

The 8.7 Kb plasmids found in MC1 and MC23 (pMC1.2 and pMC23.2) were identical (accession number MK531537), with a GC content of 34.3% (**Figure 5**). This small plasmid has often been found in IC1 *A. baumannii* isolates (Lean and Yeo, 2017). Annotation of this plasmid revealed ORFs encoding for a RepB replicon (Rep-3 superfamily, GR2) (Bertini et al., 2010; Lean and Yeo, 2017) a toxin-antitoxin system (BrnT-BrnA), that is involved in vertical stability; TonB-dependent receptor, related to the transmission of signals from the outside of the cell leading to transcriptional activation of target genes; a *septicolysin* gene encoding a cytolytic enzyme toward eukaryotic cells and is involved in pathogenesis; as well as *sel1* gene that encodes for a protein that has been described in diverse prokaryotic genera and has an important role in virulence.

pMC23.1

The largest plasmid in MC23 was the 67.5 Kb pMC23.1 (accession number MK531538) (**Figure 6**). It belonged to GR6 according to its replicase, *repAci6*. Its GC content was 33.7% and almost all of its putative protein encoding genes were related to conjugative plasmid transfer in a *tra* locus, some of them are part of a type IV (T4SS) secretion system. This T4SS is able to secrete or take up both proteins and DNA, and possibly is involved in natural competence, a feature of *A. baumannii* (Salto et al., 2018). Two toxin encoding genes were present in the plasmid,

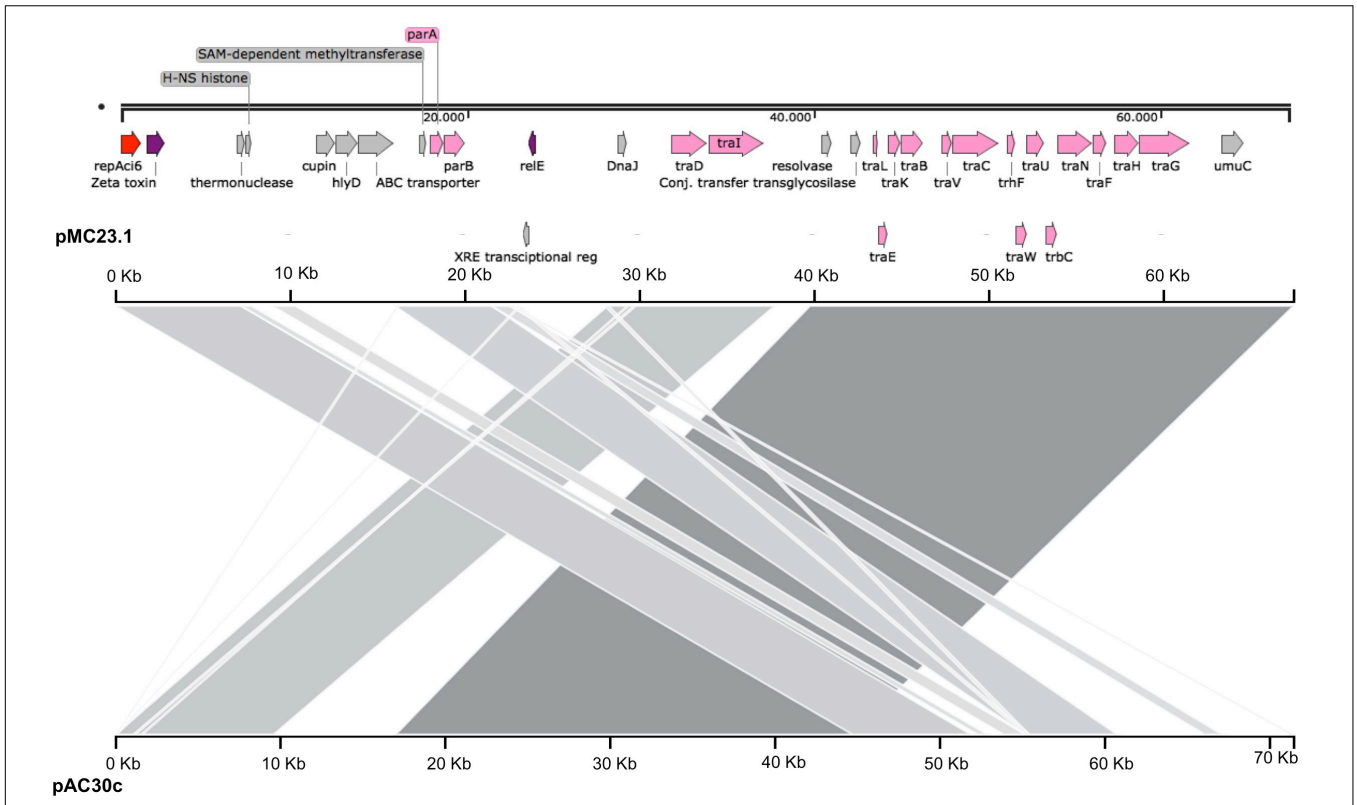

FIGURE 7 | Comparison of plasmids pMC23.1 and pAC30c. The top axis represents the pMC23.1, the bottom axis represents pAC30c. Gray shaded regions show the homologous regions between the two plasmids.

relE and zeta toxin, but no antitoxins were found, although they were present in a very similar plasmid (pAC30c) in an *A. baumannii* isolate belonging to ST195 (IC2) (**Figure 7**; Lean et al., 2016). In addition, the partition genes *parA/parB* were also encoded on pMC23.1. The backbone of pMC23.1 and pAC30c were very similar, with only a few differences. pMC23.1 lacked some hypothetical proteins present in pAC30c, and the region encoding for tellurite resistance (*telA* gene and IS*66*); while *traD*, a cupin-like protein (that is a superfamily of enzymes including dioxygenases, decarboxylases, hydrolases, or isomerases); HlyD protein, that exports proteins from the cytosol to the outside of the cell, and an ABC transporter were not present in pAC30.

pMC23.3

A 6 Kb small plasmid was present in the isolate MC23, pMC23.3 (accession number MK531539), 39.2% GC content, and was found to have 100% similarity with an already described plasmid, pRAY from an isolate in South Africa, encoding resistance to gentamicin, kanamycin and tobramycin (*aadB* gene) together with *mobA* and *mobC* genes, which are thought to encode mobilization proteins (Lean and Yeo, 2017). Many similar plasmids have been found in diverse *A. baumannii* isolates from different ICs and countries, suggesting a common origin and subsequent diversification in their evolution. Concurrent with other studies, no *rep* gene was found in the plasmid sequence, supporting the idea of the presence of a mechanism of replication relying in the host RNA polymerase (Lean and Yeo, 2017).

pMC75.1

Analysis of pMC75.1 (accession number MK531540) a large plasmid of 150 Kb revealed that it was very similar to pMC1.1 (sharing 80% of their sequences), it also carried a Tn*6172,* in which antimicrobial resistance genes such as *sul2, strB,* and *strA* are encoded, but lacking *tet(B)* and *arsR* that were present in pMC1.1 (**Figure 8**). The *mer* operon was also found in this plasmid, and many genes encoding conjugative transfer proteins. The BREX type 1 system was also present. A *stbA* gene was found, the protein encoded by this gene plays a role in plasmid stability as well as *parA/parB*. Several IS elements were also present, i.e., IS*Aba1*, IS*Aba125*, IS*Aba14*, IS*Aba42*, IS*1007*, and IS*Aha2*. However, this plasmid lacked the transposon carrying *aac(3)-IIa* and *aac(6′)-Ian*.

pMC75.2

The 13.9 Kb plasmid, pMC75.2 (accession number MK531541) (**Figure 9**) with a GC content of 40.3%, carried the broad-spectrum β-lactamase $bla_{\mathrm{TEM-1B}}$ and the aminoglycoside resistance gene *aac(3)-IIa* flanked on both sides by IS15DIV; a toxin-antitoxin system, *brnT/brnA*; a TonB-dependant receptor, a septicolysin gene and *mobA/mobS*, which are involved in plasmid mobility. Conjugation experiments revealed that

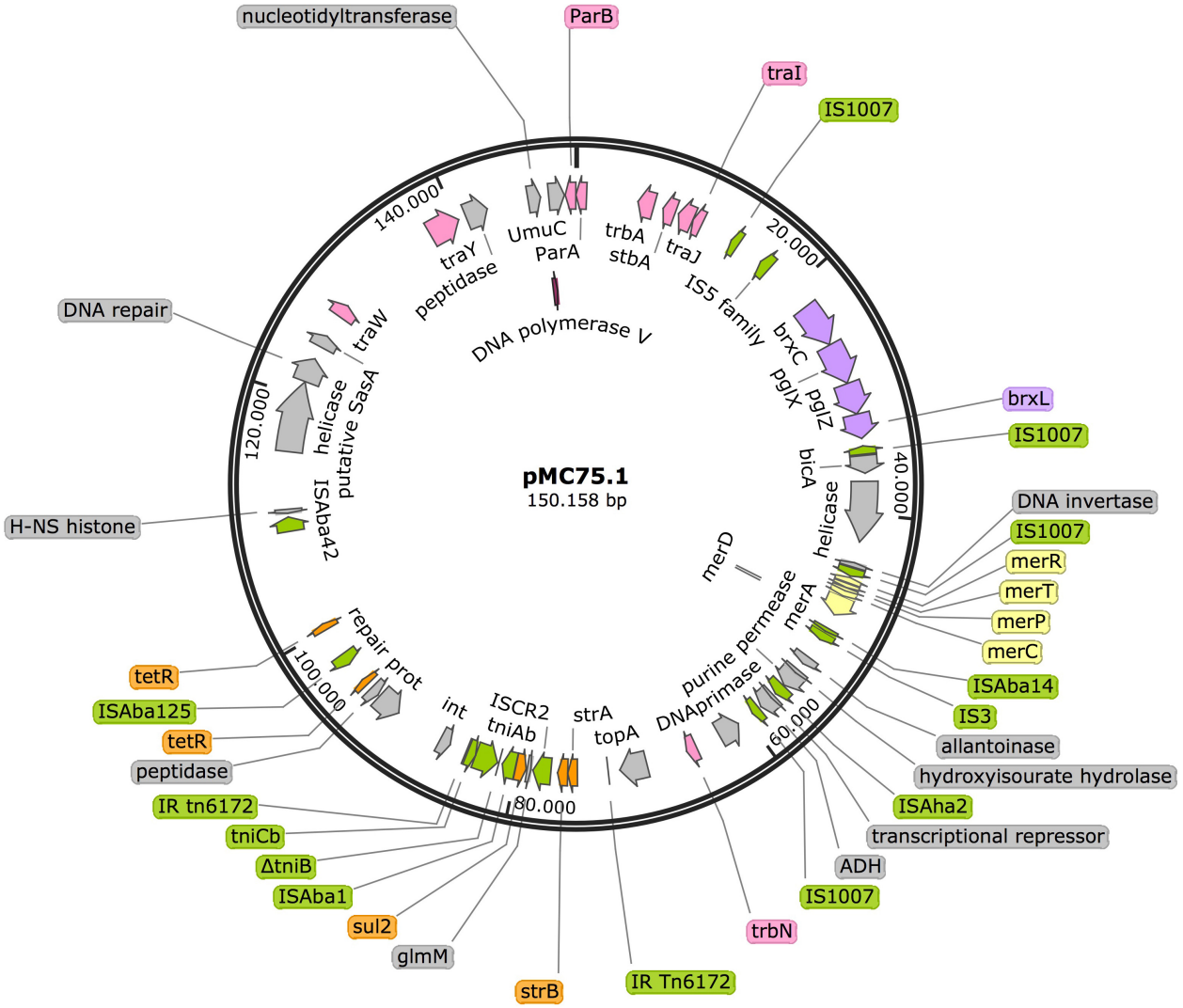

FIGURE 8 | Plasmid pMC75.1 in isolate MC75. Arrows represent predicted ORFs and the direction of the arrow represents the direction of transcription. Resistance genes are shown by orange arrows and transposon-related genes, recombinases and insertion sequences are indicated by green arrows. Transfer protein encoding genes, conjugal transfer protein encoding genes, and genes involved in plasmid partition and replication are shown in pink. The mercury resistance operon genes are indicated by yellow arrows and the BREX type 1 system is shown in purple. Other genes are indicated by gray arrows. Hypothetical proteins are not shown.

pMC75.2 was transferable into *A. baumannii* BM4547 but it was unstable and was lost after several passages. The replicon of this plasmid belonged to the RepB (Rep_3) superfamily with 100% homology. This plasmid shares a great homology with pMC1.2/pMC23.2, same RepB, toxin-antitoxin system, TonB-dependant receptor and septicolysin; it seems that one of them has lost or alternatively acquired the integron carrying the antimicrobial resistance genes and the mobility genes.

Recently, two similar plasmids to pMC75.1 and pMC75.2 were described in a Brazilian *A. baumannii* isolate representing the same ST (ST15). This illustrates that these plasmids can be very plastic by acquiring or losing genes, but can also be conserved within a ST (Matos et al., 2019).

The two carbapenem-resistant isolates carried the bla_{OXA-23} gene in Tn*2008*, which has been previously described in diverse ICs (Nigro and Hall, 2016; Ewers et al., 2017) including IC7 isolates recovered from a hospital in the same city, Cochabamba (Sennati et al., 2016). The Tn*2008* contributes to the overexpression of the carbapenemase encoding gene and to its mobilization. In addition, all three isolates harbored three aminoglycoside resistance genes such as *aac(3)-IIa*, *strA,* and *strB*; and *sul2* conferring resistance to sulphonamides; MC1 carried *tetB* conferring resistance to tetracycline as well. All the genes were found to be associated with IS elements, constituting transposons that lead to their mobilization and make genetic rearrangements more likely to happen. These genes were found both in the chromosome and in plasmids, demonstrating the plasticity of the *A. baumannii* genome and the mobility of these antimicrobial resistance

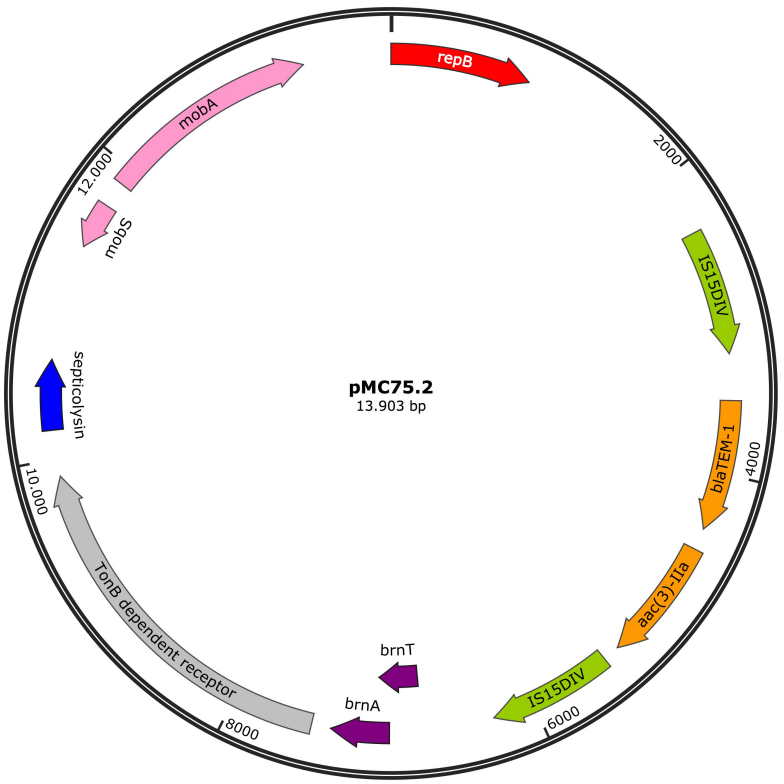

FIGURE 9 | Plasmid pMC75.2 in isolate MC75. Arrows represent predicted ORFs and the direction of the arrow represents the direction of transcription. Resistance genes are shown by orange arrows and insertion sequences are indicated by green arrows. Genes involved in plasmid mobility are shown in pink. The toxin-antitoxin system is shown in violet. Blue represents virulence genes. Other genes are indicated by gray arrows. Hypothetical proteins are not shown. Red arrow is used for the replicon.

determinants within MGEs such as transposons or plasmids.

CONCLUSION

In summary, these data further confirm that *A. baumannii* has a great ability to acquire antimicrobial resistance determinants and become a threat in hospitals. These are associated with different plasmids and many different IS elements, of which some are found in multiple genera. For these reasons it is important to study the dynamics and resistomes of the bacterial populations in order to understand the situation in each hospital or unit. The fact that some of these plasmids have been found in diverse *A. baumannii* clonal lineages mirrors the transfer and prevalence of these MGEs contributing to the spread of antimicrobial resistance worldwide.

DATA AVAILABILITY STATEMENT

The datasets generated for this study can be found in the GenBank, MK531536, MK531538, MK531537, MK531539, MK531540, and MK531541.

AUTHOR CONTRIBUTIONS

MC, KX, JW, and PH contributed to the design of the experiments. MC, KX, and JW performed the experiments. MC, KX, JW, OK, HS, LG, and PH analyzed and interpreted the data. MC, KX, and PH wrote the manuscript. All authors contributed to critical manuscript revision, read, and approved the submitted version.

FUNDING

This work was supported by the Basque Government 1129 and University of the Basque Country [Grupo Consolidado del Sistema Universitario Vasco (IT1097-16)/UPV/EHU GIC15/143]. PH was supported by the German Research Council (DFG) – FOR2251 (www.acinetobacter.de). This work was supported by the German Center for Infection Research (DZIF).

ACKNOWLEDGMENTS

We would like to thank Yvonne Pfeifer for providing the conjugation protocol and also Rémy A. Bonnin for providing the *A. baumannii* BM4547 strain.

REFERENCES

Adams, M. D., Chan, E. R., Molyneaux, N. D., and Bonomo, R. A. (2010). Genomewide analysis of divergence of antibiotic resistance determinants in closely related isolates of *Acinetobacter baumannii*. *Antimicrob. Agents Chemother.* 54, 3569–3577. doi: 10.1128/AAC.00057-10

Antipov, D., Korobeynikov, A., Mclean, J. S., and Pevzner, P. A. (2016). Genome analysis HYBRIDSPADES: an algorithm for hybrid assembly of short and long reads. *Bioinformatics* 32, 1009–1015. doi: 10.1093/bioinformatics/btv688

Bertini, A., Poirel, L., Mugnier, P. D., Villa, L., Nordmann, P., and Carattoli, A. (2010). Characterization and PCR-based replicon typing of resistance plasmids in *Acinetobacter baumannii*. *Antimicrob. Agents Chemother.* 54, 4168–4177. doi: 10.1128/AAC.00542-10

Carattoli, A. (2013). Plasmids and the spread of resistance. *Int. J. Med. Microbiol.* 303, 298–304. doi: 10.1016/j.ijmm.2013.02.001

Cayô, R., Rodrigues-Costa, F., Pereira Matos, A., Godoy Carvalhaes, C., Dijkshoorn, L., and Gales, A. C. (2016). Old clinical isolates of *Acinetobacter seifertii* in Brazil producing OXA-58. *Antimicrob. Agents Chemother.* 60, 2589–2591. doi: 10.1128/AAC.01957-15

Cerezales, M., Ocampo-Sosa, A. A., Álvarez Montes, L., Díaz Ríos, C., Bustamante, Z., Santos, J., et al. (2018). High prevalence of extensively drug-resistant *Acinetobacter baumannii* at a children hospital in Bolivia. *Pediatr. Infect. Dis. J.* 37, 1118–1123. doi: 10.1097/INF.0000000000001962

Cerezales, M., Xanthopoulou, K., Wille, J., Bustamante, Z., Seifert, H., Gallego, L., et al. (2019). *Acinetobacter baumannii* analysis by core genome MLST in two hospitals in Bolivia: endemicity of international clone 7 isolates (CC25). *Int. J. Antimicrob. Agents* 53, 844–849. doi: 10.1016/j.ijantimicag.2019.03.019

Chen, Y., Gao, J., Zhang, H., and Ying, C. (2017). Spread of the blaOXA-23-containing Tn2008 in carbapenem-resistant *Acinetobacter baumannii* isolates grouped in CC92 from China. *Front. Microbiol.* 8:163. doi: 10.3389/fmicb.2017.00163

Ewers, C., Klotz, P., Leidner, U., Stamm, I., Prenger-Berninghoff, E., Göttig, S., et al. (2017). OXA-23 and IS*Aba1* –OXA-66 class D β-lactamases in *Acinetobacter baumannii* isolates from companion animals. *Int. J. Antimicrob. Agents* 49, 37–44. doi: 10.1016/j.ijantimicag.2016.09.033

Genomics, B., Aziz, R. K., Bartels, D., Best, A. A., DeJongh, M., Disz, T., et al. (2008). The RAST server: rapid annotations using subsystems technology. *BMC Genomics* 9:75 doi: 10.1186/1471-2164-9-75

Goldfarb, T., Sberro, H., Weinstock, E., Cohen, O., Doron, S., Charpak-Amikam, Y., et al. (2015). BREX is a novel phage resistance system widespread in microbial genomes. *EMBO J.* 34, 169–183. doi: 10.15252/embj.201489455

Gonzalez-Villoria, A. M., and Valverde-Garduno, V. (2016). Antibiotic-resistant *Acinetobacter baumannii* increasing success remains a challenge as a nosocomial pathogen. *J. Pathog.* 2016:7318075. doi: 10.1155/2016/7318075

Göttig, S., Gruber, T. M., Higgins, P. G., Wachsmuth, M., Seifert, H., and Kempf, V. A. J. (2014). Detection of pan drug-resistant *Acinetobacter baumannii* in Germany. *J. Antimicrob. Chemother.* 69, 2578–2579. doi: 10.1093/jac/dku170

Hamidian, M., Ambrose, S. J., and Hall, R. M. (2016). A large conjugative *Acinetobacter baumannii* plasmid carrying the *sul2* sulphonamide and *strAB* streptomycin resistance genes. *Plasmid* 87–88, 43–50. doi: 10.1016/j.plasmid.2016.09.001

Hamidian, M., and Hall, R. M. (2016). The resistance gene complement of D4, a multiply antibiotic-resistant ST25 *Acinetobacter baumannii* isolate, resides in two genomic islands and a plasmid. *J. Antimicrob. Chemother.* 71, 1730–1741. doi: 10.1093/jac/dkw041

Higgins, P. G., Dammhayn, C., Hackel, M., and Seifert, H. (2010). Global spread of carbapenem-resistant *Acinetobacter baumannii*. *J. Antimicrob. Chemother.* 65, 233–238. doi: 10.1093/jac/dkp428

Koren, S., Walenz, B. P., Berlin, K., Miller, J. R., Bergman, N. H., and Phillippy, A. M. (2017). Canu: scalable and accurate long-read assembly via adaptive *k* -mer weighting and repeat separation. *Genome Res.* 27, 722–736. doi: 10.1101/gr.215087.116

Lean, S. S., and Yeo, C. C. (2017). Small, enigmatic plasmids of the nosocomial pathogen, *Acinetobacter baumannii*: good, bad, who knows? *Front. Microbiol.* 8:1547. doi: 10.3389/fmicb.2017.01547

Lean, S.-S., Yeo, C. C., Suhaili, Z., and Thong, K.-L. (2016). Comparative genomics of two ST 195 carbapenem-resistant *Acinetobacter baumannii* with different susceptibility to polymyxin revealed underlying resistance mechanism. *Front. Microbiol.* 6:1445. doi: 10.3389/fmicb.2015.01445

Manchanda, V., Sanchaita, S., and Singh, N. (2010). Multidrug resistant *Acinetobacter*. *J. Glob. Infect. Dis.* 2, 291–304. doi: 10.4103/0974-777X.68538

Matos, A. P., Cayô, R., Almeida, L. G. P., Streling, A. P., Nodari, C. S., Martins, W. M. B. S., et al. (2019). Genetic characterization of plasmid-borne *bla* OXA-58 in distinct *Acinetobacter* Species. *mSphere* 4:e00376-19. doi: 10.1128/mSphere.00376-19

Mugnier, P. D., Poirel, L., and Nordmann, P. (2009). Functional analysis of insertion sequence IS*Aba1*, responsible for genomic plasticity of *Acinetobacter baumannii*. *J. Bacteriol.* 191, 2414–2418. doi: 10.1128/JB.01258-08

Nigro, S. J., and Hall, R. M. (2016). Structure and context of *Acinetobacter* transposons carrying the *oxa23* carbapenemase gene. *J. Antimicrob. Chemother.* 71, 1135–1147. doi: 10.1093/jac/dkv440

Peleg, A. Y., Seifert, H., and Paterson, D. L. (2008). *Acinetobacter baumannii*: emergence of a successful pathogen. *Clin. Microbiol. Rev.* 21, 538–582. doi: 10.1128/CMR.00058-07

Roca, I., Espinal, P., Vila-Farrés, X., and Vila, J. (2012). The *Acinetobacter baumannii* oxymoron: commensal hospital dweller turned pan-drug-resistant menace. *Front. Microbiol.* 3:148. doi: 10.3389/fmicb.2012.00148

Salto, I. P., Torres Tejerizo, G., Wibberg, D., Pühler, A., Schlüter, A., and Pistorio, M. (2018). Comparative genomic analysis of *Acinetobacter* spp. plasmids originating from clinical settings and environmental habitats. *Science* 8:7783. doi: 10.1038/s41598-018-26180-3

Sennati, S., Villagran, A. L., Bartoloni, A., Rossolini, G. M., and Pallecchi, L. (2016). OXA-23-producing ST25 *Acinetobacter baumannii*?: first report in Bolivia. *J. Glob. Antimicrob. Resist.* 4, 70–71. doi: 10.1016/j.jgar.2015.10.007

Toleman, M. A., Bennett, P. M., and Walsh, T. R. (2006). ISCR elements: novel gene-capturing systems of the 21st century? *Microbiol. Mol. Biol. Rev.* 70, 296–316. doi: 10.1128/MMBR.00048-05

Vilacoba, E., Almuzara, M., Gulone, L., Traglia, G. M., Figueroa, S. A., Sly, G., et al. (2013). Emergence and spread of plasmid-borne tet(B)::ISCR2 in minocycline-resistant *Acinetobacter baumannii* isolates. *Antimicrob. Agents Chemother.* 57, 651–654. doi: 10.1128/AAC.01751-12

Wintersinger, J. A., and Wasmuth, J. D. (2015). Kablammo: an interactive, web-based BLAST results visualizer. *Bioinformatics* 31, 1305–1306. doi: 10.1093/bioinformatics/btu808

Conflict of Interest: The authors declare that the research was conducted in the absence of any commercial or financial relationships that could be construed as a potential conflict of interest.

frontiers in Microbiology

ORIGINAL RESEARCH
published: 25 May 2020
doi: 10.3389/fmicb.2020.00926

Chromosome Architecture and Gene Content of the Emergent Pathogen *Acinetobacter haemolyticus*

*Semiramis Castro-Jaimes[1], Elena Bello-López[2], Consuelo Velázquez-Acosta[3], Patricia Volkow-Fernández[3], Patricia Lozano-Zarain[2], Santiago Castillo-Ramírez[1] and Miguel Angel Cevallos[1]**

[1] Centro de Ciencias Genómicas, Programa de Genómica Evolutiva, Universidad Nacional Autónoma de México, Cuernavaca, Mexico, [2] Centro de Investigaciones en Ciencias Microbiológicas, Posgrado en Microbiología, Instituto de Ciencias, Benemérita Universidad Autónoma de Puebla, Puebla, Mexico, [3] Departamento de Infectología, Instituto Nacional de Cancerología, Ciudad de México, Mexico

Acinetobacter haemolyticus is a Gammaproteobacterium that has been involved in serious diseases frequently linked to the nosocomial environment. Most of the strains causing such infections are sensitive to a wide variety of antibiotics, but recent reports indicate that this pathogen is acquiring very efficiently carbapenem-resistance determinants like the *bla*NDM-1 gene, all over the world. With this work we contribute with a collection set of 31 newly sequenced nosocomial *A. haemolyticus* isolates. Genome analysis of these sequences and others collected from RefSeq indicates that their chromosomes are organized in 12 syntenic blocks that contain most of the core genome genes. These blocks are separated by hypervariable regions that are rich in unique gene families, but also have signals of horizontal gene transfer. Genes involved in virulence or encoding different secretion systems are located inside syntenic regions and have recombination signals. The relative order of the synthetic blocks along the *A. haemolyticus* chromosome can change, indicating that they have been subject to several kinds of inversions. Genomes of this microorganism show large differences in gene content even if they are in the same clade. Here we also show that *A. haemolyticus* has an open pan-genome.

Keywords: *Acinetobacter haemolyticus*, chromosome architecture, emerging pathogen, opportunistic pathogen, horizontal gene transfer, open pangenome

OPEN ACCESS

Edited by:
Ludmila Chistoserdova, University of Washington, United States

Reviewed by:
Alexandr Nemec, National Institute of Public Health (NIPH), Czechia
Zhi Ruan, Zhejiang University, China

****Correspondence:***
Miguel Angel Cevallos
mac@ccg.unam.mx

Specialty section:
This article was submitted to Evolutionary and Genomic Microbiology, a section of the journal Frontiers in Microbiology

Received: *13 January 2020*
Accepted: *20 April 2020*
Published: *25 May 2020*

Citation:
Castro-Jaimes S, Bello-López E, Velázquez-Acosta C, Volkow-Fernández P, Lozano-Zarain P, Castillo-Ramírez S and Cevallos MA (2020) Chromosome Architecture and Gene Content of the Emergent Pathogen Acinetobacter haemolyticus. Front. Microbiol. 11:926. doi: 10.3389/fmicb.2020.00926

INTRODUCTION

Species of *Acinetobacter* are widespread in nature. They can be isolated from different environments, such as soil, water, and food, and as commensals of many animals, including humans (Bouvet and Grimont, 1986; Doughari et al., 2011; Fyhrquist et al., 2014). Unfortunately, some *Acinetobacter* species are dangerous opportunistic pathogens of humans. The *Acinetobacter baumannii* – *Acinetobacter calcoaceticus* (ABC) complex is composed of closely related species that cause serious infections in the hospital setting and, less frequently, in the community (Gerner-Smidt and Tjernberg, 1993; Cosgaya et al., 2016; Nemec et al., 2015). The ability of *A. baumannii*, the most clinically relevant member of the ABC complex, to acquire antibiotic resistance genes has favored the appearance of multidrug-resistant (MDR) clones, and this characteristic combined

with its capacity to form biofilms and to survive desiccation allows the species to persist in the hospital environment and promote the emergence of outbreaks (Antunes et al., 2014; Doi et al., 2015). Infection by *A. baumannii* leads to worse clinical outcomes than those associated with other ABC complex species (Chuang et al., 2011; Fitzpatrick et al., 2015; Chen et al., 2018; Wisplinghoff et al., 2012; Lee et al., 2013; Park et al., 2013).

Acinetobacter haemolyticus belongs to the haemolytic clade; the members of this clade show beta-haemolysis halos in blood-agar media, and sometimes they can also degrade gelatin; *A. haemolyticus* shows both phenotypes (Bouvet and Grimont, 1986; Tayabali et al., 2012; Touchon et al., 2014; Nemec et al., 2016). The haemolytic clade has 13 named species (and 3 genospecies) to date, which have been isolated from humans, water and soil (Touchon et al., 2014; Nemec et al., 2016; Nemec et al., 2017, 2019), in contrast with six named species in the ACB clade, most of which are of clinical origin, but some have been isolated from soil (Nemec et al., 2011, 2019). *A. haemolyticus* has been implicated in serious infections, frequently in those linked to the nosocomial environment (Ko et al., 2007; Gundi et al., 2009; Turton et al., 2010; Fu et al., 2012; Schleicher et al., 2013; Wang et al., 2014; Jeong et al., 2016). Moreover, recent reports indicate that this pathogen is acquiring very efficient carbapenem-resistance determinants, such as the *bla*NDM-1 gene, worldwide (Fu et al., 2012; Jones et al., 2015; Bello-López et al., 2019; Jiang et al., 2019). All these characteristics suggest that *A. haemolyticus* may have the potential to become a threatening pathogen, following a path similar to that of *A. baumannii*.

In this work, we analyzed the genome sequences of a collection of 31 newly sequenced *A. haemolyticus* isolates obtained from different Mexican hospitals and a previously sequenced Mexican strain (Bello-López et al., 2019). Additionally, we added 12 complete genomes of *A. haemolyticus* isolates from other parts of the world from RefSeq. With all these data, we examined the genomic diversity of the collection and the evolutionary forces that have shaped the genome architecture of this species, with a particular focus on the roles of horizontal gene transfer (HGT) and gene gain and loss. This analysis contributes to our understanding of how the emergent pathogen *A. haemolyticus* evolves.

MATERIALS AND METHODS

The *A. haemolyticus* Collection

Mexican *A. haemolyticus* strains were obtained from different hospitals in different years, and only one sample per patient was considered, regardless of the antibiotic susceptibility profile. Considering that no previous data on the clonal relationship between strains and there were no studies on the diversity of Mexican strains circulating among hospitals, we kept all strains that fulfilled the above-mentioned criteria. Species identity was initially determined by querying the NCBI's nt database with the Sanger sequence of the cloned PCR product of a fragment of *rpo*B (Zone-1) with an identity cutoff of 97%; the results were the same if the cutoff was more strict (99%) (La Scola et al., 2006). Additionally, we downloaded all putative *A. haemolyticus* genomes available in the National Center for Biotechnology Information (NCBI) RefSeq until October 30th, 2018, including their associated clinical data.

Genome Sequencing and Assembly of Mexican *A. haemolyticus* Strains

Mexican isolates were sequenced with paired-end Illumina MiSeq 2 × 300 bp sequencing (except for strain 11616, which was sequenced with HiSeq 2 × 150 bp sequencing) by Macrogen, Korea, and Instituto Nacional de Medicina Genómica (INMEGEN), Mexico. Some genomes were sequenced with the PacBio RSII or PacBio Sequel platform at Yale and SNPsaurus; all reads are available in SRA under accessions SRR10672463–SRR10672503 (**Supplementary Table S1**).

Illumina reads were adapter filtered with Trimmomatic (Bolger et al., 2014) against a custom database with Illumina adapter sequences up to 2018 (document # 1000000002694 v04, January 2018). The resulting reads were quality trimmed with DynamicTrim, which is part of the SolexaQA suite (Cox et al., 2010); final quality was inspected with FastQC[1].

Filtered and trimmed Illumina reads were assembled using ABySS 2.0.1 (Simpson et al., 2009), SPAdes 3.9.0 (Bankevich et al., 2012), and Velvet 1.2.10 (Zerbino and Birney, 2008) with various kmers. The best assembly obtained with each program was selected for further use with Metassembler 1.5 (Wences and Schatz, 2015). Hybrid assembly was performed with SPAdes (Bankevich et al., 2012) and Unicycler (Wick et al., 2017). All assemblies were inspected for various metrics, such as N50, average contig length, and total assembly size with getAssemblyStats.py, available from GitHub[2].

Core Genome Phylogeny and Diversity Analyses

The Average Nucleotide Identity (ANI) of all the genomes in our collection was assessed with pyANI (Pritchard et al., 2016) with a relaxed cutoff of 93% (Rosselló-Móra and Amann, 2015) and a strict 96% cutoff (Richter and Rosselló-Móra, 2009) to determine which genomes were *A. haemolyticus*. We built a Maximum Likelihood (ML) phylogenetic tree with the core monocopy protein-coding genes from the complete dataset of each species with RAxML, excluding sequences with recombination signals (Stamatakis, 2014). We inspected the tree to select one or two genomes per clade. We further sequenced the selected Mexican strains with long reads to finish those genomes, and we kept the complete genomes available from NCBI. In this way, we focused the genome structure analyses only on complete chromosomes.

For Single Nucleotide Variant (SNV) analysis, we obtained the VCF file from core genome alignments with Parsnp and Gingr (Treangen et al., 2014) and converted it to hierBAPS format with PGDSpider (Lischer and Excoffier, 2012) and Perl. We ran Principal Component Analysis (PCA) with gdsfmt and SNPRelate (Zheng et al., 2017, 2012); Bayesian analysis was

[1]http://www.bioinformatics.babraham.ac.uk/projects/fastqc/

[2]https://github.com/semiramisCJ/spotsAhaem

performed with rhierbaps (Cheng et al., 2013), ape version 5.3 (Paradis and Schliep, 2019) and phytools version 0.6–99 (Revell, 2012), also in R 3.6.1 (R Core Team, 2019).

Genome Annotation

Initial genome annotation was performed with Prokka (Seemann, 2014), but the final annotations of the submitted genomes were performed by the NCBI staff with PGAP; all accession numbers are listed in **Supplementary Table S1**. Antibiotic resistance determinants were identified using the Comprehensive Antibiotic Resistance Database (CARD) (Jia et al., 2016). Virulence factors were identified by using the Virulence Factor of Bacteria Database (VFDB) (Chen et al., 2016) and searching for secretion systems in the TXSSCAN profiles (Abby et al., 2014; Abby and Rocha, 2017). The capsule and outer core of lipooligosaccharide (LOS) loci from the genome sequences of *A. baumannii* strains A85 (KC118540.6), A91 (JN968483.3), D13 (HM590877.5), and SDF (BK010760.1) were analyzed separately. Iron-acquisition systems were curated from the literature (Dorsey, 2003; Zimbler et al., 2009; Antunes et al., 2011; Eijkelkamp et al., 2011; Hasan et al., 2015; Penwell et al., 2015) and cross-referred with the genomes of *A. baumannii* strains ACICU (NC_010611.1), AYE (CU459141.1), and 8399 (AY149472.1). Clusters of Orthologous Groups (COG) and Non-supervised orthologous group (NOG) functional annotation was performed with the eggNOG mapper (Huerta-Cepas et al., 2017, 2016).

To identify mobile genetic elements in the representative genomes, we used other specialized databases and tools: we queried the Mobile Genetic Elements Database (MGE DB) (Pärnänen et al., 2018) and, to identify integrative and conjugative elements (ICEs), ICEberg database version 2.0 (Liu et al., 2019) with the local version of ICEfinder (Hong Yu), which requires the EMBOSS suite (Rice et al., 2000). We searched for insertion sequences (ISs) with ISEScan 1.6 (Xie and Tang, 2017) and ISFinder (Siguier et al., 2006). Phages were analyzed with PHASTER (Arndt et al., 2016) and VirSorter (Roux et al., 2015). To detect signals of HGT via the nucleotide composition of each genome, we used AlienHunter (Vernikos and Parkhill 2006) and a custom python script to calculate the GC content for each replicon.

Syntenic Block (Spot) Delimitation

The code used for spot delimitation is available from GitHub see text footnote 2. We based our analysis on the methodology proposed by Oliveira et al. (2017), with the following modifications: first, we separated protein-coding genes into orthologous groups with PanOCT (Fouts et al., 2012). Next, we focused on single-copy core orthologs, and if the vicinity of a defined gene was shared by all the strains, the genes were said to be in an interval. This analysis was performed for overlapping sliding windows with a step of one gene. The vicinity was set to five genes upstream and five genes downstream of the middle (query) gene (a total of 11 genes at a time), and the vicinity had to share at least three other genes (a total of at least four genes in common), no matter the order; moreover, the genes at the extremes of the interval had to belong to the same gene family, allowing for permutations (**Figure 5**).

Overlapping intervals of each strain were combined into superintervals to avoid redundancy. To map equivalent superintervals between strains, we used the intersection of gene families and kept a link table; in our analysis, all the mappings resulted in 1-to-1 agreement, with each superinterval mapping to one superinterval and no splits.

Finally, we added the non-core genes to the superintervals to obtain the complete syntenic blocks (spots), and the genes outside spots were said to be in hypervariable regions. Spots were consecutively named as encountered by the script. If the spots shared the identifier, they were said to be equivalent. Hypervariable regions were named on the basis of the surrounding spots to keep track of their genomic context in each strain.

Recombination Signal Detection

To detect gene families with recombination signals, we first aligned the proteins with Clustal Omega (Sievers et al., 2014) and used RevTrans 1.4 (Wernersson and Pedersen, 2003) to guide nucleotide alignment and keep the alignments in frame. Then, we used Phi-pack (Bruen et al., 2006) to test for recombination; if the *p*-value of the phi test with permutation was less than 0.05, we considered the alignment to have signals of recombination, as in Wang et al. (2016).

Context and Comparison of Common Gene Families

To determine how many times each gene family was represented in each spot or hypervariable region and how similar the genetic compositions of the family members were, we searched each gene family, accounting for paralogs, among all locations between all strains. The Jaccard index was computed as the overlap (intersection) between sets; thus, a value of 1 meant complete overlap, and 0, complete dissimilarity. Jaccard indexes were computed among equivalent spots and among hypervariable regions with the same genetic context (flanked by the same spots).

Category Enrichment

The enrichment of some categories was assessed by hypergeometric tests, corrected for multiple testing, in R 3.6.1 (R Core Team, 2019). For each category (spot or hypervariable region), we searched for COG/NOG functional enrichment, virulence factors, phages, genes with a recombination signal, and atypical nucleotide composition, the last of which was determined by both AlienHunter and GC content.

Data Visualization

The ML phylogenetic tree was annotated with iTOL (Letunic and Bork, 2019). Plots of genome features per genomic position were constructed with matplotlib (Hunter, 2007) in Python 3. The rest of the plots were constructed in R 3.6.1 (R Core Team, 2019). All heatmaps were created with ComplexHeatmap (Gu et al., 2016); scatterplots and violin plots were created with ggplot2 (Wickham, 2009). Additional R packages used included

dplyr, ggrepel, GGally, paletteer and RColorBrewer (Neuwirth, 2014; Schloerke et al., 2018; Hvitfeldt, 2019; Slowikowski, 2019; Wickham et al., 2019).

RESULTS AND DISCUSSION

Genome Collection

To study the genome architecture of the emerging pathogen *A. haemolyticus*, we constructed a data set consisting of the genome sequences of 31 Mexican isolates described here and a previously sequenced Mexican *A. haemolyticus* (Bello-López et al., 2019) (in total, 9 Mexican strains now have finished chromosomes) and 19 putative *A. haemolyticus* complete genome sequences available in NCBI RefSeq database (4 of them were finished assemblies), which were isolated from hospitals in different countries. To confirm the species designation of all the genomes in the collection, and to detect equivalent strains, we calculated the average nucleotide identity (ANI) between all genome pairs. Our results confirmed that all but two isolates were correctly assigned to *A. haemolyticus* (**Supplementary Figure S1** and **Supplementary Table S2**). The two exceptions were isolates JKSF06 and KCRI-45, which were excluded from the final data set because they had around 84% ANI values (**Supplementary Figure S1** and **Supplementary Table S2**), far below the species designation cutoffs of 93–96% (Richter and Rosselló-Móra, 2009; Rosselló-Móra and Amann, 2015). We excluded strain TG19602 because its genome assembly was very fragmented and could introduce noise in the genome content analysis: it had 382 contigs (the largest of all the collection) and the lowest average contig length. To avoid redundancy and to work only with good quality data, we only kept the assembly with the best quality when there were equivalent strains; in those cases, the ANI values were of 99.9% (**Supplementary Table S2**). Thus, CIP 64.3 (the type strain of the species) represented assemblies of MTCC 9819, NBRC 109758, and TG19599, whereas the assembly of ATCC 27244 represented the TG21157 genome (Marcus et al., 1969; Khatri et al., 2014; Touchon et al., 2014).). After applying all these filters, our final data set consisted of 44 genomes. Their corresponding assembly status (finished or draft), isolation year, isolation country, and accession numbers are listed in **Table 1**.

Mexican *A. haemolyticus* strains were isolated from different patients, sources, hospitals, and hospital units in different years, irrespective of antibiogram results. Most of the isolates were collected from secondary and tertiary care institutions located in Puebla and Mexico City. Most of the patients were admitted to the Internal Medicine Unit (10), Oncology (7) or Emergencies (6), but some patients were also in Surgery (2) or Intensive Therapy (2), and 1 patient was HIV+. The average and median ages of hosts were 25 and 15.5 years, respectively, because more than half of the samples (18/32) were from pediatric hospitals. Twelve of the patients were female. Isolation year ranged from 1998 to 2016. The most common isolation sources were peritoneal dialysis fluid (14), blood (6), and bronchial secretion (4).

Many of the NCBI genome sequences were from China (4). In addition, one of the sequences was from the Czechia, one was from Tanzania, and one was from the United States; the remaining strains (5) did not have information about the country from which they were isolated. The most common isolation source was sputum (6). Our collection also included an isolate (HW-2A) obtained from an E-waste recycling plant, in contrast to the rest of the strains, which had a clinical origin and isolation dates ranging from 1962 to 2017.

General Features of the Genomes in the Collection

Draft genomes of all Mexican isolates were obtained with an Illumina platform. Additionally, the genome sequences of eight of them were completed with the aid of PacBio reads (see section "Materials and Methods"; **Supplementary Table S1**). This genome collection represents the largest data set of sequenced clinical *A. haemolyticus* isolates to date and an important step in our understanding of an emergent pathogen that has received little attention due to misidentification with routine techniques and because most of its isolates tend to be antibiotic sensitive.

Genome size was similar among all the strains, with a median of 3.5 Mb. The assembly size of Mexican *A. haemolyticus* genomes in the collection ranged from 3 264 943 to 3 694 983 bp (*sd* = 117 494.84 bp), whereas that of NCBI genomes ranged from 3 291 819 to 3 715 198 bp (*sd* = 127 635 bp). Among the complete genomes, chromosome size ranged from 3.3 to 3.7 Mb (*sd* = 1.1 Mb), and some strains had up to six plasmids (mean = 3). Plasmid size ranged from 4 280 to 107 843 bp (*sd* = 3 0532.56 bp).

The *A. haemolyticus* genomes analyzed here contained 3 028 to 3 720 protein-coding genes (*sd* = 162) and could be organized into 10 866 gene families, only 1 893 of which formed the core genome and 4 941 were singletons (**Supplementary Figure S2**). We also performed a sampling analysis in which we monitored the increase in pangenome size when more genomes were included (**Supplementary Figure S3**). These data indicated that *A. haemolyticus* has an open pangenome.

Diversity, Distribution, and Grouping of the Strains

To evaluate the relationships between the strains, we analyzed the SNVs in the core genome (regardless of whether they were in non-coding or coding regions), and we built a ML phylogenetic tree with all monocopy core protein-coding genes without recombination signals. The number of SNVs in the complete core genome between most pairs of strains were in the order of thousands, which highlights the diversity of the dataset. The exceptions were a few cases of closely related strains: 3 SNVs between AN43 and AN59 even if they were from the same hospital, but isolated from different patients at different years; 6 SNVs between CIP 64.3 and strains NCTC 10305 and NCTC 12155, which are also very similar at the ANI values; 10 SNVs between AN4 and 10633 even if they were isolated from different hospitals, in different parts of Mexico, at different years (**Table 1** and **Supplementary Table S3**). In the ML phylogenetic tree (**Figure 1** and **Supplementary Figure S4**), the Mexican and Chinese strains were interspersed. The isolates from the same Mexican hospital belonged to different clades,

TABLE 1 | Assembly status, isolation country, isolation year, and assembly accession numbers of *A. haemolyticus* genomes analyzed in this work.

Notes	Strain	Country	Year	Assembly accession numbers	References
Mexican strains, finished					
	INNSZ174	Mexico	1998	CP031998 - CP032001	This study
	11616	Mexico	2012	CP032002 - CP032008	This study
	AN43	Mexico	2015	CP031976 - CP031978	This study
	AN54	Mexico	2016	CP041224 - CP041229	Bello-López et al., 2019
	AN59	Mexico	2016	CP031972 - CP031975	This study
	2126ch	Mexico	2011	CP031991 – CP031997	This study
	5227	Mexico	2014	CP031988 – CP031990	This study
	AN3	Mexico	2010	CP031984 – CP031987	This study
	AN4	Mexico	2010	CP031979 – CP031983	This study
NCBI's strains, finished					
	TJS01	China	2012	NZ_CP018871 – NZ_CP018873	
	XH900	China	2016	NZ_CP018260 – NZ_CP018261	
	HW-2A	China	2017	NZ_CP030880	
	sz1652	China	2017	CP032135 – CP032137	Jiang et al., 2019
Mexican strains, draft					
	2227	Mexico	2011	WTTY00000000	This study
	3275	Mexico	2012	WTTX00000000	This study
	3281	Mexico	2012	WTTW00000000	This study
	5439	Mexico	2014	WTTV00000000	This study
	10633	Mexico	2013	WTTU00000000	This study
	11650	Mexico	2013	WTTT00000000	This study
	11652	Mexico	2010	WTTS00000000	This study
	11654	Mexico	2008	WTTR00000000	This study
	11658	Mexico	2008	WTTQ00000000	This study
	978H	Mexico	2016	WTTP00000000	This study
	AN10	Mexico	2012	WTTO00000000	This study
	AN11	Mexico	2012	WTTN00000000	This study
	AN13	Mexico	2012	WTTM00000000	This study
	AN20	Mexico	2013	WTTL00000000	This study
	AN27	Mexico	2014	WTTK00000000	This study
	AN34	Mexico	2014	WTTJ00000000	This study
	AN44	Mexico	2015	WTTI00000000	This study
	AN5	Mexico	2011	WTTH00000000	This study
	AN60	Mexico	2016	WTTG00000000	This study
	AN61	Mexico	2016	WTTF00000000	This study
	AN63	Mexico	2016	WTTE00000000	This study
	AN7	Mexico	2011	WTTD00000000	This study
	DIV33	Mexico	2016	WTTC00000000	This study
NCBI's strains, draft					
	ATCC 19194			NZ_GG770435.1 – NZ_GG770495.1	Baumann et al., 1968
	ATCC 27244	United States		NZ_GG665949.1 – NZ_GG666013.1	Marcus et al., 1969
	CIP 64.3 T			NZ_KB849798.1 – NZ_KB849812.1	Baumann et al., 1968; Touchon et al., 2014
	NIPH 261	Czechia	1993	NZ_KB849813.1 – NZ_KB849819.1	Nemec et al., 2000; Touchon et al., 2014
	KCRI-348C	Tanzania	2014	NZ_OVCN01000001.1 – NZ_OVCN01000043.1	
	NCTC 10305		1962	NZ_UFRR01000001.1 – NZ_UFRR01000006.1	
	NCTC 10306		1962	NZ_UFRT01000001.1 – NZ_UFRT01000004.1	
	NCTC 12155		1987	NZ_UAPN01000001.1 – NZ_UAPN01000032.1	

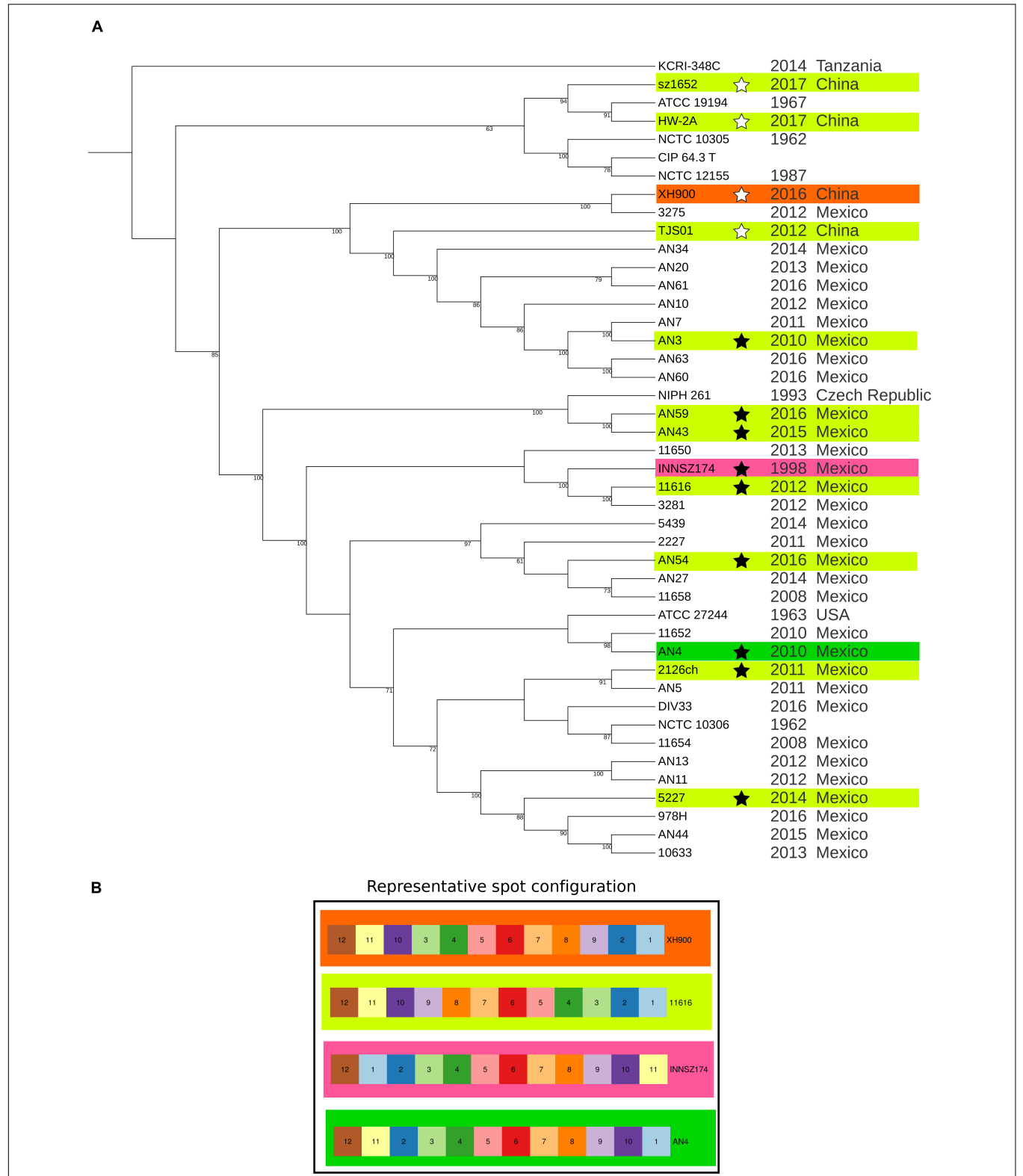

FIGURE 1 | Maximum likelihood phylogeny of core protein-coding genes and spot configuration in representative genomes. **(A)** Maximum likelihood phylogeny. The ML tree was built with the 955 core monocopy orthologous protein-coding genes without recombination signals between the 44 analyzed A. haemolyticus genomes. The tree was drawn with iTOL. Annotation includes isolation year and isolation country. Stars mark representative genomes. Branch length is not to scale. Bootstrap values above 60% are shown. **(B)** Graphic representation of spot configuration of representative genomes. The background color is used to clarify where the spot configuration is located in the representative genomes in the phylogeny.

and strains obtained in the same year were located in different positions on the tree (**Figure 1**). We also found that there were multiple, distantly related lineages circulating in Chinese hospitals. These data showed that *A. haemolyticus* clones were introduced to Mexican and Chinese hospitals during multiple independent events.

We analyzed the SNVs present in the complete core genome with two approaches, PCA and a Bayesian method (rhierbaps). The results of the two strategies were consistent, but the Bayesian method tended to split PCA clusters into many subpopulations. The results of both SNV analyses were consistent with the bipartitions of the ML tree because they showed the same patterns (**Supplementary Figure S5**): some strains formed clusters clearly separated from others by isolation year or isolation country. A few strains were very different from the rest of the strains in the collection, and the others did not form sharply delimited clusters. The first scenario was illustrated by two clusters: some strains isolated in 1962 (NCTC 10305 and NCTC 12155) formed a tight group with the type strain of *A. haemolyticus* (CIP 64.3), also isolated in the 1960s (Baumann et al., 1968). Most of the strains isolated in Puebla (Mexico) from 2011 to 2016 (AN3, AN7, AN10, AN20, AN34, AN60, AN61, and AN63) were more similar to each other than to members of the other clusters. The rest of the Mexican *A. haemolyticus* strains grouped more tightly with each other than with the strains from other countries. The most heterogeneous strains were those isolated in Tanzania (KCRI-348C) and China (HW-2A, XH900, sz1652 and TJS01) from 2012 to 2017. This analysis showed that most *A. haemolyticus* genomes were grouped by isolation country; nonetheless, we identified a cluster of closely related strains grouped by isolation year.

Genome Architecture of Representative Strains

We randomly selected at least one genome per clade and defined it as the representative genome of each clade. We excluded two clades (CIP 64.3 and KCRI-348C) from the genome architecture analyses because none of the chromosome sequences of their members were finished. To evaluate the differences in genome architecture between members of our *A. haemolyticus* collection, we first identified the syntenic regions in all of them using, with some modifications, a previously suggested method based on the proximity of orthologous protein-coding genes (Oliveira et al., 2017). Briefly, we identified all the orthologous genes among all the genomes and focused on monocopy core orthologous genes to determine if they were present within the same region in a defined window in all genomes. At this point, we omitted all multicopy and accessory genes. A set of core genes with a conserved position formed an "interval." Then, we reincorporated multicopy and accessory genes into the intervals to generate "spots." The zones between spots were named "hypervariable regions." The hypervariable regions were composed of genes that did not pass the synteny criteria. Importantly, we limited our analysis to protein-coding genes and excluded pseudogenes. This method identifies syntenic regions based only on the conservation of core orthologous genes, regardless of the accessory genome content, and is flexible because the accessory genes do not obscure the conserved regions.

With the implemented method, we identified 12 spots (syntenic regions) and 7 to 9 hypervariable regions (zones in the genome flanked by spots) in the *A. haemolyticus* genomes, as in some strains, a few pairs of spots were not separated by hypervariable regions. The spots were always larger than the hypervariable regions. Most (2 608 to 3 038 genes; *sd* = 120) of the genes were located within spots comprising 93 to 97% of the genes on the chromosome. Each spot contained 43 to 555 genes (*sd* = 150). On the other hand, hypervariable regions contained, in total, between 85 and 221 genes (*sd* = 42) per chromosome, and each hypervariable region included 1 to 102 genes (*sd* = 24) (**Supplementary Figure S6**).

The relative order of the spots tended to be conserved. However, we observed various inversions that always involved spots 1, 2, 10, and 11, which led to four different spot configurations (**Supplementary Figure S7** and **Figure 1**); in contrast, spot 12 always had the same relative orientation in all the chromosomes. The most frequent spot configuration, represented by strain 11616, was present in multiple clades, and the other three configurations detected in distinct clades indicated that rearrangements were possible but infrequent.

Gene Order Inside Spots

To analyze the order of core genes inside equivalent spots, we selected a genome from each of the four spot configurations described above as references, namely, INNSZ174, AN4, XH900 and a strain with the most common configuration (11616).

Almost all the strains with the same spot configuration as 11616 had the exact same order of core genes; strains AN3 and TJS01 were the exceptions because they had a complete inversion of spot 6 (**Figure 1**). When we compared strain 11616 with strain INNSZ174, which belonged to the same clade but had a different spot configuration, we found that the *relative* core gene order in all spots was conserved (**Figure 1**). When we compared strain 11616 with strain AN4, which belonged to a neighboring clade, the inversions inside the spots reflected the inversions between the spots, as the only conserved core gene positions were those of spots 1, 11, and 12, which had the same order (**Figure 1**). Finally, when we compared strain 11616 with strain XH900, which belonged to a more distant clade, we saw that again, the spots with the same order also had conserved core gene positions inside them; this was the case for spots 1, 2, 6, 10, 11, and 12, but the rest had complete inversions (**Figure 1**). All these data showed that the relative order inside spots was conserved and that the most common rearrangements (inversions) involved multiple spots.

Gene Content in Spots and Hypervariable Regions

To evaluate how similar the spots were in terms of gene content and to determine how many genes in the hypervariable regions were shared among strains, we computed the Jaccard index, which indicates how similar two datasets are, with 1 indicating identical and 0 indicating completely dissimilar.

Two equivalent spots contain the same core genes; however, they can differ in the type and number of accessory genes. To assess how similar the spots were, we compared their total gene contents. All spots shared at least 50% of their genes, but others were nearly 100% percent identical (**Figure 2**). At least 50% of the shared genes comprised the monocopy core orthologous genes that were used to identify the spots.

We also found that some spots were more similar in global gene content than others, irrespective of size. For example, spots 2 and 12 (median sizes of 96 and 47 genes, respectively) were the most conserved spots in all the strains, and spots 6 and 7 (median sizes of 369 and 135 genes, respectively) were the most conserved in more closely related clades. The most heterogeneous spots were spots 3, 5, and 8 (median gene contents of 63, 507, and 288, respectively).

These findings indicated that accessory genes are the drivers of diversity in gene content among spots and that even if two equivalent spots have similar sizes, their gene contents can be very different.

Next, we analyzed the gene content of hypervariable regions flanked by the same spots, i.e., with the same genetic context, in different strains. We found a range of patterns (**Figure 3**): at one extreme, there were no regions separating spots, and in other cases, there were similar gene contents within equivalent hypervariable regions; at the other extreme, there were equivalent hypervariable regions that were completely different in terms of gene content, or there were unique hypervariable regions present in only one or two strains.

The first scenario occurred when a pair of spots were always together but without hypervariable regions in between. Spots 9 and 10 exemplified this case. These spots formed separate entities because they were in different configurations in some strains (**Supplementary Figure S7** and **Figure 1**), considering that they could not form a larger spot overall and thus did not comply with the synteny criteria.

Five hypervariable regions with the same genetic context also possessed equivalent genes. Some of them shared only one or two genes, as in the case of the hypervariable region between spots 1 and 12; meanwhile, others shared a larger gene set among all or a subgroup of strains. The latter case sometimes also occurred when a gene context could not be present in other strains because the involved spots were not near each other; for example, the hypervariable region between spots 2 and 3 was present in most of the genomes but absent in strain sz1652, whereas these spots were separated in strain XH900 because they were not consecutive in its genome.

We identified four hypervariable regions with the same genetic context but with very different gene contents. For example, the hypervariable region between spots 1 and 2 was very heterogeneous: in some of the genomes, it was composed of 1 to 8 genes, but in strain AN54, it contained 58 genes, many of which were related to transposases associated with ISs. Furthermore, this region was absent in strain HW-2A (see **Supplementary Figure S8**).

We identified two hypervariable regions that were unique on the basis of either gene content or genetic context. One was the hypervariable region between spots 5 and 6; it included two genes (a hypothetical protein and a transposase) and was present only in strains AN3 and TJS01. These two regions shared a hypothetical protein, but they had different transposases. The other case was a hypervariable region between spots 2 and 11 in strain AN4; this arrangement was unique because only this strain exhibited these spots as adjacent fragments. The region consisted of a gene coding for a transposase and another coding for a hypothetical protein; the latter was also found in the hypervariable region between spots 1 and 2 in seven strains (2126ch, AN3, AN43, AN59, INNSZ174, sz1652, and TJS01).

All these results highlighted that hypervariable regions, which are located along the entire chromosome, are the most susceptible regions to gene gain and loss. Hypervariable regions can be highly heterogeneous in both gene content and size. These regions might be hotspots for gene content variation, in some cases, due to site-specific recombination driven by transposases.

Functional Categories in Spots and Hypervariable Regions

To obtain a general overview of the functions of the protein-coding genes within spots and hypervariable regions, we performed enrichment analysis of general functional annotations with COG and NOG categories. We found that two general metabolic categories were overrepresented among spots: "(C) Energy production and conversion" and "(J) Translation, ribosomal structure and biogenesis." In contrast, in hypervariable regions, there were both an excess of genes without functional annotation and enrichment in the category "(L) Replication, recombination and repair," which is frequently linked to regions with HGT signals.

Mobile Genetic Elements and Other Horizontal Gene Transfer Signals

Horizontal gene transfer is an important contributor of genes associated with phenotypes of clinical concern in gram-negative bacteria that cause opportunistic infections, such as antibiotic resistance genes and virulence factors (Dobrindt et al., 2004). Foreign regions such as genomic islands have an atypical nucleotide composition, a skewed GC content, and one or more hallmarks of mobility, such as ISs, transposons, integrase attachment sites, integrases and even conjugation machinery (Dobrindt et al., 2004). Moreover, finding a specific genome segment within other genomic contexts in different strains or even species provides additional and strong evidence that it has a foreign origin (Ploswiki et al., 2015). Thus, to identify mobile genetic elements or chromosomal regions with HGT signals in representative genomes, we followed three steps. First, we used specialized software that may suggest HGT events of genomic regions, such as recombination signals (pairwise homoplasy index, phi), GC content and nucleotide composition (AlienHunter). In addition, we quantified the number of unique gene families, i.e., those present in only one strain. Then, we built non-redundant databases of HGT regions to obtain only a representative of each genomic fragment and then performed BLASTn searches against the non-redundant nucleotide database, excluding either the species *A. haemolyticus*

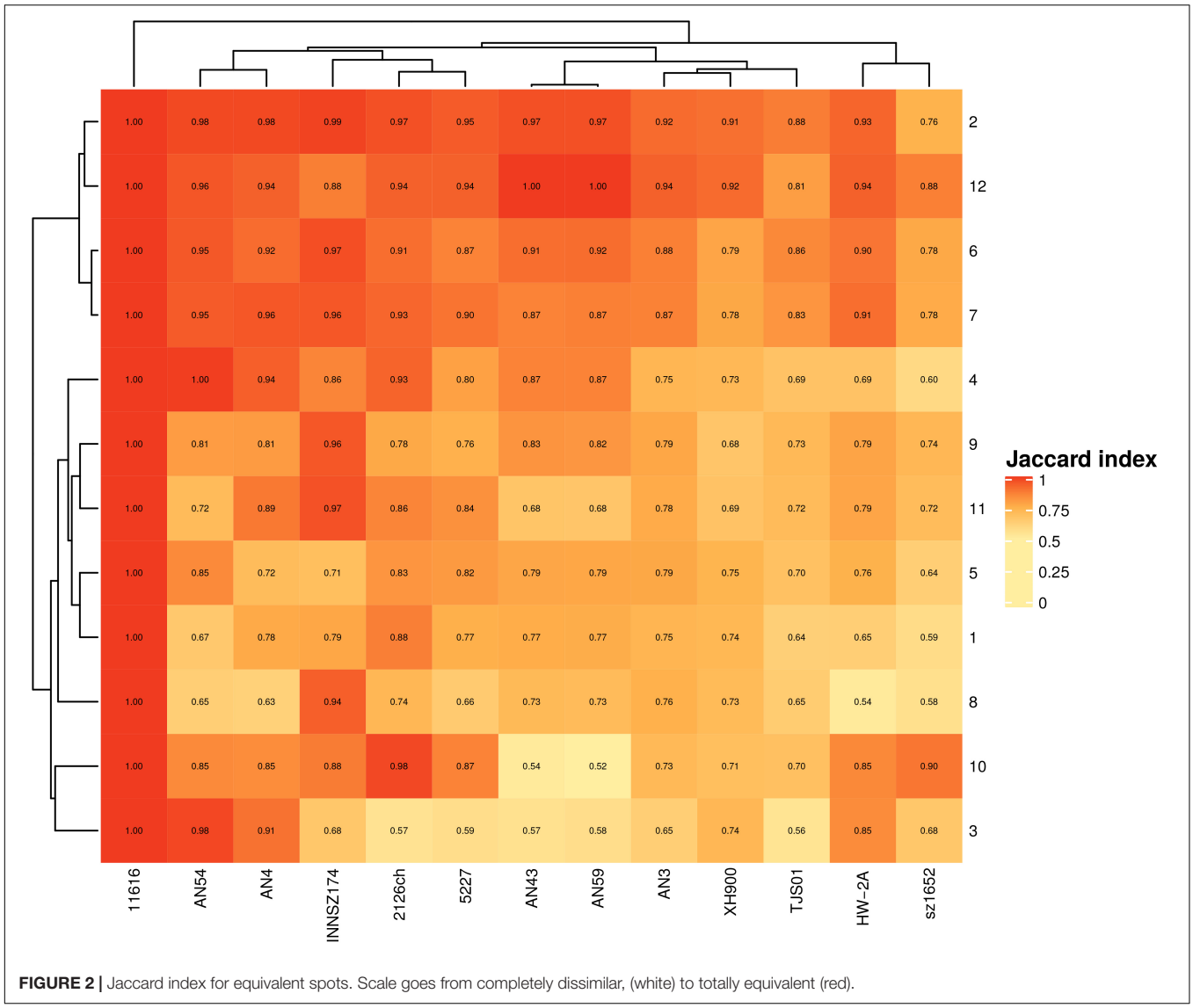

FIGURE 2 | Jaccard index for equivalent spots. Scale goes from completely dissimilar, (white) to totally equivalent (red).

or the genus *Acinetobacter*. Furthermore, we consulted databases of mobile genetic elements such as ISs, phages, and ICEs.

We found 695 to 797 (*sd* = 32) genes with recombination signals (detected by the phi test) per chromosome. Larger spots tended to have more genes with recombination signals (**Supplementary Figure S9**). Genes with recombination signals were overrepresented in spots of strains 11616, 2126ch, 5227, AN 3, AN 54, and sz1652. This observation showed that the presence of genes with recombination signals was related to spot size, such that the spots grew via the integration of genes by homologous recombination and gene duplication.

We also quantified gene families that were present in only one strain; these were considered unique gene families and were present in either one or multiple copies in the same genome. We found 29 to 374 unique gene families per chromosome, and they were present in both spots and hypervariable regions. We discovered regions without unique gene families but also hypervariable regions composed almost entirely of unique gene families (**Supplementary Figure S10**). Indeed, unique gene families were overrepresented in hypervariable regions in almost all representative strains (8/13). This finding showed that there is extensive gene content variation in *A. haemolyticus* chromosomes, mainly in hypervariable regions.

AlienHunter detected, in the chromosomes, putative HGT zones that varied from 5 to 15 Kb in size and overlapped with regions of atypical GC content (**Supplementary Figure S8**). These regions were almost always overrepresented in hypervariable regions compared with spots. The exception was strain HW-2A (with no enrichment), possibly because this strain also contained a high density of putative HGT regions along all regions of the chromosome; therefore, no enrichment was detected in any zone. We found that only a few of these regions were outside the genus *Acinetobacter*. One of these regions was the transposon that harbors the NDM-1 Metallo-beta-lactamase gene, which is present in two *A. haemolyticus* strains, namely, AN54 (plasmid) and sz1659 (chromosome), and found in a

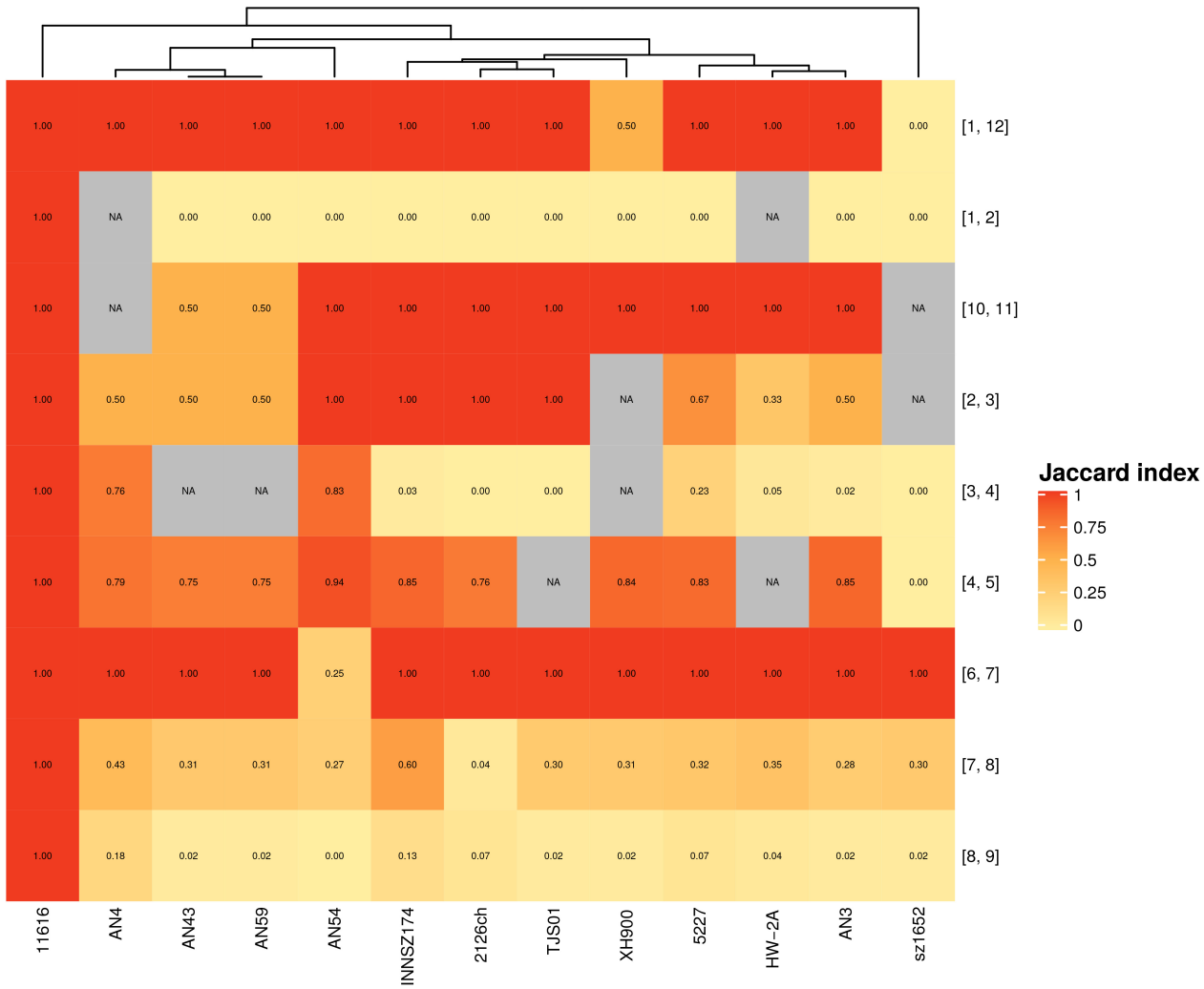

FIGURE 3 | Jaccard index for hypervariable regions between equivalent spots. Scale goes from completely dissimilar, (white) to totally equivalent (red); NA (gray)- Not applicable. Numbers in brackets represent the spots flanking each hypervariable region.

variety of bacterial species. The other region was present in strain 11616 and matched a chromosomal region of an uncharacterized gamma-proteobacterium isolated from the bee gut. Regarding the genus *Acinetobacter*, the putative HGT regions identified with AlienHunter were mainly found in *Acinetobacter junii* and *A. baumannii* plasmids and comprised hypothetical proteins, oxidoreductases, and transposases. These observations suggested that *Acinetobacter* species are donors of foreign genetic material with potential clinical relevance, such as the NDM-1 transposon, to *A. haemolyticus*.

Integrative and Conjugative Elements

Integrative and conjugative elements encode transposases but can also contain a variety of genes, and they are flanked by repeats (*att* sites) necessary for site-specific recombination. ICEs are inserted into the bacterial genome and encode all the elements required for their transfer by conjugation (Johnson and Grossman, 2015). In contrast to ICEs, integrative and mobile elements (IMEs) do not have complete conjugation machinery but can be transferred if the lacking mobile elements are provided by another ICE or plasmid (Delavat et al., 2017). We found some IMEs, which ranged in size from 3 688 to 79 964 bp (*sd* = 23171) and differed in both sequence and gene annotation, except in strains AN43 and AN59, which shared the same IME on the same chromosome. Additionally, none of these regions were found outside the *Acinetobacter* genus.

We found one to four putative IMEs in the chromosomes of nine strains: 11616 (1), 2126ch (1), 5227 (1), AN43 (1), AN59 (1), INNSZ174 (4), sz1652 (1), TJS01 (2), and XH900 (1). Chromosomal IMEs were located in spots 3 (INNSZ174), 5 (AN43, AN59, INNSZ174, and TJS01), 8 (11616, 2126ch, 5227, INNSZ174, sz1652, and TJS01), and 11 (XH900) or in a hypervariable region (between spots 3 and 4 in INNSZ174) (**Supplementary Figure S8**). In addition, ICEfinder detected 1 putative IME, without its characteristic flanking direct repeats, in the plasmids of two strains (plasmid unnamed2 of sz1652 and

pAHTJS2 of TJS01), which seemed to be conjugative plasmids. The conjugation machinery encoded in plasmid unnamed2 was very similar to that found in *A. baumannii* plasmids such as pACICU2 and pAba3207b, suggesting that *A. haemolyticus* can acquire and maintain plasmids present in *A. baumannii*.

Phages

PHASTER found 1 to 8 (*sd* = 2) putative phages in all strains. In contrast, VirSorter predicted only the largest plasmid (80 Kb) of strain 11616 (pAhae11616_f) as a putative phage region, probably because the plasmid is abundant in transposases; thus, we discarded VirSorter results in downstream analyses. Putative phage regions also overlapped with atypical GC content, which supported the foreign origin of these genomic fragments.

Transposases and Insertion Sequences

The mobile genetic elements database (MGE DB) identified only a transposase, tnpA-like, in each genome. However, there were 7 to 107 (*sd* = 33) genes annotated as transposases per chromosome. Therefore, we did not consider these results in further analyses.

Insertion sequences are DNA sequences composed of flanking sequences for site-specific recombination and a gene that codes for a transposase, which can be used to classify these elements into different families (Patricia Siguier et al., 2015). ISs are widely distributed in *A. haemolyticus* genomes; we identified 10 to 202 elements (*sd* = 61) per chromosome. The most abundant families were IS66, IS1, IS701, IS30, IS4, IS5, and IS3 because they were present in multiple copies, ranging from 2 to 13 copies (*sd* = 5) for IS66 and from 5 to 71 copies (*sd* = 24) for IS3. IS66 is a promiscuous IS with no sequence specificity (Patricia Siguier et al., 2015); this might explain why it is so frequent in the *A. haemolyticus* chromosome. IS66 has been found to interrupt a competence gene (*comEC*) in *A. baumannii* isolated in Italy (Gaiarsa et al., 2019). IS1 has been found in an *A. baumannii* transposon that harbors a gene that codes for a chloramphenicol acetyl-transferase (Elisha and Steyn, 1991); it is also present in Enterobacteriaceae plasmids (Nyman et al., 1981) and chromosomes (Lee et al., 2016), where it can mediate, in combination with IS3, IS4 and IS5, large insertions and deletions, some of the latter of which are mediated by recombination between adjacent ISs of the same family.

ISAba11, a member of the IS701 family (Rieck et al., 2012), in *A. baumannii* has been implicated in colistin resistance achieved by disruption of either of two genes important for lipid A biosynthesis (Moffatt et al., 2011). In addition, ISAba11 mediates the transposition of a genomic island that confers sulfonamide resistance from a plasmid to the *A. baumannii* chromosome (Hamidian and Hall, 2017).

IS18, a member of the IS30 family, activates an aminoglycoside resistance gene in *A. baumannii* by providing a functional promoter (Rudant et al., 1998). In a similar way, ISAba1, a member of the IS4 family, when located upstream, can potentiate the expression of intrinsic beta-lactamases, thus conferring an antibiotic resistance phenotype; for example, when ISAba1 is inserted upstream of $bla_{\mathrm{OXA-23}}$, the strain can be resistant to carbapenems (Nigro and Hall, 2016), and when ISAba1 is located upstream of *ampC*, the strain can be resistant to cephalosporins (Hamidian and Hall, 2014). In contrast, disruption of the *ampC* gene by insertion of IS5 (Said et al., 2018) or disruption of $bla_{\mathrm{OXA-75}}$ by IS3 (Li et al., 2015) results in strains susceptible to cephalosporin and, in the absence of other carbapenemases, the generation of carbapenem-susceptible isolates, respectively.

In summary, regions with atypical nucleotide features and unique gene families are overrepresented in hypervariable regions, whereas genes with recombination signals are more common in spots. IMEs are commonly found in spots, whereas ISs are scattered along the entire chromosome, are present in multiple copies, and can provide the substrate for genome rearrangements and modify distinct phenotypes.

Antibiotic Resistance Determinants in All *A. haemolyticus* Strains

We searched for antibiotic resistance determinants in the Comprehensive Antibiotic Resistance Database (CARD), and for Mexican *A. haemolyticus* strains, we contrasted the antibiotic resistance genes with their *in vitro* antibiograms. The antibiograms of the Mexican strains are presented in **Figure 4** and **Supplementary Table S4**.

We found that all *A. haemolyticus* genomes had an aminoglycoside acetyl-transferase gene [AAC(6′)-Ig] in the same location (in spot 5). In addition, only six strains harbored extra aminoglycoside-modifying enzymes in different locations; the majority were aminoglycoside phosphotransferases, two of which were observed in the representative genome sz1652 [APH(3″)-Ib and APH(6)-Id] in the hypervariable region between spots 7 and 8, near some conjugation proteins (TraA and TraB). This points to the role of hypervariable regions as a platform for the acquisition of novel genes by HGT.

All *A. haemolyticus* genomes had either a full-length or a fragment of a chromosomal oxacillinase, which could be $bla_{\mathrm{OXA-214}}$ or $bla_{\mathrm{OXA-215}}$ (**Supplementary Table S4**). The gene variant was not related to the position of the strain in the phylogeny (**Figure 1**). Moreover, both genes were in similar contexts (in representative strains, they were located in spot 11), and for each variant, there were point mutations in some strains but also large deletions that spanned multiple codons and resulted in truncated proteins. This could be the result of multiple mutations that occurred during independent events.

On the other hand, most *A. haemolyticus* strains isolated in Puebla (Mexico) (AN5, AN7, AN10, AN11, AN13, AN20, AN27, AN34, AN44, AN60, AN61, and AN63) and three strains from Mexico City (2227, 3281, DIV33, and 978) had a $bla_{\mathrm{TEM-116}}$ beta-lactamase, but none of the representative genomes had this gene (**Supplementary Table S4**). These observations indicated that the acquisition of $bla_{\mathrm{TEM-116}}$ occurred during multiple independent events along the phylogeny and that the insertion occurred in distinct locations in the genome.

Notably, two strains (AN54 and sz1652) had a transposon that carries an NDM-1 Metallo-beta-lactamase, which confers resistance to all beta-lactams, including carbapenems (Khan et al., 2017). In strain AN54, this gene resided in a plasmid, and in

FIGURE 4 | Antibiograms for Mexican *A. haemolyticus* strains. PIP, Piperacillin; TIC, Ticarcillin; AMC, Amoxicillin/Clavulanate; SAM, Ampicillin/Sulbactam; TZP, Piperacillin/Tazobactam; TIM, Ticarcillin/Clavulanate; CAZ, Ceftazidime; CTX, Cefotaxime; CRO, Ceftriaxone; FEP, Cefepime; IPM, Imipenem; MEM, Meropenem; ETP, Ertapenem; AZT, Aztreonam; GM, Gentamicin; AN, Amikacin; TOB, Tobramycin; TE, Tetracycline; CIP, Ciprofloxacin; LVX, Levofloxacin; SXT, Trimethoprim/Sulfamethoxazole. This data is also available in **Supplementary Table S4**.

strain sz1652, it was located in the chromosome. Additionally, in strain sz1652, there were two macrolide resistance genes (*msr*E and *mph*E) in the chromosome. This highlighted that *A. haemolyticus* is already acquiring antibiotic resistance genes of clinical concern.

The majority of the Mexican strains were susceptible to most antibiotics used to treat *Acinetobacter* infections, such as penicillins, either alone or in combination with beta-lactamase inhibitors, 3rd- and 4th-generation cephalosporins, carbapenems, monobactams, tetracyclines, fluoroquinolones, and sulfonamides (**Figure 4** and **Supplementary Table S4**). Overall, there was a decrease in susceptibility for aminoglycosides, which could be explained by the presence of different aminoglycoside-modifying enzymes. Additionally, of notable concern, there were some MDR strains resistant to three or more antibiotic families (Magiorakos et al., 2012) isolated in various years: AN3 (2010), 2227 (2011), 2126ch (2011), 3275 (2012), 3281 (2012), 10633 (2013), 5227 (2014), and AN54 (2016). However, the MDR phenotype could not be explained solely by the presence of antibiotic resistance genes because some strains harbored the same genes but were antibiotic sensitive, such as strains AN7 (antibiotic sensitive) and 3281 (MDR). Conversely, a strain could be MDR and lack some genes, such as strain 5227, which had neither extra aminoglycoside-modifying enzymes nor $bla_{\mathrm{TEM-116}}$ (**Supplementary Table S4**). Additionally, the MDR phenotype was interspersed throughout the phylogeny. All of this highlighted the relevance of HGT in the acquisition of novel genes, as well as the role of the regulation of efflux pumps, or

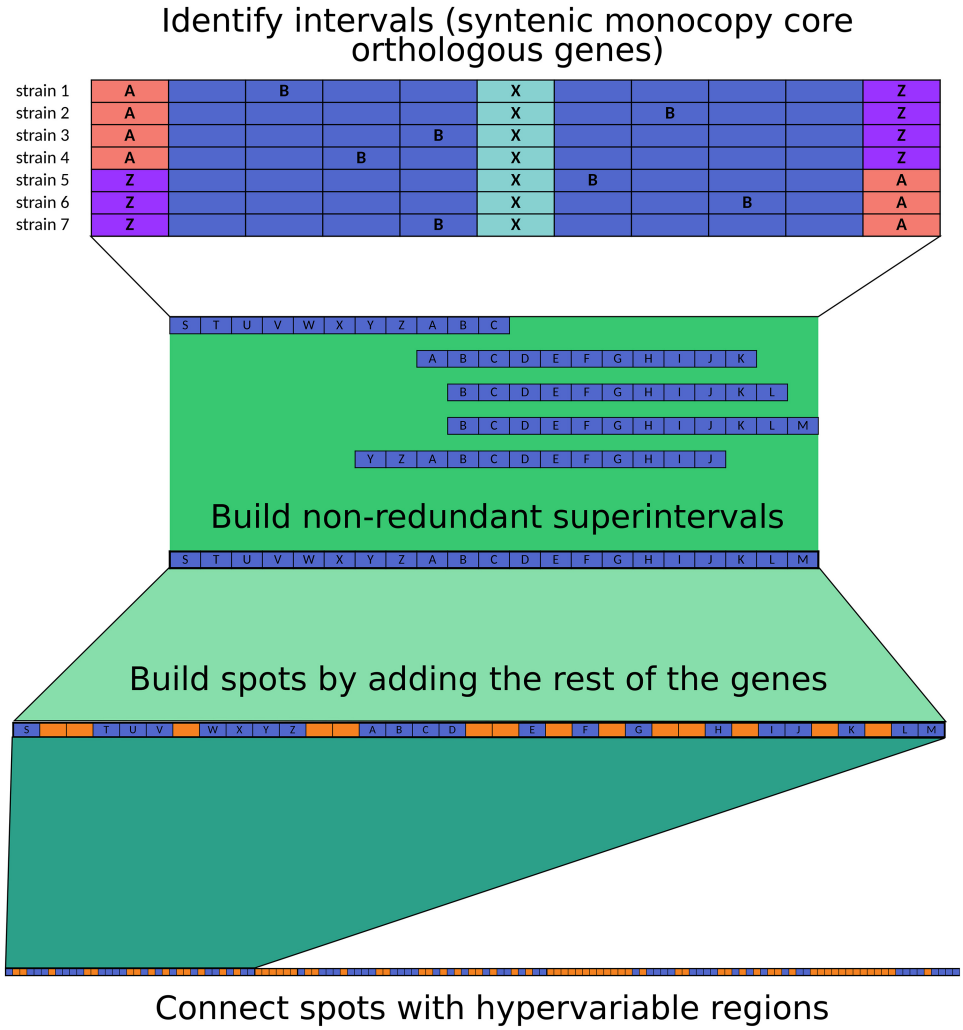

FIGURE 5 | Methodology used for spot and hypervariable region delimitation.

point mutations in either regulatory regions or genes that code for antibiotic-modifying enzymes.

Virulence Factors and Secretion Systems in all *A. haemolyticus* Strains

We also searched for protein-coding genes that were relevant for pathogens, such as virulence factors and secretion systems, in the specialized databases VFDB and TXSSCAN (Abby et al., 2014; Chen et al., 2016; Abby and Rocha, 2017) and two curated databases from the literature: one of siderophores and iron-acquisition systems and one of capsule *loci* (KLs) (see section "Materials and Methods"). Virulence factors can be grouped by function, either as immunogenic proteins, adherence factors for attachment to host and inert surfaces, capsules for protection from the environment, and siderophores and other micronutrient acquisition systems. In addition, some type-II secretion systems release effectors that damage host cells (Dobrindt et al., 2004; Wong et al., 2016; Weber et al., 2017).

The *A. haemolyticus* strains harbored multiple copies of the gene *omp*A, which codes for a porin that is one of the most abundant surface proteins in *Acinetobacter*. *A. baumannii* OmpA is immunogenic, can induce apoptosis of host cells, and is related to biofilm formation and persistence (C.-R. Wong et al., 2016; Lee et al., 2017; Weber et al., 2017). Therefore, *omp*A in *A. haemolyticus* could have the same functions and promote damage to the host. Moreover, in the representative genomes, some copies of *omp*A were in putative HGT regions defined by AlienHunter or in regions with atypical GC content, and some also had recombination signals. In addition, *omp*A copies were located in multiple spots but also in hypervariable regions. This result highlighted the high variation in this gene in *A. haemolyticus*.

The type-I secretion system (T1SS) was present in multiple copies in all *A. haemolyticus* genomes, and it formed part of the core genome. The T1SS consists of an ABC transporter, a membrane fusion protein, and an outer membrane protein (Abby and Rocha, 2017; Harding et al., 2018). In the representative

genomes, we identified two copies of the ABC transporter in spot 6, a copy of the membrane fusion protein in spot 8, and a copy of the outer membrane protein in spots 8 and 9. The T1SS exports Bap (Biofilm-associated protein) in *A. baumannii* (Harding et al., 2018), but we did not find a close homolog of this virulence factor in the *A. haemolyticus* genomes; instead, there might be other uncharacterized adhesins that are secreted by the T1SS. In addition, all strains possessed the two genes that code for BfmRS (except ATCC_19194, where only the bfmR gene was detected), a two-component system that regulates Csu (Chaperone-usher) *pili*, which are important for biofilm formation, adherence to abiotic surfaces, and capsule production (Weber et al., 2016; Lee et al., 2017). However, most of the Csu *pilus* components were annotated as hypothetical proteins (CsuA/B, CsuC, and CsuE). These results suggested that *A. haemolyticus* can form a biofilm, but the specific genes involved in its production and regulation remain to be elucidated.

All *A. haemolyticus* genomes harbor protein-coding genes for LOS biosynthesis (*lpx* genes). In the representative genomes, these genes were interspersed within spots 1, 6, 8, and 9, and almost all had recombination signals. LOSs have been implicated in serum resistance because of their role in the evasion of complement-mediated mortality and promotion of bacterial survival in host tissues (Wong et al., 2016; Geisinger et al., 2019). Importantly, in contrast to other gram-negative pathogens such as *Escherichia coli*, *Acinetobacter* members do not produce lipopolysaccharides (LPSs) because their genomes lack a ligase for LPS biosynthetic pathways (Singh et al., 2019); therefore, there are no exotoxin-like properties for these *Acinetobacter* surface structures.

The capsule is an important surface structure that in *Acinetobacter* contributes to resistance to desiccation, the ability to survive long after periods of drought, and a survival strategy linked to persistence on abiotic surfaces such as medical equipment and hospital surfaces, but it has also been linked to increased virulence, complement-mediated mortality resistance, and biofilm formation (Wong et al., 2016; Harding et al., 2018; Geisinger et al., 2019). All capsule genes in the representative genomes were located in spot 1. The KLs in *A. baumannii* exhibit great compositional variation (Harding et al., 2018); thus, it was not surprising that there were only three protein-coding genes of KLs in the core genome that also had recombination signals: *gal*U, *gdr*, and *gpi*; these genes are involved in the synthesis of oligosaccharide repeat units that will form the capsule. Notably, we also found one of the genes that commonly flanks the KLs in the core genome of *A. baumannii* (*fkp*A). The rest of the protein-coding genes involved in capsule synthesis also had recombination signals: *gne*1, *pgm*, and *ugd* (for oligosaccharide synthesis), *qhb*B (an aminotransferase), and *wza* and *wzc* (for polysaccharide export). However, we did not identify homologs of genes involved in the synthesis of the outer core of LOSs (OCL), but flanking genes (*ilv*E and *asp*S) were present (in representative genomes, they were in spot 9, such as some LOS biosynthesis genes). Among the genes flanked by *ilv*E and *asp*S, we recognized only hypothetical proteins and other enzymes annotated as having functions similar to those of the OCL, namely, an O-acetyltransferase, a capsular polysaccharide phosphotransferase, and a UDP-glucose 6-dehydrogenase. Therefore, *A. haemolyticus* produces a capsule and modifies LOSs with enzymes different from those in *A. baumannii*, but some of them are shared.

On the other hand, the type-IV pilus (T4P) is important for adhesion and twitching motility (Geisinger et al., 2019). Indeed, all strains had genes encoding twitching motility proteins (PilTU) in the same genetic context, but the regulators (PilGH) were in distinct locations. Together, these data suggested that *A. haemolyticus* can use strategies similar to those of *A. baumannii* for resistance to desiccation and survival on hospital and host surfaces.

The type-II secretion system (T2SS) can export proteins that cause host damage, for example, lipases and proteases (Weber et al., 2017; Harding et al., 2018). All strains had a complete T2SS and a phospholipase D in the same genetic context; in the representative genomes, they were located in spot 10. In addition, 10 strains (2227, 978H, AN4, CIP 64.3, KCRI-348C, MTCC 9819, NBRC 109758, NCTC 10305, NCTC 12155, and TG19599) also encoded a phospholipase C in the same genetic location, but it was present in only one representative genome (AN4) in spot 1. This finding highlighted that *A. haemolyticus* can produce a variety of enzymes that are important for the acquisition of nutrients and lysis of host cells.

Hosts can inhibit bacterial growth by sequestration of iron; however, to overcome this limitation, bacteria harbor iron-transport and iron-acquisition systems (Antunes et al., 2011). To date, the following systems have been described in *Acinetobacter*: an ABC-transporter system for ferrous iron (FeoABC) (Antunes et al., 2011); at least three siderophore clusters for iron acquisition: acinetobactin (Zimbler et al., 2009; Hasan et al., 2015), baumanoferrin (Antunes et al., 2011; Eijkelkamp et al., 2011; Penwell et al., 2015), and enterobactin (Dorsey, 2003; Antunes et al., 2011); and two clusters for hemin uptake, used to sequester iron from the host (Antunes et al., 2011). FeoABC was located in the core genome and, in the representative genomes, was located in spot 1; feoB and feoC had recombination signals. Consequently, FeoABC can serve as a platform for the acquisition of novel genes by recombination if the cluster is not lost.

Fourteen strains (AN43, AN59, ATCC 19194, ATCC 27244, CIP 64.3, HW-2A, MTCC 9819, NBRC 109758, NCTC 10305, NCTC 10306, NCTC 12155, NIPH 61, TG19599, and TG21157) contained most of the protein-coding genes needed for the biosynthesis and transport of acinetobactin (14 to 16 of 18 genes); in three representative genomes (AN43, AN59, and HW-2A), this cluster was located in spot 8, but it was absent in the rest of the genomes. Inside this region in strains AN43 and AN59, signals of HGT were detected by AlienHunter and two IS66 transposases, whereas in strain HW-2A, we detected only unique gene families. These data showed that the acinetobactin biosynthesis cluster had a foreign origin, as is the case in *A. baumannii* (Antunes et al., 2011).

Genes involved in enterobactin synthesis were not found; therefore, *A. haemolyticus* might not produce this siderophore.

Only a few genes for the synthesis of baumanoferrin were present (2 or 3 of 11), and two of them were in the core genome; in the representative genomes, all were located in spot 6. Therefore, *A. haemolyticus* might produce neither enterobactin nor baumanoferrin but have the potential to acquire the genes necessary for their production or the production of novel siderophores. Alternatively, this species might already produce them, in which case their characterization is pending.

All but 6 strains (AN60, AN61, AN63, HW-2A, KCRI-348C, and TJS01) harbored almost all the components of a hemin cluster (10 or 11 of 11 genes), but only one gene was located in the core genome (ACICU_RS08290). In the representative genomes, these genes were located in spot 4 (but one gene was located in spot 6), and only two genes had recombination signals. On the other hand, all but 9 strains (11654, ATCC 19194, CIP 64.3, MTCC 9819, NBRC 109758, NCTC 10305, NCTC 12155, TG19599, and XH900) contained almost all the components of another hemin cluster (5 to 7 of 8 genes). These genes were also located in spot 6 in the representative strains, and two of them had recombination signals (ACICU_RS04580 and ACICU_RS04605). All these data showed that *A. haemolyticus* can uptake hemin for iron acquisition and that the gene clusters had been integrated via recombination with neighboring genes.

Regarding virulence factors characterized in other gram-negative bacteria, we found that all strains had a superoxide dismutase (*sod*) and that all but three strains (11616, 3281, and KCRI-348C) had a gene that codes for a catalase/peroxidase (*kat*B); both enzymes provide resistance to reactive oxygen species-induced killing via immune system cells (Heindorf et al., 2014; Harding et al., 2018). The *sod* gene can be flanked by different genes, even though in the representative genomes it was always located in spot 5, however, the gene had recombination signals, and in a couple of strains (5227 and AN54), AlienHunter detected it as a region of putative foreign origin. *kat*B was located in spot 2 in the representative genomes and in similar genetic contexts in the rest of the genomes, but there was also slight variation in gene content in this region; this could also be explained by the fact that the *kat*B gene also had recombination signals.

Finally, TXSSCAN identified two elements of the flagellum, but they were false positives because *Acinetobacter* does not have flagella. Indeed, the elements identified were a transcriptional terminator and a subunit of an ATP synthase, which could have distinct functions in the biology of this organism.

In general, in the *A. haemolyticus* genomes, we found most of the virulence factors previously characterized in *A. baumannii* but also signs of the foreign origin of these systems. However, some elements were absent in these genes, even if the strains were associated with human infections. This can be explained by the "damage-response framework," which highlights that virulence is mediated by bacterium, host characteristics and other factors (Casadevall and Pirofski, 2019). The patients' clinical data showed that their health was compromised because of immunosuppression or because host barriers were broken by invasive procedures; thus, it is possible that the presence of additional virulence factors exacerbated the infection in most susceptible hosts.

CONCLUSION

In this work, we analyzed 47 genomes of the opportunistic pathogen *A. haemolyticus*, 31 of which were contributed by us. We found that multiple lineages of *A. haemolyticus* are circulating in Mexican and Chinese hospitals and that Mexican strains are more closely related than strains isolated from other countries. We also pointed out that the *A. haemolyticus* chromosome is fragmented into large syntenic regions (spots) and hypervariable regions that can span one to hundreds of genes. Most of the core monocopy orthologs lie in spots, many of which have recombination signals and thus serve as receptors of novel genes introduced by homologous recombination. Hypervariable regions are platforms of gene acquisition, for example, mediated by transposition. Finally, we found that *A. haemolyticus* strains are already acquiring antibiotic resistance determinants and virulence factors, which may complicate treatment and exacerbate illness in infected hosts. The virulence factors were located only in chromosomes, but as antibiotic resistance determinants are located in both chromosomes and plasmids, surveillance and analysis of *A. haemolyticus* plasmids are also warranted.

DATA AVAILABILITY STATEMENT

The genome assembly accession numbers are listed in **Table 1** and the reads are listed in **Supplementary Table S1**.

ETHICS STATEMENT

The protocol for this study was approved by the Committee of Hospital para el Niño Poblano (Registry Number: HNP/ENS/177/2016), the committee waived the need for written informed consent from patients.

AUTHOR CONTRIBUTIONS

SC-J contributed to the initial species designation by *rpoB*, genome assembly, bioinformatic analyses, data visualization, and manuscript writing. EB-L helped with the initial species designation by *rpoB* and antibiograms. CV-A performed the antibiograms and provided the clinical data. PV-F and PL-Z provided isolates, clinical data, and resources. SC-R gave feedback for some bioinformatic analyses, and manuscript editing. MC designed the study, acquired the funding, and wrote and edited manuscript.

FUNDING

This work was supported by Programa de Apoyo a Proyectos de Investigación e Innovación Tecnológica (PAPIIT) grant number 200318 and Consejo Nacional de Ciencia y Tecnología (CONACyT) grant number 253070. SC-J was a doctoral student from Programa de Doctorado en Ciencias Biomédicas,

Universidad Nacional Autónoma de México (UNAM) and received fellowship 606188 from CONACYT.

ACKNOWLEDGMENTS

We would like to thank M. C. Zita Gutiérrez-Cazares and M. C. María del Rocío López Álvarez for their help providing clinical strains, B.Cs. Alfredo Hernández and Unidad de Apoyo Bioinformático (UAB) for technical assistance and the installation of software used in this work. We also thank B.Sc. Patricia Bustos for her help finishing a genome assembly and to M. C. Ángeles Pérez-Oseguera for her technical assistance. We would also thank to Unidad de Secuenciación of Instituto Nacional de Medicina Genómica, Yale's Sequencing Facility, Macrogen, and SNPsaurus for their services. We would also thank the reviewers for their comments to improve the manuscript.

SUPPLEMENTARY MATERIAL

The Supplementary Material for this article can be found online at: https://www.frontiersin.org/articles/10.3389/fmicb.2020.00926/full#supplementary-material

REFERENCES

Abby, S. S., Néron, B., Ménager, H., Touchon, M., and Rocha, E. P. C. (2014). MacSyFinder: a program to mine genomes for molecular systems with an application to CRISPR-Cas systems. *PLoS One* 9:e110726. doi: 10.1371/journal.pone.0110726

Abby, S. S., and Rocha, E. P. C. (2017). Identification of protein secretion systems in bacterial genomes using MacSyFinder. *Methods Mol. Biol.* 1615, 1–21. doi: 10.1007/978-1-4939-7033-9_1

Antunes, L. C. S., Imperi, F., Towner, K. J., and Visca, P. (2011). Genome-assisted identification of putative iron-utilization genes in *Acinetobacter baumannii* and their distribution among a genotypically diverse collection of clinical isolates. *Res. Microbiol.* 162, 279–284. doi: 10.1016/j.resmic.2010.10.010

Antunes, L. C. S., Visca, P., and Towner, K. J. (2014). *Acinetobacter baumannii*: evolution of a global pathogen. *Pathog. Dis.* 71, 292–301. doi: 10.1111/2049-632X.12125

Arndt, D., Grant, J. R., Marcu, A., Sajed, T., Pon, A., Liang, Y., et al. (2016). PHASTER: a better, faster version of the PHAST phage search tool. *Nucleic Acids Res.* 44, W16–W21. doi: 10.1093/nar/gkw387

Bankevich, A., Nurk, S., Antipov, D., Gurevich, A. A., Dvorkin, M., Kulikov, A. S., et al. (2012). SPAdes: a new genome assembly algorithm and its applications to single-cell sequencing. *J. Comput. Biol.* 19, 455–477. doi: 10.1089/cmb.2012.0021

Baumann, P., Doudoroff, M., and Stanier, R. Y. (1968). A study of the *Moraxella* group. II. Oxidative-negative species (genus *Acinetobacter*). *J. Bacteriol.* 95, 1520–1541.

Bello-López, E., Castro-Jaimes, S., Cevallos, M. Á, Rocha-Gracia, R. D. C., Castañeda-Lucio, M., Sáenz, Y., et al. (2019). Resistome and a novel bla NDM-1 -harboring plasmid of an *Acinetobacter haemolyticus* strain from a children's hospital in Puebla, Mexico. *Microb. Drug Resist.* 25, 1023–1031. doi: 10.1089/mdr.2019.0034

Bolger, A. M., Lohse, M., and Usadel, B. (2014). Trimmomatic: a flexible trimmer for illumina sequence data. *Bioinformatics* 30, 2114–2120. doi: 10.1093/bioinformatics/btu170

Bouvet, P. J. M., and Grimont, P. A. D. (1986). Taxonomy of the genus *Acinetobacter* with the recognition of *Acinetobacter baumannii* sp. nov., *Acinetobacter haemolyticus* sp. nov., *Acinetobacter johnsonii* sp. nov., and *Acinetobacter junii* sp. nov. and emended descriptions of *Acinetobacter calcoaceticusa*. *Int. J. Syst. Bacteriol.* 36, 228–240. doi: 10.1099/00207713-36-2-228

Bruen, T. C., Philippe, H., and Bryant, D. (2006). A simple and robust statistical test for detecting the presence of recombination. *Genetics* 172, 2665–2681. doi: 10.1534/genetics.105.048975

Casadevall, A., and Pirofski, L. (2019). Benefits and costs of animal virulence for microbes. *mBio* 10, e00863-19. doi: 10.1128/mBio.00863-19

Chen, L., Zheng, D., Liu, B., Yang, J., and Jin, Q. (2016). VFDB 2016: hierarchical and refined dataset for big data analysis—10 years on. *Nucleic Acids Res.* 44, D694–D697. doi: 10.1093/nar/gkv1239

Chen, L., Yuan, J., Xu, Y., Zhang, F., and Chen, Z. (2018). Comparison of clinical manifestations and antibiotic resistances among three genospecies of the Acinetobacter calcoaceticus-*Acinetobacter baumannii* complex. *PLoS One* 13:e0191748. doi: 10.1371/journal.pone.0191748

Cheng, L., Connor, T. R., Siren, J., Aanensen, D. M., and Corander, J. (2013). Hierarchical and spatially explicit clustering of DNA sequences with BAPS software. *Mol. Biol. Evol.* 30, 1224–1228. doi: 10.1093/molbev/mst028

Chuang, Y.-C., Sheng, W.-H., Li, S.-Y., Lin, Y.-C., Wang, J.-T., Chen, Y.-C., et al. (2011). Influence of genospecies of *Acinetobacter baumannii* complex on clinical outcomes of patients with *Acinetobacter bacteremia*. *Clin. Infect. Dis.* 52, 352–360. doi: 10.1093/cid/ciq154

Cosgaya, C., Marí-Almirall, M., Van Assche, A., Fernández-Orth, D., Mosqueda, N., Telli, M., et al. (2016). *Acinetobacter dijkshoorniae* sp. nov., a member of the *Acinetobacter calcoaceticus–Acinetobacter baumannii* complex mainly recovered from clinical samples in different countries. *Int. J. Syst. Evol. Microbiol.* 66, 4105–4111. doi: 10.1099/ijsem.0.001318

Cox, M. P., Peterson, D. A., and Biggs, P. J. (2010). SolexaQA: at-a-glance quality assessment of illumina second-generation sequencing data. *BMC Bioinform.* 11:485. doi: 10.1186/1471-2105-11-485

Delavat, F., Miyazaki, R., Carraro, N., Pradervand, N., and van der Meer, J. R. (2017). The hidden life of integrative and conjugative elements. *FEMS Microbiol. Rev.* 41, 512–537. doi: 10.1093/femsre/fux008

Dobrindt, U., Hochhut, B., Hentschel, U., and Hacker, J. (2004). Genomic islands in pathogenic and environmental microorganisms. *Nat. Rev. Microbiol.* 2, 414–424. doi: 10.1038/nrmicro884

Doi, Y., Murray, G., and Peleg, A. (2015). *Acinetobacter baumannii*: evolution of antimicrobial resistance—treatment options. *Semin. Respir. Crit. Care Med.* 36, 085–098. doi: 10.1055/s-0034-1398388

Dorsey, C. W. (2003). Genetic organization of an *Acinetobacter baumannii* chromosomal region harbouring genes related to siderophore biosynthesis and transport. *Microbiology* 149, 1227–1238. doi: 10.1099/mic.0.26204-0

Doughari, H. J., Ndakidemi, P. A., Human, I. S., and Benade, S. (2011). The ecology, biology and pathogenesis of *Acinetobacter* spp.: an overview. *Microbes Environ.* 26, 101–112. doi: 10.1264/jsme2.ME10179

Eijkelkamp, B. A., Hassan, K. A., Paulsen, I. T., and Brown, M. H. (2011). Investigation of the human pathogen *Acinetobacter baumannii* under iron limiting conditions. *BMC Genomics* 12:126. doi: 10.1186/1471-2164-12-126

Elisha, B. G., and Steyn, L. M. (1991). Identification of an *Acinetobacter baumannii* gene region with sequence and organizational similarity to Tn2670. *Plasmid* 25, 96–104. doi: 10.1016/0147-619X(91)90020-W

Fitzpatrick, M. A., Ozer, E., Bolon, M. K., and Hauser, A. R. (2015). Influence of ACB complex genospecies on clinical outcomes in a U.S. hospital with high rates of multidrug resistance. *J. Infect.* 70, 144–152. doi: 10.1016/j.jinf.2014.09.004

Fouts, D. E., Brinkac, L., Beck, E., Inman, J., and Sutton, G. (2012). PanOCT: automated clustering of orthologs using conserved gene neighborhood for pan-genomic analysis of bacterial strains and closely related species. *Nucleic Acids Res.* 40:e172. doi: 10.1093/nar/gks757

Fu, Y., Du, X., Ji, J., Chen, Y., Jiang, Y., and Yu, Y. (2012). Epidemiological characteristics and genetic structure of blaNDM-1 in non-baumannii *Acinetobacter* spp. in China. *J. Antimicrob. Chemother.* 67, 2114–2122. doi: 10.1093/jac/dks192

Fyhrquist, N., Ruokolainen, L., Suomalainen, A., Lehtimäki, S., Veckman, V., Vendelin, J., et al. (2014). Acinetobacter species in the skin microbiota protect

against allergic sensitization and inflammation. *J. Allergy Clin. Immunol.* 134, 1301–1309.e11. doi: 10.1016/j.jaci.2014.07.059

Gaiarsa, S., Bitar, I., Comandatore, F., Corbella, M., Piazza, A., Scaltriti, E., et al. (2019). Can insertion sequences proliferation influence genomic plasticity? Comparative analysis of *Acinetobacter baumannii* sequence type 78, a persistent clone in Italian Hospitals. *Front. Microbiol.* 10:2080. doi: 10.3389/fmicb.2019.02080

Geisinger, E., Huo, W., Hernandez-Bird, J., and Isberg, R. R. (2019). *Acinetobacter baumannii*: envelope determinants that control drug resistance, virulence, and surface variability. *Annu. Rev. Microbiol.* 73, 481–506. doi: 10.1146/annurev-micro-020518-115714

Gerner-Smidt, P., and Tjernberg, I. (1993). Acinetobacter in Denmark: II. Molecular studies of the *Acinetobacter calcoaceticus-Acinetobacter baumannii* complex. *APMIS* 101, 826–832.

Gu, Z., Eils, R., and Schlesner, M. (2016). Complex heatmaps reveal patterns and correlations in multidimensional genomic data. *Bioinformatics* 32, 2847–2849. doi: 10.1093/bioinformatics/btw313

Gundi, V. A. K. B., Dijkshoorn, L., Burignat, S., Raoult, D., and La Scola, B. (2009). Validation of partial rpoB gene sequence analysis for the identification of clinically important and emerging *Acinetobacter* species. *Microbiology* 155, 2333–2341. doi: 10.1099/mic.0.026054-0

Hamidian, M., and Hall, R. M. (2014). Tn6168, a transposon carrying an ISAba1-activated ampC gene and conferring cephalosporin resistance in *Acinetobacter baumannii*. *J. Antimicrob. Chemother.* 69, 77–80. doi: 10.1093/jac/dkt312

Hamidian, M., and Hall, R. M. (2017). *Acinetobacter baumannii* ATCC 19606 carries GI sul2 in a genomic island located in the chromosome. *Antimicrob. Agents Chemother.* 61:e01991-16. doi: 10.1128/AAC.01991-16

Harding, C. M., Hennon, S. W., and Feldman, M. F. (2018). Uncovering the mechanisms of *Acinetobacter baumannii* virulence. *Nat. Rev. Microbiol.* 16, 91–102. doi: 10.1038/nrmicro.2017.148

Hasan, T., Choi, C. H., and Oh, M. H. (2015). Genes involved in the biosynthesis and transport of Acinetobactin in *Acinetobacter baumannii*. *Genomics Inform.* 13:2. doi: 10.5808/GI.2015.13.1.2

Heindorf, M., Kadari, M., Heider, C., Skiebe, E., and Wilharm, G. (2014). Impact of *Acinetobacter baumannii* superoxide dismutase on motility, virulence, oxidative stress resistance and susceptibility to antibiotics. *PLoS One* 9:e101033. doi: 10.1371/journal.pone.0101033

Huerta-Cepas, J., Forslund, K., Coelho, L. P., Szklarczyk, D., Jensen, L. J., von Mering, C., et al. (2017). Fast genome-wide functional annotation through orthology assignment by eggNOG-mapper. *Mol. Biol. Evol.* 34, 2115–2122. doi: 10.1093/molbev/msx148

Huerta-Cepas, J., Szklarczyk, D., Forslund, K., Cook, H., Heller, D., Walter, M. C., et al. (2016). eggNOG 4.5: a hierarchical orthology framework with improved functional annotations for eukaryotic, prokaryotic and viral sequences. *Nucleic Acids Res.* 44, D286–D293. doi: 10.1093/nar/gkv1248

Hunter, J. D. (2007). Matplotlib: a 2D graphics environment. *Comput. Sci. Eng.* 9, 90–95. doi: 10.1109/MCSE.2007.55

Hvitfeldt, E. (2019). *Paletteer: Comprehensive Collection of Color Palettes*. Available online at: https://cran.r-project.org/package=paletteer (accessed April, 2020).

Jeong, S., Hong, J. S., Kim, J. O., Kim, K.-H., Lee, W., Bae, I. K., et al. (2016). Identification of *Acinetobacter* species using matrix-assisted laser desorption ionization-time of flight mass spectrometry. *Ann. Lab. Med.* 36:325. doi: 10.3343/alm.2016.36.4.325

Jia, B., Raphenya, A. R., Alcock, B., Waglechner, N., Guo, P., Tsang, K. K., et al. (2016). CARD 2017: expansion and model-centric curation of the comprehensive antibiotic resistance database. *Nucleic Acids Res.* 45, D566–D573. doi: 10.1093/nar/gkw1004

Jiang, L., Yunmei, Y., Zeng, W., Guo, J., Lv, F., Wang, X., et al. (2019). Whole-genome analysis of New Delhi metallo-beta-lactamase-1-producing *Acinetobacter haemolyticus* from China. *J. Glob. Antimicrob. Resist.* 20, 204–208. doi: 10.1016/j.jgar.2019.05.012

Johnson, C. M., and Grossman, A. D. (2015). Integrative and conjugative elements (ICEs): what they do and how they work. *Annu. Rev. Genet.* 49, 577–601. doi: 10.1146/annurev-genet-112414-055018

Jones, L. S., Carvalho, M. J., Toleman, M. A., White, P. L., Connor, T. R., Mushtaq, A., et al. (2015). Characterization of plasmids in extensively drug-resistant acinetobacter strains isolated in India and Pakistan. *Antimicrob. Agents Chemother.* 59, 923–929. doi: 10.1128/AAC.03242-14

Khan, A. U., Maryam, L., and Zarrilli, R. (2017). Structure, genetics and worldwide spread of New Delhi Metallo-β-lactamase (NDM): a threat to public health. *BMC Microbiol.* 17:101. doi: 10.1186/s12866-017-1012-8

Khatri, I., Singh, N. K., Subramanian, S., and Mayilraj, S. (2014). Genome sequencing and annotation of *Acinetobacter haemolyticus* strain MTCC 9819T. *Genomics Data* 2, 10–12. doi: 10.1016/j.gdata.2013.10.004

Ko, K. S., Suh, J. Y., Kwon, K. T., Jung, S.-I., Park, K.-H., Kang, C. I., et al. (2007). High rates of resistance to colistin and polymyxin B in subgroups of *Acinetobacter baumannii* isolates from Korea. *J. Antimicrob. Chemother.* 60, 1163–1167. doi: 10.1093/jac/dkm305

La Scola, B., Gundi, V. A. K. B., Khamis, A., and Raoult, D. (2006). Sequencing of the rpoB Gene and flanking spacers for molecular identification of *Acinetobacter* species. *J. Clin. Microbiol.* 44, 827–832. doi: 10.1128/JCM.44.3.827-832.2006

Lee, C.-R., Lee, J. H., Park, M., Park, K. S., Bae, I. K., Kim, Y. B., et al. (2017). Biology of *Acinetobacter baumannii*: pathogenesis, antibiotic resistance mechanisms, and prospective treatment options. *Front. Cell. Infect. Microbiol.* 7:55. doi: 10.3389/fcimb.2017.00055

Lee, H., Doak, T. G., Popodi, E., Foster, P. L., and Tang, H. (2016). Insertion sequence-caused large-scale rearrangements in the genome of *Escherichia coli*. *Nucleic Acids Res.* 44, 7109–7119. doi: 10.1093/nar/gkw647

Lee, Y.-T., Kuo, S.-C., Yang, S.-P., Lin, Y.-T., Chiang, D.-H., Tseng, F.-C., et al. (2013). Bacteremic nosocomial pneumonia caused by *Acinetobacter baumannii* and *Acinetobacter nosocomialis*: a single or two distinct clinical entities? *Clin. Microbiol. Infect.* 19, 640–645. doi: 10.1111/j.1469-0691.2012.03988.x

Letunic, I., and Bork, P. (2019). Interactive tree of life (iTOL) v4: recent updates and new developments. *Nucleic Acids Res.* 47, W256–W259. doi: 10.1093/nar/gkz239

Li, P., Yang, C., Xie, J., Liu, N., Wang, H., Zhang, L., et al. (2015). *Acinetobacter calcoaceticus* from a fatal case of pneumonia harboring blaNDM-1 on a widely distributed plasmid. *BMC Infect. Dis.* 15:131. doi: 10.1186/s12879-015-0870-7

Lischer, H. E. L., and Excoffier, L. (2012). PGDSpider: an automated data conversion tool for connecting population genetics and genomics programs. *Bioinformatics* 28, 298–299. doi: 10.1093/bioinformatics/btr642

Liu, M., Li, X., Xie, Y., Bi, D., Sun, J., Li, J., et al. (2019). ICEberg 2.0: an updated database of bacterial integrative and conjugative elements. *Nucleic Acids Res.* 47, D660–D665. doi: 10.1093/nar/gky1123

Magiorakos, A.-P., Srinivasan, A., Carey, R. B., Carmeli, Y., Falagas, M. E., Giske, C. G., et al. (2012). Multidrug-resistant, extensively drug-resistant and pandrug-resistant bacteria: an international expert proposal for interim standard definitions for acquired resistance. *Clin. Microbiol. Infect.* 18, 268–281. doi: 10.1111/j.1469-0691.2011.03570.x

Marcus, B. B., Samuels, S. B., Pittman, B., and Cherry, W. B. (1969). A serologic study of *Herellea vaginicola* and its identification by immunofluorescent staining. *Am. J. Clin. Pathol.* 52, 309–319. doi: 10.1093/ajcp/52.3.309

Moffatt, J. H., Harper, M., Adler, B., Nation, R. L., Li, J., and Boyce, J. D. (2011). Insertion sequence IS Aba11 is involved in colistin resistance and loss of lipopolysaccharide in *Acinetobacter baumannii*. *Antimicrob. Agents Chemother.* 55, 3022–3024. doi: 10.1128/AAC.01732-10

Nemec, A., Dijkshoorn, L., and Ježek, P. (2000). Recognition of two novel phenons of the genus *Acinetobacter* among non-glucose-acidifying isolates from human specimens. *J. Clin. Microbiol.* 38, 3937–3941.

Nemec, A., Krizova, L., Maixnerova, M., Sedo, O., Brisse, S., and Higgins, P. G. (2015). *Acinetobacter seifertii* sp. nov., a member of the *Acinetobacter calcoaceticus-Acinetobacter baumannii* complex isolated from human clinical specimens. *Int. J. Syst. Evol. Microbiol.* 65(Pt 3), 934–942. doi: 10.1099/ijs.0.000043

Nemec, A., Krizova, L., Maixnerova, M., van der Reijden, T. J. K., Deschaght, P., Passet, V., et al. (2011). Genotypic and phenotypic characterization of the *Acinetobacter calcoaceticus–Acinetobacter baumannii* complex with the proposal of *Acinetobacter pittii* sp. nov. (formerly *Acinetobacter* genomic species 3) and *Acinetobacter nosocomialis* sp. nov. (formerly Ac. *Res. Microbiol.* 162, 393–404. doi: 10.1016/j.resmic.2011.02.006

Nemec, A., Radolfová-Křížová, L., Maixnerová, M., Nemec, M., Clermont, D., Bzdil, J., et al. (2019). Revising the taxonomy of the *Acinetobacter lwoffii* group: the description of *Acinetobacter pseudolwoffii* sp. nov. and emended description of *Acinetobacter lwoffii*. *Syst. Appl. Microbiol.* 42, 159–167. doi: 10.1016/j.syapm.2018.10.004

Nemec, A., Radolfová-Křížová, L., Maixnerova, M., and Sedo, O. (2017). *Acinetobacter colistiniresistens* sp. nov. (formerly genomic species 13 sensu Bouvet and Jeanjean and genomic species 14 sensu Tjernberg and Ursing), isolated from human infections and characterized by intrinsic resistance to polymyxins. *Int. J. Syst. Evol. Microbiol.* 67, 2134–2141. doi: 10.1099/ijsem.0.001903

Nemec, A., Radolfová-Křížová, L., Maixnerova, M., Vrestiakova, E., Jezek, P., and Sedo, O. (2016). Taxonomy of haemolytic and/or proteolytic strains of the genus *Acinetobacter* with the proposal of *Acinetobacter courvalinii* sp. nov. (genomic species 14 sensu Bouvet & Jeanjean), *Acinetobacter dispersus* sp. nov. (genomic species 17), *Acinetobacter modestu*. *Int. J. Syst. Evol. Microbiol.* 66, 1673–1685. doi: 10.1099/ijsem.0.000932

Neuwirth, E. (2014). *RColorBrewer: ColorBrewer Palettes*. Available online at: https://cran.r-project.org/package=RColorBrewer (accessed April, 2020).

Nigro, S. J., and Hall, R. M. (2016). Structure and context of *Acinetobacter* transposons carrying the oxa23 carbapenemase gene. *J. Antimicrob. Chemother.* 71, 1135–1147. doi: 10.1093/jac/dkv440

Nyman, K., Nakamura, K., Ohtsubo, H., and Ohtsubo, E. (1981). Distribution of the insertion sequence IS1 in gram-negative bacteria. *Nature* 289, 609–612. doi: 10.1038/289609a0

Oliveira, P. H., Touchon, M., Cury, J., and Rocha, E. P. C. (2017). The chromosomal organization of horizontal gene transfer in bacteria. *Nat. Commun.* 8:841. doi: 10.1038/s41467-017-00808-w

Paradis, E., and Schliep, K. (2019). ape 5.0: an environment for modern phylogenetics and evolutionary analyses in R. *Bioinformatics* 35, 526–528. doi: 10.1093/bioinformatics/bty633

Park, K.-H., Shin, J.-H., Lee, S. Y., Kim, S. H., Jang, M. O., Kang, S.-J., et al. (2013). The clinical characteristics, carbapenem resistance, and outcome of *Acinetobacter bacteremia* according to genospecies. *PLoS One* 8:e65026. doi: 10.1371/journal.pone.0065026

Pärnänen, K., Karkman, A., Hultman, J., Lyra, C., Bengtsson-Palme, J., Larsson, D. G. J., et al. (2018). Maternal gut and breast milk microbiota affect infant gut antibiotic resistome and mobile genetic elements. *Nat. Commun.* 9:3891. doi: 10.1038/s41467-018-06393-w

Penwell, W. F., DeGrace, N., Tentarelli, S., Gauthier, L., Gilbert, C. M., Arivett, B. A., et al. (2015). Discovery and characterization of new hydroxamate siderophores, baumannoferrin A and B, produced by *Acinetobacter baumannii*. *Chembiochem* 16, 1896–1904. doi: 10.1002/cbic.201500147

Ploswiki, F., Ravenhall, M., Lassalle, F., and Dessimoz, C. (2015). Inferring horizontal gene transfer. *PLoS Comput. Biol.* 11:e1004095. doi: 10.1371/journal.pcbi.1004095

Pritchard, L., Glover, R. H., Humphris, S., Elphinstone, J. G., and Toth, I. K. (2016). Genomics and taxonomy in diagnostics for food security: soft-rotting enterobacterial plant pathogens. *Anal. Methods* 8, 12–24. doi: 10.1039/C5AY02550H

R Core Team (2019). *R: A Language and Environment for Statistical Computing*. Available online at: https://www.r-project.org/ (accessed April, 2020).

Revell, L. J. (2012). phytools: an R package for phylogenetic comparative biology (and other things). *Methods Ecol. Evol.* 3, 217–223. doi: 10.1111/j.2041-210X.2011.00169.x

Rice, P., Longden, I., and Bleasby, A. (2000). EMBOSS: the european molecular biology open software suite. *Trends Genet*. 16, 276–277. doi: 10.1016/S0168-9525(00)02024-2

Richter, M., and Rosselló-Móra, R. (2009). Shifting the genomic gold standard for the prokaryotic species definition. *Proc. Natl. Acad. Sci. U. S. A.* 106, 19126–19131. doi: 10.1073/pnas.0906412106

Rieck, B., Tourigny, D. S., Crosatti, M., Schmid, R., Kochar, M., Harrison, E. M., et al. (2012). *Acinetobacter* insertion sequence is aba11 belongs to a novel family that encodes transposases with a signature HHEK motif. *Appl. Environ. Microbiol.* 78, 471–480. doi: 10.1128/AEM.05663-1

Rosselló-Móra, R., and Amann, R. (2015). Past and future species definitions for Bacteria and Archaea. *Syst. Appl. Microbiol.* 38, 209–216. doi: 10.1016/j.syapm.2015.02.001

Roux, S., Enault, F., Hurwitz, B. L., and Sullivan, M. B. (2015). VirSorter: mining viral signal from microbial genomic data. *PeerJ* 3:e985. doi: 10.7717/peerj.985

Rudant, E., Courvalin, P., and Lambert, T. (1998). Characterization of IS 18, an element capable of activating the silent aac(6′)-Ij gene of *Acinetobacter* sp. 13 Strain BM2716 by transposition. *Antimicrob. Agents Chemother.* 42, 2759–2761. doi: 10.1128/AAC.42.10.2759

Said, H. S., Benmahmod, A. B., and Ibrahim, R. H. (2018). Co-production of AmpC and extended spectrum beta-lactamases in cephalosporin-resistant *Acinetobacter baumannii* in Egypt. *World J. Microbiol. Biotechnol.* 34:189. doi: 10.1007/s11274-018-2571-z

Schleicher, X., Higgins, P. G., Wisplinghoff, H., Körber-Irrgang, B., Kresken, M., and Seifert, H. (2013). Molecular epidemiology of *Acinetobacter baumannii* and *Acinetobacter nosocomialis* in Germany over a 5-year period (2005–2009). *Clin. Microbiol. Infect.* 19, 737–742. doi: 10.1111/1469-0691.12026

Schloerke, B., Crowley, J., Cook, D., Briatte, F., Marbach, M., Thoen, E., et al. (2018). *GGally: Extension to "ggplot2."*. Available online at: https://cran.r-project.org/package=GGally

Seemann, T. (2014). Prokka: rapid prokaryotic genome annotation. *Bioinformatics* 30, 2068–2069. doi: 10.1093/bioinformatics/btu153

Sievers, F., Wilm, A., Dineen, D., Gibson, T. J., Karplus, K., Li, W., et al. (2014). Fast, scalable generation of high-quality protein multiple sequence alignments using Clustal Omega. *Mol. Syst. Biol.* 7, 539–539. doi: 10.1038/msb.2011.75

Siguier, P., Perochon, J., Lestrade, L., Mahillon, J., and Chandler, M. (2006). ISfinder: the reference centre for bacterial insertion sequences. *Nucleic Acids Res.* 34, D32–D36. doi: 10.1093/nar/gkj014

Siguier, P., Gourbeyre, E., Varani, A., Ton-Hoang, B., and Chandler, M. (2015). Everyman's guide to bacterial insertion sequences. *Microbiol. Spectr.* 3:MDNA3-0030-2014. doi: 10.1128/microbiolspec.MDNA3-0030-2014

Simpson, J. T., Wong, K., Jackman, S. D., Schein, J. E., Jones, S. J. M., and Birol, I. (2009). ABySS: a parallel assembler for short read sequence data. *Genome Res.* 19, 1117–1123. doi: 10.1101/gr.089532.108

Singh, J. K., Adams, F. G., and Brown, M. H. (2019). Diversity and function of capsular polysaccharide in *Acinetobacter baumannii*. *Front. Microbiol.* 9:3301. doi: 10.3389/fmicb.2018.03301

Slowikowski, K. (2019). *ggrepel: Automatically Position Non-Overlapping Text Labels with "ggplot2."*. Available online at: https://cran.r-project.org/package=ggrepel (accessed April, 2020).

Stamatakis, A. (2014). RAxML version 8: a tool for phylogenetic analysis and post-analysis of large phylogenies. *Bioinformatics* 30, 1312–1313. doi: 10.1093/bioinformatics/btu033

Tayabali, A. F., Nguyen, K. C., Shwed, P. S., Crosthwait, J., Coleman, G., and Seligy, V. L. (2012). Comparison of the virulence potential of *Acinetobacter* strains from clinical and environmental sources. *PLoS One* 7:e37024. doi: 10.1371/journal.pone.0037024

Touchon, M., Cury, J., Yoon, E.-J., Krizova, L., Cerqueira, G. C., Murphy, C., et al. (2014). The genomic diversification of the whole *Acinetobacter* genus: origins, mechanisms, and consequences. *Genome Biol. Evol.* 6, 2866–2882. doi: 10.1093/gbe/evu225

Treangen, T. J., Ondov, B. D., Koren, S., and Phillippy, A. M. (2014). The Harvest suite for rapid core-genome alignment and visualization of thousands of intraspecific microbial genomes. *Genome Biol.* 15:524. doi: 10.1186/s13059-014-0524-x

Turton, J. F., Shah, J., Ozongwu, C., and Pike, R. (2010). Incidence of *Acinetobacter* species other than a. baumannii among clinical isolates of *Acinetobacter*: evidence for emerging species. *J. Clin. Microbiol.* 48, 1445–1449. doi: 10.1128/JCM.02467-09

Wang, J., Ruan, Z., Feng, Y., Fu, Y., Jiang, Y., Wang, H., et al. (2014). Species distribution of clinical *Acinetobacter* isolates revealed by different identification techniques. *PLoS One* 9:e104882. doi: 10.1371/journal.pone.0104882

Wang, Y.-C., Hao, X.-Y., Wang, L., Bin Xiao, Wang, X.-C., and Yang, Y.-J. (2016). Diverse colletotrichum species cause anthracnose of tea plants (*Camellia sinensis* (L.) O. Kuntze) in China. *Sci. Rep.* 6:35287. doi: 10.1038/srep35287

Weber, B. S., Harding, C. M., and Feldman, M. F. (2016). Pathogenic *Acinetobacter*: from the cell surface to infinity and beyond. *J. Bacteriol.* 198, 880–887. doi: 10.1128/JB.00906-15

Weber, B. S., Kinsella, R. L., Harding, C. M., and Feldman, M. F. (2017). The secrets of *Acinetobacter* secretion. *Trends Microbiol.* 25, 532–545. doi: 10.1016/j.tim.2017.01.005

Wences, A. H., and Schatz, M. C. (2015). Metassembler: merging and optimizing de novo genome assemblies. *Genome Biol.* 16:207. doi: 10.1186/s13059-015-0764-4

Wernersson, R., and Pedersen, A. G. (2003). Revtrans: multiple alignment of coding DNA from aligned amino acid sequences. *Nucleic Acids Res.* 31, 3537–3539.

Wick, R. R., Judd, L. M., Gorrie, C. L., and Holt, K. E. (2017). Unicycler: resolving bacterial genome assemblies from short and long sequencing reads. *PLoS Comput. Biol.* 13:e1005595. doi: 10.1371/journal.pcbi.1005595

Wickham, H. (2009). *ggplot2. Elegant Graphics for Data Analysis*. New York, NY: Springer, doi: 10.1007/978-0-387-98141-3

Wickham, H., François, R., Henry, L., and Müller, K. (2019). *dplyr: A Grammar of Data Manipulation*. Available online at: https://cran.r-project.org/package=dplyr (accessed April, 2020).

Wisplinghoff, H., Paulus, T., Lugenheim, M., Stefanik, D., Higgins, P. G., Edmond, M. B., et al. (2012). Nosocomial bloodstream infections due to *Acinetobacter baumannii*, *Acinetobacter pittii* and *Acinetobacter nosocomialis* in the United States. *J. Infect.* 64, 282–290. doi: 10.1016/j.jinf.2011.12.008

Wong, D., Nielsen, T. B., Bonomo, R. A., Pantapalangkoor, P., Luna, B., and Spellberg, B. (2016). Clinical and pathophysiological overview of *Acinetobacter* infections: a century of challenges. *Clin. Microbiol. Rev.* 30, 409–447. doi: 10.1128/CMR.00058-16

Xie, Z., and Tang, H. (2017). ISEScan: automated identification of insertion sequence elements in prokaryotic genomes. *Bioinformatics* 33, 3340–3347. doi: 10.1093/bioinformatics/btx433

Zerbino, D. R., and Birney, E. (2008). Velvet: algorithms for de novo short read assembly using de Bruijn graphs. *Genome Res.* 18, 821–829. doi: 10.1101/gr.074492.107

Zheng, X., Gogarten, S. M., Lawrence, M., Stilp, A., Conomos, M. P., Weir, B. S., et al. (2017). SeqArray—a storage-efficient high-performance data format for WGS variant calls. *Bioinformatics* 33, 2251–2257. doi: 10.1093/bioinformatics/btx145

Zheng, X., Levine, D., Shen, J., Gogarten, S. M., Laurie, C., and Weir, B. S. (2012). A high-performance computing toolset for relatedness and principal component analysis of SNP data. *Bioinformatics* 28, 3326–3328. doi: 10.1093/bioinformatics/bts606

Zimbler, D. L., Penwell, W. F., Gaddy, J. A., Menke, S. M., Tomaras, A. P., Connerly, P. L., et al. (2009). Iron acquisition functions expressed by the human pathogen *Acinetobacter baumannii*. *BioMetals* 22, 23–32. doi: 10.1007/s10534-008-9202-3

Conflict of Interest: The authors declare that the research was conducted in the absence of any commercial or financial relationships that could be construed as a potential conflict of interest.

frontiers in Microbiology

ORIGINAL RESEARCH
published: 09 June 2020
doi: 10.3389/fmicb.2020.01134

Phenotypic Variation and Carbapenem Resistance Potential in OXA-499-Producing *Acinetobacter pittii*

Linyue Zhang[1,2†], Ying Fu[2,3†], Xinhong Han[1,2†], Qingye Xu[1,2], Shanshan Weng[1,2], Biyong Yan[4], Lilin Liu[1,2], Xiaoting Hua[1,2], Yan Chen[1,2] and Yunsong Yu[1,2*]*

[1] Department of Infectious Diseases, Sir Run Run Shaw Hospital, College of Medicine, Zhejiang University, Hangzhou, China, [2] Key Laboratory of Microbial Technology and Bioinformatics of Zhejiang Province, Hangzhou, China, [3] Department of Clinical Laboratory, Sir Run Run Shaw Hospital, College of Medicine, Zhejiang University, Hangzhou, China, [4] Department of Laboratory Medicine, The Second Affiliated Hospital of Zhejiang University School of Medicine, Hangzhou, China

OPEN ACCESS

Edited by:
Benjamin Andrew Evans, University of East Anglia, United Kingdom

Reviewed by:
Martina Barchitta, University of Catania, Italy
Ignasi Roca Subirà, Instituto Salud Global Barcelona (ISGlobal), Spain

***Correspondence:**
Yan Chen
chenyan@zju.edu.cn
Yunsong Yu
yvys119@zju.edu.cn

[†]These authors have contributed equally to this work

Specialty section:
This article was submitted to Antimicrobials, Resistance and Chemotherapy, a section of the journal Frontiers in Microbiology

Received: 28 January 2020
Accepted: 05 May 2020
Published: 09 June 2020

Citation:
Zhang L, Fu Y, Han X, Xu Q, Weng S, Yan B, Liu L, Hua X, Chen Y and Yu Y (2020) Phenotypic Variation and Carbapenem Resistance Potential in OXA-499-Producing Acinetobacter pittii. Front. Microbiol. 11:1134. doi: 10.3389/fmicb.2020.01134

Acinetobacter pittii is increasingly recognized as a clinically important species. Here, we identified a carbapenem-non-resistant *A. pittii* clinical isolate, A1254, harboring $bla_{OXA-499}$, $bla_{OXA-826}$, and $bla_{ADC-221}$. The $bla_{OXA-499}$ genetic environment in A1254 was identical to that of another OXA-499-producing, but carbapenem-resistant, *A. pittii* isolate, YMC2010/8/T346, indicating the existence of phenotypic variation among OXA-499-producing *A. pittii* strains. Under imipenem-selective pressure, the A1254 isolate developed resistance to carbapenems in 60 generations. Two carbapenem-resistant mutants (CAB009 and CAB010) with mutations in the $bla_{OXA-499}$ promoter region were isolated from two independently evolved populations (CAB001 and CAB004). The CAB009 mutant, with a mutation at position −14 (A to G), exhibited a four-fold higher carbapenem minimum inhibitory concentration (MIC) and a 4.53 ± 0.19 $\log_2$ fold change higher expression level of $bla_{OXA-499}$ than the ancestor strain, A1254. The other mutant, CAB010, with a mutation at position −42 (G to A), showed a two-fold higher carbapenem MIC and a 1.65 ± 0.25 $\log_2$ fold change higher $bla_{OXA-499}$ expression level than the ancestor strain. The $bla_{OXA-499}$ gene and its promoter region were amplified from the wild-type strain and two mutant isolates and then individually cloned into the pYMAb2-Hyg^r vector and expressed in *Acinetobacter baumannii* ATCC 17978, *A. pittii* LMG 1035, and *A. pittii* A1254. All the transformed strains were resistant to carbapenem, irrespective of whether they harbored the initial or an evolved promoter sequence, and transformed strains expressing the promoter from the most resistant mutant, CAB009, showed the highest carbapenem MICs, with values of 32–64 μg/ml for imipenem and 128 μg/ml for meropenem. RNA sequencing was performed to confirm the contribution of $bla_{OXA-499}$ to the development of carbapenem resistance. Although the CAB009 and CAB010 transcriptional patterns were different, $bla_{OXA-499}$ was the only differentially expressed gene shared by the two mutants.

Our results indicate that carbapenem-non-resistant *Acinetobacter* spp. strains carrying bla_{OXA} genes have the potential to develop carbapenem resistance and need to be further investigated and monitored to prevent treatment failure due to the development of resistance.

Keywords: *Acinetobacter pittii*, carbapenem resistance, OXA-499, oxacillinase, carbapenemase, phenotypic variation

INTRODUCTION

Acinetobacter spp. are increasingly raising serious concern because of their ability to rapidly develop resistance to a wide range of antimicrobials. Among these species, *Acinetobacter baumannii*, *Acinetobacter nosocomialis*, and *Acinetobacter pittii* are the most frequently isolated in hospitals globally (Weber et al., 2015). In the last few decades, relatively few studies have investigated non-*baumannii Acinetobacter* spp., likely owing to their low prevalence and resistant rates (Chen et al., 2019). However, non-*baumannii Acinetobacter* spp. are increasingly being found in clinical specimens and deserve more attention. This is true of *A. pittii*, previously called *Acinetobacter* genomic species three, which is increasingly found in food, clinical patients, and healthy individuals (Yang et al., 2012; Al Atrouni et al., 2016; Silva et al., 2018). Among *Acinetobacter* spp., *A. pittii* is the most commonly identified causative agent of nosocomial infections in patients hospitalized both in general ward and in intensive care units (ICUs) in Germany and is the most prevalent species identified among hospital-acquired *A. calcoaceticus–A. baumannii* (ACB) complex bloodstream isolates in France (Schleicher et al., 2013; Pailhories et al., 2018).

The ability of bacteria to rapidly acquire resistance poses crucial challenges to clinical treatment. We have previously shown that *A. baumannii* strains developed greater resistance with within-host evolution, thereby limiting the treatment options (Hua et al., 2017). Similar effects have also been observed for other species. For example, *Pseudomonas aeruginosa* showed rapid and large increases in resistance to carbapenem during antibiotic therapy that were likely due to *de novo* evolution and/or the selection of resistant subpopulations, indicating a potential risk for the rapid spread of antimicrobial resistance (Tueffers et al., 2019). Development of carbapenem resistance in sequential clinical isolates of *Raoultella ornithinolytica* carrying $bla_{OXA-232}$ in a hospitalized patient during the course of ertapenem therapy was recently reported, highlighting the diagnostic challenges posed by strains producing inefficient types of carbapenemase (Iovleva et al., 2019). A more comprehensive understanding of resistance development would provide a molecular basis for improving the treatment of infections. However, to the best of our knowledge, no study to date has investigated the potential for the development of carbapenem resistance in *A. pittii*.

The emergence of carbapenem-resistant *A. pittii* has been reported worldwide. The rate of carbapenem resistance in *A. nosocomialis* and *A. pittii* isolates increased from 7.5% in 2010 to 22% in 2014 (Chen et al., 2019). Carbapenem resistance in *A. pittii* is mainly associated with the production of the carbapenem-hydrolyzing class D β-lactamases (CHDLs), such as OXA-23, OXA-58, OXA-72, OXA-143, and their variants (Zander et al., 2014a; D'Souza et al., 2017; Singkham-In and Chatsuwan, 2018; Chen et al., 2019). Besides, NDM-1-producing *A. pittii* isolates have also been reported in several cases (Yang et al., 2012; Hammerum et al., 2015; Pailhories et al., 2017; Deglmann et al., 2019). The emergence of carbapenem resistance in *A. pittii* reflects its ability to acquire and spread resistance genes, posing a challenge to the management of carbapenem-resistant non-*baumannii Acinetobacter* spp.

In this study, we characterized the *A. pittii* A1254 clinical isolate, which carries $bla_{OXA-499}$, intrinsic $bla_{OXA-826}$, and $bla_{ADC-221}$, but is susceptible to imipenem and intermediate susceptible to meropenem. The carbapenem resistance profile of A1254 was different from that of another OXA-499 producing *A. pittii* strain, YMC2010/8/T346, even though the $bla_{OXA-499}$ genetic environment was identical in the two strains, indicating the existence of phenotypic variation among OXA-499-producing *A. pittii* strains. Thus, we investigated the effect of imipenem exposure in the A1254 isolate to reveal its potential to develop carbapenem resistance.

MATERIALS AND METHODS

Bacterial Isolates and Culture Conditions

Acinetobacter pittii A1254 is a clinical strain isolated from the sputum sample of a patient with chronic obstructive pulmonary disease from the People's Hospital of Quzhou, Zhejiang Province, China, in 2010. The A1254 isolate was initially described in our previous study on the prevalence of carbapenem-hydrolyzing class D β-lactamase genes in *Acinetobacter* spp. isolates (Ji et al., 2014). *A. baumannii* reference strain ATCC 17978, *A. pittii* reference strain LMG1035, and *Escherichia coli* DH5α were employed for cloning experiments. The liquid medium used was Luria–Bertani (LB) broth (Oxford, United Kingdom). The medium was supplemented with imipenem (0.75 μg/ml) as required.

Antimicrobial Susceptibility Testing

The minimum inhibitory concentrations (MICs) of imipenem and meropenem were evaluated using the broth microdilution method according to the guidelines of the Clinical and Laboratory Standards Institute (CLSI, 2018). Simultaneously, carbapenem MICs against A1254 were evaluated with Etest strips (bioMérieux, Marcy-l'Étoile, France). *E. coli* strain ATCC 25922 was used as quality control. The results were interpreted in accordance with the CLSI breakpoints.

Experimental Evolution Under Imipenem Selective Pressure

Four single colonies of the *A. pittii* A1254 ancestor strain were inoculated in LB broth supplemented with imipenem (0.75 μg/ml). This concentration was maintained throughout the experimental evolution. All the evolved lineages were passaged daily and independently with shaking (200 rpm) at 37°C. A 20-μl volume of overnight culture was collected and inoculated at a 1:100 dilution daily for 9 days, and the generations were calculated (∼6.64 generations a day) with reference to Nicoloff et al. (2019). The four evolved populations were designated as CAB001, CAB002, CAB003, and CAB004. A different single colony was passaged daily in antibiotic-free LB broth as a blank control.

Whole-Genome Sequencing and Sequence Analysis

Genomic DNA of the four evolved populations (CAB001–CAB004) was extracted on day 9 using a QIAamp DNA Mini Kit (Qiagen, Valencia, CA, United States) following the manufacturer's recommendations. The quality and quantity of genomic DNA were determined by agarose gel electrophoresis and a NanoDrop spectrophotometer. A 300-bp library for Illumina paired-end sequencing was constructed from 5 μg of DNA using a Paired-End DNA Sample Prep Kit (Illumina, San Diego, CA, United States). The ancestor strain, *A. pittii* A1254, was sequenced by both long-read nanopore sequencing (Oxford Nanopore Technologies, Oxford, United Kingdom) and Illumina paired-end sequencing. Reads obtained from Illumina paired-end sequencing were used to correct the result of the nanopore sequencing using the Unicycler assembly pipeline (Wick et al., 2017). Paired-end sequence reads were assembled by SPAdes (Bankevich et al., 2012) and the *de novo* assemblies were subsequently annotated using the Prokka pipeline (Seemann, 2014). The genome of A1254 was input to the CGE web server for detection of resistance genes (selected% ID threshold, 90%; selected minimum length, 60%)[1] (Zankari et al., 2012). Breseq was used to find mutations in evolved populations compared with A1254 (Deatherage and Barrick, 2014). Detected mutations were confirmed by PCR and Sanger sequencing. The primers used are listed in **Table 1**.

Cloning and Transformation

Fragments of $bla_{OXA-499}$ with or without the promoter region were amplified from the wild-type *A. pittii* A1254 strain and the CAB009 and CAB010 mutants. Additionally, $bla_{OXA-826}$ was also amplified, with or without its promoter region, but only from *A. pittii* A1254. The products were cloned into the *Bam*HI and *Sal*I-digested shuttle vector PYMAb2-Hyg^r using the ClonExpress® II One Step Cloning Kit (Vazyme Biotech Co., Ltd., Nanjing, China) following the manufacturer's recommendations. Cloning was performed based on recombination. Briefly, PYMAb2-Hyg^r was digested with *Bam*HI and *Sal*I. Using the primer pairs shown in **Table 1**, PCR products comprising the target fragment flanked by the recombination sequences were obtained. Then, the linearized vector, purified PCR product, buffer, and enhanced recombinase (Exnase II) were mixed and incubated for 30 min, yielding the recombinant vectors. The recombinant vectors were transformed into *A. baumannii* ATCC 17978, *A. pittii* LMG1035, and A1254 by electroporation.

Quantitative Reverse Transcription PCR

Quantitative reverse transcription PCR (RT-qPCR) was performed to measure the expression level of $bla_{OXA-499}$ and $bla_{OXA-826}$ in *A. pittii* A1254 and the CAB009 and CAB010 mutants submitted or not to imipenem selection. Total RNA was extracted using the RNeasy Mini Kit (Qiagen). RNA was reverse transcribed using random hexamers from Invitrogen (Carlsbad, CA, United States) and a reverse transcriptase from Takara Bio (Ôtsu, Japan), according to the manufacturer's instructions. Quantitative PCR was performed using the SYBR® Premix Ex Taq™ PCR Kit (Takara Bio) in a LightCycler 480 system (Roche Molecular Diagnostics, Rotkreuz, Switzerland). The Ct value of each sample was measured under the following conditions: 95°C for 5 min, followed by 40 amplification cycles at 95°C for 10 s, 52°C for 30 s, and 72°C for 30 s. The *rpoB* gene was used as an internal reference. The primers used are listed in **Table 1**. Triplicate samples were included in each run, and RT-qPCR was performed three times independently. Data were calculated based on the ΔΔCt method (Livak and Schmittgen, 2001). Log_2 fold change was used to evaluate the expression levels. Genes were identified as differentially expressed when the $|\log_2$ fold change$|$ was >1.5 (Wright et al., 2017). Differences in expression levels were assessed by two-tailed Student's *t*-tests. $P < 0.05$ was considered significant.

RNA-Sequencing (RNA-Seq)

Three single colonies of each isolate (A1254, CAB009, and CAB010) were grown overnight in LB broth, diluted 1:100 in 100 ml of fresh LB medium, and harvested at the mid-log growth phase. The subsequent RNA extraction, library construction, and transcriptomic analysis were performed by staff at MAGIGENE (Guangzhou, China). RNA was extracted using TRIzol Reagent (Invitrogen) and treated with DNase. rRNA was removed using a Ribo-Zero rRNA Removal Kit (Illumina). Paired-end RNA-sequencing (RNA-Seq) libraries were constructed with the NEBNext® Ultra II™ Directional RNA Library Prep Kit (New England Biolabs, Inc., Ipswich, MA, United States) and sequenced on the Illumina HiSeq/MiSeq NextSeq platform (Illumina). Raw reads were filtered by fastp (version 0.19.7) (Chen et al., 2018). After quality control, the reads were compared with ribosomal RNA (rRNA) sequences in the Rfam database, and unmapped reads were used for subsequent analysis. Filtered reads were mapped to the A1254 genome (GenBank accession number: CP049806-CP049810) using Hisat2 (version 2.1.0) (Kim et al., 2015). The read counts were calculated by RSEM (version 1.3.1) (Li and Dewey, 2011). The output data were analyzed by edgeR (version 3.20.2) (Robinson et al., 2010) and differences in the expression profiles of CAB009 and CAB010 were assessed by the expression ratio of each gene between the mutant and A1254. Genes were considered to be differentially expressed if

[1] https://cge.cbs.dtu.dk/services/ResFinder/

TABLE 1 | Primers used in the study.

Name	Primer sequence (5′–3′)	Target gene/region	Use
499AG F	CTTTCTGCAAACGATGTACT	$bla_{OXA-499}$ upstream region	Verify detected mutations
499AG R	GAGCCTTTTTCAGCAGTT		
499-C-F	tgcggccgcaagcttgtcgacATGAAAAAATTTATACTTCCTATCTTCAGC*	$bla_{OXA-499}$ with (499P-C-F)/without (499-C-F) the upstream region	Recombinant vector construction
499P-C-F	tgcggccgcaagcttgtcgacAAGCTCCATTTAACATAATGGGCG*		
499/P-C-R	cagcaaatgggtcgcggatccTTATATAATCCCTAAATTTTCTAATG*		
826-C-F	tgcggccgcaagcttgtcgacATGACTAAAAAAGCTCTTTTCTTTGC*	$bla_{OXA-826}$ with (826P-C-F)/without (826-C-F) the upstream region	Recombinant vector construction
826P-C-F	tgcggccgcaagcttgtcgacTGACCCAACCCTACCTAA*		
826/P-C-R	cagcaaatgggtcgcggatccCTATAAAATACCGAGTTGTTCCAATCC*		
rpoB-Q-F	TACCTACAAGCGGTTTATCC	*rpoB*	RT-qPCR
rpoB-Q-R	TGTTCGTCATCAAGGTGAAT	*rpoB*	RT-qPCR
499-Q-F	AGCTACAACAACTGAGATTTTC	$bla_{OXA-499}$	RT-qPCR
499-Q-R	CTTGTGTCCCGATGTTCATA	$bla_{OXA-499}$	RT-qPCR
826-Q-F	CATAAAGCAACACCAACTGAA	$bla_{OXA-826}$	RT-qPCR
826-Q-R	AACCAATATCAGCATTACCGA	$bla_{OXA-826}$	RT-qPCR

**Lowercase letters indicate sequences for recombination, capital letters indicate primers for amplification.*

their false discovery rate (FDR) was <0.05 and the $|\log_2$ fold change$|$ was >1.5.

RESULTS

Resistance Genes and the Genetic Environment of $bla_{OXA-499}$ in *A. pittii* A1254

Based on CLSI guidelines, *A. pittii* A1254 was susceptible to imipenem (MIC, 2 μg/ml) and intermediate susceptible to meropenem (MIC, 4 μg/ml) using the broth microdilution method. However, when determined by Etest strips, A1254 was susceptible to both imipenem (MIC, 1.5 μg/ml) and meropenem (MIC, 2 μg/ml), consistent with the result reported for when A1254 was first described (Ji et al., 2014). Although there was a one-fold difference, the MIC of meropenem evaluated by the two methods was the breakpoint for susceptibility and intermediate susceptibility, respectively. Because in this study we also employed the broth microdilution method to determine the MICs for the other strains, we adopted 4 μg/ml as the meropenem MIC against A1254 and determined the strain to be intermediate susceptible to meropenem.

A1254 carries four plasmids in addition to its 4,065,905-bp-long chromosome. We identified two oxacillinase (OXA) genes in A1254: $bla_{OXA-499}$ and a variant of $bla_{OXA-500}$. $bla_{OXA-499}$ is a variant of $bla_{OXA-143}$ identified in 2017 and is reported to confer resistance to carbapenem (D'Souza et al., 2017). The $bla_{OXA-500}$ variant was submitted to National Center for Biotechnology information (NCBI) as a member of the OXA-213 family, and NCBI designated it as $bla_{OXA-826}$. The phylogenetic tree of relative OXA variants is shown in **Figure 1**. However, according to a recent study, it might be more appropriate to classify OXA-826 into the OXA-272-like family, which may be the intrinsic *A. pittii* OXA (Kamolvit et al., 2014; D'Souza et al., 2017). We also found and submitted a variant of bla_{ADC-25}, which was designated as $bla_{ADC-221}$ by NCBI. $bla_{OXA-499}$, $bla_{OXA-826}$, and $bla_{ADC-221}$ are all located on the chromosome. No other resistance genes were detected in A1254.

We compared the genetic environment of $bla_{OXA-499}$ in A1254 with that in the *A. pittii* isolate YMC2010/8/T346 in which $bla_{OXA-499}$ was first identified (GenBank accession number: CP017938). In the YMC2010/8/T346 isolate, $bla_{OXA-499}$ is located within a 4,085-bp genomic fragment insertion consisting of a putative peptidase gene, $bla_{OXA-499}$, and a TonB-dependent receptor plug domain, along with Xer C/D like recombination sites (D'Souza et al., 2017). The same fragment was identified in A1254 (100% identity).

Carbapenem-Resistant Evolved Populations and Mutations

We serially passaged four populations independently for 9 days (∼6.64 generations per day). On day 9 (∼60 generations), we found that two of the four populations (CAB001 and CAB004) had become resistant to both imipenem and meropenem. For population 1, CAB001, the imipenem MIC increased to 32 μg/ml (a four-fold increase) and that of meropenem increased to 64 μg/ml (also a four-fold increase). For population 4, CAB004, the imipenem MIC increased to 8 μg/ml (a two-fold increase) while that of meropenem increased to 32 μg/ml (a three-fold increase).

To identify the mutations responsible for the increased MICs (at least two-fold) against CAB001 and CAB004, we compared the genome of each evolved population to the genome sequence of the A1254 ancestor strain. Mutations with a frequency $>70\%$ are listed in **Supplementary Table S1**. Mutations occurring in population two (CAB002) and population three (CAB003) where the imipenem MIC showed only a one-fold increase (4 μg/ml) were excluded from further analysis. Therefore, the mutation in the promoter region of $bla_{OXA-499}$, with a frequency of 100%, was the only mutation in CAB001 remaining for further analysis. A colony from the CAB001 population harboring this mutation was isolated and designated as CAB009.

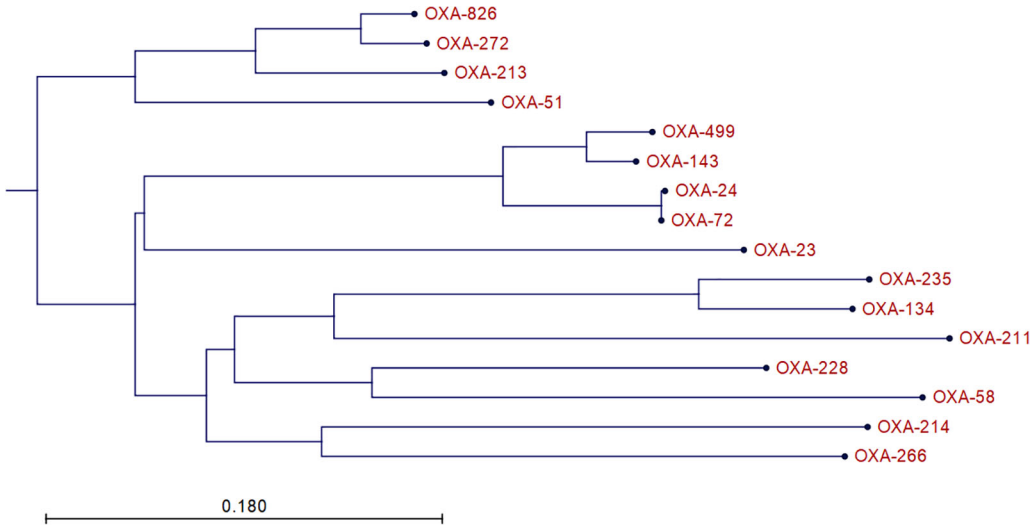

FIGURE 1 | Phylogenetic tree of relative OXA variants. The neighbor-joining tree was generated using CLC Main Workbench 8.5.1 (QIAGEN Bioinformatics).

Based on the evidence from CAB001, we suspected that the mutation in the promoter region of $bla_{OXA-499}$ might be responsible for the increased carbapenem MICs in the population. To explore whether this mutation also existed in other populations, we isolated single colonies from CAB002–CAB004 and analyzed the sequence of the $bla_{OXA-499}$ promoter region in each colony by PCR and Sanger sequencing. We identified another mutation in the promoter region of $bla_{OXA-499}$ in a CAB004-derived colony, and we designated this mutant as CAB010. No mutations were found in the promoter region of $bla_{OXA-499}$ in CAB002- and CAB003-derived colonies. Carbapenem MICs against the ancestor strain and the mutants are listed in **Table 2**.

Thus, we identified two mutations in the promoter region of $bla_{OXA-499}$ in CAB009 and CAB010 that might mediate carbapenem resistance. The promoter region of $bla_{OXA-499}$ was defined based on a previous study (Zander et al., 2014a). In the *A. pittii* CAB009 mutant from population one, we identified an A to G base substitution located one base upstream of the −10 region (position −14) (**Figure 2**), yielding a 5′-TG-3′ motif in the extended −10 element. In the *A. pittii* CAB010 mutant from population 4, we identified a G to A base substitution upstream of the −35 hexamer (position −42) within the upstream (UP) element (**Figure 2**).

Relative Expression Levels of $bla_{OXA-499}$ and $bla_{OXA-826}$ in the Mutants

We next performed RT-qPCR to determine how the mutations affected the expression levels of $bla_{OXA-499}$ and $bla_{OXA-826}$. The results revealed that the expression level of $bla_{OXA-499}$ increased significantly in CAB009, both in antibiotic-free LB broth (4.53 ± 0.19) and in LB broth supplemented with 0.75 μg/ml imipenem (4.68 ± 0.60). However, the difference between the two conditions was not significant (P = 0.6931) (**Figure 3A**). In CAB010, a more significant increase in $bla_{OXA-499}$ expression was observed under 0.75 μg/ml imipenem pressure (2.54 ± 0.15) compared with that in antibiotic-free LB broth (1.65 ± 0.25) (P = 0.006) (**Figure 3A**). The higher expression level of $bla_{OXA-499}$ in CAB009 might explain why it was more resistant to carbapenem than CAB010 (**Table 2**). Under imipenem selection pressure, there was a significant decrease in the expression level of $bla_{OXA-826}$ in CAB010 but not CAB009 (**Figure 3B**). However, based on the $|\log_2$ fold-change$|$ threshold (>1.5), only $bla_{OXA-499}$ was identified as being differentially expressed in both CAB009 and CAB010. The RT-qPCR results indicated that $bla_{OXA-499}$, but not $bla_{OXA-826}$, played an important role in the development of carbapenem resistance. **Supplementary Table S2** depicts the fold changes normalized by *rpoB* and $bla_{OXA-826}$, respectively.

The Results of Cloning and Transformation

To examine how the mutations affect carbapenem resistance, we amplified a sequence containing either $bla_{OXA-499}$ alone or $bla_{OXA-499}$ together with an upstream 114-bp segment that included the promoter region, from A1254, CAB009, and CAB010. The sequence of $bla_{OXA-826}$ with or without an upstream segment (446 bp in total, comprising a putative promoter region) was amplified from A1254. All the amplified products were cloned into the pYMAb2-Hyg^r vector. The recombinant vectors were electroporated into *A. baumannii* ATCC 17978, *A. pittii* LMG 1035, and *A. pittii* A1254 for expression analysis. The strains carrying the corresponding recombinant vectors and their MICs are listed in **Table 2**.

The results were similar among the transformed strains with different genetic backgrounds. $bla_{OXA-499}$ could not confer resistance to carbapenem without the upstream sequence. However, all the recombinant strains harboring $bla_{OXA-499}$ with its original promoter became resistant to imipenem (MIC, 16 μg/ml) and meropenem (MIC, 64–128 μg/ml). Similar MICs

TABLE 2 | Minimum inhibitory concentrations (MICs) for strains and transformants harboring recombinant vectors.

Strain and (recombinant) plasmid	MIC (μg/mL)	
	Imipenem	Meropenem
Acinetobacter pittii A1254	2	4
A. pittii CAB009	32	64
A. pittii CAB010	8	16
A. pittii A1254 + pYMAb2_Hyg^r	2	4
A. pittii A1254 + pYMAb2_Hyg^r:OXA499	2	4
A. pittii A1254 + pYMAb2_Hyg^r:OXA499_P[a]	16	64
A. pittii A1254 + pYMAb2_Hyg^r:OXA499_P009[b]	32	128
A. pittii A1254 + pYMAb2_Hyg^r:OXA499_P010[c]	16	64
A. pittii A1254 + pYMAb2_Hyg^r:OXA826	2	8
A. pittii A1254 + pYMAb2_Hyg^r:OXA826_P[d]	2	8
Acinetobacter baumannii ATCC 17978	0.125	0.25
A. baumannii ATCC 17978 + pYMAb2_Hyg^r	0.125	0.5
A. baumannii ATCC 17978 + pYMAb2_Hyg^r:OXA499	0.125	0.5
A. baumannii ATCC 17978 + pYMAb2_Hyg^r:OXA499_P	16	128
A. baumannii ATCC 17978 + pYMAb2_Hyg^r:OXA499_P009	32	128
A. baumannii ATCC 17978 + pYMAb2_Hyg^r:OXA499_P010	32	128
A. baumannii ATCC 17978 + pYMAb2_Hyg^r:OXA826	0.25	0.25
A. baumannii ATCC 17978 + pYMAb2_Hyg^r:OXA826_P	0.25	0.25
A. pittii LMG 1035	0.06	0.25
A. pittii LMG 1035 + pYMAb2_Hyg^r	0.125	0.125
A. pittii LMG 1035 + pYMAb2_Hyg^r:OXA499	0.125	0.25
A. pittii LMG 1035 + pYMAb2_Hyg^r:OXA499_P	16	64
A. pittii LMG 1035 + pYMAb2_Hyg^r:OXA499_P009	64	128
A. pittii LMG 1035 + pYMAb2_Hyg^r:OXA499_P010	16	64
A. pittii LMG 1035 + pYMAb2_Hyg^r:OXA826	0.125	0.25
A. pittii LMG 1035 + pYMAb2_Hyg^r:OXA826_P	0.125	0.25

[a]*OXA499_P indicates bla$_{OXA-499}$ with its natural promoter cloned from A1254.* [b]*OXA499_P009 indicates bla$_{OXA-499}$ with its mutated promoter cloned from CAB009.* [c]*OXA499_P010 indicates bla$_{OXA-499}$ with its mutated promoter cloned from CAB010.* [d]*OXA826_P indicates bla$_{OXA-826}$ with its natural promoter cloned from A1254.*

were observed for recombinant strains harboring *bla*$_{OXA-499}$ containing the promoter from CAB010 (P010), except for OXA-499_P010-transformed *A. baumannii* ATCC 17978, showing a one-fold higher imipenem MIC (32 μg/ml) than OXA-499_P-transformed strains (16 μg/ml). Among the *A. baumannii* and *A. pittii* strains, *bla*$_{OXA-499}$ containing the CAB009 promoter (P009) conferred the highest imipenem MICs (32–64 μg/ml, one- to two-fold change) when compared with the recombinant strains harboring the original promoter. Increased meropenem MICs were only observed for *A. pittii* A1254 and LMG 1035 (128 μg/ml, one-fold).

Transcriptomic Analysis

Differentially expressed genes between A1254 and CAB009 or CAB010 were identified based on the defined threshold. Overall, although the transcriptional patterns of CAB009 and CAB010 were different, *bla*$_{OXA-499}$ was the only differentially expressed gene shared by the two mutants.

Eighty-eight differentially expressed genes were identified in CAB009 (**Table 3**). Among them, 82 were upregulated and six downregulated. A stress-induced protein-encoding gene G8E09_11565 showed a 5.22 $\log_2$ fold change higher expression level in CAB009 than in A1254, ranking first in the expression profile. This was followed by *bla*$_{OXA-499}$, which showed a 4.70 $\log_2$ fold change higher expression level. We only identified three genes that were differentially expressed between CAB010 and A1254 (**Table 4**). The expression of *bla*$_{OXA-499}$ was 2.04 $\log_2$ fold change higher in CAB010 than in A1254. G8E09_06800 (encoding a LysR family transcriptional regulator) and G8E09_06805 (encoding a type one glutamine amidotransferase domain-containing protein) showed 1.73 and 1.62 $\log_2$ fold change higher expression levels than A1254, respectively.

DISCUSSION

Acinetobacter pittii, a member of the ACB complex, is increasingly recognized as a clinically important species following an improvement in identification methods that can better discriminate between *A. pittii* and *A. baumannii* (Yang et al., 2012). Here, we identified a carbapenem-non-resistant *A. pittii* clinical isolate, A1254, carrying *bla*$_{OXA-499}$, intrinsic *bla*$_{OXA-826}$, and *bla*$_{ADC-221}$. OXA-499 was first identified in a carbapenem-resistant *A. pittii* clinical isolate, YMC2010/8/T346, recovered from a patient in South Korea in 2010 and reported in 2017 (D'Souza et al., 2017). A1254 was also isolated in 2010. YMC2010/8/T346 is susceptible to imipenem (MIC, 2 μg/ml) but resistant to meropenem (MIC, 16 μg/ml). We compared the 4,085-bp *bla*$_{OXA-499}$ genetic environment between A1254 and YMC2010/8/T346 and found them to be identical. However, A1254 is susceptible to imipenem and intermediate-susceptible to meropenem based on the microbroth dilution method and even susceptible to meropenem when the Etest is used. The different MICs among *A. pittii* strains sharing an identical *bla*$_{OXA-499}$ genetic environment indicate that *bla*$_{OXA-499}$ expression might vary according to host and result in phenotypic variation, which might be due to the presence of additional related mechanisms that influence the phenotype.

However, when cloned into a vector, *bla*$_{OXA-499}$ containing either the initial or mutated promoter could confer carbapenem resistance in host strains. A similar result was reported by Zander et al. (2014a), who found that, although OXA-255 did not confer carbapenem resistance to the *A. pittii* clinical isolate AF726, OXA-255-transformed *A. baumannii* ATCC 17978 and *A. pittii* SH024 were resistant to carbapenem. Similar to OXA-499, OXA-255 is also a member of the OXA-143 family and the 2,239-bp genomic fragment containing *bla*$_{OXA-255}$ (GenBank accession number, KC479325) in *A. pittii* AF726 is similar to that of *bla*$_{OXA-499}$ in A1254 and YMC2010/8/T346 (99% identities). Considering that the genes were cloned into a shuttle vector and transformed into different *Acinetobacter* spp. strains by electroporation, we suspect that, apart from the genetic background of transformed strains, the introduction of the vector might also have influenced the expression level by providing

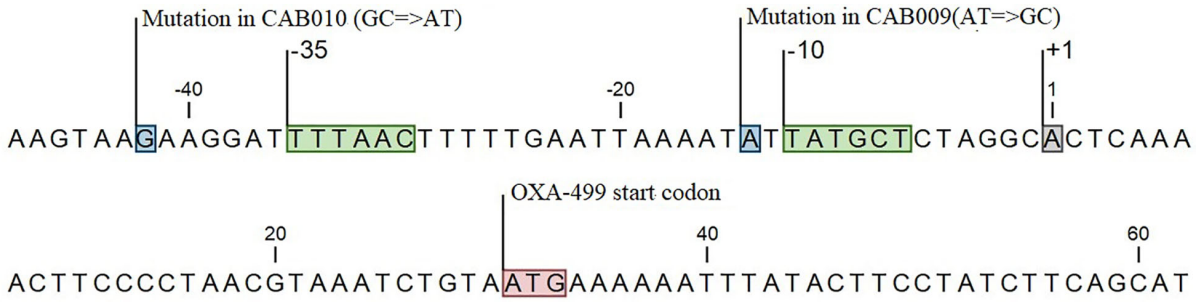

FIGURE 2 | Locations of mutations in the carbapenem-resistant mutants CAB009 and CAB010 (boxed in blue). The start codon (boxed in red), the transcription initiation site (boxed in gray), and the −10 and −35 regions (boxed in green) are also indicated.

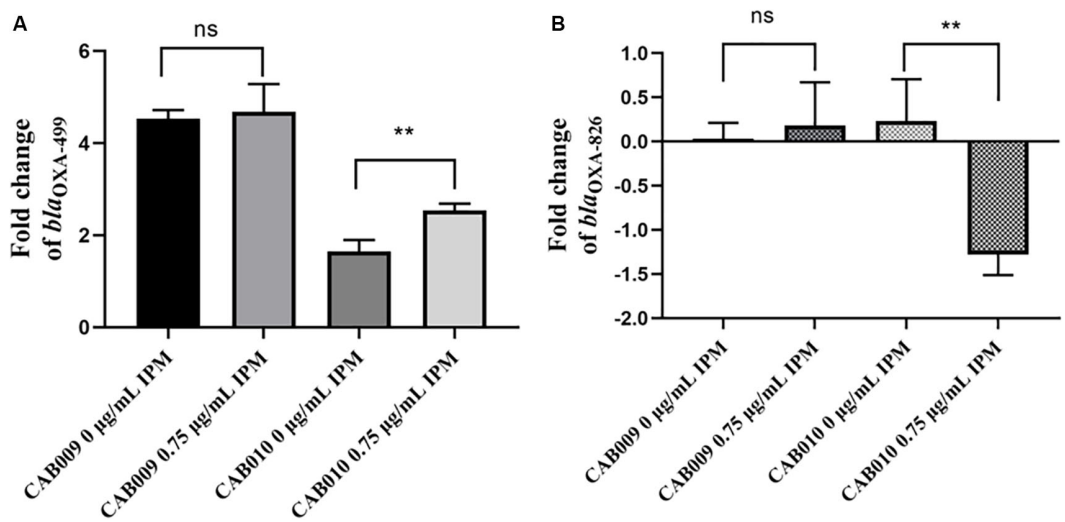

FIGURE 3 | Log_2 fold changes of **(A)** $bla_{OXA-499}$ and **(B)** $bla_{OXA-826}$ expression levels in mutants undergoing or not imipenem selection pressure. RT-qPCR analysis was performed with three biological and technical replicates per experiment. The $2^{-\Delta\Delta Ct}$ method was applied to calculate the fold change using *rpoB* as the reference gene and *Acinetobacter pittii* A1254 as the reference strain. The expression level was calculated as the log_2 fold change. The bars represent means ± SD from triplicate biological repeats. The *P*-values (each mutant undergoing or not imipenem selection pressure) were determined by two-tailed Student's *t*-tests. $^{**}P < 0.008$; ns, not significant. IPM, imipenem.

multiple copies of the gene (dose effect), whereas in A1254, $bla_{OXA-499}$ was located on the chromosome and as a single copy.

RT-qPCR and RNA-Seq results (log_2 fold changes) for $bla_{OXA-499}$ showed the same trend, although RNA-Seq data showed higher values. There was a significant difference in the number of differently expressed genes between CAB009 and CAB010 when compared with A1254. As CAB009 and CAB010 were isolated from two independently evolved populations, both mutants might harbor additional mutations besides the base substitutions in the promoter region of $bla_{OXA-499}$. The different genotypes of CAB009 and CAB010 might explain the differences in the transcriptional profiles.

Subinhibitory concentrations of antibiotics can lead to gene expression changes and promote resistance (Bernier and Surette, 2013; Chen et al., 2017). In this study, we demonstrated that a carbapenem-non-resistant strain, *A. pittii* A1254, which tends to be neglected in the clinical microbiology laboratory, can rapidly develop resistance to carbapenems when cultured in broth containing a low concentration of imipenem. Here, we evaluated the possible mechanisms underlying the increased expression level of $bla_{OXA-499}$ by analyzing the sequence of the promoter region. The mutant CAB009 isolate harbored an A to G transition at position −14, causing a base combination transformation from 5′-TA-3′ to 5′-TG-3′ one base upstream of the −10 region. The importance of the 5′-TG-3′ motif in the extended -10 element has been demonstrated in *E. coli* (Prost and Cozzone, 1999; Burr et al., 2000; Mitchell et al., 2003). It is well known that the −10 and −35 regions are where RNA polymerase (RNAP) contacts, resulting in promoter recognition and initiation of transcription. There is an additional promoter element, the "extended −10 element," located one base upstream of the −10 region, with the major 5′-TG-3′ determinant positioned at −15/−14 with respect to the transcription start site (Mitchell et al., 2003). The 5′-TG-3′ motif is an important determinant of promoter activity (Voskuil and Chambliss, 2002; Prost and Cozzone, 1999; Burr et al., 2000). In our study, we suspect that it was the

TABLE 3 | Differentially expressed genes in CAB009 compared with A1254.

Gene_ID	Description	log_2 FC[a]	*P*-value	FDR
G8E09_11565	Stress-induced protein	5.22	0.0000	0.0004
G8E09_16100	OXA-143 family carbapenem-hydrolyzing class D beta-lactamase OXA-499	4.70	0.0000	0.0000
G8E09_11570	Hypothetical protein	3.78	0.0000	0.0000
G8E09_11590	Damage-inducible protein CinA	3.59	0.0000	0.0001
G8E09_08710	Muconolactone Delta-isomerase	3.37	0.0000	0.0000
G8E09_09185	Hypothetical protein	3.27	0.0002	0.0095
G8E09_12900	Benzoate 1,2-dioxygenase small subunit	3.21	0.0000	0.0000
G8E09_12895	Benzoate 1,2-dioxygenase large subunit	3.08	0.0000	0.0000
G8E09_10220	Hypothetical protein	3.05	0.0000	0.0000
G8E09_07105	Hypothetical protein	3.04	0.0001	0.0043
G8E09_12625	DUF4142 domain-containing protein	3.00	0.0000	0.0000
G8E09_09755	Hypothetical protein	2.94	0.0000	0.0001
G8E09_11585	Iron-containing redox enzyme family protein	2.92	0.0001	0.0047
G8E09_03990	BapA prefix-like domain-containing protein	2.85	0.0000	0.0000
G8E09_14955	Trehalose-phosphatase	2.82	0.0000	0.0000
G8E09_08715	Muconate cycloisomerase	2.69	0.0000	0.0000
G8E09_11610	Hypothetical protein	2.68	0.0000	0.0000
G8E09_09795	Hypothetical protein	2.66	0.0000	0.0003
G8E09_08150	SOS response-associated peptidase	2.66	0.0000	0.0000
G8E09_12315	Hypothetical protein	2.63	0.0000	0.0011
G8E09_08605	MFS transporter	2.60	0.0000	0.0016
G8E09_07245	DNA breaking-rejoining protein	2.58	0.0000	0.0004
G8E09_12905	Ring-hydroxylating dioxygenase ferredoxin reductase family protein	2.49	0.0000	0.0000
G8E09_10205	Hypothetical protein	2.45	0.0022	0.0488
G8E09_08615	Amidase	2.45	0.0010	0.0278
G8E09_08625	IacB protein	2.40	0.0001	0.0048
G8E09_14200	Hypothetical protein	2.39	0.0001	0.0044
G8E09_08105	Hypothetical protein	2.39	0.0001	0.0061
G8E09_08620	Acyl-CoA dehydrogenase	2.39	0.0004	0.0138
G8E09_08600	OprD family porin	2.37	0.0000	0.0000
G8E09_11790	Acyl-CoA dehydrogenase	2.35	0.0000	0.0013
G8E09_14960	Trehalose-6-phosphate synthase	2.33	0.0012	0.0314
G8E09_12910	1,6-dihydroxycyclohexa-2,4-diene-1-carboxylatedehydrogenase	2.25	0.0000	0.0009
G8E09_10090	2-oxo acid dehydrogenase subunit E2	2.24	0.0000	0.0012
G8E09_07160	Type 1 glutamine amidotransferase	2.23	0.0001	0.0076
G8E09_14205	Non-heme iron oxygenase ferredoxin subunit	2.22	0.0004	0.0151
G8E09_08630	Nuclear transport factor 2 family protein	2.22	0.0002	0.0092
G8E09_09095	Type 1 glutamine amidotransferase domain-containing protein	2.19	0.0000	0.0003
G8E09_08650	Oxidoreductase	2.15	0.0000	0.0037
G8E09_12920	Aromatic acid/H + symport family MFS transporter	2.15	0.0000	0.0000
G8E09_08635	Aromatic ring-hydroxylating dioxygenase subunit alpha	2.12	0.0001	0.0073
G8E09_10085	Dihydrolipoyl dehydrogenase	2.12	0.0000	0.0018
G8E09_11775	Enoyl-CoA hydratase	2.10	0.0006	0.0196
G8E09_08705	Catechol 1,2-dioxygenase	2.10	0.0000	0.0008
G8E09_00265	DUF1328 domain-containing protein	2.08	0.0004	0.0151
G8E09_09085	NAD(P)H-binding protein	2.06	0.0000	0.0000
G8E09_08640	Hypothetical protein	2.02	0.0019	0.0437
G8E09_10100	Thiamine pyrophosphate-dependent dehydrogenaseE1 component subunit alpha	2.02	0.0001	0.0064
G8E09_10095	Alpha-ketoacid dehydrogenase subunit beta	2.02	0.0001	0.0065
G8E09_14195	Aromatic ring-hydroxylating dioxygenase subunit alpha	1.97	0.0007	0.0205
G8E09_08645	SDR family oxidoreductase	1.94	0.0002	0.0089
G8E09_03110	Peroxiredoxin	1.93	0.0000	0.0003
G8E09_07120	Molecular chaperone	1.91	0.0000	0.0014

(Continued)

TABLE 3 | Continued

Gene_ID	Description	log_2 FC[a]	*P*-value	FDR
G8E09_07115	Spore coat protein U domain-containing protein	1.90	0.0006	0.0189
G8E09_07200	Minor capsid protein	1.88	0.0016	0.0387
G8E09_07955	Hypothetical protein	1.85	0.0000	0.0004
G8E09_17600	Serine hydrolase family protein	1.83	0.0012	0.0314
G8E09_11605	Hypothetical protein	1.81	0.0005	0.0182
G8E09_12810	Hypothetical protein	1.79	0.0006	0.0198
G8E09_04225	Transglycosylase SLT domain-containing protein	1.79	0.0008	0.0229
G8E09_09750	Hypothetical protein	1.76	0.0000	0.0024
G8E09_14055	Hypothetical protein	1.76	0.0002	0.0089
G8E09_06975	Hypothetical protein	1.76	0.0000	0.0014
G8E09_11740	Enoyl-CoA hydratase	1.76	0.0003	0.0124
G8E09_12805	LysE family transporter	1.75	0.0000	0.0004
G8E09_08700	3-oxoacid CoA-transferase subunit A	1.74	0.0001	0.0044
G8E09_11745	SDR family oxidoreductase	1.74	0.0012	0.0318
G8E09_12925	OprD family porin	1.73	0.0001	0.0064
G8E09_10340	Hypothetical protein	1.72	0.0001	0.0067
G8E09_19180	GlsB/YeaQ/YmgE family stress response membrane protein	1.71	0.0020	0.0463
G8E09_01795	Hemerythrin domain-containing protein	1.71	0.0008	0.0244
G8E09_12835	Heavy-metal-associated domain-containing protein	-1.70	0.0002	0.0091
G8E09_07185	Hypothetical protein	1.67	0.0008	0.0229
G8E09_18175	Flavodoxin family protein	-1.65	0.0001	0.0044
G8E09_12485	Hypothetical protein	1.64	0.0000	0.0033
G8E09_08655	Flavin reductase family protein	1.63	0.0000	0.0017
G8E09_09715	Fimbria/pilus periplasmic chaperone	-1.61	0.0000	0.0012
G8E09_12830	Copper-translocating P-type ATPase	-1.59	0.0001	0.0076
G8E09_18170	DUF2938 domain-containing protein	-1.56	0.0001	0.0047
G8E09_10080	Acetoin reductase	1.56	0.0003	0.0119
G8E09_08695	CoA transferase subunit B	1.56	0.0001	0.0056
G8E09_13275	3-(3-hydroxy-phenyl)propionate transporter MhpT	1.56	0.0003	0.0119
G8E09_06835	3-hydroxyacyl-CoA dehydrogenase	1.56	0.0002	0.0083
G8E09_07815	Siderophore biosynthesis protein	-1.53	0.0005	0.0160
G8E09_09965	CoA transferase subunit A	1.52	0.0013	0.0324
G8E09_11795	MFS transporter	1.51	0.0000	0.0027
G8E09_06685	Transglutaminase family protein	1.51	0.0012	0.0307
G8E09_17135	DMT family transporter	1.50	0.0001	0.0048

[a]*log_2 FC, log_2 fold change; FDR, false discovery rate.*

TABLE 4 | Differentially expressed genes in CAB010 compared with A1254.

Gene_ID	Description	log2FC[a]	*P*-value	FDR
G8E09_16100	OXA-143 family carbapenem-hydrolyzing class D beta-lactamase OXA-499	2.04	0.0000	0.0014
G8E09_06800	LysR family transcriptional regulator	1.73	0.0000	0.0001
G8E09_06805	type 1 glutamine amidotransferase domain-containing protein	1.62	0.0000	0.0014

[a]*log_2FC, log_2 fold change; FDR, false discovery rate.*

presence of the 5′-TG-3′ motif in the extended −10 element of the $bla_{OXA-499}$ promoter of the CAB009 mutant that led to the increased expression of $bla_{OXA-499}$, resulting in resistance to carbapenem. Another mutant, CAB010, exhibited a G to A transition at position −42, upstream of the −35 region. The UP element, located upstream of the −35 element (from approximately −40 to −60), can be recognized by RNAP and facilitates its initial binding as well as the subsequent steps in transcription initiation (Estrem et al., 1999; Presnell et al., 2019). A consensus UP element sequence consists almost exclusively of A and T residues and leads to increased promoter activity (Estrem et al., 1998). For the wild-type strain, *A. pittii* A1254, the proximal site of the UP element, contains a near-perfect A tract from position −39 to −44, interrupted only by a G at position −42. Following the transition from G to A at position −42, the proximal site in the CAB010 mutant became a perfect A tract.

In this study, we employed whole-genome sequencing (WGS) to identify putative resistance genes in the ancestor strain and mutations in the populations obtained from the experimental evolution. For clinical use, comprehensive databases of known resistant genes and related mutations are necessary for the successful prediction of antibiotic-resistance phenotypes. It is known that the accumulation of one or more single-nucleotide variants (SNVs) in genes encoding antibiotic targets or transposon insertions can lead to antibiotic resistance (Schurch and van Schaik, 2017). Published carbapenem resistance-related mechanisms in *A. pittii* include plasmid-borne bla_{OXA-23}, bla_{OXA-72}, or bla_{OXA-58}; AbaR4-located bla_{OXA-23} on the chromosome; plasmid-borne class I integron containing bla_{IMP-1} (Montealegre et al., 2012; Silva et al., 2018; Chen et al., 2019); and a composite transposon containing bla_{NDM-1} (Yang et al., 2012). In addition, it has been proposed that *A. pittii* may be a resistance reservoir for the dissemination of NDM-1 (Bogaerts et al., 2013; Huang et al., 2015). Overexpression of bla_{OXA} is typically mediated through promoters provided by insertion sequence (IS) elements, although OXA-40 and OXA-143 appear to be exceptions to this (Higgins et al., 2009). The association with IS elements and frequent presence in plasmids highlight the potential of bla_{OXA} genes to spread within *Acinetobacter* spp. via transposition events and horizontal gene transfer (Zander et al., 2014b). For OXA-143-like and OXA-40-like, $bla_{OXA-499}$ is flanked by XerC/XerD-like recombinase sites in both *A. pittii* A1254 and YMC2010/8/T346, suggesting that this gene was acquired through recombination. This recombination system is exploited by mobile DNA elements to integrate into the host genome (Midonet and Barre, 2014). A similar genetic context was also reported for other *A. pittii* isolates, in which the resistance gene was flanked by XerC/XerD-like recombinase sites (Cayo et al., 2014; Ruan et al., 2017; Brasiliense et al., 2019). This suggests that *A. pittii* may be an important source of resistance genes and contribute to their dissemination among species.

Here, we report for the first time that mutations in the promoter region of $bla_{OXA-499}$ can contribute to the development of carbapenem resistance, complementing other known carbapenem resistance mechanisms in *A. pittii*. Enhanced resistance to β-lactam resulting from promoter mutations has also been reported in *Staphylococcus aureus* (Basuino et al., 2018). Additionally, loss of *pncA* expression due to promoter mutation conferred pyrazinamide resistance in multidrug-resistant tuberculosis isolates (Pang et al., 2017). This indicated that predicting resistance phenotypes based on the presence of resistance genes may be inaccurate in some circumstances; mutations on non-coding regions such as the promoter region should also be taken into consideration. One limitation of our study was that we failed to introduce a mutation in the wild-type A1254 strain due to technical restrictions. Moreover, we did not elucidate the specific mechanisms underlying the different carbapenem MICs between *A. pittii* strains harboring $bla_{OXA-499}$.

In conclusion, to the best of our knowledge, our study represents the first investigation on the development of carbapenem resistance in an OXA-499-harboring, but carbapenem-non-resistant, *A. pittii* isolate. The genetic environment of $bla_{OXA-499}$ was identical to that of a previously reported carbapenem-resistant *A. pittii* strain, indicating the existence of phenotypic variation in OXA-499-producing strains. We demonstrated that carbapenem-non-resistant *A. pittii* A1254 could become resistant to carbapenem under imipenem selective pressure and that a single-base substitution in the promoter region of $bla_{OXA-499}$ contributed to the carbapenem-resistance phenotype. This highlights the need to monitor the potential development of carbapenem resistance when treating infections caused by non-resistant strains. The potential risk of resistance development requires that more attention be paid to the type, courses, and doses of antibiotics prescribed.

DATA AVAILABILITY STATEMENT

The GenBank accession number of $bla_{OXA-826}$ is MK810442 (https://www.ncbi.nlm.nih.gov/nuccore/MK810442). The GenBank accession number of $bla_{ADC-221}$ is MN654470 (https://www.ncbi.nlm.nih.gov/nuccore/MN654470.1). The GenBank accession number of *A. pittii* A1254 is CP049806-CP049810 (BioProject: PRJNA610163). The SRA accession numbers for populations CAB001–CAB004 are SRR11306746, SRR11306745, SRR11306744, and SRR11306743, respectively (BioProject: PRJNA610163). The SRA accession numbers for raw reads of RNA-Seq are SRR11648396–SRR11648404 (BioProject: PRJNA610163).

AUTHOR CONTRIBUTIONS

YC, YY, and XHu designed the study. LZ, YF, XHa, and QX performed the experiments. XH, SW, BY, and LL analyzed the bioinformatics data. LZ and XHa wrote the manuscript.

FUNDING

This work was supported by the National Natural Science Foundation of Zhejiang Province (grant number LQ17H190003) and the National Natural Science Foundation of China (grant numbers 81702041 and 31970128).

ACKNOWLEDGMENTS

We thank Mrs. Haiping Wang (Zhejiang University) and Mrs. Ping Zhang (Zhejiang University) for kindly experiment assisting in this study.

SUPPLEMENTARY MATERIAL

The Supplementary Material for this article can be found online at: https://www.frontiersin.org/articles/10.3389/fmicb.2020.01134/full#supplementary-material

REFERENCES

Al Atrouni, A., Joly-Guillou, M. L., Hamze, M., and Kempf, M. (2016). Reservoirs of non-baumannii *Acinetobacter* species. *Front. Microbiol.* 7:49. doi: 10.3389/fmicb.2016.00049

Bankevich, A., Nurk, S., Antipov, D., Gurevich, A. A., Dvorkin, M., Kulikov, A. S., et al. (2012). SPAdes: a new genome assembly algorithm and its applications to single-cell sequencing. *J. Comput. Biol.* 19, 455–477. doi: 10.1089/cmb.2012.0021

Basuino, L., Jousselin, A., Alexander, J. A. N., Strynadka, N. C. J., Pinho, M. G., Chambers, H. F., et al. (2018). PBP4 activity and its overexpression are necessary for PBP4-mediated high-level beta-lactam resistance. *J. Antimicrob. Chemother.* 73, 1177–1180. doi: 10.1093/jac/dkx531

Bernier, S. P., and Surette, M. G. (2013). Concentration-dependent activity of antibiotics in natural environments. *Front. Microbiol.* 4:20. doi: 10.3389/fmicb.2013.00020

Bogaerts, P., Huang, T. D., Rezende de Castro, R., Bouchahrouf, W., and Glupczynski, Y. (2013). Could Acinetobacter pittii act as an NDM-1 reservoir for *Enterobacteriaceae*? *J. Antimicrob. Chemother.* 68, 2414–2415. doi: 10.1093/jac/dkt201

Brasiliense, D. M., Lima, K. V. B., Perez-Chaparro, P. J., Mamizuka, E. M., de Oliveira Souza, C., Dutra, L. M. G., et al. (2019). Emergence of carbapenem-resistant *Acinetobacter pittii* carrying the blaOXA-72 gene in the Amazon region. *Brazil. Diagn. Microbiol. Infect. Dis.* 93, 82–84. doi: 10.1016/j.diagmicrobio.2018.07.017

Burr, T., Mitchell, J., Kolb, A., Minchin, S., and Busby, S. (2000). DNA sequence elements located immediately upstream of the -10 hexamer in *Escherichia coli* promoters: a systematic study. *Nucleic Acids Res.* 28, 1864–1870. doi: 10.1093/nar/28.9.1864

Cayo, R., Merino, M., Ruiz Del Castillo, B., Cano, M. E., Calvo, J., Bou, G., et al. (2014). OXA-207, a novel OXA-24 variant with reduced catalytic efficiency against carbapenems in *Acinetobacter pittii* from Spain. *Antimicrob. Agents Chemother.* 58, 4944–4948. doi: 10.1128/AAC.02633-13

Chen, F. J., Huang, W. C., Liao, Y. C., Wang, H. Y., Lai, J. F., Kuo, S. C., et al. (2019). Molecular epidemiology of emerging carbapenem resistance in acinetobacter nosocomialis and acinetobacter pittii in Taiwan, 2010 to 2014. *Antimicrob. Agents Chemother.* 63:e02007-18. doi: 10.1128/AAC.02007-18

Chen, S., Zhou, Y., Chen, Y., and Gu, J. (2018). fastp: an ultra-fast all-in-one FASTQ preprocessor. *Bioinformatics* 34, i884–i890. doi: 10.1093/bioinformatics/bty560

Chen, X., Meng, X., Gao, Q., Zhang, G., Gu, H., and Guo, X. (2017). Meropenem selection induced overproduction of the intrinsic carbapenemase as well as phenotype divergence in *Acinetobacter baumannii*. *Int. J. Antimicrob. Agents* 50, 419–426. doi: 10.1016/j.ijantimicag.2017.04.015

CLSI (2018). *Performance Standards for Antimicrobial Susceptibility Testing; 28th Informational Supplement. CLSI Document M100*. Wayne, PA: CLSI.

Deatherage, D. E., and Barrick, J. E. (2014). Identification of mutations in laboratory-evolved microbes from next-generation sequencing data using breseq. *Methods Mol. Biol.* 1151, 165–188. doi: 10.1007/978-1-4939-0554-6_12

Deglmann, R. C., Kobs, V. C., Oliveira, D., Burgardt, P., Franca, P. H. C., and Pillonetto, M. (2019). Earliest identification of New Delhi metallo-beta-lactamase 1 (NDM-1) in *Acinetobacter pittii* in Brazil. *Rev. Soc. Bras. Med. Trop.* 52:e20180348. doi: 10.1590/0037-8682-0348-2018

D'Souza, R., Pinto, N. A., Higgins, P. G., Hwang, I., Yong, D., Choi, J., et al. (2017). First report of the carbapenemase gene blaOXA-499 in *Acinetobacter pittii*. *Antimicrob. Agents Chemother.* 61:e02676-16. doi: 10.1128/AAC.02676-16

Estrem, S. T., Gaal, T., Ross, W., and Gourse, R. L. (1998). Identification of an UP element consensus sequence for bacterial promoters. *Proc. Natl. Acad. Sci. U.S.A.* 95, 9761–9766. doi: 10.1073/pnas.95.17.9761

Estrem, S. T., Ross, W., Gaal, T., Chen, Z. W., Niu, W., Ebright, R. H., et al. (1999). Bacterial promoter architecture: subsite structure of UP elements and interactions with the carboxy-terminal domain of the RNA polymerase alpha subunit. *Genes Dev.* 13, 2134–2147. doi: 10.1101/gad.13.16.2134

Hammerum, A. M., Hansen, F., and Littauer, P. (2015). Use of whole-genome sequencing for characterisation of a ST119 NDM-1-producing *Acinetobacter pittii* from a patient in Denmark with no history of recent travel. *Int. J. Antimicrob. Agents* 46, 351–352. doi: 10.1016/j.ijantimicag.2015.05.005

Higgins, P. G., Poirel, L., Lehmann, M., Nordmann, P., and Seifert, H. (2009). OXA-143, a novel carbapenem-hydrolyzing class D beta-lactamase in *Acinetobacter baumannii*. *Antimicrob. Agents Chemother.* 53, 5035–5038. doi: 10.1128/AAC.00856-09

Hua, X., Zhou, Z., Yang, Q., Shi, Q., Xu, Q., Wang, J., et al. (2017). Evolution of *Acinetobacter baumannii in vivo*: international clone II, more resistance to ceftazidime, mutation in ptk. *Front. Microbiol.* 8:1256. doi: 10.3389/fmicb.2017.01256

Huang, T. W., Lauderdale, T. L., Liao, T. L., Hsu, M. C., Chang, F. Y., Chang, S. C., et al. (2015). Effective transfer of a 47 kb NDM-1-positive plasmid among *Acinetobacter* species. *J. Antimicrob. Chemother.* 70, 2734–2738. doi: 10.1093/jac/dkv191

Iovleva, A., Mettus, R. T., McElheny, C. L., Griffith, M. P., Mustapha, M. M., Pasculle, A. W., et al. (2019). High-level carbapenem resistance in OXA-232-producing raoultella ornithinolytica triggered by ertapenem therapy. *Antimicrob. Agents Chemother.* 64:e01335-19. doi: 10.1128/AAC.01335-19

Ji, S., Chen, Y., Ruan, Z., Fu, Y., Ji, J., Fu, Y., et al. (2014). Prevalence of carbapenem-hydrolyzing class D beta-lactamase genes in *Acinetobacter* spp. isolates in China. *Eur. J. Clin. Microbiol. Infect. Dis.* 33, 989–997. doi: 10.1007/s10096-013-2037-z

Kamolvit, W., Higgins, P. G., Paterson, D. L., and Seifert, H. (2014). Multiplex PCR to detect the genes encoding naturally occurring oxacillinases in *Acinetobacter* spp. *J. Antimicrob. Chemother.* 69, 959–963. doi: 10.1093/jac/dkt480

Kim, D., Langmead, B., and Salzberg, S. L. (2015). HISAT: a fast spliced aligner with low memory requirements. *Nat. Methods* 12, 357–360. doi: 10.1038/nmeth.3317

Li, B., and Dewey, C. N. (2011). RSEM: accurate transcript quantification from RNA-Seq data with or without a reference genome. *BMC Bioinformatics* 12:323. doi: 10.1186/1471-2105-12-323

Livak, K. J., and Schmittgen, T. D. (2001). Analysis of relative gene expression data using real-time quantitative PCR and the 2(-Delta Delta C(T)) Method. *Methods* 25, 402–408. doi: 10.1006/meth.2001.1262

Midonet, C., and Barre, F. X. (2014). Xer site-specific recombination: promoting vertical and horizontal transmission of genetic information. *Microbiol. Spectr.* 2, 163–182. doi: 10.1128/microbiolspec.MDNA3-0056-2014

Mitchell, J. E., Zheng, D., Busby, S. J., and Minchin, S. D. (2003). Identification and analysis of 'extended -10' promoters in *Escherichia coli*. *Nucleic Acids Res.* 31, 4689–4695. doi: 10.1093/nar/gkg694

Montealegre, M. C., Maya, J. J., Correa, A., Espinal, P., Mojica, M. F., Ruiz, S. J., et al. (2012). First identification of OXA-72 carbapenemase from *Acinetobacter pittii* in Colombia. *Antimicrob. Agents Chemother.* 56, 3996–3998. doi: 10.1128/aac.05628-11

Nicoloff, H., Hjort, K., Levin, B. R., and Andersson, D. I. (2019). The high prevalence of antibiotic heteroresistance in pathogenic bacteria is mainly caused by gene amplification. *Nat. Microbiol.* 4, 504–514. doi: 10.1038/s41564-018-0342-0

Pailhories, H., Hadjadj, L., Mahieu, R., Crochette, N., Rolain, J. M., and Kempf, M. (2017). Fortuitous diagnosis of NDM-1-producing *Acinetobacter pittii* carriage in a patient from France with no recent history of travel. *J. Antimicrob. Chemother.* 72, 942–944. doi: 10.1093/jac/dkw505

Pailhories, H., Tiry, C., Eveillard, M., and Kempf, M. (2018). *Acinetobacter pittii* isolated more frequently than *Acinetobacter baumannii* in blood cultures: the experience of a French hospital. *J. Hosp. Infect.* 99, 360–363. doi: 10.1016/j.jhin.2018.03.019

Pang, Y., Zhu, D., Zheng, H., Shen, J., Hu, Y., Liu, J., et al. (2017). Prevalence and molecular characterization of pyrazinamide resistance among multidrug-resistant Mycobacterium tuberculosis isolates from Southern China. *BMC Infect. Dis.* 17:711. doi: 10.1186/s12879-017-2761-6

Presnell, K. V., Flexer-Harrison, M., and Alper, H. S. (2019). Design and synthesis of synthetic UP elements for modulation of gene expression in *Escherichia coli*. *Synth. Syst. Biotechnol.* 4, 99–106. doi: 10.1016/j.synbio.2019.04.002

Prost, J. F., and Cozzone, A. J. (1999). Detection of an extended-10 element in the promoter region of the pckA gene encoding phosphoenolpyruvate carboxykinase in *Escherichia coli*. *Biochimie* 81, 197–200. doi: 10.1016/s0300-9084(99)80052-2

Robinson, M. D., McCarthy, D. J., and Smyth, G. K. (2010). edgeR: a Bioconductor package for differential expression analysis of digital gene expression data. *Bioinformatics* 26, 139–140. doi: 10.1093/bioinformatics/btp616

Ruan, Z., Chen, Y., and Wang, J. (2017). Glimpse into the genome sequence of a multidrug-resistant *Acinetobacter pittii* ST950 clinical isolate carrying the

blaOXA-72 and blaOXA-533 genes in China. *Mem. Inst. Oswaldo Cruz.* 112, 723–727. doi: 10.1590/0074-02760170019

Schleicher, X., Higgins, P. G., Wisplinghoff, H., Korber-Irrgang, B., Kresken, M., and Seifert, H. (2013). Molecular epidemiology of *Acinetobacter baumannii* and *Acinetobacter nosocomialis* in Germany over a 5-year period (2005–2009). *Clin. Microbiol. Infect.* 19, 737–742. doi: 10.1111/1469-0691.12026

Schurch, A. C., and van Schaik, W. (2017). Challenges and opportunities for whole-genome sequencing-based surveillance of antibiotic resistance. *Ann. N. Y. Acad. Sci.* 1388, 108–120. doi: 10.1111/nyas.13310

Seemann, T. (2014). Prokka: rapid prokaryotic genome annotation. *Bioinformatics* 30, 2068–2069. doi: 10.1093/bioinformatics/btu153

Silva, L., Mourao, J., Grosso, F., and Peixe, L. (2018). Uncommon carbapenemase-encoding plasmids in the clinically emergent *Acinetobacter pittii*. *J. Antimicrob. Chemother.* 73, 52–56. doi: 10.1093/jac/dkx364

Singkham-In, U., and Chatsuwan, T. (2018). Mechanisms of carbapenem resistance in *Acinetobacter pittii* and *Acinetobacter nosocomialis* isolates from Thailand. *J. Med. Microbiol.* 67, 1667–1672. doi: 10.1099/jmm.0.000845

Tueffers, L., Barbosa, C., Bobis, I., Schubert, S., Hoppner, M., Ruhlemann, M., et al. (2019). *Pseudomonas aeruginosa* populations in the cystic fibrosis lung lose susceptibility to newly applied beta-lactams within 3 days. *J. Antimicrob. Chemother.* 74, 2916–2925. doi: 10.1093/jac/dkz297

Voskuil, M. I., and Chambliss, G. H. (2002). The TRTGn motif stabilizes the transcription initiation open complex. *J. Mol. Biol.* 322, 521–532. doi: 10.1016/s0022-2836(02)00802-1

Weber, B. S., Harding, C. M., and Feldman, M. F. (2015). Pathogenic acinetobacter: from the cell surface to infinity and beyond. *J. Bacteriol.* 198, 880–887. doi: 10.1128/JB.00906-15

Wick, R. R., Judd, L. M., Gorrie, C. L., and Holt, K. E. (2017). Unicycler: resolving bacterial genome assemblies from short and long sequencing reads. *PLoS Comput. Biol.* 13:e1005595. doi: 10.1371/journal.pcbi.1005595

Wright, M. S., Jacobs, M. R., Bonomo, R. A., and Adams, M. D. (2017). Transcriptome remodeling of *Acinetobacter baumannii* during infection and treatment. *mBio* 8:e02193-16. doi: 10.1128/mBio.02193-16

Yang, J., Chen, Y., Jia, X., Luo, Y., Song, Q., Zhao, W., et al. (2012). Dissemination and characterization of NDM-1-producing *Acinetobacter pittii* in an intensive care unit in China. *Clin. Microbiol. Infect.* 18, E506–E513. doi: 10.1111/1469-0691.12035

Zander, E., Bonnin, R. A., Seifert, H., and Higgins, P. G. (2014a). Characterization of blaOXA-143 variants in *Acinetobacter baumannii* and *Acinetobacter pittii*. *Antimicrob. Agents Chemother.* 58, 2704–2708. doi: 10.1128/aac.02618-13

Zander, E., Fernandez-Gonzalez, A., Schleicher, X., Dammhayn, C., Kamolvit, W., Seifert, H., et al. (2014b). Worldwide dissemination of acquired carbapenem-hydrolysing class D beta-lactamases in *Acinetobacter* spp. *other than Acinetobacter baumannii*. *Int. J. Antimicrob. Agents* 43, 375–377. doi: 10.1016/j.ijantimicag.2014.01.012

Zankari, E., Hasman, H., Cosentino, S., Vestergaard, M., Rasmussen, S., Lund, O., et al. (2012). Identification of acquired antimicrobial resistance genes. *J. Antimicrob. Chemother.* 67, 2640–2644. doi: 10.1093/jac/dks261

Conflict of Interest: The authors declare that the research was conducted in the absence of any commercial or financial relationships that could be construed as a potential conflict of interest.

frontiers in Microbiology

ORIGINAL RESEARCH
published: 17 June 2020
doi: 10.3389/fmicb.2020.01176

Comparative Genomics of *Acinetobacter baumannii* Clinical Strains From Brazil Reveals Polyclonal Dissemination and Selective Exchange of Mobile Genetic Elements Associated With Resistance Genes

*Nilma C. Leal[1], Túlio L. Campos[1], Antonio M. Rezende[1], Cássia Docena[1], Carina L. Mendes-Marques[1], Felipe L. de Sá Cavalcanti[1,2], Gabriel L. Wallau[1], Igor V. Rocha[1], Carmelita L. B. Cavalcanti[3], Dyana L. Veras[1], Lilian R. Alves[4], Mariana Andrade-Figueiredo[1], Maria P. Silva de Barros[1], Alzira M. Paiva de Almeida[1], Marcia M. Camargo de Morais[2], Tereza C. Leal-Balbino[1], Danilo E. Xavier[1] and Osvaldo P. de-Melo-Neto[1]**

[1] Aggeu Magalhães Institute (IAM), Fundação Oswaldo Cruz (Fiocruz), Recife, Brazil, [2] Department of Pathology, Institute of Biological Sciences, University of Pernambuco, Recife, Brazil, [3] Laboratory of Immunopathology Keizo Asami, Federal University of Pernambuco, Recife, Brazil, [4] Department of Tropical Medicine, Federal University of Pernambuco, Recife, Brazil

OPEN ACCESS

Edited by:
Santiago Castillo Ramírez, National Autonomous University of Mexico, Mexico

Reviewed by:
Mohammad Hamidian, University of Technology Sydney, Australia
Raffaele Zarrilli, University of Naples Federico II, Italy

***Correspondence:**
Osvaldo P. de-Melo-Neto
opmn@cpqam.fiocruz.br

Specialty section:
This article was submitted to Evolutionary and Genomic Microbiology, a section of the journal Frontiers in Microbiology

Received: 03 January 2020
Accepted: 08 May 2020
Published: 17 June 2020

Citation:
Leal NC, Campos TL, Rezende AM, Docena C, Mendes-Marques CL, de Sá Cavalcanti FL, Wallau GL, Rocha IV, Cavalcanti CLB, Veras DL, Alves LR, Andrade-Figueiredo M, de Barros MPS, de Almeida AMP, de Morais MMC, Leal-Balbino TC, Xavier DE and de-Melo-Neto OP (2020) Comparative Genomics of Acinetobacter baumannii Clinical Strains From Brazil Reveals Polyclonal Dissemination and Selective Exchange of Mobile Genetic Elements Associated With Resistance Genes. Front. Microbiol. 11:1176. doi: 10.3389/fmicb.2020.01176

Acinetobacter baumannii is an opportunistic bacterial pathogen infecting immunocompromised patients and has gained attention worldwide due to its increased antimicrobial resistance. Here, we report a comparative whole-genome sequencing and analysis coupled with an assessment of antibiotic resistance of 46 *Acinetobacter* strains (45 *A. baumannii* plus one *Acinetobacter nosocomialis*) originated from five hospitals from the city of Recife, Brazil, between 2010 and 2014. An average of 3,809 genes were identified per genome, although only 2,006 genes were single copy orthologs or core genes conserved across all sequenced strains, with an average of 42 new genes found per strain. We evaluated genetic distance through a phylogenetic analysis and MLST as well as the presence of antibiotic resistance genes, virulence markers and mobile genetic elements (MGE). The phylogenetic analysis recovered distinct monophyletic *A. baumannii* groups corresponding to five known (ST1, ST15, ST25, ST79, and ST113) and one novel ST (ST881, related to ST1). A large number of ST specific genes were found, with the ST79 strains having the largest number of genes in common that were missing from the other STs. Multiple genes associated with resistance to β-lactams, aminoglycosides and other antibiotics were found. Some of those were clearly mapped to defined MGEs and an analysis of those revealed known elements as well as a novel Tn*7*-Tn*3* transposon with a clear ST specific distribution. An association of selected resistance/virulence markers with specific STs was indeed observed, as well as the recent spread of the OXA-253 carbapenemase encoding gene. Virulence

genes associated with the synthesis of the capsular antigens were noticeably more variable in the ST113 and ST79 strains. Indeed, several resistance and virulence genes were common to the ST79 and ST113 strains only, despite a greater genetic distance between them, suggesting common means of genetic exchange. Our comparative analysis reveals the spread of multiple STs and the genomic plasticity of *A. baumannii* from different hospitals in a single metropolitan area. It also highlights differences in the spread of resistance markers and other MGEs between the investigated STs, impacting on the monitoring and treatment of *Acinetobacter* in the ongoing and future outbreaks.

Keywords: *Acinetobacter baumannii*, antimicrobial resistance, virulence, mobile genetic elements, Brazil

INTRODUCTION

Acinetobacter baumannii is an opportunistic Gram-negative bacterium considered one of the most prevalent pathogens associated to nosocomial infections, especially among immunocompromised patients. Its ability to survive in hostile conditions, its high level of intrinsic and acquired antimicrobial resistance and the ease with which it spreads within and between health care units worldwide has made *A. baumannii* a successful pathogen in hospital settings (McConnell et al., 2013; Wong et al., 2017; Hamidian and Nigro, 2019). The genus *Acinetobacter* has also gained attention due to the increasing number of reported multi-drug resistant (MDR) clinical strains. These represent a great challenge in terms of treatment of infections and the elimination of pathogenic *Acinetobacter* species. The genome plasticity of *A. baumannii* further enhances its ability to adapt and persist in hospital environments and has facilitated the emergence of global MDR strains (Imperi et al., 2011; McConnell et al., 2013; Elhosseiny and Attia, 2018; Rocha et al., 2018).

Acinetobacter baumannii exhibits intrinsic resistance to many classes of antimicrobial agents and is further capable of developing resistance to virtually all other classes of agents used in the clinical practices to treat Gram-negative infections (Esterly et al., 2011; Leclercq et al., 2013; Nowak and Paluchowska, 2016; Lee et al., 2017). Considering the β-lactam antimicrobials, specially the carbapenems, one of the main therapeutic options for infections caused by most Gram-negative pathogens and which have been regarded as one of the last line agents for the infection therapy, a rapid increase in carbapenem-resistant *A. baumannii* (CRAb) has been observed (Pogue et al., 2013; Piperaki et al., 2019). In *A. baumannii*, a major mechanism of carbapenem resistance is related to carbapenemase enzymes belonging to the Ambler A, B, and D classes of β-lactamases (Patel and Bonomo, 2013; Rahman et al., 2018). Carbapenem-hydrolyzing class D β-lactamases (CHDL) are the most common in *A. baumannii* strains and these are referred as OXA-type carbapenemases (Nowak and Paluchowska, 2016). Other mechanisms that have been related to decreased carbapenem-susceptibility in *A. baumannii* include: decreased permeability due to changes in porin expression, especially CarO and OprD-like; overexpression of efflux pumps; changes in penicillin-binding proteins; and overexpression of intrinsic *Acinetobacter*-derived cephalosporinases (Fernández-Cuenca et al., 2003; Hu et al., 2007; Catel-Ferreira et al., 2011; Jeon et al., 2014). In MDR strains more than one of these mechanisms can work synergically (Sen and Joshi, 2016).

The sequencing of several *A. baumannii* genomes revealed a wide repertoire of antimicrobial resistance genes, many of which associated with transposable elements and insertion sequences and which might be found in genomic islands (GIs), known as AbaR (Zhu et al., 2013; Liu et al., 2014; Bi et al., 2019). Several AbaR islands have been described which can vary in size and are dynamically reshaped mainly due to the activity of transposases, recombinases and integrases (Krizova et al., 2011; Li et al., 2015; Hamidian and Hall, 2018; Bi et al., 2019). Resistance genes can also be found within plasmids, which can be exchanged intra- and interspecies (Leungtongkam et al., 2018; Wibberg et al., 2018) and even by prophages (Wachino et al., 2019). In contrast to the better understood resistance genes, few virulence mechanisms and associated genes have been identified in *A. baumannii* involved in the establishment and progression of infection (Morris et al., 2019). Nevertheless, some determinants have been found related to *Acinetobacter* virulence and these include factors involved in biofilm formation, secretion systems, surface glycoconjugates and micronutrient acquisition systems (Penwell et al., 2012; Carruthers et al., 2013; Kenyon and Hall, 2013; Weber et al., 2017; Harding et al., 2018; Morris et al., 2019). Even though some studies have suggested that *Acinetobacter* elaborates a lipooligosaccharide (LOS) layer instead of lipopolysaccharides (LPS) on their cell surface, the diversity of the biosynthesized LOS core has also been implicated in its survival and virulence (Weber et al., 2016).

Considering the *A. baumannii* genetic diversity, their strains have been typed by the multilocus sequence typing method (MLST) to distinguish between different clonal lineages. Based on two existing MLST schemes, Pasteur (Diancourt et al., 2010) and Oxford (Bartual et al., 2005), clinical isolates of *A. baumannii* have been clustered into several clonal complexes (CCs) that group genetically and phenotypically related strains that are generally fairly widespread across the globe. More recently the Pasteur scheme has been shown to me more reliable and appropriate for evaluations concerning epidemiological studies (Gaiarsa et al., 2019). Eighteen of those clonal complexes were early on considered international clones since they were been found in more than one continent, while the remaining were suspected to be restricted to Europe and Asia (Karah et al., 2012). In Brazil, many multidrug resistant clinical strains of *A. baumannii* collected from several states have been studied

(Pagano et al., 2017) and at least six clonal complexes were identified (Chagas et al., 2014). The CC79, CC1, CC15, and CC113, complexes (named according to the Pasteur scheme) have been more frequently reported among Brazilian clinical strains of *A. baumannii*, but only CC79 remains predominantly restricted to South America, while the others are considered international clones (Karah et al., 2012; Chagas et al., 2014; Girlich et al., 2014).

Although *Acinetobacter* MDR strains belonging to different clonal complexes have been reported from Brazil (Chagas et al., 2015; Turano et al., 2016; Pagano et al., 2017; Da Silva et al., 2018), no comprehensive genome-wide comparative analysis of Brazilian strains has been conducted and a need for further sequencing from South American strains has recently been pointed out (Hamidian and Nigro, 2019). In the present study, we sequenced the genomes of 46 *Acinetobacter* clinical strains from five different hospitals located in Recife, a large metropolitan area of Northeastern Brazil, to reveal the genetic features and the outbreak potential of multiple clonal lineages and circulating strains of this pathogen. An extensive genome-wide comparative analysis based on the sequenced genomes was carried out, leading to the identification of key genetic determinants associated with antimicrobial resistance, virulence and associated transposable elements.

MATERIALS AND METHODS

Bacterial Isolates, Growth Conditions and Antimicrobial Susceptibility Testing

This study evaluated a total of 45 carbapenem-resistant *A. baumannii* (CRAb) strains and a single pan-susceptible clinical strain of *A. nosocomialis* (Acb_11) (**Supplementary Table S1**). These strains were collected between 2010 and 2014 from patients hospitalized at five different tertiary hospitals located in Recife, Brazil. A single *A. baumannii* strain per patient was included in this study and those were recovered from upper respiratory tract infections (n = 13); bloodstream (n = 10), cerebrospinal fluid (CSF, n = 09), peritoneal fluid (n = 03); catheter tip (n = 03); urinary tract (n = 02); bone (n = 01); soft tissues (n = 1), and rectal swab cultures (n = 04). The strains were stored at −80°C in commercial Brain-Heart Infusion (BHI) broth supplemented with 20% glycerol for preservation and were grown in BHI medium at 35 ± 2°C.

Species identification was verified by Biotyper MALDI-TOF mass spectrometry (Marí-Almirall et al., 2017). Clinical and Laboratory Standards Institute (CLSI) broth microdilution susceptibility testing was performed to determine the minimal inhibitory concentration (MIC) to ampicillin/sulbactam (1/0.5–128/64 μg/ml); ceftriaxone (1–128 μg/ml); ceftazidime (1–128 μg/ml); cefepime (1–128 μg/ml); imipenem (0.5–64 μg/ml); meropenem (0.5–64 μg/ml); ciprofloxacin (0.25–32 μg/ml); levofloxacin (0.25–32 μg/ml); amikacin (2–256 μg/ml); gentamicin (0.5–64 μg/ml), and polymyxin B sulfate (0.25–32 μg/ml). *Pseudomonas aeruginosa* ATCC 27853 and *Escherichia coli* ATCC 25922 strains were used as quality controls in this assay (Clinical and Laboratory Standards Institute [CLSI], 2015, 2018).

Library Preparation and Sequencing

Total DNA from each strain was extracted employing the DNeasy® Blood and Tissue kit (QIAGEN®, Hilden, Germany) following the manufacturer's instructions. After DNA extraction, the DNA was quantified with the QUBIT fluorometric device (Thermo Fisher®, Waltham, MA, United States) using the Qubit dsDNA BR Assay Kit (Thermo Fisher®, Waltham, MA, United States). Adapter-ligated sequencing libraries were prepared using the Nextera XT DNA Library Prep Kit (Illumina, San Diego, CA, United States) with 1 ng input of genomic DNA for each sample. Oligonucleotides used as indexes were added by PCR amplification according to the manufacturer's instructions. Unique index-tagged libraries were generated for each strain and pooled to generate a multiplexed library which was sequenced on Illumina MiSeq in a single run, using MiSeq Reagent Kit v3, 2 × 300 base pair run. The raw sequencing data generated in the present study is publicly available at the European Nucleotide Archive (ENA), accession: PRJEB12754[1].

Genome Assembly, Gene Prediction, and Annotation

Prior to genome assembly, the quality of the raw sequencing reads was first evaluated using the FastQC package[2], followed by sequence trimming using the Trimmomatic v0.32 program (Bolger et al., 2014) with the following parameters: LEADING:3 TRAILING:3 SLIDINGWINDOW:4:15 MINLEN:50 CROP:240. For each strain, the trimmed paired-end data was then used to perform genomic *de novo* assembly with the VelvetOptimiser[3] script for Velvet (Zerbino, 2010), setting N50 optimization function for *k*-mer length selection. For protein prediction and annotation the Prokka pipeline (Seemann, 2014) was used along with a database containing all *A. baumannii* proteins available at NCBI Refseq, to enhance this annotation (parameters: –genus and –gram neg).

In order to visualize genomic contexts, a synteny map was created using the Mauve software (Darling, 2004) to align all 46 sequenced genomes. The produced alignment was then converted to the ClustalW format (Thompson et al., 2003) and the GBrowse Syn framework (McKay et al., 2010) used to upload it to a relational database and to visualize the synteny maps in an Internet browser.

All draft assemblies and annotations produced in the present study are available at https://doi.org/10.6084/m9.figshare.12144855.

Phylogenetic Tree and MLST Analysis

To predict the ortholog protein groups used in this study, the fourteen *A. baumannii* reference proteomes available at the time of the last collection of our samples were downloaded from NCBI and used as input for ORTHOMCL (Li et al., 2003) along with the Prokka-predicted proteomes of all the strains sequenced here. To generate a phylogenetic tree using an alignment-free

[1]https://www.ebi.ac.uk/ena/browser/view/PRJEB12754

[2]http://www.bioinformatics.babraham.ac.uk/projects/fastqc

[3]http://bioinformatics.net.au/software.velvetoptimiser.shtml

approach, first we generated 1,000 datasets using a bootstrap approach (bootstrap sampling with replacement), picking 1740 ORTHOMCL groups with replacement (the number of orthologs identified for all the strains used in the analyses), using the *sample* function in R - http://www.R-project.org. Each ortholog group included one protein for each sample present in this analysis, and these groups were defined as the list of core proteins. For each bootstrap, amino-acid sequences for each ortholog group were extracted from the predicted proteome of each strain. Each pool of protein sequences in each bootstrap was then used as input for CVTree (Qi et al., 2004; Xu and Hao, 2009; Zuo and Hao, 2015), a software that generates phylogenies based on a composition vector approach and that uses alignment-free whole genome comparisons, yielding 1,000 distance matrices. The Neighbor program from the PHYLIP package (Retief, 2000) was then used to generate a phylogenetic tree for each distance matrix, with the Consense program, also from PHYLIP, used to compute a consensus tree by the majority-rule consensus tree method, followed by tree visualization and figure generation using the iTOL software (Letunic and Bork, 2016). The pan-susceptible *A. nosocomialis* Acb_11 clinical strain was used as an outgroup.

Multilocus sequence typing (MLST) analysis was performed using SRST2 (Inouye et al., 2014). The MLST profiles were assigned *in silico* using the marker sequences available at the *A. baumannii* MLST Databases, PubMLST[4] for the Pasteur (Diancourt et al., 2010) scheme. Allele sequences were extracted from each *Acinetobacter* genome using the BLASTN tool and were then submitted to the pubMLST database for the assignment to both existing and new sequence types (STs).

NCBI accession numbers for the reference *A. baumannii* genomes included in the present study: AB0057 - GCA_000021245; AB307-0294 - GCA_000021145; AYE - GCA_000069245; BJAB0715 - GCA_000419405; D1279779 - GCA_000186665; ZW85-1 - GCA_000505685; BJAB0868 - GCA_000419425; BJAB07104 - GCA_000419385; MDR-ZJ06 - GCA_000226275; MDR-TJ - GCA_000187205; TYTH-1 - GCA_000302575; 1656-2 - GCA_000188215; ACICU - GCA_000018445; ATCC 17978 - GCA_000015425.

Identification of Antibiotic Resistance and Virulence Genes and Features

In order to identify the resistance genes, we queried the predicted protein sequences against the ResFinder (Zankari et al., 2012) using *blastp* (*e*-value cutoff 1*e*-5) (Altschul et al., 1990), keeping only genes that displayed coverage higher than 90% and identity values above 70%. The *blaADC* alleles genes and their association with ISAba-like elements were confirmed through PCR and DNA sequencing, as previously described (Ruiz et al., 2007). To search for virulence related genes in the sequenced genomes, as well as in the reference *A. baumannii* genomes selected for this study, we carried out BLAST searches for genes classified within the virulence factor of pathogenic bacteria database (VFDB) for the *Acinetobacter* genus with the VFanalyzer online tool (Chen, 2004; Liu et al., 2019). Genes encoding the BfmRS two-component regulatory system (Geisinger and Isberg, 2015) were also investigated. A presence/absence table was generated based on the selected resistance and virulence related genes found. This table was used as input for iTOL (Letunic and Bork, 2016) for visualization alongside the phylogenetic tree.

Analysis of Capsule (K) and O-Antigen (OC) Biosynthetic Gene Clusters

To characterize predicted protein sequences from the K and OC loci, a preliminary assessment was carried out using both *blastp* (Altschul et al., 1990) and Pfam (Bateman, 2002), for gene identification, and Artemis (Rutherford et al., 2000), to compare gene arrangement. Modules A and B from the K loci and the OC loci were first identified using *blastp* queries against the flanking *fkpA*/*lldP*, and *ilvE*/*aspS* genes, respectively, as described previously (Kenyon and Hall, 2013; Kenyon et al., 2014; Holt et al., 2016). Variable genes encoding proteins predicted to be involved in sugar synthesis were examined for homology to the *A. baumannii* reference sequences. KL and OCL types were subsequently defined using the *Kaptive* tool (Wick et al., 2018) and the curated databases of annotated reference sequences for *A. baumannii* K and OC loci, recently described (Wyres et al., 2020). For the gene encoding the WaaL O-antigen ligase, we searched for homologs to the *P. aeruginosa* PAO1 [GenPept accession NP_253686.1] and to WaaL ligases from *E. coli* core types K12, R1, R2, R3, and R4. Similar searches were carried out for the gene encoding the PglL *O*-oligosaccharyltransferase.

Search for Genomic Islands and Mobile Genetic Elements (MGEs)

Nucleotide sequences encoding published genomic islands (GIs) were downloaded from PAIDB (Yoon et al., 2015). For the identification of GIs within our strains, two different approaches were then applied. First, a homology-based search method against known islands was followed by a second approach which evaluated the flanking sequences of known insertion hotspots. Fragments with high similarity to AbaR0 (KF483599) and AbGRI1[5] were thus identified and aTRAM (Allen et al., 2015) was used to map the sequenced reads from identified resistance genes and virulence factors onto these GIs. Mapping coverage was also evaluated to identify the potentially most similar GIs present in each strain.

Nucleotide sequences annotated by the Prokka software that encode transposases were also recovered and used in an alignment search with the *blastp* tool (with default parameters) against the ISfinder database (Siguier, 2006). This was performed in order to identify the corresponding IS family of transposases. If no homolog could be detected in the ISfinder database, we then performed a complementary search against the NCBI non-redundant database. In order to access the copy number of each element *per* strain, we used the Prokka annotated transposases to perform *blastn* searches against contigs from all 46 strains and the 14 reference genomes.

Prophages derived sequences were detected using the PhiSpy software (Akhter et al., 2012) which uses an *ab initio* approach to find phage genome related segments.

[4]http://pubmlst.org/abaumannii/

[5]http://www.paidb.re.kr/view_pai_from_genome.php?pa=NC_021729_R1

RESULTS

Strain Selection and Antimicrobial Susceptibility Profile

In order to investigate *Acinetobacter* clinical strains associated with hospital acquired human infection in Northeastern Brazil, we selected 46 *Acinetobacter* strains from patients hospitalized in five hospitals from Recife. Forty-five of those were carbapenem-resistant *A. baumannii* strains isolated from different sources or body fluids. A single pan-susceptible strain of *A. nosocomialis* (Acb_11), a related nosocomial species from the *Acinetobacter calcoaceticus-baumannii* complex, was isolated from a bloodstream infection. All strains were identified by MALDI-TOF (Marí-Almirall et al., 2017), with the species identification subsequently confirmed by the genome sequence analysis, as described below. The *A. nosocomialis* strain (Acb_11) was maintained in our analysis considering that it turned out to be an efficient outgroup species for the phylogenetic studies carried out.

Prior to any genetic analysis, we opted to determine the antimicrobial susceptibility profile exhibited by the 46 *Acinetobacter* clinical strains against eleven different antimicrobial agents using the CLSI broth microdilution method (results summarized in the **Supplementary Table S1**). As expected, the *A. nosocomialis* Acb_11 was the sole strain susceptible to all tested antimicrobial agents. In contrast, after testing with imipenem and meropenem, the carbapenem-resistance phenotype was confirmed for all 45 *A. baumannii* strains. Among these clinical strains, nearly all were also resistant to the first two cephalosporins tested, ceftriaxone and ceftazidime, with two thirds also found to be resistant to a third cephalosporin, cefepime. A reduced susceptibility to cefepime was, nevertheless, observed for most of the remaining strains (30%, 13/45), with only a single strain (Acb_41) being susceptible to the three cephalosporins tested.

The totality of the strains included in this study showed *in vitro* susceptibility to ampicillin/sulbactam. In contrast, distinct results were observed regarding resistance to the two aminoglycosides tested, amikacin and gentamicin. Full resistance to amikacin was found in 60% of the strains, with 20% classified as susceptible and the remaining 20% having an intermediate resistance phenotype, while for gentamicin a resistance phenotype was found for ∼50% of the strains, with ∼40% classified as susceptible. Cross-resistance was observed for the gentamicin resistant strains only, since those also had reduced susceptibility to amikacin, while eight of the amikacin-resistant strains were nevertheless susceptible to gentamicin. Regarding the fluoroquinolones tested, ciprofloxacin, and levofloxacin, all 45 strains were resistant to ciprofloxacin and even the highest concentration tested (32 μg/ml) was incapable of inhibiting the growth of most of the strains. In contrast, levofloxacin resistance was observed for only ∼13% of the strains. The last antimicrobial agent investigated was polymyxin B, which was found to be active against all tested *A. baumannii* strains. Overall, the antibiotic resistance profile from the selected *A. baumannii* strains confirm a diverse pattern of resistance to cephalosporins, fluoroquinolones, and aminoglycosides, while displaying full resistance to the two carbapenems tested and susceptibility to the ampicillin/sulbactam combination and to polymyxin B.

Acinetobacter Genomic Features

To evaluate the genetic diversity of the clinical strains selected for this study as well as to define their phylogenetic relationships and understand the genetic basis for their diverse antibiotic resistance profiles, we performed next generation sequencing, draft genome assembly and annotation for all 46 strains. The assembly metrics and statistics for the sequenced genomes can be found in the **Supplementary Table S2**. We identified an average of 3,809 genes per genome but only 2,006 genes were single copy orthologs, or core genes that are conserved across all 46 *Acinetobacter* strains sequenced, similar to results derived from other analysis (Imperi et al., 2011; Chan et al., 2015). The average number of accessory genes per genome was 2,106 highlighting the high degree of diversity in gene repertoire between different strains. This is better visualized through an ortholog group accumulation curve (shown in **Supplementary Figure S1A**) where the total number of ortholog groups identified are plotted according to the total number of strains sequenced. The curve shows a continuous increase in the number of ortholog groups that does not reach a plateau even after adding all 46 genomes sequenced, indicating that each new strain adds new genes that are not found in the previously added genomes. Indeed, an average number of 42 new orphan genes were identified per strain and plotting only these orphan genes generate a straight line confirming the addition of new genes by each sequential strain sequenced (**Supplementary Figure S1B**). These analyses are consistent with an active process of adaptation by the *Acinetobacter* strains with a constant acquisition of new genes by different strains and a more limited number of core sequences responsible for house-keeping functions. They also indicate that as more genomes are sequenced, more strain-specific genes are expected to be found, as well as other strains which share the so far strain-specific genes.

MLST, Clonal Complexes and Phylogeny

With the availability of the full set of gene sequences available for the *Acinetobacter* strains investigated here, a MLST analysis was carried out for the 46 sequenced genomes in order to define how the various strains are related to each other. The Pasteur scheme Sequence Type (ST) identified a total of six *A. baumannii* STs circulating in the hospitals investigated and belonging to four clonal complexes previously reported as widespread among clinical isolates from this species: ST1 (5 strains, clonal complex CC1); ST15 (10 strains, CC15); ST25 (1 strain, CC113); ST79 (14 strains, CC79); ST113 (13 strains, CC113); and the new ST881 (CC1), which is represented by two strains having a *rpoB* single locus variant from ST1 (**Supplementary Table S3**). The *A. nosocomialis* strain (Acb_11) also displayed a previously non-described MLST profile with a new *fusA* allele and had a new ST assigned (ST882).

Next, we performed a phylogenomic analysis comparing the 46 genomes reported here with the first 14 *Acinetobacter* reference genomes. This analysis was based on an alignment-free

phylogenetic tree created with the sequences of 1,740 core proteins common to all these 60 genomes. It revealed the existence of seven well supported monophyletic groups (bootstrap support > 800) corresponding to related clonal complexes (**Figure 1**), as previously defined (Karah et al., 2012). Two of these groups contained only references genomes belonging to CC2 and CC10 while a third group included seven of newly sequenced strains (five ST1-red and the two ST881-orange strains) and three reference genomes, all belonging to complex CC1. Comprising only strains sequenced here, two other groups were based on strains from CC79 (ST79-yellow in the figure) and CC15 (ST15-blue), while one more group, corresponding to CC113, included the thirteen ST113-green strains and the single ST25-pink strain (Acb_41). The seventh group included in the figure is represented by the *A. nosocomialis* Acb_11 plus the reference genome of *A. baumannii* ATCC 17978 (ST437), isolated from a French infant patient in 1951 (Smith et al., 2007). The phylogenetic analysis (also shown in **Figure 2**) highlights the CC1 strains as a basal group, with CC79 as its sister clade. Nearly all the *A. baumannii* reference strains included here were found within a larger clade, which also included the CC1 and CC79 strains from this study. The CC15 and CC113 *A. baumannii* strains were more divergent, with the CC113 strains forming a well-supported sister clade to all other confirmed *A. baumannii* strains.

The reduced number of single-copy orthologs or core genes conserved across all sequenced strains in this study, which in a few cases could be a possible consequence of the fragmented nature of the genomes, prompted us to investigate the degree of conservation/divergence in gene content seen between strains belonging to different STs, in order to identify possible lineage-specific genes. Indeed, a considerable, but variable, number of core genes were therefore found to be ST or lineage-specific (also shown in **Supplementary Table S3**). For instance, 164 genes were found common to all the ST1 strains that were not found in any of the *A. baumannii* strains belonging to other STs. Remarkably, for the ST15 (505 genes in common), ST79 (706 genes) and ST113 (897 genes), a much larger number of ST specific genes were seen, contrasting even with the *A. nosocomialis* strain,

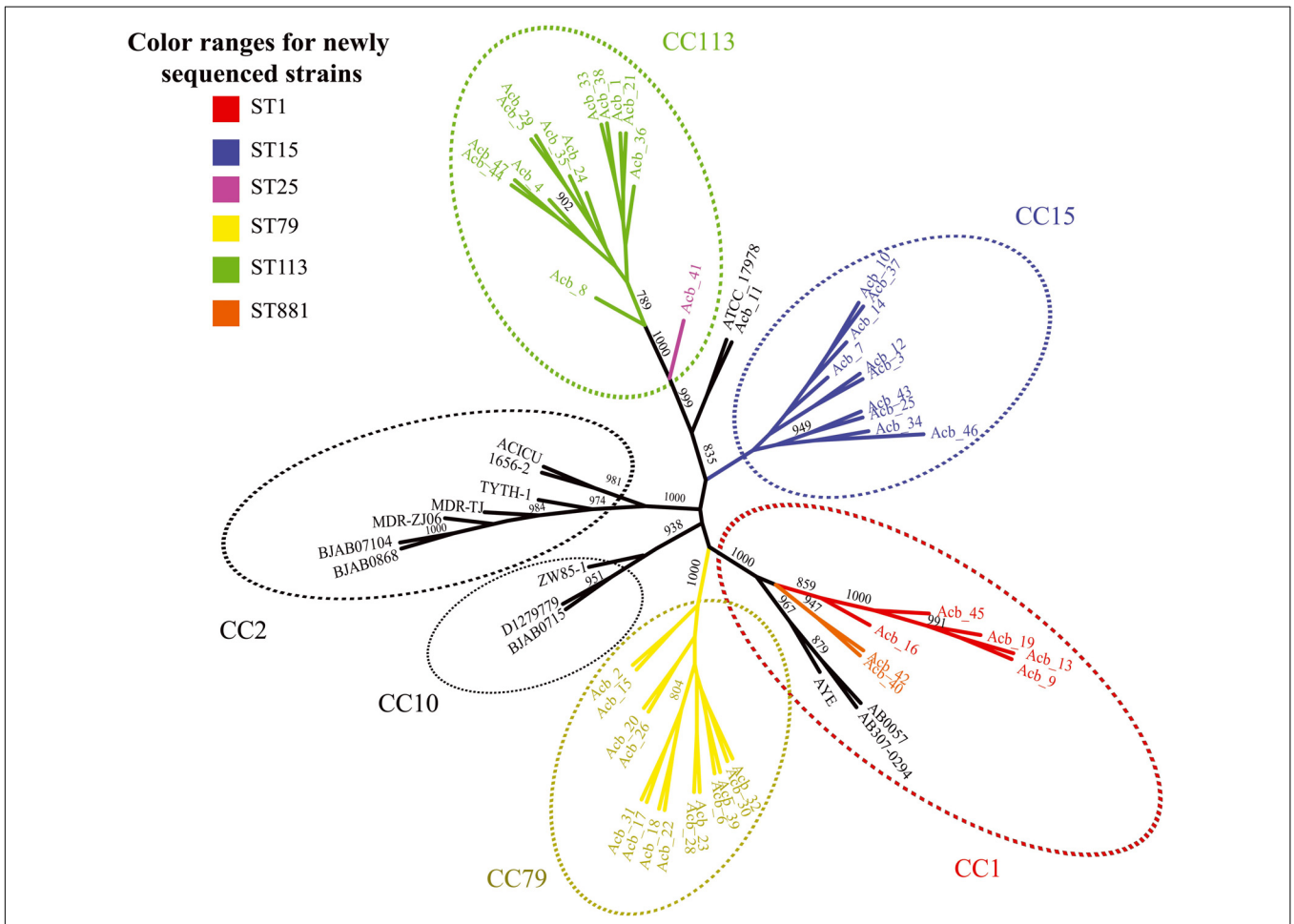

FIGURE 1 | Phylogenetic evaluation of the genomes sequenced here and in comparisons with selected reference genomes. An unrooted tree was built with the core genome of all *Acinetobacter baumannii* strains sequenced in this study and selected reference published genomes. Colors scheme follow the sequence type (ST) determined in the Pasteur's MLST scheme. The numbers near the branches are supporting bootstrap values with only the bootstrap values higher than 700 shown. Acb - *Acinetobacter baumannii*.

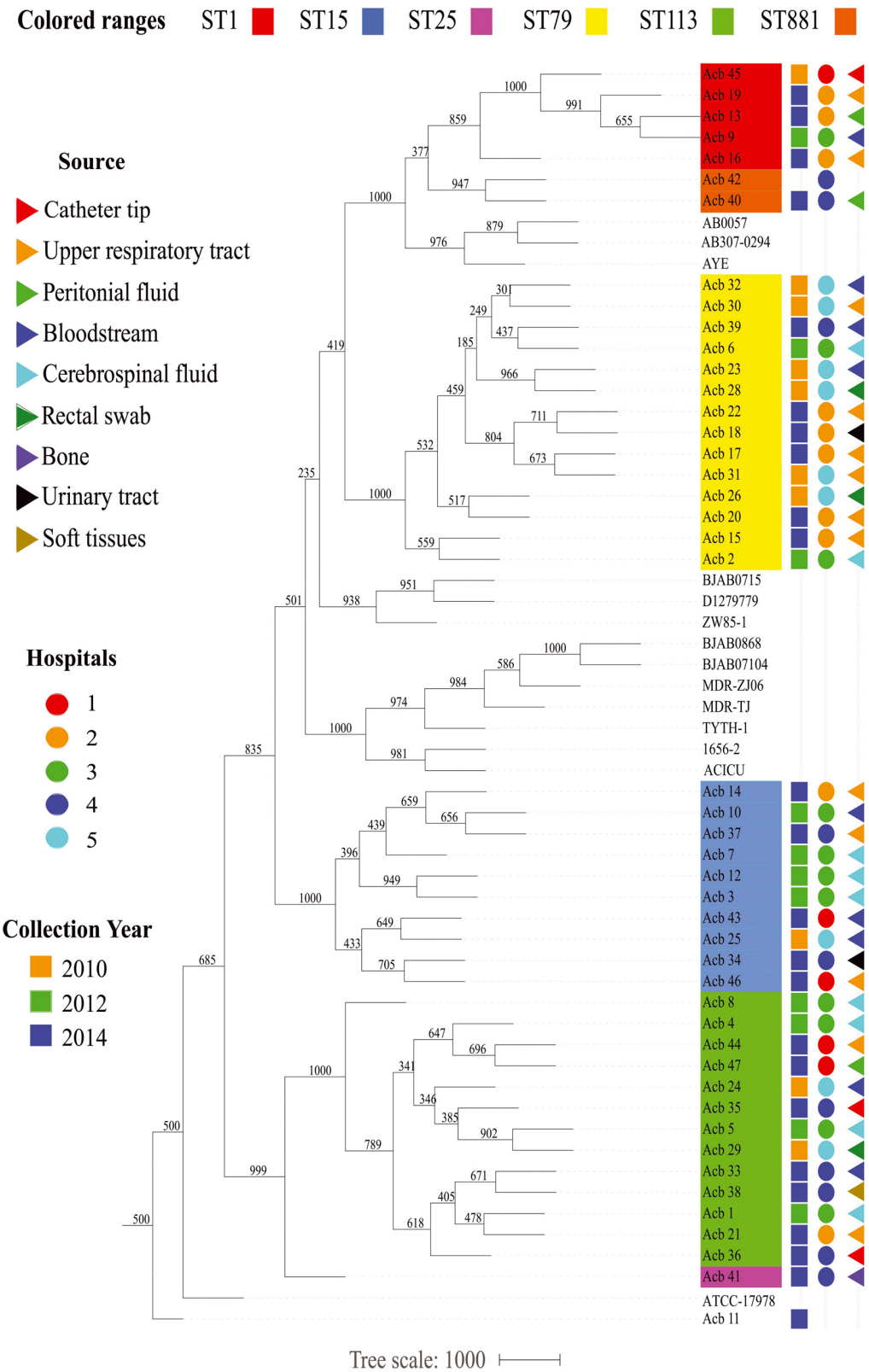

FIGURE 2 | Epidemiological features of the *Acinetobacter* strains characterized in this study. The source of the bacterial samples, the hospitals from where the strains were isolated and the year of sample collections are displayed at the right and represented by colored triangles, circles or squares, respectively. A phylogenetic tree comparing all strains sequenced here, and with selected reference genomes, is included in the right, color coded as in **Figure 1**.

Acb_11, which has only 256 genes not found in the other strains investigated here. These numbers reflect the remarkable ability of the *A. baumannii* strains to acquire new genes which can be maintained in a ST (or clonal lineage) specific manner.

ST Distribution, Date and Place of Isolation and Collection Method

Prior to any detailed genetic analysis, and based on the ST identification results, we next investigated any association between specific *A. baumannii* STs and variables such as date and place of isolation and collection methods. As summarized in the **Figure 2**, except for the strains from hospital 1, collected both in 2010 and 2014, bacterial samples from individual hospitals were generally collected from a single year so it is not possible to evaluate changes in frequencies for the various STs over different years for specific hospitals. Nevertheless, four out of six STs investigated here (ST1, ST79, ST113, and ST15) were collected over all the 3 years sampled (2010, 2012, and 2014), while the single ST25 and both ST881 *A. baumannii* strains were isolated only in 2014. *A. baumannii* strains belonging to ST113 and ST15 were isolated from all five hospitals studied, while ST79 grouped strains from four different hospitals and the ST1 strains are derived from three of the five hospitals. The same hospital where the single ST25 strain was isolated was also found to have strains from ST15, ST79, and ST113, as well as the two ST881 strains. The other four hospitals were found to harbor strains from three or four of the STs identified in this study. No correlation between the collection method used for strain isolation and the different STs was found. Overall, we can observe that despite the diversity in circulating *A. baumannii* STs identified in this study, all six STs have been simultaneously circulating at least since 2014, and multiple STs were found in each of the different hospitals investigated, with no clear indication of changes in ST frequency within the municipality during the time frame analyzed.

Antibiotic Resistance Determinants and Related Genes

The diverse profile of antibiotic resistance observed for the strains studied here prompted us to perform a detailed analysis of the resistance associated genes present in the draft genomes evaluated in this study. These include intrinsic and acquired β-lactamases encoding genes and allelic variants, even though not all may be necessarily be required for resistance, as well as genes which confer resistance to aminoglycosides, fluoroquinolones, chloramphenicol, macrolides, rifampicin, trimethoprim/sulfamethoxazole and tetracycline (**Figure 3**). Strains assigned to ST79 and ST113 accumulated a higher number of antimicrobial resistance and related genes than ST1 or ST15. If only genes found in more than one strain of the same ST are taken into account, seven gene variants were found for ST1 and six for ST15 strains, compared to 15 and 13 genes seen for ST79 and ST113, respectively. Nevertheless, with the exception of the resistance phenotype to gentamicin, where the ST15 strains were markedly more susceptible to this drug than the strains from other STs, no significant increase in antimicrobial susceptibility was seen for the ST1 or ST15 strains when compared to the remaining STs studied here, as discussed below. Also, a further analysis of the distribution of the more abundant resistance genes from ST79 and ST113 strains, based on their mode of action, showed that there is no enrichment for any particular type of antimicrobial resistance. Instead, redundant genes seemed to occur multiple times in related strains. For instance, most ST79 strains had four β-lactamase and four aminoglycoside resistance genes, with, respectively, four and three genes also seen for most ST113 strains, while three β-lactamase and two or one aminoglycoside resistant genes were seen in multiple strains from ST1 or ST15. Importantly, several genes involved in resistance, or genes related to those, were commonly shared by both sets of ST79 and ST113 strains. This is relevant considering their greater divergence and the fact that these genes might be missing from ST1 and ST15 strains, more closely related to ST79. This observation suggests that selected genes were either being preferentially exchanged between strains belonging to ST79 and ST113 or being selectively acquired by these strains only.

For the β-lactamase encoding genes we opted to first investigate genes for the different Ambler classes independently of them having a defined role in resistance. For the Ambler class A β-lactamases, two genes were found in the strains sequenced in this study with a clear ST specific pattern for one of them, $bla_{\text{TEM-1}}$. This gene was found within all genomes of the ST79 and ST113 strains but in none of the other STs, a first evidence indicating a preferential exchange of resistance genes between these two STs or independent acquisition events restricted to them. In contrast, the second class A β-lactamase gene, $bla_{\text{TEM-209}}$, was found in the single ST25 strain (Acb_41). Two other class A genes, $bla_{\text{TEM-171}}$ and $bla_{\text{PER-1}}$, were found only in reference strains belonging to CC2. Regarding the class B β-lactamase genes, none were found in the strains from Recife, although one gene ($bla_{\text{IMP-37}}$) was found in several reference strains belonging to the globally spread CC2 group and that also harbor the class A $bla_{\text{PER-1}}$ gene. A single gene encoding an intrinsic class C *Acinetobacter*-derived cephalosporinases, the AmpC (or ADC) enzyme, was recovered from all *Acinetobacter* genomes analyzed here, including the reference strains and the one classified as *A. nosocomialis* (Acb_11), always associated with an ISAba1 insertion (discussed further in the last section). After comparisons with available databases (Karah et al., 2017; Naas et al., 2017), specific alleles were identified which were found to be differentially distributed among the various strains and were generally absent from the genomes used as references. The $bla_{\text{ADC-182}}$ allele was by far the most widely distributed, found in 32 strains from five of the six *A. baumannii* STs identified (also shown in **Figure 3** and detailed in **Supplementary Table S4**). This was the sole allele found for the ST113 and ST881 strains and it was also present in thirteen of the fourteen ST79 strains. The second most frequent allele, more closely related to $bla_{\text{ADC-5}}$/$bla_{\text{ADC-183}}$, was mainly found in the ST1 and ST15 strains and in Acb_11 (from ST79). Two other alleles were also found, $bla_{\text{ADC-26}}$, in Acb_16 (ST1), and $bla_{\text{ADC-195}}$, in the ST25 strain (Acb_41). Intrinsic class D β-lactamases genes $bla_{\text{OXA-51}}$ or $bla_{\text{OXA-51}}$-like were also detected in all *A. baumannii* strains sequenced, but for these a clear association was found between

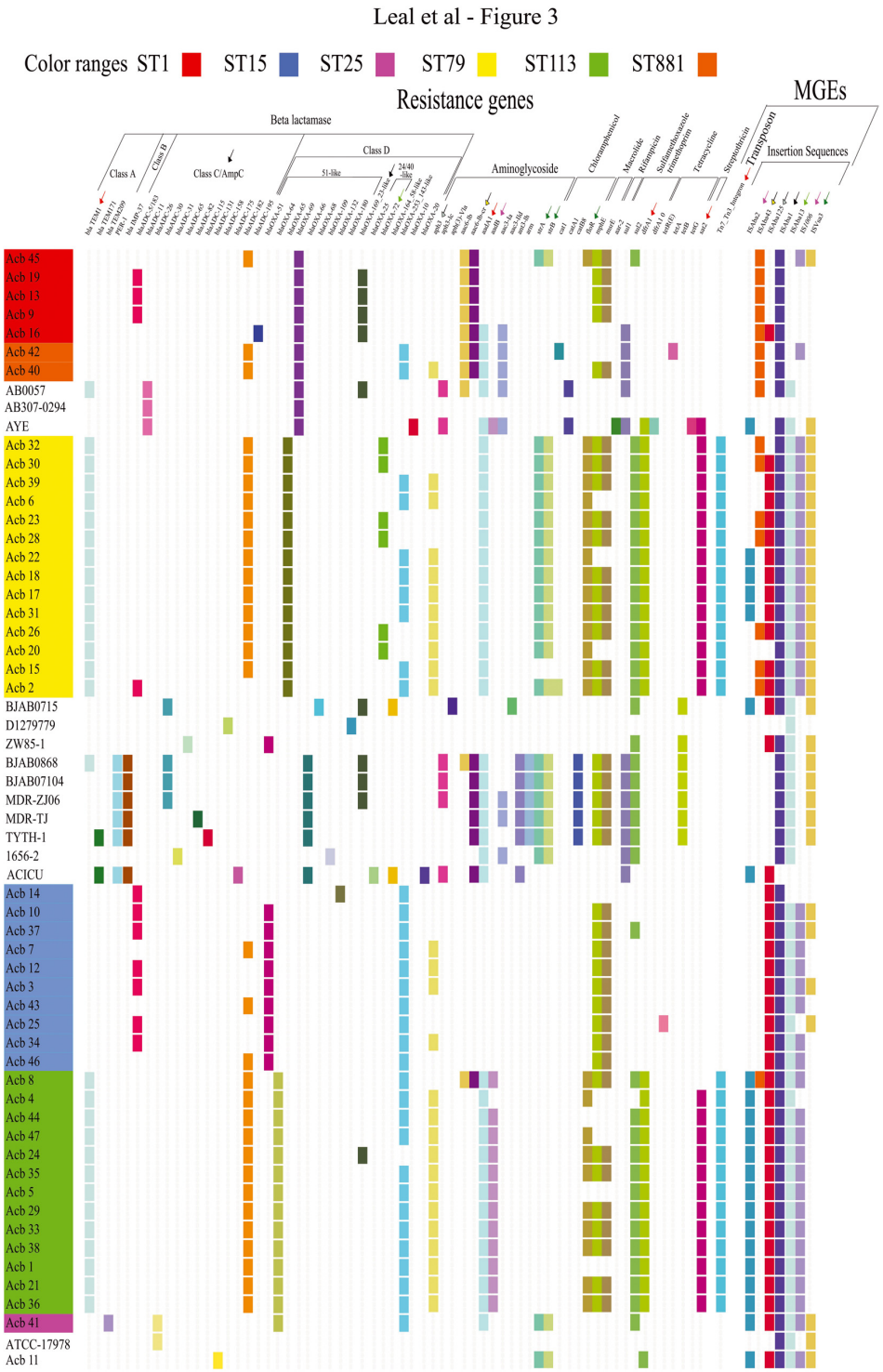

FIGURE 3 | Overview of the resistance genes identified as well as selected mobile genetic elements (MGEs). The *Acinetobacter* strains are sequentially ordered according to their STs and the phylogenetic relationship previously defined (**Figure 2** and **Supplementary Figure S1**) and color-coded as in **Figure 2**. The identification of the resistance genes was carried out with the sequences from the ResFinder database (*e*-value cutoff $1 \times E^{-5}$, coverage ≥0.9, identity ≥0.9). A positive match in the figure is indicated by a colored rectangle, with different genes colored differently. Negative matches are shown as blank spaces. Resistance genes are sorted by antibiotic classes to which they confer resistance. A selection list of mobile genetic elements (MGEs) characterized by homology search with the ISFinder database and linked to specific resistance genes is also displayed in the right side of the figure (more detailed in **Supplementary Figure S2**), with the transposon separated from insertion sequences (IS) and these sorted according to the IS family to which they belong to. Similarly colored arrows above resistance genes and MGEs indicate the association found between them.

the allelic variant of the *bla*$_{\text{OXA-51}}$-like identified and a specific ST or phylogenetic group, reinforcing the ST identification and phylogenetic analysis, although these genes are not likely to be associated with the resistance phenotype. For instance, *bla*$_{\text{OXA-69}}$ was found in ST1 and in the related ST881 and reference strains, *bla*$_{\text{OXA-65}}$ in ST79, *bla*$_{\text{OXA-64}}$ in ST113 and *bla*$_{\text{OXA-51}}$ in the ST15 strains.

With the exception of Acb_45, all strains, independent of ST, included one additional gene coding for a D class β-lactamase known to have a carbapenemase activity and which might be associated with a resistance phenotype, the acquired carbapenem-hydrolyzing class D β-lactamases (CHDL): most ST1 strains and one ST113 strain had the *bla*$_{\text{OXA-169}}$; some ST79 strains only had *bla*$_{\text{OXA-72}}$; and strains from five of the studied STs (ST15, ST25, ST79, ST113, and ST881) were found associated with *bla*$_{\text{OXA-253}}$. The presence of the *bla*$_{\text{OXA-253}}$ gene in strains from nearly all *A. baumannii* STs sequenced here but not in the reference genome sequences, indicates a recent spread of this more recently reported OXA-carbapenemase gene between the different STs or the spread of clones carrying this gene over different hospitals, as recently reported by some of us (de Sá Cavalcanti et al., 2017). Indeed, for ST79 only, the evidence indicates a chronological replacement of OXA-72 producing *A. baumannii* clinical isolates for OXA-253 producers in the more recent years, since most of the strains collected in 2010 have the acquired *bla*$_{\text{OXA-72}}$, a variant of the *bla*$_{\text{OXA-24}}$ gene, while those collected in 2012 and 2014 in general have *bla*$_{\text{OXA-253}}$. Regarding cephalosporin resistance, when the resistance profile obtained for the various strains included in the present study was superimposed with the ST identification derived from the genome sequencing effort (summarized in the **Supplementary Table S5**), a mixed pattern was observed regarding antibiotic resistance and ST that depends on the drug evaluated. The only *A. baumannii* strain susceptible to all three cephalosporin drugs tested was the single ST25 strain investigated here, while the strains showing intermediate resistance to cefepime were mostly found among the ST15 and ST113 strains, contrasting with the ST1 strains that were all resistant to this drug. The sequenced data, however, reveals no clear explanation for these differences in the cephalosporin resistance profile.

A different picture emerged regarding the aminoglycoside resistance genes and their distribution among the strains from the different STs. Most of the ST1, ST881, and ST113 strains displayed resistance to the amikacin, with a mixed profile observed for both sets of ST15 and ST79 strains (**Supplementary Table S5**). In contrast, a clear association between ST and resistance was seen for the second aminoglycoside gentamicin, since all ST1, ST881, and nearly all ST113 (12/13) strains were resistant to this drug, while all ST15 strains were susceptible and only the ST79 strains were of a mixed phenotype. Genes encoding aminoglycoside modifying enzymes, including acetyltransferases, phosphotransferases, and adenylyltransferases were found distributed among the different phylogenetic groups and STs and these were more frequently found for strains belonging to ST79 and ST113. Indeed, an association between the presence of the *aph3* gene and resistance to amikacin was seen for nearly all ST15, ST79, and ST113 strains. The two exceptions were the ST79 Acb_28 and the ST113 Acb_08 strains, which lacked the *aph3* gene despite displaying resistance to amikacin. Acb_08, however, was the sole ST113 strain having both *aac6-Ib* and *aac6-Ib-cr* genes, also found in the ST1 and ST881 strains, all displaying some resistance to amikacin but missing *aph3*. In contrast, Acb_41, the single ST25 strain, also displayed some resistance to amikacin despite the absence of any of these three genes. For the second aminoglycoside, gentamicin, a clear correlation between the presence of the *aadB* gene, associated with resistance to this drug (Hamidian et al., 2012), was seen for the ST113 strains, but no similar correlation was observed for strains belonging to the other STs where the *aadB* gene was notably missing. For the aminoglycoside resistance, then, most but not all resistance phenotypes can be explained by the presence or absence of previously characterized genes in the sequenced genomes.

The QRDR (Quinolone-Resistance Determinant Region) of *Acinetobacter* strains was also analyzed in order to identify modifications in the genes for the DNA gyrase subunit A (*gyr*A) and topoisomerase IV subunit C (*par*C), which have been associated with high levels of fluoroquinolone resistance (summarized in the **Supplementary Table S6**). All 45 *A. baumannii* clinical strains had the GyrA modification S83L, associated with high level of ciprofloxacin resistance (Vila et al., 1994, 1997) and in agreement with their resistance profile to this drug. Other modifications encoding the G81C and E87G substitutions were observed in the *gyr*A gene from two strains displaying cross-resistance to levofloxacin, the ST1 Acb_16 and the ST113 Acb_21 strains, both isolated in 2014. The S80L mutation targeting the topoisomerase IV ParC was observed in most of the newly sequenced strains, with the exception of those belonging to ST79, but it does not correlate with any significant increase in resistance. For the ST79 strains, several of those had a S80Y ParC substitution that also does not correlate with levofloxacin resistance, while others had a E84K substitution that might be associated with a reduced susceptibility to this drug. However, since other ST79 strains lacking this substitution also displayed some resistance to levofloxacin, it does not fully explain the changes seen in resistance. Likewise, the resistant profile to levofloxacin observed for the Acb_40 (ST881), Acb_10 (ST15), and Acb_08 (ST113) strains is not associated with the mutations investigated in both *gyr*A and *par*C genes.

Several other antimicrobial resistance genes were identified in our search of the sequenced genomes but whose resistance profile to the corresponding antimicrobial agents are not available for the different strains, since we needed to focus on a selected set of tested drugs, chosen mainly for their clinical relevance. Nevertheless, genes associated with resistance to chloramphenicol, tetracycline and others were identified in the analysis carried out and the search results are shown in **Figure 3**. Many of those were differentially associated with the various STs and include several that were specifically present only in ST79 and ST113 (*sul2*, *dfrA1*, and *sat2*, for example), but were otherwise missing from nearly all other strains included in the analysis. Noteworthy, there were also two genes responsible for the resistance to the aminoglycoside streptomycin (*strA* and *strB*) which were selectively missing from the ST15, ST113, ST881, and nearly all ST1 strains.

Selected Virulence Factors

Selected genes encoding factors from the *Acinetobacter* virulence factor database (VFDB) plus a few others were also investigated regarding their presence/absence among the newly sequenced strains, with the relevant results summarized in **Figure 4**. Acinetobactin genes cluster and *hemO*, related to iron uptake, were generally present in almost all strains investigated here, with the notable exception of the *A. nosocomialis* Acb_11 strain. Genes coding the phospholipases C and D were present in all strains, while the *cpaA* gene, encoding the secreted coagulation targeting metallo-endopeptidase (CpaA) and related to reduced coagulation of human plasma (Waack et al., 2018), was found only in *A. nosocomialis* strain (Acb_11) and the *A. baumannii* Acb_41. In contrast, the catalase gene (*katA*), which protects bacteria from superoxidants produced by leukocytes as a host defense mechanism (Sun et al., 2016), was present in most of the sequenced strains, with the exception of those from ST1/ST881 and ST15. Also found in all or nearly all strains investigated here was the *pbpG* (penicillin-binding protein) gene.

Porins such as CarO and OprD, channels for influx of carbapenems, and the outer membrane protein A (OmpA), were investigated here with other virulence factors. The *omp*A gene was found in all strains, but *carO* and *oprD* were alternatively absent from multiple strains belonging to ST1 (only *oprD*) and ST79 (both genes absent from different strains) as well as single strains from ST15 and ST113 (*carO* only), with the *oprD* also missing from Acb_11. Another virulence *locus* investigated was the one coding for the CDI system, but among the sequenced strains those from ST79 (and also the single ST25 strain, Acb_41) were unique in having these genes. Regarding type IV pili formation, also investigated here, all strains from this study as well as the reference strains had the three *pil* genes.

Multiple biofilm-related virulence genes known from *A. baumannii* were also investigated and, in general, genes encoding proteins involved in biofilm and pili formation, adherence, and quorum sensing were found in almost all the sequenced strains. Indeed, all strains from this study had the genes encoding the AdeFGH efflux pump, as well as the *pgaABCD* locus, required for intercellular adhesin synthesis, and the chaperone-usher assembly system of *csu* pili. In contrast, genes encoding the Biofilm Associated Protein (*bap*) were also investigated but could not be found in the single ST25 and in most ST113 strains. These genes, however, are complex in nature, with very long coding sequence containing variable repetitive regions (De Gregorio et al., 2015), and the fragmented nature of the genomes sequenced here would require a more detailed analysis to better define their diversity and distribution. Curiously, only strains from ST79 have confirmed genes encoding both Bap and the RTX-serralysin-like toxin, with the latter gene found in most, but not all ST79 strains, and in none of the other strains targeted in this study. Additionally, we searched for two quorum sensing genes (*abaI* and *abaR*), found to be missing only for some of the ST79 strains, and for the two-component system *bfmRS* (*rstBA*). These last two genes were found in nearly all sequenced strains, with the single exception of Acb_3, where the histidine kinase *bfmS* gene was absent.

Lipopolysaccharide (LPS)/Lipooligosaccharide (LOS) Biosynthesis

The LPS/LOS component of the outer membrane of Gram-negative bacteria is a major virulence component whose synthesis is dependent on several biosynthetic pathways (Wang and Quinn, 2010). As expected, the locus responsible for the synthesis of its hydrophobic lipid component, the conserved lipid A (*lpxABCDLM*), was present in all sequenced strains, with the single exception being Acb_40 where the *lpxA* gene was not found (not shown). No WaaL ligase was found in any of the sequenced strains but, with the exception of Acb_11 and Acb_31, all other sequenced strains had the PglL *O*-oligosaccharyltransferase enzyme, a putative substitute for WaaL ligase (Kenyon and Hall, 2013). Curiously, only in ST113 and ST25 the *pglL* gene open reading frame is complete having its three domains: pglLA, wzyC, and wzyC2. In strains from other STs, either pglLA plus wzyC or wzyC alone are found.

The variable carbohydrate component of LPS/LOS is encoded by the outer core *locus* (OC), which comprises genes involved in the synthesis, assembly and export of complex oligosaccharides that are then linked to lipid A to form the LPS/LOS (Wang and Quinn, 2010; Kenyon and Hall, 2013). The OC *locus* (OCL) is flanked by the *ilvE* (aminotransferase) and *aspS* (aspartate-tRNA ligase) genes and both are found in all sequenced genomes. Different OCL variants have been reported, which vary according to the presence or absence of genes encoding multiple glycosyltransferases and other enzymes (Kenyon et al., 2014). The complete OC gene cluster was not contiguously assembled for all strains sequenced here, although their OCL-type could be tentatively defined using recently described tools (Wick et al., 2018; Wyres et al., 2020), as summarized in **Figure 4** and also in the **Supplementary Table S7**. All the analyzed *Acinetobacter* CC1 strains (from ST1 and ST881) had the OCL1 variant, while all the ST79 strains were found to have the OCL10 type from Group A. In contrast, OCL variants belonging to Group B were found for the remaining sequenced strains with the ST15 and ST113 strains, and also the *A. nosocomialis* Acb_11, having OCL7, while the single ST25 strain had the OCL6 variant. Overall, the OCL types observed for the sequenced strains were tightly linked to their ST-classification as well as their phylogenetic relationships, with different types generally associated to strains from different STs, the exception being those belonging to the ST15 and ST113 strains.

Genes Associated With the K Antigen Synthesis

The K *locus* also determines the production of complex oligosaccharides units that are exported to the outer membrane of Gram-negative bacteria and includes genes responsible for the synthesis of the exopolysaccharide capsule, the K antigen (Iwashkiw et al., 2012; Kenyon and Hall, 2013; Senchenkova et al., 2015; Holt et al., 2016; Shashkov et al., 2016, 2017; Kenyon et al., 2017, 2019). Despite having the flanking *fkpA* and *lldP* genes, none of the strains sequenced here exhibited a unique and fully assembled K locus contig (not shown). Module A (*wza*, *wzb*,

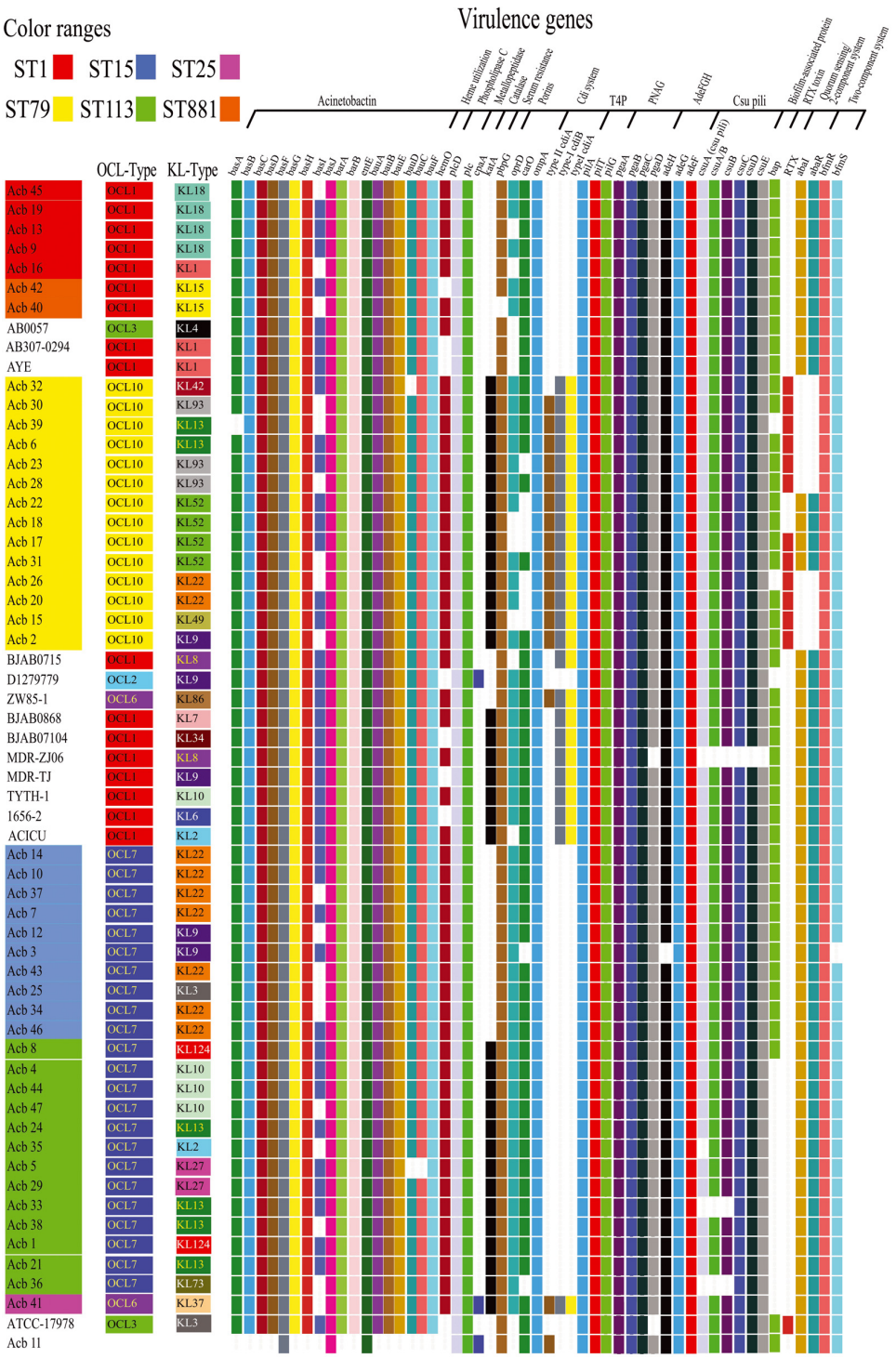

FIGURE 4 | Overview of the virulence genes identified and definition of the OC/K loci for the strains investigated here. As for **Figure 3**, the *Acinetobacter* strains are also sequentially ordered according to their STs and the phylogenetic relationship previously defined (**Figure 2** and **Supplementary Figure S1**), with a positive match indicated by a colored rectangle and negative matches are shown as blank spaces. The virulence genes were identified comparing the annotation made with PROKKA to Vfdb database (*e*-value cutoff $1E^{-5}$, coverage ≥0.9, identity ≥0.9). In the figure, these genes are sorted by the mechanistic feature that they likely confer to *A. baumannii* strains. The predicted *Acinetobacter* OCL and KL-types for each strain are also indicated in the figure and were defined as shown in the **Supplementary Table S7**.

and *wzc*) is nevertheless present in all strains sequenced here, as well as the *gna* gene, positioned immediately after it, and module B (*galU*, *udg*, *gpi*, *gne1*, *pgm*, and *lldP*). The KL gene cluster was also evaluated and found within multiple contigs of the draft genomes, with several genes appearing to be interrupted by frameshifts and/or insertion sequence. It was not always possible to clearly define distinct KL groups for the sequenced strains and these would require complementary studies. However, a tentative classification was also made based on the presence/absence of previously defined genes, as described for the OCL-types (summarized in **Figure 4** and in the **Supplementary Table S7**).

Four of the five ST1 strains likely have the KL18 cluster, with the fifth strain, Acb_16, having genes belonging to KL1, a closely related cluster, and both ST881 strains having KL15. The ST79 strains are much more diverse, with seven different KL-types identified for the 14 strains: KL9 (Acb_2), KL13 (Acb_6 and Acb_39), KL22 (Acb_20 and Acb_26), KL42 (Acb_32), KL49 (Acb_15), KL52 (Acb_17, Acb_18, Acb_22, and Acb_31), and KL93 (Acb_23, Acb_28, and Acb_30). For the ST15 strains, three KL types were identified, with seven strains found having the KL22 (Acb_7, Acb_10, Acb_14, Acb_34, Acb_37, Acb_43, and Acb_46), two with KL9 (Acb_3 and Acb_12), and one with KL3 (Acb_25). Six KL-types were found for the ST113 strains: KL2 (Acb_35), KL10 (Acb_4, Acb_44, and Acb_47), KL13 (Acb_21, Acb_24, Acb_33, and Acb_38), KL27 (Acb_5 and Acb_29), KL73 (Acb_36), and KL124 (Acb_1 and Acb_8). Lastly, the single ST25 strain, Acb_41, was classified as having the KL37-type cluster. The ST79 and ST113 strains then are more variable in terms of KL-types when compared with the other STs. The data also highlights the KL-types shared by newly sequenced strains belonging to more than one of ST, such as KL22, found in both ST79 and ST15 strains, and KL13, found in strains belonging to the more distantly related ST79 and ST113 strains.

Mobilome

Searches for known mobile genetic elements (MGEs), including genomic islands, insertions sequences and transposons, were also carried out here using the available sequences (results summarized in **Figure 3** and **Supplementary Figure S2**). Considering the genomic islands, we first investigated regions mapping to AbaR0-type islands [recently reviewed by Hamidian and Hall (2018)]. In addition to two of the reference CC1 strains (AB0057 and AYE), segments belonging to these islands were clearly found in all ST1 and in both ST881 strains sequenced here (**Supplementary Figure S3A**), with disrupted *comM* gene sequences. When only the AbaR0 backbone is considered, based on the Tn*6019*::*Tn6018* transposons, most assemblies were fragmented into one or more contigs, missing several segments, with the exception of those from Acb_19 and Acb_13 (detailed in the **Supplementary Figure S3B**). Three ST79 strains (Acb_22, Acb_18, and Acb_17) also have a disrupted *comM* gene split by an AbaR0-like prototype, with only six genes related to transposases as well as two stress related genes (also shown in **Supplementary Figure S3B**). Regions homologous to AbGRI1-type islands (Nigro et al., 2013; Zhu et al., 2013; Blackwell et al., 2016) displayed a more dispersed distribution among the sequenced strains, with contigs bearing several genes originally mapped to this island found in all five ST1 strains as well as in several ST15 (8/10), ST79 (3/14), and ST113 strains (3/13) (**Supplementary Figure S2** – genomic islands). A major difference between the ST1 and ST881 strains then was the absence of the AbGRI1-type segments from the ST881 strains. More detailed information about the genes found associated to these islands is included in **Supplementary Figures S4, S5**. Regarding the other sequenced genomes, most of them harbor an intact *comM* gene and no regions homologous to the investigated islands.

Next, a search for composite transposons revealed a single Tn*3* and two Tn*7* transposons plus a chimeric transposon having both Tn*3* and Tn*7* features. These were found distributed among the different genome sequenced with a substantial variation in copy number, from 27 to 81. The Tn*3* element (MGEs section from **Figure 3** and **Supplementary Figure S2**) was found in some of the reference genomes as well as in all the ST79 and ST113 strains and in one of the two ST881 strains (Acb_42). In contrast, the first Tn*7* transposon was found in all the genomes analyzed here, including the *A. nosocomialis* strain, with a higher copy number for ST79. The second Tn*7* transposon was also found in all ST1, ST15, ST25, and ST881 strains and in most of the reference genomes but was missing from several of the ST79 and ST113 strains. The fourth transposon element, having both Tn*3* and Tn*7* features, however, showed a more restricted distribution and was found strictly in the ST79 and ST113 strains (see the following section).

A total of 18 insertion sequences (IS) from 10 different families were also found in the different genomes (**Supplementary Figure S2**): IS*1*, IS*3*, ISL*3*, IS*4*, IS*5*, IS*6*, IS*30*, IS*66*, IS*91*, and IS*256*. Those ISs varied in copy number from 6 to 14. They also varied in distribution with some being widely distributed among the genomes investigated, such as ISAba1, and others much more restricted, including ISAba17, which is restricted to ST113 strains, and ISAba31, mostly found in ST15 strains.

Regarding phage related sequences, complete or almost complete prophage genomes were detected in several of our samples. Examples are the genomes for the Haemop_SuMu_NC_019455 phage, found in 38 of the 47 strains, and those for the Acinet_Bphi_B1251_NC_019541 phage, found in 41 of the 47 genomes sequenced here (data not shown). Since virulence or resistance genes were not found to be associated with any of the phages detected, we will not discuss them further in this manuscript.

Genetic Basis for the Transfer of Resistance Determinants

A search was also carried out to investigate specific associations between the various resistance genes and different MGEs, aiming to clarify how the antibiotic resistance genes were being affected by these elements (results summarized in **Figure 3** and also in **Supplementary Figure S2**). The first MGE linked to resistance genes here was the novel Tn*7*-Tn*3* element found to be specifically associated with the ST79 and ST113 strains. A more detailed analysis of its sequence revealed that its 3′ region includes a 12 Kb Tn*7* transposon harboring three hypothetical

ORFs and five genes related to the Tn*7* transposition process plus a 5′ integron consisting of three resistance gene cassettes (*drfA1*, *sat2*, and *aadA1*) and the *Intl2* gene. These are essentially identical to an MGE previously reported from Argentina (Ramirez et al., 2005), but the element identified here is missing the 5′ end of the previously described element, consisting of three ORFs encoding resistance genes. In its place a novel 5′ region ∼6.9 kb in length is found, which harbors three genes related to a Tn*3* transposition machinery, a bla_{TEM1} resistance gene and two hypothetical ORFs (**Figures 5A,B**). At least eight strains (one from ST79 and seven from ST113) have this element inserted in a known hotspot for Tn*7* transposons, between genes *racE* (Glutamate racemase 1) and *glmS* (Glutamine–fructose-6-phosphate aminotransferase). Contigs encompassing the full length ∼19 Kb element, but missing *racE* and *glmS* flanking genes, were also generated from thirteen other strains from ST79 and ST113. Only fragments of this integron, split into many contigs, were found for the remaining strains from these two STs, probably due to the lack of proper assembly, but again the presence of the integron sequences remained restricted to both these STs only.

At least seven others different MGEs have some association to resistance genes. All 46 strains sequenced have an ISAba1 insertion upstream of the *ampC* (bla_{ADC}) gene (**Figure 6A**, indicated by black arrows in **Figure 3**), a carbapenem resistance gene. Moreover, an ISAba1 insertion could also be identified upstream of another carbapenem resistant gene variant the $bla_{OXA-169}$ gene (**Figure 6B**, also indicated in **Figure 3**) found in Acb_16 (ST1) and Acb_24 (ST113). Yet another carbapenem resistance gene linked to a MGE is the bla_{OXA-72} (a bla_{OXA-24} gene variant), encoding a OXA-72 carbapenemase, associated with a replication initiation gene (*repE*) and flanked by two transporter (*tonB*) genes and two ISAba13 insertion sequences 151 bp in length (**Figure 6C**, light green arrows in **Figure 3**). Those IS could not be identified as full length elements (IS containing coding region and terminal repeats) and hence were fragmented at the end of assembled contigs, since the limited size of the sequenced fragments and the presence of multiple identical elements prevented an adequate assemblage of the fragments downstream. However, their 151 bp extremities were intact, indicating that this composite IS is probably capable of mobilization in the presence of a transposase *in trans* encoded by any coding full-length element inserted in the genome and independently of any transposases being encoded by a downstream ORF.

Twenty-six strains from three different STs (ST15, ST79, and ST113) showed the aminoglycoside resistance gene *aph3* flanked by two ISAba125 fragments ∼140 bp long, also suggesting a potential mobilizable unity in the presence of transposases (**Figure 6D**, light gray arrows in **Figure 3**). In Acb_18 (ST79), a cassette of three resistance genes (*strB*, *strA*, and *floR*), the first two of which are associated with resistance to streptomycin, were found in association to an integrase, a transposase and a 5′ ISVsa3 motif 288 bp long (**Figure 6E**, dark green arrows in **Figure 3**).

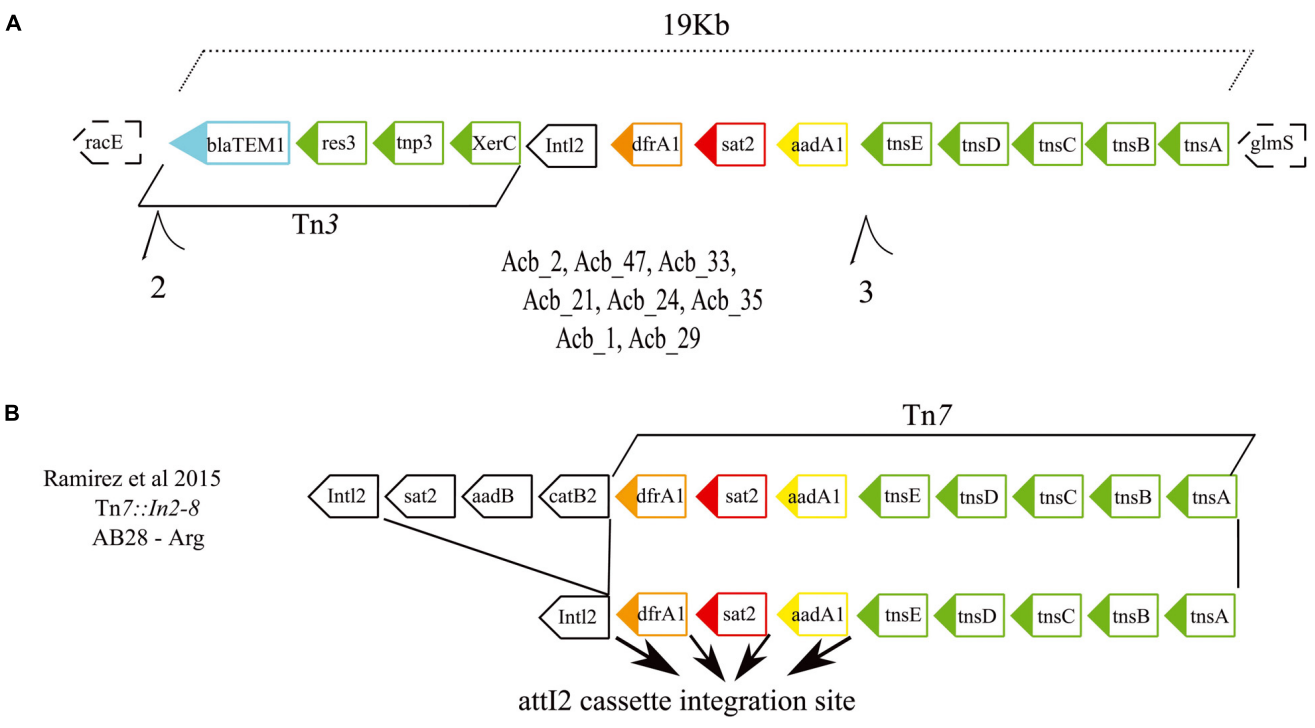

FIGURE 5 | Gene structure of the novel Tn*7*-Tn*3* transposable element. **(A)** Schematic representation of the integron discovered in this study formed by the fused Tn*7* and Tn*3* transposons found in the American STs 79 and 113. The dashed boxes correspond to the integron flanking genes. **(B)** Schematic representations of the previously described Tn*7* transposons (Ramirez et al., 2005) related to the one reported here. Such integrons carry four resistance genes highlighted in light blue, orange, red, and yellow. Genes responsible for the transposition/recombination process are in green. Black arrows denote the *attI2* cassette integration site.

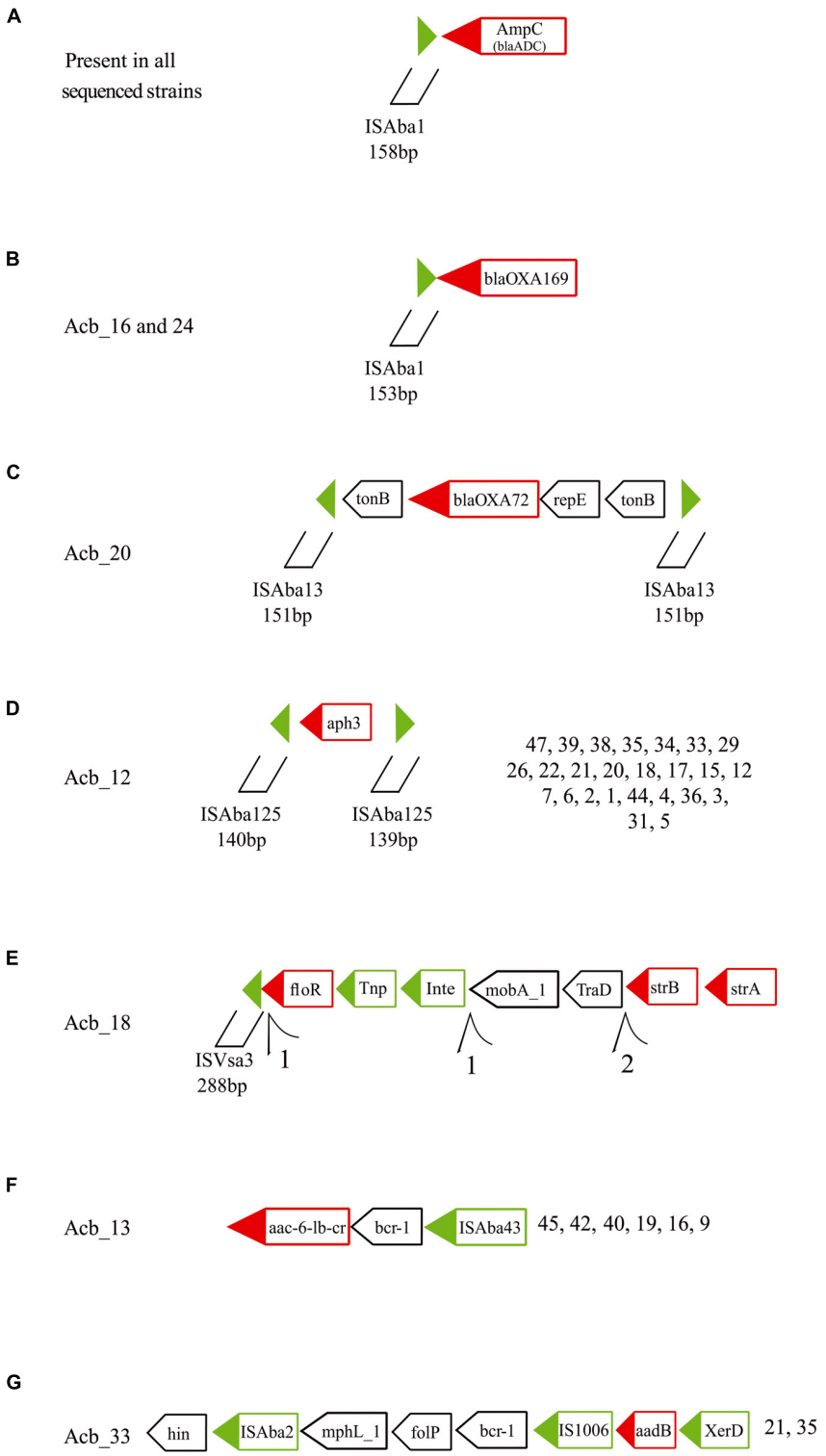

FIGURE 6 | Schematic representation of other resistance genes associated with transposable elements found in the *A. baumannii* strains sequenced in this study. Green triangles are inverted terminal repeats of insertion sequences flanking resistance genes. Green boxes are genes related with the transposition process and red boxes are resistance and virulence genes. *Tnp*, transposase; *Int*, Integrase; and *XerD*, tyrosine recombinase. Further structures of selected resistance genes and associated TEs can be found in the **Supplementary Figure S6**. **(A)** The *ampC* (bla_{ADC}) gene and its upstream ISAba1. **(B)** The $bla_{OXA-169}$ gene with the identified upstream ISAba1. **(C)** The bla_{OXA-72} gene with flanking genes and ISAba13 insertions. **(D)** The *aph3* gene with flanking ISAba125 fragments. **(E)** The *strB*, *strA* and *floR* genes with associated ISVsa3 motifs. **(F)** The *acc-6-lb-c* and *bcr-1* genes and their association with ISAba43. **(G)** The *aadB* and proximal genes in association with ISAba2 and IS1006.

Several rearrangements and fragmented contigs related to this cassette were also observed, mainly in assemblies from other ST79 strains (exemplified in the **Supplementary Figure S6A**). Another aminoglycoside resistance gene, *acc-6-lb-cr*, was found associated with an ISAba43 in all ST1 and ST881 strains (**Figure 6F**, yellow arrows in **Figure 3**) and the same is also likely the case for a single ST113 strain (Acb_8), but here the sequence data is incomplete. In between the *acc-6-lb-c* gene and ISAba43 one more antibiotic resistance gene was always found, *bcr-1*, and indeed seven other strains belonging to ST79 have the *brc-1* gene next to the ISAba43 insertion in the absence of *acc-6-lb-c* (**Supplementary Figure S6B**). In addition, the 5′ upstream region of the *brc-1* gene is flanked by a mutator transposase coding sequence, reinforcing that there is a distinct *brc-1*/ISAba43 specific structure within the genomes from these strains. Yet another aminoglycoside resistance gene, *aadB* found only in ST113 strains, was identified with two insertion sequences, *ISAba2* and *IS1006* (**Figure 6G**, pink arrows in **Figure 3**), along with the gene encoding the tyrosine recombinases XerD and also a *brc-1* gene (**Supplementary Figure S6C**).

The contigs assembled here for the various *A. baumannii* strains, using short reads, were generally not long enough to produce or identify complete or near-complete plasmids associated with the sequenced strains. For the $bla_{\text{OXA-253}}$ gene, however, whose genetic environment has been studied in more detail in these strains and has been the focus of a separate publication by us, a plasmid localization for this gene from most, if not all, strains is validated by the analysis carried out, since contigs encompassing up to 97% of the previously described plasmid were found (de Sá Cavalcanti et al., 2017). This is compatible with the broad distribution of the $bla_{\text{OXA-253}}$ gene among five of the six STs investigated here, with the sole exception of ST1. Nevertheless, at this stage, plasmid localization could not be implied from the sequenced genomes for other genes known to be plasmid-based.

DISCUSSION

The data reported here confirms that at least four different CCs are circulating in the different hospitals from a single metropolitan area from Northeastern Brazil, with no obvious association found between any of the CCs/STs and variables such as hospitals, collection years or sampling methods. This is in contrast with other studies which usually reports outbreaks of either a single ST or closely related ones (Mosqueda et al., 2013; Wright et al., 2014; Li et al., 2015; Ou et al., 2015), although a recent report from Latin America has also found multiple lineages of MDR *A. baumannii* coexisting within the same hospital (Graña-Miraglia et al., 2020). Among those CCs founds here, CC1, CC15, and CC113 (ST25) are considered globally spread *Acinetobacter* clonal complexes, having been isolated from different parts of the world for more than 20 years (Diancourt et al., 2010; Di Nocera et al., 2011; Di Popolo et al., 2011; Karah et al., 2012; Sahl et al., 2015; Gaiarsa et al., 2019). In contrast, CC79 strains have been described mostly from North and South America but also in Europe (Karah et al., 2012; Villalón et al., 2013; Chagas et al., 2014; Wright et al., 2014; Bado et al., 2018; Da Silva et al., 2018; Levy-Blitchtein et al., 2018; Graña-Miraglia et al., 2020), while ST113 (also belonging to CC113) was described originally in the Middle East but has more recently mostly been reported from South America (Bonnin et al., 2013; Clímaco et al., 2013; Girlich et al., 2014). Here, the availability of draft genome sequences from multiple strains from various STs and clonal complexes co-existing in the same environments allowed a large-scale comparison of the multiple elements associated with their antibiotic resistance and virulence. Our results confirm previous analyses highlighting the diversity in *A. baumannii* gene content and in antibiotic-resistant genes as well as the high efficiency with which this bacteria acquires novel genetic elements (Imperi et al., 2011; Liu et al., 2014; Wright et al., 2014; Chan et al., 2015). It also suggests that the ability to exchange certain genetic elements between strains is not uniform for all STs, with strains from some STs being more prone to exchange these elements than others, as discussed below.

Multidrug resistant *A. baumannii* is a serious threat to immunologically compromised and critically ill patients under intensive care worldwide (Nowak and Paluchowska, 2016; Wong et al., 2017). This is also the case in Brazil and researchers have been using PCR based detection methods in order to access the resistance gene profile of hospital isolates (Adams-Haduch et al., 2008; Clímaco et al., 2013; Chagas et al., 2014; Da Silva et al., 2018) and even in isolates from environmental samples (Turano et al., 2016). Accumulation of resistance determinants to multiple classes of antimicrobials was observed among the genomes sequenced here, some clearly capable of being transferred between strains, independent of their ST, while others more associated with specific STs. Indeed, four resistance genes (*frA1*, *sat2*, *aadA1*, and $bla_{\text{TEM-1}}$) were found to be inherited together due to the new MGE found here only in ST79 and ST113 strains and related to an element described from Argentina, carrying six resistance genes (Ramirez et al., 2005). Likewise, a wide distribution was observed for the $bla_{\text{OXA-253}}$ gene, more recently described from Honduras, Brazil, and Peru (Girlich et al., 2014; Zander et al., 2014; Levy-Blitchtein et al., 2018). This gene, most likely plasmid encoded, was found among different STs comprising >70% of the *A. baumannii* strains sequenced here, as previously reported (de Sá Cavalcanti et al., 2017). Indeed, the recent expansion of the $bla_{\text{OXA-253}}$ gene and its replacement of $bla_{\text{OXA-72}}$ could be more clearly observed here in the ST79 strains isolated from different time periods, highlighting the speed with which these MGEs and associated resistance genes can be acquired. In contrast, the data available suggests that the genomic islands, although present in many of the strains sequenced here, might not be the main determinant for the spread of resistance, due to the lack of identifiable resistance genes in the islands found here. This is even more so for many of the ST79- and ST113-resistant strains, where genomic islands could not be found, in agreement with what has been previously reported with ST79 strains from North America (Wright et al., 2014).

In most instances the genetic analysis carried out here is consistent with the antibiotic resistance profile observed for the

strains included in the present study. The presence of different $bla_{\text{OXA-51}}$-like allelic variant associated with specific STs is in agreement with previous reports, where, $bla_{\text{OXA-69}}$ has been found in ST1 strains, for example, while $bla_{\text{OXA-69}}$ is associated with ST79, $bla_{\text{OXA-51}}$ with ST15 and $bla_{\text{OXA-64}}$ with ST25 (Karah et al., 2012). As expected, an acquired class D β-lactamase gene was nearly always found in all carbapenem resistant strains, such as $bla_{\text{OXA-72}}$, $bla_{\text{OXA-253}}$ and so on. Other genes associated with the aminoglycoside and fluoroquinolone resistance profiles were also observed for nearly all strains sequenced. However, some cases of antibiotic resistance in strains closely related to susceptible ones could not be linked to specific genes and these should be better investigated, since they might be associated with novel, yet uncharacterized, resistance mechanisms.

A noteworthy observation reported here is the identification of specific MGEs, as well as virulence and resistance genes, shared between the ST79 and ST113 strains only. Strains from ST113 are more distantly related from the ST79 strains than, for instance, the ST1 strains. However, the new Tn*7*-Tn*3* element, with associated resistance genes, is found only in the ST79 and ST113 strains. Likewise, the related KL13 genes associated with the K antigen synthesis, also likely interchanged between different *A. baumannii* strains, are only found in strains from these two STs and in none of the others investigated here. Other MGEs, however, are more widely distributed among the sequenced STs and more promiscuous, such as the MGE associated to $bla_{\text{OXA-253}}$ (de Sá Cavalcanti et al., 2017). Even then, however, there is a noticeable absence of this gene from the ST1 strains, some isolated in the same hospital and year than some of the ST79 ones. These results suggest selective gene exchanges between strains from specific STs, perhaps associated with the presence of specific shared genetic elements. Indeed, a search for genes common only to strains from ST79 and ST113 revealed 159 genes shared by strains from these two STs which are not found in the other genomes investigated here. In contrast, only 34 genes are found in common between the ST79 and the more closely related ST1, with 29 genes in common between ST113 and ST1. It is possible then that among the genes shared only by the ST79 and ST113 strains there might be some involved with specific genetic exchange mechanisms that need to be further investigated.

Overall, our data revealed that in Recife, hospital physicians might be dealing with *A. baumannii* outbreaks of multiple clonal complexes, and which vary substantially in their resistance and virulence profile. The trend observed for the recent spread of the $bla_{\text{OXA-253}}$ gene and maybe the genes associated with quinolone resistance, associated with the continuous increase in bacterial resistance in the clinics, further restricts the therapeutic options available for empirical treatment and the chance of achieving clinical success in infections caused by *A. baumannii*. This study emphasizes once again the need for the diversity in *A. baumannii* resistance mechanisms to be carefully considered in future monitoring strategies and in the decision-making regarding patients' treatment by practicing physicians. It also highlights the need for further monitoring of *A. baumannii* isolated from the hospitals through the use of genetic methods, in addition to phenotypic tests.

DATA AVAILABILITY STATEMENT

The datasets generated for this study can be found in the https://www.ebi.ac.uk/ena/browser/view/PRJEB12754.

AUTHOR CONTRIBUTIONS

NL, AA, MM, TL-B, and Od-M-N contributed to the conception and design of the study. DX and IR carried out the antimicrobial susceptibility testing. CM-M and FS did all DNA extraction and the $bla_{\text{OXA-51}}$ gene amplification while CD, CM-M, and FS performed the whole-genome sequencing. AR and TC organized and curated the database and performed the initial bioinformatics analysis. CM-M, CC, CD, DX, DV, FS, GW, IR, LA, NL, MB, and MA-F contributed with the identification and analysis of different genes or gene sets. AR, CD, DX, FS, TC, and GW wrote sections of the preliminary document. Od-M-N reviewed and edited the manuscript. All authors reviewed and approved the submitted version.

FUNDING

This work was mainly supported by institutional funding from the Oswaldo Cruz Foundation (Fiocruz, Brazil). NL also received financial support from PROEP/FACEPE/Fiocruz (APQ-1628-2.12/15). CM-M was funded by a PNPD/CAPES/PPGBBS institutional grant. Studentships and fellowships to the graduate students and post-doctoral fellows were granted by the Ministry of Education and the Pernambuco state funding agencies, Capes and FACEPE, respectively.

ACKNOWLEDGMENTS

We thank the Core Facilities Program from IAM/Fiocruz for the use of its Next-Generation DNA Sequencing facilities as well as the Bioinformatic support. We thank the Centro de Tecnologias Estratégicas do Nordeste (CETENE), for assistance with bacterial species identification through MALDI-TOF. This work could not be carried out without the support by Dr. Maria Amélia Maciel and the laboratories of clinical microbiology from the hospitals involved, responsible for the collection of clinical samples and bacterial isolation.

SUPPLEMENTARY MATERIAL

The Supplementary Material for this article can be found online at: https://www.frontiersin.org/articles/10.3389/fmicb.2020.01176/full#supplementary-material

FIGURE S1 | Evaluation of overall gene content from the genomes sequenced in this study. **(A)** Cumulative curve of *Acinetobacter baumannii* pan-genome using as proxy the number of new ortholog group of genes detected by ORTHOMCL software with 100 replicates. **(B)** Cumulative graph showing the number of unique genes after the addition of each new strain, 1,000 replicates.

FIGURE S2 | Full list of mobile genetic elements (MGEs) characterized by the homology search with ISFinder database are displayed in the right side of the figure and including genomic islands, transposons and insertion sequences (IS), the latter sorted according to the IS family to which they belong to. Since the MGEs can be found in multiple copies in each genome, the width of the colored rectangles reflects the number of copies found for each. The STs follow the colors displayed in **Figure 1**.

FIGURE S3 | Regions from AbaR0 genomic islands found in the five ST1 and two ST881 strains. **(A)** Circular plot with regions with high identity from pair wise Blast comparisons between a reference AbaR0 island first detected in a *A. baumannii* strain from Australia (Hamidian et al., 2014) and the contigs derived from the sequenced Recife strains. **(B)** Striking examples of the AbaR0-like island dynamics found in a single contig flanked by the *comM* gene. A schematic representation of the AbaR0 island backbone transposons found in Acb_19 and Acb_13 (both ST1 strains) as well as Acb_22, Acb_18, and Acb_17 (all from ST79) is shown. Green boxes are MGEs related genes, red boxes define the resistance related genes, and yellow boxes represent the genes found in the islands sequenced in this study, but which are absent from the original AbaR0. It is important to note that, unless stated, this representation of the segments homologous to the AbaR0 and AbGRI1 islands found in the sequenced strains should not be interpreted as contiguous contigs. Only the presence or absence of genes originally found in an island should be considered. Any new gene present only in the newly sequenced strains will not be depicted in this figure.

FIGURE S4 | Regions from AbGRI1 genomic islands found in ST1 and ST79 strains. Only the presence or absence of genes originally found in an island should be considered. Any new gene present only in the newly sequenced strains will not be depicted in this figure.

FIGURE S5 | Regions from AbGRI1 genomic islands homologs found in ST113 and ST15 strains. Only the presence or absence of genes originally found in an island should be considered. Any new gene present only in the newly sequenced strains will not be depicted in this figure. Based on this analysis, for the ST113 strains, only Acb_21, Acb_33, and Acb_38 strains were considered to have true segments of an AbGRI1 island.

FIGURE S6 | Other resistance and virulence genes found associated (in the same contigs) with transposition related genes and their assembly variability among the strains sequenced in this study. **(A)** Variations associated with the streptomycin (*strB* and *strA*) resistance genes, linked or not to ISVsa3 and transposable elements. **(B)** Variations associated with the *bcr-1* gene and the ISAba43 insertion. **(C)** Alternative profiles for the elements flanking the *aadB* resistance gene.

TABLE S1 | Summary of the antimicrobial susceptibility profile exhibited by the single *Acinetobacter nosocomialis* and 45 *Acinetobacter baumannii* clinical strains investigated here against 11 different antimicrobial agents using the CLSI broth microdilution method. The background colors are derived from **Figure 2** and represent the different STs to which the 45 *A. baumannii* clinical strains belong.

TABLE S2 | Summary of the assembly and annotation statistics for the genomes from all strains sequenced in this study.

TABLE S3 | Summary of the ST identification data for all strains sequenced in this study, with counts for shared single copy orthologs or lineage-specific core genes.

TABLE S4 | Summary of the bla_{ADC}/*ampC* identification analysis data for all strains sequenced in this study, comparing the identified alleles with the $bla_{\text{OXA-51}}$-like alleles.

TABLE S5 | Comparison of the ST identification and antimicrobial susceptibility profile for all 46 *A. baumannii* strains sequenced here.

TABLE S6 | Mutations associated with the quinolone-resistance determinant region for the sequenced *Acinetobacter* strains.

TABLE S7 | Summary of the gene identification data for the OC and K antigen gene clusters for the various sequenced *Acinetobacter* strains with definition of likely OCL and KL-types. The relevant output results from the *Kaptive* tool (Wick et al., 2018) using the curated databases of annotated reference sequences for *A. baumannii* K and OC loci (Wyres et al., 2020) were added to the table with the relevant OCL and KL-types listed, as shown also in **Figure 4**.

REFERENCES

Adams-Haduch, J. M., Paterson, D. L., Sidjabat, H. E., Pasculle, A. W., Potoski, B. A., Muto, C. A., et al. (2008). Genetic basis of multidrug resistance in *Acinetobacter baumannii* clinical isolates at a tertiary medical center in Pennsylvania. *Antimicrob. Agents Chemother.* 52, 3837–3843. doi: 10.1128/AAC.00570-08

Akhter, S., Aziz, R. K., and Edwards, R. A. (2012). PhiSpy: a novel algorithm for finding prophages in bacterial genomes that combines similarity-and composition-based strategies. *Nucleic Acids Res.* 40:e126. doi: 10.1093/nar/gks406

Allen, J. M., Huang, D. I., Cronk, Q. C., and Johnson, K. P. (2015). aTRAM - automated target restricted assembly method: a fast method for assembling loci across divergent taxa from next-generation sequencing data. *BMC Bioinformatics* 16:98. doi: 10.1186/s12859-015-0515-2

Altschul, S. F., Gish, W., Miller, W., Myers, E. W., and Lipman, D. J. (1990). Basic local alignment search tool. *J. Mol. Biol.* 215, 403–410. doi: 10.1016/S0022-2836(05)80360-2

Bado, I., Papa-Ezdra, R., Delgado-Blas, J. F., Gaudio, M., Gutiérrez, C., Cordeiro, N. F., et al. (2018). Molecular characterization of carbapenem-resistant *Acinetobacter baumannii* in the intensive care unit of Uruguay's University hospital identifies the first rmtC gene in the species. *Microb. Drug Resist.* 24, 1012–1019. doi: 10.1089/mdr.2017.0300

Bartual, S. G., Seifert, H., Hippler, C., Luzon, M. A. D., Wisplinghoff, H., and Rodriguez-Valera, F. (2005). Development of a Multilocus Sequence Typing scheme for characterization of clinical isolates of *Acinetobacter baumannii*. *J. Clin. Microbiol.* 43, 4382–4390. doi: 10.1128/JCM.43.9.4382-4390.2005

Bateman, A. (2002). The Pfam protein families database. *Nucleic Acids Res.* 30, 276–280. doi: 10.1093/nar/30.1.276

Bi, D., Xie, R., Zheng, J., Yang, H., Zhu, X., Ou, H.-Y., et al. (2019). Large-scale identification of AbaR-type Genomic Islands in *Acinetobacter baumannii* reveals diverse insertion sites and clonal lineage-specific antimicrobial resistance gene profiles. *Antimicrob. Agents Chemother.* 63:e02526-18. doi: 10.1128/AAC.02526-18

Blackwell, G. A., Nigro, S. J., and Hall, R. M. (2016). Evolution of AbGRI2-0, the progenitor of the AbGRI2 resistance island in global clone 2 of *Acinetobacter baumannii*. *Antimicrob. Agents Chemother.* 60, 1421–1429. doi: 10.1128/AAC.02662-15

Bolger, A. M., Lohse, M., and Usadel, B. (2014). Trimmomatic: a flexible trimmer for Illumina sequence data. *Bioinformatics* 30, 2114–2120. doi: 10.1093/bioinformatics/btu170

Bonnin, R. A., Rotimi, V. O., Al Hubail, M., Gasiorowski, E., Al Sweih, N., Nordmann, P., et al. (2013). Wide dissemination of GES-type carbapenemases in *Acinetobacter baumannii* isolates in Kuwait. *Antimicrob. Agents Chemother.* 57, 183–188. doi: 10.1128/AAC.01384-12

Carruthers, M. D., Nicholson, P. A., Tracy, E. N., and Munson, R. S. (2013). *Acinetobacter baumannii* utilizes a Type VI Secretion System for bacterial competition. *PLoS One* 8:e59388. doi: 10.1371/journal.pone.0059388

Catel-Ferreira, M., Coadou, G., Molle, V., Mugnier, P., Nordmann, P., Siroy, A., et al. (2011). Structure–function relationships of CarO, the carbapenem resistance-associated outer membrane protein of *Acinetobacter baumannii*. *J. Antimicrob. Chemother.* 66, 2053–2056. doi: 10.1093/jac/dkr267

Chagas, T. P. G., Carvalho, K. R., de Oliveira Santos, I. C., Carvalho-Assef, A. P. D. D., and Asensi, M. D. (2014). Characterization of carbapenem-resistant *Acinetobacter baumannii* in Brazil (2008-2011): countrywide spread of OXA-23-producing clones (CC15 and CC79). *Diagn. Microbiol. Infect. Dis.* 79, 468–472. doi: 10.1016/j.diagmicrobio.2014.03.006

Chagas, T. P. G., Silveira, M. C., Albano, R. M., Carvalho-Assef, A. P. D., and Asensi, M. D. (2015). Draft genome sequence of a multidrug-resistant *Acinetobacter baumannii* ST15 (CC15) isolated from Brazil. *Mem. Inst. Oswaldo Cruz* 110, 691–692. doi: 10.1590/0074-02760150158

Chan, A. P., Sutton, G., DePew, J., Krishnakumar, R., Choi, Y., Huang, X.-Z., et al. (2015). A novel method of consensus pan-chromosome assembly and large-scale comparative analysis reveal the highly flexible pan-genome

of *Acinetobacter baumannii*. *Genome Biol.* 16:143. doi: 10.1186/s13059-015-0701-6

Chen, L. (2004). VFDB: a reference database for bacterial virulence factors. *Nucleic Acids Res.* 33, D325–D328. doi: 10.1093/nar/gki008

Clímaco, E. C., Oliveira, M. L., de Pitondo-Silva, A., Oliveira, M. G., Medeiros, M., Lincopan, N., et al. (2013). Clonal complexes 104, 109 and 113 playing a major role in the dissemination of OXA-carbapenemase-producing *Acinetobacter baumannii* in Southeast Brazil. *Infect. Genet. Evol.* 19, 127–133. doi: 10.1016/j.meegid.2013.06.024

Clinical and Laboratory Standards Institute [CLSI] (2015). *Performance Standards for Antimicrobial Disk Susceptibility Tests; Approved Standard—Twelfth Edition*. Wayne, PA: CLSI.

Clinical and Laboratory Standards Institute [CLSI] (2018). *Performance Standards for Antimicrobial Susceptibility Testing. 28th ed. CLSI supplement M100*. Wayne, PA: Clinical and Laboratory Standards Institute.

Da Silva, K. E., Maciel, W. G., Croda, J., Cayˆo, R., Ramos, A. C., De Sales, R. O., et al. (2018). A high mortality rate associated with multidrug-resistant *Acinetobacter baumannii* ST79 and ST25 carrying OXA-23 in a Brazilian intensive care unit. *PLoS One* 13:e0209367. doi: 10.1371/journal.pone.0209367

Darling, A. C. E. (2004). Mauve: multiple alignment of conserved genomic sequence with rearrangements. *Genome Res.* 14, 1394–1403. doi: 10.1101/gr.2289704

De Gregorio, E., Del Franco, M., Martinucci, M., Roscetto, E., Zarrilli, R., and Di Nocera, P. P. (2015). Biofilm-associated proteins: news from *Acinetobacter*. *BMC Genomics* 16:933. doi: 10.1186/s12864-015-2136-6

de Sá Cavalcanti, F. L., Mendes-Marques, C. L., Vasconcelos, C. R. D. S., de Lima Campos, T., Rezende, A. M., Xavier, D. E., et al. (2017). High frequency of OXA-253-producing *Acinetobacter baumannii* in different hospitals in Recife, Brazil. *Antimicrob. Agents Chemother.* 61, e1309–e1316. doi: 10.1128/AAC.01309-16

Di Nocera, P., Rocco, F., Giannouli, M., Triassi, M., and Zarrilli, R. (2011). Genome organization of epidemic *Acinetobacter baumannii* strains. *BMC Microbiol.* 11:224. doi: 10.1186/1471-2180-11-224

Di Popolo, A., Giannouli, M., Triassi, M., Brisse, S., and Zarrilli, R. (2011). Molecular epidemiological investigation of multidrug-resistant *Acinetobacter baumannii* strains in four Mediterranean countries with a multilocus sequence typing scheme. *Clin. Microbiol. Infect.* 17, 197–201. doi: 10.1111/j.1469-0691.2010.03254.x

Diancourt, L., Passet, V., Nemec, A., Dijkshoorn, L., and Brisse, S. (2010). The population structure of *Acinetobacter baumannii*: expanding multiresistant clones from an ancestral susceptible genetic pool. *PLoS One* 5:e10034. doi: 10.1371/journal.pone.0010034

Elhosseiny, N. M., and Attia, A. S. (2018). *Acinetobacter*: an emerging pathogen with a versatile secretome. *Emerg. Microbes Infect.* 7, 1–15. doi: 10.1038/s41426-018-0030-4

Esterly, J. S., Richardson, C. L., Eltoukhy, N. S., Qi, C., and Scheetz, M. H. (2011). Genetic mechanisms of antimicrobial resistance of *Acinetobacter baumannii*. *Ann. Pharmacother.* 45, 218–228. doi: 10.1345/aph.1P084

Fernández-Cuenca, F., Martínez-Martínez, L., Conejo, M. C., Ayala, J. A., Perea, E. J., and Pascual, A. (2003). Relationship between beta-lactamase production, outer membrane protein and penicillin-binding protein profiles on the activity of carbapenems against clinical isolates of *Acinetobacter baumannii*. *J. Antimicrob. Chemother.* 51, 565–574. doi: 10.1093/jac/dkg097

Gaiarsa, S., Biffignandi, G. B., Esposito, E. P., Castelli, M., Jolley, K. A., Brisse, S., et al. (2019). Comparative analysis of the two *Acinetobacter baumannii* multilocus sequence typing (MLST) schemes. *Front. Microbiol.* 10:930. doi: 10.3389/fmicb.2019.00930

Geisinger, E., and Isberg, R. R. (2015). Antibiotic modulation of capsular exopolysaccharide and virulence in *Acinetobacter baumannii*. *PLoS Pathog.* 11:e1004691. doi: 10.1371/journal.ppat.1004691

Girlich, D., Damaceno, Q. S., Oliveira, A. C., and Nordmann, P. (2014). OXA-253, a variant of the carbapenem-hydrolyzing class D beta-lactamase OXA-143 in *Acinetobacter baumannii*. *Antimicrob. Agents Chemother.* 58, 2976–2978. doi: 10.1128/AAC.02640-13

Graña-Miraglia, L., Evans, B. A., López-Jácome, L. E., Hernández-Durán, M., Colín-Castro, C. A., Volkow-Fernández, P., et al. (2020). Origin of OXA-23 variant OXA-239 from a recently emerged lineage of *Acinetobacter baumannii* international clone V. *mSphere* 5, 1–9. doi: 10.1128/msphere.00801-19

Hamidian, M., and Hall, R. M. (2018). The AbaR antibiotic resistance islands found in *Acinetobacter baumannii* global clone 1 – Structure, origin and evolution. *Drug Resist. Updat.* 41, 26–39. doi: 10.1016/j.drup.2018.10.003

Hamidian, M., Holt, K. E., Pickard, D., Dougan, G., and Hall, R. M. (2014). A GC1 *Acinetobacter baumannii* isolate carrying AbaR3 and the aminoglycoside resistance transposon TnaphA6 in a conjugative plasmid. *J. Antimicrob. Chemother.* 69, 955–958. doi: 10.1093/jac/dkt454

Hamidian, M., and Nigro, S. J. (2019). Emergence, molecular mechanisms and global spread of carbapenem-resistant *Acinetobacter baumannii*. *Microb. Genomics* 5:e000306. doi: 10.1099/mgen.0.000306

Hamidian, M., Nigro, S. J., and Hall, R. M. (2012). Variants of the gentamicin and tobramycin resistance plasmid pRAY are widely distributed in *Acinetobacter*. *J. Antimicrob. Chemother.* 67, 2833–2836. doi: 10.1093/jac/dks318

Harding, C. M., Hennon, S. W., and Feldman, M. F. (2018). Uncovering the mechanisms of *Acinetobacter baumannii* virulence. *Nat. Rev. Microbiol.* 16, 91–102. doi: 10.1038/nrmicro.2017.148

Holt, K., Kenyon, J. J., Hamidian, M., Schultz, M. B., Pickard, D. J., Dougan, G., et al. (2016). Five decades of genome evolution in the globally distributed, extensively antibiotic-resistant *Acinetobacter baumannii* global clone 1. *Microb. Genomics* 2:e000052. doi: 10.1099/mgen.0.000052

Hu, W. S., Yao, S.-M., Fung, C.-P., Hsieh, Y.-P., Liu, C.-P., and Lin, J.-F. (2007). An OXA-66/OXA-51-like carbapenemase and possibly an efflux pump are associated with resistance to imipenem in *Acinetobacter baumannii*. *Antimicrob. Agents Chemother.* 51, 3844–3852. doi: 10.1128/AAC.01512-06

Imperi, F., Antunes, L. C. S., Blom, J., Villa, L., Iacono, M., Visca, P., et al. (2011). The genomics of *Acinetobacter baumannii*: insights into genome plasticity, antimicrobial resistance and pathogenicity. *IUBMB Life* 63, 1068–1074. doi: 10.1002/iub.531

Inouye, M., Dashnow, H., Raven, L.-A., Schultz, M. B., Pope, B. J., Tomita, T., et al. (2014). SRST2: rapid genomic surveillance for public health and hospital microbiology labs. *Genome Med.* 6:90. doi: 10.1186/s13073-014-0090-6

Iwashkiw, J. A., Seper, A., Weber, B. S., Scott, N. E., Vinogradov, E., Stratilo, C., et al. (2012). Identification of a general O-linked protein glycosylation system in *Acinetobacter baumannii* and its role in virulence and biofilm formation. *PLoS Pathog.* 8:e1002758. doi: 10.1371/journal.ppat.1002758

Jeon, J. H., Hong, M. K., Lee, J. H., Lee, J. J., Park, K. S., Karim, A. M., et al. (2014). Structure of ADC-68, a novel carbapenem-hydrolyzing class C extended-spectrum β-lactamase isolated from *Acinetobacter baumannii*. *Acta Crystallogr. Sect. D Biol. Crystallogr.* 70, 2924–2936. doi: 10.1107/S1399004714019543

Karah, N., Jolley, K. A., Hall, R. M., and Uhlin, B. E. (2017). Database for the ampC alleles in *Acinetobacter baumannii*. *PLoS One* 12:e0176695. doi: 10.1371/journal.pone.0176695

Karah, N., Sundsfjord, A., Towner, K., and Samuelsen, Ø (2012). Insights into the global molecular epidemiology of carbapenem non-susceptible clones of *Acinetobacter baumannii*. *Drug Resist. Updat.* 15, 237–247. doi: 10.1016/j.drup.2012.06.001

Kenyon, J. J., and Hall, R. M. (2013). Variation in the complex carbohydrate biosynthesis loci of *Acinetobacter baumannii* genomes. *PLoS One* 8:e62160. doi: 10.1371/journal.pone.0062160

Kenyon, J. J., Kasimova, A. A., Notaro, A., Arbatsky, N. P., Speciale, I., Shashkov, A. S., et al. (2017). *Acinetobacter baumannii* K13 and K73 capsular polysaccharides differ only in K-unit side branches of novel non-2-ulosonic acids: di- N -acetylated forms of either acinetaminic acid or 8-epiacinetaminic acid. *Carbohydr. Res.* 452, 149–155. doi: 10.1016/j.carres.2017.10.005

Kenyon, J. J., Nigro, S. J., and Hall, R. M. (2014). Variation in the OC locus of *Acinetobacter baumannii* genomes predicts extensive structural diversity in the lipooligosaccharide. *PLoS One* 9:e107833. doi: 10.1371/journal.pone.0107833

Kenyon, J. J., Senchenkova, S. N., Shashkov, A. S., Shneider, M. M., Popova, A. V., Knirel, Y. A., et al. (2019). K17 capsular polysaccharide produced by *Acinetobacter baumannii* isolate G7 contains an amide of 2-acetamido-2-deoxy-d-galacturonic acid with d-alanine. *Int. J. Biol. Macromol.* 144, 857–862. doi: 10.1016/j.ijbiomac.2019.09.163

Krizova, L., Dijkshoorn, L., and Nemec, A. (2011). Diversity and evolution of AbaR genomic resistance islands in *Acinetobacter baumannii* strains of European clone I. *Antimicrob. Agents Chemother.* 55, 3201–3206. doi: 10.1128/AAC.00221-11

Leclercq, R., Cantón, R., Brown, D. F. J., Giske, C. G., Heisig, P., MacGowan, A. P., et al. (2013). EUCAST expert rules in antimicrobial susceptibility testing. *Clin. Microbiol. Infect.* 19, 141–160. doi: 10.1111/j.1469-0691.2011.03703.x

Lee, C.-R., Lee, J. H., Park, M., Park, K. S., Bae, I. K., Kim, Y. B., et al. (2017). Biology of *Acinetobacter baumannii*: pathogenesis, antibiotic resistance mechanisms, and prospective treatment options. *Front. Cell. Infect. Microbiol.* 7:55. doi: 10.3389/fcimb.2017.00055

Letunic, I., and Bork, P. (2016). Interactive tree of life (iTOL) v3: an online tool for the display and annotation of phylogenetic and other trees. *Nucleic Acids Res.* 44, W242–W245. doi: 10.1093/nar/gkw290

Leungtongkam, U., Thummeepak, R., Tasanapak, K., and Sitthisak, S. (2018). Acquisition and transfer of antibiotic resistance genes in association with conjugative plasmid or class 1 integrons of *Acinetobacter baumannii*. *PLoS One* 13:e0208468. doi: 10.1371/journal.pone.0208468

Levy-Blitchtein, S., Roca, I., Plasencia-Rebata, S., Vicente-Taboada, W., Velásquez-Pomar, J., Muñoz, L., et al. (2018). Emergence and spread of carbapenem-resistant *Acinetobacter baumannii* international clones II and III in Lima, Peru article. *Emerg. Microbes Infect.* 7:119. doi: 10.1038/s41426-018-0127-9

Li, H., Liu, F., Zhang, Y., Wang, X., Zhao, C., Chen, H., et al. (2015). Evolution of carbapenem-resistant *Acinetobacter baumannii* revealed through whole-genome sequencing and comparative genomic analysis. *Antimicrob. Agents Chemother.* 59, 1168–1176. doi: 10.1128/AAC.04609-14

Li, L., Stoeckert, C. J., and Roos, D. S. (2003). OrthoMCL: identification of ortholog groups for eukaryotic genomes. *Genome Res.* 13, 2178–2189. doi: 10.1101/gr.1224503

Liu, B., Zheng, D., Jin, Q., Chen, L., and Yang, J. (2019). VFDB 2019: a comparative pathogenomic platform with an interactive web interface. *Nucleic Acids Res.* 47, D687–D692. doi: 10.1093/nar/gky1080

Liu, F., Zhu, Y., Yi, Y., Lu, N., Zhu, B., and Hu, Y. (2014). Comparative genomic analysis of *Acinetobacter baumannii* clinical isolates reveals extensive genomic variation and diverse antibiotic resistance determinants. *BMC Genomics* 15:1163. doi: 10.1186/1471-2164-15-1163

Marí-Almirall, M., Cosgaya, C., Higgins, P. G., Van Assche, A., Telli, M., Huys, G., et al. (2017). MALDI-TOF/MS identification of species from the *Acinetobacter baumannii* (Ab) group revisited: inclusion of the novel *A. seifertii* and *A. dijkshoorniae* species. *Clin. Microbiol. Infect.* 23, 210.e1–210.e10. doi: 10.1016/j.cmi.2016.11.020

McConnell, M. J., Actis, L., and Pachón, J. (2013). *Acinetobacter baumannii*: human infections, factors contributing to pathogenesis and animal models. *FEMS Microbiol. Rev.* 37, 130–155. doi: 10.1111/j.1574-6976.2012.00344.x

McKay, S. J., Vergara, I. A., and Stajich, J. E. (2010). Using the generic synteny browser (GBrowse_syn). *Curr. Protoc. Bioinformatics* 31, 9.12.1–9.12.25.

Morris, F. C., Dexter, C., Kostoulias, X., Uddin, M. I., and Peleg, A. Y. (2019). The mechanisms of disease caused by *Acinetobacter baumannii*. *Front. Microbiol.* 10:1601. doi: 10.3389/fmicb.2019.01601

Mosqueda, N., Espinal, P., Cosgaya, C., Viota, S., Plasensia, V., Álvarez-Lerma, F., et al. (2013). Globally expanding carbapenemase finally appears in Spain: nosocomial outbreak of *Acinetobacter baumannii* producing plasmid-encoded OXA-23 in Barcelona, Spain. *Antimicrob. Agents Chemother.* 57, 5155–5157. doi: 10.1128/AAC.01486-13

Naas, T., Oueslati, S., Bonnin, R. A., Dabos, M. L., Zavala, A., Dortet, L., et al. (2017). Beta-lactamase database (BLDB) – structure and function. *J. Enzyme Inhib. Med. Chem.* 32, 917–919. doi: 10.1080/14756366.2017.1344235

Nigro, S. J., Farrugia, D. N., Paulsen, I. T., and Hall, R. M. (2013). A novel family of genomic resistance islands, AbGRI2, contributing to aminoglycoside resistance in *Acinetobacter baumannii* isolates belonging to global clone 2. *J. Antimicrob. Chemother.* 68, 554–557. doi: 10.1093/jac/dks459

Nowak, P., and Paluchowska, P. (2016). *Acinetobacter baumannii*: biology and drug resistance - role of carbapenemases. *Folia Histochem. Cytobiol.* 54, 61–74. doi: 10.5603/FHC.a2016.0009

Ou, H.-Y., Kuang, S. N., He, X., Molgora, B. M., Ewing, P. J., Deng, Z., et al. (2015). Complete genome sequence of hypervirulent and outbreak-associated *Acinetobacter baumannii* strain LAC-4: epidemiology, resistance genetic determinants and potential virulence factors. *Sci. Rep.* 5:8643. doi: 10.1038/srep08643

Pagano, M., Rocha, L., Sampaio, J. L. M., Martins, A. F., and Barth, A. L. (2017). Emergence of OXA-72-producing *Acinetobacter baumannii* belonging to high-risk clones (CC15 and CC79) in different Brazilian states. *Infect. Control Hosp. Epidemiol.* 38, 252–254. doi: 10.1017/ice.2016.287

Patel, G., and Bonomo, R. A. (2013). "Stormy waters ahead": global emergence of carbapenemases. *Front. Microbiol.* 4:48. doi: 10.3389/fmicb.2013.00048

Penwell, W. F., Arivett, B. A., and Actis, L. A. (2012). The *Acinetobacter baumannii entA* gene located outside the Acinetobactin cluster is critical for siderophore production, iron acquisition and virulence. *PLoS One* 7:e36493. doi: 10.1371/journal.pone.0036493

Piperaki, E.-T., Tzouvelekis, L. S., Miriagou, V., and Daikos, G. L. (2019). Carbapenem-resistant *Acinetobacter baumannii*: in pursuit of an effective treatment. *Clin. Microbiol. Infect.* 25, 951–957. doi: 10.1016/j.cmi.2019.03.014

Pogue, J. M., Mann, T., Barber, K. E., and Kaye, K. S. (2013). Carbapenem-resistant *Acinetobacter baumannii*: epidemiology, surveillance and management. *Expert Rev. Anti. Infect. Ther.* 11, 383–393. doi: 10.1586/eri.13.14

Qi, J., Luo, H., and Hao, B. (2004). CVTree: a phylogenetic tree reconstruction tool based on whole genomes. *Nucleic Acids Res.* 32, W45–W47. doi: 10.1093/nar/gkh362

Rahman, S., Ali, T., Ali, I., Khan, N. A., Han, B., and Gao, J. (2018). The growing genetic and functional diversity of extended spectrum Beta-Lactamases. *Biomed Res Int.* 2018:9519718. doi: 10.1155/2018/9519718

Ramirez, M. S., Quiroga, C., and Centron, D. (2005). Novel rearrangement of a Class 2 integron in two non-epidemiologically related isolates of *Acinetobacter baumannii*. *Antimicrob. Agents Chemother.* 49, 5179–5181. doi: 10.1128/AAC.49.12.5179-5181.2005

Retief, J. D. (2000). Phylogenetic analysis using PHYLIP. *Methods Mol. Biol.* 132, 243–258. doi: 10.1385/1-59259-192-2:243

Rocha, I. V., Xavier, D. E., Almeida, K. R. H., de Oliveira, S. R., and de Leal, N. C. (2018). Multidrug-resistant *Acinetobacter baumannii* clones persist on hospital inanimate surfaces. *Brazilian J. Infect. Dis.* 22, 438–441. doi: 10.1016/j.bjid.2018.08.004

Ruiz, M., Marti, S., Fernandez-Cuenca, F., Pascual, A., and Vila, J. (2007). Prevalence of ISAba1 in epidemiologically unrelated *Acinetobacter baumannii* clinical isolates. *FEMS Microbiol. Lett.* 274, 63–66. doi: 10.1111/j.1574-6968.2007.00828.x

Rutherford, K., Parkhill, J., Crook, J., Horsnell, T., Rice, P., Rajandream, M.-A., et al. (2000). Artemis: sequence visualization and annotation. *Bioinformatics* 16, 944–945. doi: 10.1093/bioinformatics/16.10.944

Sahl, J. W., Del Franco, M., Pournaras, S., Colman, R. E., Karah, N., Dijkshoorn, L., et al. (2015). Phylogenetic and genomic diversity in isolates from the globally distributed *Acinetobacter baumannii* ST25 lineage. *Sci. Rep.* 5, 1–12. doi: 10.1038/srep15188

Seemann, T. (2014). Prokka: rapid prokaryotic genome annotation. *Bioinformatics* 30, 2068–2069. doi: 10.1093/bioinformatics/btu153

Sen, B., and Joshi, S. G. G. (2016). Studies on *Acinetobacter baumannii* involving multiple mechanisms of carbapenem resistance. *J. Appl. Microbiol.* 120, 619–629. doi: 10.1111/jam.13037

Senchenkova, S. N., Popova, A. V., Shashkov, A. S., Shneider, M. M., Mei, Z., Arbatsky, N. P., et al. (2015). Structure of a new pseudaminic acid-containing capsular polysaccharide of *Acinetobacter baumannii* LUH5550 having the KL42 capsule biosynthesis locus. *Carbohydr. Res.* 407, 154–157. doi: 10.1016/j.carres.2015.02.006

Shashkov, A. S., Kenyon, J. J., Senchenkova, S. N., Shneider, M. M., Popova, A. V., Arbatsky, N. P., et al. (2016). *Acinetobacter baumannii* K27 and K44 capsular polysaccharides have the same K unit but different structures due to the presence of distinct wzy genes in otherwise closely related K gene clusters. *Glycobiology* 26, 501–508. doi: 10.1093/glycob/cwv168

Shashkov, A. S., Liu, B., Kenyon, J. J., Popova, A. V., Shneider, M. M., Senchenkova, S. N., et al. (2017). Structures of the K35 and K15 capsular polysaccharides of *Acinetobacter baumannii* LUH5535 and LUH5554 containing amino and diamino uronic acids. *Carbohydr. Res.* 448, 28–34. doi: 10.1016/j.carres.2017.05.017

Siguier, P. (2006). ISfinder: the reference centre for bacterial insertion sequences. *Nucleic Acids Res.* 34, D32–D36. doi: 10.1093/nar/gkj014

Smith, M. G., Gianoulis, T. A., Pukatzki, S., Mekalanos, J. J., Ornston, L. N., Gerstein, M., et al. (2007). New insights into *Acinetobacter baumannii* pathogenesis revealed by high-density pyrosequencing and transposon mutagenesis. *Genes Dev.* 21, 601–614. doi: 10.1101/gad.1510307

Sun, D., Crowell, S. A., Harding, C. M., De Silva, P. M., Harrison, A., Fernando, D. M., et al. (2016). KatG and KatE confer *Acinetobacter resistance* to hydrogen peroxide but sensitize bacteria to killing by phagocytic respiratory burst. *Life Sci.* 148, 31–40. doi: 10.1016/j.lfs.2016.02.015

Thompson, J. D., Gibson, T. J., and Higgins, D. G. (2003). Multiple sequence alignment using ClustalW and ClustalX. *Curr. Protoc. Bioinformatics* 2, 2.3.1–2.3.22. doi: 10.1002/0471250953.bi0203s00

Turano, H., Gomes, F., Medeiros, M., Oliveira, S., Fontes, L. C., Sato, M. I. Z., et al. (2016). Presence of high-risk clones of OXA-23-producing *Acinetobacter baumannii* (ST79) and SPM-1-producing *Pseudomonas aeruginosa* (ST277) in environmental water samples in Brazil. *Diagn. Microbiol. Infect. Dis.* 86, 80–82. doi: 10.1016/j.diagmicrobio.2016.06.005

Vila, J., Ruiz, J., Goni, P., Jimenez, and de Anta, T. (1997). Quinolone-resistance mutations in the topoisomerase IV *parC* gene of *Acinetobacter baumannii*. *J. Antimicrob. Chemother.* 39, 757–762. doi: 10.1093/jac/39.6.757

Vila, J., Ruiz, J., Marco, F., Barcelo, A., Goni, P., Giralt, E., et al. (1994). Association between double mutation in *gyrA* gene of ciprofloxacin-resistant clinical isolates of *Escherichia coli* and MICs. *Antimicrob. Agents Chemother.* 38, 2477–2479. doi: 10.1128/AAC.38.10.2477

Villalón, P., Valdezate, S., Medina-Pascual, M. J., Carrasco, G., Vindel, A., and Saez-Nieto, J. A. (2013). Epidemiology of the *Acinetobacter*-derived cephalosporinase, carbapenem-hydrolysing oxacillinase and metallo-β-lactamase genes, and of common insertion sequences, in epidemic clones of *Acinetobacter baumannii* from Spain. *J. Antimicrob. Chemother.* 68, 550–553. doi: 10.1093/jac/dks448

Waack, U., Warnock, M., Yee, A., Huttinger, Z., Smith, S., Kumar, A., et al. (2018). CpaA is a glycan-specific Adamalysin-like protease secreted by *Acinetobacter baumannii* that inactivates coagulation factor XII. *mBio* 9:e01606-18. doi: 10.1128/mBio.01606-18

Wachino, J., Jin, W., Kimura, K., and Arakawa, Y. (2019). Intercellular transfer of chromosomal antimicrobial resistance genes between *Acinetobacter baumannii* strains mediated by prophages. *Antimicrob. Agents Chemother.* 63, E334–E319. doi: 10.1128/AAC.00334-19

Wang, X., and Quinn, P. J. (2010). Lipopolysaccharide: biosynthetic pathway and structure modification. *Prog. Lipid Res.* 49, 97–107. doi: 10.1016/j.plipres.2009.06.002

Weber, B. S., Harding, C. M., and Feldman, M. F. (2016). Pathogenic *Acinetobacter*: from the cell surface to infinity and beyond. *J. Bacteriol.* 198, 880–887. doi: 10.1128/JB.00906-15

Weber, B. S., Kinsella, R. L., Harding, C. M., and Feldman, M. F. (2017). The secrets of *Acinetobacter* secretion. *Trends Microbiol.* 25, 532–545. doi: 10.1016/j.tim.2017.01.005

Wibberg, D., Salto, I. P., Eikmeyer, F. G., Maus, I., Winkler, A., Nordmann, P., et al. (2018). Complete genome sequencing of *Acinetobacter baumannii* strain K50 discloses the large conjugative plasmid pK50a encoding carbapenemase OXA-23 and extended-spectrum β-Lactamase GES-11. *Antimicrob. Agents Chemother.* 62, e212–e218. doi: 10.1128/AAC.00212-18

Wick, R. R., Heinz, E., Holt, K. E., and Wyres, K. L. (2018). Kaptive web: user-friendly capsule and lipopolysaccharide serotype prediction for *Klebsiella* genomes. *J. Clin. Microbiol.* 56:e00197-18. doi: 10.1128/JCM.00197-18

Wong, D., Nielsen, T. B., Bonomo, R. A., Pantapalangkoor, P., Luna, B., and Spellberg, B. (2017). Clinical and pathophysiological overview of *Acinetobacter* infections: a century of challenges. *Clin. Microbiol. Rev.* 30, 409–447. doi: 10.1128/CMR.00058-16

Wright, M. S., Haft, D. H., Harkins, D. M., Perez, F., Hujer, K. M., Bajaksouzian, S., et al. (2014). New insights into dissemination and variation of the health care-associated pathogen *Acinetobacter baumannii* from genomic analysis. *mBio* 5, 1–13. doi: 10.1128/mBio.00963-13

Wyres, K. L., Cahill, S. M., Holt, K. E., Hall, R. M., and Kenyon, J. J. (2020). Identification of *Acinetobacter baumannii* loci for capsular polysaccharide (KL) and lipooligosaccharide outer core (OCL) synthesis in genome assemblies using curated reference databases compatible with Kaptive. *Microb. genomics* 6:e000339. doi: 10.1099/mgen.0.000339

Xu, Z., and Hao, B. (2009). CVTree update: a newly designed phylogenetic study platform using composition vectors and whole genomes. *Nucleic Acids Res.* 37, W174–W178. doi: 10.1093/nar/gkp278

Yoon, S. H., Park, Y.-K., and Kim, J. F. (2015). PAIDB v2.0: exploration and analysis of pathogenicity and resistance islands. *Nucleic Acids Res.* 43, D624–D630. doi: 10.1093/nar/gku985

Zander, E., Bonnin, R. A., Seifert, H., and Higgins, P. G. (2014). Characterization of blaOXA-143 variants in *Acinetobacter baumannii* and *Acinetobacter pittii*. *Antimicrob. Agents Chemother.* 58, 2704–2708. doi: 10.1128/AAC.02618-13

Zankari, E., Hasman, H., Cosentino, S., Vestergaard, M., Rasmussen, S., Lund, O., et al. (2012). Identification of acquired antimicrobial resistance genes. *J. Antimicrob. Chemother.* 67, 2640–2644. doi: 10.1093/jac/dks261

Zerbino, D. R. (2010). Using the Velvet de novo assembler for short-read sequencing technologies. *Curr. Protoc. Bioinformatics* 31, 11.5.1–11.5.12. doi: 10.1002/0471250953.bi1105s31

Zhu, L., Yan, Z., Zhang, Z., Zhou, Q., Zhou, J., Wakeland, E. K., et al. (2013). Complete genome analysis of three *Acinetobacter baumannii* clinical isolates in China for insight into the diversification of drug resistance elements. *PLoS One* 8:e66584. doi: 10.1371/journal.pone.0066584

Zuo, G., and Hao, B. (2015). CVTree3 Web Server for whole-genome-based and alignment-free prokaryotic phylogeny and taxonomy. *Genomics Proteomics Bioinformatics* 13, 321–331. doi: 10.1016/j.gpb.2015.08.004

Conflict of Interest: The authors declare that the research was conducted in the absence of any commercial or financial relationships that could be construed as a potential conflict of interest.

frontiers in Microbiology

ORIGINAL RESEARCH
published: 18 June 2020
doi: 10.3389/fmicb.2020.01283

Structure and Evolution of *Acinetobacter baumannii* Plasmids

*Abraham D. Salgado-Camargo[1], Semiramis Castro-Jaimes[1], Rosa-Maria Gutierrez-Rios[2], Luis F. Lozano[1], Luis Altamirano-Pacheco[1], Jesús Silva-Sanchez[3], Ángeles Pérez-Oseguera[1], Patricia Volkow[4], Santiago Castillo-Ramírez[1] and Miguel A. Cevallos[1]**

[1] Programa de Genómica Evolutiva, Centro de Ciencias Genómicas, Universidad Nacional Autónoma de México, Cuernavaca, Mexico, [2] Departamento de Microbiología Molecular, Instituto de Biotecnología, Universidad Nacional Autónoma de México, Cuernavaca, Mexico, [3] Grupo de Resistencia Bacteriana, Centro de Investigaciones Sobre Enfermedades Infecciosas, Instituto Nacional de Salud Pública, Cuernavaca, Mexico, [4] Departamento de Infectología, Instituto Nacional de Cancerología, Mexico City, Mexico

OPEN ACCESS

Edited by:
Feng Gao,
Tianjin University, China

Reviewed by:
Chew Chieng Yeo,
Sultan Zainal Abidin University, Malaysia
Mark D. Adams,
The Jackson Laboratory for Genomic Medicine, United States

***Correspondence:**
Miguel A. Cevallos
mac@ccg.unam.mx

Specialty section:
This article was submitted to Evolutionary and Genomic Microbiology, a section of the journal Frontiers in Microbiology

Received: *15 January 2020*
Accepted: *20 May 2020*
Published: *18 June 2020*

Citation:
Salgado-Camargo AD, Castro-Jaimes S, Gutierrez-Rios R-M, Lozano LF, Altamirano-Pacheco L, Silva-Sanchez J, Pérez-Oseguera Á, Volkow P, Castillo-Ramírez S and Cevallos MA (2020) Structure and Evolution of Acinetobacter baumannii Plasmids. Front. Microbiol. 11:1283. doi: 10.3389/fmicb.2020.01283

Acinetobacter baumannii is an emergent bacterial pathogen that provokes many types of infections in hospitals around the world. The genome of this organism consists of a chromosome and plasmids. These plasmids vary over a wide size range and many of them have been linked to the acquisition of antibiotic-resistance genes. Our bioinformatic analyses indicate that *A. baumannii* plasmids belong to a small number of plasmid lineages. The general structure of these lineages seems to be very stable and consists not only of genes involved in plasmid maintenance functions but of gene sets encoding poorly characterized proteins, not obviously linked to survival in the hospital setting, and opening the possibility that they improve the parasitic properties of plasmids. An analysis of genes involved in replication, suggests that members of the same plasmid lineage are part of the same plasmid incompatibility group. The same analysis showed the necessity of classifying the Rep proteins in ten new groups, under the scheme proposed by Bertini et al. (2010). Also, we show that some plasmid lineages have the potential capacity to replicate in many bacterial genera including those embracing human pathogen species, while others seem to replicate only within the limits of the *Acinetobacter* genus. Moreover, some plasmid lineages are widely distributed along the *A. baumannii* phylogenetic tree. Despite this, a number of them lack genes involved in conjugation or mobilization functions. Interestingly, only 34.6% of the plasmids analyzed here possess antibiotic resistance genes and most of them belong to fourteen plasmid lineages of the twenty one described here. Gene flux between plasmid lineages appears primarily limited to transposable elements, which sometimes carry antibiotic resistance genes. In most plasmid lineages transposable elements and antibiotic resistance genes are secondary acquisitions. Finally, broad host-range plasmids appear to have played a crucial role.

Keywords: *A. baumannii*, plasmids, Rep proteins, antibiotic resistance genes, plasmid maintenance functions, IS

INTRODUCTION

Acinetobacter baumannii is a global emergent nosocomial pathogen that causes a wide variety of infections, especially in severely ill patients, in intensive care units. This pathogen is a major cause of morbidity and mortality in hospitals worldwide, and the recent success of this species as a pathogen seems to be linked to the ability of this organism to acquire antibiotic resistance genes, form biofilms and resist desiccation; these characteristics facilitate the persistence of this bacterium in the hospital setting and promote the emergence of outbreaks (Antunes et al., 2014). A large fraction of the nosocomial outbreaks in Europe, Asia, and North America are produced by a limited number of strains belonging to three different international clones (IC-I, IC-II, and IC-III) (Zarrilli et al., 2013). Most of these international clones are resistant to antibiotics belonging to three or more different families, a characteristic that defines these clones as being multidrug resistant (MDR) (Diancourt et al., 2010; Roca et al., 2012).

Plasmids are extrachromosomal DNA molecules, usually circular, that replicate independently of the chromosome and have the potential to be transferred frequently, but not exclusively by conjugation, not only to members of the same species but also to distantly related bacteria (Partridge et al., 2018). Plasmids play a leading role in the spread of antibiotic resistance genes among bacterial pathogens that cause community- or hospital-acquired infections, including *A. baumannii* (Carattoli, 2013; San Millan, 2018). A wide variety of *A. baumannii* plasmids carrying antibiotic resistance genes with different sizes and characteristics have been described in recent literature. There has been particular interest in plasmids carrying genes encoding serine carbapenemases (OXA-type beta-lactamases), which facilitate the most predominant mechanism for carbapenem resistance in this species (Higgins et al., 2010; Mosqueda et al., 2014; Hujer et al., 2017; Cameranesi et al., 2018; Wibberg et al., 2018).

Despite the apparent importance of plasmids in the spread of virulence and antibiotic resistance genes among *A. baumannii* isolates, only a few papers that have analyzed the structures, relationships and evolution of *A. baumannii* plasmids as a whole have been published (Fondi et al., 2010; Lean and Yeo, 2017; Salto et al., 2018). In this work, taking advantage of the increasing interest in *A. baumannii* and the large number of complete genome sequences for this organism that have been deposited in GenBank in the last decade, we performed a comparative plasmid sequence analysis to gain insights into the structures, relatedness, and evolution of these plasmids. We were able to determine that the *A. baumannii* plasmids belong to a small number of plasmid lineages, some of them widely distributed among the different *A. baumannii* clades, while others seem to be restricted to a small number of clades. Surprisingly, some widespread plasmids do not have genes linked to conjugation or plasmid mobilization, suggesting that other mechanisms or horizontal transfer play an important role in the dissemination of *A. baumannii* plasmids. Genes encoding initiator replication proteins and the corresponding surrounding DNA sequences within each plasmid lineage are similar enough to suggest that each lineage represents plasmids of the same incompatibility group. This suggestion is also supported by the observation that plasmids of the same strain have different replication proteins. Each plasmid lineage possesses a common gene set that contains not only genes involved in plasmid maintenance but also a set of genes encoding hypothetical or poorly characterized proteins. Despite the antibiotic or metal resistance genes that some plasmids possess, the remaining genes that are not involved in plasmid maintenance are not obviously linked with properties that allow survival in the hospital setting, suggesting that these genes could be associated with plasmid survival functions. Additionally, we determined that gene transfer from one plasmid lineage to another is highly limited and restricted to a few gene classes.

RESULTS AND DISCUSSION

The Plasmid Collection

Next-generation sequencing platforms have been a crucial means to obtain the complete sequences of all types of bacterial genomes, including those of many important human pathogens. We took advantage of the large amount of information generated in this manner to analyze the structure and evolution of the *A. baumannii* plasmids. For this purpose, we used the 155 complete plasmid sequences deposited in NCBI as of August 14, 2017. However, considering that most of these plasmid sequences were obtained from isolates of international clones and/or from a restricted set of countries, we incorporated the sequences of 18 plasmids obtained from the genome sequences of 10 nosocomial strains that represent some of the most prevalent STs circulating in Mexico to increase the plasmid diversity included in our investigation (see Materials and Methods). In total, our study collection comprised 173 plasmids of a wide variety of sizes, ranging from 1,109 to 216,780 bp. Moreover, our plasmid set originated from 103 different isolates, each carrying up to six plasmids. These isolates belonged to at least 47 different STs and originated from 17 countries (see **Supplementary Table S1**).

A. baumannii Plasmids Belong to a Very Restricted Number of Plasmid Lineages

Plasmids have been visualized as molecules that possess genes involved in self-maintenance (plasmid backbone) and genes that could be important for the ability of bacteria to exploit new ecological niches or acquire new capabilities (Frost et al., 2005). These genes are commonly described as plasmid *cargo*. Antibiotic resistance genes are a perfect example of such genes, particularly for organisms in hospital settings (Tschäpe, 1994; Carattoli, 2013; San Millan, 2018).

To understand how plasmids are organized and to define which are the relationship between them, several plasmid classification systems have been proposed. Some of these systems relay in the phenotypic features that plasmids confer, assuming that plasmids sharing such characteristics are phylogenetically related. Plasmid incompatibility or the inability of two plasmids to reside in the same cell has been another way to classify plasmids. Plasmids belonging to the same incompatibility group have identical or very similar replication and/or segregation gene

modules (Novick, 1987; Austin and Nordström, 1990). With this idea in mind, some authors have developed typing systems based on the nucleotide sequence identity of the genes encoding replication initiation proteins. Other authors designed methods to classify conjugative plasmids based on the sequence of the relaxase, a gene crucial for conjugation. The problem with these classification systems is that they are based on a limited number of genes or traits. However, considering the diversity of genes carried on plasmids and the different mechanisms that plasmid use for their maintenance makes a futile dream to design a universal plasmid taxonomy system. Nevertheless, we can design a classification system that takes into account, in an unbiased way, the whole gene content of plasmids, to determine which are the relationships between them and to have a picture of how these plasmids evolve. This was the approach that we follow in this work.

Plasmid evolution can be thought to occur via two basic pathways: first, plasmids are entities that are prone to rapid loss and gain of genes such that, in a short period of time, descendants of one plasmid are only recognizable because they share the same set of genes involved in the basic maintenance functions of the plasmid (Hülter et al., 2017; Brandt et al., 2019). Second, the ability of plasmids to gain or lose genetic information can be assumed to be more or less limited, and the plasmids persist for long durations within bacterial populations as plasmid lineages, where plasmid lineages are groups of plasmids that are closely related by gene content, including, but not restricted to, genes responsible for plasmid maintenance (Yau et al., 2010).

Our first interest was to evaluate, precisely, the type of evolution undergone by *A. baumannii* plasmids. For this purpose, our strategy was to compare the degree and extent of DNA sequence identity between the plasmids in our collection. We used nucleotide MEGABLAST (BLASTn) searches instead of Protein BLAST (BLASTp), as described by other authors, for two reasons: first, BLASTn comparisons are less sensitive to sequencing errors introduced during the assembly process (false frame shifts or incorrect stop codons) than BLASTp, and second, a BLASTp approach does not take into consideration intergenic regions and regions essential for plasmid function, such as the origin of replication. We made pairwise MEGABLAST (BLASTn) comparisons of each plasmid of our collection against the others. To filter BLAST results, we constructed networks with the following rule: two plasmids are linked if at least 85% of the regions of the largest plasmid (for each comparison) are covered by the smaller plasmid, and those regions exhibit at least 90% of DNA sequence identity. To belong to a specific network, one plasmid must fulfill the above-mentioned cutoff values of identity and coverage not with all, but with at least one member of the group. Being a member of a specific network does no mean that all plasmids of this network have at least 85% coverage with the rest of the members. The minimal requirement is to accomplish the cutoff values with at least one member of the network, for example, the shortest with the next in size.

After these analyses, we determined that 124 *A. baumannii* plasmids were organized into 23 groups, and 39 plasmids remained without an assigned group. The plasmid composition of each group is listed in **Supplementary Table S1**. As shown in **Supplementary Figure S1**, the plasmid networks constructed as mentioned above are densely interconnected, and all members of a determined group have the same or a very closely related gene encoding a DNA replication initiator (Rep) protein. Notably, plasmids within a group share, in general, several genes that are involved in plasmid maintenance.

To evaluate the coherence of these groups, we repeated the analysis, raising plasmid coverage to 90% again, with 90% DNA sequence identity. In general, the groups remained almost the same (some groups lost a few members). On the one hand, lowering coverage to 50% and retaining 90% of DNA sequence identity, allows the incorporation of some orphans into different groups and led to the fusion of six lineages: Group_17 with Group_22, Group_7 with Group_8 and Group_3 with Group_14. Members of lineages Group_17 share sequence identity of approximately 70% with components of Group_22, including the replication module and nearby sequences. This grouping suggest that Group_17 and Group_22 have a common evolutionary origin. Likewise, members of Group_3_and Group_14 have similar but not identical Rep proteins, indicating also that they have a hypothetical common ancestor. In contrast, members of Group_8 do not have the same replication module as those belonging to Group_7 and for this reason we do not contemplate them having a common ancestry.

Groups formed using 85% coverage and 90% of sequence identity as cutoff values represent a useful method for identification of *A. baumannii* plasmid lineages. Lowering the coverage cutoff value to 50% may be useful to recognize ancestral relationships, as long as the shared sequences include the replication/maintenance module. Therefore, hereinafter, we will consider each one of the groups identified with this methodology as a plasmid lineage.

However, to indicate that Group_3_and Group_14 had a common origin but now each one of the groups has a different evolutionary path, these were named as plasmid lineages LN_3A and LN_3B, respectively. With these considerations, members of our plasmid collection belong to 21 plasmid lineages and 39 plasmids remain as orphans (not assigned to a plasmid lineage). Interestingly, 88 plasmids, or 50.8% of our collection, were clustered in only four plasmid lineages: LN-1, LN_2; LN_3 and LN_4. The other 17 groups are very small, as most of them contained only two members (**Supplementary Figure S1**).

With only one exception, we elected the largest and most interconnected member of the group as the representative plasmid of each lineage. The exception is lineage 2 (LN_2), in which the largest and most interconnected member has a very large duplicated region. The duplicated regions include the replication genes indicating that this sequence has assembly problems, considering that plasmids with duplicated replication regions are highly unstable and they are rapidly eliminated of the population (Summers et al., 1993). Therefore, the second largest most interconnected plasmid (pPKAB07) was selected as the representative of this particular lineage. In conjunction, these analyses indicate that *A. baumannii* plasmids evolve as lineages

and that most of the *A. baumannii* plasmids in circulation worldwide belong to a few lineages.

The general structure of the members of each one of the plasmid lineages is very stable, considering that some of the strains were isolated many years ago. For example, strain A1 was isolated in 1982, and one of the plasmids of this strain, pA1-1, belongs to lineage LN_2. This plasmid has a very similar gene content and organization as other plasmids isolated in 2015 that belong to the same lineage (plasmid unnamed2, GenBank accession number CP014293). Similarly, plasmid pALAC4-2 of LN_4 belongs to a strain isolated in 1997 and has a very similar structure to other plasmids of the same lineage isolated a decade later (i.e., plasmid pMRSN3527-6, GenBank accession number NZ_CM003318.1). Additionally, plasmid p4ABAYE (GenBank accession number NC_010403.1), described in 2001, shared 98% sequence identity with pMRSN58-2.7 (GenBank accession number NZ_CM003316.1), isolated in 2013. Members of LN_19 are almost identical. The oldest member of the lineage was isolated in 2001 and the most recent in 2010 (**Supplementary Table S1**).

The *A. baumannii* plasmid sequences deposited in NCBI have increased since we last performed the analyses. On April 28, 2020, this database embraced the complete sequence of 422 A baumannii plasmids. To make a rapid evaluation of the prevalence of plasmid lineages LN_1, LN_2, LN_3A, LN_3B, and LN_4, we performed BLASTn on all members of these lineages against the new database. Using this strategy 30 new plasmids were incorporated in LN_1, 23 in LN_2, 12 in LN_3A+3B, and finally, 10 new plasmids were included in LN_4. Now, these lineages contain 38.4% of the *A baumannii* plasmids. However, we must say that the only way to identify all new members of the plasmid lineages is by reconstructing the networks with the rules mentioned above. These observations confirm that a few plasmid lineages encompass most of *A. baumannii* plasmids.

Plasmid Lineage Gene Composition

Comparisons of all members of a particular plasmid lineage with their representative plasmid show that the genome core of a plasmid lineage includes genes that are not involved in plasmid maintenance functions (the backbone) (**Figure 1** and **Supplementary Figures S2–S12**).

To obtain a general picture of the gene composition of our plasmid collection, we assigned a functional class (COG) to each of the protein products encoded by these plasmids. This analysis showed that these proteins fall within 23 functional classes; however, we were unable to assign a functional class (not in COG) to 74.15% of the proteins (**Figure 2**). In total, 3.53% of the encoded proteins have only a general function prediction (class R), and 3.5% are classified within class S (function unknown). Nevertheless, these 2497 uncharacterized or poorly characterized proteins were grouped in 242 orthologous groups [Remained Orthologous Groups (ROGs)] (Taboada et al., 2010). Therefore, it is not possible to predict whether some of these hypothetical proteins play a role in the nosocomial setting. However, given that the genes encoding these proteins are highly conserved within each plasmid lineage; the general structure of plasmids belonging to each one of the different lineages is stable during time and that the plasmids replicate in very different genetic backgrounds (even in different species), we suggest that these genes may play a role in reducing the fitness cost for the host to maintain the plasmids, thereby improving the favorability of the plasmids as parasite molecules.

We also found, as expected, a set of genes encoding proteins that are typically associated with plasmids: 7.28% of the proteins fall under class L (replication, recombination and repair), which includes replication initiation proteins, transposases, site-specific recombinases, and other proteins involved in recombination. Additionally, 1.31% of the proteins belong to class V (defense mechanisms), which includes proteins involved in plasmid stability (toxin-antitoxin modules) and restriction modification and proteins conferring antibiotic resistance. In the following sections, we will describe genes that play a crucial role in plasmid maintenance and that are usually associated with plasmid functions (**Figure 2**).

Classification of New Replication Initiation Protein (Rep) Genes

An absolute requirement for the survival of a plasmid is the presence of a replication module. These modules consist of an origin of replication, one gene encoding a replication initiator (Rep gene) and the factors and DNA sites involved in regulation of the expression of this gene, which is located near the Rep gene (del Solar et al., 1998). Our bioinformatic analysis indicates that from the 173 plasmids in our collection, 143 had an intact Rep gene and 13 plasmids had Rep pseudogenes, because we found on them premature stop codons or frameshifts generated, probably, during the sequencing and/or assembly processes. Nevertheless, in 27 plasmids, we could not find a Rep protein by annotation or BLAST searches; thus, as already noted by other authors, an experimental approach is needed to identify such replication regions (Lean and Yeo, 2017).

Rep genes of *A. baumannii* plasmids have been mainly identified by bioinformatic analyses, which have indicated that these proteins can be classified into five different categories: the most common Rep proteins belong to the Rep_3 superfamily (Pfam:01051) and are usually annotated as RepB. The next most frequent Rep proteins are those annotated as *replicases*, and these proteins have two distinctive domains: one is a replicase domain (pfam:03090), and the other is an alpha-helical domain that is also present at the C termini of primases (PriCT_1 superfamily). Other *A. baumannii* plasmids have Rep proteins belonging to the Rep_1 superfamily (Pfam01446). Several plasmids have a protein with a helix-turn-helix (HTH) domain annotated as a replication protein, and finally, one plasmid has an initiator protein classified as belonging to the RepC superfamily (Pfam:06504). Recently, the functionality of some of these replication regions was tested experimentally (Salto et al., 2018). Nevertheless, as mentioned above, many plasmids do not have an identifiable Rep protein. **Figure 3** and **Supplementary Figure S13** show the phylogenies of the replicases with the most members, separated by the domains identified by Pfam (Rep3 and replicase-PriCT). Some proteins were not included because either these proteins did not have

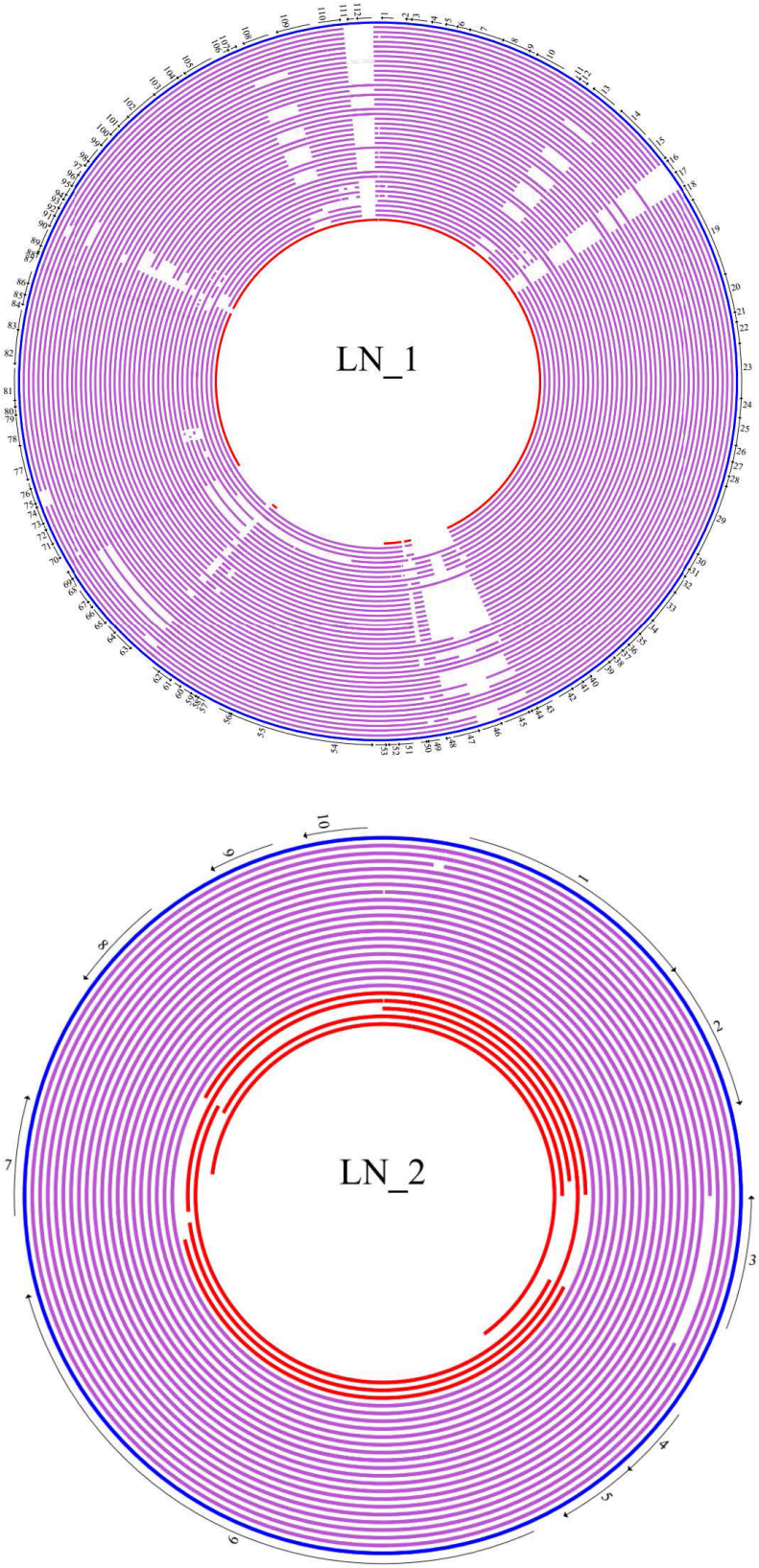

FIGURE 1 | Continued

FIGURE 1 | Cicular map of members of plasmid lineage LN_1 and linear map of members of LN_2. Plasmid sequences of each lineage were compared with its reference with BLASTn and mapped using GenVision a component of DNASTAR's Lasergene Core Suite. The genes core are in bold letters. The representative plasmid of LN_1 is plasmid AB34299 (blue ring) and numbers around this plasmid indicate the position of the following genes: **1. Nuclease; 2. Hypothetical protein; 3. Hypothetical protein; 4. Hypothetical protein; 5. Hypothetical protein; 6. Hypothetical protein; 7. Zeta-antitoxin; 8. Zeta-Toxin; 9. Hypothetical protein; 10. Plasmid replicase; 11. Hypothetical protein**; 12. Hypothetical protein; 13. Hypothetical protein; 14. DNA polymerase; 15. Hypothetical protein; 16. ISAba1; 17. ISAba1; **18. Transglycosylase; 19. Conjugal protein TraG; 20. Conjugal protein TraH; 21. Hypothetical protein; 22. Conjugal protein TraF; 23. Conjugal protein TraN; 24. Conjugal protein TrbC; 25. Conjugal protein TraU; 26. Conjugal protein TraW; 27. Peptidase; 28. Hypothetical protein; 29. Conjugal protein TraC; 30. Conjugal protein Tra; 31. Hypothetical protein; 32. Protein-disulfide isomerase; 33. Conjugal protein TraB; 34. Conjugal protein TraK; 35. Conjugal protein TraE; 36. Conjugal protein TraL; 37. Hypothetical protein; 38. Hypothetical protein; 39. Murein transglycosylase; 40. Hypothetical protein; 41. Hypothetical protein; 42. Resolvase; 43. Hypothetical protein**; 44. Hypothetical protein; 45. ISAba125; 46. Aminoglycoside phosphotransferase; 47. ISAba125; 48. Hypothetical protein; 49. Hypothetical protein; 50. Hypothetical protein; **51. Hypothetical protein**; 52. Hypothetical protein; 53. Hypothetical protein; 54. Relaxase MOBF; 55. Type IV secretion system protein VirD4; 56. Hypothetical protein; 57. Hypothetical protein; 58. Hypothetical protein; 59. Hypothetical protein; 60. Hypothetical protein; 61. Molecular chaperone DnaJ; 62. Hypothetical protein; 63. Hypothetical protein; 64. Hypothetical protein; 65. Hypothetical protein; 66. Hypothetical protein; 67. Hypothetical protein; 68. Addiction module toxin; 69. DNA-binding protein; **70. Hypothetical protein; 71. Hypothetical protein;** 72. Hypothetical protein; 73. Hypothetical protein; **74. Hypothetical protein**; 75. Hypothetical protein; 76. Hypothetical protein; 77. Hypothetical protein; **78. Toxic anion resistance protein TelA; 79. Hypothetical protein; 80. Hypothetical protein; 81. Hypothetical protein; 82. ParB family partition protein; 83. ParA family protein; 84. Hypothetical protein; 85. Hypothetical protein; 86. Hypothetical protein; 87. Hypothetical protein; 88. Hypothetical protein**; 89. Hypothetical protein; 90. Hypothetical; protein; 91. Hypothetical protein; 92. Hypothetical protein; 93. Hypothetical protein; 94. DNA-binding protein; 95. Nuclease; **96. Hypothetical protein; 97. Hypothetical protein; 98. Hypothetical protein; 99. Hypothetical protein; 100. Hypothetical protein; 101. Hypothetical protein; 102. Zeta-antitoxin; 103. Zeta-toxin; 104. Hypothetical protein; 105. Hypothetical protein; 106. Hypothetical protein; 107. Hypothetical protein**; 108. Hypothetical protein; **109. DNA polymerase**; 110. Hypothetical protein; 111. Transposase; 112. Transposase. Purple rings: Purple rings: from outside to inside: pNaval18-74, p2ABTCDC0715, pAC30c, pAba10042b,pAba9102a, pAba7847b, pACICU2, ABKp1, p1ABST2, pNaval81-67, pOIFC143-70, pIS123-67, pABUH1-74, p1AB5075, pAB04-2, plasmid YU-R612, pAba3207b, pCMCVTAb2-Ab4, plasmid CMC-CR-MDR-Ab66, plasmid KAB01, plasmid KAB02, plasmidKAB03, plasmid KAB04, plasmid KAB05, plasmid KAB06, pSSA12_1, pSSMA17_1,pJBA13_1, p15A34_1, pUSA2_1, pUSA15_1, pA85-3, pCS01A, pCS01B, pCR17A,pCR17B, pAba7835b, plasmid KAB07, plasmid KAB08, p15A5_1. Additional orphan plasmid is in red ring: pAC29b. LN_2. The representative plasmid of lineage LN_2 is pPKAB07 (blue bar). Numbers along this bar indicate the position of genes: **1. RepB family plasmid replication initiator protein; 2. DNA-binding protein**; 3. Hypothetical protein; 4. Toxin-Antitoxin system spITA (COG3514); 5 Toxin-Antitoxin system spITA (DUF497); 6. TonB dependent receptor; 7. Hypothetical protein; 8. Hypothetical protein; 9. Hypothetical protein; 10. Hypothetical protein. Purple bars: from top to bottom: p1ABTCDC0715, pAC12, pAC30a, p2ABAYE, pAB0057, p1BJAB0868, pCanadaBC5-8.7, pABUH6a-8.8, pMRSN7339-8.7, pMRSN58-8.7, pAB0057, plasmid_2 AB34299, p2AB5075, pAC29a, pA1-1, p15A5_2, pSSA12_2, pA85-2, pAB5075. Additional orphan plasmids are in red bars: from top to bottom: pAB2, p1ABST78, pORAB01-3, p MEX11594, pYU-R612.

any Pfam domain assigned in the database or there were not enough members to perform comparisons, as in the extreme case of the RepC domain, with only one protein assigned to this domain(El-Gebali et al., 2019).

In 2010, Bertini and coworkers designed a classification system for the *A. baumannii* plasmids based on the nucleotide identity of the Rep genes (Bertini et al., 2010). Rep genes that shared at least 74% nucleotide identity were pooled in the same group. With this scheme, the authors identified 19 homology groups (GR1 to GR19). Subsequently, Lean and Yeo, studying A. *baumannii* plasmids of less than 10 kb, proposed a new group based on Rep phylogenetic analyses: GR20, which is closely related to GR2; however, the members of this group form a clear separate clade (Lean and Yeo, 2017). Recently, Cameranesi and collaborators analyzed *A. baumannii* plasmids from Argentina and determined that some Rep genes of these plasmids required the formation of three additional groups: GR21, GR22 and GR23 (Cameranesi et al., 2018). However, the analysis of the genes annotated as Rep proteins from our plasmid collection showed that the current classification system was not sufficient to include all the Rep proteins. Therefore, by following the scheme proposed by Bertini and coworkers, ten additional groups were constructed (GR24-GR33). These replication gene groups can be visualized as a network in which one gene encoding a replication protein is part of a group if its DNA sequence shares at least 74% identity and 90% coverage with another member of the same group. For each new Rep group (GR), we chose the most interconnected member as the representative sequence of the group. However, we identified some unusual Rep proteins that showed nucleotide sequence identity higher than 74% with members of two different groups. This inconsistency was provoked because some authors named new replication homology groups, using a different set of rules of those originally proposed by Bertini and coworkers. Examples, the representative protein of GR23 is identical to that of GR8_1 proposed by Bertini and coworkers or the representative members of groups GR2 and GR20 have a DNA sequence identity higher than 74%. (Fondi et al., 2010; Cameranesi et al., 2018). In these cases, we assigned the unusual protein to the group with which this element shared the highest nucleotide identity (**Supplementary Table S2**). The assignations of all the replication proteins encoded in our plasmid set are listed in **Supplementary Table S1**. Seven of the new groups harbor DNA initiator proteins of the Rep_3 family (GR26, GR27, GR28, GR29, GR30, GR31, GR32); two of these groups are composed of proteins of the Replicase_PriCT family (GR25 and GR32), but the representative member of GR25 has an HTH_29 additional conserved domain (Pfam13551) and finally, one plasmid carries a Rep protein of the RepC family (GR33). We were incapable of identifying a gene encoding a Rep protein in three plasmid lineages (LN_4, LN_7 and LN_18) and in 14 orphan plasmids. On the other hand, four plasmid lineages, namely, LN_2, LN_11, LN_13 and LN_20, exhibited the same organization in their replication modules. This module consists of a bicistronic operon, in which the first gene encodes an initiator protein of the Rep_3 family (or RepB), and the second gene of the operon encodes a protein with an HTH motif that on

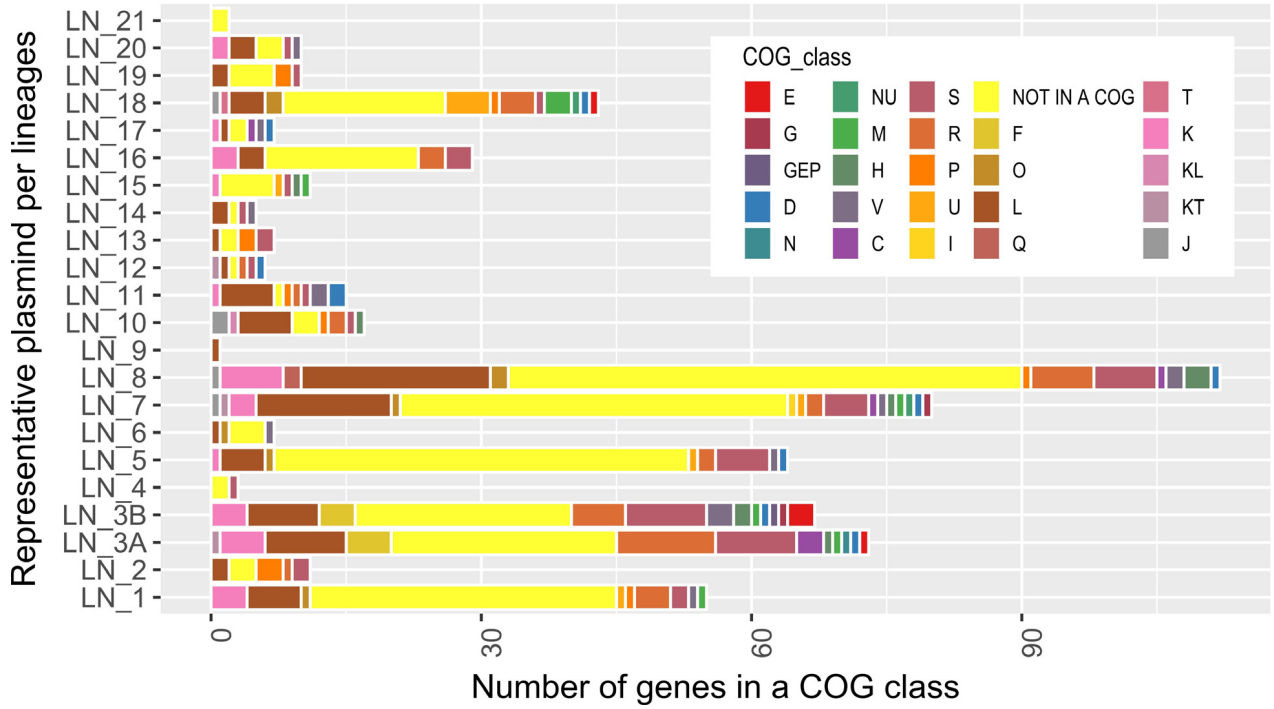

FIGURE 2 | Number of genes assigned to a functional class (COG) present in the representative plasmid of each lineage. Classes: CO, energy production and conversion, posttranslational modification, protein turnover, chaperones. DJ, cell cycle control, cell division, chromosome partitioning, translation, ribosomal structure and biogenesis. Q, secondary metabolites biosynthesis, transport and catabolism I, Lipid transport and metabolism. GEP, carbohydrate transport and metabolism, amino acid transport and metabolism, inorganic ion transport and metabolism. KT, transcription, signal transduction mechanisms. NU, cell motility, intracellular trafficking, secretion, and vesicular transport. G, carbohydrate transport and metabolism. KL, transcription, replication, recombination and repair. J, translation, ribosomal structure and biogenesis. T, signal transduction mechanisms. E, amino acid transport and metabolism. D, cell cycle control, cell division, chromosome partitioning. H, coenzyme transport and metabolism. F, nucleotide transport and metabolism. C, energy production and conversion. M, cell wall/membrane/envelope biogenesis. U, intracellular trafficking, secretion, and vesicular transport. O, posttranslational modification, protein turnover, chaperones. P, inorganic ion transport and metabolism. V, defense mechanisms. K, transcription. S, function unknown. R, general function prediction only. L, Replication, recombination and repair. NOT IN A COG, COG not defined.

some occasions has been wrongly annotated as a putative Rep protein, for example, in the homology group GR17. We traced the error source to an obvious mistake in GenBank: plasmid pAB1 (GenBank accession number CP000522.1) carries a gene annotated as encoding a DNA replication protein (protein_id ABO13850.1) which is precisely the representative member of GR17. This putative DNA replication protein carries an HTH_17 conserved domain (Pfam12728). However, a BLAST search indicates that the gene upstream to that encoding the HTH-carrying protein encodes a protein belonging to the Rep_3 superfamily (protein_id ABO13860.1) which is identical to other *A. baumannii* replication proteins. Unfortunately, this gene is annotated as encoding a hypothetical protein. To facilitate future work, Rep proteins sequences and the genes that codify them are listed in **Supplementary Materials S1**, **S2**. Be careful: these lists still include the representative member of GR17 described above.

Iterons in the New GR Replication Homology Groups

It has been shown that *iterons*, which are small repetitive DNA sequences located near the Rep gene, usually in tandem, play a crucial role in the control of plasmid replication in many plasmids (Chattoraj, 2000; Wegrzyn et al., 2016). These sequences have been bioinformatically identified in some *A. baumannii* plasmids; therefore, we searched for the presence of these sequences in the representative Rep genes and their surrounding sequences in each of the new GR groups (GR24-GR33) (Lean and Yeo, 2017; Salto et al., 2018). We could identify such tandem repeats near the initial codon of the Rep protein in six of these groups (GR24, GR26-GR30). The putative iterons of each one of the new groups are shown in **Supplementary Table S3**. Interestingly, in these cases, we also identified a region rich in A+T near these tandem repeats, which is a typical characteristic of plasmid replication origins. Of course, these presumptions must be tested in the laboratory. In contrast, GR25, GR31, GR32, and GR33 do not have iterons, at least not near the Rep gene. The first two Rep genes belong to the Rep_PriCT family and GR33 is the only member of the RepC family in our collection. Plasmid pD36-4 is a bireplicon that encodes two Rep proteins of the Rep_3 superfamily: RepA1 (WP_000140303.1) (GR31) and RepA2 (protein_id WP_000786839.1) (Hamidian and Hall, 2018a). The RepA2 gene is preceded by three copies of a 19 bp iteron

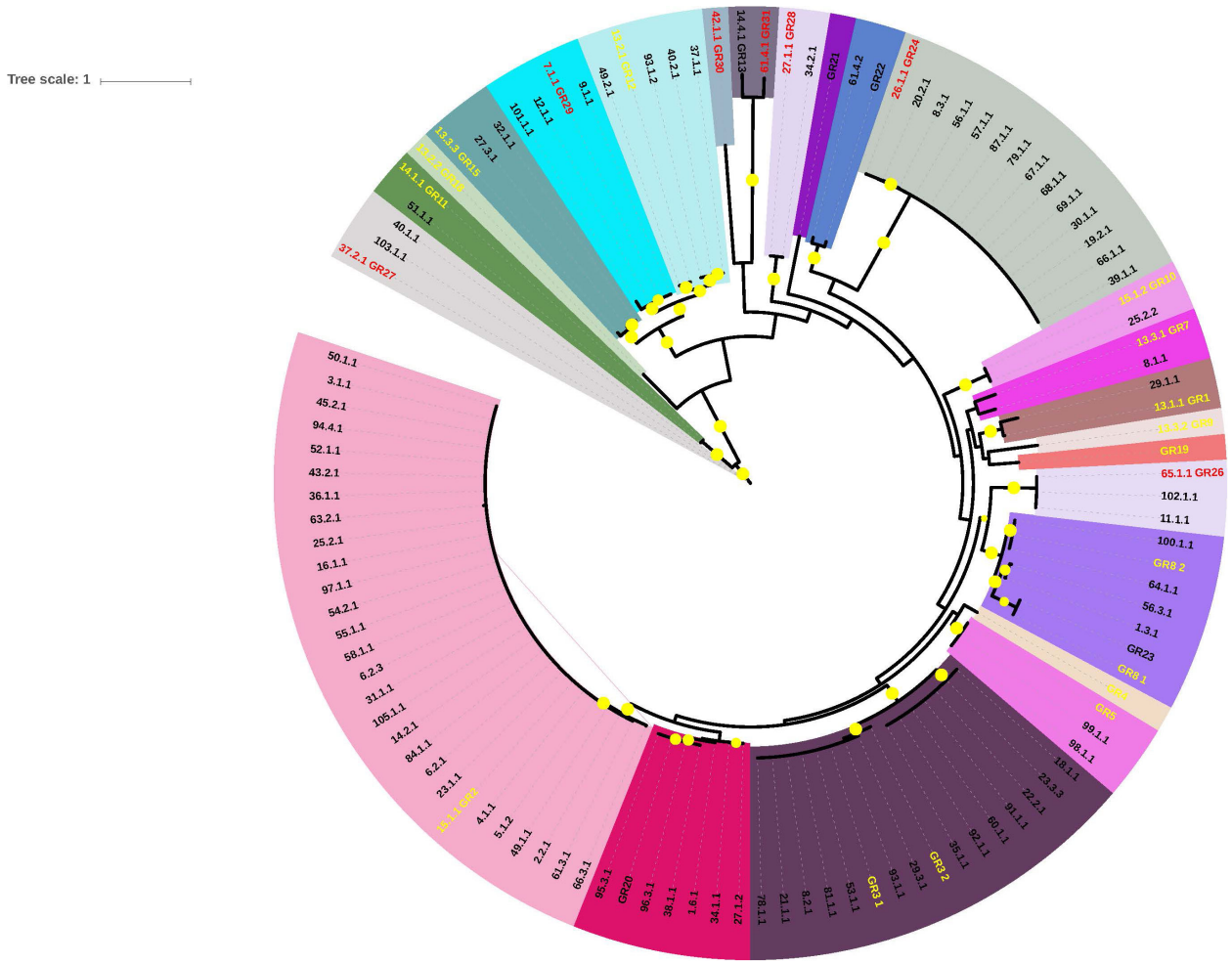

FIGURE 3 | Phylogenetic tree of genes encoding replicase proteins belonging to the Rep_3 family. Gene codons were aligned guided by protein alignments. In this figure we are using the replicase_ID numbers listed in **Supplementary Table S2**. Each color embrace members of one clade. Names with yellow letters indicate the reference genes used by Bertini et al. (2010) to construct GR homology groups. Names with red letters show the reference genes used by us to construct the new GR homology groups. Bootstrap values higher than 70% are marked in the figure with yellow circles.

sequence, but surprisingly, RepA1 does not possess iterons at least 500 bp upstream of the initiation codon, 500 bp downstream of the stop codon or within the Rep coding region, suggesting that this protein is no longer responsible for pD36-4 replication(Hamidian and Hall, a).

Plasmid Incompatibility and Initiator Proteins

Plasmid incompatibility has been defined as the inability of two replicons to coexist in the same cell line. This phenomenon occurs when some elements of the replication or partitioning machineries of a plasmid interfere with the maintenance functions of a second plasmid (Novick, 1987; Austin and Nordström, 1990). Thus, different plasmids that are stably maintained in the same bacterial cell belong, by definition, to different incompatibility groups. On the other hand, plasmids that are mutually incompatible are classified within the same incompatibility group and, very frequently, are phylogenetically closely related.

An inspection of the initiator genes in each of the plasmid lineages with only one Rep gene shows that all members of the same plasmid lineage share a replication initiator protein, classified within the same Rep homology group as defined by Bertini and coworkers (Bertini et al., 2010). For example, Rep proteins of lineage 1 belong to Rep group GR6; Rep proteins of lineage 2 belong to GR2; Rep proteins of lineage 3 belong to GR24, and those of LN_5 are classified within GR25 (**Supplementary Table S1**). In many cases, Rep proteins of the same GR group have amino acid sequences that are identical or almost identical: for example, all Rep proteins within LN_2 or LN_3A are identical, and those of LN_1 share 99.1% sequence identity among each other.

Plasmid lineages (LN_8, LN_10, LN_16) share Rep proteins of the same GR homology group (GR3); however, a protein

alignment performed with Clustal Omega indicates that Rep proteins of LN_8 and LN_10 are almost identical (>99.6%). Differences between LN_8 and LN_10 and LN16 is 80.2%. In our collection, members of these plasmid lineages are never located in the same bacterial isolate; however, differences in the sequences of Rep proteins between these two groups could be significant enough to represent two incompatibility groups. Recently, Blackwell and Hall (2019) showed that plasmids pS32-1 and pS21-a are compatible and that these plasmids contain Rep proteins of the Rep_3 superfamily. Interestingly, these proteins share a protein sequence identity of 85.4% (Blackwell and Hall, 2019). Nevertheless, an experimental approach is needed to resolve these problems. Our analysis indicates that plasmids of the same isolate belong to different plasmid lineages, with two exceptions, namely, isolates CR17 and CS01, which are almost identical in sequence. Each isolate possesses three plasmids, and two of the plasmids in each strain belong to LN_1; however, we were unable to identify complete Rep genes in these four plasmids; we could identify only truncated Rep genes or pseudogenes. Therefore, we could not elucidate the mechanisms via which these plasmids replicate or coexist in the same isolates. Taken together, these observations suggest that members of a plasmid lineage belong to the same incompatibility group.

Bi- and Trireplicons

It has been previously observed that some *A. baumannii* plasmids contain more than one gene encoding a Rep protein. In fact, there are some examples of such plasmids in our collection: 5 plasmids possess two Rep genes, and one plasmid, p3ABSDF, contains 3 Rep genes (**Supplementary Table S4**). Each one of the Rep genes residing in the same plasmid belongs to a different Rep group. Some of the isolates that have bi- or trireplicons also contain other companion plasmids; these companion plasmids always include replication modules belonging to different Rep groups, between each other and with those present in the multireplicon plasmid. The French isolate SDF is an extreme example present in our collection. This isolate has three plasmids: p1ABSDF, p2ABSDF and p3ABSDF. The first plasmid possesses a replication module classified within Rep group GR1. The second plasmid, p2ABSDF, has two replication modules, one belonging to GR12 and the other to GR18. The third plasmid has 3 replication modules that belong to different Rep groups: GR7, GR9 and GR15. All the GR homology groups present in each isolate differ, preventing potential functional interference between the groups. These observations reinforce our hypothesis that each plasmid lineage belongs to a different incompatibility group and also suggest that these plasmids are the products of ancient plasmid cointegrations.

We also identified a plasmid lineage, LN_3 with a Rep protein belonging to homology group GR24. Members of this lineage contain a large set of phage-related genes, including several that could be implicated in replication, such as a DNA primase, a DNA helicase, a DNA ligase, the catalytic domain of DNA polymerase III (subunit α), and exonucleases, as already observed by Huang and coworkers (Huang et al., 2014). Plasmids that are capable of using phage-related proteins in replication can be considered bireplicons.

Partitioning Modules

Plasmids of high molecular weight and low copy number require an active segregation machinery to ensure that newly replicated plasmids are adequately segregated into the daughter cells. To date, three different active segregation machinery types have been identified, all of which consist of an NTPase, a centromere-like binding protein and at least one centromere-like sequence. These segregation machineries have been classified into three types according to their NTPase proteins: type I, which has a Walker-type ATPase (ParA); type II, which contains actin-like ATPases (ParM); and type III, which possesses a GTPase similar to tubulin (TubZ) (Baxter and Funnell, 2014). However, by far, the most common segregation machinery is that belonging to type I. This type consists of three different elements: ParA, a Walker-type ATPase; ParB, which is a centromere-like binding protein; and a DNA centromere-like site (*parS*). These systems are usually organized in an operon in which the first gene is *parA*, followed by *parB*, and the *parS* site is usually located near the *parA/parB* genes. Generally, plasmids that use this segregation system possess only one copy of the operon (Bignell and Thomas, 2001).

Of the *A. baumannii* plasmids studied here, lines LN_1, LN_5, LN_7 and LN_8 have *parA/parB* genes in the classic conformation, but members of LN_8 contain duplicates of these genes. In contrast, other lineages possess incomplete *parA/parB* systems: LN_3 members have one copy of *parA* and two copies of *parB*; LN_11 contains only one *parA* gene per plasmid and LN_18 members contain one *parB* copy. Interestingly, all members of LN_8 also encode a ParM-like protein, suggesting that these plasmids may possess a second segregation system belonging to type II. These observations revealed an extensive diversity of plasmid segregation systems in *A. baumannii* (**Supplementary Table S1**).

Toxin-Antitoxin Modules

Plasmids have developed several genetic modules to ensure their persistence within a bacterial population, and some of these modules are classified as toxin-antitoxin (TA) modules. These modules consist of two genes: one encoding a toxin and the other its cognate antitoxin. Toxins are more stable than antitoxins; therefore, cells that lose a plasmid encoding one of these modules are eventually eliminated from the population (Hayes and Van Melderen, 2011; Unterholzner et al., 2013). The presence of these modules on plasmids not only ensures the persistence of the plasmids within a cell line but may also play a role in bacterial virulence (Lobato-Márquez et al., 2016). TA modules been previously described in *A. baumannii* plasmids; therefore, we searched for the presence of these modules in our 173 plasmids (Jurenaite et al., 2013; Sužiedėlienė et al., 2016; Armalytė et al., 2018). We determined that 108 of them have TA modules belonging to nine different classes. Eight of these modules were TA modules of type II: ZetaTA (43.5%), SplTA (30.5%) and HigB/A (11.1%), and other TA modules that were less well represented (13.9%, in total), including YafQ/RelB, RelB/E, HicAB, HipA/B, and Phd/YoeB. Four plasmids have the

TA module AbiEii/AbiGii (type IV). Plasmids with TA modules exhibit the general tendency to have one per plasmid, with one exception: the orphan plasmid p3ABAYE has three different TA systems, namely, HigB/A, HipA/B, and RelB/E. Plasmids with the same TA module, in general, do not coexist. We have two isolates, namely, CR17 and CS01, that each possess one plasmid of the same lineage and with the same TA modules (**Supplementary Figure S14** and **Supplementary Table S5**).

Plasmid-carried restriction-modification modules play a role in plasmid stabilization via postsegregational killing (Kulakauskas et al., 1995) therefore, we searched for these modules in the plasmid collection, and only 7.9% of the plasmids harbor these modules. We showed that only five members of LN_1 and two plasmids of LN_3B have these modules. Three orphan plasmids, namely, pOIFC032-101, p2ABSDF and p3ABSDF, also have restriction-modification modules. Some plasmids, such as those belonging to LN_8 and the orphan plasmid pHWBA8_1, encode only for the DNA methyltransferase. These results suggest that some members of LN_1 and LN_3B acquired restriction-modification modules after the origination and diversification of the lineages.

Conjugation Modules

Conjugation is probably the most efficient process for dissemination of plasmids among strains of the same species or even to not closely related species. This process requires two gene sets: one involved in mating pair formation, which encompasses all genes required for the synthesis of a specialized type 4 secretion system that is essential for establishment of contacts between donor and receptor cells. The second gene set encodes products required for DNA processing and replication. Plasmids with these two functional gene sets are self-transmissible. However, other plasmids, containing only a transfer origin (*oriT*), a relaxase gene and some genes encoding nicking accessory proteins, require for mobilization of their proteins a specialized type 4 secretion system encoded by a second (helper) plasmid. These plasmids are known as mobilizable plasmids (Smillie et al., 2010; Cabezón et al., 2015). We performed a bioinformatic search for genes involved in conjugation in our plasmid collection, and the results are summarized in **Supplementary Table S5**. We discovered that only two plasmid lineages, namely, LN_1 and LN_5, have large sets of conjugation genes (>10 genes), but only members of LN_1 have been experimentally shown to be capable of conjugation (Di Venanzio et al., 2019). One of the 39 orphan plasmids, pKBN10P02143, has a large set of conjugation genes, suggesting that this plasmid is also conjugative. We also found some plasmids that have a small set of six conjugation genes but not a gene encoding a relaxase, such as members of lineages LN_7 and LN_8, suggesting that in the mobilization capacity was lost during evolution.

Eight of the 21 plasmid lineages identified in this work have the potential to be mobilizable, considering that these lineages have relaxase genes and their cognate *oriT* sequences. Six of these plasmid lineages (LN_12, LN_14, LN_15, LN_17, LN_18 and LN_3B) have relaxase genes belonging to the MOB_Q family, and all of these genes are closely related to other relaxases described only for *A. baumannii* plasmids (Salto et al., 2018). Lineages LN_1 and LN_5 have relaxase genes of the MOB_F family, and members of LN_4 possess a relaxase gene of the MOB_H family. Thirteen orphan plasmids have MOB_Q relaxase genes and only one relaxase gene of the MOB_P family. Notably, 14 plasmid lineages do not have relaxase genes; however, some of these lineages are dispersed throughout the A baumannii phylogenetic tree constructed with ribosomal genes not containing recombination signals. However, it has been shown that some *Staphylococcus aureus* plasmids, even in the absence of a relaxase and relaxase accessory genes, have sequences that mimic *oriT* sequences and that can be used for mobilization when they coexist with a conjugative plasmid that encodes Mob proteins able to recognize these oriT sequences (O'Brien et al., 2015a,b). Recently, Blackwell and Hall (2019) showed that the conjugative plasmid (pAb-G7-2) was capable to mobilize plasmid pS32-1, which lacks Mob encoding genes, through a relaxase *in trans* mechanism (Blackwell and Hall, 2019). Making sequence comparisons, these authors suggest that plasmid pS32-1 has a 32 pb DNA sequence that closely matches in sequence and organization the *oriT* of plasmid R388, an IncW plasmid whose *oriT* has been experimentally dissected. Blackwell and Hall also showed that the putative *oriT* and their adjacent sequences are present in other *A. baumannii* plasmids (Blackwell and Hall, 2019). To expand these observations, we search for the presence of these sequences in our plasmid collection set and here we show that they are present in all members of LN_2, LN_11, LN_19, LN_20 and some other plasmid, including a couple of orphans, indicating that potentially this mechanism is the responsible to disperse this plasmid lineages through different *A. baumannii* clades. DNA alignment of the putative *oriT* sequences located in these plasmids is shown in **Figure 4**. Nevertheless, these observations in conjunction also suggest that other plasmid transmission mechanisms that are not dependent on type IV secretion systems, such as transduction, transformation or outer membrane vesicles may play an important role in the spread of plasmids between *A. baumannii* populations (Rumbo et al., 2011; Chatterjee et al., 2017).

All *A. baumannii* strains studied here contain in their chromosomes genes encoding a type VI secretion system (T6SS) that is used to eliminate nonkin bacteria (Weber et al., 2013). An essential requirement for conjugation and T6SS functioning requires a tight cell-to-cell contact, and for this reason, conjugation can only take place when the T6SS is repressed, otherwise, the receptors for conjugation will be killed. Weber et al. (2015) demonstrated that large *A. baumannii* conjugative plasmids, all belonging to LN_1, encode two proteins TetR1 and TetR2 that repress the expression of the T6SS system and in this way promoting the dissemination not only of LN_1 plasmids but also of those mobilizable plasmids that coexist with them (Weber et al., 2015; Di Venanzio et al., 2019). These observations explain why LN_1 plasmids are widely distributed along many *A. baumannii* strains.

Insertion Sequences

IS elements and transposons are mobile genetic elements that can move from one location to another on the same replicon or between replicons of the same cell, but if linked

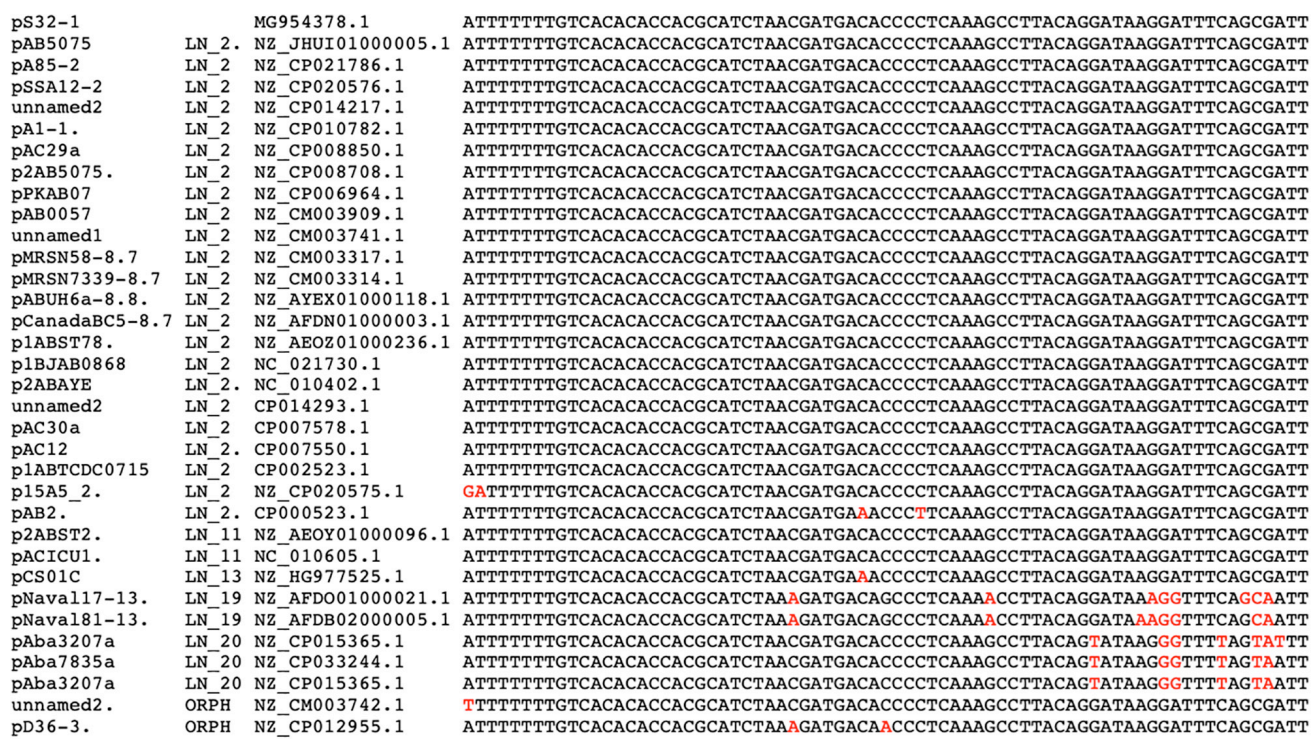

FIGURE 4 | DNA sequence alignment of *oriT* regions (73 bp) located in *A. baumannii* plasmids. At the left, plasmid names followed by the plasmid lineages and by their accession numbers. Letters in red are the nucleotides that show differences with the *oriT* of plasmid pS32.1 (at the top).

to other mobile elements such as plasmids or phages, these elements can be horizontally transmitted to other genomes (Siguier et al., 2014). These elements play an essential role in genome plasticity and gene expression and play a crucial role in bacterial pathogens because antibiotic resistance genes are frequently linked to these elements (Partridge et al., 2018). However, 47.3% of the plasmids in our collection do not have IS elements. The remaining plasmids analyzed here have at least one IS element of the 41 different IS elements identified in the collection (**Supplementary Table S6**). The most common IS elements were IS*Aba1* (13.1%) and IS*Aba125* (12.6%). The plasmid lineages exhibit contrasting features in terms of the number and diversity of IS elements: some plasmid lineages do not contain IS elements, such as LN_2 and LN_4. However, all the members of some lineages have IS elements. Some of these plasmids share the same IS elements or set of IS elements located in the same region (LN_10), while members of other lineages include different IS elements (i.e., LN_7). In conjunction, some lineages have members that lack IS elements; others have members with one IS; and the remaining include several IS elements of different kinds scattered along their DNA sequences. One of these lineages is LN_1. This lineage includes 42 members. Eight of these members do not possess IS elements; 22 members have only one element (the most frequent element being IS*Aba125*); and the remaining members have 2-4 IS elements. This observation clearly shows that IS elements are secondary acquisitions in the genomes of the members of this lineage. The plasmid lineages with a high number of IS elements and which exhibit high diversity in IS families are LN_8 and LN_7.

XerCD Recombinase and *Pdif* Sites

XerCD recombinases and their action sites (*dif* or XerC/D and XerD/C sites) have an important role resolving chromosome and plasmid dimers to monomers, but also in other site-specific reactions like the integration of the phage CTX at the *dif1* site of *Vibrio cholerae* chromosome I (Summers and Sherratt, 1988; Val et al., 2005). The presence of homologous *dif* sequences (*pdif*) has been found in many *A. baumannii* plasmids and they consist of stretches of 28 bp that contain the binding sites for the XerC and XerD recombinases (11 bp each) separated by a variable 6 bp linker. It has been proposed that these sites play a role in the mobilization of discrete DNA modules between *A. baumannii* replicons (D'Andrea et al., 2009; Blackwell and Hall, 2017). These modules have an important role in the dissemination of antibiotic resistance genes, since some of them embrace antibiotic-resistant genes like OXA-58 and OXA-24/40 (Poirel and Nordmann, 2006; Merino et al., 2010; Grosso et al., 2012), genes involved in tetracycline resistance (*tet39*), or the *msrE* and *mphE* macrolide resistance genes (Blackwell and Hall, 2017). We evaluated the presence of these sites in our plasmid set using as query the *pdif* sites of plasmid pS30-1 described by Blackwell and Hall (2017). Many plasmids of our collection possess at least one XerC/D site and others, but not necessarily the same plasmids, have one or several XerD/C sites, but only 15 plasmids have

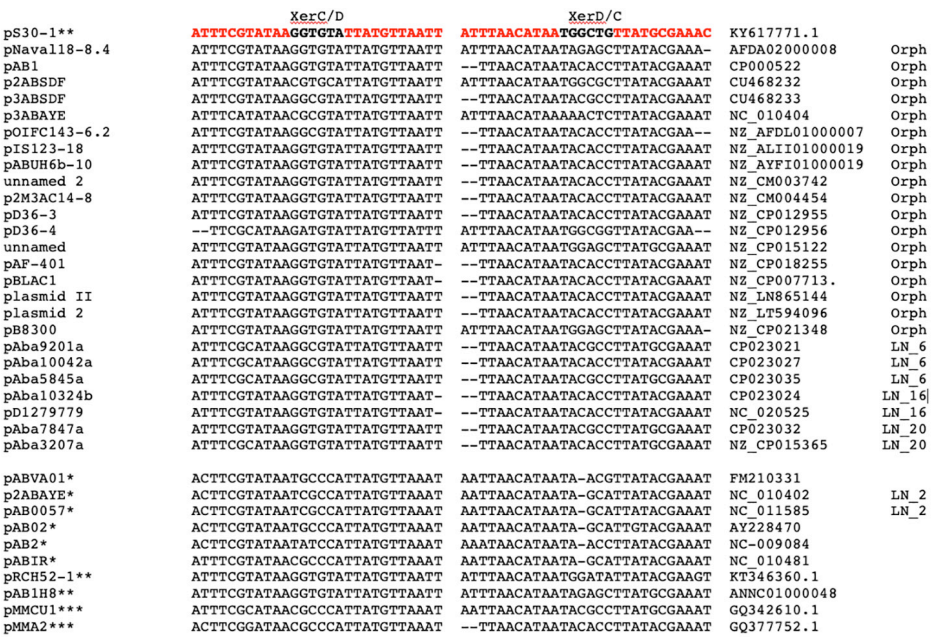

	XerC/D	XerD/C		
pS30-1**	ATTTCGTATAAGGTGTATTATGTTAATT	ATTTAACATAATGGCTGTTATGCGAAAC	KY617771.1	
pNaval18-8.4	ATTTCGTATAAGGTGTATTATGTTAATT	ATTTAACATAATAGAGCTTATACGAAA-	AFDA02000008	Orph
pAB1	ATTTCGTATAAGGTGTATTATGTTAATT	--TTAACATAATACACCTTATACGAAAT	CP000522	Orph
p2ABSDF	ATTTCGTATAACGTGCATTATGTTAATT	ATTTAACATAATGGCGCTTATACGAAAT	CU468232	Orph
p3ABSDF	ATTTCGTATAAGGCGTATTATGTTAATT	--TTAACATAATACGCCTTATACGAAAT	CU468233	Orph
p3ABAYE	ATTTCATATAACGCGTATTATGTTAATT	ATTTAACATAAAAACTCTTATACGAAAT	NC_010404	Orph
pOIFC143-6.2	ATTTCGTATAAGGCGTATTATGTTAATT	--TTAACATAATACACCTTATACGAA--	NZ_AFDL01000007	Orph
pIS123-18	ATTTCGTATAAGGTGTATTATGTTAATT	--TTAACATAATACACCTTATACGAAAT	NZ_ALII01000019	Orph
pABUH6b-10	ATTTCGTATAAGGTGTATTATGTTAATT	--TTAACATAATACACCTTATACGAAAT	NZ_AYFI01000019	Orph
unnamed 2	ATTTCGTATAAGGTGTATTATGTTAATT	--TTAACATAATACACCTTATACGAAAT	NZ_CM003742	Orph
p2M3AC14-8	ATTTCGTATAAGGTGTATTATGTTAATT	--TTAACATAATACACCTTATACGAAAT	NZ_CM004454	Orph
pD36-3	ATTTCGTATAAGGTGTATTATGTTAATT	--TTAACATAATACACCTTATACGAAAT	NZ_CP012955	Orph
pD36-4	--TTCGCATAAGATGTATTATGTTATTT	ATTTAACATAATGGCGGTTATACGAA--	NZ_CP012956	Orph
unnamed	ATTTCGTATAAGGTGTATTATGTTAATT	ATTTAACATAATGGAGCTTATGCGAAAT	NZ_CP015122	Orph
pAF-401	ATTTCGTATAAGGTGTATTATGTTAAT-	--TTAACATAATACACCTTATACGAAAT	NZ_CP018255	Orph
pBLAC1	ATTTCGTATAAGGTGTATTATGTTAAT-	--TTAACATAATACACCTTATACGAAAT	NZ_CP007713.	Orph
plasmid II	ATTTCGTATAAGGTGTATTATGTTAATT	--TTAACATAATACACCTTATACGAAAT	NZ_LN865144	Orph
plasmid 2	ATTTCGTATAAGGTGTATTATGTTAATT	--TTAACATAATACACCTTATACGAAAT	NZ_LT594096	Orph
pB8300	ATTTCGTATAAGGTGTATTATGTTAATT	ATTTAACATAATGGAGCTTATACGAAA-	NZ_CP021348	Orph
pAba9201a	ATTTCGCATAAGGCGTATTATGTTAATT	--TTAACATAATACGCCTTATGCGAAAT	CP023021	LN_6
pAba10042a	ATTTCGCATAAGGCGTATTATGTTAATT	--TTAACATAATACACCTTATACGAAAT	CP023027	LN_6
pAba5845a	ATTTCGCATAAGGCGTATTATGTTAATT	--TTAACATAATACGCCTTATGCGAAAT	CP023035	LN_6
pAba10324b	ATTTCGTATAAGGTGTATTATGTTAAT-	--TTAACATAATACACCTTATACGAAAT	CP023024	LN_16
pD1279779	ATTTCGTATAAGGTGTATTATGTTAAT-	--TTAACATAATACACCTTATACGAAAT	NC_020525	LN_16
pAba7847a	ATTTCGTATAAGGTGTATTATGTTAATT	--TTAACATAATACGCCTTATGCGAAAT	CP023032	LN_20
pAba3207a	ATTTCGCATAAGGTGTATTATGTTAATT	--TTAACATAATACACCTTATGCGAAAT	NZ_CP015365	LN_20
pABVA01*	ACTTCGTATAATGCCCATTATGTTAAAT	AATTAACATAATA-ACGTTATACGAAAT	FM210331	
p2ABAYE*	ACTTCGTATAATCGCCATTATGTTAAAT	AATTAACATAATA-GCATTATACGAAAT	NC_010402	LN_2
pAB0057*	ACTTCGTATAATCGCCATTATGTTAAAT	AATTAACATAATA-GCATTATACGAAAT	NC_011585	LN_2
pAB02*	ACTTCGTATAATGCCCATTATGTTAAAT	AATTAACATAATA-GCATTGTACGAAAT	AY228470	
pAB2*	ACTTCGTATAATATCCATTATGTTAAAT	AAATAACATAATA-ACCTTATACGAAAT	NC-009084	
pABIR*	ATTTCGTATAACGCCCATTATGTTAAAT	AATTAACATAATA-GCATTATACGAAAT	NC_010481	
pRCH52-1**	ATTTCGTATAAGGTGTATTATGTTAATT	ATTTAACATAATGGATATTATACGAAGT	KT346360.1	
pAB1H8**	ATTTCGTATAAGGTGTATTATGTTAATT	ATTTAACATAATAGAGCTTATGCGAAAT	ANNC01000048	
pMMCU1***	ATTTCGCATAACGCCCATTATGTTAAAT	AATTAACATAATACGCCTTATGCGAAAT	GQ342610.1	
pMMA2***	ACTTCGGATAACGCCCATTATGTTAAAT	--TTAACATAATACACCTTATACGAAAT	GQ377752.1	

FIGURE 5 | Alignment of left *pdif* (XerC/D) and right *pdif* (XerC/D) plasmids sites (in red) and their flanking sequences. At the top sequences used as query. At the left, plasmid names followed by XerC/D and XerC/D sequences. Next, column list GenBank accession numbers followed by the lineage number. At the bottom and marked with asterisks are plasmid and *pdif* sites defined by other authors: D'Andrea et al. (2009); Merino et al. (2010), and Blackwell and Hall (2017).

matches with both sequences. The list of the plasmids possessing these sites and the DNA sequence alignment of these sites are shown in **Figure 5**. In this work, we analyzed the *pdif* modules with antibiotic resistance genes. This analysis revealed some of the gene modules described by other authors in new plasmids. For example, the module of plasmid pS30-1 carrying *tetR* and *tet39* genes and involved in tetracycline resistance is also present in the orphan plasmid pNaval18-8.4 (Blackwell and Hall, 2017). However, in plasmids of the Mexican isolates, we found two new *pdif* modules. One of them of 967bp contains an OXA-72 gene and was identified in the members of LN_6. The second was present in plasmids pAba7847a and pAba3207a of LN_20 and consists in a 5260 bp module with four genes: OXA-58, two IS30 family transposases, and a hypothetical protein. However, more work must be done to identify other *pdif* modules carrying genes not related to antibiotic resistance.

Which Plasmids Carry Antibiotic Resistance Genes?

As vehicles of horizontal gene transfer, plasmids play a crucial role in the dissemination of antibiotic resistance genes within pathogenic bacterial populations (San Millan, 2018; Carattoli, 2013). To evaluate the role of *A. baumannii* plasmids in the dispersion of antibiotic resistance genes, we searched for the presence of acquired resistance genes in our plasmid set using the ResFinder database (Zankari et al., 2012). In this manner, we identified not only plasmids that carry antibiotic resistance genes but also the plasmids lineages associated with these genes (**Supplementary Table S7**). Only 35.2% of our plasmid collection possesses antibiotic resistance genes, and of these plasmids, thirty-eight contain only one antibiotic resistance gene. Fifteen plasmids have two antibiotic resistance genes, and eight plasmids have three or more of these genes. The most frequent antibiotic resistance genes were those involved in resistance to aminoglycosides, which were present in 60.6% of the plasmids carrying antibiotic resistance, followed by plasmids with genes conferring resistance to beta-lactam antibiotics (49.1%). Sulfonamide resistance genes were also present in 26.2% of the plasmids with antibiotic resistance, and 14.7% have genes implicated in macrolide resistance.

Of the twenty-three plasmid lineages, only thirteen have members with antibiotic resistance genes. However, most commonly, only a few members of a plasmid lineage possess this type of gene, suggesting that these genes were secondary acquisitions after the origination of the lineage. With a few exceptions, antibiotic resistance genes are closely linked to one or two IS elements, in some cases to class 1 integrons, and in three plasmids, namely, pA85-3, pAB04-2 and pUSA15-1, all of which are members of LN_1, the antibiotic resistance genes are linked to an AbaR4 element (Hamidian et al., 2014; Hamidian and Hall, 2018b). A good example of this situation is lineage LN_1. This lineage has 42 members, but only 14 have antibiotic resistance genes, and of these plasmids, nine carry one antibiotic resistance gene; three plasmids have two resistance genes; and plasmid p1AB5075 carries eleven of these genes. One gene is an aminoglycoside resistance gene (*aph(3')-Via*) surrounded by two IS*Aba25* elements, and the remaining antibiotic resistance genes are class 1 integrons. The other twelve plasmids have antibiotic resistance genes tightly linked to IS*Aba1* or IS*Aba25* elements. These observations suggest that the IS elements and

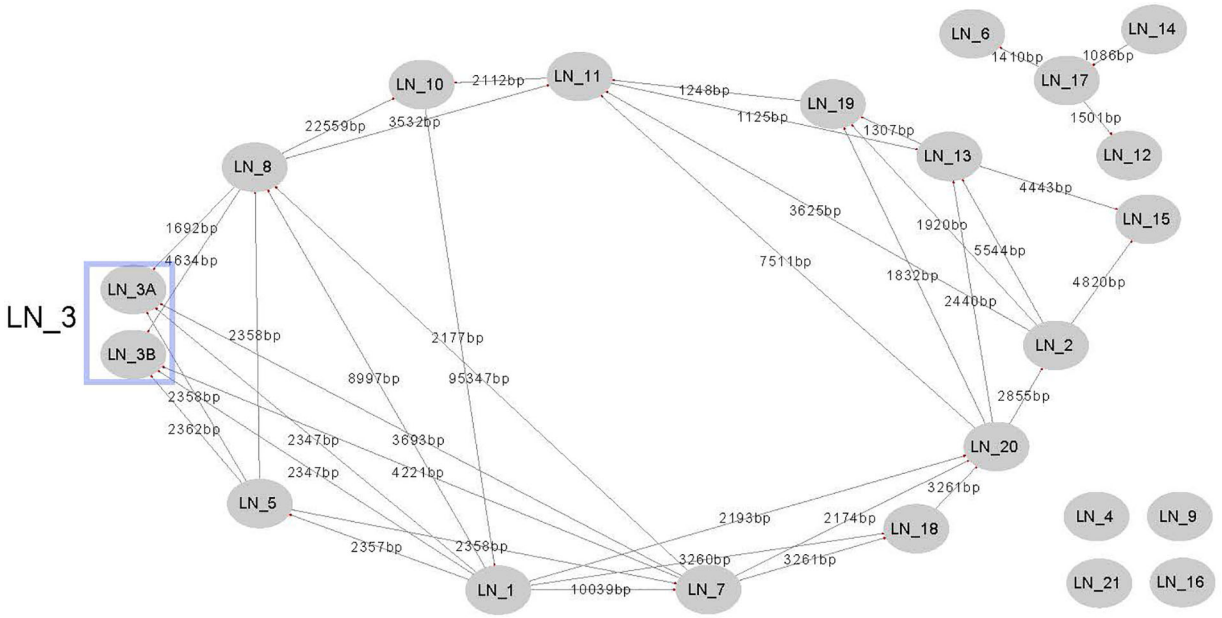

FIGURE 6 | Gene flux between plasmid lineages. Edges connect plasmid lineages that share at least 1Kb of DNA with an identity of 90%. Numbers in edges represent the total amount of different DNA sequences that members of one plasmid lineage have in common with members of the other plasmid lineage.

antibiotic resistance genes were acquired after the origin of this plasmid lineage.

The most predominant mechanism for carbapenem resistance in *A. baumannii* is the activity of OXA-type beta-lactamases (serine carbapenemases), some of which are encoded in plasmids (Da Silva and Domingues, 2016). In the analyzed plasmids, we found seven lineages with members carrying *bla*OXA genes: seven members of LN_1 carry *bla*OXA-23 genes as well as two members of LN_5. The four members of LN_6, all obtained from Mexican isolates, have *bla*OXA-72 genes. All members of LN_11 and LN21 possess *bla*OXA-58 genes, and one member of LN_14 and another from LN_17 contain *bla*OXA-24 genes.

Gene Flux Between Plasmid Lineages

To evaluate the gene flux between plasmid lineages or the amount of gene information that is shared between plasmid lineages, we performed BLASTn comparisons using the representative plasmid of one lineage as a query against all plasmids belonging to the other lineages. With this approach, we identified all DNA regions of 1 kb or higher with an identity of at least 90% and recorded the genes that remained in such regions. The results of this analysis are summarized in **Supplementary Table S8**. The amount of sequence information that two plasmid lineages can share varies dramatically (**Figure 6**). As described above, the lineage pair LN_7 and LN_8 share at least 90% sequence identity and coverage higher than 50% but lower than 85%. In contrast, lineages LN_4, LN_9, LN_16 and LN_21 do not share DNA sequences higher than 1 kb with any other plasmid lineage. Interestingly, plasmid members of these lineages are embedded in different genomic backgrounds, as illustrated in the phylogenetic tree shown in **Figure 7**. The remaining lineages share information with at least three and up to seven other plasmid lineages (**Supplementary Table S8**). Most of the DNA sequences that are shared between plasmid lineages, as expected, contain transposable elements, commonly but not exclusively IS*Aba1* and IS*Aba125*. Sets of antibiotic resistance genes are also frequently shared between plasmid lineages, and these genes are frequently linked to transposable elements such as IS elements and antibiotic resistance islands (AbaR4), suggesting that these elements frequently travel together (**Supplementary Table S6**).

Beyond *A. baumannii* and *Acinetobacter*

It has been shown that plasmids play a crucial role in disseminating virulence and antibiotic resistance genes in pathogenic bacteria. However, not all plasmids have the same potential to act as vectors for these purposes. One property that imposes limits on this potential is the replication host range. Some plasmids are capable of replicating in one or a few related species (narrow host range), while others are capable of replicating in an ample range of species and even genera (wide host range) (Jain and Srivastava, 2013). To evaluate the potential plasmid host ranges of the different *A. baumannii* plasmid lineages, we follow two strategies: first, we explored the NCBI nr (nonredundant) database by BLASTp analysis. We searched for proteins identical in sequence to those annotated as Rep proteins in our plasmid collection but excluded those identified in *A. baumannii* or *Acinetobacter*. Second, we also performed a BLASTn analysis of the NCBI nr (nonredundant) database, using the DNA sequences of the representative plasmids of each lineage and all orphan plasmids as queries but, again, excluding matches within *A. baumannii* or within the *Acinetobacter* genus.

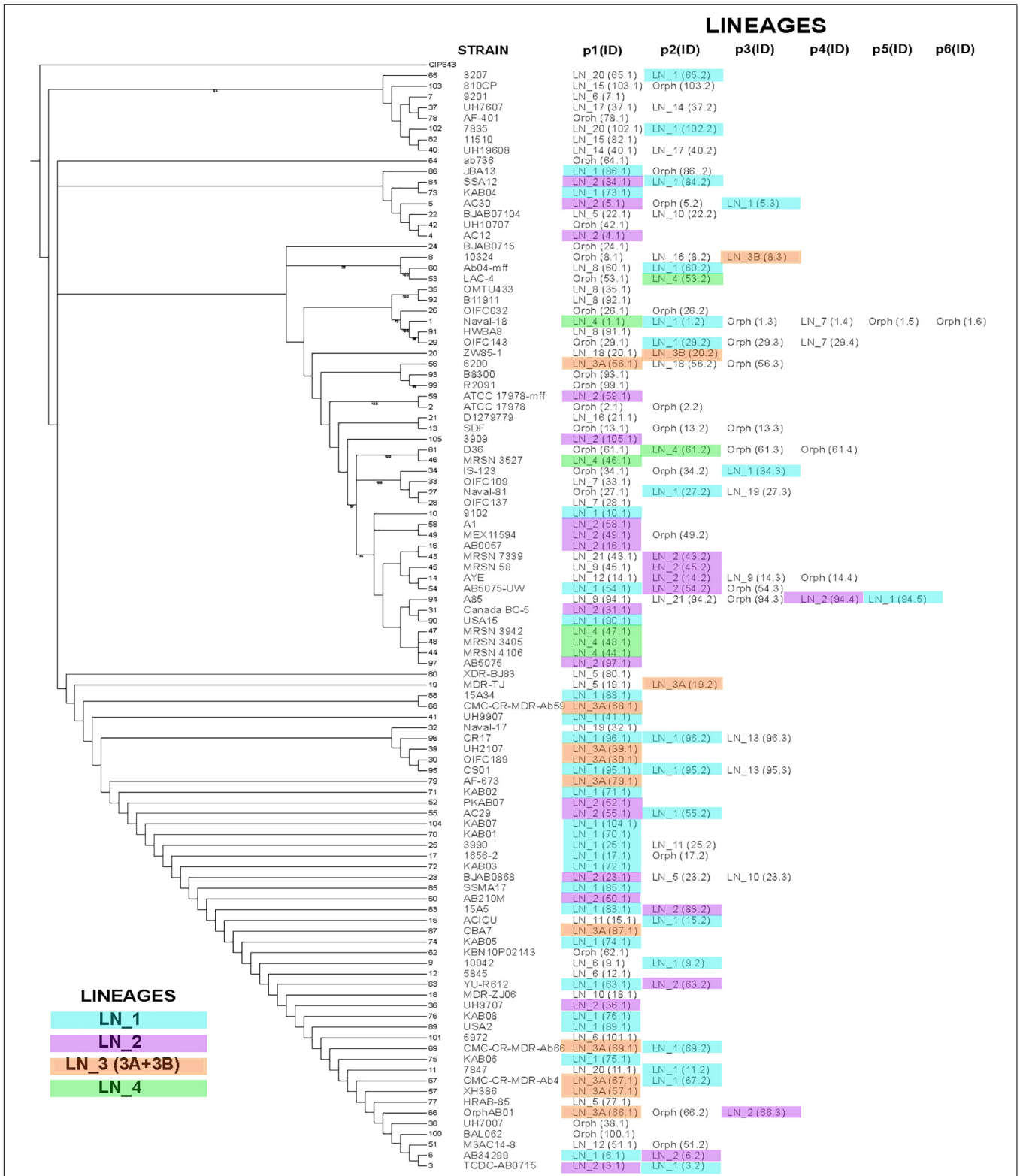

FIGURE 7 | Phylogenetic Tree of strains carrying the plasmids analyzed here. The tree was constructed using unicopy ribosomal protein genes without recombination signals. Bootstrap values higher than 70% are indicated in the tree. Strains containing our plasmid collection harbors a different numbers of plasmids, between one and six (p1..p6). At the right of each strain name shows the plasmids that that particular strain contains, using the alias plasmid name listed in **Supplementary Table S1** and the plasmid lineage that they belong. Plasmids marked in color belong to LN_1, LN_2, LN_3 or LN_4. Orph, indicates that the plasmid is an orphan.

A summary of our findings is presented in **Supplementary Table S9**. The Rep protein that seems to have a broad host range is encoded in the orphan plasmid pAB3 and can be found in the genomes of twelve genera of Gammaproteobacteria, ten genera of Betaproteobacteria, and three genera of Alphaproteobacteria and even in the actinobacterial species *Mycobacteroides abscessus*. This protein belongs to the RepC family. Some replication proteins of the GR3 homology group are also found in a wide variety of bacteria. For example, Rep proteins of the plasmids pB11911 (LN_8) and pMDR-ZJ06 (LN_10) were also identified in twelve different genera, all within Gammaproteobacteria. Similarly, the GR3 Rep protein of the orphan plasmid pHWBA8_1 was also found in the genomes of ten different genera of Gammaproteobacteria. Some Rep proteins of homology group GR2 were identified in, in addition to *A. baumannii, Enterococcus faecium, Klebsiella pneumoniae* and *Providencia rettgeri*. Some other Rep proteins were identified outside of Gammaproteobacteria; for example, some Rep proteins of LN_12 (GR11) and LN_14 (GR27) were located in *Neisseria meningitidis* (Betaproteobacteria). Additionally, the Rep protein of the orphan plasmid pIS123-12 (GR20) was present in the betaproteobacterial species *Nakamurella silvestris*. The remaining Rep proteins of the other GR groups seem to have a limited host range, being found in only *Acinetobacter*.

Intriguingly, some plasmids in our collection are very similar to other plasmids that are not closely related to *Acinetobacter*. For example, pMDR-ZJ06, which is the representative plasmid of LN_10, shares ≥ 75% coverage and 99% DNA sequence identity with the plasmid pEA49-KPC (GenBank: KU318419.1) of *Enterobacter aerogenes,* the plasmid RCS40_p (GenBank: LT985241.1) of *E. coli*, the plasmid pPMK1-NDM (GenBank: NZ_CP008933.1) of *K. pneumoniae* and the plasmid unnamed1 of *Citrobacter* sp. Similarly, plasmid pKP-NCGM38-1 (GenBank: AB825955.1) of *K. pneumoniae* shares 86% coverage and 99% identity with the representative plasmid of LN_13, indicating that this plasmid belongs to LN_13. The representative plasmid of LN_18 is almost identical to the plasmid p3SP-NDM (GenBank: KP900015.1) of *E. aerogenes* strain p3SP and shares 75% coverage and 99% identity with the plasmid p06-1619-NDM (GenBank: KX832928.1) of *P. rettgeri*.

The smallest plasmid in our collection, the orphan plasmid pJBA13_2 (1,109 bp), is almost identical to other very small plasmids belonging to other bacterial classes. This plasmid shares 100% coverage and 100% identity with an unnamed plasmid (GenBank: NZ_CP021055.1) from *Methylobacterium zatmanii* strain PSBB041 and with the plasmid unnamed6 (GenBank: NZ_CP023042.1) from *Komagataeibacter saccharivorans* CV1, both belonging to Alphaproteobacteria. Additionally, with plasmid unnamed2 (GenBank: NZ_CP013938.1) from *Weissella cibaria* strain CMU (Firmicutes) and with unnamed plasmid2 (GenBank: NZ_CP021993.1) from *Cryobacterium* sp. LW097 (Actinobacteria). Finally, orphan plasmid pJBA13_2 is almost identical to plasmids from *Salmonella enterica* subsp. *enterica* serovar Kentucky str. SA20030505 (GenBank: NZ_CP022501.1), *Pantoea ananatis* strain YJ76 (GenBank: NZ_CP022430.1) and *E. coli* strain HB-Coli0 (GenBank: NZ_CP020935.1) (Gammaproteobacteria). These observations indicate that the *A. baumannii* plasmid replication systems vary widely in host range; some seem to replicate only in *Acinetobacter* species, while others are capable of replicating in bacteria of different families and even different bacterial classes.

Pandemic and Epidemic Plasmids

We took two different approaches to evaluate whether our plasmid lineages are pandemic, that is, capable of existing in a wide range of chromosomal backgrounds, or epidemic, that is, only found in a few closely related chromosomes. For this purpose, we first determined the number of STs (Oxford and Pasteur MLST schemes) containing members of a specific plasmid lineage (listed in **Supplementary Table S1**). We found that a majority of our plasmid lineages occurred in more than one ST. Moreover, most of the plasmid lineages are present not only in isolates belonging to the International Clones but also out of these clonal complexes. For example, members of LN_1 are present in 20 different STs, and members of LN_2 are present in 9 STs. These lineages are clearly pandemic; however, members of some plasmid lineages seem to be epidemic, considering that these plasmids are restricted to a few STs; for instance, LN_3A, possessing 11 members, is represented in only 3 STs, mostly in ST208, and members of LN_4 are located in 3 STs. Lineages LN_9, LN_11, LN_14, LN_15, and LN_17 are present in one ST, but these lineages have only two or three members each, and in these circumstances, it is not possible to determine whether these lineages have a restricted chromosomal range.

Our second approach was to construct a phylogenetic tree using single-copy ribosomal genes without recombination signals of the strains including our plasmid collection and map the different plasmid lineages in this tree. In **Figure 5** we show the locations in the tree of our entire plasmid set, indicating the corresponding plasmid lineages. In **Figure 5**, we show evidence that the members of the four largest lineages (LN_1 to LN_4) are scattered throughout the phylogenetic tree, indicating that these plasmids are capable of replicating in a wide range of chromosomal backgrounds that are not necessarily closely related. However, notably, despite the wide distribution of plasmids belonging to LN_2 and LN_3A, these plasmids do not possess genes annotated as part of the conjugation or mobilization machineries. Nevertheless, as mentioned above, all members of LN_2 have *oriT*-like sequences that probably can be used for mobilization when they co-reside with a compatible conjugative helper plasmid.

Our bioinformatics analyses suggest that *A. baumannii* plasmids have diverse host ranges: plasmid lineages containing a Rep protein of homology group GR3, have the potential to replicate in an extensive range of bacterial genera, including some important pathogens such as *K. pneumoniae, E. coli,* and *Salmonella enterica.* As described above, the representative plasmid of LN_10 is very similar in sequence and gene content to previously described plasmids of *E. aerogenes, E. coli* and *K. pneumoniae.* All these plasmids of presumably of very wide host ranges are located in not closely related clades in the phylogenetic tree, suggesting that these plasmids were introduced into the *A. baumannii* populations in different independent

events. The remaining plasmids seem to replicate only within *Acinetobacter* (restricted host range).

A notable feature that we want to point out is the behavior of plasmids as antibiotic resistance gene carriers: members of lineages LN_4, LN_6, LN_7, LN_8, LN_10, LN_11, LN_3B, LN_18 and LN_20 all carry antibiotic resistance genes. As mentioned above, lineages LN_8 and LN_10 can probably also replicate in *K. pneumoniae*, a pathogen that has been identified as an important reservoir of antibiotic resistance genes (Wyres and Holt, 2018). In contrast, lineages LN_2, LN_3A LN_12, LN_13, LN_15, LN_16A, LN_19, and LN_21 do not carry genes of this type. We also found plasmids with intermediate behavior, in which some members of the lineage carry antibiotic resistance genes, while others do not (LN_1, LN_5, LN_14 and LN_17). At least in LN_1 and LN_5, antibiotic resistant genes are closely linked with IS elements.

Evolution of *A. baumannii* Plasmids in the Nosocomial Environment

Considering all these observations as a whole, we want to propose the following hypothesis to explain the evolution of *A. baumannii* plasmids in the nosocomial environment: before the advent of antibiotics, *A. baumannii* plasmids were parasites of this organism. The gene of these plasmids were involved not only in maintenance functions but also in reducing the fitness cost of plasmid replication. The stability of the structure and gene content of these plasmids over long periods of time in several genetic backgrounds within each of plasmid lineage is probably a product of this condition. When *A. baumannii* arrived in the nosocomial environment, this species began to interact with other bacterial pathogens, such as *K. pneumoniae* or *E. coli,* which already contained plasmids with antibiotic resistance genes. At this point, *A. baumannii* acquired a subset of these plasmids with broad host ranges, probably containing Rep proteins of the homology group GR3. The coexistence of these broad-host-range plasmids with the *A. baumannii* genome allowed the dispersion of new transposable elements with or without antibiotic resistance genes. The acquisition of IS elements permitted some plasticity in *A. baumannii* plasmids. In other words, we propose that at the beginning, *A. baumannii* plasmids were specialized to replicate in this microorganism with a minimal fitness cost, but the acquisition of new broad-host-range plasmids that already contained antibiotic resistance genes native to other microbial pathogens allowed *A. baumannii* to survive easily in the nosocomial environment and become a pathogen of concern.

A Note Regarding Plasmid Nomenclature

During this study, we found that the nomenclature of *Acinetobacter* plasmids does not follow any type of rule. Moreover, adding an additional layer of complexity, some plasmids do not have official names and are simple referred to in GenBank as unnamed plasmids or tagged as p1, p2, etc. This evident lack of convention imposes unnecessary challenges during a systematic study of plasmids. We need names that easily link a plasmid with its strain/isolate ID and with the species name. For these reasons, we strongly suggest naming *Acinetobacter* plasmids by following the nomenclature rules proposed for the *Agrobacterium* and *Rhizobium* cryptic plasmids: first, all plasmid names must begin with letter "p" followed by the first letter of the genus name and the first two letters of the species name. Then, the strain/isolate ID number is added, followed by a lower-case letter, using "a" for the smallest plasmid, "b" for the next plasmid and so on. For example, the name of the smallest plasmid of *A. haemolyticus* MC1956 would be pAhaMC1956a. The plasmid that is next in size in the same strain will be pAhaMC1956b, and so on.

The annotation of plasmid genes is also confusing and not uniform, and genes are often annotated by using the name of the best BLAST hit and not the true biological function of the gene in the plasmid. Recently, Christopher M. Thomas and coworkers published a paper addressing all these problems and suggested methods to resolve these issues. We encourage scientists interested in plasmid biology to follow those recommendations (Thomas et al., 2017).

CONCLUSION

Acinetobacter baumannii plasmids belong to a limited number of plasmid lineages and their structure seem to be very stable, in contrast to the observations made in the so-called mosaic plasmids. Mosaic plasmids are composed of genetic elements from distinct sources and they are highly dynamic in acquisition and loss of genes (Pesesky et al., 2019).

Core genomes of *A. baumannii* plasmid lineages contain more genes to those required for plasmid maintenance functions and these genes seems to be not related to the nosocomial environment, open the possibility that they could have other functions and opening the possibility that they reduce fitness cost in the plasmid host. Evidence showed here, suggest that each plasmid lineage represents a plasmid incompatibility group and that the largest plasmid lineages are widely distributed along the phylogenetic tree even though, some of them lack identifiable mobilization systems. In most plasmid lineages transposable elements and antibiotic resistance genes are secondary acquisitions. Plasmids of broad host range have a crucial role in the acquisition of antibiotic resistance genes in *A. baumannii.*

MATERIALS AND METHODS

Plasmid Collection

Our collection included all the complete plasmids (with the "assembled molecule" status) of *A. baumannii* available in the RefSeq and GenBank databases (NCBI) on August 14th, 2017. We parsed the GenBank and fasta files with the SeqIO Biopython module (Cock et al., 2009) in Python 2.7 for all subsequent analyses.

To increase the diversity of our plasmid collection, we obtained the complete genome sequences of 10 Mexican isolates using the PacBio RSII and Illumina NextSeq platforms.

The genome sequences of three isolates, namely, 7804, 810CP and 3207, have previously been reported by some of the authors of this manuscript (Castro-Jaimes et al., 2016; Pérez-Oseguera et al., 2017).

For the other eight isolates, we constructed hybrid assemblies with reads from both platforms using SPAdes v3.9.0 or Unicycler v0.4.1 (Bankevich et al., 2012; Wick et al., 2017). We performed functional annotation with the NCBI Prokaryotic Genome Annotation Pipeline. The GenBank accession numbers of the genomes of the Mexican isolates are listed in **Supplementary Table S10**. Therefore, in total, we analyzed 173 complete plasmids, and the complete list of plasmids and strains is shown in **Supplementary Table S1**.

Plasmid Lineage Delimitation

We performed paired BLASTn (Camacho et al., 2009) searches between all 173 complete plasmids in our collection. We built different plasmid networks, each based on a defined range of coverage (from 40 to 90%). For each plasmid pair, we placed a link between the plasmids if the smallest plasmid covered at least a defined percentage of the other plasmid, where coverage was determined by the sum of alignment lengths with greater than 90% identity Then, we extracted the islands or "connected components" with NetworkX (Hagberg et al., 2008) in Python 2.7. For each connected component, we extracted the most connected plasmid (hub) to use as a reference. When there was more than one hub, we sorted the hubs by size and selected the largest plasmid. The plasmid lineages and the associated references are listed in **Supplementary Table S1**.

Extraction of Plasmid Replication Proteins

We used an annotation-based approach to extract the plasmid initiation replication proteins. By using the plasmid GenBank files, we performed a case-insensitive search for the following keywords in the products: "replication protein", "plasmid replication initiator", "plasmid replication", "DNA replication", "plasmid replicase", "replication a", "replication b", "replication c", "RepB", "rolling circle", "replication initiation", "replicase". Then, we extracted both the nucleotide and protein sequences and excluded partial genes and pseudogenes. Additionally, we extracted 500 nucleotides upstream and downstream of the Rep gene for further analyses. This entire process was performed with Python 2.7 and the Biopython SeqIO module (Cock et al., 2009).

Reference Proteins for Homology Group Designation

We compiled all replication (Rep) proteins that were reported by Bertini et al. (2010); (Bertini et al., 2010) by gene name, plasmid name and plasmid accession number when available. For those cases in which the Rep proteins did not have a locus tag or gene name, we added an artificial locus tag built using the replicon ID and the replicase name. When the replicase name was not available, we assigned the word 'rep' followed by a number in the order of appearance in the GenBank file to distinguish between replicases. In some cases, when there were two replication proteins in the same plasmid, to correctly assign these proteins as references for certain homology groups, we performed a BLAST search of these proteins against the GenBank nr database to identify corresponding hits outside the *Acinetobacter* genus reported in **Supplementary Table S1** in Bertini et al. (2010). Two proteins could not be identified: the Aci3 replicase from plasmid Ab599 (member of GR3), because the plasmid sequence was not deposited in databases, and the Aci2 replicase from the MAD plasmid, because the plasmid had a partial sequence that did not include the replicase. Therefore, we omitted these proteins from our analyses and examined other members of the same homology groups instead. As reported by Lean and Yeo (2017), the GR2 homology group should be split into two groups; therefore, we separated the proteins that represent GR2 from those of the newly formed GR20. Additionally, (Cameranesi et al., 2017) recently reported new homology groups; thus, we downloaded the plasmids that harbored the replicases that represent these groups and extracted those genes. **Supplementary Table S2** lists all proteins used as references in this work, including the origins, accessions, numbers and headers used in the multi-FASTA files included in **Supplementary Materials S1**, **S2**.

Homology Group Assignation for Rep Proteins

First, we performed paired BLASTn (Camacho et al., 2009) searches between all genes encoding replication initiation proteins present in our plasmid collection. We retained hits with more than 74% nucleotide identity and that covered at least 90% of the query. Then, if the query coding sequence (CDS) mapped to only one homology group, we designated the sequence as belonging to that group, whereas if there was more than one hit for different homology groups, we assigned the query to the GR with the highest percentage identity. We discarded the GR23 homology group because the associated reference (KY984047_repAci23) was 100% identical to one of the references of GR8 (GU979000.1_p11921_repA).

Plasmid Rep Protein Phylogenetic Analysis and Designation of New Homology Groups

We built a network in which each gene encoding a Rep protein was connected to another if the two genes shared at least 74% nucleotide identity and 90% coverage. Then, for the islands or connected components that did not have a Rep protein in the reference table, we selected the hub as a reference and added it to **Supplementary Table S1**. Additionally, we built plasmid replication initiation protein phylogenies to validate current assignations and new homology groups. We searched for the associated Pfam domains in the Pfam database (El-Gebali et al., 2019), accessed on February 21st, 2018, to separate the proteins by conserved domains and perform alignments separately because these proteins are very different. We used Clustal Omega (Sievers et al., 2014) to align amino acids and RevTrans (Wernersson and Pedersen, 2003) to guide the nucleotide alignment by the translated CDS. Then, we ran jModelTest2 (Darriba et al., 2012) to search for an adequate evolutionary model and built the

phylogenetic tree with PHYML (Guindon and Gascuel, 2003) with the selected model. By visual inspection, we validated the references of new homology groups, selected proteins that may be representative of new clades and designated these proteins as new homology groups, as detailed in **Supplementary Table S2**.

Phylogenetic Analysis of Ribosomal Proteins and MLST

We used Roary (Page et al., 2015) to extract monocopy genes encoding ribosomal proteins belonging to the core genome and that had the exact same size in all the strains to avoid gaps in the alignment. We aligned the ribosomal proteins with Clustal Omega (Sievers et al., 2014) to guide the nucleotide alignment with RevTrans (Wernersson and Pedersen, 2003). We discarded sequences with recombination signals detected with RDP4 (Martin et al., 2015). We concatenated the remaining nucleotide alignments with FASconCAT-G (Kück and Longo, 2014) and used jModelTest2 (Darriba et al., 2012) to select the evolutionary model to build a phylogenetic tree with PHYML (Guindon and Gascuel, 2003). We used the ribosomal proteins of the *Acinetobacter haemolyticus* CIP 64.3 strain as an outgroup. The sequence type (ST) assignation of each *A. baumannii* isolate, under Oxford and Pasteur MLST schemes, were obtained from the PubMLST database[1] (Bartual et al., 2005; Diancourt et al., 2010).

Identification of Secretion Systems, Antibiotic Resistance Genes, and Insertion Sequences on Plasmids

We used MacSyFinder with the TXSSCAN profiles (Abby and Rocha, 2017) to identify secretion systems on the plasmid collection and ResFinder to identify the acquired antibiotic resistance genes present in our plasmid set (Zankari et al., 2012). We identified the insertion sequence (IS) elements present in the plasmids using the ISfinder database at[2] (Siguier et al., 2006).

Identification of *pdif* Sites (XerC/D and Xer D/C) on Plasmids

To identify the *pdif* sites in our plasmid set, we made a BLASTn analysis using as queries the *pdif* sites of plasmid pS30-1: XerC/D, ATTTCGTATAAGGTGTATTAT- GTTAATT and XerD/C, ATTTAACATAATGGCTGTTATGCGAAAC (Blackwell and Hall, 2017).

COG Assignments

We determined homologous gene assignments for each plasmid based on hidden Markov model (HMM) searches using the *hmmsearch* program (Eddy, 2011). This HMM search process employs a previously constructed model set that represents each of the 4873 COGs and 8539 Remained Orthologous Groups (ROGs) (Tatusov et al., 2003; Taboada et al., 2010). Then, using Perl scripts, we classified each assigned COG by using the general classification scheme of Tatusov [66]. We calculated the frequency of each gene per class and plotted the results using ggplot2 R scripts[3] (Wickham, 2009).

[1]https://pubmlst.org

[2]http://www-is.biotoul.fr

DATA AVAILABILITY STATEMENT

Genome sequences were deposited in NCBI/GenBank with the following accession numbers: Isolate 7847: NZ_CP023031.1, CP023032.1, CP023033.1. Isolate 7835: CP033243.1, CP03 3244.1, CP033245.1. Isolate 9102: CP023029.1, CP023030.1. Isolate 5845: NZ_CP023034.1, CP023035.1. Isolate 10042: NZ_CP023026.1, CP023027.1, CP023028.1. Isolate 10324: NZ_CP023022.1, CP023023.1, CP023024.1, CP023025.1. Isolate 9201: NZ_CP023020.1, CP023021.1.

AUTHOR CONTRIBUTIONS

MC conceived, designed, and coordinated the study. ÁP-O made plasmid profile analysis and genome analysis of Mexican isolates. AS-C and SC-J made genome assemblies, genome annotation, network analysis, and bioinformatics analysis, and made bioinformatic analysis. AS-C designed figures and most of the tables of the manuscript. R-MG-R made COG analysis and statistics. LA-P made the analysis of Rep proteins. LL made bioinformatic analysis and made many pf Perl scripts used in this work. PV contributed with the Mexican isolates, participated in the manuscript drafting and in the general discussion. SC-R and JS-S had a crucial role in the general discussion. All authors contributed to manuscript revision, read and approved the submitted version.

FUNDING

This work was partially supported by PAPIIT grant number 200318 (Universidad Nacional Autónoma de México) and Consejo Nacional de Ciencia y Tecnología (CONACyT) grant number 253070.

ACKNOWLEDGMENTS

We would like to thank Ricardo Grande and Gloria Tanahiry Vazquez Castro for the sequencing support as part of the *Unidad de Secuenciación Masiva y Bioinformática* (UNAM). AS-C made his Ph.D. studies in Programa de Doctorado en Ciencias Biomédicas (Universidad Nacional Autónoma de México, UNAM) and was supported by CONACyT with a scholarship (244044).

SUPPLEMENTARY MATERIAL

The Supplementary Material for this article can be found online at: https://www.frontiersin.org/articles/10.3389/fmicb.2020.01283/full#supplementary-material

[3]http://www.R-project.org/

FIGURE S1 | Plasmid networks.

FIGURE S2 | Circular maps of members of plasmid lineage LN_3.

FIGURE S3 | Circular maps of members of plasmid lineages LN_4 and LN_5.

FIGURE S4 | Circular maps of members of plasmid lineages LN_6 and LN_7.

FIGURE S5 | Circular maps of members of plasmid lineage LN_8.

FIGURE S6 | Circular maps of members of plasmid lineages LN_9, LN_10.

FIGURE S7 | Maps of members of plasmid LN_11 and LN_12.

FIGURE S8 | Linear maps of members of plasmid lineages LN_13, and LN_14.

FIGURE S9 | Linear maps of members of plasmid lineages LN_15, and LN_16.

Figure S10 | Maps of members of plasmid lineages LN_17 and LN_18.

FIGURE S11 | Linear maps of members of plasmid lineages LN_19, and LN_20.

FIGURE S12 | Linear maps of members of plasmid lineage LN_21.

FIGURE S13 | Phylogenetic tree of Rep proteins belonging to the Pri_CT family.

FIGURE S14 | Phylogenetic Tree of strains carrying the plasmids analyzed here and their associated Toxin-Antitoxin modules.

TABLE S1 | List of plasmids belonging to lineages and their general characteristics.

TABLE S2 | Replicases used to assign GR homology groups.

TABLE S3 | Replicon-associated iterons identified in new GR members.

TABLE S4 | Plasmids encoding two or more replication proteins.

TABLE S5 | Conjugation genes and Toxin-Antitoxin system present in plasmids.

TABLE S6 | IS elements present in plasmids.

TABLE S7 | Antibiotic resistance genes located in plasmids.

TABLE S8 | Gene flux between plasmid lineages.

TABLE S9 | Replication proteins of A. baumannii plasmids which are identical in sequence to replication proteins in the genomes of other Acinetobacterspecies and in other genera.

TABLE S10 | GenBank accession numbers of Mexican isolates and their Sequence type following Oxfordand Pasteur schemes.

MATERIAL S1 | List in fasta format of genes encoding representative replication proteins of each one of the GR homology groups.

MATERIAL S2 | List in fasta format of the representative replication proteins of each one of the GR homology groups.

REFERENCES

Abby, S. S., and Rocha, E. P. C. (2017). Identification of protein secretion systems in bacterial genomes using MacSyFinder. *Methods Mol. Biol.* 1615, 1–21. doi: 10.1007/978-1-4939-7033-9_1

Antunes, L. C. S., Visca, P., and Towner, K. J. (2014). *Acinetobacter baumannii*: evolution of a global pathogen. *Pathog. Dis.* 71, 292–301. doi: 10.1111/2049-632X.12125

Armalytė, J., Jurėnas, D., Krasauskas, R., Čepauskas, A., and Sužiedėlienė, E. (2018). The higBA toxin-antitoxin module from the opportunistic pathogen *Acinetobacter baumannii* - regulation, activity, and evolution. *Front. Microbiol.* 9:732. doi: 10.3389/fmicb.2018.00732

Austin, S., and Nordström, K. (1990). Partition-mediated incompatibility of bacterial plasmids. *Cell* 60, 351–354. doi: 10.1016/0092-8674(90)90584-2

Bankevich, A., Nurk, S., Antipov, D., Gurevich, A. A., Dvorkin, M., Kulikov, A. S., et al. (2012). SPAdes: a new genome assembly algorithm and its applications to single-cell sequencing. *J. Comput. Biol.* 19, 455–477. doi: 10.1089/cmb.2012.0021

Bartual, S. G., Seifert, H., Hippler, C., Luzon, M. A. D., Wisplinghoff, H., and Rodríguez-Valera, F. (2005). Development of a multilocus sequence typing scheme for characterization of clinical isolates of *Acinetobacter baumannii*. *J. Clin. Microbiol.* 43, 4382–4390. doi: 10.1128/JCM.43.9.4382-4390.2005

Baxter, J. C., and Funnell, B. E. (2014). Plasmid partition mechanisms. *Microbiol. Spectr.* 2:6. doi: 10.1128/microbiolspec.PLAS-0023-2014

Bertini, A., Poirel, L., Mugnier, P. D., Villa, L., Nordmann, P., and Carattoli, A. (2010). Characterization and PCR-based replicon typing of resistance plasmids in *Acinetobacter baumannii*. *Antimicrob. Agents Chemother.* 54, 4168–4177. doi: 10.1128/AAC.00542-10

Bignell, C., and Thomas, C. M. (2001). The bacterial ParA-ParB partitioning proteins. *J. Biotechnol.* 91, 1–34. doi: 10.1016/s0168-1656(01)00293-0

Blackwell, G. A., and Hall, R. M. (2017). The tet39 determinant and the msrE-mphE genes in *Acinetobacter* plasmids are each part of discrete modules flanked by inversely oriented pdif (XerC-XerD) sites. *Antimicrob. Agents Chemother.* 61:e00780-17. doi: 10.1128/AAC.00780-17

Blackwell, G. A., and Hall, R. M. (2019). Mobilisation of a small *Acinetobacter* plasmid carrying an oriT transfer origin by conjugative RepAci6 plasmids. *Plasmid* 103, 36–44. doi: 10.1016/j.plasmid.2019.04.002

Brandt, C., Viehweger, A., Singh, A., Pletz, M. W., Wibberg, D., Kalinowski, J., et al. (2019). Assessing genetic diversity and similarity of 435 KPC-carrying plasmids. *Sci. Rep.* 9:11223. doi: 10.1038/s41598-019-47758-5

Cabezón, E., Ripoll-Rozada, J., Peña, A., de la Cruz, F., and Arechaga, I. (2015). Towards an integrated model of bacterial conjugation. *FEMS Microbiol. Rev.* 39, 81–95. doi: 10.1111/1574-6976.12085

Camacho, C., Coulouris, G., Avagyan, V., Ma, N., Papadopoulos, J., Bealer, K., et al. (2009). BLAST+: architecture and applications. *BMC Bioinformatics* 10:421. doi: 10.1186/1471-2105-10-421

Cameranesi, M. M., Limansky, A. S., Morán-Barrio, J., Repizo, G. D., and Viale, A. M. (2017). Three novel *Acinetobacter baumannii* plasmid replicase-homology groups inferred from the analysis of a multidrug-resistant clinical strain isolated in Argentina. *J. Infect. Dis. Epidemiol.* 3:46 doi: 10.23937/2474-3658/1510046

Cameranesi, M. M., Morán-Barrio, J., Limansky, A. S., Repizo, G. D., and Viale, A. M. (2018). Site-specific recombination at XerC/D sites mediates the formation and resolution of plasmid co-integrates carrying a blaOXA-58- and TnaphA6-Resistance module in *Acinetobacter baumannii*. *Front. Microbiol.* 9:66. doi: 10.3389/fmicb.2018.00066

Carattoli, A. (2013). Plasmids and the spread of resistance. *Int. J. Med. Microbiol.* 303, 298–304. doi: 10.1016/j.ijmm.2013.02.001

Castro-Jaimes, S., Salgado-Camargo, A. D. A. D., Graña-Miraglia, L., Lozano, L., Bocanegra-Ibarias, P., Volkow-Fernández, P., et al. (2016). Complete genome sequence of a multidrug-resistant *Acinetobacter baumannii* isolate obtained from a mexican hospital (Sequence Type 422). *Genome Announc.* 4:e00583-16. doi: 10.1128/genomeA.00583-16

Chatterjee, S., Mondal, A., Mitra, S., and Basu, S. (2017). *Acinetobacter baumannii* transfers the blaNDM-1 gene via outer membrane vesicles. *J. Antimicrob. Chemother.* 72, 2201–2207. doi: 10.1093/jac/dkx131

Chattoraj, D. K. (2000). Control of plasmid DNA replication by iterons: no longer paradoxical. *Mol. Microbiol.* 37, 467–476. doi: 10.1046/j.1365-2958.2000.01986.x

Cock, P. J. A., Antao, T., Chang, J. T., Chapman, B. A., Cox, C. J., Dalke, A., et al. (2009). Biopython: freely available Python tools for computational molecular biology and bioinformatics. *Bioinformatics* 25, 1422–1423. doi: 10.1093/bioinformatics/btp163

Da Silva, G. J., and Domingues, S. (2016). Insights on the horizontal gene transfer of carbapenemase determinants in the opportunistic pathogen *Acinetobacter baumannii*. *Microorganisms* 4:29. doi: 10.3390/microorganisms4030029

D'Andrea, M. M., Giani, T., D'Arezzo, S., Capone, A., Petrosillo, N., Visca, P., et al. (2009). Characterization of pABVA01, a plasmid encoding the OXA-24 carbapenemase from Italian isolates of *Acinetobacter baumannii*. *Antimicrob. Agents Chemother.* 53, 3528–3533. doi: 10.1128/AAC.00178-09

Darriba, D., Taboada, G. L., Doallo, R., and Posada, D. (2012). jModelTest 2: more models, new heuristics and parallel computing. *Nat. Methods* 9, 772–772. doi: 10.1038/nmeth.2109

del Solar, G., Giraldo, R., Ruiz-Echevarría, M. J., Espinosa, M., and Díaz-Orejas, R. (1998). Replication and control of circular bacterial plasmids. *Microbiol. Mol. Biol. Rev.* 62, 434–464. doi: 10.1128/mmbr.62.2.434-464.1998

Di Venanzio, G., Moon, K. H., Weber, B. S., Lopez, J., Ly, P. M., Potter, R. F., et al. (2019). Multidrug-resistant plasmids repress chromosomally encoded T6SS to enable their dissemination. *Proc. Natl. Acad. Sci. U.S.A.* 116, 1378–1383. doi: 10.1073/pnas.1812557116

Diancourt, L., Passet, V., Nemec, A., Dijkshoorn, L., and Brisse, S. (2010). The population structure of *Acinetobacter baumannii*: expanding multiresistant clones from an ancestral susceptible genetic pool. *PLoS One* 5:e10034. doi: 10.1371/journal.pone.0010034

Eddy, S. R. (2011). Accelerated profile HMM searches. *PLoS Comput. Biol.* 7:e1002195. doi: 10.1371/journal.pcbi.1002195

El-Gebali, S., Mistry, J., Bateman, A., Eddy, S. R., Luciani, A., Potter, S. C., et al. (2019). The Pfam protein families database in 2019. *Nucleic Acids Res.* 47, D427–D432. doi: 10.1093/nar/gky995

Fondi, M., Bacci, G., Brilli, M., Papaleo, M. C., Mengoni, A., Vaneechoutte, M., et al. (2010). Exploring the evolutionary dynamics of plasmids: the *Acinetobacter* pan-plasmidome. *BMC Evol. Biol.* 10:59. doi: 10.1186/1471-2148-10-59

Frost, L. S., Leplae, R., Summers, A. O., and Toussaint, A. (2005). Mobile genetic elements: the agents of open source evolution. *Nat. Rev. Microbiol.* 3, 722–732. doi: 10.1038/nrmicro1235

Grosso, F., Quinteira, S., Poirel, L., Novais, Â, and Peixe, L. (2012). Role of common blaOXA-24/OXA-40-carrying platforms and plasmids in the spread of OXA-24/OXA-40 among *Acinetobacter* species clinical isolates. *Antimicrob. Agents Chemother.* 56, 3969–3972. doi: 10.1128/AAC.06255-11

Guindon, S., and Gascuel, O. (2003). A simple, fast, and accurate algorithm to estimate large phylogenies by maximum likelihood. *Syst. Biol.* 52, 696–704. doi: 10.1080/10635150390235520

Hagberg, A. A., Schult, D. A., and Swart, P. J. (2008). "Exploring network structure, dynamics, and function using NetworkX," in *Proceedings of the 7th Python in Science Conference (SciPy2008)*, eds G. Varoquaux, T. Vaught, and J. Millman (Pasadena, CA), 11–15.

Hamidian, M., and Hall, R. M. (2018a). Genetic structure of four plasmids found in *Acinetobacter baumannii* isolate D36 belonging to lineage 2 of global clone 1. *PLoS One* 13:e0204357. doi: 10.1371/journal.pone.0204357

Hamidian, M., and Hall, R. M. (2018b). The AbaR antibiotic resistance islands found in *Acinetobacter baumannii* global clone 1 - Structure, origin and evolution. *Drug Resist. Updat.* 41, 26–39. doi: 10.1016/j.drup.2018.10.003

Hamidian, M., Kenyon, J. J., Holt, K. E., Pickard, D., and Hall, R. M. (2014). A conjugative plasmid carrying the carbapenem resistance gene blaOXA-23 in AbaR4 in an extensively resistant GC1 *Acinetobacter baumannii* isolate. *J. Antimicrob. Chemother.* 69, 2625–2628. doi: 10.1093/jac/dku188

Hayes, F., and Van Melderen, L. (2011). Toxins-antitoxins: diversity, evolution and function. *Crit. Rev. Biochem. Mol. Biol.* 46, 386–408. doi: 10.3109/10409238.2011.600437

Higgins, P. G., Dammhayn, C., Hackel, M., and Seifert, H. (2010). Global spread of carbapenem-resistant *Acinetobacter baumannii*. *J. Antimicrob. Chemother.* 65, 233–238. doi: 10.1093/jac/dkp428

Huang, H., Dong, Y., Yang, Z.-L., Luo, H., Zhang, X., and Gao, F. (2014). Complete sequence of pABTJ2, a plasmid from *Acinetobacter baumannii* MDR-TJ, carrying many phage-like elements. *Genomics Proteomics Bioinformatics* 12, 172–177. doi: 10.1016/j.gpb.2014.05.001

Hujer, A. M., Higgins, P. G., Rudin, S. D., Buser, G. L., Marshall, S. H., Xanthopoulou, K., et al. (2017). Nosocomial outbreak of extensively drug-resistant *Acinetobacter baumannii* isolates containing blaOXA-237 carried on a plasmid. *Antimicrob. Agents Chemother.* 61:e00797-17. doi: 10.1128/AAC.00797-17

Hülter, N., Ilhan, J., Wein, T., Kadibalban, A. S., Hammerschmidt, K., and Dagan, T. (2017). An evolutionary perspective on plasmid lifestyle modes. *Curr. Opin. Microbiol.* 38, 74–80. doi: 10.1016/j.mib.2017.05.001

Jain, A., and Srivastava, P. (2013). Broad host range plasmids. *FEMS Microbiol. Lett.* 348, 87–96. doi: 10.1111/1574-6968.12241

Jurenaite, M., Markuckas, A., and Suziedeliene, E. (2013). Identification and characterization of type II toxin-antitoxin systems in the opportunistic pathogen *Acinetobacter baumannii*. *J. Bacteriol.* 195, 3165–3172. doi: 10.1128/JB.00237-13

Kück, P., and Longo, G. C. (2014). FASconCAT-G: extensive functions for multiple sequence alignment preparations concerning phylogenetic studies. *Front. Zool.* 11:81. doi: 10.1186/s12983-014-0081-x

Kulakauskas, S., Lubys, A., and Ehrlich, S. D. (1995). DNA restriction-modification systems mediate plasmid maintenance. *J. Bacteriol.* 177, 3451–3454. doi: 10.1128/jb.177.12.3451-3454.1995

Lean, S. S., and Yeo, C. C. (2017). Small, enigmatic plasmids of the nosocomial pathogen, *Acinetobacter baumannii*: good, bad, who knows? *Front. Microbiol.* 8:1547. doi: 10.3389/fmicb.2017.01547

Lobato-Márquez, D., Díaz-Orejas, R., and García-Del Portillo, F. (2016). Toxin-antitoxins and bacterial virulence. *FEMS Microbiol. Rev.* 40, 592–609. doi: 10.1093/femsre/fuw022

Martin, D. P., Murrell, B., Golden, M., Khoosal, A., and Muhire, B. (2015). RDP4: Detection and analysis of recombination patterns in virus genomes. *Virus Evol.* 1:vev003. doi: 10.1093/ve/vev003

Merino, M., Acosta, J., Poza, M., Sanz, F., Beceiro, A., Chaves, F., et al. (2010). OXA-24 carbapenemase gene flanked by XerC/XerD-like recombination sites in different plasmids from different *Acinetobacter* species isolated during a nosocomial outbreak. *Antimicrob. Agents Chemother.* 54, 2724–2727. doi: 10.1128/AAC.01674-09

Mosqueda, N., Gato, E., Roca, I., López, M., de Alegría, C. R., Fernández Cuenca, F., et al. (2014). Characterization of plasmids carrying the blaOXA-24/40 carbapenemase gene and the genes encoding the AbkA/AbkB proteins of a toxin/antitoxin system. *J. Antimicrob. Chemother.* 69, 2629–2633. doi: 10.1093/jac/dku179

Novick, R. P. (1987). Plasmid incompatibility. *Microbiol. Rev.* 51, 381–395.

O'Brien, F. G., Ramsay, J. P., Monecke, S., Coombs, G. W., Robinson, O. J., Htet, Z., et al. (2015a). Staphylococcus aureus plasmids without mobilization genes are mobilized by a novel conjugative plasmid from community isolates. *J. Antimicrob. Chemother.* 70, 649–652. doi: 10.1093/jac/dku454

O'Brien, F. G., Yui Eto, K., Murphy, R. J. T., Fairhurst, H. M., Coombs, G. W., Grubb, W. B., et al. (2015b). Origin-of-transfer sequences facilitate mobilisation of non-conjugative antimicrobial-resistance plasmids in *Staphylococcus aureus*. *Nucleic Acids Res.* 43, 7971–7983. doi: 10.1093/nar/gkv755

Page, A. J., Cummins, C. A., Hunt, M., Wong, V. K., Reuter, S., Holden, M. T. G., et al. (2015). Roary: Rapid large-scale prokaryote pan genome analysis. *Bioinformatics* 31, 3691–3693. doi: 10.1093/bioinformatics/btv421

Partridge, S. R., Kwong, S. M., Firth, N., and Jensen, S. O. (2018). Mobile genetic elements associated with antimicrobial resistance. *Clin. Microbiol. Rev.* 31:e00088-17. doi: 10.1128/CMR.00088-17

Pérez-Oseguera, Á, Castro-Jaimes, S., Salgado-Camargo, A. D., Silva-Sanchez, J., Garza-González, E., Castillo-Ramírez, S., et al. (2017). Complete genome sequence of a blaOXA-58-producing *Acinetobacter baumannii* strain isolated from a mexican hospital. *Genome Announc.* 5:e00949-17. doi: 10.1128/genomeA.00949-17

Pesesky, M. W., Tilley, R., and Beck, D. A. C. (2019). Mosaic plasmids are abundant and unevenly distributed across prokaryotic taxa. *Plasmid* 102, 10–18. doi: 10.1016/j.plasmid.2019.02.003

Poirel, L., and Nordmann, P. (2006). Genetic structures at the origin of acquisition and expression of the carbapenem-hydrolyzing oxacillinase gene blaOXA-58 in *Acinetobacter baumannii*. *Antimicrob. Agents Chemother.* 50, 1442–1448. doi: 10.1128/AAC.50.4.1442-1448.2006

Roca, I., Espinal, P., Vila-Farrés, X., and Vila, J. (2012). The *Acinetobacter baumannii* oxymoron: commensal hospital dweller turned pan-drug-resistant menace. *Front. Microbiol.* 3:148. doi: 10.3389/fmicb.2012.00148

Rumbo, C., Fernández-Moreira, E., Merino, M., Poza, M., Mendez, J. A., Soares, N. C., et al. (2011). Horizontal transfer of the OXA-24 carbapenemase gene via outer membrane vesicles: a new mechanism of dissemination of carbapenem resistance genes in *Acinetobacter baumannii*. *Antimicrob. Agents Chemother.* 55, 3084–3090. doi: 10.1128/AAC.00929-10

Salto, I. P., Torres Tejerizo, G., Wibberg, D., Pühler, A., Schlüter, A., and Pistorio, M. (2018). Comparative genomic analysis of *Acinetobacter* spp. plasmids originating from clinical settings and environmental habitats. *Sci. Rep.* 8:7783. doi: 10.1038/s41598-018-26180-3

San Millan, A. (2018). Evolution of plasmid-mediated antibiotic resistance in the clinical context. *Trends Microbiol.* 26, 978–985. doi: 10.1016/j.tim.2018.06.007

Sievers, F., Wilm, A., Dineen, D., Gibson, T. J., Karplus, K., Li, W., et al. (2014). Fast, scalable generation of high-quality protein multiple sequence alignments using Clustal Omega. *Mol. Syst. Biol.* 7, 539–539. doi: 10.1038/msb.2011.75

Siguier, P., Gourbeyre, E., and Chandler, M. (2014). Bacterial insertion sequences: their genomic impact and diversity. *FEMS Microbiol. Rev.* 38, 865–891. doi: 10.1111/1574-6976.12067

Siguier, P., Perochon, J., Lestrade, L., Mahillon, J., and Chandler, M. (2006). ISfinder: the reference centre for bacterial insertion sequences. *Nucleic Acids Res.* 34, D32–D36. doi: 10.1093/nar/gkj014

Smillie, C., Garcillán-Barcia, M. P., Francia, M. V., Rocha, E. P. C., and de la Cruz, F. (2010). Mobility of plasmids. *Microbiol. Mol. Biol. Rev.* 74, 434–452. doi: 10.1128/MMBR.00020-10

Summers, D. K., Beton, C. W., and Withers, H. L. (1993). Multicopy plasmid instability: the dimer catastrophe hypothesis. *Mol. Microbiol.* 8, 1031–1038. doi: 10.1111/j.1365-2958.1993.tb01648.x

Summers, D. K., and Sherratt, D. J. (1988). Resolution of ColE1 dimers requires a DNA sequence implicated in the three-dimensional organization of the cer site. *EMBO J.* 7, 851–858. doi: 10.1002/j.1460-2075.1988.tb02884.x

Sužiedėlienė, E., Jurėnaitė, M., and Armalytė, J. (2016). "Identification and characterization of type II toxin-antitoxin systems in the opportunistic pathogen *Acinetobacter baumannii*," in *Stress and Environmental Regulation of Gene Expression and Adaptation in Bacteria*, ed. F. J. de Bruijn (Hoboken, NJ: John Wiley & Sons, Inc), 454–462. doi: 10.1002/9781119004813.ch41

Taboada, B., Verde, C., and Merino, E. (2010). High accuracy operon prediction method based on STRING database scores. *Nucleic Acids Res.* 38:e130. doi: 10.1093/nar/gkq254

Tatusov, R. L., Fedorova, N. D., Jackson, J. D., Jacobs, A. R., Kiryutin, B., Koonin, E. V., et al. (2003). The COG database: an updated version includes eukaryotes. *BMC Bioinformatics* 4:41. doi: 10.1186/1471-2105-4-41

Thomas, C. M., Thomson, N. R., Cerdeño-Tárraga, A. M., Brown, C. J., Top, E. M., and Frost, L. S. (2017). Annotation of plasmid genes. *Plasmid* 91, 61–67. doi: 10.1016/j.plasmid.2017.03.006

Tschäpe, H. (1994). The spread of plasmids as a function of bacterial adaptability. *FEMS Microbiol. Ecol.* 15, 23–31. doi: 10.1016/0168-6496(94)90022-1

Unterholzner, S. J., Poppenberger, B., and Rozhon, W. (2013). Toxin-antitoxin systems: Biology, identification, and application. *Mob. Genet. Elements* 3:e26219. doi: 10.4161/mge.26219

Val, M.-E., Bouvier, M., Campos, J., Sherratt, D., Cornet, F., Mazel, D., et al. (2005). The single-stranded genome of phage CTX is the form used for integration into the genome of *Vibrio cholerae*. *Mol. Cell* 19, 559–566. doi: 10.1016/j.molcel.2005.07.002

Weber, B. S., Ly, P. M., Irwin, J. N., Pukatzki, S., and Feldman, M. F. (2015). A multidrug resistance plasmid contains the molecular switch for type VI secretion in *Acinetobacter baumannii*. *Proc. Natl. Acad. Sci. U.S.A.* 112, 9442–9447. doi: 10.1073/pnas.1502966112

Weber, B. S., Miyata, S. T., Iwashkiw, J. A., Mortensen, B. L., Skaar, E. P., Pukatzki, S., et al. (2013). Genomic and functional analysis of the type VI secretion system in *Acinetobacter*. *PLoS One* 8:e55142. doi: 10.1371/journal.pone.0055142

Wegrzyn, K. E., Gross, M., Uciechowska, U., and Konieczny, I. (2016). Replisome assembly at bacterial chromosomes and iteron plasmids. *Front. Mol. Biosci.* 3:39. doi: 10.3389/fmolb.2016.00039

Wernersson, R., and Pedersen, A. G. (2003). RevTrans: Multiple alignment of coding DNA from aligned amino acid sequences. *Nucleic Acids Res.* 31, 3537–3539. doi: 10.1093/nar/gkg609

Wibberg, D., Salto, I. P., Eikmeyer, F. G., Maus, I., Winkler, A., Nordmann, P., et al. (2018). Complete genome sequencing of *Acinetobacter baumannii* strain K50 discloses the large conjugative plasmid pK50a encoding carbapenemase OXA-23 and extended-spectrum β-Lactamase GES-11. *Antimicrob. Agents Chemother.* 62:e00212-18. doi: 10.1128/AAC.00212-18

Wick, R. R., Judd, L. M., Gorrie, C. L., and Holt, K. E. (2017). Unicycler: Resolving bacterial genome assemblies from short and long sequencing reads. *PLoS Comput. Biol.* 13:e1005595. doi: 10.1371/journal.pcbi.1005595

Wickham, H. (2009). *ggplot2*. New York, NY: Springer.

Wyres, K. L., and Holt, K. E. (2018). *Klebsiella pneumoniae* as a key trafficker of drug resistance genes from environmental to clinically important bacteria. *Curr. Opin. Microbiol.* 45, 131–139. doi: 10.1016/j.mib.2018.04.004

Yau, S., Liu, X., Djordjevic, S. P., and Hall, R. M. (2010). RSF1010-like plasmids in Australian *Salmonella enterica* serovar Typhimurium and origin of their sul2-strA-strB antibiotic resistance gene cluster. *Microb. Drug Resist.* 16, 249–252. doi: 10.1089/mdr.2010.0033

Zankari, E. E., Hasman, H., Cosentino, S., Vestergaard, M., Rasmussen, S., Lund, O., et al. (2012). Identification of acquired antimicrobial resistance genes. *J. Antimicrob. Chemother.* 67, 2640–2644. doi: 10.1093/jac/dks261

Zarrilli, R., Pournaras, S., Giannouli, M., and Tsakris, A. (2013). Global evolution of multidrug-resistant *Acinetobacter baumannii* clonal lineages. *Int. J. Antimicrob. Agents* 41, 11–19. doi: 10.1016/j.ijantimicag.2012.09.008

Conflict of Interest: The authors declare that the research was conducted in the absence of any commercial or financial relationships that could be construed as a potential conflict of interest.

frontiers in Microbiology

MINI REVIEW
published: 06 October 2020
doi: 10.3389/fmicb.2020.589234

The Outer Membrane Proteins OmpA, CarO, and OprD of *Acinetobacter baumannii* Confer a Two-Pronged Defense in Facilitating Its Success as a Potent Human Pathogen

*Siva R. Uppalapati, Abhiroop Sett and Ranjana Pathania**

Department of Biotechnology, Indian Institute of Technology Roorkee, Roorkee, India

OPEN ACCESS

Edited by:
Benjamin Andrew Evans, University of East Anglia, United Kingdom

Reviewed by:
Brock Aaron Arivett, Middle Tennessee State University, United States
Shakiba Darvish Alipour Astaneh, Semnan University, Iran

***Correspondence:**
Ranjana Pathania
ranjana.pathania@bt.iitr.ac.in

Specialty section:
This article was submitted to Antimicrobials, Resistance and Chemotherapy, a section of the journal Frontiers in Microbiology

Received: *31 July 2020*
Accepted: *11 September 2020*
Published: *06 October 2020*

Citation:
Uppalapati SR, Sett A and Pathania R (2020) The Outer Membrane Proteins OmpA, CarO, and OprD of Acinetobacter baumannii Confer a Two-Pronged Defense in Facilitating Its Success as a Potent Human Pathogen. Front. Microbiol. 11:589234. doi: 10.3389/fmicb.2020.589234

Of all the *ESKAPE* pathogens, carbapenem-resistant and multidrug-resistant *Acinetobacter baumannii* is the leading cause of hospital-acquired and ventilator-associated pneumonia. *A. baumannii* infections are notoriously hard to eradicate due to its propensity to rapidly acquire multitude of resistance determinants and the virulence factor cornucopia elucidated by the bacterium that help it fend off a wide range of adverse conditions imposed upon by host and environment. One such weapon in the arsenal of *A. baumannii* is the outer membrane protein (OMP) compendium. OMPs in *A. baumannii* play distinctive roles in facilitating the bacterial acclimatization to antibiotic- and host-induced stresses, albeit following entirely different mechanisms. OMPs are major immunogenic proteins in bacteria conferring bacteria host-fitness advantages including immune evasion, stress tolerance, and resistance to antibiotics and antibacterials. In this review, we summarize the current knowledge of major *A. baumannii* OMPs and discuss their versatile role in antibiotic resistance and virulence. Specifically, we explore how OmpA, CarO, and OprD-like porins mediate antibiotic and amino acid shuttle and host virulence.

Keywords: OmpA, CARO, OprD, antibiotic resistance, virulence

INTRODUCTION

The Gram-negative coccobacillus *Acinetobacter baumannii* is an aerobic opportunistic pathogen responsible for some of the most morbid hospital-acquired infections (Bouvet and Grimont, 1987; Peleg et al., 2008; Lin and Lan, 2014; Lee et al., 2017). The global threat from this pathogen comes from its high rate of resistance gene acquisition leading to rapid emergence of multidrug-resistant (MDR) clinical isolates (Abbott et al., 2013; Giammanco et al., 2017; Rodloff and Dowzicky, 2017). Increasing number of studies show frequent isolation of carbapenem and colistin-resistant strains of *A. baumannii* from clinical settings (Garnacho-Montero et al., 2005; Asadollahi et al., 2012; Zhao et al., 2015; Benmahmod et al., 2019; Pormohammad et al., 2020). Swift accumulation and dispersion of antibiotic resistance markers along with the ability to cause urinary tract infections, skin and soft tissue infections and wound infections (Sievert et al., 2013;

Weiner et al., 2016; Giammanco et al., 2017) makes *A. baumannii*, a pathogen of great significance for both humans and animals (Sen and Joshi, 2016; van der Kolk et al., 2019). In light of this, the World Health Organization (WHO) categorized this organism as a priority-1 critical pathogen for which discovery of new treatment options is of utmost importance (World Health Organization [WHO], 2017). The potency of *A. baumannii* as a successful pathogen can be elaborated by the high number of deaths associated with its infection. A recent finding showed that bacteremia caused by multidrug-resistant (MDR) *A. baumannii* exhibited 56.2% mortality rate among infected patients (Zhou et al., 2019).

A plethora of virulence factors are elucidated by *A. baumannii* (Harding et al., 2018), some of which include, but are not limited to, porin proteins, efflux pumps, outer membrane vesicles, metal acquisition systems, secretion systems, phospholipases, and capsular polysaccharides (Lee et al., 2017; Sharma et al., 2019; Skariyachan et al., 2019). Recent advances in research have not only provided better knowledge of these determinants, but also shed light on how these can be used as potential drug targets (Bhattacharyya et al., 2017; Iyer et al., 2018). However, growth conditions like temperature, oxygen content, osmolarity, and media components regulate the expression of porins in *A. baumannii* (Hwa et al., 2010; Fernando and Kumar, 2012; Bazyleu and Kumar, 2014). Transcriptional and post-transcriptional regulatory networks (Kuo et al., 2017; Sharma et al., 2018) also determine the virulence and antibiotic resistance of *A. baumannii*.

Among the vast diversity of antibiotic resistance and virulence determinants and *A. baumannii* specific regulatory networks, one group of bacterial proteins, termed outer membrane proteins (OMPs) due to their localization, have been studied with utmost interest due to their distribution, functional relevance and stipulated role in both antibiotic resistance and virulence (Sato et al., 2017; Nie et al., 2020). OMPs in general are beta barrel-shaped monomeric or trimeric porins (**Table 1**) that allow diffusion of small molecules into and out of periplasmic space of Gram-negative bacteria (Nitzan et al., 1999; Nikaido, 2003; Slusky and Dunbrack, 2013). *A. baumannii* outer membrane holds scores of OMPs including OmpA, CarO, OprD- like OMPs, Omp 33-36 kDa, AbuO, TolB, DcaP, Oma87/BamA, NmRmpM, CadF, OprF, etc. (Borneleit and Kleber, 1991; Park et al., 2012; Srinivasan et al., 2015; Lee et al., 2017; Bhamidimarri et al., 2019; Rasooli et al., 2020). OMPs participate in a wide range of functions that assist the bacterium in enduring the harsh environmental conditions, in combating the threat posed by antimicrobial compounds (Limansky et al., 2002; del Mar Tomás et al., 2005; Dupont et al., 2005; Mussi et al., 2007; Choi et al., 2008a; Srinivasan et al., 2015; Wang et al., 2015), host (Choi et al., 2008b,c; Lee et al., 2008; Gaddy, 2010), and surprisingly, in degrading crude oil (Hanson et al., 1994). Immunization with *A. baumannii* OMPs ensued significant rise in protective immune parameters (McConnell et al., 2011; Alzubaidi and Alkozai, 2015; Bazmara et al., 2019) and antibodies against OMPs passively protected experimental animals (Goel and Kapil, 2001). Clinical studies frequently identify differential expression of OMPs in antibiotic resistant *A. baumannii* strains, establishing their role in conferring resistance (Cuenca et al., 2003; Yun et al., 2008; Vashist et al., 2010; Moganty et al., 2011; Mostachio et al., 2012). Here, we explore and summarize how antibiotic resistance and virulence in *A. baumannii* is mediated by different OMPs like OmpA, CarO and OprD.

OmpA

OmpA, a beta barrel-shaped monomeric protein (Park et al., 2011) is one of the most abundant OMPs (Gribun et al., 2003), which has been reported to impart drug resistance to *A. baumannii* by allowing slower diffusion of negatively charged beta-lactam antibiotics (Nitzan et al., 2002) and virulence (Sato and Nakae, 1991; Sato et al., 2017; Sánchez-Encinales et al., 2017) by its toxicity to host cells. Clinical isolates of *A. baumannii* overexpressing OmpA arbitrate higher morbidity and even mortality in patients (Sato et al., 2017; Sánchez-Encinales et al., 2017). The global repressor H-NS binds to the promoter region of OmpA gene and gene locus A1S_0316 and the two component system BfmSR function as a possible anti-repressor and repressor of OmpA in *A. baumannii*, respectively (Liou et al., 2014; Oh et al., 2020).

Role of OmpA in Antibiotic Resistance in *A. baumannii*

Being the most abundant porin in *A. baumannii*, the role of OmpA in antibiotic resistance was more prominent in disruption mutants of the gene, which showed increased susceptibility to nalidixic acid, chloramphenicol, aztreonam, imipenem, and meropenem. Besides diffusion, research indicates that OmpA possibly couples with efflux pumps and forces out antibacterial compounds from the periplasm (Smani et al., 2013; Fahmy et al., 2018; Tsai et al., 2020). OmpA also couples to *A. baumannii* peptidoglycan (PG) via its C-terminal region, where Asp271 and Arg286 bind to diaminopimelic acid of PG (Park et al., 2012). This binding may regulate outer membrane vesicle (OMV) production and the membrane stability in the bacteria (Moon et al., 2012). OMVs with OmpA in their membrane (Walzer et al., 2006; Jin et al., 2011; Yun et al., 2018) mediate antibiotic resistance by actively siphoning extracellular drugs (Agarwal et al., 2019). Recently, resistance to colistin, a last-resort antibiotic, was also attributed to the presence of OmpA in *A. baumannii*. An isogenic mutant of OmpA resulted in loss of cell wall integrity, thus making the bacterium 20-fold more sensitive to colistin (Kwon et al., 2019) and 5.3 fold more sensitive to trimethoprim (Kwon et al., 2017) than wild type *A. baumannii*. The distinctive role of OmpA in conferring antibiotic resistance thrusts researchers to discover novel antibacterials against the protein. In one study, a novel diazabicyclooctenone beta-lactamase inhibitor that inhibits major classes of carbapenemases and in turn potentiates sulbactam activity was shown to be OmpA-dependent (Iyer et al., 2018). OmpA blockers can function synergistically with last resort antibiotics like colistin in eradicating MDR strains of *A. baumannii* (Vila-Farrés et al., 2017; Parra-Millán et al., 2018). OmpA also interacts with antimicrobial peptides (AMPs) of diverse origin and confers resistance against them (Lin et al., 2015; Guo Y. et al., 2018). Minimum inhibitory

TABLE 1 | Structure and function of major outer membrane proteins of *A. baumannii*.

Name of porin	Molecular weight	Structure	Proposed role in *A. baumannii*	References
OmpA	28–36 kDa	Eight-stranded Beta barrel shaped	Cytotoxic protein. Mediates attachment to host cells via fibronectin.	Choi et al., 2005; Smani et al., 2012; Confer and Ayalew, 2013
CarO	25/29 kDa	Eight-stranded beta barrel shaped	Uptake of glycine and ornithine. Also implicated in carbapenem resistance.	Limansky et al., 2002; Siroy et al., 2005; Zahn et al., 2015; Zhu et al., 2019
OprD/OccAB1	43 kDa	Eighteen-stranded beta-barrel shaped	Allows diffusion of basic amino acids and beta-lactam class of antibiotics into the cell.	Dupont et al., 2005; Zahn et al., 2016
Omp33-36	33–36 kDa	Yet to be studied	Implicated in imipenem resistance. Induces apoptosis in host cells by activating caspases 3 and 9.	Clark, 1996; Rumbo et al., 2014
AbuO	50.2 kDa (Theoretical)	Three domains—four-stranded beta barrel, α-helical barrel and α- β mixed barrel	Homolog of *E. coli* TolC protein. Involved in pH and bile salt tolerance.	Srinivasan et al., 2015
DcaP	47–50 kDa	Sixteen-stranded beta-barrel shaped	An Omp with preference for anionic compounds. Involved in transport of phthalates into the cell.	Bhamidimarri et al., 2019
OmpW	Yet to be studied	Eight-stranded beta-barrel shaped. (Theoretical)	Serves as a colistin binding site. Facilitates iron uptake into the cell.	Catel-Ferreira et al., 2016

concentrations of human AMP LL-37 and bovine AMP BMAP-28 increased upon binding to N-terminal region of OmpA. The multifaceted role of OmpA in *A. baumannii* membrane permeability and cell wall integrity indicates its potential as a candidate for novel antibacterial development *via* chemical genetic screens.

Role of OmpA in *A. baumannii* Adherence and Invasion of Host Cells

Besides their distinguishable role in antibiotic resistance, OMPs confer virulence to *A. baumannii*. The bacterium is capable of invading and persisting in host epithelial and immune cells (**Figure 1**). The primary requisite for invasion is to adhere to the host cells, which is mediated by many virulence factors expressed by *A. baumannii viz*., OmpA (Nie et al., 2020), BapA (Brossard and Campagnari, 2012), fimbrial like protrusions (Mortensen and Skaar, 2012). *A. baumannii* adherence to host cells can be both host cell and bacterial sequence-type specific. For instance, two types of adherence patterns have been elucidated in *A. baumannii*; dispersed adherence of bacteria to the host cells, and adherence of clusters of bacteria at localized areas of the host cells (Lee et al., 2006). Bacterial clusters can be a result of amyloidogenic BAP protein mediated biofilm formation. Interestingly, OmpA specifically mediates bacterial binding to healthy cells than cancerous cells (Choi et al., 2008c). *A. baumannii* cells devoid of OmpA were found to be less virulent to human airway epithelium due to decreased adherence to cells (Gaddy, 2010) and formed weaker biofilms (Gaddy et al., 2009; Lin et al., 2020).

Following adherence to host cells, *A. baumannii* invades into the cell cytoplasm. The bacterial penetration into epithelial cells is microfilament- and microtubule-dependent following zipper-like mechanism (Choi et al., 2008c). Upon internalization, *A. baumannii* cells localize to membrane-bound vacuoles and finally traffic to the nucleus. Bacterial cells actively divide and finally kill the host cell to release into the blood stream. In this process, OmpA actively assists bacterial invasion, although by unknown mechanisms (Kim et al., 2016). Iron homeostasis is found to be a key factor regulating the survival of *A. baumannii* in the cytoplasm (Gaddy, 2010). Other adherence factors like BapA are not found to mediate invasion of *A. baumannii* (Brossard and Campagnari, 2012; De Gregorio et al., 2015) indicating that OmpA specific pathways regulate *A. baumannii* virulence. The functional dynamics of such a feature for a protein can be emphasized succinctly by looking into immune responses in the host.

Immune Response Configuration Against *A. baumannii* OmpA

In healthy individuals, *A. baumannii* cells in the blood stream and airways are actively phagocytosed by circulatory or tissue-resident immune cells like macrophages, neutrophils, dendritic cells (DCs), etc. (Harding et al., 2018) before leading to fulminant *A. baumannii* sepsis, although the latter is the case frequently encountered in immunocompromised patients. *A. baumannii* induces host cell cytotoxicity by targeting mitochondrial system and nuclear localization. In epithelial cells, OmpA induces the surface expression of Toll-like receptor 2 and the production of inducible nitric oxide synthase (Kim et al., 2008). Phagocytosed bacteria release several structural and cytoplasmic proteins that induce cytotoxicity directly (e.g., Type VI secretion system effector enzymes, and toxins) or indirectly by activating caspases (e.g., OmpA). In macrophages and epithelial cells, OmpA triggers autophagy, albeit incomplete, by preventing the fusion of autophagosomes with lysosomes, activating MAPK/JNK signaling pathway (Kim et al., 2008; An and Su, 2019) and enhancing the levels of phosphorylated JNK, p38, ERK and c-Jun (An et al., 2019). Early response in DCs treated with OmpA includes augmenting the expression of CD40, CD54, CD80, CD86 and MHC-I and II surface markers. The marker expression is accompanied by

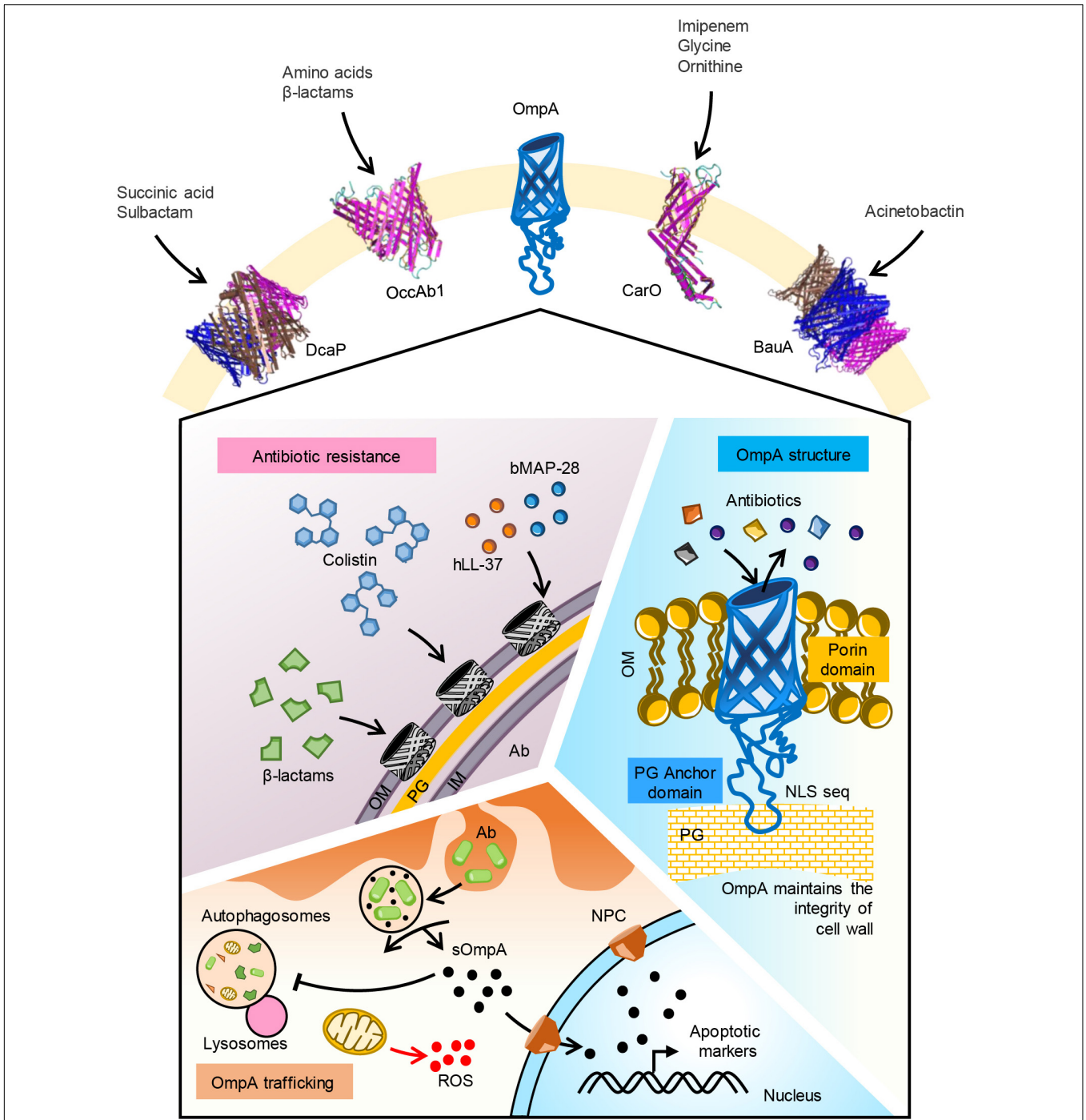

FIGURE 1 | Function of major OMPs in *A. baumannii*. Five major OMPs with their substrate specificity is shown. OmpA porin mediates uptake of β-lactam and colistin antibiotics. Human antimicrobial peptide LL-37 and bovine AMP BMAP-28 may bind to the porin. OmpA pore size is optimal for uptake of iron siderophores like acenitobactin. A coiled loop in the C-terminal region of the protein binds to peptidoglycan maintaining the membrane integrity. Phagocytosed A. baumannii releases OmpA into the cytoplasm of host cells. Secreted OmpA inhibits lysosome fusion to autophagosomes, enters into mitochondria inducing ROS generation. Secreted OmpA actively localizes to nucleus via nuclear pore complex where it activates apoptotic markers like caspases. *Ab, A. baumannii*; OM, outer membrane; PG, peptidoglycan; IM, inner membrane; sOmpA, secreted OmpA; ROS, reactive oxygen species.

secretion of Th-1 promoting IL-12 (Lee et al., 2007). However, upon prolonged exposure, secreted OmpA in DCs targets mitochondria and induces production of reactive oxygen species (ROS) (Lee et al., 2008 and 2010). ROS stimulates early-onset apoptosis and delayed-onset necrosis in DCs, thus impairing T-cell response against *A. baumannii*. Besides induction of ROS,

OmpA in conjunction with carbonic anhydrase IX stimulates DCs to generate potent anti-tumor immune response against renal cell carcinoma (Kim B.R. et al., 2011; Kim D.Y. et al., 2011; Kim et al., 2012).

All these observations in the host indicate that OmpA might be toxic in nature, unlike other outer membrane proteins. The toxicity of *A. baumannii* OmpA can be attributed to its unique structural features and vast diversity of alleles (Viale and Evans, 2020) with conserved domains. OmpA protein is comprised of two domains; an N-terminal 8-stranded β-barrel domain and a C-terminal periplasmic peptidoglycan binding domain. OmpA possesses a basic amino-acid rich signal termed nuclear localization signal (NLS) 'KTKEGRAMNRR' (Choi et al., 2007) on its C-terminal domain. Karyopherin β family proteins on nuclear pore complex recognize the NLS via its lysine (K) residues and shuttle OmpA to nucleus from cytoplasm. It can thus be speculated that OmpA devoid of NLS can be a non-toxic variant. Studies to reduce the host cell toxicity of recombinant *A. baumannii* revealed the importance of both N and C-terminal regions and the importance of lysine residues in NLS sequence. A synthetic OmpA with mutations at K320 and K322 to Alanine, replacing "NADEEFWN" sequence with "YKYDFDGVNRGTRGTSEEGTL" and deleting N-terminal signal sequence and "VVQPGQEAAAPAAAQ" at C-terminal resulted in least toxic but highly immunogenic OmpA (Jahangiri et al., 2017). In addition to NLS, the N-terminal region of OmpA is bioinformatically predicted to be more immunogenic (Darbandian and Sefid, 2016). The epitopes "QIQDSEHSGKMVAKRQ" at position 100–115 and "HTSFDKLPEGGRAT" at position 125–138 are delineated best by Ellipro software. A peptide at N-terminal region located at 24–50 position, "VTVTPLLLGYTFQDSQHNNGGKDGNLT" alone is immunogenic and elicited similar levels serum antibodies like OmpA (Mehdinejadiani et al., 2019). It is clear that OmpA is toxic to host when secreted and when intact, it provides antibiotic resistance to the bacterium. Whether these observations can be implied to the clinical manifestations of *A. baumannii* is yet to be elucidated.

CarO

Carbapenem susceptibility porin or CarO was first reported in imipenem (IMP) sensitive *A. baumannii* isolates that acquired resistance upon the loss of a 29 kDa protein (Limansky et al., 2002). CarO is an 8-stranded beta barrel-shaped outer membrane channel protein that does not have a continuous channel (Mussi et al., 2005 and 2011; Siroy et al., 2005; Zahn et al., 2015) but mediates influx of beta lactams (selectively imipenem) into *A. baumannii* (Mussi et al., 2005). However, contradicting these observations, liposome model system embedded with CarO revealed its ability to transport small amino acids such as glycine and ornithine, but not carbapenem antibiotics (Zahn et al., 2016). Despite this lonesome tangential observation, the excessive evidence from diverse research groups denotes the role of CarO in antibiotic resistance.

CarO is classified into two sub-groups; CarOa and CarOb; of which CarOb exhibits a two-fold greater specificity for IMP (Catel-Ferreira et al., 2011). However, there has been a recent call to rethink the CarO classification system based on phylogenetic analysis (Catel-Ferreira et al., 2011; Novovic et al., 2015). So far, at least six polymorphic variants of CarO have been reported to co-exist in *A. baumannii* populations with varied specificities to imipenem, highlighting the importance of the protein. The alterations in CarO gene are posited to be a result of rapid adaptation of *A. baumannii* to diverse habitats and hosts. Besides gene alterations, conformational changes in primary structure, intra-genic insertion sequences (Lee et al., 2011), posttranscriptional (Kuo et al., 2017) and transcriptional (Fonseca et al., 2013; Cardoso et al., 2016) regulation dramatically affect CarO function (summarized in **Supplementary Table 1**). The recent identification that CarO is significantly up-regulated in an Hfq deletion mutant strain of *A. baumannii* indicate that it is kept under post-transcriptional control by the bacterium to regulate its expression in response to the changing environment (Kuo et al., 2017). Finally, the occasional isolation of antibiotic resistant strains with a loss of CarO gene signifies the diversity of resistance mechanisms in *A. baumannii* (Li et al., 2015). In contrast to these studies linking carbapenem resistance to the loss of CarO, there are a few reports of the presence of CarO porin on the OM of carbapenem resistant clinical isolates of *A. baumannii*. However, this can possibly be explained by the "porin-localized toxin inactivation" model, where carbapenemases like Oxa-23 interact with the periplasmic region of OMPs like CarO or OmpA to act as an efficient selective filter to inactivate incoming antibacterial compounds (Li et al., 2015; Wu et al., 2016; Royer et al., 2018).

The clinical relevance of CarO has also been ascertained by many hospital epidemiological studies. These revealed that there is a prevalence of CarO deficiency amongst carbapenem resistant isolates expressing Bla_{OXA} (Pajand et al., 2013; Abbasi et al., 2020) and TEM-1 (Nan et al., 2018) genes among the hospital isolates of *A. baumannii*. Various carbapenem resistant clinical isolates demonstrated a disruption in the CarO gene by insertion sequences like ISAba1, ISAba125, ISAba825, ISAba10, ISAba15, and ISAba36 (Mussi et al., 2005; Lee et al., 2011; Ravasi et al., 2011; Kim and Ko, 2015; Khorsi et al., 2018; Mirshekar et al., 2018). When exposed to a high concentration of monovalent cations, *A. baumannii* release a variety of OMPs including CarO into the surrounding media and becomes more tolerant to IMP stress. This finding implicated that MICs of antibiotics determined *in vitro* may not help eradicate *A. baumannii* infection from within the host system, especially in the case of urinary tract infections where there is the presence of a high concentration of monovalent cations like NaCl and KCl (Hood et al., 2010).

The immunological role of CarO protein in *A. baumannii* is studied inadequately. Sato et al. (2017) showed that clinical *A. baumannii* isolates expressing higher CarO mRNA levels negatively regulated TNF-α, IL-6 and IL-8 in lung epithelial cells. Recently, CarO has been linked to *A. baumannii* adhesion and virulence in host cells via inhibition of NF-kβ signaling (Zhang et al., 2019). However, the significance of this observation is debatable as the strain used in the study is ATCC 19606 where expression of CarO is significantly lesser than that of clinical strains (Sato et al., 2017).

OprD

OprD was first identified during outer membrane investigations of carbapenem resistant *A. baumannii* isolates (Dupont et al., 2005). It is an orthologous protein to a porin involved in the basic amino acid and imipenem transport in *Pseudomonas aeruginosa* (Hancock and Brinkman, 2002). Crystallographic studies of a conserved *P. aeruginosa* OprD revealed a monomeric 18-stranded β-barrel structure characterized by a very narrow pore constriction (Biswas et al., 2007). The amino acid conservation at structural domains between *A. baumannii* and *P. aeruginosa* OprD porins indicate its putative function in *A. baumannii*. However, sequence and homology analysis of *A. baumannii* OprD showed that it belongs to *P. aeruginosa* OprQ, a protein involved in resisting low-iron or magnesium and low oxygen stresses (Catel-Ferreira et al., 2012). Recombinant *A. baumannii* OprD did not conduct antibiotics but partially bound to Fe^{2+} and Mg^{2+} cations. An isogenic deletion mutant of *A. baumannii* OprD did not affect MICs of β-lactams (Smani and Pachón, 2013), but in *A. baylyi* spp., a significant reduction in MIC of imipenem, ertapenem and meropenem is observed (Morán-Barrio et al., 2017). Despite these two heralding reports on lack of relationship between OprD and antibiotic resistance in *A. baumannii*, single nucleotide polymorphisms and insertional elements in OprD have been frequently identified in MDR A. *baumannii* signifying its role in resistance. For instance, Yang et al., 2015; Liu et al., 2016 and Lai et al., 2018 showed SNP clusters in OprD in MDR and tigecycline-resistant *A. baumannii,* respectively. Downregulation of OprD was observed in MDR (Asai et al., 2014) and pan drug-resistant (Cuenca et al., 2011) *A. baumannii* clinical strains. Insertion of mobile element ISAba1 upstream to the gene was also associated with increased carbapenem MICs of *A. baumannii* sequence type 107 strains (Costa et al., 2019). OprD was renamed to OccAB1 by Zahn et al. (2016), while solving its crystal structure. In their work, Zahn et al., resolved structures of four carboxylate channels OccAB1, 2, 3, and 4 and showed that OccAB1 has the largest channel size with corresponding high rates of small-molecule shuttle, including amino acids, sugars, and antibiotics, contrary to previous observations. The particularly large pore size of OccAB1 facilitates the objective translocation of both positive and negative substrates at low energy cost (Benkerrou and Ceccarelli, 2018). On the other hand, OccAB2, OccAB3, and OccAB4 mediate hydroxycinnamate (Smith et al., 2003), vanillate (Segura et al., 1999), and benzoate (Clark et al., 2002) transport, respectively. Being induced by limitation of metal ions, it can be presumed that OccAB1 may play a significant role in combating host-induced nutritional immunity and stress survival.

Diversity in *A. baumannii* OMP Architecture, Expression, and Function

Besides the above three OMPs, a variety of proteins are identified in the outer membrane of *A. baumannii* with varied expressions and distinctive roles. One of the most abundant OMPs in *A. baumannii* is Omp33. Crystal structure of the protein revealed its function as a putative gated channel contributing to low permeability of the outer membrane (Abellón-Ruiz et al., 2018). Intracellular *A. baumannii* in the host cell expresses DcaP OMP in abundance. Crystallographic studies on DcaP revealed a trimeric porin structure with affinity to dicarboxylic acids and sulbactam (Bhamidimarri et al., 2019). The most abundant OMP under osmotic stress in *A. baumannii* is Omp38 (Jyothisri et al., 1999). Intracellular *A. baumannii* secretes Omp38, which localizes to the mitochondria stimulating the release of proapoptotic molecules such as cytochrome c and apoptosis-inducing factor (Choi et al., 2005). Oxidative stress in *A. baumannii* induces expression of AbuO, a homolog of *Escherichia coli* TolC OMP involved in resistance to amikacin, carbenicillin, ceftriaxone, meropenem, streptomycin, and tigecycline, and hospital-based disinfectants like benzalkonium chloride and chlorhexidine (Srinivasan et al., 2015). Under iron-limiting conditions, a 76-kDa iron-repressible OMP termed fhuE was overexpressed in *A. baumannii* to facilitate uptake of xenosiderophores desferricoprogen, rhodotorulic acid and desferrioxamine B (Funahashi et al., 2012). Besides fhuE, two other siderophore (acinetobactin) uptake proteins, BfnH and BauA are also elucidated in the outer membrane of *A. baumannii* (Sefid and Rasooli, 2012; Aghajani et al., 2019). The translation initiation factor EF-Tu, typically a cytoplasmic protein, is also found to localize in the outer membrane in *A. baumannii* (Dallo et al., 2012). Membrane associated EF-Tu binds to DsbA protein in the periplasm and assists in disulfide bonding during protein folding (Premkumar et al., 2014). Externally, EF-Tu binds to fibronectin thus mediating host cell adhesion (Dallo et al., 2012; Harvey et al., 2019). Decreased expression of a 33–36 kDa OMP (Clark, 1996; del Mar Tomás et al., 2005) and a 29 kDa (Jeong et al., 2009) is associated with imipenem resistance among *A. baumannii*. Serodiagnostic studies revealed an antigenic 34.4-kDa OMP specific to sera from *A. baumannii* infected patients (Islam et al., 2011). Upregulation of this protein along with downregulation of CarO and OprD was found to mediate imipenem resistance (Luo et al., 2011). The protein along with OmpA and TonB-dependant copper receptor was identified as fibronectin binding protein during infection (Smani et al., 2012). *In silico* exploration into the genome of *A. baumannii* revealed a nuclease (NucAb), BamA (Oma87), FilF, and TolB in the outer membrane as potential vaccine targets. Immunization with these recombinant proteins protected mice from lethal challenge with *A. baumannii* (Singh et al., 2014, 2016 and Singh et al., 2017; Garg et al., 2016; Song et al., 2018; Rasooli et al., 2020). In another effort toward developing a subunit vaccine against *A. baumannii* infections, a fusion protein of OmpK and Omp22 was synthesized which provided significantly greater protection against *A. baumannii* challenge in mice than those immunized with either of the two proteins individually (Huang et al., 2016; Guo et al., 2017; Guo S.J. et al., 2018).

CONCLUSION

One of the critical gaps in combating *A. baumannii* is deciphering its overall membrane permeability. Significant progress has been

made during the last decade in our understanding of how *A. baumannii* OMPs mediate antibiotic resistance and virulence in the host cells. Remarkable breakthroughs have also been made in understanding the regulatory mechanisms behind OMP expression and the mechanisms of antibiotic uptake. However, these efforts fall short in many aspects. The knowledge about *in vitro* or *in vivo* OMP assembly and folding dynamics in lipid bilayers is scarce. The crystal structure of most studied *A. baumannii* OMP, OmpA is still elusive, although NLS domain structure has been resolved. Due to its complex structure and hydrophobic loops in its structure, expression and purification of recombinant OmpA presents various hurdles. The solution of crystal structure is decisive in molecular dynamic studies tracking the antibiotic entry and exit through OMPs. Many questions still remain unanswered. How does the beta barrel assembly complex in *A. baumannii* function? What are the different chaperones mediating OMP folding in *A. baumannii*? Does the expression of OMPs in *A. baumannii* depend on transcription factors alone or is it small RNA mediated? Although in small number, concerted efforts are directed toward solving these problems. Crystal structures of CarO1, CarO2, OccAB1 through 4, DcaP, PiuA, Omp33 BauA have been resolved. Understanding the magnitude of posttranscriptional regulation in *A. baumannii* OMP synthesis is a necessary goal, as this aspect has been overlooked till date. In the next few years, it is likely that *A. baumannii* OMP compendium will be resolved with novel insights into its structure, diversity, biogenesis, and expression, furthering our efforts in confronting antibiotic resistance and virulence in *A. baumannii*.

AUTHOR CONTRIBUTIONS

SU, AS, and RP conceptualized the manuscript and contributed the ideas on the texts. SU and AS wrote the first draft of the manuscript. SU and RP edited the subsequent versions. All authors read and approved the final manuscript.

SUPPLEMENTARY MATERIAL

The Supplementary Material for this article can be found online at: https://www.frontiersin.org/articles/10.3389/fmicb.2020.589234/full#supplementary-material

REFERENCES

Abbasi, E., Goudarzi, H., Hashemi, A., Chirani, A. S., Ardebili, A., Goudarzi, M., et al. (2020). Decreased carO gene expression and OXA-type carbapenemases among extensively drug-resistant *Acinetobacter baumannii* strains isolated from burn patients in Tehran, Iran. *Acta Microbiol. Immunol Hung.* doi: 10.1556/030.2020.01138 [Epub ahead of print].

Abbott, I., Cerqueira, G. M., Bhuiyan, S., and Peleg, A. Y. (2013). Carbapenem resistance in *Acinetobacter baumannii*: laboratory challenges, mechanistic insights and therapeutic strategies. *Expert Rev. Anti. Infect. Ther.* 11, 395–409. doi: 10.1586/eri.13.21

Abellón-Ruiz, J., Zahn, M., Baslé, A., and van den Berg, B. (2018). Crystal structure of the *Acinetobacter baumannii* outer membrane protein Omp33. *Acta Crystallogr D Struct. Biol. Struct. Biol.* 74(Pt 9), 852–860. doi: 10.1107/S205979831800904X

Agarwal, B., Karthikeyan, R., Gayathri, P., RameshBabu, B., Ahmed, G., and Jagannadham, M. V. (2019). Studies on the mechanism of multidrug resistance of *Acinetobacter baumannii* by proteomic analysis of the outer membrane vesicles of the bacterium. *J. Proteins Proteo* 10, 1–15. doi: 10.1007/s42485-018-0001-4

Aghajani, Z., Rasooli, I., and Mousavi Gargari, S. L. (2019). Exploitation of two siderophore receptors, BauA and BfnH, for protection against *Acinetobacter baumannii* infection. *APMIS* 127, 753–763. doi: 10.1111/apm.12992

Alzubaidi, A. N., and Alkozai, Z. M. (2015). Immunogenic properties of outer membrane protein of *Acinetobacter baumannii* that loaded on chitosan nanoparticles. *Am. J. Bio Med.* 3, 59–74.

An, Z., Huang, X., Zheng, C., and Ding, W. (2019). *Acinetobacter baumannii* outer membrane protein A induces HeLa cell autophagy via MAPK/JNK signaling pathway. *Int. J. Med. Microbiol.* 309, 97–107. doi: 10.1016/j.ijmm.2018.12.004

An, Z., and Su, J. (2019). *Acinetobacter baumannii* outer membrane protein 34 elicits NLRP3 inflammasome activation via mitochondria-derived reactive oxygen species in RAW264. 7 macrophages. *Microbes Infect.* 21, 143–153. doi: 10.1016/j.micinf.2018.10.005

Asadollahi, P., Akbari, M., Soroush, S., Taherikalani, M., Asadollahi, K., Sayehmiri, K., et al. (2012). Antimicrobial resistance patterns and their encoding genes among *Acinetobacter baumannii* strains isolated from burned patients. *Burns* 38, 1198–1203. doi: 10.1016/j.burns.2012.04.008

Asai, S., Umezawa, K., Iwashita, H., Ohshima, T., Ohashi, M., Sasaki, M., et al. (2014). An outbreak of blaOXA-51-like- and blaOXA-66-positive *Acinetobacter baumannii* ST208 in the emergency intensive care unit. *J. Med. Microbiol.* 63(Pt 11), 1517–1523. doi: 10.1099/jmm.0.077503-0

Bazmara, H., Rasooli, I., Jahangiri, A., Sefid, F., Astaneh, S. D. A., and Payandeh, Z. (2019). Antigenic properties of iron regulated proteins in *Acinetobacter baumannii*: an *in silico* approach. *Int. J. Pept. Res. Ther.* 25, 205–213. doi: 10.1007/s10989-017-9665-6

Bazyleu, A., and Kumar, A. (2014). Incubation temperature, osmolarity, and salicylate affect the expression of resistance-nodulation-division efflux pumps and outer membrane porins in *Acinetobacter baumannii* ATCC19606T. *FEMS Microbiol. Lett.* 357, 136–143. doi: 10.1111/1574-6968.12530

Benkerrou, D., and Ceccarelli, M. (2018). Free energy calculations and molecular properties of substrate translocation through OccAB porins. *Phys. Chem. Chem. Phys.* 20, 8533–8546. doi: 10.1039/c7cp08299a

Benmahmod, A. B., Said, H. S., and Ibrahim, R. H. (2019). Prevalence and Mechanisms of Carbapenem Resistance among *Acinetobacter baumannii* clinical isolates in Egypt. *Microb. Drug Resist.* 25, 480–488. doi: 10.1089/mdr.2018.0141

Bhamidimarri, S. P., Zahn, M., Prajapati, J. D., Schleberger, C., Söderholm, S., Hoover, J., et al. (2019). A multidisciplinary approach toward identification of antibiotic scaffolds for *Acinetobacter baumannii*. *Structure* 27, 268.e6–280.e6. doi: 10.1016/j.str.2018.10.021

Bhattacharyya, T., Sharma, A., Akhter, J., and Pathania, R. (2017). The small molecule IITR08027 restores the antibacterial activity of fluoroquinolones against multidrug-resistant *Acinetobacter baumannii* by efflux inhibition. *Int. J. Antimicrob. Agents* 50, 219–226. doi: 10.1016/j.ijantimicag.2017.03.005

Biswas, S., Mohammad, M. M., Patel, D. R., Movileanu, L., and van den Berg, B. (2007). Structural insight into OprD substrate specificity. *Nat. Struct. Mol. Biol.* 14, 1108–1109. doi: 10.1038/nsmb1304

Borneleit, P., and Kleber, H. P. (1991). "The outer membrane of acinetobacter: structure-function relationships," in *The Biology of Acinetobacter*, *Federation of European Microbiological Societies Symposium Series*, Vol. 57, eds K. J. Towner, E. Bergogne-Bérézin, and C. A. Fewson (Boston, MA: Springer). doi: 10.1007/978-1-4899-3553-3_18

Bouvet, P. J., and Grimont, P. A. (1987). Identification and biotyping of clinical isolates of *Acinetobacter*. *Ann. Inst. Pasteur Microbiol.* 138, 569–578. doi: 10.1016/0769-2609(87)90042-1

Brossard, K. A., and Campagnari, A. A. (2012). The *Acinetobacter baumannii* biofilm-associated protein plays a role in adherence to human epithelial cells. *Infect. Immun.* 80, 228–233. doi: 10.1128/IAI.05913-11

Cardoso, J. P., Cayô, R., Girardello, R., and Gales, A. C. (2016). Diversity of mechanisms conferring resistance to β-lactams among OXA-23-producing *Acinetobacter baumannii* clones. *Diagn. Microbiol. Infect. Dis.* 85, 90–97. doi: 10.1016/j.diagmicrobio.2016.01.018

Catel-Ferreira, M., Coadou, G., Molle, V., Mugnier, P., Nordmann, P., Siroy, A., et al. (2011). Structure-function relationships of CarO, the carbapenem resistance-associated outer membrane protein of *Acinetobacter baumannii*. *J. Antimicrob. Chemother.* 66, 2053–2056. doi: 10.1093/jac/dkr267

Catel-Ferreira, M., Nehmé, R., Molle, V., Aranda, J., Bouffartigues, E., Chevalier, S., et al. (2012). Deciphering the function of the outer membrane protein OprD homologue of *Acinetobacter baumannii*. *Antimicrob. Agents Chemother.* 56, 3826–3832. doi: 10.1128/AAC.06022-11

Catel-Ferreira, M., Marti, S., Guillon, L., Jara, L., Coadou, G., Molle, V., et al. (2016). The outer membrane porin OmpW of *Acinetobacter baumannii* is involved in iron uptake and colistin binding. *FEBS Lett.* 590, 224–231. doi: 10.1002/1873-3468.12050

Choi, C. H., Hyun, S. H., Kim, J., Lee, Y. C., Seol, S. Y., Cho, D. T., et al. (2008a). Nuclear translocation and DNAse I-like enzymatic activity of *Acinetobacter baumannii* outer membrane protein A. *FEMS Microbiol. Lett.* 288, 62–67. doi: 10.1111/j.1574-6968.2008.01323.x

Choi, C. H., Hyun, S. H., Lee, J. Y., Lee, J. S., Lee, Y. S., Kim, S. A., et al. (2008b). *Acinetobacter baumannii* outer membrane protein A targets the nucleus and induces cytotoxicity. *Cell Microbiol.* 10, 309–319. doi: 10.1111/j.1462-5822.2007.01041.x

Choi, C. H., Lee, J. S., Lee, Y. C., Park, T. I., and Lee, J. C. (2008c). *Acinetobacter baumannii* invades epithelial cells and outer membrane protein A mediates interactions with epithelial cells. *BMC Microbiol.* 8:216. doi: 10.1186/1471-2180-8-216

Choi, C. H., Lee, E. Y., Lee, Y. C., Park, T. I., Kim, H. J., Hyun, S. H., et al. (2005). Outer membrane protein 38 of *Acinetobacter baumannii* localizes to the mitochondria and induces apoptosis of epithelial cells. *Cell Microbiol.* 7, 1127–1138. doi: 10.1111/j.1462-5822.2005.00538.x

Choi, C. H., Lee, J. S., and Lee, J. C. (2007). "A versatile role of outer membrane protein a in pathogenesis of *Acinetobacter baumannii*," in *Proceedings of the Microbiological Society of Korea Conference*, (South Korea: The Microbiological Society of Korea), 107–108.

Clark, R. B. (1996). Imipenem resistance among *Acinetobacter baumannii*: association with reduced expression of a 33-36 kDa outer membrane protein. *J. Antimicrob. Chemother.* 38, 245–251. doi: 10.1093/jac/38.2.245

Clark, T. J., Momany, C., and Neidle, E. L. (2002). The benPK operon, proposed to play a role in transport, is part of a regulon for benzoate catabolism in *Acinetobacter* sp. strain ADP1. *Microbiology* 148(Pt 4), 1213–1223. doi: 10.1099/00221287-148-4-1213

Confer, A. W., and Ayalew, S. (2013). The OmpA family of proteins: roles in bacterial pathogenesis and immunity. *Vet. Microbiol.* 163, 207–222. doi: 10.1016/j.vetmic.2012.08.019

Costa, R. F., Cayô, R., Matos, A. P., Girardello, R., Martins, W., Carrara-Marroni, F. E., et al. (2019). Temporal evolution of *Acinetobacter baumannii* ST107 clone: conversion of blaOXA-143 into blaOXA-231 coupled with mobilization of ISAba1 upstream occAB1. *Res. Microbiol.* 170, 53–59. doi: 10.1016/j.resmic.2018.07.001

Cuenca, F. F., Pascual, A., Martínez, L. M., Conejo, M. C., and Perea, E. J. (2003). Evaluation of SDS-polyacrylamide gel systems for the study of outer membrane protein profiles of clinical strains of *Acinetobacter baumannii*. *J. Basic Microbiol.* 43, 194–201. doi: 10.1002/jobm.200390022

Cuenca, F. F., Smani, Y., Gómez-Sánchez, M. C., Docobo-Pérez, F., Caballero-Moyano, F. J., Domínguez-Herrera, J., et al. (2011). Attenuated virulence of a slow-growing pandrug-resistant *Acinetobacter baumannii* is associated with decreased expression of genes encoding the porins CarO and OprD-like. *Int. J. Antimicrob. Agents* 38, 548–549. doi: 10.1016/j.ijantimicag.2011.08.002

Dallo, S. F., Zhang, B., Denno, J., Hong, S., Tsai, A., Haskins, W., et al. (2012). Association of *Acinetobacter baumannii* EF-Tu with cell surface, outer membrane vesicles, and fibronectin. *ScientificWorldJournal* 2012:128705. doi: 10.1100/2012/128705

Darbandian, P., and Sefid, F. (2016). Evaluation of OMP A (Outer Membrane Protein A) linear and conformational epitopes in *Acinetobacter baumannii*. *Int. J. Adv. Biotechnol. Res.* 7:3.

De Gregorio, E., Del Franco, M., Martinucci, M., Roscetto, E., Zarrilli, R., and Di Nocera, P. P. (2015). Biofilm-associated proteins: news from *Acinetobacter*. *BMC Genomics* 16:933. doi: 10.1186/s12864-015-2136-6

del Mar Tomás, M., Beceiro, A., Pérez, A., Velasco, D., Moure, R., Villanueva, R., et al. (2005). Cloning and functional analysis of the gene encoding the 33- to 36-kilodalton outer membrane protein associated with carbapenem resistance in *Acinetobacter baumannii*. *Antimicrob. Agents Chemother.* 49, 5172–5175. doi: 10.1128/AAC.49.12.5172-5175.2005

Dupont, M., Pagès, J. M., Lafitte, D., Siroy, A., and Bollet, C. (2005). Identification of an OprD homologue in *Acinetobacter baumannii*. *J. Proteome Res.* 4, 2386–2390. doi: 10.1021/pr050143q

Fahmy, I. L., Amin, M. H., Mohamed, F. A., and Hashem, A. G. (2018). Colonization of multi-drug resistant (MDR) *Acinetobacter baumannii* isolated from tertiary hospitals in Egypt and the possible role of the outer membrane protein (OmpA.). *Int. Res. J. Pharm.* 9, 103–110.

Fernando, D., and Kumar, A. (2012). Growth phase-dependent expression of RND efflux pump- and outer membrane porin-encoding genes in *Acinetobacter baumannii* ATCC 19606. *J. Antimicrob. Chemother.* 67, 569–572. doi: 10.1093/jac/dkr519

Fonseca, E. L., Scheidegger, E., Freitas, F. S., Cipriano, R., and Vicente, A. C. (2013). Carbapenem-resistant *Acinetobacter baumannii* from Brazil: role of CarO alleles expression and blaOXA-23 gene. *BMC Microbiol.* 13:245. doi: 10.1186/1471-2180-13-245

Funahashi, T., Tanabe, T., Mihara, K., Miyamoto, K., Tsujibo, H., and Yamamoto, S. (2012). Identification and characterization of an outer membrane receptor gene in *Acinetobacter baumannii* required for utilization of desferricoprogen, rhodotorulic acid, and desferrioxamine B as xenosiderophores. *Biol. Pharm. Bull.* 35, 753–760. doi: 10.1248/bpb.35.753

Gaddy, J. A. (2010). *Acinetobacter baumannii Virulence Attributes: The Roles of Outer Membrane Protein A, Acinetobactin-mediated Iron Acquisition Functions, and Blue Light Sensing Protein A*. Doctoral dissertation, Miami University, Oxford.

Gaddy, J. A., Tomaras, A. P., and Actis, L. A. (2009). The *Acinetobacter baumannii* 19606 OmpA protein plays a role in biofilm formation on abiotic surfaces and in the interaction of this pathogen with eukaryotic cells. *Infect. Immun.* 77, 3150–3160. doi: 10.1128/IAI.00096-09

Garg, N., Singh, R., Shukla, G., Capalash, N., and Sharma, P. (2016). Immunoprotective potential of *in silico* predicted *Acinetobacter baumannii* outer membrane nuclease. NucAb. *Int. J. Med. Microbiol.* 306, 1–9. doi: 10.1016/j.ijmm.2015.10.005

Garnacho-Montero, J., Ortiz-Leyba, C., Fernández-Hinojosa, E., Aldabó-Pallás, T., Cayuela, A., Marquez-Vácaro, J. A., et al. (2005). *Acinetobacter baumannii* ventilator-associated pneumonia: epidemiological and clinical findings. *Intensive Care Med.* 31, 649–655. doi: 10.1007/s00134-005-2598-0

Giammanco, A., Calà, C., Fasciana, T., and Dowzicky, M. J. (2017). Global assessment of the activity of tigecycline against multidrug-resistant gram-negative pathogens between 2004 and 2014 as part of the tigecycline evaluation and surveillance trial. *mSphere* 2:e00310-16. doi: 10.1128/mSphere.00310-16

Goel, V. K., and Kapil, A. (2001). Monoclonal antibodies against the iron regulated outer membrane proteins of *Acinetobacter baumannii* are bactericidal. *BMC Microbiol.* 1:16. doi: 10.1186/1471-2180-1-16

Gribun, A., Nitzan, Y., Pechatnikov, I., Hershkovits, G., and Katcoff, D. J. (2003). Molecular and structural characterization of the HMP-AB gene encoding a pore-forming protein from a clinical isolate of *Acinetobacter baumannii*. *Curr. Microbiol.* 47, 434–443. doi: 10.1007/s00284-003-4050-4

Guo, S. J., Ren, S., and Xie, Y. E. (2017). Recombinant expression and purification of the OmpK outer membrane protein of *Acinetobacter baumannii*. *J. Pathog. Biol.* 12, 837–839.

Guo, S. J., Ren, S., and Xie, Y. E. (2018). Evaluation of the protective efficacy of a fused OmpK/Omp22 protein vaccine Candidate against *Acinetobacter baumannii* Infection in Mice. *Biomed. Environ. Sci.* 31, 155–158. doi: 10.3967/bes2018.019

Guo, Y., Xun, M., and Han, J. (2018). A bovine myeloid antimicrobial peptide (BMAP-28) and its analogs kill pan-drug-resistant *Acinetobacter baumannii* by interacting with outer membrane protein A (OmpA). *Medicine* 97:e12832. doi: 10.1097/MD.0000000000012832

Hancock, R. E., and Brinkman, F. S. (2002). Function of *Pseudomonas* porins in uptake and efflux. *Annu. Rev. Microbiol.* 56, 17–38. doi: 10.1146/annurev.micro.56.012302.160310

Hanson, K. G., Kale, V. C., and Desai, A. J. (1994). The possible involvement of cell surface and outer membrane proteins of *Acinetobacter* sp. A3 in crude oil degradation. *FEMS Microbiol. Lett.* 122, 275–279. doi: 10.1111/j.1574-6968.1994.tb07180.x

Harding, C. M., Hennon, S. W., and Feldman, M. F. (2018). Uncovering the mechanisms of *Acinetobacter baumannii* virulence. *Nat. Rev. Microbiol.* 16, 91–102. doi: 10.1038/nrmicro.2017.148

Harvey, K. L., Jarocki, V. M., Charles, I. G., and Djordjevic, S. P. (2019). The diverse functional roles of elongation factor Tu (EF-Tu) in microbial pathogenesis. *Front. Microbiol.* 10:2351. doi: 10.3389/fmicb.2019.02351

Hood, M. I., Jacobs, A. C., Sayood, K., Dunman, P. M., and Skaar, E. P. (2010). *Acinetobacter baumannii* increases tolerance to antibiotics in response to monovalent cations. *Antimicrob. Agents Chemother.* 54, 1029–1041. doi: 10.1128/AAC.00963-09

Huang, W., Yao, Y., Wang, S., Xia, Y., Yang, X., Long, Q., et al. (2016). Immunization with a 22-kDa outer membrane protein elicits protective immunity to multidrug-resistant *Acinetobacter baumannii*. *Sci. Rep.* 6:20724. doi: 10.1038/srep20724

Hwa, W. E., Subramaniam, G., Mansor, M. B., Yan, O. S., Gracie, Anbazhagan, D., et al. (2010). Iron regulated outer membrane proteins (IROMPs) as potential targets against carbapenem-resistant *Acinetobacter* spp. isolated from a Medical Centre in Malaysia. *Indian J. Med. Res.* 131, 578–583.

Islam, A. H., Singh, K. K., and Ismail, A. (2011). Demonstration of an outer membrane protein that is antigenically specific for *Acinetobacter baumannii*. *Diagn. Microbiol. Infec.t Dis.* 69, 38–44. doi: 10.1016/j.diagmicrobio.2010.09.008

Iyer, R., Moussa, S. H., Durand-Réville, T. F., Tommasi, R., and Miller, A. (2018). *Acinetobacter baumannii* OmpA is a selective antibiotic permeant porin. *ACS Infect. Dis.* 4, 373–381. doi: 10.1021/acsinfecdis.7b00168

Jahangiri, A., Rasooli, I., Owlia, P., Fooladi, A. A., and Salimian, J. (2017). *In silico* design of an immunogen against *Acinetobacter baumannii* based on a novel model for native structure of outer membrane protein A. *Microb. Pathog.* 105, 201–210. doi: 10.1016/j.micpath.2017.02.028

Jeong, H. W., Cheong, H. J., Kim, W. J., Kim, M. J., Song, K. J., Song, J. W., et al. (2009). Loss of the 29-kilodalton outer membrane protein in the presence of OXA-51-like enzymes in *Acinetobacter baumannii* is associated with decreased imipenem susceptibility. *Microb. Drug Resist.* 15, 151–158. doi: 10.1089/mdr.2009.0828

Jin, J. S., Kwon, S. O., Moon, D. C., Gurung, M., Lee, J. H., Kim, S. I., et al. (2011). *Acinetobacter baumannii* secretes cytotoxic outer membrane protein A via outer membrane vesicles. *PLoS One* 6:e17027. doi: 10.1371/journal.pone.0017027

Jyothisri, K., Deepak, V., and Rajeswari, M. R. (1999). Purification and characterization of a major 40 kDa outer membrane protein of *Acinetobacter baumannii*. *FEBS lett.* 443, 57–60. doi: 10.1016/s0014-5793(98)01679-2

Khorsi, K., Messai, Y., Ammari, H., Hamidi, M., and Bakour, R. (2018). ISAba36 inserted into the outer membrane protein gene carO and associated with the carbapenemase gene blaOXA-24-like in *Acinetobacter baumannii*. *J. Glob. Antimicrob. Resist.* 15, 107–108. doi: 10.1016/j.jgar.2018.08.020

Kim, B. R., Yang, E. K., Kim, D. Y., Kim, S. H., Moon, D. C., Lee, J. H., et al. (2012). Generation of anti-tumour immune response using dendritic cells pulsed with carbonic anhydrase IX-*Acinetobacter baumannii* outer membrane protein A fusion proteins against renal cell carcinoma. *Clin. Exp. Immunol.* 167, 73–83. doi: 10.1111/j.1365-2249.2011.04489.x

Kim, B. R., Yang, E. K., Kim, S. H., Moon, D. C., Kim, H. J., Lee, J. C., et al. (2011). Immunostimulatory activity of dendritic cells pulsed with carbonic anhydrase IX and *Acinetobacter baumannii* outer membrane protein A for renal cell carcinoma. *J. Microbiol.* 49, 115–120. doi: 10.1007/s12275-011-1037-x

Kim, D. Y., Kim, B., Kim, S. H., Lee, J., Kim, J. C., Park, C. H., et al. (2011). 242 *Acinetobacter baumannii* outer membrane protein a enhance immune responses to renal cell carcinoma vaccines targeting carbonic anhydrase IX. *J. Urol.* 185:e98. doi: 10.1016/j.juro.2011.02.311

Kim, D. H., and Ko, K. S. (2015). ISAba15 inserted into outer membrane protein gene carO in *Acinetobacter baumannii*. *J. Bacteriol. Virol.* 45, 51–53. doi: 10.4167/jbv.2015.45.1.51

Kim, S. A., Yoo, S. M., Hyun, S. H., Choi, C. H., Yang, S. Y., Kim, H. J., et al. (2008). Global gene expression patterns and induction of innate immune response in human laryngeal epithelial cells in response to *Acinetobacter baumannii* outer membrane protein A. *FEMS Immunol. Med. Microbiol.* 54, 45–52. doi: 10.1111/j.1574-695X.2008.00446.x

Kim, S. W., Oh, M. H., Jun, S. H., Jeon, H., Kim, S. I., Kim, K., et al. (2016). Outer membrane Protein A plays a role in pathogenesis of *Acinetobacter* nosocomialis. *Virulence* 7, 413–426. doi: 10.1080/21505594.2016.1140298

Kuo, H. Y., Chao, H. H., Liao, P. C., Hsu, L., Chang, K. C., Tung, C. H., et al. (2017). Functional Characterization of *Acinetobacter baumannii* Lacking the RNA Chaperone Hfq. *Front. Microbiol.* 8:2068. doi: 10.3389/fmicb.2017.02068

Kwon, H. I., Kim, S., Oh, M. H., Na, S. H., Kim, Y. J., Jeon, Y. H., et al. (2017). Outer membrane protein A contributes to antimicrobial resistance of *Acinetobacter baumannii* through the OmpA-like domain. *J. Antimicrob. Chemother.* 72, 3012–3015. doi: 10.1093/jac/dkx257

Kwon, H. I., Kim, S., Oh, M. H., Shin, M., and Lee, J. C. (2019). Distinct role of outer membrane protein A in the intrinsic resistance of *Acinetobacter baumannii* and *Acinetobacter* nosocomialis. *Infect. Genet. Evol.* 67, 33–37. doi: 10.1016/j.meegid.2018.10.022

Lai, C. C., Chen, C. C., Lu, Y. C., Chuang, Y. C., and Tang, H. J. (2018). In vitro activity of cefoperazone and cefoperazone-sulbactam against carbapenem-resistant *Acinetobacter baumannii* and *Pseudomonas aeruginosa*. *Infect. Drug. Resist.* 12, 25–29. doi: 10.2147/IDR.S181201

Lee, C. R., Lee, J. H., Park, M., Park, K. S., Bae, I. K., Kim, Y. B., et al. (2017). Biology of *Acinetobacter baumannii*: pathogenesis, antibiotic resistance mechanisms, and prospective treatment options. *Front. Cell Infect. Microbiol.* 7:55. doi: 10.3389/fcimb.2017.00055

Lee, J. C., Koerten, H., van den Broek, P., Beekhuizen, H., Wolterbeek, R., van den Barselaar, M., et al. (2006). Adherence of *Acinetobacter baumannii* strains to human bronchial epithelial cells. *Res. Microbiol.* 157, 360–366. doi: 10.1016/j.resmic.2005.09.011

Lee, J. S., Choi, C. H., Kim, J. W., and Lee, J. C. (2010). *Acinetobacter baumannii* outer membrane protein A induces dendritic cell death through mitochondrial targeting. *J. Microbiol.* 48, 387–392. doi: 10.1007/s12275-010-0155-1

Lee, J. S., Kim, J. W., Choi, C. H., Lee, W. K., Chung, H. Y., and Lee, J. C. (2008). Anti-tumor activity of *Acinetobacter baumannii* outer membrane protein A on dendritic cell-based immunotherapy against murine melanoma. *J. Microbiol.* 46, 221–227. doi: 10.1007/s12275-008-0052-z

Lee, J. S., Lee, J. C., Lee, C. M., Jung, I. D., Jeong, Y. I., Seong, E. Y., et al. (2007). Outer membrane protein A of *Acinetobacter baumannii* induces differentiation of CD4+ T cells toward a Th1 polarizing phenotype through the activation of dendritic cells. *Biochem. Pharmacol.* 74, 86–97. doi: 10.1016/j.bcp.2007.02.012

Lee, Y., Kim, C. K., Lee, H., Jeong, S. H., Yong, D., and Lee, K. (2011). A novel insertion sequence, ISAba10, inserted into ISAba1 adjacent to the bla(OXA-23) gene and disrupting the outer membrane protein gene CarO in *Acinetobacter baumannii*. *Antimicrob. Agents Chemother.* 55, 361–363. doi: 10.1128/AAC.01672-09

Li, Q., Li, Z., Qu, Y., Li, H., Xing, J., and Hu, D. (2015). A study of outer membrane protein and molecular epidemiology of carbapenem-resistant *Acinetobacter baumannii*. *Zhonghua Wei Zhong Bing Ji Jiu Yi Xue* 27, 611–615. doi: 10.3760/cma.j.issn.2095-4352.2015.07.014

Limansky, A. S., Mussi, M. A., and Viale, A. M. (2002). Loss of a 29-kilodalton outer membrane protein in *Acinetobacter baumannii* is associated with imipenem resistance. *J. Clin. Microbiol.* 40, 4776–4778. doi: 10.1128/jcm.40.12.4776-4778.2002

Lin, M. F., and Lan, C. Y. (2014). Antimicrobial resistance in *Acinetobacter baumannii*: From bench to bedside. *World J. Clin. Cases* 2, 787–814. doi: 10.12998/wjcc.v2.i12.787

Lin, M. F., Lin, Y. Y., and Lan, C. Y. (2020). Characterization of biofilm production in different strains of *Acinetobacter baumannii* and the effects of chemical compounds on biofilm formation. *PeerJ* 8:e9020. doi: 10.7717/peerj.9020

Lin, M. F., Tsai, P. W., Chen, J. Y., Lin, Y. Y., and Lan, C. Y. (2015). OmpA binding mediates the effect of antimicrobial peptide LL-37 on *Acinetobacter baumannii*. *PLoS One* 10:e0141107. doi: 10.1371/journal.pone.0141107

Liou, M. L., Soo, P. C., Ling, S. R., Kuo, H. Y., Tang, C. Y., and Chang, K. C. (2014). The sensor kinase BfmS mediates virulence in *Acinetobacter baumannii*. *Microbiol. Immunol. Infec.* 47, 275–281. doi: 10.1016/j.jmii.2012.12.004

Liu, L., Cui, Y., Zheng, B., Jiang, S., Yu, W., Shen, P., et al. (2016). Analysis of tigecycline resistance development in clinical *Acinetobacter baumannii* isolates through a combined genomic and transcriptomic approach. *Sci. Rep.* 6:26930. doi: 10.1038/srep26930

Luo, L., Jiang, X., Wu, Q., Wei, L., Li, J., and Ying, C. (2011). Efflux pump overexpression in conjunction with alternation of outer membrane protein may induce *Acinetobacter baumannii* resistant to imipenem. *Chemotherapy* 57, 77–84. doi: 10.1159/000323620

McConnell, M. J., Domínguez-Herrera, J., Smani, Y., López-Rojas, R., Docobo-Pérez, F., and Pachón, J. (2011). Vaccination with outer membrane complexes elicits rapid protective immunity to multidrug-resistant *Acinetobacter baumannii*. *Infect. Immun.* 79, 518–526. doi: 10.1128/IAI.00741-10

Mehdinejadiani, K., Bandehpour, M., Hashemi, A., Ranjbar, M. M., Taheri, S., Jalali, S. A., et al. (2019). *In Silico* design and evaluation of *Acinetobacter baumannii* outer membrane protein a antigenic peptides as vaccine candidate in immunized mice. *Iran J. Allergy Asthma Immunol.* 18, 655–663. doi: 10.18502/ijaai.v18i6.2178

Mirshekar, M., Shahcheraghi, F., Azizi, O., Solgi, H., and Badmasti, F. (2018). Diversity of Class 1 integrons, and disruption of carO and dacD by insertion sequences among *Acinetobacter baumannii* Isolates in Tehran. Iran. *Microb. Drug. Resist.* 24, 359–366. doi: 10.1089/mdr.2017.0152

Moganty, R. R., Vashistt, J., Tiwari, V., and Kapil, A. (2011). Differential expression of Outer membrane proteins in early stages of meropenem-resistance in *Acinetobacter baumannii*. *J. Integrat. OMICS* 1, 281–287. doi: 10.5584/jiomics.v1i2.67

Moon, D. C., Choi, C. H., Lee, J. H., Choi, C. W., Kim, H. Y., Park, J. S., et al. (2012). *Acinetobacter baumannii* outer membrane protein A modulates the biogenesis of outer membrane vesicles. *J. Microbiol.* 50, 155–160. doi: 10.1007/s12275-012-1589-4

Morán-Barrio, J., Cameranesi, M. M., Relling, V., Limansky, A. S., Brambilla, L., and Viale, A. M. (2017). The *Acinetobacter* outer membrane contains multiple specific channels for carbapenem β-lactams as revealed by kinetic characterization analyses of imipenem permeation into *Acinetobacter baylyi* Cells. *Antimicrob. Agents Chemother.* 61:e01737-16. doi: 10.1128/AAC.01737-16

Mortensen, B. L., and Skaar, E. P. (2012). Host-microbe interactions that shape the pathogenesis of *Acinetobacter baumannii* infection. *Cell Microbiol.* 14, 1336–1344. doi: 10.1111/j.1462-5822.2012.01817.x

Mostachio, A. K., Levin, A. S., Rizek, C., Rossi, F., Zerbini, J., and Costa, S. F. (2012). High prevalence of OXA-143 and alteration of outer membrane proteins in carbapenem-resistant *Acinetobacter* spp. isolates in Brazil. *Int. J. Antimicrob. Agents* 39, 396–401. doi: 10.1016/j.ijantimicag.2012.01.021

Mussi, M. A., Limansky, A. S., Relling, V., Ravasi, P., Arakaki, A., Actis, L. A., et al. (2011). Horizontal gene transfer and assortative recombination within the *Acinetobacter baumannii* clinical population provide genetic diversity at the single carO gene, encoding a major outer membrane protein channel. *J. Bacterial.* 193, 4736–4748. doi: 10.1128/JB.01533-10

Mussi, M. A., Limansky, A. S., and Viale, A. M. (2005). Acquisition of resistance to carbapenems in multidrug-resistant clinical strains of *Acinetobacter baumannii*: natural insertional inactivation of a gene encoding a member of a novel family of beta-barrel outer membrane proteins. *Antimicrob. Agents Chemother.* 49, 1432–1440. doi: 10.1128/AAC.49.4.1432-1440.2005

Mussi, M. A., Relling, V. M., Limansky, A. S., and Viale, A. M. (2007). CarO, an *Acinetobacter baumannii* outer membrane protein involved in carbapenem resistance, is essential for L-ornithine uptake. *FEBS Lett.* 581, 5573–5578. doi: 10.1016/j.febslet.2007.10.063

Nan, L. I., Zhang, H. J., Wang, Y., Meng, Q. I., Guo, W. X., Wang, Z., et al. (2018). Study on the drug resistance of clinical strain of *Acinetobacter baumannii* mediated by TEM-1 beta-lactamases and porin CarO. *Tianjin Med. J.* 46, 246–250.

Nie, D., Hu, Y., Chen, Z., Li, M., Hou, Z., Luo, X., et al. (2020). Outer membrane protein A (OmpA) as a potential therapeutic target for *Acinetobacter baumannii* infection. *J. Biomed. Sci.* 27:26. doi: 10.1186/s12929-020-0617-7

Nikaido, H. (2003). Molecular basis of bacterial outer membrane permeability revisited. *Microbiol. Mol. Biol. Rev.* 67, 593–656. doi: 10.1128/mmbr.67.4.593-656.2003

Nitzan, Y., Deutsch, E. B., and Pechatnikov, I. (2002). Diffusion of beta-lactam antibiotics through oligomeric or monomeric porin channels of some gram-negative bacteria. *Curr. Microbiol.* 45, 446–455. doi: 10.1007/s00284-002-3778-6

Nitzan, Y., Pechatnikov, I., Bar-El, D., and Wexler, H. (1999). Isolation and characterization of heat-modifiable proteins from the outer membrane of *Porphyromonas asaccharolytica* and *Acinetobacter baumannii*. *Anaerobe* 5, 43–50. doi: 10.1006/anae.1998.0181

Novovic, K., Mihajlovic, S., Vasiljevic, Z., Filipic, B., Begovic, J., and Jovcic, B. (2015). Carbapenem-resistant *Acinetobacter baumannii* from Serbia: revision of CarO classification. *PLoS One* 10:e0122793. doi: 10.1371/journal.pone.0122793

Oh, K. W., Kim, K., Islam, M. M., Jung, H. W., Lim, D., Lee, J. C., et al. (2020). Transcriptional Regulation of the Outer Membrane Protein A in *Acinetobacter baumannii*. *Microorganisms* 8:706. doi: 10.3390/microorganisms8050706

Pajand, O., Rezaee, M. A., Nahaei, M. R., Mahdian, R., Aghazadeh, M., Soroush, M. H., et al. (2013). Study of the carbapenem resistance mechanisms in clinical isolates of *Acinetobacter baumannii*: comparison of burn and non-burn strains. *Burns* 39, 1414–1419. doi: 10.1016/j.burns.2013.03.024

Park, J. S., Lee, W. C., Choi, S., Yeo, K. J., Song, J. H., Han, Y. H., et al. (2011). Overexpression, purification, crystallization and preliminary X-ray crystallographic analysis of the periplasmic domain of outer membrane protein A from *Acinetobacter baumannii*. *Acta Crystallogr. Sect. F Struct. Biol. Cryst. Commun.* 67(Pt 12), 1531–1533. doi: 10.1107/S1744309111038401

Park, Y. K., Jung, S. I., Park, K. H., Kim, S. H., and Ko, K. S. (2012). Characteristics of carbapenem-resistant *Acinetobacter* spp. other than Acinetobacter baumannii in South Korea. *Int. J. Antimicrob. Agents* 39, 81–85. doi: 10.1016/j.ijantimicag.2011.08.006

Parra-Millán, R., Vila-Farrés, X., Ayerbe-Algaba, R., Varese, M., Sánchez-Encinales, V., Bayó, N., et al. (2018). Synergistic activity of an OmpA inhibitor and colistin against colistin-resistant *Acinetobacter baumannii*: mechanistic analysis and in vivo efficacy. *J. Antimicrob. Chemother.* 73, 3405–3412. doi: 10.1093/jac/dky343

Peleg, A. Y., Seifert, H., and Paterson, D. L. (2008). *Acinetobacter baumannii*: emergence of a successful pathogen. *Clin. Microbiol. Rev.* 21, 538–582. doi: 10.1128/CMR.00058-07

Pormohammad, A., Mehdinejadiani, K., Gholizadeh, P., Nasiri, M. J., Mohtavinejad, N., Dadashi, M., et al. (2020). Global prevalence of colistin resistance in clinical isolates of *Acinetobacter baumannii*: a systematic review and meta-analysis. *Microb. Pathog.* 139:103887. doi: 10.1016/j.micpath.2019.103887

Premkumar, L., Kurth, F., Duprez, W., Grøftehauge, M. K., King, G. J., Halili, M. A., et al. (2014). Structure of the *Acinetobacter baumannii* dithiol oxidase DsbA bound to elongation factor EF-Tu reveals a novel protein interaction site. *J. Biol. Chem.* 289, 19869–19880. doi: 10.1074/jbc.M114.571737

Rasooli, I., Abdolhamidi, R., Jahangiri, A., and Darvish Alipour Astaneh, S. (2020). Outer membrane protein, Oma87 Prevents *Acinetobacter baumannii* Infection. *Int. J. Pept. Res. Ther.* 1–8. doi: 10.1007/s10989-020-10056-0 [Epub ahead of print].

Ravasi, P., Limansky, A. S., Rodriguez, R. E., Viale, A. M., and Mussi, M. A. (2011). ISAba825, a functional insertion sequence modulating genomic plasticity and bla(OXA-58) expression in *Acinetobacter baumannii*. *Antimicrob. Agents Chemother.* 55, 917–920. doi: 10.1128/AAC.00491-10

Rodloff, A. C., and Dowzicky, M. J. (2017). Antimicrobial susceptibility among european gram-negative and gram-positive isolates collected as part of the tigecycline evaluation and surveillance Trial (2004-2014). *Chemotherapy* 62, 1–11. doi: 10.1159/000445022

Royer, S., de Campos, P. A., Araújo, B. F., Ferreira, M. L., Gonçalves, I. R., Batistão, D., et al. (2018). Molecular characterization and clonal dynamics of nosocomial blaOXA-23 producing XDR *Acinetobacter baumannii*. *PLoS One* 13:e0198643. doi: 10.1371/journal.pone.0198643

Rumbo, C., Tomás, M., Moreira, E. F., Soares, N. C., Carvajal, M., Santillana, E., et al. (2014). The *Acinetobacter baumannii* Omp33-36 porin is a virulence factor that induces apoptosis and modulates autophagy in human cells. *Infect. Immun.* 82, 4666–4680. doi: 10.1128/IAI.02034-14

Sánchez-Encinales, V., Álvarez-Marín, R., Pachón-Ibáñez, M. E., Fernández-Cuenca, F., Pascual, A., Garnacho-Montero, J., et al. (2017). Overproduction of outer membrane protein A by *Acinetobacter baumannii* as a risk factor for nosocomial pneumonia. Bacteremia, and Mortality Rate Increase. *J. Infect. Dis.* 215, 966–974. doi: 10.1093/infdis/jix010

Sato, K., and Nakae, T. (1991). Outer membrane permeability of *Acinetobacter calcoaceticus* and its implication in antibiotic resistance. *J. Antimicrob. Chemother.* 28, 35–45. doi: 10.1093/jac/28.1.35

Sato, Y., Unno, Y., Kawakami, S., Ubagai, T., and Ono, Y. (2017). Virulence characteristics of *Acinetobacter baumannii* clinical isolates vary with the expression levels of omps. *J. Med. Microbiol.* 66, 203–212. doi: 10.1099/jmm.0.000394

Sefid, F., and Rasooli, I. (2012). "Cleft analysis Of BauA outer membrane protein in *Acinetobacter Baumannii*," in *Bioinformatics conference*, (Tehran: Shahed University).

Segura, A., Bünz, P. V., D'Argenio, D. A., and Ornston, L. N. (1999). Genetic analysis of a chromosomal region containing vanA and vanB, genes required for conversion of either ferulate or vanillate to protocatechuate in *Acinetobacter*. *J. Bacteriol.* 181, 3494–3504.

Sen, B., and Joshi, S. G. (2016). Studies on *Acinetobacter baumannii* involving multiple mechanisms of carbapenem resistance. *J. Appl. Microbiol.* 120, 619–629. doi: 10.1111/jam.13037

Sharma, A., Dubey, V., Sharma, R., Devnath, K., Gupta, V. K., Akhter, J., et al. (2018). The unusual glycine-rich C terminus of the *Acinetobacter baumannii* RNA chaperone Hfq plays an important role in bacterial physiology. *J. Biol. Chem.* 293, 13377–13388. doi: 10.1074/jbc.RA118.002921

Sharma, M., Sapkota, J., Jha, B., Mishra, B., and Bhatt, C. P. (2019). Biofilm formation and extended-spectrum beta-lactamase producer among *Acinetobacter* species isolated in a tertiary care hospital: a descriptive cross-sectional study. *JNMA J. Nepal. Med. Assoc.* 57, 424–428.

Sievert, D. M., Ricks, P., Edwards, J. R., Schneider, A., Patel, J., Srinivasan, A., et al. (2013). Antimicrobial-resistant pathogens associated with healthcare-associated infections: summary of data reported to the National Healthcare Safety Network at the centers for disease control and prevention, 2009-2010. *Infect. Control Hosp. Epidemiol.* 34, 1–14. doi: 10.1086/668770

Singh, R., Capalash, N., and Sharma, P. (2017). Immunoprotective potential of BamA, the outer membrane protein assembly factor, against MDR *Acinetobacter baumannii*. *Sci. Rep.* 7:12411. doi: 10.1038/s41598-017-12789-3

Singh, R., Garg, N., Capalash, N., Kumar, R., Kumar, M., and Sharma, P. (2014). *In silico* analysis of *Acinetobacter baumannii* outer membrane protein BamA as a potential immunogen. *Int. J. Pure Appl. Sci. Technol.* 21, 32–39.

Singh, R., Garg, N., Shukla, G., Capalash, N., and Sharma, P. (2016). Immunoprotective efficacy of *Acinetobacter baumannii* outer membrane protein. FilF, Predicted *In silico* as a potential vaccine candidate. *Front. Microbiol.* 7:158. doi: 10.3389/fmicb.2016.00158

Siroy, A., Molle, V., Lemaître-Guillier, C., Vallenet, D., Pestel-Caron, M., Cozzone, A. J., et al. (2005). Channel formation by CarO, the carbapenem resistance-associated outer membrane protein of *Acinetobacter baumannii*. *Antimicrob. Agents Chemother.* 49, 4876–4883. doi: 10.1128/AAC.49.12.4876-4883.2005

Skariyachan, S., Taskeen, N., Ganta, M., and Venkata Krishna, B. (2019). Recent perspectives on the virulent factors and treatment options for multidrug-resistant *Acinetobacter baumannii*. *Crit. Rev. Microbiol.* 45, 315–333. doi: 10.1080/1040841X.2019.1600472

Slusky, J. S., and Dunbrack, R. L. Jr. (2013). Charge asymmetry in the proteins of the outer membrane. *Bioinformatics* 29, 2122–2128. doi: 10.1093/bioinformatics/btt355

Smani, Y., Dominguez-Herrera, J., and Pachón, J. (2013). Association of the outer membrane protein Omp33 with fitness and virulence of *Acinetobacter baumannii*. *J. Infect. Dis.* 208, 1561–1570. doi: 10.1093/infdis/jit386

Smani, Y., McConnell, M. J., and Pachón, J. (2012). Role of fibronectin in the adhesion of *Acinetobacter baumannii* to host cells. *PLoS One* 7:e33073. doi: 10.1371/journal.pone.0033073

Smani, Y., and Pachón, J. (2013). Loss of the OprD homologue protein in *Acinetobacter baumannii*: impact on carbapenem susceptibility. *Antimicrob. Agents Chemother.* 57:677. doi: 10.1128/AAC.01277-12

Smith, M. A., Weaver, V. B., Young, D. M., and Ornston, L. N. (2003). Genes for chlorogenate and hydroxycinnamate catabolism (hca) are linked to functionally related genes in the dca-pca-qui-pob-hca chromosomal cluster of *Acinetobacter* sp. strain ADP1. *Appl. Environ. Microbiol.* 69, 524–532. doi: 10.1128/aem.69.1.524-532.2003

Song, X., Zhang, H., Zhang, D., Xie, W., and Zhao, G. (2018). Bioinformatics analysis and epitope screening of a potential vaccine antigen TolB from *Acinetobacter baumannii* outer membrane protein. *Infect. Genet. Evol.* 62, 73–79. doi: 10.1016/j.meegid.2018.04.019

Srinivasan, V. B., Vaidyanathan, V., and Rajamohan, G. (2015). AbuO, a TolC-like outer membrane protein of *Acinetobacter baumannii*, is involved in antimicrobial and oxidative stress resistance. *Antimicrob. Agents Chemother.* 59, 1236–1245. doi: 10.1128/AAC.03626-14

Tohidinia, M., Moshtaghioun, S. M., Sefid, F., and Falahati, A. (2019). Functional exposed amino acids of CarO analysis as a potential vaccine candidate in *Acinetobacter Baumannii*. *Int. J. Peptide Res. Thera.* 26, 1185–1197. doi: 10.1007/s10989-019-09923-2

Tsai, Y. K., Liou, C. H., Lin, J. C., Fung, C. P., Chang, F. Y., and Siu, L. K. (2020). Effects of different resistance mechanisms on antimicrobial resistance in *Acinetobacter baumannii*: a strategic system for screening and activity testing of new antibiotics. *Int. J. Antimicrob. Agents* 55:105918. doi: 10.1016/j.ijantimicag.2020.105918

van der Kolk, J. H., Endimiani, A., Graubner, C., Gerber, V., and Perreten, V. (2019). Acinetobacter in veterinary medicine, with an emphasis on *Acinetobacter baumannii*. *J. Glob. Antimicrob. Resist.* 16, 59–71. doi: 10.1016/j.jgar.2018.08.011

Vashist, J., Tiwari, V., Kapil, A., and Rajeswari, M. R. (2010). Quantitative profiling and identification of outer membrane proteins of beta-lactam resistant strain of *Acinetobacter baumannii*. *Proteome Res.* 9, 1121–1128. doi: 10.1021/pr9011188

Viale, A. M., and Evans, B. A. (2020). Microevolution in the major outer membrane protein OmpA of *Acinetobacter baumannii*. *Microb. Genom.* 6:e000381. doi: 10.1099/mgen.0.000381

Vila-Farrés, X., Parra-Millán, R., Sánchez-Encinales, V., Varese, M., Ayerbe-Algaba, R., Bayó, N., et al. (2017). Combating virulence of Gram-negative bacilli by OmpA inhibition. *Sci. Rep.* 7, 14683. doi: 10.1038/s41598-017-14972-y

Walzer, G., Rosenberg, E., and Ron, E. Z. (2006). The *Acinetobacter* outer membrane protein A (OmpA) is a secreted emulsifier. *Environ. Microbiol.* 8, 1026–1032. doi: 10.1111/j.1462-2920.2006.00994.x

Wang, T., Yuan, Q., and Ling, B. (2015). Analysis of the expression of the outer membrane protein in carbapenem-resistant *Acinetobacter baumannii*. *Int. J. Lab. Med.* 2015, 2295–2296.

Weiner, L. M., Webb, A. K., Limbago, B., Dudeck, M. A., Patel, J., Kallen, A. J., et al. (2016). Antimicrobial-resistant pathogens associated with healthcare-associated infections: summary of data reported to the national healthcare safety network at the centers for disease control and prevention, 2011-2014. *Infect. Control Hosp. Epidemiol.* 37, 1288–1301. doi: 10.1017/ice.2016.174

World Health Organization [WHO] (2017). *Global Priority list of Antibiotic-Resistant Bacteria to Guide Researach, Discovery and Development of New Antibiotics*. Geneva: WHO.

Wu, X., Chavez, J. D., Schweppe, D. K., Zheng, C., Weisbrod, C. R., Eng, J. K., et al. (2016). In vivo protein interaction network analysis reveals porin-localized antibiotic inactivation in *Acinetobacter baumannii* strain AB5075. *Nat. Commun.* 7:13414. doi: 10.1038/ncomms13414

Yang, H., Huang, L., Barnie, P. A., Su, Z., Mi, Z., Chen, J., et al. (2015). Characterization and distribution of drug resistance associated β-lactamase, membrane porin and efflux pump genes in MDR A. baumannii isolated from Zhenjiang. China. *Int. J. Clin. Exp. Med.* 8, 15393–15402.

Yun, S. H., Choi, C. W., Park, S. H., Lee, J. C., Leem, S. H., Choi, J. S., et al. (2008). Proteomic analysis of outer membrane proteins from *Acinetobacter baumannii* DU202 in tetracycline stress condition. *J. Microbiol.* 46, 720–727. doi: 10.1007/s12275-008-0202-3

Yun, S. H., Park, E. C., Lee, S. Y., Lee, H., Choi, C. W., Yi, Y. S., et al. (2018). Antibiotic treatment modulates protein components of cytotoxic outer membrane vesicles of multidrug-resistant clinical strain, *Acinetobacter baumannii* DU202. *Clin. Proteomics* 15:28. doi: 10.1186/s12014-018-9204-2

Zahn, M., Bhamidimarri, S. P., Baslé, A., Winterhalter, M., and van den Berg, B. (2016). Structural insights into outer membrane permeability of *Acinetobacter baumannii*. *Structure* 24, 221–231. doi: 10.1016/j.str.2015.12.009

Zahn, M., D'Agostino, T., Eren, E., Baslé, A., Ceccarelli, M., and van den Berg, B. (2015). Small-molecule transport by CarO, an abundant eight-stranded β-Barrel outer membrane protein from *Acinetobacter baumannii*. *J. Mol. Biol.* 427, 2329–2339. doi: 10.1016/j.jmb.2015.03.016

Zhang, L., Liang, W., S-G, Xu, Mei, J., Di, Y. Y., Lan, H. H., et al. (2019). CarO promotes adhesion and colonization of *Acinetobacter baumannii* through inhibiting NF-êB pathways. *Int. J. Clin. Exp. Med.* 12, 2518–2524.

Zhao, S. Y., Jiang, D. Y., Xu, P. C., Zhang, Y. K., Shi, H. F., Cao, H. L., et al. (2015). An investigation of drug-resistant *Acinetobacter baumannii* infections

in a comprehensive hospital of East China. *Ann. Clin. Microbiol. Antimicrob.* 14:7. doi: 10.1186/s12941-015-0066-4

Zhou, H., Yao, Y., Zhu, B., Ren, D., Yang, Q., Fu, Y., et al. (2019). Risk factors for acquisition and mortality of multidrug-resistant *Acinetobacter baumannii* bacteremia: a retrospective study from a Chinese hospital. *Medicine* 98:e14937. doi: 10.1097/MD.0000000000014937

Zhu, L. J., Chen, X. Y., and Hou, P. F. (2019). Mutation of CarO participates in drug resistance in imipenem-resistant *Acinetobacter baumannii*. *J. Clin. Lab. Anal.* 33:e22976. doi: 10.1002/jcla.22976

Conflict of Interest: The authors declare that the research was conducted in the absence of any commercial or financial relationships that could be construed as a potential conflict of interest.

frontiers in Microbiology

ORIGINAL RESEARCH
published: 15 October 2020
doi: 10.3389/fmicb.2020.576673

Molecular Epidemiology of *Acinetobacter calcoaceticus-Acinetobacter baumannii* Complex Isolated From Children at the Hospital Infantil de México Federico Gómez

Jetsi Mancilla-Rojano[1,2], Sara A. Ochoa[1], Juan Pablo Reyes-Grajeda[3], Víctor Flores[4], Oscar Medina-Contreras[5], Karina Espinosa-Mazariego[1], Israel Parra-Ortega[6], Daniela De La Rosa-Zamboni[7], María del Carmen Castellanos-Cruz[6], José Arellano-Galindo[8], Miguel A. Cevallos[9], Rigoberto Hernández-Castro[10], Juan Xicohtencatl-Cortes[1] and Ariadnna Cruz-Córdova[1]**

[1]*Laboratorio de Investigación en Bacteriología Intestinal, Subdirección de Gestión de la Investigación, Hospital Infantil de México Federico Gómez, CDMX, Mexico,* [2]*Facultad de Medicina, Posgrado en Ciencias Biológicas, Universidad Nacional Autónoma de México, CDMX, Mexico,* [3]*Subdirección de Desarrollo de Aplicaciones Clínicas, Instituto Nacional de Medicina Genómica, Ciudad de México, Mexico,* [4]*Unidad de Genómica Avanzada, Laboratorio Nacional de Genómica para la Biodiversidad, Irapuato, Mexico,* [5]*Unidad de Investigación Epidemiológica en Endocrinología y Nutrición, Hospital Infantil de México Federico Gómez, CDMX, Mexico,* [6]*Departamento de Laboratorio Clínico, Laboratorio Central, Hospital Infantil de México Federico Gómez, CDMX, Mexico,* [7]*Departamento de Epidemiología Hospitalaria, Hospital Infantil de México Federico Gómez, CDMX, Mexico,* [8]*Unidad de investigación en Enfermedades Infecciosas, Subdirección de Gestión de la Investigación, Hospital Infantil de México Federico Gómez, CDMX, Mexico,* [9]*Centro de Ciencias Genómicas, Programa de Genómica Evolutiva, Universidad Nacional Autónoma de México, Cuernavaca, Mexico,* [10]*Departamento de Ecología de Agentes Patógenos, Hospital General Dr. Manuel Gea González, CDMX, Mexico*

The *Acinetobacter calcoaceticus-baumannii* (*Acb*) complex is regarded as a group of phenotypically indistinguishable opportunistic pathogens responsible for mainly causing hospital-acquired pneumonia and bacteremia. The aim of this study was to determine the frequency of isolation of the species that constitute the *Acb* complex, as well as their susceptibility to antibiotics, and their distribution at the Hospital Infantil de Mexico Federico Gomez (HIMFG). A total of 88 strains previously identified by Vitek 2®, 40 as *Acinetobacter baumannii* and 48 as *Acb* complex were isolated from 52 children from 07, January 2015 to 28, September 2017. *A. baumannii* accounted for 89.77% (79/88) of the strains; *Acinetobacter pittii*, 6.82% (6/88); and *Acinetobacter nosocomialis*, 3.40% (3/88). Most strains were recovered mainly from patients in the intensive care unit (ICU) and emergency wards. Blood cultures (BC) provided 44.32% (39/88) of strains. The 13.63% (12/88) of strains were associated with primary bacteremia, 3.4% (3/88) with secondary bacteremia, and 2.3% (2/88) with pneumonia. In addition, 44.32% (39/88) were multidrug-resistant (MDR) strains and, 11.36% (10/88) were extensively drug-resistant (XDR). All strains amplified the $bla_{\text{OXA-51}}$ gene; 51.13% (45/88), the $bla_{\text{OXA-23}}$ gene; 4.54% (4/88), the $bla_{\text{OXA-24}}$ gene; and 2.27% (2/88), the $bla_{\text{OXA-58}}$ gene. Plasmid profiles showed that the strains had 1–6 plasmids. The strains were distributed in 52 pulsotypes, and 24 showed identical restriction patterns, with a correlation coefficient of 1.0. Notably, some strains with the

OPEN ACCESS

Edited by:
Benjamin Andrew Evans, University of East Anglia, United Kingdom

Reviewed by:
Andres Felipe Opazo-Capurro, University of Concepcion, Chile
Clndy Shuan Ju Teh, University of Malaya, Malaysia
Leena Al-Hassan, Brighton and Sussex Medical School, United Kingdom

***Correspondence:**
Juan Xicohtencatl-Cortes
juanxico@yahoo.com
Ariadnna Cruz-Córdova
ariadnnacruz@yahoo.com.mx

Specialty section:
This article was submitted to Antimicrobials, Resistance and Chemotherapy, a section of the journal Frontiers in Microbiology

Received: *26 June 2020*
Accepted: *08 September 2020*
Published: *15 October 2020*

Citation:
Mancilla-Rojano J, Ochoa SA, Reyes-Grajeda JP, Flores V, Medina-Contreras O, Espinosa-Mazariego K, Parra-Ortega I, Rosa-Zamboni DDL, Castellanos-Cruz MdC, Arellano-Galindo J, Cevallos MA, Hernández-Castro R, Xicohtencatl-Cortes J and Cruz-Córdova A (2020) Molecular Epidemiology of Acinetobacter calcoaceticus-Acinetobacter baumannii Complex Isolated From Children at the Hospital Infantil de México Federico Gómez. Front. Microbiol. 11:576673. doi: 10.3389/fmicb.2020.576673

same pulsotype were isolated from different patients, wards, or years, suggesting the persistence of more than one clone. Twenty-seven sequence types (STs) were determined for the strains based on a Pasteur multilocus sequence typing (MLST) scheme using massive sequencing; the most prevalent was ST 156 (27.27%, 24/88). The Clustered Regularly Interspaced Short Palindromic Repeats (CRISPR)-Cas I-Fb system provided amplification in *A. baumannii* and *A. pittii* strains (22.73%, 20/88). This study identified an increased number of MDR strains and the relationship among strains through molecular typing. The data suggest that more than one strain could be causing an infection in some patient. The implementation of molecular epidemiology allowed the characterization of a set of strains and identification of different attributes associated with its distribution in a specific environment.

Keywords: *Acinetobacter baumannii*, *Acinetobacter calcoaceticus-Acinetobacter baumannii* complex, intensive care unit, resistance, molecular typing

INTRODUCTION

The *Acinetobacter* genus includes species widely disseminated in nature, mostly in water and soil; some of these species are considered opportunistic pathogens that are relevant for their association with health-care associated infections (HAIs). The clinically important species in this genus are *Acinetobacter pittii*, *Acinetobacter nosocomialis*, and *Acinetobacter baumannii*, with the last being the most important epidemiologically and frequently isolated from the intensive care unit (ICU), causing infections such as ventilator-associated pneumonia, bacteremia, urinary tract infection, meningitis, and wound infection (Dexter et al., 2015; Wong et al., 2017).

The *Acinetobacter calcoaceticus-baumannii* complex (*Acb*) harbored six species: *A. calcoaceticus*, *A. baumannii*, *A. pittii*, *A. nosocomialis*, *Acinetobacter seifertii*, and *Acinetobacter dijkshoorniae* (Gerner-Smidt et al., 1991; Nemec et al., 2011, 2015). The *Acb* complex cause hospital-acquired pneumonia and bacteremia in critically ill or immunocompromised patients (Wong et al., 2017; Vazquez and Kollef, 2018). The species of the complex are phenotypically indistinguishable and molecular methods are required for its correct identification (Gerner-Smidt et al., 1991). The participation of *A. calcoaceticus* in clinical infections remains unclear compared with other species, in which clinical importance has been demonstrated (Peleg et al., 2008; Nemec et al., 2015; Cosgaya et al., 2016). *A. baumannii* is one of the most difficult bacteria to contain in a hospital environment. Additionally, it is included in the list of priority pathogens resistant to antibiotics, owing to the resistance it has acquired to different antibiotics such as carbapenems and cephalosporins limiting the therapeutic options for the treatment of infections caused by this pathogen (Higgins et al., 2010; Shrivastava et al., 2018).

The pulsed-field gel electrophoresis (PFGE), multilocus sequence typing (MLST), and amplified fragment length polymorphism (AFLP) methods have been used to type clinical strains of *A. baumanni* (Limansky et al., 2004; Rafei et al., 2014). In hospitals in Spain and Germany, a total of 20 allelic profiles or sequence types (STs) were identified through MLST, and these results agreed with those generated by PFGE, suggesting MLST as a tool for the molecular epidemiological study of clinical strains of *A. baumannii* (Bartual et al., 2005). However, there are other studies where according to the tool used, the typing of the strains differs completely; the relationships between clinical isolates that were determined through PFGE revealed that isolates were not closely related (Evans et al., 2008). Through nucleotide analysis of the $bla_{\text{OXA-51}}$ gene sequence, two closely related groups were identified. The sequencing of the $bla_{\text{OXA-51}}$ gene, being only one genetic element, yielded a less-defined clonal relationship than PFGE analyses, where the whole genome is digested and analyzed to establish whether there is a clonal relationship between the strains under study (Evans et al., 2008).

The Clustered Regularly Interspaced Short Palindromic Repeats (CRISPR)-Cas system has been proposed for typing bacterial strains. Two CRISPR-Cas systems have been identified in strains of *A. baumannii* from military and children's hospitals. An analysis of the nucleotide sequences of the CRISPR-Cas systems (CRISPR-AYE and *Acinetobacter baylyi* ADP systems) grouped the isolates into two clonal complexes and provided information about the evolution of these complexes (Hauck et al., 2012). At the same time, the CRISPR-Cas I-Fb system has been proposed for the subtyping of strains (Karah et al., 2015).

Genome sequencing is used to characterize and establish genetic relationships among isolates. Clinical strains identified as *Acb* complex were typed using PFGE, MLST, and single nucleotide polymorphism (SNP) analyses. SNP analysis was more discriminatory than those obtained by PFGE and MLST for the identification of clones and their association with outbreaks (Fitzpatrick et al., 2016).

A. baumannii mortality is approximately 14.5% and it has been associated with HAIs in tertiary level hospitals in Mexico (Bocanegra-Ibarias et al., 2015). Furthermore, the Mexican strains that have been characterized are distinguished by their resistance to imipenem and meropenem, as well as being associated with the amplification of carbapenemases such as OXA-23, OXA-239, and OXA-58. An epidemiological aspect of relevance is the different STs distributed among Mexican

hospitals, belonging to clonal complexes 636 and 92, presenting ST208, ST369, and ST758 (Alcántar-Curiel et al., 2014; Tamayo-Legorreta et al., 2014; Gonzalez-Villoria et al., 2016). However, information about other species related to the *Acb* complex has not been available. The *Acb* complex poses a major challenge to this genus, suggesting a very recent diversification of those species, and events of homologous recombination can probably be contributed to a homogenous gene composition (Mateo-Estrada et al., 2019).

The aim of this study was to determine the frequency of isolation of the species that constitute the *Acb* complex, as well as the susceptibility to antibiotics, and their distribution at the Hospital Infantil de Mexico Federico Gomez (HIMFG). To achieve this aim, the *Acinetobacter* species were distinguished when the strains were identified as the *Acb* complex using a collection of 88 strains from 52 children from 07, January 2015 to 28, September 2017, previously identified as the *A. baumannii* and *Acb* complex. Then, after the susceptibility profile was determined, four of the most frequent bla_{OXA} genes were detected, the plasmid profile, pulsotype, and sequence type were established and the CRISPR-Cas system was carried out for all strains.

MATERIALS AND METHODS

Identification by MALDI-TOF Biotyper

In this study, all strains among 07, January 2015 to 28, September 2017 were considered and identified as the *A. baumannii* or *Acb* complex, from patients with or without HAIs. If one patient had more than one strain, all strains were included in this study. The strains were previously identified at the Central Clinical Laboratory at the HIMFG using the Vitek® 2 automated system (BioMérieux, Marcy l'Étoile France), and they were subsequently reidentified by matrix-assisted laser desorption/ionization time-of-flight (MALDI-TOF) Biotyper (mass spectrometer, Bremen, Germany). Each strain was spread onto Brucella blood agar (BD Difco, Madrid, Spain), and one colony was placed on a metallic card for analysis (Bruker Daltonics Ultraflextreme, Bremen, Germany). The sample allowed to dry at room temperature; 1 µl of formic acid (70%) was placed on each well to dry at room temperature, and 1 µl of matrix [saturated solution of α-cyano-4-hydroxycinnamic acid (HCCA; Bruker Daltonics Ultraflextreme, Bremen, Germany) in 50% acetonitrile (Sigma, California, United States) and 2.5% trifluoroacetic acid were subsequently added (Sigma, California, United States)]. The spectra were analyzed using the MALDI Biotyper software Bruker Daltonics Ultraflextreme 3.1 (Bremen, Germany) and were compared with a database using identification criteria at the species level with a score between 1.7 and 1.9.

Antibiotic Susceptibility Test

Antibiotic susceptibility testing was performed using a Vitek® 2 automated system (BioMériux, Marcy l'Étoile, France). The antibiotics considered included penicillins (piperacillin); β-lactam combination agents (ampicillin-sulbactam and piperacillin-tazobactam); cephems (cefepime and ceftriaxone); carbapenems (imipenem); a lipopeptide (colistin); aminoglycosides (gentamicin); fluoroquinolones (ciprofloxacin); and folate pathway antagonists (trimethoprim-sulfamethoxazole), according to the Clinical and Laboratory Standards Institute (CLSI, 2018). Colistin susceptibility by the broth microdilution method according to CLSI was determined. *Escherichia coli* ATCC®25922 and *Pseudomonas aeruginosa* ATCC®27853 were used as quality controls; including *A. baumannii* ATCC®19606 as an internal control. Susceptibility to tigecycline was interpreted according to the United States Food and Drug Administration (FDA) breakpoints for *Enterobacteriaceae*. The multidrug-resistant (MDR) profile was defined as the strains resistant to three or more antimicrobial classes, and the extensively drug-resistant (XDR) profile was defined as the strains nonsusceptible to ≥1 agent in all but ≤2 categories (Magiorakos et al., 2012).

Amplification of $bla_{\text{OXA-LIKE}}$ Genes

Genomic DNA of strains was obtained with the Quick-DNA Universal kit (Zymo, Irvine, California, United States). $bla_{\text{OXA-LIKE}}$ genes were amplified by PCR using the specific primers listed in **Table 1**. PCR assays were performed using the following thermocycling conditions: 94°C for 5 min; 30 cycles at 94°C for 25 s, 52°C for 40 s, and 72°C for 50 s; and a final step at 72°C for 6 min. *A. baumannii* ATCC®19606 was used as a positive control for $bla_{\text{OXA-51}}$.

Plasmid DNA Profiles

The extraction of plasmid DNA was performed using the technique of Eckhardt (1978). A colony of each strain grown first on Brucella blood agar was cultured in 3 ml of Luria-Bertani (LB) broth (BD Difco, Madrid, Spain) with constant stirring (200 rpm) at 37°C for 15 h. Subsequently, 100 µl of this bacterial culture was incubated in 5 ml of LB broth under agitation at 37°C for 2.5 h. Finally, 1 ml bacterial culture was taken and centrifuged for 8 min at 14,000 rpm. The pellet was dissolved in 500 µl of cold sterile water, mixed with 1 ml of 0.3% sarcosyl solution, and then centrifuged at 14,000 rpm for 6 min. The pellet was incubated with 40 µl of 20% Ficoll in 10:1 TE buffer, kept on ice for 15 min and mixed with 20 µl of lysis solution [0.4 mg/ml RNase, 1 mg/ml bromophenol blue, 80 µl lysozyme (20 mg/ml in water)]. After 30 µl of SDS (10%) was added to each well, the samples were run on a 0.75% agarose gel (Promega, Wisconsin, United States) under

TABLE 1 | Primers used to amplify $bla_{\text{OXA-LIKE}}$ genes.

Gene	Sequence 5' – 3'	Amplified size (bp)	Reference
$bla_{\text{OXA-23}}$	F: GATCGGATTGGAGAA CAGA R: ATTTCTGACCGCATTTCCAT	501	Hujer et al. (2006)
$bla_{\text{OXA-24}}$	F: GGTTAGTTGGCCCCCTTAAA R: AGTTGACGCAAAAGGGGATT	246	Hujer et al. (2006)
$bla_{\text{OXA-51}}$	F: TAATGCTTTGATCGGCCTTG R: TGCATTGCACTTCATCTTGG	353	Hujer et al. (2006)
$bla_{\text{OXA-58}}$	F: AAGTATTGGGGCTTGTGCTG R: CCCCTCTGCGCTCTACATAC	599	Hujer et al. (2006)

OXA-23 ($bla_{\text{OXA-23}}$), OXA-24 ($bla_{\text{OXA-24}}$), OXA-51 ($bla_{\text{OXA-51}}$), and OXA-58 ($bla_{\text{OXA-58}}$).

the following conditions: 100 V for 15 min in 1X TBE buffer (AMRESCO, United States) without completely covering the gel and with the negative polarity inverted. After this time, 1X TBE was added to the chamber in a cold room until the gel was covered, and the samples were placed. The electrophoretic shift was performed with the poles in the standard orientation at 40 V for 90 min and thereafter at 100 V for 21 h. The gel was stained with ethidium bromide for visualization.

PFGE Assay

The 88 strains were seeded and incubated at 37°C for 18 h. PFGE assay was performed for all strains as described by Mancilla-Rojano et al. (2019). Briefly, colonies cultured on Brucella blood agar were selected and suspended in 1 ml of negative Gram suspension buffer (100 mM Tris-HCl and 100 mM EDTA 100 pH 8). The bacterial suspension was embedded into 1% agarose plugs (SeaKem, Cambrex, Rockland, United States) and lysed with 5 ml of lysis buffer at pH 8.0 [0.5 M Tris-HCl, 0.5 M EDTA, 1% N-lauryl sarcosine sodium salt, and 25 µl of proteinase K (20 mg/ml)]. Afterward, the samples were digested with the ApaI enzyme (Promega, Wisconsin, United States), and the chromosomal DNA obtained was subjected to electrophoresis on 1% agarose gels (Bio-Rad, Hercules, California, United States) using in the CHEF MAPPER system (Bio-Rad, Hercules, California, United States) using 0.5X TBE (AMRESCO, United States) under the following conditions: initial time 5.0 s, final time 30.0 s, 6 V/cm, inclination angle 120, and running time 24 h. The lambda marker (Biolabs, Hertfordshire, England, United Kingdom) was used as a molecular weight marker. The electrophoresis gels were stained with 0.5 mg/ml ethidium bromide for 40 min and visualized under UV light. The DNA fragment patterns generated by PFGE were analyzed and compared using NTSYS software version 2.2 (Applied Biostatistics, Setauket, New York, United States) with the unweighted pair group method using the arithmetic average (UPGMA) algorithm and the DICE correlation coefficient. The relatedness degree was assessed according to the criteria established by Tenover et al. (1995).

MLST Assay

Amplification of the fragments was carried out according to the MLST protocol with some modifications (Diancourt et al., 2010). The primers to amplify the *fusA* (elongation factor EF-G) gene were designed using the genome of *A. baumannii* AYE (GCA_000069245.1). To perform massive sequencing, the following adaptors were incorporated in each primer: F: 5'- TCG TCG GCA GCG TCA GAT GTG TAT AAG AGA CAG-3' and R: 5'- GTC TCG TGG GCT CGG AGA TGT GTA TAA GAG ACA-3' (**Table 2**).

TABLE 2 | Primers used to amplify genes to determine STs by multilocus sequence typing (MLST).

Gene	Sequence 5'-3'	Amplified size (bp)	
cpn60	F: TCG TCG GCA GCG TCA GAT GTG TAT AAG AGA CAG ACT GTA CTT GCT CAA GC	480	Diancourt et al. (2010)
	R: GTC TCG TGG GCT CGG AGA TGT GTA TAA GAG ACA GTT CAG CGA TGA TAA GAA GTG G		
fusA	F: TCG TCG GCA GCG TCA GAT GTG TAT AAG AGA CAG ACA ATT ACC TCT GCT GCA ACA	633	This study
	R: GTC TCG TGG GCT CGG AGA TGT GTA TAA GAG ACA TCA TCG CAG GTT TAC GTG CT		
gltA	F: TCG TCG GCA GCG TCA GAT GTG TAT AAG AGA CAG AGA TGT ATT GGC CTC AGG TCA CTT	545	Diancourt et al. (2010)
	R: GTC TCG TGG GCT CGG AGA TGT GTA TAA GAG ACG GGT TTA CTT TGT AGT CAC GGT CTG		
pyrG	F: TCG TCG GCA GCG TCA GTA GTG TAT AAG AGA CAG GGT GTT GTT TCA TCA CTA GGW AAA GG	434	Diancourt et al. (2010)
	R: GTC TCG TGG GCT CGG AGA TGT GTA TAA GAG ACA GAT AAA TGG TAA AGA YTC GAT RTC ACC		
recA	F: TCG TCG GCA GCG TCA GAT GTG TAT AAG AGA CAG CCT GAA TCT TCY GGT AAA AC	425	Diancourt et al. (2010)
	R: GTC TCG TGG GCT CGG AGA TGT GTA TAA GAG ACA GGT TTC TGG GCT GCC AAA CAT TAC		
rplB	F: TCG TCG GCA GCG TCA GAT GTG TAT AAG AGA CAG GTA GAG CGT ATT GAA TAC GAT CCT AAC C	472	Diancourt et al. (2010)
	R: GTC TCG TGG GCT CGG AGA TGT GTA TAA GAG ACA GCA CCA CCA CCR TGY GGG TGA TC		
rpoB	F: TCG TCG GCA GCG TCA GAT GTG TAT AAG AGA CAG GGC TTC TGA AGT ACG TGA CGT	502	Diancourt et al. (2010)
	R: GTC TCG TGG GCT CGG AGA TGT GTA TAA GAG ACG TCA CGT GCA ACG TTC GCT T		

Citrate synthase (gltA); DNA gyrase subunit B (gyrB); glucose dehydrogenase B (gdhB); homologous recombination factor (recA); 60-kDa chaperonin (cpn60); glucose-6 phosphate isomerase (gpi); and RNA polymerase sigma factor (rpoD).

The genes were amplified from genomic DNA (1 μg), and PCR was performed under the following conditions: 94°C for 2 min, 35 cycles at 94°C for 30 s, 50°C for 30 s, and 72°C for 30 s, and a final step of 72°C for 5 min. To verify the amplified products *via* electrophoresis, 1.8% agarose gel electrophoresis was run using 1X TAE buffer at 120 V, and then the gel was stained with ethidium bromide to observe the amplified products with a transilluminator (Bio-Rad, CA, United States).

Constitutive gene sequencing was carried out using the Illumina Nextseq500 platform on 1 μg of genomic DNA. The readings obtained for each of the strains were analyzed through the bioinformatics tool FASTQC (Andrews, 2010) and were filtered with AfterQC (Chen et al., 2017). The sequences that had a depth of less than 20X and those that did not have the necessary length for the analysis were eliminated. Assembly of the readings was carried out from the sequences deposited in PubMLST using the aTRAM 2.0 program (Allen et al., 2018) with default parameters for paired readings and was verified by mapping the raw readings using BWA software (Li and Durbin, 2009). The mapped readings were filtered with SAMtools (Li et al., 2009) with the -m3 option to preserve only those readings that properly mapped onto the sequences, and the mappings were edited using SeaView (Gouy et al., 2010). The sequences obtained from each gene and the concatemer were analyzed using the database for *A. baumannii*.[1] Each strain was characterized by a pattern of numbers that define its ST.

CRISPR-Cas System Identification

The CRISPR-Cas I-Fb system (95°C for 5 min, 30 cycles at 95°C for 1 min, 58°C for 1 min, 72°C for 7 min, and a final step of 72°C for 10 min), the CRISPR AYE system (95°C for 5 min, 30 cycles at 95°C for 1 min, 45°C for 1 min, 72°C for 7 min, and a final step of 72°C for 10 min), and the gene *cas1* (95°C for 5 min, 35 cycles at 95°C for 30 s, 48°C for 30 s, 72°C for 30 s, and a final step of 72°C for 7 min) were identified by PCR (**Table 3**). To verify the presence of the amplified DNA, electrophoresis was performed on a 1% agarose gel using 1X TBE buffer at 120 V, and then the gel was stained with ethidium bromide to observe the amplification products with a transilluminator. The PCR products were purified and subsequently sequenced by capillary electrophoresis following the Sanger method. The sequences obtained were compared with the sequence of the CRISPR loci in strains of *A. baumannii*, which is available on the CRISPR web server.[2] This server has 12 genomes of *A. baumannii* with structures confirmed by the CRISPR systems. The repeated sequences were analyzed by multiple alignments using the MultAlin interface page[3] to determine the similarity between the strains.

[1]http://pubmlst.org/abaumannii/

TABLE 3 | Primers used to amplify CRISPR-Cas systems.

Gene	Sequence 5'-3'	Reference
aye-cris	F: CCGTAGTTGAATCAACACGTA	Hauck et al. (2012)
	R: TTTGATTGGGTAAAATGCCAAA	
aye-cas1	F: TCAAGCTGCGATGCGAATGT	Hauck et al. (2012)
	R: ATCCGGGCAAATTGAAACGC	
ab-cris	F: AGTCCCAGAGTTTTGACCCA	Karah et al. (2015)
	R: TTGGATTGGGTCATCATTGGT	

aye-cris: CRISPR-AYE system, aye-cas1: cas1 gene, ab-cris: CRISPR-Cas I-Fb system.

Statistical Analysis

The data were analyzed using the chi square test to evaluate the relationship between variables, with $p < 0.05$ considered significant. The descriptive statistics included percentages and frequencies.

RESULTS

The MALDI-TOF-MS Biotyper Allowed the Differentiation of *Acb* Complex

The eighty-eight strains firstly identified as *A. baumannii* and 48 as *Acb* complex were reidentified with the MALDI-TOF-MS Biotyper, allowing us to differentiate between the species with the *Acb* complex. Additionally, 89.77% (79/88) of the strains were identified as *A. baumannii*, 6.82% (6/88) as *A. pittii*, and 3.40% (3/88) as *A. nosocomialis*.

Patients in the Intensive Care Unit and Blood Culture Samples Were the Most Frequent Sources of *A. baumannii* Isolation

In this study was included 52 patients (children between 1 and 15 years old) retained in 14 wards at the HIMFG from January 2015 to September 2017. Patients located in the ICU and emergency wards [26.92% (14/52)] made up the largest number of patients carrying the *Acinetobacter* strain (**Figure 1**).

From the 52 patients were recovered 88 strains with 37.5% (33/88), 25% (22/88), and 37.5% (33/88) obtained from the 2015, 2016, and 2017 samples, respectively. *A. baumannii* strains were identified in patients from several services wards, but mainly in emergency (13.63%, 12/88) and ICU (27.27%, 24/88). *A. pittii* strains were recovered from samples from patients in emergency, nephrology, and infectology. *A. nosocomialis* strains were obtained from samples from patients in surgery, gastroenterology, and internal medicine (**Supplementary Table 1**).

The isolation frequency by sample origin was as follows: 44.32% (39/88) from BC, 36.36% (32/88) from different (D) samples (including bronchial aspirate, catheter, mediastinal tissue, cholesteatoma culture, and peritoneal fluid), 13.63% (12/88) from urine cultures (UC), 2.27% (2/88) from a stool culture (SC) and an autopsy (A), and 1.14% (1/88) from cerebrospinal fluid (CSF, **Figure 1**).

According to the epidemiology analysis from 2015, nine strains (568BC, 173BC, 180BC, 181BC, 49BC, 50BC, 470BC, 471BC, and 800D) isolated from five patients were related to HAIs. Eight strains (219BC, 182BC, 183BC, 144D, 600BC, 928BC, 940BC, and 136BC) isolated from five patients were

[2]https://crispr.i2bc.paris-saclay.fr/
[3]http://multalin.toulouse.inra.fr/multalin/

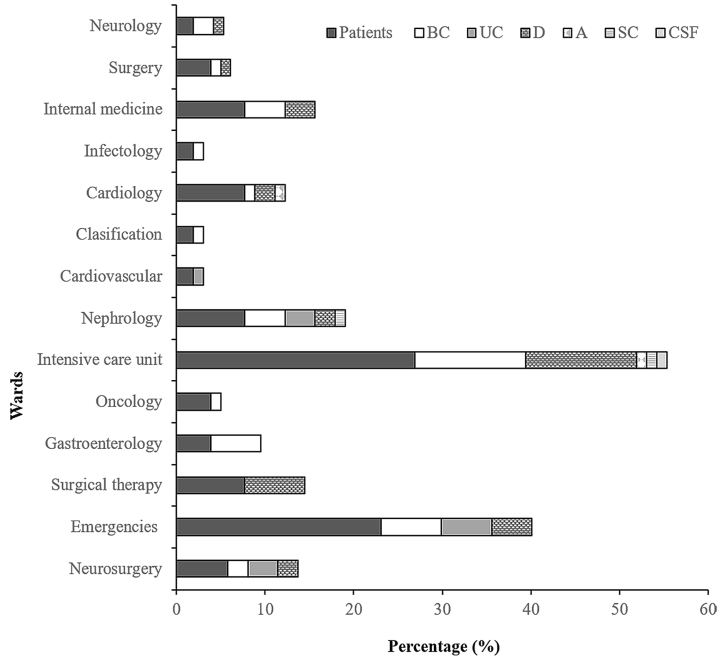

FIGURE 1 | Frequency of isolation of the *Acinetobacter baumannii*, *Acinetobacter pittii*, and *Acinetobacter nosocomialis* strains. Percentage of patients from wards in which at least one of the strains was isolated in the period of study. BC, blood cultures; D, different samples; UC, urine cultures; SC, stool culture; A, autopsy; and CSF, cerebrospinal fluid.

related to HAIs in 2017. The 13.63% (12/88) of strains were associated with primary bacteremia, 3.4% (3/88) with secondary bacteremia, and 2.3% (2/88) with pneumonia. The aforementioned infections were caused by identified strains such as *A. baumannii*, with the exception of one strain of *A. nosocomialis* (182BC) that was associated with primary bacteremia. Unlike these years in 2016, no HAIs were associated with *Acinetobacter* species.

The *A. baumannii* and *A. pittii* Strains Were Multidrug Resistant

The resistance profile was as follows: 97.73% (86/88) to a penicillin (piperacillin), 50% (44/88) to β-lactam combination agents (ampicillin-sulbactam), 35.23% (31/88) to β-lactam combination agents (piperacillin-tazobactam), 87.5% (77/88) to a third-generation cephem (ceftriaxone), 42.05% (37/88) to a fourth-generation cephem (cefepime), 38.64% (34/88) to a carbapenem (imipenem), 14.77% (13/88) to aminoglycosides (gentamicin), 40.91% (36/88) to fluoroquinolone (ciprofloxacin), 26.14% (23/88) to folate pathway antagonists (SXT), and 31.82% (28/88) to a glycylcycline (tigecycline; **Figure 2**). All strains were susceptible to colistin.

Additionally, 44.32% (39/88) of the strains showed a MDR resistance profile. The MDR profile distribution according to species was as follows: 94.87% (37/39) for *A. baumannii* and 5.13% (2/39) for *A. pittii* strains (**Figure 3**; **Supplementary Table 1**). Interestingly, the number of resistant strains for imipenem and tigecycline increased ($p < 0.05$) during 2017 (**Supplementary Table 2**). This is in contrast to folate pathway antagonists, for decreases in the number of resistant strains were observed ($p < 0.05$). On the other hand, 11.36% (10/88) of strains showed an XDR profile. Interestingly, all strains with this profile were identified as *A. baumannii* (**Figure 3**; **Supplementary Table 1**).

The $bla_{\text{OXA-23}}$ Gene Was Amplified in the *A. baumannii* and *A. pittii* Strains

The presence of $bla_{\text{OXA-LIKE}}$ genes related to carbapenem resistance was determined by PCR. All strains amplified the $bla_{\text{OXA-51}}$ gene, 51.13% (45/88) the $bla_{\text{OXA-23}}$ gene, 4.54% (4/88) the $bla_{\text{OXA-24}}$ gene, and 2.27% (2/88) the $bla_{\text{OXA-58}}$ gene (**Figure 3**). Interestingly, the $bla_{\text{OXA-23}}$ gene was amplified in two species (*A. pittii* and *A. baumannii*). The $bla_{\text{OXA-24}}$ and $bla_{\text{OXA-58}}$ genes were amplified only *A. baumannii* strains (**Figure 3**; **Supplementary Table 1**).

One to Six Plasmids Were Identified in *A. baumannii*, *A. pittii*, and *A. nosocomialis* Strains

The plasmid profiles obtained through the Eckardt method showed that the strains had from one to six plasmids with sizes between 2.4 and 121 kb. The results were the following: 37.5% (33/88) of the strains presented two plasmids, 34.09% (30/88) presented three plasmids, and only one of the strains presented six plasmids; however, in 7.95% (7/88) of the strains, these mobile elements were not detected (**Figure 3**; **Supplementary Table 1**). Briefly, *A. baumannii* strains carried one to six plasmids, *A. pittii* strains carried two or three plasmids, and *A. nosocomialis* carried one or three plasmids. No correlation was found between the resistance profile and the plasmid number; however, the largest number of MDR strains harbored between two or three plasmids.

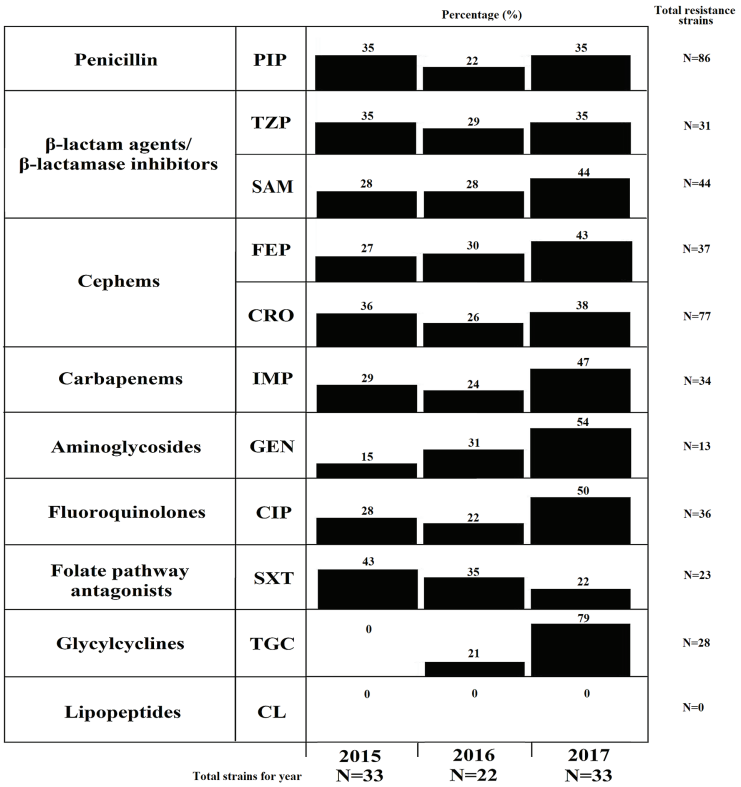

FIGURE 2 | Resistance profiles of the *A. baumannii*, *A. pittii*, and *A. nosocomialis* strains. Percentages of strains resistant to at least one antibiotic in the following groups: penicillins (piperacillin), β-lactam agents/beta-lactamase inhibitors (ampicillin-sulbactam and piperacillin-tazobactam), third- and fourth-generation cephalosporins (cefepime and ceftriaxone), carbapenems (imipenem), aminoglycosides (gentamicin), fluoroquinolones (ciprofloxacin), folates (trimethoprim/sulfamethoxazole), glycylcyclines (tigecycline), and lipopeptides (colistin). PIP, piperacillin; TZP, piperacillin/tazobactam; SAM, ampicillin-sulbactam; FEP, cefepime; CRO, ceftriaxone; IMP, imipenem; GEN, gentamicin; CIP, ciprofloxacin; SXT, trimethoprim/sulfamethoxazole; TGC, tigecycline; and CL, colistin.

The *A. baumannii* Strains Were Genetically Diverse in Comparison to *A. pittii*, *A. nosocomialis*

Macrorestriction patterns obtained by PFGE showed between 16 and 23 fragments with sizes of 48–339 kb. For construction of a dendrogram, a sensitive strain (434S), and the ATCC®19606 strain were included. In agreement with the macrorestriction pattern, the strains were distributed in 52 pulsotypes, and 24 showed were closely related with a correlation coefficient of 1.0 (**Figure 3**). Most of the strains maintained a correlation between the number of plasmids obtained by the Eckard technique and its pulsotype.

Strains recovered from the same patient were grouped into pulsotypes 6, 7, 10, 12, 19, 25, 37, 49, and 51 (**Figure 3**). The isolation period of these strains in the same patient was a maximum of 5 days according to PFGE and other determinants analyzed (resistance profile, $bla_{\text{oxa-like}}$ genes, plasmid number, ST, and CRISPR-Cas system) in this study, suggesting the presence of the same strain.

Interestingly, 12 pulsotypes (2, 11, 17, 21, 22, 31, 33, 34, 38, 46, 47, and 48) harbored strains with an identical macrorestriction pattern, which were isolated from at least two different patients with a minimum difference of 1 month between each strain. However, some changes were observed between these strains, mainly in profile resistance and $bla_{\text{oxa-like}}$ gene amplification.

Notably, some of the strains grouped in the same pulsotypes were isolated from different patients and/or wards and in some cases from samples from different years, such as, pulsotypes 17, 21, 31, and 45, suggesting the persistence of more than one clone in the hospital environment (**Figure 3**).

A. pittii strains were clustered into pulsotypes 1, 6, 35, and 49; while *A. nosocomialis* strains were clustered into pulsotypes 10, 13, and 14. Interestingly, all *A. nosocomialis* strains were closely related to *A. baumannii* strains. In addition, pulsotypes 2, 14, 15, 16, 18, 25, 31, 33, 34, 36, 46, 48, 50, and 51 harbored the strains related with HAIs (**Figure 3**; **Supplementary Table 1**).

ST 156 Was Widely Distributed in the *A. baumannii* Strains

MLST results from *Acinetobacter* strains showed 27 STs, of which the most prevalent was ST 156, at 27.27% (24/88), followed by ST 132, 7.95% (7/88); STs 1296 and 282, 5.68% (5/88); STs 2, 1285, and 1314, 4.54% (4/88); STs 338, 462, 667, and 1166, 3.41% (3/88); STs 20, 206, 398, 1072, 1094, 1312, and 1328, 2.27% (2/88); and STs 163, 744, 870, 907, 1256, 1264, 1277, 1281, and 1468, 1.14% (1/88).

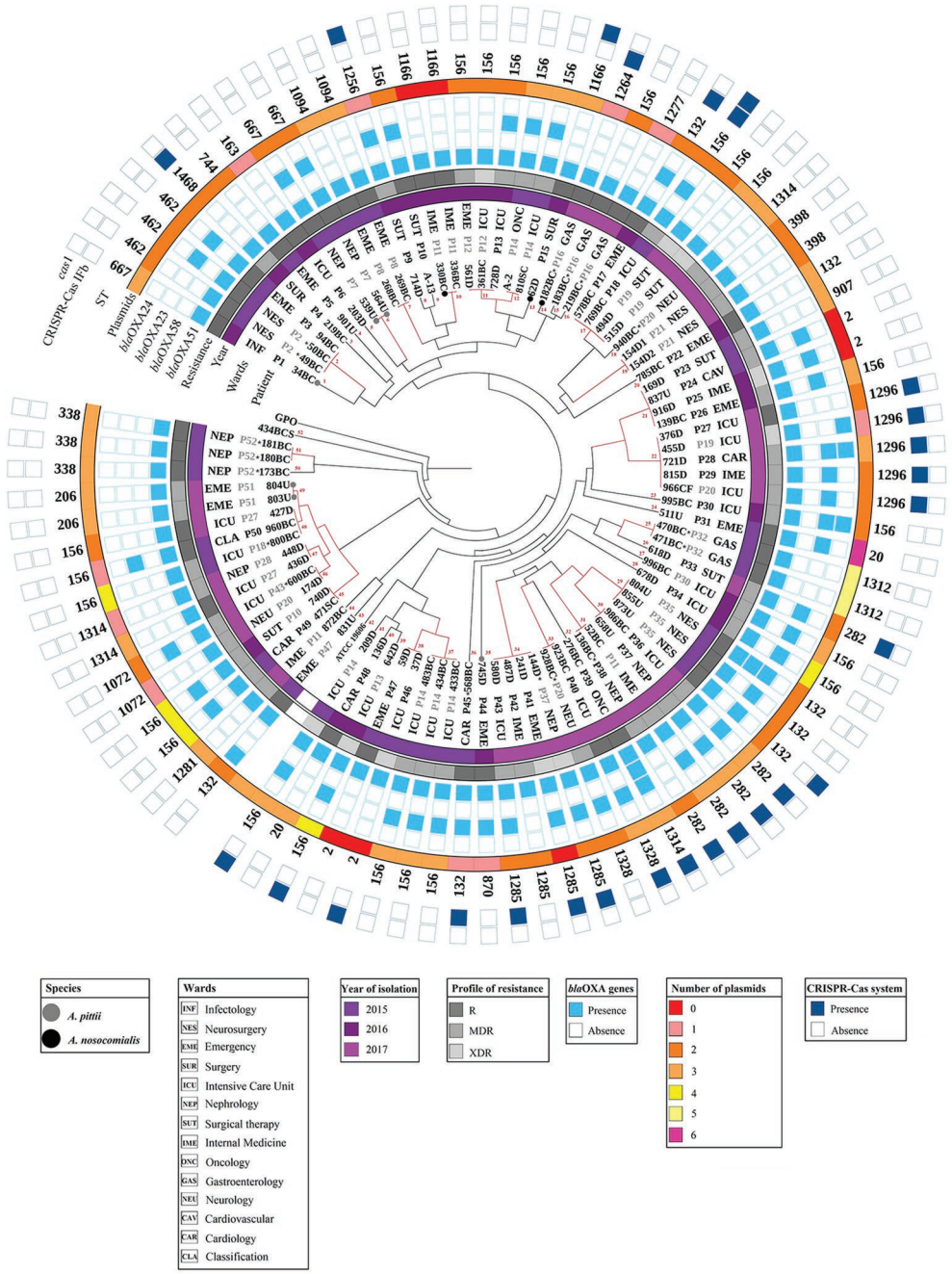

FIGURE 3 | Dendrogram profile of the *A. baumannii*, *A. pittii*, and *A. nosocomialis* complex strains. Dendrogram profile displaying the genetic relatedness among the 88 strains based on the pulsed-field gel electrophoresis (PFGE) pattern. The red line represents the strains with the same pulsotype. The species other than *A. baumannii* are shown with circles in gray (*A. pittii*) and black (*A. nosocomialis*). Internal data represent strain with the origin of isolation, followed by the patient and the ward of origin for each strain. The asterisk symbol shows the strains associated with HAIs (bacteremia and pneumonia). The first band represents the year of isolation, and the second represents the profile of resistance: Resistant (R), multidrug-resistant (MDR), and extensively drug-resistant (XDR). The strains with a R profile showed resistance to PIP, SAM, or TZP. The detection of *blaoxa* genes is represented by clear blue clear squares and the amplification of the CRISPR-Cas system with dark blue squares. The number of plasmids associated with each strain is shown in the third band. The type sequences (ST) for each strain were added. The color codes for each analyzed characteristic are shown in the legends below the figure. The visualization was performed with the iTol program (Letunic and Bork, 2007).

The relationships between the STs obtained in this study were analyzed through eBURST, which found that they belong to 12 clonal complexes (CC20, CC64, CC79, CC132, CC163, CC214, CC462, CC629, CC782, CC1094, CC1264, and CC2), and the last clonal complex (CC2) harbored most of the STs (**Figure 3**; **Supplementary Table 1**). The results obtained with

MLST remained correlated with the data generated data through the other typing tools used in this study. The strains that presented the same plasmid, pulsotype, and resistance profiles also showed the same STs. Two inconsistencies were found between the PFGE and MLST results; more than one ST in the strains grouped into 17 and 21 pulsotypes, suggesting the presence of different strains in the same pulsotype.

In relation to the *A. pittii* strains, three STs (206, 667, and 870) were identified and regarding the *A. nosocomialis* strains, two STs (1166 and 1264) were identified (**Figure 3**; **Supplementary Table 1**). Interestingly, ST 1166 identified in *A. nosocomialis* (strains 330BC and 62D) has been described for *A. baumannii*, and according to the pulsotypes, these strains showed a macrorestriction pattern related to *A. baumannii* strains (pulsotypes 10 and 13). *A. nosocomialis* ST 1264 was associated with CC1264, while in *A. pittii*, only ST 667 was found in CC21; the other ST has not been associated with a CC.

Strains associated with HAIs showed STs 132, 462, 1312, 156, 338, 282, 1264, 1277, 1285, 1072, 1314, and 1328 (**Figure 3**; **Supplementary Table 1**)[4].

CRISPR-Cas I-Fb Systems Were Identified in the *A. baumannii*, and *A. nosocomialis* Strains

The CRISPR-Cas I-Fb system was amplified in 22.73% (20/88) of the *A. baumannii* and *A. nosocomialis* strains; however, the other CRISPR-AYE system was not amplified (**Figure 3**; **Supplementary Table 1**). The *cas1* gene was identified in 7.95% (7/88) of the strains.

The CRISPR-Cas I-Fb system was identified based on the sizes of the amplified PCR products, which was determined through sequencing spacers and repeated sequences. The sizes of the amplified sequences were approximately 700 bp (data not shown). Thereafter, they were sequenced, and when the bioinformatics search was carried out on the CRISPR server, it was found that the CRISPR-Cas I-Fb system sequences had 10 spacers with identical sequences to the nucleotide sequences of the strains in which they were performed[5].

DISCUSSION

A. baumannii is an opportunistic pathogen that is associated with severe infections worldwide and is related to the different attributes that allow it to emerge as a nosocomial microorganism, i.e., mainly resistance to antibiotics and its ability to persist in hospital environments due to its ability to resist drying (Antunes et al., 2014; Harding et al., 2017).

The genus *Acinetobacter* have six species with very similar phenotypes they and have been grouped into the *Acb* complex. Of this complex, *A. pittii*, *A. nosocomialis* and *A. baumannii* are the species associated with a greater number of infections and mortality; in addition, the isolation frequency of *A. pittii* and *A. nosocomialis* strains as etiological agents of HAIs is high (Wisplinghoff et al., 2012). The mortality rates of *A. pittii* are greater than those of *A. nosocomialis* but lower than those of *A. baumannii*, suggesting that a future *A. pittii* strain could also emerge as an important nosocomial pathogen (Yang et al., 2012). For this reason, the molecular typing of the *Acb* complex using different techniques is essential to generate information about the epidemiology of this complex and to learn more about the distribution of these species in hospital environments. The differentiation of *Acb* complex strains was carried out through MALDI-TOF MS in this study. This method allowed for the identification of the *A. baumannii* strains and differentiation between the species that belong to the *Acb* complex (Lin et al., 2008); three species were identified in this study: *A. baumannii*, *A. pittii*, and *A. nosocomialis*.

The ward with the highest recurrence of *A. baumannii* was the ICU, which corresponded to the data from other regions such as Europe, Asia, the United States, Latin America, and Morocco (Martins et al., 2009; Vincent et al., 2009; Uwingabiye et al., 2017). The high recurrence of isolating *A. baumannii* in the ICU has been attributed to risk factors for the development of infections, including invasive procedures, catheter placement, and intubation endotracheal, which may cause urinary tract and respiratory tract infections (Cisneros et al., 1996; Lynch et al., 2017). However, the development of *A. baumannii* infections is also related to the immune systems of patients since it has been observed in individuals with serious diseases such as hematological malignancies and diabetes mellitus, and even those subjected to prolonged antimicrobial therapy with broad-spectrum antibiotics (Vincent et al., 2009; Kempf and Rolain, 2012; Lin et al., 2016). *A. pittii* and *A. nosocomialis* strains were identified in patients at the HIMFG, but none of these strains were isolated from the ICU ward. The resistance percentage found in this study was low compared with those in other studies (Alcántar-Curiel et al., 2014, 2019; Xie et al., 2018).

The low resistance percentages could be associated with the source of strains from pediatric patients; however, an increase in the number of imipenem-resistant strains was found in 2017. The frequency of MDR strains in this study was high (44.32%), and this phenotype was identified in *A. baumannii*, and *A. pittii* strains. This MDR profile contrasted with the XDR profile, as only *A. baumannii* strains had this phenotype, and resistance has been associated with high epidemic potential and high mortality (Song et al., 2011; Lee et al., 2014). The main mechanism of *A. baumannii* resistance to β-lactams is enzymatic degradation by β-lactamases; oxacillinases (OXAs) give it the ability to hydrolyze oxacillin (Evans and Amyes, 2014). In this study, the $bla_{\text{OXA-51}}$ gene, in addition to the $bla_{\text{OXA-23}}$, $bla_{\text{OXA-24}}$ and $bla_{\text{OXA-58}}$ genes (identified more frequently in *A. baumannii*), were identified by PCR. All of the strains amplified the $bla_{\text{OXA-51}}$ gene, which has been reported to be intrinsic in *A. baumannii*, with $bla_{\text{OXA-69}}$ (Brown et al., 2005). The chromosomal location and the detection of these genes allow for identification at the species level (Turton et al., 2006).

Strains with an amplified $bla_{\text{OXA-23}}$ gene formed the first group identified in *A. baumannii*, and the production of this enzyme is sufficient to confer resistance to carbapenems. This group is mostly distributed and has been detected in clinical strains in

[4]https://github.com/JetsiMancilla/MLST-A.baumannii
[5]https://github.com/JetsiMancilla/CRISPR-Cas-System

Brazil, Belgium, Singapore, and France, where have been related to outbreaks. In addition, the presence of the $bla_{\text{OXA-23}}$ gene is limited to not only clinical strains but also environmental isolates, suggesting that the propagation of these genes occurs in different environments and under different selective pressures (Girlich et al., 2010). Moreover, 27% of the strains (*A. pittii* and *A. baumannii*) that amplified the $bla_{\text{OXA-23}}$ gene showed resistance to imipenem, which have been reported in Latin America and Mexico. Other determinants of resistance have been associated with these species, such as the $bla_{\text{OXA-58}}$ gene and metallo-β-lactamases, which are predominantly responsible for carbapenems resistance in *A. nosocomialis* and *A. pittii*; however, $bla_{\text{OXA-23}}$ and $bla_{\text{OXA-24}}$ have recently become more common in carbapenems resistance for both species (Yang et al., 2012; Cayô et al., 2014; Silva et al., 2018).

Most of the elements that encode for resistance can be found in mobile elements, such as plasmids. The determination of plasmid profiles has been used for comparisons of strains, since these can be found in identical numbers, sizes, and molecular weights in bacteria with different isolation origins. Our results agreed with other studies in which the authors included the characterization of 132 clinical strains of *A. baumannii* harboring of 1 to 7 plasmids (Singh et al., 2006). Furthermore, the strains that presented the same pulsotype, and ST had identical numbers of plasmids and molecular weights, with the exception of pulsotypes 17, 22, and 34, which showed the same type sequence and pulsotype but different in resistance profiles, $bla_{\text{OXA-LIKE}}$ genes, and plasmid profiles. The plasmid profile has been used as a complementary typing method to others such as PFGE; in this study, we observed congruence between the results obtained through each one; however, one of the limitations of this method is the use of mobile elements to carry out the typing of strains. Nevertheless, it provides a general overview of whether the strains can be carriers of mobile elements, from which their roles can be determined as mechanisms underlying the transfer of virulence and resistance determinants based on their sequencing.

Due to its high reproducibility, one of the most commonly used tools in the typing of clinical strains is PFGE. According to Tenover et al. (1995), when isolates do not differ in band pattern, they are considered indistinguishable, and therefore, the strains can be related. We found that 24 pulsotypes presented identical macrorestriction patterns; some strains were recovered from the same patient, but the others were isolated from different patients. The results of PFGE were consistent with the plasmid profiles, but when the advantages and disadvantages of these methods were compared, PFGE is clearly a technique that can be time consuming, laborious and expensive with respect to the profiling of plasmids; however, the results by PFGE were more accurate in terms of the typing of the strains, its reproducibility is high, and we can also obtain information regarding genetic diversity and clonal relationships.

Another one of the most common tools for typing *A. baumannii* strains is MLST, which is based on sequencing the variable regions of seven genes. For *A. baumannii*, two protocols based on different constitutive genes have been proposed, with some discrepancies (Tomaschek et al., 2016; Gaiarsa et al., 2019). Among the disadvantages that have been reported when using this method is the consideration of only seven constitutive genes of the total chromosomal information of *A. baumannii* strains, a bacterium with high genetic variation and would be disadvantageous to consider only a portion of the total information (Wang et al., 2013; Feng et al., 2016; Castillo-Ramírez and Graña-Miraglia, 2019). In this study, the strains were analyzed using the modified Pasteur protocol because in the case of the Oxford scheme, complications have been reported in the amplification of genes such as *gdhB* and *gpi* (Hamouda et al., 2010; Hamidian et al., 2017; Gaiarsa et al., 2019). The nucleotide sequences for the determination of STs were obtained through massive sequencing using next-generation platforms. However, under the Pasteur protocol, it was difficult to amplify and sequence the *fusA* gene; therefore, we designed other primers that allowed us to sequence this gene.

The most prevalent STs were STs 156, 132, 1296, 2, 282, 1285, and 1314. Interestingly, ST 156 belongs to the CC79 complex, which has been associated with outbreaks in several countries (Mexico, Canada, Honduras, Colombia, and even in Europe) and is epidemiologically important in Mexico (Loewen et al., 2014; Kubo et al., 2015; López-Leal et al., 2019). ST 156 strains are producers of carbapenemases ($bla_{\text{OXA-23}}$) and recently included was the new variant OXA-239 (Tamayo-Legorreta et al., 2014; Graña-Miraglia et al., 2017; Mancilla-Rojano et al., 2019). According to our results, there is an association between ST 156 and $bla_{\text{OXA-23}}$ gene amplification and between MDR and XDR profiles. Interestingly, ST 156 was identified during all 3 years of this study, which indicates that this lineage has been maintained and distributed within the hospital. However, other STs were associated with strains of a specific year. These data suggest that there is more than one strain distributed simultaneously within the HIMFG. STs 132 and particularly ST 2 the most common clone globally, are distributed in Europe, Asia, and Latin America, associated with outbreaks and resistance to carbapenems due to the presence of the $bla_{\text{OXA-66}}$ and $bla_{\text{OXA-120}}$ genes (Bakour et al., 2014; Dahdouh et al., 2017; Nowak et al., 2017; Levy-Blitchtein et al., 2018; Villalón et al., 2019). Conversely, we report a strain associated with ST 1468 that has recently been entered into the MLST *A. baumannii* database.

This technique has been used to distinguish the species of the *Acb* complex and designed to study the population of various bacteria, showing the presence of different clonal lineages, which could, for example, be associated with different species of the *Acb* complex (Bartual et al., 2005; Yamada et al., 2016). This finding agrees with our results, since the STs obtained for *A. pittii* were described in the MLST database for this species. Interestingly, the STs identified for *A. pittii* and *A. nosocomialis* are associated with different clonal complexes from those associated with *A. baumannii*. The MLST protocol is expensive and time consuming, and the analysis of the data can be slow; however, it should be noted that it allows the typing of strains and the differentiation of some species of the *Acb* complex (such as *A. pittii*). Similarly, the comparison with strains in other parts of the world enabled us to recognize the STs and clonal complexes associated with this hospital, determining that ST 156 is a clone that persists in the HIMFG.

The PFGE results were consistent with the MLST results, the strains with the same pulsotype presented the same ST, and except for the strains with pulsotypes 17 and 21, which were related despite being associated with different patients and years. The pulsotypes 17 and 21were grouped with the same restriction patterns; nevertheless, we could observe that they differed with respect to their resistance profile, plasmid profile, and amplification of bla_{OXA} genes. However, the determination of different STs allows us to suggest that these pulsotypes group different strains; the opposite occurred in some of the strains that were isolated from different patients, since there were cases in which, according to the agreement of the data obtained by PFGE, the same patient could harbor different pulsotypes; nevertheless, they could present the same ST (P14, and P30).

Recently, the polymorphism observed between CRISPR-Cas systems has been used to genotype strains and establish phylogenetic relationships in different bacterial species; although, in some cases the spacers can be too diverse, hindering their use as a method for subtyping. On the other hand, the CRISPR-Cas system has been implemented as a successful typing method in species such as *Salmonella enterica* and *Yersinia pestis* (Cui et al., 2008; Shariat et al., 2015). The use of this system has also separated other bacteria such as *Erwinia amylovora* into different groups depending on their geographical origin (Rezzonico et al., 2011). Two systems have been described in *A. baumannii*: CRISPR-AYE and CRISPR-Cas subtype I-Fb (Hauck et al., 2012; Karah et al., 2015). In this study, the CRISPR-Cas subtype I-Fb system was identified in only 20 strains. Despite the amplification of the CRISPR-AYE system with primers reported previously by Karah et al. (2015), when the PCR products were sequenced, the nucleotide analyses did not show any homology with the CRISPR-Cas systems.

Despite the successful implementation of the CRISPR-Cas system as a typing method in other studies, we were unable to use it because not all of the strains had this system; however, two phenomena were observed. The first was that some strains that amplified the CRISPR-Cas I-Fb system had been grouped in the same pulsotypes and possessed the same STs. The second was that some strains had the same pulsotype but differed in STs or CRISPR-Cas system; interestingly, they provide us with information on the diversity within each of the subgroups obtained by PFGE and MLST. There was no ST that was specifically associated with some type of these systems, but interestingly, the CRISPR-Cas I-Fb system was identified with more frequency in strains recovered during 2017.

On the other hand, approximately 70% (14/20) of the strains with a CRISPR-Cas I-Fb system presented MDR and XDR profiles, which has not been observed in other studies since there is no correlation between the previous profiles (Hauck et al., 2012). Amazingly, we found that the strains that amplify the CRISPR-Cas I-Fb system presented from 1 to 4 plasmids. According to Mangas et al. (2019), there is an association between the presence of the CRISPR-Cas system and the absence of plasmids in *A. baumannii* genomes; as we could see in our results; these systems would limit the transfer of mobile elements such as plasmids.

In addition, the gene encoding the Cas1 protein of the CRISPR-Cas system was also identified only in seven strains. The gene encoding the Cas1 protein is one of the most conserved and is involved in the acquisition of spacers and it has been proposed that the gene evolves slower than other *cas* genes (Takeuchi et al., 2012; Makarova and Koonin, 2015). The strains that amplified this gene did not amplify any CRISPR-Cas system, so we could suggest the presence of another system different from those sought in this study. In contrast, 26 strains amplified at least one system but not the *cas* gene. For *Enterococcus faecium* strains, the *cas1* gene has not been identified with CRISPR-Cas IIA systems, suggesting that these systems have lost their ability to acquire different spacers (van Schaik and Willems, 2010; Lyons et al., 2015), which could also have occurred in our strains. However, it is necessary to carry out other studies to demonstrate this hypothesis.

The amplified spacers were larger in the CRISPR-Cas I-Fb system. Strains that had more spacers in their CRISPR systems have been related to evolution in the environment (Hauck et al., 2012). The detection of these systems through PCR and amplification sequencing seems to be simple; however, something that must be highlighted is the probable implication of these systems in other processes. CRISPR-Cas systems in *E. coli* are related to the repair of DNA damage (Babu et al., 2011); this would be relevant in *A. baumannii*, since microorganisms are subjected to a series of environmental agents or possess resistance to desiccation. An important contribution of our work is the identification of the CRISPR-Cas system in clinical strains.

In the case of patients, there were two interesting conditions. First, in patients (14, 20, 27, 28, 37, 43, and 47), more than one strain was isolated, some with differences of days or 1 month. These strains were all different, locating themselves into different pulsotypes, STs, and with differences in the rest of the characteristics evaluated, suggesting the presence of different strains in the same patient over a short temporality. In the second case, was observed that patients (11, 16, and 19) had more than one strain; however, they were divided into two groups in the same patient that were identical, and that were not same in the characteristics evaluated, suggesting once again the presence of more than one strain over a longer period. In 11 patients, the strains were obtained on the same date but corresponded to different samples, presenting cases, in which the strains showed the same characteristics with respect to the pulsotype, $bla_{OXA\text{-}LIKE}$ genes, plasmid profile, and type sequence. Nevertheless, five patients (P16, P18, P27, P30, and P47) provided samples on the same date but with phenotypic and genotypic characteristics that were completely different. Also, there were cases presented in which the samples obtained more than 1 day apart exhibited the same characteristics.

Only 17 strains were associated with HAIs, such as bacteremia and pneumonia. According to the results, the patients: 2 (49BC and 50BC), 32 (470BC and 471BC), and 52 (173BC, 180BC, and 181BC) related with bacteremia, had more than one strain. The strains were distributed along the tree and only clustered when they were from the same patient such as pulsotypes 2 and 25, for which all of the phenotypic and genotypic characteristics were identical, with the exception of strain 173BC recovered from the patient 52, the only difference that had with the other two strains (189BC and 181BC) isolated of this patient was his

macrorestriction pattern. Patients 18 (800BC) and 38 (136BC) developed bacteremia; while, patients 37 (144D), 43 (600BC), and 45 (568BC) developed pneumonia, the strains were randomly distributed in different pulsotypes, but apparently there was no related between them. Finally, patients 16 (182BC, 183BC, and 219BC) and 20 (928BC and 940BC) with bacteremia were all different from each other. Interestingly, these features were observed for strains identified as *A. baumannii*, with the exception of one strain of *A. nosocomialis* that was associated with a primary bacteremia. The latter was isolated together with two strains of *A. baumannii* from the same patient (P16) on the same date; however, they presented different genetic characteristics, which suggest that more than one different strain could be causing an infection in the patient. These strains were collected from a total of 10 patients and are genetically diverse since they presented different plasmid profiles, type sequences, and pulsotypes.

According to the results obtained in this study, an increase was identified an increase in the number of resistant carbapenems strains. The molecular typing methods allowed us to determine the relationships between clinical strains. PFGE data demonstrated that different patients could be infected by the same strain (identical pulsotypes were harbored by more than one patient). MLST showed that the strains in one group, i.e., pulsotypes 17 and 21, showed different STs and thus were not the same strain. ST 156 is a persistent clone at HIMFG. Finally, the CRISPR-Cas system identified in a low percentage of these strains could be associated with the nosocomial environment. The severity of the disease and the difference between strains that are closely related to those associated with HAIs shown in this study, were related to the immunocompromise patient and virulence factors of the strain, which were not determined in this study and will be examined in a future study. The clinical importance of *A. baumannii* in ICUs isolated from BCs has been well documented. *A. baumannii* infections (i.e., nosocomial pneumonia) tend to be more serious than those caused by *A. nosocomialis* and *A. pittii* (Lee et al., 2013). Therefore, it is necessary to identify and differentiate the species in the *Acb* complex to determine their epidemiological and clinical importance. The implementation of molecular epidemiology allows the characterization of a set of strains and identification of different attributes associated with their distribution in a specific environment. This study will allow future interventions for the recognition of risk factors related to opportunistic pathogens such as *A. baumannii*.

DATA AVAILABILITY STATEMENT

The datasets presented in this study can be found in online repositories. The names of the repository/repositories and accession number(s) can be found in the article/**Supplementary Material**.

ETHICS STATEMENT

The Research Committee (Dr. Juan Garduño Espinosa), Ethics Committee (Dr. Luis Jasso Gutiérrez), and Biosecurity Committee (Dr. Marcela Salazar García) of the HIMFG granted approval for the development of the protocol HIM/2017/003 SSA.1299, HIM/2018/038 SSA.1513. The strains were provided by the Central Laboratory of the HIMFG, with prior informed consent of the patients to obtain the samples. Written informed consent was not required for this study according to the institutional ethical, biosecurity and investigation committees because the Central Laboratory from the HIMFG provided the *A. baumannii* clinical strain isolates from the child included in this study.

AUTHOR CONTRIBUTIONS

AC-C had the initial idea and developed it into a project together with JX-C. JM-R done the experiments. AC-C, JX-C, SO, VF, and JA-G analyzed the data. OM-C performed identification by MALDI-TOF Biotyper. DR-Z reviewed the clinical data. AC-C, JX-C, SO, KE-M, MC, JR-G, JA-G, RH-C, and OM-C contributed reagents and materials. IP-O supplied the *A. baumannii* strains. MC-C carried out susceptibility. AC-C and JX-C wrote the manuscript, read and approved the final version. All authors contributed to the article and approved the submitted version.

FUNDING

JM-R received support from the Consejo Nacional de Ciencia y Tecnología, México, PDCPN 605309. This work was supported by Federal Founds HIM/2017/003 SSA.1299, HIM/2018/038 SSA.1513 at the HIMFG.

ACKNOWLEDGMENTS

The authors acknowledge Gerardo Escalona Venegas and Isabel Franco Hernández for their technical assistance. Miriam Bobadilla del Valle and Francisco Leal Vega for sequencing support. Consejo Nacional de Ciencia y Tecnología, México for SNI EXP. AYTE17734.

SUPPLEMENTARY MATERIAL

The Supplementary Material for this article can be found online at: https://www.frontiersin.org/articles/10.3389/fmicb.2020.576673/full#supplementary-material

REFERENCES

Alcántar-Curiel, M. D., García-Torres, L. F., González-Chávez, M. I., Morfín-Otero, R., Gayosso-Vázquez, C., Jarillo-Quijada, M. D., et al. (2014). Molecular mechanisms associated with nosocomial carbapenem-resistant *Acinetobacter baumannii* in Mexico. *Arch. Med. Res.* 45, 553–560. doi: 10.1016/j.arcmed.2014.10.006

Alcántar-Curiel, M. D., Rosales-Reyes, R., Jarillo-Quijada, M. D., Gayosso-Vázquez, C., Fernández-Vázquez, J. L., Toledano-Tableros, J. E., et al. (2019). Carbapenem-resistant *Acinetobacter baumannii* in three tertiary

care hospitals in Mexico: virulence profiles, innate immune response and clonal dissemination. *Front. Microbiol.* 10:2116. doi: 10.3389/fmicb.2019.02116

Allen, J. M., LaFrance, R., Folk, R. A., Johnson, K. P., and Guralnick, R. P. (2018). aTRAM 2.0: an improved, flexible locus assembler for NGS data. *Evol. Bioinforma.* 14:117693431877454. doi: 10.1177/1176934318774546

Andrews, S. (2010). FastQC: una herramienta de control de calidad para datos de secuencia de alto rendimiento. Available at: http://www.bioinformatics.babraham.ac.uk/projects/fastqc (Accessed April 2, 2020).

Antunes, L. C. S., Visca, P., and Towner, K. J. (2014). *Acinetobacter baumannii*: evolution of a global pathogen. *Pathog. Dis.* 71, 292–301. doi: 10.1111/2049-632X.12125

Babu, M., Beloglazova, N., Flick, R., Graham, C., Skarina, T., Nocek, B., et al. (2011). A dual function of the CRISPR-Cas system in bacterial antivirus immunity and DNA repair. *Mol. Microbiol.* 79, 484–502. doi: 10.1111/j.1365-2958.2010.07465.x

Bakour, S., Alsharapy, S. A., Touati, A., and Rolain, J. M. (2014). Characterization of *Acinetobacter baumannii* clinical isolates carrying blaOXA-23 carbapenemase and 16S rRNA methylase armA genes in Yemen. *Microb. Drug Resist.* 20, 604–609. doi: 10.1089/mdr.2014.0018

Bartual, S. G., Seifert, H., Hippler, C., Luzon, M. A. D., Wisplinghoff, H., and Rodriguez-Valera, F. (2005). Development of a multilocus sequence typing scheme for characterization of clinical isolates of *Acinetobacter baumannii*. *J. Clin. Microbiol.* 43, 4382–4390. doi: 10.1128/JCM.43.9.4382-4390.2005

Bocanegra-Ibarias, P., Peña-López, C., Camacho-Ortiz, A., Llaca-Díaz, J., Silva-Sánchez, J., Barrios, H., et al. (2015). Genetic characterisation of drug resistance and clonal dynamics of *Acinetobacter baumannii* in a hospital setting in Mexico. *Int. J. Antimicrob. Agents* 45, 309–313. doi: 10.1016/j.ijantimicag.2014.10.022

Brown, S., Young, H. K., and Amyes, S. G. B. (2005). Characterisation of OXA-51, a novel class D carbapenemase found in genetically unrelated clinical strains of *Acinetobacter baumannii* from Argentina. *Clin. Microbiol. Infect.* 11, 15–23. doi: 10.1111/j.1469-0691.2004.01016.x

Castillo-Ramírez, S., and Graña-Miraglia, L. (2019). Inaccurate multilocus sequence typing of *Acinetobacter baumannii*. *Emerg. Infect. Dis.* 25, 186–187. doi: 10.3201/eid2501.180374

Cayô, R., Merino, M., Ruiz del Castillo, B., Cano, M. E., Calvo, J., Bou, G., et al. (2014). OXA-207, a novel OXA-24 variant with reduced catalytic efficiency against carbapenems in *Acinetobacter pittii* from Spain. *Antimicrob. Agents Chemother.* 58, 4944–4948. doi: 10.1128/AAC.02633-13

Chen, S., Huang, T., Zhou, Y., Han, Y., Xu, M., and Gu, J. (2017). AfterQC: automatic filtering, trimming, error removing and quality control for fastq data. *BMC Bioinform.* 18:80. doi: 10.1186/s12859-017-1469-3

Cisneros, J. M., Reyes, M. J., Pachon, J., Becerril, B., Caballero, F. J., Garcia-Garmendia, J. L., et al. (1996). Bacteremia due to *Acinetobacter baumannii*: epidemiology, clinical findings, and prognostic features. *Clin. Infect. Dis.* 22, 1026–1032. doi: 10.1093/clinids/22.6.1026

Clinical and Laboratory Standards Institute (CLSI) (2018). *Performance standards for antimicrobial susceptibility testing*. Wayne, Pennsylvania: Clinical and Laboratory Standards Institute.

Cosgaya, C., Marí-Almirall, M., Van Assche, A., Fernández-Orth, D., Mosqueda, N., Telli, M., et al. (2016). *Acinetobacter dijkshoorniae* sp. nov., a member of the *Acinetobacter calcoaceticus-Acinetobacter baumannii* complex mainly recovered from clinical samples in different countries. *Int. J. Syst. Evol. Microbiol.* 66, 4105–4111. doi: 10.1099/ijsem.0.001318

Cui, Y., Li, Y., Gorgé, O., Platonov, M. E., Yan, Y., Guo, Z., et al. (2008). Insight into microevolution of *Yersinia pestis* by clustered regularly interspaced short palindromic repeats. *PLoS One* 3:e2652. doi: 10.1371/journal.pone.0002652

Dahdouh, E., Gómez-Gil, R., Pacho, S., Mingorance, J., Daoud, Z., and Suárez, M. (2017). Clonality, virulence determinants, and profiles of resistance of clinical *Acinetobacter baumannii* isolates obtained from a Spanish hospital. *PLoS One* 12:e0176824. doi: 10.1371/journal.pone.0176824

Dexter, C., Murray, G. L., Paulsen, I. T., and Peleg, A. Y. (2015). Community-acquired *Acinetobacter baumannii*: clinical characteristics, epidemiology and pathogenesis. *Expert Rev. Anti-Infect. Ther.* 13, 567–573. doi: 10.1586/14787210.2015.1025055

Diancourt, L., Passet, V., Nemec, A., Dijkshoorn, L., and Brisse, S. (2010). The population structure of *Acinetobacter baumannii*: expanding multiresistant clones from an ancestral susceptible genetic pool. *PLoS One* 5:e10034. doi: 10.1371/journal.pone.0010034

Eckhardt, T. (1978). A rapid method for the identification of plasmid desoxyribonucleic acid in bacteria. *Plasmid* 1, 584–588. doi: 10.1016/0147-619x(78)90016-1

Evans, B. A., and Amyes, S. G. B. (2014). OXA β-lactamases. *Clin. Microbiol. Rev.* 27, 241–263. doi: 10.1128/CMR.00117-13

Evans, B. A., Hamouda, A., Towner, K. J., and Amyes, S. G. B. (2008). OXA-51-like β-lactamases and their association with particular epidemic lineages of *Acinetobacter baumannii*. *Clin. Microbiol. Infect.* 14, 268–275. doi: 10.1111/j.1469-0691.2007.01919.x

Feng, Y., Ruan, Z., Shu, J., Chen, C. L., and Chiu, C. H. (2016). A glimpse into evolution and dissemination of multidrug-resistant *Acinetobacter baumannii* isolates in East Asia: a comparative genomics study. *Sci. Rep.* 6:24342. doi: 10.1038/srep24342

Fitzpatrick, M. A., Ozer, E. A., and Hauser, A. R. (2016). Utility of whole-genome sequencing in characterizing *Acinetobacter* epidemiology and analyzing hospital outbreaks. *J. Clin. Microbiol.* 54, 593–612. doi: 10.1128/JCM.01818-15

Gaiarsa, S., Batisti Biffignandi, G., Esposito, E. P., Castelli, M., Jolley, K. A., Brisse, S., et al. (2019). Comparative analysis of the two *Acinetobacter baumannii* multilocus sequence typing (MLST) schemes. *Front. Microbiol.* 10:930. doi: 10.3389/fmicb.2019.00930

Gerner-Smidt, P., Tjiernberg, I., and Ursing, J. (1991). Reliability of phenotypic tests for identification of *Acinetobacter* species. *J. Clin. Microbiol.* 29, 277–282. doi: 10.1128/JCM.29.2.277-282.1991

Girlich, D., Poirel, L., and Nordmann, P. (2010). First isolation of the blaOXA-23 carbapenemase gene from an environmental *Acinetobacter baumannii* isolate. *Antimicrob. Agents Chemother.* 54, 578–579. doi: 10.1128/AAC.00861-09

Gonzalez-Villoria, A. M., Tamayo-Legorreta, E., Garza-Ramos, U., Barrios, H., Sanchez-Pérez, A., Rodríguez-Medina, N., et al. (2016). A multicenter study in Mexico finds *Acinetobacter baumannii* clinical isolates belonging to clonal complexes 636B (113B) and 92B harboring OXA-72, OXA-239, and OXA-469. *Antimicrob. Agents Chemother.* 60, 2587–2588. doi: 10.1128/AAC.02042-15

Gouy, M., Guindon, S., and Gascuel, O. (2010). SeaView version 4: a multiplatform graphical user interface for sequence alignment and phylogenetic tree building. *Mol. Biol. Evol.* 27, 221–224. doi: 10.1093/molbev/msp259

Graña-Miraglia, L., Lozano, L. F., Velázquez, C., Volkow-Fernández, P., Pérez-Oseguera, Á., Cevallos, M. A., et al. (2017). Rapid gene turnover as a significant source of genetic variation in a recently seeded population of a healthcare-associated pathogen. *Front. Microbiol.* 8:1817. doi: 10.3389/fmicb.2017.01817

Hamidian, M., Nigro, S. J., and Hall, R. M. (2017). Problems with the oxford multilocus sequence typing scheme for *Acinetobacter baumannii*: do sequence type 92 (ST92) and ST109 exist? *J. Clin. Microbiol.* 55, 2287–2289. doi: 10.1128/JCM.00533-17

Hamouda, A., Evans, B. A., Towner, K. J., and Amyes, S. G. B. (2010). Characterization of epidemiologically unrelated *Acinetobacter baumannii* isolates from four continents by use of multilocus sequence typing, pulsed-field gel electrophoresis, and sequence-based typing of blaOXA-51-like genes. *J. Clin. Microbiol.* 48, 2476–2483. doi: 10.1128/JCM.02431-09

Harding, C. M., Hennon, S. W., and Feldman, M. F. (2017). Uncovering the mechanisms of *Acinetobacter baumannii* virulence. *Nat. Rev. Microbiol.* 16, 91–102. doi: 10.1038/nrmicro.2017.148

Hauck, Y., Soler, C., Jault, P., Mérens, A., Gérome, P., Nab, C. M., et al. (2012). Diversity of *Acinetobacter baumannii* in four French military hospitals, as assessed by multiple locus variable number of tandem repeats analysis. *PLoS One* 7:e44597. doi: 10.1371/journal.pone.0044597

Higgins, P. G., Dammhayn, C., Hackel, M., and Seifert, H. (2010). Global spread of carbapenem-resistant *Acinetobacter baumannii*. *J. Antimicrob. Chemother.* 65, 233–238. doi: 10.1093/jac/dkp428

Hujer, K. M., Hujer, A. M., Hulten, E. A., Bajaksouzian, S., Adams, J. M., Donskey, C. J., et al. (2006). Analysis of antibiotic resistance genes in multidrug-resistant *Acinetobacter* sp. isolates from military and civilian patients treated at the Walter reed Army medical Center. *Antimicrob. Agents Chemother.* 50, 4114–4123. doi: 10.1128/AAC.00778-06

Karah, N., Samuelsen, Ø., Zarrilli, R., Sahl, J. W., Wai, S. N., and Uhlin, B. E. (2015). CRISPR-cas subtype I-Fb in *Acinetobacter baumannii*: evolution and utilization for strain subtyping. *PLoS One* 10:e0118205. doi: 10.1371/journal.pone.0118205

Kempf, M., and Rolain, J. M. (2012). Emergence of resistance to carbapenems in *Acinetobacter baumannii* in Europe: clinical impact and therapeutic options. *Int. J. Antimicrob. Agents* 39, 105–114. doi: 10.1016/j.ijantimicag.2011.10.004

Kubo, Y., Komatsu, M., Tanimoto, E., Sugimoto, K., Tanaka, S., Migita, S., et al. (2015). Spread of OXA-23-producing *Acinetobacter baumannii* ST2

and ST246 in a hospital in Japan. *J. Med. Microbiol.* 64, 739–744. doi: 10.1099/jmm.0.000077

Lee, H. Y., Chen, C. L., Wu, S. R., Huang, C. W., and Chiu, C. H. (2014). Risk factors and outcome analysis of *Acinetobacter baumannii* complex bacteremia in critical patients. *Crit. Care Med.* 42, 1081–1088. doi: 10.1097/CCM.0000000000000125

Lee, Y. T., Kuo, S. C., Yang, S. P., Lin, Y. T., Chiang, D. H., Tseng, F. C., et al. (2013). Bacteremic nosocomial pneumonia caused by *Acinetobacter baumannii* and *Acinetobacter nosocomialis*: a single or two distinct clinical entities? *Clin. Microbiol. Infect.* 19, 640–645. doi: 10.1111/j.1469-0691.2012.03988.x

Letunic, I., and Bork, P. (2007). Interactive tree of life (iTOL): an online tool for phylogenetic tree display and annotation. *Bioinformatics* 23, 127–128. doi: 10.1093/bioinformatics/btl529

Levy-Blitchtein, S., Roca, I., Plasencia-Rebata, S., Vicente-Taboada, W., Velásquez-Pomar, J., Muñoz, L., et al. (2018). Emergence and spread of carbapenem-resistant *Acinetobacter baumannii* international clones II and III in Lima, Peru. *Emerg. Microbes Infect.* 7:119. doi: 10.1038/s41426-018-0127-9

Li, H., and Durbin, R. (2009). Fast and accurate short read alignment with burrows-wheeler transform. *Bioinformatics* 25, 1754–1760. doi: 10.1093/bioinformatics/btp324

Li, H., Handsaker, B., Wysoker, A., Fennell, T., Ruan, J., Homer, N., et al. (2009). The sequence alignment/map format and SAMtools. *Bioinformatics* 25, 2078–2079. doi: 10.1093/bioinformatics/btp352

Limansky, A. S., Zamboni, M. I., Guardati, M. C., Rossignol, G., Campos, E., and Viale, A. M. (2004). Evaluation of phenotypic and genotypic markers for clinical strains of *Acinetobacter baumannii*. *Medicina* 64, 306–312.

Lin, C. Y., Chen, Y. M., Lin, M. C., Chang, Y. P., Chao, T. Y., Wang, C. C., et al. (2016). Risk factors of multidrug-resistant *Acinetobacter baumannii* recurrence after successful eradication in ventilated patients. *Biom. J.* 39, 130–138. doi: 10.1016/j.bj.2015.07.001

Lin, Y. C., Sheng, W. H., Chang, S. C., Wang, J. T., Chen, Y. C., Wu, R. J., et al. (2008). Application of a microsphere-based array for rapid identification of *Acinetobacter* spp. with distinct antimicrobial susceptibilities. *J. Clin. Microbiol.* 46, 612–617. doi: 10.1128/JCM.01798-07

Loewen, P. C., Alsaadi, Y., Fernando, D., and Kumar, A. (2014). Genome sequence of an extremely drug-resistant clinical isolate of *Acinetobacter baumannii* strain AB030. *Genome Announc.* 2, e01035–e01114. doi: 10.1128/genomeA.01035-14

López-Leal, G., Zuniga-Moya, J. C., Castro-Jaimes, S., Graña-Miraglia, L., Pérez-Oseguera, Á., Reyes-García, H. S., et al. (2019). Unexplored genetic diversity of multidrug- and extremely drug-resistant *Acinetobacter baumannii* isolates from tertiary hospitals in Honduras. *Microb. Drug Resist.* 25, 690–695. doi: 10.1089/mdr.2018.0311

Lynch, J., Zhanel, G., and Clark, N. (2017). Infections due to *Acinetobacter baumannii* in the ICU: treatment options. *Semin. Respir. Crit. Care Med.* 38, 311–325. doi: 10.1055/s-0037-1599225

Lyons, C., Raustad, N., Bustos, M. A., and Shiaris, M. (2015). Incidence of type II CRISPR1-Cas systems in enterococcus is species-dependent. *PLoS One* 10:e0143544. doi: 10.1371/journal.pone.0143544

Magiorakos, A. P., Srinivasan, A., Carey, R. B., Carmeli, Y., Falagas, M. E., Giske, C. G., et al. (2012). Multidrug-resistant, extensively drug-resistant and pandrug-resistant bacteria: an international expert proposal for interim standard definitions for acquired resistance. *Clin. Microbiol. Infect.* 18, 268–281. doi: 10.1111/j.1469-0691.2011.03570.x

Makarova, K., and Koonin, E. (2015). Annotation and classification of CRISPR-Cas systems. *Methods Mol. Biol.* 1311, 47–75. doi: 10.1007/978-1-4939-2687-9_4

Mancilla-Rojano, J., Castro-Jaimes, S., Ochoa, S. A., Bobadilla del Valle, M., Luna-Pineda, V. M., Bustos, P., et al. (2019). Whole-genome sequences of five *Acinetobacter baumannii* strains from a child with leukemia M2. *Front. Microbiol.* 10:132. doi: 10.3389/fmicb.2019.00132

Mangas, E. L., Rubio, A., Álvarez-Marín, R., Labrador-Herrera, G., Pachón, J., Pachón-Ibáñez, M. E., et al. (2019). Pangenome of *Acinetobacter baumannii* uncovers two groups of genomes, one of them with genes involved in CRISPR/Cas defence systems associated with the absence of plasmids and exclusive genes for biofilm formation. *Microb. Genom.* 5:e000309. doi: 10.1099/mgen.0.000309

Martins, A. F., Kuchenbecker, R., Sukiennik, T., Boff, R., Reiter, K. C., Lutz, L., et al. (2009). Carbapenem-resistant *Acinetobacter baumannii* producing the OXA-23 enzyme: dissemination in Southern Brazil. *Infection* 37, 474–476. doi: 10.1007/s15010-009-9003-9

Mateo-Estrada, V., Graña-Miraglia, L., López-Leal, G., and Castillo-Ramírez, S. (2019). Phylogenomics reveals clear cases of misclassification and genus-wide phylogenetic markers for *Acinetobacter*. *Genome Biol. Evol.* 11, 2531–2541. doi: 10.1093/gbe/evz178

Nemec, A., Krizova, L., Maixnerova, M., Sedo, O., Brisse, S., and Higgins, P. (2015). *Acinetobacter seifertii* sp. nov., a member of the *Acinetobacter calcoaceticus – Acinetobacter baumannii* complex isolated from human clinical specimens. *Int. J. Syst. Evol. Microbiol.* 65, 934–942. doi: 10.1099/ijs.0.000043

Nemec, A., Krizova, L., Maixnerova, M., van der Reijden, T. J. K., Deschaght, P., Passet, V., et al. (2011). Genotypic and phenotypic characterization of the *Acinetobacter calcoaceticus-Acinetobacter baumannii* complex with the proposal of *Acinetobacter pittiii* sp. nov. (formerly *Acinetobacter* genomic species 3) and *Acinetobacter nosocomialis* sp. nov (formerly *Acinetobacter* genomic species 13TU). *Res. Microbiol.* 162, 393–404. doi: 10.1016/j.resmic.2011.02.006

Nowak, J., Zander, E., Stefanik, D., Higgins, P. G., Roca, I., Vila, J., et al. (2017). High incidence of pandrug-resistant *Acinetobacter baumannii* isolates collected from patients with ventilator-associated pneumonia in Greece, Italy and Spain as part of the MagicBullet clinical trial. *J. Antimicrob. Chemother.* 72, 3277–3282. doi: 10.1093/jac/dkx322

Peleg, A. Y., Seifert, H., and Paterson, D. L. (2008). *Acinetobacter baumannii*: emergence of a successful pathogen. *Clin. Microbiol. Rev.* 21, 538–582. doi: 10.1128/CMR.00058-07

Rafei, R., Kempf, M., Eveillard, M., Dabboussi, F., Hamze, M., and Joly-Guillou, M. L. (2014). Current molecular methods in epidemiological typing of *Acinetobacter baumannii*. *Future Microbiol.* 9, 1179–1194. doi: 10.2217/fmb.14.63

Rezzonico, F., Smits, T. H. M., and Duffy, B. (2011). Diversity, evolution, and functionality of clustered regularly interspaced short palindromic repeat (CRISPR) regions in the fire blight pathogen *Erwinia amylovora*. *Appl. Environ. Microbiol.* 77, 3819–3829. doi: 10.1128/AEM.00177-11

Shariat, N., Timme, R. E., Pettengill, J. B., Barrangou, R., and Dudley, E. G. (2015). Characterization and evolution of *Salmonella* CRISPR-Cas systems. *Microbiology* 161, 374–386. doi: 10.1099/mic.0.000005

Shrivastava, S., Shrivastava, P., and Ramasamy, J. (2018). World health organization releases global priority list of antibiotic-resistant bacteria to guide research, discovery, and development of new antibiotics. *J. Med. Soc.* 32, 76–77. doi: 10.4103/jms.jms_25_17

Silva, L., Mourão, J., Grosso, F., and Peixe, L. (2018). Uncommon carbapenemase-encoding plasmids in the clinically emergent *Acinetobacter pittii*. *J. Antimicrob. Chemother.* 73, 52–56. doi: 10.1093/jac/dkx364

Singh, A., Goering, R. V., Simjee, S., Foley, S. L., and Zervos, M. J. (2006). Application of molecular techniques to the study of hospital infection. *Clin. Microbiol. Rev.* 19, 512–530. doi: 10.1128/CMR.00025-05

Song, J. Y., Cheong, H. J., Choi, W. S., Heo, J. Y., Noh, J. Y., and Kim, W. J. (2011). Clinical and microbiological characterization of carbapenem-resistant *Acinetobacter baumannii* bloodstream infections. *J. Med. Microbiol.* 60, 605–611. doi: 10.1099/jmm.0.029439-0

Takeuchi, N., Wolf, Y. I., Makarova, K. S., and Koonin, E. V. (2012). Nature and intensity of selection pressure on CRISPR-associated genes. *J. Bacteriol.* 194, 1216–1225. doi: 10.1128/JB.06521-11

Tamayo-Legorreta, E. M., Garza-Ramos, U., Barrios-Camacho, H., Sanchez-Perez, A., Galicia-Paredes, A., Meza-Chavez, A., et al. (2014). Identification of OXA-23 carbapenemases: novel variant OXA-239 in *Acinetobacter baumannii* ST758 clinical isolates in Mexico. *New Microbes New Infect.* 2, 173–174. doi: 10.1002/nmi2.60

Tenover, F. C., Arbeit, R. D., Goering, R. V., Mickelsen, P. A., Murray, B. E., Persing, D. H., et al. (1995). Interpreting chromosomal DNA restriction patterns produced by pulsed-field gel electrophoresis: criteria for bacterial strain typing. *J. Clin. Microbiol.* 33, 2233–2239. doi: 10.1128/JCM.33.9.2233-2239.1995

Tomaschek, F., Higgins, P. G., Stefanik, D., Wisplinghoff, H., and Seifert, H. (2016). Head-to-head comparison of two multi-locus sequence typing (MLST) schemes for characterization of *Acinetobacter baumannii* outbreak and sporadic isolates. *PLoS One* 11:e0153014. doi: 10.1371/journal.pone.0153014

Turton, J. F., Kaufmann, M. E., Gill, M. J., Pike, R., Scott, P. T., Fishbain, J., et al. (2006). Comparison of *Acinetobacter baumannii* isolates from the United Kingdom and the United States that were associated with repatriated casualties of the Iraq conflict. *J. Clin. Microbiol.* 44, 2630–2634. doi: 10.1128/JCM.00547-06

Uwingabiye, J., Lemnouer, A., Baidoo, S., Frikh, M., Kasouati, J., Maleb, A., et al. (2017). Intensive care unit-acquired *Acinetobacter baumannii* infections

in a Moroccan teaching hospital: epidemiology, risk factors and outcome. *Germs* 7, 193–205. doi: 10.18683/germs.2017.1126

van Schaik, W., and Willems, R. J. (2010). Genome-based insights into the evolution of enterococci. *Clin. Microbiol. Infect.* 16, 527–532. doi: 10.1111/j.1469-0691.2010.03201.x

Vazquez, C., and Kollef, M. H. (2018). *Acinetobacter* pneumonia: improving outcomes with early identification and appropriate therapy. *Clin. Infect. Dis.* 67, 1455–1462. doi: 10.1093/cid/ciy375

Villalón, P., Ortega, M., Sáez-Nieto, J. A., Carrasco, G., Medina-Pascual, M. J., Garrido, N., et al. (2019). Dynamics of a sporadic nosocomial *Acinetobacter calcoaceticus – Acinetobacter baumannii* complex population. *Front. Microbiol.* 10:593. doi: 10.3389/fmicb.2019.00593

Vincent, J. L., Rello, J., Marshall, J., Silva, E., and Anzueto, A. (2009). International study of the prevalence and outcomes of infection in intensive care units. *JAMA* 302, 2323–2329. doi: 10.1001/jama.2009.1754

Wang, X., Qiao, F., Yu, R., Gao, Y., and Zong, Z. (2013). Clonal diversity of *Acinetobacter baumannii* clinical isolates revealed by a snapshot study. *BMC Microbiol.* 13:234. doi: 10.1186/1471-2180-13-234

Wisplinghoff, H., Paulus, T., Lugenheim, M., Stefanik, D., Higgins, P. G., Edmond, M. B., et al. (2012). Nosocomial bloodstream infections due to *Acinetobacter baumannii*, *Acinetobacter pittii* and *Acinetobacter nosocomialis* in the United States. *J. Inf. Secur.* 64, 282–290. doi: 10.1016/j.jinf.2011.12.008

Wong, D., Nielsen, T. B., Bonomo, R. A., Pantapalangkoor, P., Luna, B., and Spellberg, B. (2017). Clinical and pathophysiological overview of *Acinetobacter* infections: a century of challenges. *Clin. Microbiol. Rev.* 30, 409–447. doi: 10.1128/CMR.00058-16

Xie, R., Zhang, X. D., Zhao, Q., Peng, B., and Zheng, J. (2018). Analysis of global prevalence of antibiotic resistance in *Acinetobacter baumannii* infections disclosed a faster increase in OECD countries. *Emerg. Microbes Infect.* 7:31. doi: 10.1038/s41426-018-0038-9

Yamada, Y., Endo, K., Sawase, K., Anetai, M., Narita, K., Hatakeyama, Y., et al. (2016). Rapid species identification and epidemiological analysis of carbapenem-resistant *Acinetobacter* spp. by a PCR-based open reading frame typing method. *J. Med. Microbiol.* 65, 923–927. doi: 10.1099/jmm.0.000314

Yang, J., Chen, Y., Jia, X., Luo, Y., Song, Q., Zhao, W., et al. (2012). Dissemination and characterization of NDM-1-producing *Acinetobacter pittii* in an intensive care unit in China. *Clin. Microbiol. Infect.* 18, E506–E513. doi: 10.1111/1469-0691.12035

Conflict of Interest: The authors declare that the research was conducted in the absence of any commercial or financial relationships that could be construed as a potential conflict of interest.

frontiers in Microbiology

ORIGINAL RESEARCH
published: 02 November 2020
doi: 10.3389/fmicb.2020.584789

AdeABC Efflux Pump Controlled by AdeRS Two Component System Conferring Resistance to Tigecycline, Omadacycline and Eravacycline in Clinical Carbapenem Resistant *Acinetobacter nosocomialis*

Yi-Tzu Lee[1,2†], Hsing-Yu Chen[3†], Ya-Sung Yang[4], Yu-Ching Chou[5], Tein-Yao Chang[6], Wei-Jane Hsu[3], I-Chieh Lin[6], ACTION Study Group and Jun-Ren Sun[6]*

[1] Department of Emergency Medicine, Taipei Veterans General Hospital, Taipei, Taiwan, [2] Faculty of Medicine, School of Medicine, National Yang-Ming University, Taipei, Taiwan, [3] Department of Medical Techniques, Taipei City Hospital Ren-Ai Branch, Taipei, Taiwan, [4] Division of Infectious Diseases and Tropical Medicine, Department of Internal Medicine, Tri-Service General Hospital, National Defense Medical Center, Taipei, Taiwan, [5] School of Public Health, National Defense Medical Center, Taipei, Taiwan, [6] Institute of Preventive Medicine, National Defense Medical Center, Taipei, Taiwan

OPEN ACCESS

Edited by:
Ayush Kumar,
University of Manitoba, Canada

Reviewed by:
Jozsef Soki,
University of Szeged, Hungary
Zhi Ruan,
Zhejiang University, China

***Correspondence:**
Jun-Ren Sun
tsghsun@gmail.com

† These authors have contributed equally to this work

Specialty section:
This article was submitted to Antimicrobials, Resistance and Chemotherapy, a section of the journal Frontiers in Microbiology

Received: *18 July 2020*
Accepted: *06 October 2020*
Published: *02 November 2020*

Citation:
Lee Y-T, Chen H-Y, Yang Y-S, Chou Y-C, Chang T-Y, Hsu W-J, Lin I-C, ACTION Study Group and Sun J-R (2020) AdeABC Efflux Pump Controlled by AdeRS Two Component System Conferring Resistance to Tigecycline, Omadacycline and Eravacycline in Clinical Carbapenem Resistant Acinetobacter nosocomialis. Front. Microbiol. 11:584789. doi: 10.3389/fmicb.2020.584789

Carbapenem-resistant *Acinetobacter nosocomialis* (CRAn) is a significant public health concern. Tigecycline non-susceptible CRAn (Tn-CRAn) isolates have emerged worldwide. Tigecycline resistance is mainly related to the overexpression of AdeABC efflux pump controlled by AdeRS two-component system (TCS). Two novel tetracycline derivatives, omadacycline and eravacycline, may present a treatment option for CRAn. This study investigated the *in vitro* antimicrobial activity of tigecycline, omadacycline and eravacycline against clinical CRAn isolates and the contribution of efflux pumps in their resistance. Eighty-nine clinical CRAn isolates, including 57 Tn-CRAn isolates were evaluated for minimum inhibitory concentrations (MICs) by the broth microdilution. The relationship between the antimicrobial resistance and efflux pump expression was assessed by their responses to the efflux pump inhibitor 1-(1-naphthylmethyl)-piperazine (NMP). The contribution of the AdeABC efflux pump in their resistance was determined by the complementation of the AdeRS two-component system in wild-type, *adeRS* operon and *adeB* gene knockout strains. Among the 89 isolates, omadacycline and eravacycline MICs were correlated closely with those of tigecycline. They demonstrated improved potency, based on MIC_{90} values, by showing a 4 to 8-fold greater potency than tigecycline. The synergetic effects of tigecycline, omadacycline and eravacycline with NMP were observed in 57 (100%), 13 (22.8%), and 51 (89.5%) of Tn-CRAn isolates, respectively. Further analysis showed that the laboratory strain carrying the Type 1 *adeRS* operon increased the tigecycline, omadacycline and eravacycline MICs by 4–8-folds, respectively. Eravacycline demonstrated improved potency over tigecycline against populations of CRAn, including Tn-CRAn isolates.

The over-expression of AdeABC efflux pumps was directly activated by the AdeRS two-component system and simultaneously reduced the susceptibilities of tigecycline, eravacycline, and omadacycline. Omadacycline and eravacycline MICs were correlated closely with those of eravacycline.

Keywords: tigecycline, *Acinetobacter*, omadacycline, eravacycline, efflux pump

INTRODUCTION

Acinetobacter species has become a major nosocomial pathogen associated with high mortality in immunocompromised patients on account of its rapid acquisition of resistance (Ayoub Moubareck and Hammoudi Halat, 2020). When *Acinetobacter* spp. develops extended drug resistance to sulbactam, tigecycline, and colistin, the antimicrobial choices become scarce and difficult (Montana et al., 2015). New and novel antimicrobial agents are therefore needed.

Acinetobacter nosocomialis is an emerging opportunistic pathogen that is usually grouped into the *Acinetobacter calcoaceticus-baumannii* complex (Acb complex) (Vijayakumar et al., 2019). In Asia, the carbapenem resistant rate among infections caused by *A. nosocomialis* is as high as 30% (Chen et al., 2018; Singkham-In and Chatsuwan, 2018; Chen et al., 2019). Tigecycline has been regarded as one of the final armamentaria against carbapenem resistant *A. nosocomialis* (CRAn). Unfortunately, tigecycline non-susceptible *A. nosocomialis* has also increasingly emerged in recent years (Yang et al., 2019).

Resistance-nodulation-cell division (RND) efflux pumps are ubiquitous in gram-negative bacteria and have been shown to play an important role in antimicrobial resistance (Coyne et al., 2011; Li et al., 2015b). It has been shown that three efflux pumps, AdeABC, AdeFGH, and AdeIJK, are associated with tigecycline resistance in *Acinetobacter* species (Coyne et al., 2011). The expression of the AdeABC is controlled by the AdeRS two-component system (TCS). The expression of AdeFGH and AdeIJK is controlled by AdeL, a LysR-type transcriptional regulator and AdeN, a TetR-like transcriptional regulator, respectively (Xu et al., 2019). Our previous study has demonstrated that the overexpression of the AdeABC efflux pump plays a major role in exporting tigecycline in tigecycline non-susceptible *A. nosocomialis* (Yang et al., 2019). Type 1 AdeRS TCS was found to be associated with tigecycline non-susceptible in clinical *Acinetobacter nosocomialis* in isolates (Yang et al., 2019). However, the correlation between the Type 1 AdeRS TCS pattern and tigecycline resistance is still uncertain and requires further investigation.

Omadacycline and eravacycline are novel tetracycline derivatives similar to tigecycline, and they were found to have broad spectrum activity against various multi-drug resistant pathogens (Zhanel et al., 2018; Karlowsky et al., 2019; Kaushik et al., 2019). Because of the structural resemblance to tigecycline, omadacycline and eravacycline are believed to have good activity against clinical CRAn. In addition, there were no reports indicating omadacycline and eravacycline susceptibilities among tigecycline non-susceptible CRAn (Tn-CRAn). The aim of this study was to examine the antimicrobial susceptibilities of omadacycline and eravacycline against the emerging CRAn, in comparison with tigecycline. Furthermore, we also investigated the role of efflux pump-mediated resistance to omadacycline and eravacycline.

MATERIALS AND METHODS

Bacterial Strains

The bacterial strains and plasmids used in this study are listed in **Table 1**. Between 2012 and 2018, clinical CRAn isolates were collected from AntimiCrobial studies in Taiwan Operating Network (ACTION), which included six medical centers located in different parts of Taiwan, including (alphabetically) the Changhua Christian Hospital (CCH) in Central Taiwan, Kaohsiung Medical University Hospital (KMUH) in southern Taiwan, Mackay Memorial Hospital (MMH) in Northern Taiwan, National Taiwan University Hospital (NTUH) in Northern Taiwan, Taipei Veterans General Hospital (TVGH) in Northern Taiwan, Tri-Service General Hospital (TSGH) of the National Defense Medical Center (NDMC) in Northern Taiwan and National Institute of Infectious Diseases and Vaccinology, National Health Research Institute (NHRI) in Northern Taiwan. All isolates were identified by MALDI-TOF (matrix-assisted laser desorption ionization-time of flight) and confirmed by a sequence analysis of the *rpoB* gene (Bartual et al., 2005). The isolates were subjected to multi-locus sequence typing (MLST) according to the Pasteur scheme (Diancourt et al., 2010). The genetic relationship among the MLST types of Tn-CRAn isolates was reconstructed using the Phyloviz program.[1]

[1]https://online.phyloviz.net/index

TABLE 1 | Bacterial strains and plasmids used in this study.

Strains or plasmids	Relevant characteristics
***Acinetobacter nosocomialis* strains**	
An wt	*A. nosocomialis* reference strain ATCC17903
AnΔadeRS	Derived from ATCC17903. *adeRS* operon deletion
AnΔadeB	Derived from ATCC17903. *adeB* gene deletion
Plasmids	
pS01	*E. coli-Acinetobacter* shuttle plasmid; mini-CTX::laclq-PT7-lacZ
pRS-AnadeRS (wt)	Derived from pRS, mini-CTX:: adeRS-Pade-lacZ (adeRS from ATCC 17903)
pRS-AnadeRS (Type1)	Derived from pRS, mini-CTX:: adeRS-Pade-lacZ (adeRS from clinical Tn-CRAn isolate)

MIC, Minimum inhibitory concentration.

Antimicrobial Susceptibility and Efflux Pump Inhibitor Tests

Antibiotic susceptibility testing was performed using Sensititre GNX2F (Thermo Fisher Scientific, Waltham, MA, United States) following the manufacturer's protocols. Minimum inhibitory concentrations (MICs) of tigecycline, omadacycline and eravacycline were determined by broth microdilution. The U.S. Food and Drug Administration (FDA) recommendation for tigecycline susceptibility breakpoints of *Enterobacteriaceae* (susceptible MIC≤2 mg/L; intermediate >2 and <8 mg/L; resistant ≥8 mg/L) was used as the MIC interpretation criteria (Yang et al., 2019). Omadacycline and eravacycline were currently without breakpoints. *Escherichia coli* ATCC 25922 was utilized as a quality control for each series of isolates tested. The effect of 1-(1-naphthylmethyl)-piperazine (NMP) on antibiotic activity was determined by the Mueller-Hinton broth (MHB) in the presence and absence of NMP (50 mg/L), respectively. The NMP effects were interpreted and reported as follows: good effect for a 4-fold or more reduction and poor effect for a less than 2-fold reduction in the MIC value (Yang et al., 2019).

Construction of Deletion Mutations and *adeRS* Transforms

ATCC17903ΔadeRS (AnΔadeRS) and ATCC17903ΔadeB (AnΔadeB) were unmarked deletion mutants created by a previously described method for generating markerless deletions in *A. nosocomialis* strain ATCC17903 (An wt) as suggested in a previous study (Sun et al., 2017). Primers are shown in **Table 2**. Suicide plasmid pMo130-TelR was used for deleting the *adeRS* and *adeB* operons. Approximately 1-kb fragments upstream and downstream from the target genes were amplified and cloned in pMo130-TelR. Successful ATCC17903 transformants were first selected on LB agar plates containing 10 mg/L kanamycin (first crossovers). Kanamycin-resistant clones were isolated, and single homologous recombination events were screened for by PCR. Kanamycin -resistant clones were then plated on an LB agar containing 10% sucrose to be selected for the deletion of the *adeRS* operon or *adeB* gene by a second crossover and allelic replacement.

The plasmid pS01 was digested with *Sma*I and *BamH*I to delete its lacIq gene and T7 early gene promoters. The digested plasmids were ligated with the respective gene fragments to generate a series of recombinant pRS clones, including pRS-AnadeRS (wt) and pRS-AnadeRS (Type1). Recombinant plasmids were introduced by electroporation into AnΔadeRS and AnΔadeB and selected on LB agar plates containing 5 mg/L tetracycline.

Quantitative Real-Time PCR

The transcription levels of *adeB*, *adeJ*, and *adeG* genes were measured by quantitative real-time PCR assays as suggested in a previous study (Yang et al., 2019). ATCC 17903 transforms were grown in Luria-Bertani (LB) broth until mid-log phase. Total RNA was extracted using an RNeasy Mini Kit (Qiagen Sciences, Germantown, MD, United States). Reverse transcription was performed using a QuantiNova Reverse Transcription Kit (Qiagen). Real-time PCR was performed with the QuantiNova SYBR Green PCR Kit (Qiagen). The mRNA of *rpoB* gene was used as a control and ATCC 17903 as a reference to the standard expression level.

Statistical Analyses

Statistical analysis was carried out using the SPSS version 20.0 software package. The calculation of statistical differences between various groups was based on the Fisher's exact test. Pairs of outcomes (Correlation of MICs between two antibiotics) were examined for evidence of monotonic associations using Spearman's correlation coefficients. Differences were considered statistically significant when $p < 0.05$.

RESULTS

Susceptibilities Among CRAn Isolates

A total of 89 clinical CRAn isolates were collected, including 57 Tn-CRAn from ACTION medical centers. The antimicrobial

TABLE 2 | Oligonucleotides used in this study.

Primer name	Sequence	Features/purpose
An_adeRS_r_NaeI	AAGAGCCGGCAGTGAAGAGTTGTAACGCTAAGG	Cloning *adeRS* operon and promoter with engineered NaeI and BamHI site into pRS to form pRS- adeRS.
An_Apromoter_f_BamHI	CCGAGGATCCAAAAGATGCTTTTGCATACTGTC	
pMo130Tel F	TTTACCACGACCGCATTCTC	Primers specific to pMo130TelR DNA flanking the Up and Down insert; PCR product not present after single and double crossover.
pMo130Tel R	AAATAGGCGTATCACGAGGC	
AdeAUp_f (Pst1)	ACTCTGCAGGCTGATGTCGCTCAAATGAAAGCA	PCR of UP fragment containing partial AdeB region.
AdeAUp_r (BamH1)	ATGGATCCCGGAGCTACACTTGGAAAGC	
AdeBDwn_fover (BamH1)	GCTTTCCAAGTGTAGCTCCGGGATCCAT TGACCGTGAAAAGCTGAGTGCACTT	PCR of DOWN fragment containing partial AdeB region.
AdeBDwn_r (Sph1)	CAAGCATGCGCCAGAATGGTTGCTGAAATCAT	
AdeRUp_f (Pst1)	ACTCTGCAGTTCATTTGAGCGACATCAGC	PCR of UP fragment containing partial AdeR region.
AdeRUp_r (BamH1)	GATGGATCCGCCTGAACTCTAGCGACCAC	
AdeSDwn_fover (BamH1)	GTCGCTAGAGTTCAGGCGGATCCATCTTGCGAAGCGTTTCATT	PCR of DOWN fragment containing partial AdeS region.
AdeSDwn_r (Sph1)	CAAGCATGCCCTAAACCTGTACCGCCAAA	

susceptibilities of Tn-CRAn isolates are shown in **Supplementary Table S1**. Multilocus sequence typing revealed the Tn-CRAn isolates belonged to three sequence types (ST): ST410 (55 isolates), ST68 (1 isolate) and ST1272 (1 isolate) (**Supplementary Figure S1**). Tigecycline susceptible CRAn (Ts-CRAn) isolates were randomly selected with the following STs: ST1272 (14 isolates), ST433 (6 isolates), ST410 (6 isolates), ST68 (4 isolates) and ST217 (2 isolates). The overall tigecycline MICs of CRAn isolates ranged from 0.25 to 32 mg/L; omadacycline, 0.25 to 16 mg/L; and eravacycline, 0.03 to 8 mg/L (**Table 3**). Among the 57 isolates, 34 displayed lower omadacycline MICs than tigecycline MICs (**Figure 1A**) and all displayed lower eravacycline MICs than tigecycline MICs (**Figure 1B**). Correlation analysis was carried out to test the correlation between levels of resistance to the three tetracycline derivatives (**Table 4**). There was a strong correlation among MICs for the three antibiotics (Spearman's correlation coefficients = 0.829 to 0.852, both $P < 0.05$). Taken together, these data indicate that omadacycline and eravacycline showed a positive correlation with tigecycline activity, but they were not associated with the MLST profile. Eravacycline demonstrated improved potency over tigecycline, based on MIC_{90} values, showing a 4-fold and 4- to 8-fold greater potency against populations of Tn-CRAn and Ts-CRAn, respectively (**Table 5**).

Effects of NMP on Antibiotic Activity

The effects of the NMP on MICs of the three antibiotics against CRAn isolates are reported in **Table 5**. Among those, Tn-CRAn isolates showed better response to NMP in the three antibiotics than Ts-CRAn isolates (Fisher's exact test; $P < 0.05$). All Tn-CRAn isolates showed a more than 4-fold decrease in eravacycline MICs with NMP. However, only seven Tn-CRAn isolates reached such reduction in omadacycline MICs with NMP. Among the NMP effects in the three antibiotics against Tn-CRAn isolates, Tigecycline and eravacycline with NMP both showed significantly more MIC reductions than omadacycline with NMP (Fisher's exact test; $P < 0.05$).

The Contribution of AdeRS TCS in AdeABC Efflux Pump-Mediated Resistance

To confirm the roles of AdeABC efflux pumps in the resistance to the three antibiotics, *AdeRS* operon and *adeB* gene deletion mutants were generated and tested. The sequence alignment of AdeR and AdeS sequences from Type 1 AdeRS TCS (GenBank accession number MH321430) and ATCC 17903 AdeRS TCS (wt) were shown in **Supplementary Figure S2**. The two amino acid differences were found between the AdeRS patterns, which contained S16N in AdeS and T137S in AdeR. The AnΔadeRS transformed with pRS-AnadeRS (Type1) showed higher MICs of the three antibiotics in comparison with pRS-adeRS (wt) [tigecycline (1 vs. 0.13 mg/L); omadacycline (2 vs. 0.25 mg/L); eravacycline (0.25 vs. 0.06 mg/L)] (**Table 6**). The transcription levels of *adeB* genes in AnΔadeRS with pRS-AnadeRS (Type1) were higher than that with pRS-adeRS (wt) (27.4-folds vs. 1.4-folds). The increase of omadacycline and eravacycline MIC was similar to tigecycline MIC and correlated with the expression of AdeABC efflux pump in the transformant. The transcription levels of *adeJ* and *adeG* in the two transforms were not significantly different. The MICs of the three antibiotics did not increase while being transformed with those recombinant plasmids into the AnΔadeB strain. These findings suggested that AdeABC efflux pumps medicated by AdeRS TCS played a role in the resistance to the three antibiotics in *A. nosocomialis*.

DISCUSSION

This is the first study elucidating the contribution of efflux pumps in the resistance to novel tetracycline derivative antibiotics, eravacycline and omadacycline in clinical carbapenem resistant

TABLE 3 | Minimum inhibitory concentration distributions of tigecycline, omadacycline, and eravacycline in relation to multi-locus sequence typing types.

	No. of isolates with MLST pattern at various MICs (mg/L)										
Antibiotics and MLST pattern (n)	**0.03**	**0.06**	**0.13**	**0.25**	**0.5**	**1**	**2**	**4**	**8**	**16**	**32**
Tigecycline											
ST410 (61)					4		2	25	26	3	1
ST1272 (15)				1	10	2	1	1			
Other type (13)[a]				3	2	4	3		1		
Omadacycline											
ST410 (61)				1	2	4	2	50	1	1	
ST1272 (15)				11	2		1	1			
Other type (13)[a]				7	4		1	1			
Eravacycline											
ST410 (61)		4			5	27	22	2	1		
ST1272 (15)	1	8	2	3		1					
Other type (13)[a]	2	4	3	2	1		1				

[a]*ST433 (6) ST68 (5) and ST217 (2).*

MIC, Minimum inhibitory concentration; MLST, multi-locus sequence typing; OT, other type.

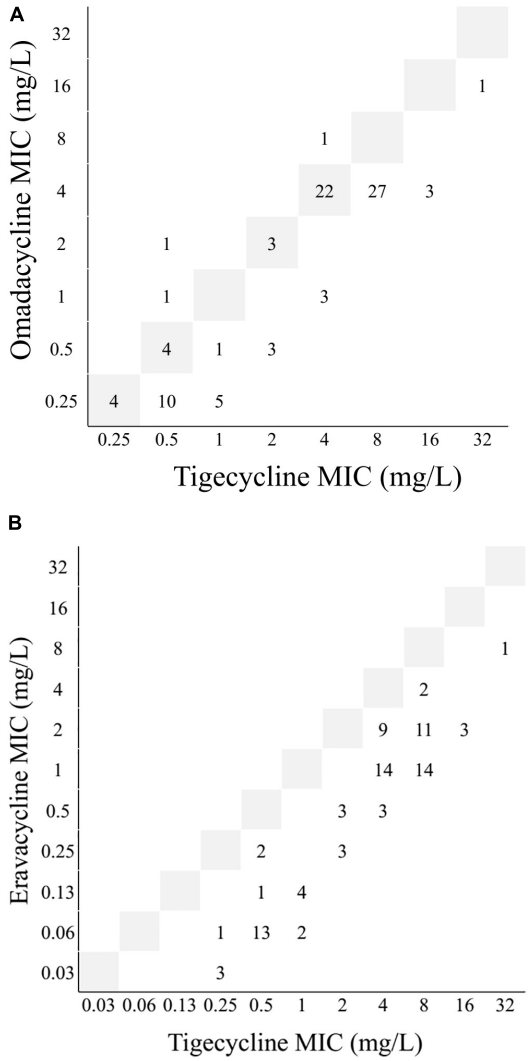

FIGURE 1 | Interrelationship between minimum inhibitory concentrations (MICs) of omadacycline, eravacycline and tigecycline against 89 *Acinetobacter nosocomialis* isolates. **(A)** omadacycline vs. tigecycline. **(B)** eravacycline vs. tigecycline. Gray boxes represented the line of equivalence. Numbers below this line indicated omadacycline or eravacycline was more active, and numbers above indicate tigecycline was more active.

TABLE 4 | Correlations between minimum inhibitory concentrations of tigecycline, omadacycline, and eravacycline against carbapenem resistant *Acinetobacter nosocomialis*[a].

	Spearman's correlation coefficient (*P*-value)		
Antibiotics	**Tigecycline**	**Omadacycline**	**Eravacycline**
Tigecycline	1.000		
Omadacycline	0.852 ($P < 0.001$)	1.000	
Eravacycline	0.852 ($P < 0.001$)	0.829 ($P < 0.001$)	1.000

[a]*Minimum inhibitory concentrations were measured from all 89 carbapenem resistant A. nosocomialis isolates.*

A nosocomialis isolates. We found that there was a strong correlation among the MICs of the two antibiotics and tigecycline. NMP pump inhibitors reduced the MICs of tigecycline and eravacycline against Tn-CRAn isolates. Since the synergistic effect with NMP for omadacycline susceptibility was poor, it suggests that other mechanisms are contributing to omadacycline resistance. Further studies confirmed that AdeRS TCS played a role in the resistance to the three antibiotics in *A. nosocomialis*.

ST410 was found to be the most dominant type in clinical Tn-CRAn isolates in Taiwan, which is consistent with our previous studies (Chen et al., 2018; Yang et al., 2019). This may indicate that there is an unknown mechanism in ST410 that provides fitness advantage in a hospital setting, which could easily transform to carbapenem and/or tigecycline resistance. Further evaluation is needed to elucidate the relationship between ST410 and tigecycline resistance, such as whole-genome sequence analysis by next generation sequencing. MICs of omadacycline and eravacycline for the ST410 Tn-CRAn isolates were unimodally distributed, with clustering at 4 vs. 1 to 2 mg/L. In previous studies, the *A. baumannii* with higher MICs of tigecycline also had a strong positive correlation with higher eravacycline MICs, and the eravacycline MICs were generally 2-fold lower than that of tigecycline (Livermore et al., 2016; Seifert et al., 2018). In this study, we observed a strong correlation among the MICs of the three antibiotics against *A. nosocomialis*. The results suggested that the resistant mechanisms of *A. nosocomialis* against these three antibiotics might be similar due to the similar tetracycline-like structures and related to the AdeABC efflux pump.

1-(1-naphthylmethyl)-piperazine is a type of naphthyl derivative and is often used as an efflux pump inhibitor (EPI) in research (Sonnet et al., 2012; Yang et al., 2019). EPI has the ability to reverse antibiotic resistance, but is partly related to the ability to inhibit the AdeABC efflux pump (Pannek et al., 2006). In the current study, we found that omadacycline with NMP has weaker synergistic activity compared to the other two antibiotics. Moreover, we found that this was not related to the overexpression of the AdeABC efflux pump system. However, other findings about NMP under sub-inhibitory concentrations have also been reported in recent years, including reduction of the mass of preformed biofilm, inhibition of virulence factors and membrane destabilization (Bina et al., 2009; Anes et al., 2018; Anes et al., 2019). During survival in an environmental stress containing NMP, *Klebsiella pneumoniae* would initiate many genes involved in repairing and maintaining membrane homeostasis, up-regulation of other efflux systems and lipopolysaccharide modification genes (Anes et al., 2019). These findings may also suggest that sub-inhibitory concentrations of NMP not only inhibit the AdeABC efflux pump, but also drive other specific mechanisms of resistance to omadacycline.

The resistant mechanisms against tigecycline in *Acinetobacter* spp. included RND efflux pump overexpression, modifications at the ribosomal binding site, and enzymatic inactivation by tetracycline monooxygenase TetX (Chen et al., 2014; Beabout et al., 2015; Li et al., 2015a; Wang et al., 2019; Yang et al., 2019).

TABLE 5 | Minimum inhibitory concentration reduction effects of 1-(1-naphthylmethyl)-piperazine (NMP) in relation to multi-locus sequence typing types between tigecycline resistant/carbapenem resistant and tigecycline susceptible/carbapenem resistant *Acinetobacter nosocomialis*.

	Tigecycline				Omadacycline				Eravacycline			
MLST profiles	**Good (≥4-folds)**	**Poor (≤2-folds)**	**MIC Range**	**MIC 50/90**	**Good (≥4-folds)**	**Poor (≤2-folds)**	**MIC Range**	**MIC 50/90**	**Good (≥4-folds)**	**Poor (≤2-folds)**	**MIC Range**	**MIC 50/90**
Tn-CRAn (57)												
ST410 (55)	55		4–32	8/8	12	43	1–16	4/4	49	6	0.5–8	1/2
ST1272 (1)	1		4	4/4	1		4	4/4	1		1	1/1
OT (1)	1		8	8/8		1	4	4/4	1		2	2/2
Ts-CRAn (32)												
ST410 (6)	2	4	0.5–2	0.5/2		6	0.25–2	0.5/2		6	0.06–0.5	0.06/0.5
ST1272 (14)	1	13	0.2–2	0.5/1	1	13	0.25–2	0.25/0.5	1	13	0.03–0.25	0.06/0.25
OT (12)	2	10	0.25–2	1/2		12	0.25–2	0.25/0.5	2	10	0.03–0.5	0.06/0.25

MIC, Minimum inhibitory concentration; MLST, multi-locus sequence typing; OT, other type; Tn-CRAn, tigecycline resistant/carbapenem resistant A. nosocomialis; Ts-CRAn, tigecycline susceptible/carbapenem resistant A. nosocomialis.

TABLE 6 | Minimum inhibitory concentrations of tigecycline, omadacycline and eravacycline against various *Acinetobacter nosocomialis* transformants.

	MIC (mg/L)			RND efflux pump expression (fold (SD))		
Strains and plasmid	**Tigecycline**	**Omadacycline**	**Eravacycline**	***adeB***	***adeJ***	***adeG***
An wt	0.13	0.25	0.06	1	1	1
AnΔadeRS::pS01 (vector only)	0.13	0.25	0.06	1.0 (0.3)	1.1 (0.4)	0.8 (0.2)
AnΔadeRS::pRSANadeRS (Type1)	1	2	0.25	27.4 (7.7)	1.1 (0.6)	0.5 (0.1)
AnΔadeRS::pRSANadeRS (wt)	0.25	0.5	0.06	1.4 (0.4)	1.1 (0.4)	0.7 (0.3)
AnΔadeB::pS01 (vector only)	0.13	0.25	0.06	-	1.1 (0.5)	0.9 (0.3
AnΔadeB::pRSANadeRS (Type1)	0.13	0.25	0.06	-	1.5 (1.2)	0.6 (0.3)
AnΔadeB::pRSANadeRS (wt)	0.13	0.25	0.03	-	1.4 (1.0)	0.6 (0.1)

Although the plasmid mediated TetX gene has been found to confer resistance to tigecycline, the overexpression of chromosomal RND efflux pumps, especially the AdeABC efflux pump is still a widespread tigecycline resistance determinant (Wang et al., 2019; Yang et al., 2019). The AdeABC efflux pump has been demonstrated to be present in most clinical *A. nosocomialis* and *A. baumannii* isolates (Yang et al., 2019; Yoon et al., 2013). The AdeABC efflux pump was confirmed to export not only tigecycline but also beta-lactam, fluoroquinolone, aminoglycoside and chloramphenicol (Coyne et al., 2011; Xu et al., 2019). As mentioned in previous studies, the overexpression of AdeABC efflux pump has been shown to be related to amino acid substitutions in AdeRS TCS (Gerson et al., 2018; Yoon et al., 2013). Our results indicated that the two amino acid substitutions in AdeRS TCS may be associated to the overexpression of AdeABC efflux pump. S16N is in the transmembrane domain of AdeS, while T137S is in the receiver domain of AdeR. Further structural and biochemical studies are needed to unravel how the two amino acid substitutions affect AdeRS TCS signal transmission.

Although, the CRAn isolates were collected from six major medical centers in Taiwan, one of the limitations in our study is that such small sample sizes may not represent the genotype distribution of CRAn in the world. Another limitation is that the contribution of potential mechanism other than efflux pump was not examined. On the basis of our current data, we suggest that Type 1 AdeRS TCS could directly stimulate the expression of the AdeABC efflux pump and is associated with eravacycline and omadacycline resistance. Thus, Type 1 AdeRS TCS could be a potential target to screen inhibitors as tetracycline derivative adjuvants for future combination therapy.

CONCLUSION

In conclusion, eravacycline and omadacycline MICs of CRAn were correlated closely with those of tigecycline and eravacycline. They demonstrated improved potency over tigecycline against populations of CRAn, including Tn-CRAn isolates. The synergistic activity of NMP on eravacycline and tigecycline was observed, but not on omadacycline. The type 1 AdeRS TCS pattern was able to reduce the susceptibilities of the three antibiotics against *A. nosocomialis* by the regulation of AdeABC efflux pumps medicated by AdeRS TCS.

MEMBERS OF THE ACTION STUDY GROUP

The members of the ACTION study group include Yea-Yuan Chang (National Yang-Ming University Hospital, Yilan, Taiwan), Y-SY (Division of Infectious Diseases and Tropical Medicine, Department of Internal Medicine, Tri-Service General Hospital, National Defense Medical Centre, Taipei, Taiwan),

Chung-Ting Chen (Department of Emergency Medicine, Taipei Veterans General Hospital, Taipei, Taiwan), Yuag-Meng Liu (Changhua Christian Hospital, Changhua, Taiwan), Shu-Chen Kuo (National Institute of Infectious Diseases and Vaccinology, National Health Research Institute, Maoli County, Taiwan), Chang-Pan Liu (MacKay Memorial Hospital, Taipei, Taiwan), Te-Li Chen (Graduate Institute of Life Sciences, National Defense Medical Centre, Taipei, Taiwan), and Y-TL (Taipei Veterans General Hospital, Taipei, Taiwan).

DATA AVAILABILITY STATEMENT

The raw data supporting the conclusions of this article will be made available by the authors, without undue reservation.

AUTHOR CONTRIBUTIONS

Y-TL, Y-SY, Y-CC, T-YC, W-JH, and I-CL conceptualized the study, performed the experiments, and analyzed the data. J-RS, H-YC and Y-TL was responsible for funding acquisition, aided in conceptualization of the study, and writing of the manuscript. All authors contributed to the article and approved the submitted version.

FUNDING

This work was supported by grants from the National Yang-Ming University Hospital (RD2019-011), Taipei City Hospital (TPCH-109-20), and the Ministry of Science and Technology (MOST 108-2320-B-016-009).

ACKNOWLEDGMENTS

This study was supported by the ACTION study group.

SUPPLEMENTARY MATERIAL

The Supplementary Material for this article can be found online at: https://www.frontiersin.org/articles/10.3389/fmicb.2020.584789/full#supplementary-material

REFERENCES

Anes, J., Martins, M., and Fanning, S. (2018). Reversing antimicrobial resistance in multidrug-resistant *Klebsiella pneumoniae* of clinical origin using 1-(1-Naphthylmethyl)-piperazine. *Microb. Drug Resist.* Online ahead of print.

Anes, J., Sivasankaran, S. K., Muthappa, D. M., Fanning, S., and Srikumar, S. (2019). Exposure to sub-inhibitory concentrations of the chemosensitizer 1-(1-naphthylmethyl)-piperazine creates membrane destabilization in multi-drug resistant *Klebsiella pneumoniae*. *Front. Microbiol.* 10:92. doi: 10.3389/fmicb.2019.00092

Ayoub Moubareck, C., and Hammoudi Halat, D. (2020). Insights into *Acinetobacter baumannii*: a review of microbiological, virulence, and resistance traits in a threatening nosocomial pathogen. *Antibiotics (Basel)* 9:119. doi: 10.3390/antibiotics9030119

Bartual, S. G., Seifert, H., Hippler, C., Luzon, M. A., Wisplinghoff, H., and Rodriguez-Valera, F. (2005). Development of a multilocus sequence typing scheme for characterization of clinical isolates of *Acinetobacter baumannii*. *J. Clin. Microbiol.* 43, 4382–4390. doi: 10.1128/jcm.43.9.4382-4390.2005

Beabout, K., Hammerstrom, T. G., Perez, A. M., Magalhaes, B. F., Prater, A. G., Clements, T. P., et al. (2015). The ribosomal S10 protein is a general target for decreased tigecycline susceptibility. *Antimicrob. Agents Chemother* 59, 5561–5566. doi: 10.1128/aac.00547-15

Bina, X. R., Philippart, J. A., and Bina, J. E. (2009). Effect of the efflux inhibitors 1-(1-naphthylmethyl)-piperazine and phenyl-arginine-beta-naphthylamide on antimicrobial susceptibility and virulence factor production in *Vibrio cholerae*. *J. Antimicrob Chemother* 63, 103–108. doi: 10.1093/jac/dkn466

Chen, F. J., Huang, W. C., Liao, Y. C., Wang, H. Y., Lai, J. F., Kuo, S. C., et al. (2019). Molecular epidemiology of emerging carbapenem resistance in *Acinetobacter nosocomialis* and *Acinetobacter pittii* in Taiwan, 2010 to 2014. *Antimicrob Agents Chemother* 63, e2007–e2018.

Chen, H. Y., Yang, Y. S., Hsu, W. J., Chou, Y. C., Huang, L. S., Wang, Y. C., et al. (2018). Emergence of carbapenem-resistant *Acinetobacter nosocomialis* strain ST410 harbouring plasmid-borne blaOXA-72 gene in Taiwan. *Clin. Microbiol. Infect.* 24, 1023–1024. doi: 10.1016/j.cmi.2018.04.009

Chen, Q., Li, X., Zhou, H., Jiang, Y., Chen, Y., Hua, X., et al. (2014). Decreased susceptibility to tigecycline in *Acinetobacter baumannii* mediated by a mutation in trm encoding SAM-dependent methyltransferase. *J Antimicrob Chemother* 69, 72–76. doi: 10.1093/jac/dkt319

Coyne, S., Courvalin, P., and Perichon, B. (2011). Efflux-mediated antibiotic resistance in *Acinetobacter spp*. *Antimicrob Agents Chemother* 55, 947–953. doi: 10.1128/aac.01388-10

Diancourt, L., Passet, V., Nemec, A., Dijkshoorn, L., and Brisse, S. (2010). The population structure of *Acinetobacter baumannii*: expanding multiresistant clones from an ancestral susceptible genetic pool. *PLoS One* 7:e10034. doi: 10.1371/journal.pone.0010034

Gerson, S., Nowak, J., Zander, E., Ertel, J., Wen, Y., Krut, O., et al. (2018). Diversity of mutations in regulatory genes of resistance-nodulation-cell division efflux pumps in association with tigecycline resistance in *Acinetobacter baumannii*. *J. Antimicrob Chemother* 73, 1501–1508. doi: 10.1093/jac/dky083

Karlowsky, J. A., Steenbergen, J., and Zhanel, G. G. (2019). Microbiology and preclinical review of omadacycline. *Clin. Infect. Dis.* 69, S6–S15.

Kaushik, A., Ammerman, N. C., Martins, O., Parrish, N. M., and Nuermberger, E. L. (2019). In vitro activity of new tetracycline analogs omadacycline and eravacycline against drug-resistant clinical isolates of *Mycobacterium abscessus*. *Antimicrob Agents Chemother* 63:e00470-19.

Li, X., Liu, L., Ji, J., Chen, Q., Hua, X., Jiang, Y., et al. (2015a). Tigecycline resistance in *Acinetobacter baumannii* mediated by frameshift mutation in plsC, encoding 1-acyl-sn-glycerol-3-phosphate acyltransferase. *Eur. J. Clin. Microbiol. Infect. Dis.* 34, 625–631. doi: 10.1007/s10096-014-2272-y

Li, X. Z., Plesiat, P., and Nikaido, H. (2015b). The challenge of efflux-mediated antibiotic resistance in Gram-negative bacteria. *Clin. Microbiol. Rev.* 28, 337–418. doi: 10.1128/cmr.00117-14

Livermore, D. M., Mushtaq, S., Warner, M., and Woodford, N. (2016). In vitro activity of eravacycline against carbapenem-resistant *Enterobacteriaceae* and *Acinetobacter baumannii*. *Antimicrob Agents Chemother* 60, 3840–3844. doi: 10.1128/aac.00436-16

Montana, S., Vilacoba, E., Traglia, G. M., Almuzara, M., Pennini, M., Fernandez, A., et al. (2015). Genetic variability of aders two-component system associated with tigecycline resistance in XDR-*Acinetobacter baumannii* isolates. *Curr. Microbiol.* 71, 76–82. doi: 10.1007/s00284-015-0829-3

Pannek, S., Higgins, P. G., Steinke, P., Jonas, D., Akova, M., Bohnert, J. A., et al. (2006). Multidrug efflux inhibition in *Acinetobacter baumannii*: comparison between 1-(1-naphthylmethyl)-piperazine and phenyl-arginine-beta-naphthylamide. *J. Antimicrob Chemother* 57, 970–974. doi: 10.1093/jac/dkl081

Seifert, H., Stefanik, D., Sutcliffe, J. A., and Higgins, P. G. (2018). In-vitro activity of the novel fluorocycline eravacycline against carbapenem non-susceptible

Acinetobacter baumannii. *Int. J. Antimicrob Agents* 51, 62–64. doi: 10.1016/j.ijantimicag.2017.06.022

Singkham-In, U., and Chatsuwan, T. (2018). Mechanisms of carbapenem resistance in *Acinetobacter pittii* and *Acinetobacter nosocomialis* isolates from Thailand. *J. Med. Microbiol.* 67, 1667–1672. doi: 10.1099/jmm.0.000845

Sonnet, P., Izard, D., and Mullie, C. (2012). Prevalence of efflux-mediated ciprofloxacin and levofloxacin resistance in recent clinical isolates of *Pseudomonas aeruginosa* and its reversal by the efflux pump inhibitors 1-(1-naphthylmethyl)-piperazine and phenylalanine-arginine-beta-naphthylamide. *Int. J. Antimicrob Agents* 39, 77–80. doi: 10.1016/j.ijantimicag.2011.08.005

Sun, J. R., Chiang, Y. S., Shang, H. S., Perng, C. L., Yang, Y. S., and Chiueh, T. S. (2017). Phenotype microarray analysis of the AdeRS two-component system in *Acinetobacter baumannii*. *Eur. J. Clin. Microbiol. Infect. Dis.* 36, 2343–2353. doi: 10.1007/s10096-017-3066-9

Vijayakumar, S., Biswas, I., and Veeraraghavan, B. (2019). Accurate identification of clinically important *Acinetobacter spp.*: *an update*. *Future Sci. OA*. 5:FSO395.

Wang, L., Liu, D., Lv, Y., Cui, L., Li, Y., Li, T., et al. (2019). Novel plasmid-mediated tet(X5) gene conferring resistance to tigecycline, eravacycline and omadacycline in clinical *Acinetobacter baumannii*. *Antimicrob Agents Chemother*. 64:e013 26-19.

Xu, C., Bilya, S. R., and Xu, W. (2019). adeABC efflux gene in *Acinetobacter baumannii*. *New Microbes New Infect.* 30:100549. doi: 10.1016/j.nmni.2019.100549

Yang, Y. S., Chen, H. Y., Hsu, W. J., Chou, Y. C., Perng, C. L., Shang, H. S., et al. (2019). Overexpression of AdeABC efflux pump associated with tigecycline resistance in clinical *Acinetobacter nosocomialis* isolates. *Clin. Microbiol. Infect.* 512, e511–e512.

Yoon, E. J., Courvalin, P., and Grillot-Courvalin, C. (2013). RND-type efflux pumps in multidrug-resistant clinical isolates of *Acinetobacter baumannii*: major role for AdeABC overexpression and AdeRS mutations. *Antimicrob Agents Chemother* 57, 2989–2995. doi: 10.1128/aac.02556-12

Zhanel, G. G., Baxter, M. R., Adam, H. J., Sutcliffe, J., and Karlowsky, J. A. (2018). In vitro activity of eravacycline against 2213 Gram-negative and 2424 Gram-positive bacterial pathogens isolated in Canadian hospital laboratories: CANWARD surveillance study 2014-2015. *Diagn. Microbiol. Infect. Dis.* 91, 55–62. doi: 10.1016/j.diagmicrobio.2017.12.013

Conflict of Interest: The authors declare that the research was conducted in the absence of any commercial or financial relationships that could be construed as a potential conflict of interest.

frontiers in Microbiology

ORIGINAL RESEARCH
published: 10 November 2020
doi: 10.3389/fmicb.2020.589253

First Report of New Delhi Metallo-β-Lactamase-6 (NDM-6) in a Clinical *Acinetobacter baumannii* Isolate From Northern Spain

*Kyriaki Xanthopoulou[1,2†], Mikel Urrutikoetxea-Gutiérrez[3†], Matxalen Vidal-Garcia[3], José-Luis Diaz de Tuesta del Arco[3], Sandra Sánchez-Urtaza[4], Julia Wille[1,2], Harald Seifert[1,2], Paul G. Higgins[1,2] and Lucía Gallego[4]**

[1]Institute for Medical Microbiology, Immunology and Hygiene, University of Cologne, Cologne, Germany, [2]German Centre for Infection Research (DZIF), Partner Site Bonn-Cologne, Cologne, Germany, [3]Servicio de Microbiología y Control de Infección, Hospital Universitario Basurto, Biocruces Bizkaia Health Research Institute, Barakaldo, Spain, [4]Department of Immunology, Microbiology, and Parasitology, Faculty of Medicine and Nursing, University of the Basque Country UPV/EHU, Bilbao, Spain

OPEN ACCESS

Edited by:
Benjamin Andrew Evans, University of East Anglia, United Kingdom

Reviewed by:
Xiaojiong Jia, Harvard Medical School, United States
Maria Soledad Ramirez, California State University, United States

***Correspondence:**
Lucía Gallego
lucia.gallego@ehu.es

[†]These authors have contributed equally to this work

Specialty section:
This article was submitted to Antimicrobials, Resistance and Chemotherapy, a section of the journal Frontiers in Microbiology

Received: *30 July 2020*
Accepted: *15 October 2020*
Published: *10 November 2020*

Citation:
Xanthopoulou K, Urrutikoetxea-Gutiérrez M, Vidal-Garcia M, Diaz de Tuesta del Arco J-L, Sánchez-Urtaza S, Wille J, Seifert H, Higgins PG and Gallego L (2020) First Report of New Delhi Metallo-β-Lactamase-6 (NDM-6) in a Clinical Acinetobacter baumannii Isolate From Northern Spain. Front. Microbiol. 11:589253. doi: 10.3389/fmicb.2020.589253

The objective of this study was the phenotypic and genotypic characterization of a carbapenem resistant *Acinetobacter baumannii* (CRAB) isolate. The isolate, recovered in Northern Spain in 2019, was identified by MALDI-TOF to the species level. Antimicrobial susceptibility testing was performed using the Phoenix BD NMIC-502 Panel, E-test, and broth microdilution methods. The presence of a metallo-β-lactamase (MBL) was verified by PCR and immunochromatographic assays. The genetic location of the MBL was confirmed using S1-pulsed-field gel electrophoresis (S1-PFGE) followed by Southern blot hybridization. Whole genome sequencing (WGS) was completed using the Miseq and MinION platforms, followed by core-genome MLST (cgMLST) and seven-locus MLST analysis. The CRAB was assigned ST85 (Pasteur scheme) and ST957 (Oxford scheme) representing international clone (IC) 9 and harbored the intrinsic β-lactamase OXA-94 with IS*Aba1* upstream of it, and the MBL bla_{NDM-6}. Hybridization experiments revealed that the bla_{NDM-6} was encoded on the chromosome. Using WGS the bla_{NDM-6} environment could be identified arranged in the following order: IS*Aba14*, *aphA6*, IS*Aba125*, bla_{NDM-6}, ble_{MBL}, *trpF*, *dsbC*, *cutA*, and IS*Aba14*. Downstream, a 10,462 bp duplication was identified, including a second copy of bla_{NDM-6} in the following genetic composition: IS*Aba125*, bla_{NDM-6}, ble_{MBL}, *trpF*, *dsbC*, *cutA*, and IS*Aba14*. To our knowledge, this is the first description of bla_{NDM-6} in *A. baumannii*. The MBL was present in two copies in the chromosome in a new genetic environment associated with IS elements highlighting the contribution of mobile genetic elements in the dissemination of this gene.

Keywords: carbapenemase, whole genome sequencing, long reads, NDM-6, *Acinetobacter baumannii*

INTRODUCTION

Infections caused by multidrug-resistant *Acinetobacter baumannii* have become a health care challenge worldwide (Peleg et al., 2008; Higgins et al., 2010). Carbapenems are often the antimicrobials of choice of treatment of *A. baumannii* infections; however, their use has led to the development of carbapenem resistance front-line antimicrobial agents (Tal-Jasper et al., 2016). In 2019, the World Health Organization (WHO) classified carbapenem resistant *A. baumannii* (CRAB) as one of the "Priority 1: Critical group" organisms for which new

antimicrobials are urgently needed.[1] Carbapenem resistance in *A. baumannii* is mainly mediated through acquired carbapenem-hydrolyzing class D ß-lactamases (oxacillinases), encoded by $bla_{\text{OXA-23-like}}$, $bla_{\text{OXA-40-like}}$, $bla_{\text{OXA-58-like}}$, $bla_{\text{OXA-143-like}}$, and $bla_{\text{OXA-235-like}}$ (Higgins et al., 2013; Evans and Amyes, 2014). There are two pillars of CRAB prevailing; the widespread international clone 2 (IC2) isolates, and the most prevalent carbapenemase in the species, OXA-23 (Higgins et al., 2010; Tomaschek et al., 2016; Müller et al., 2019). Class B metallo-β-lactamases (MBLs), such as IMP, VIM, SIM, and NDM are less frequently reported in CRAB isolates (Müller et al., 2019). Nevertheless, MBL-positive *A. baumannii* are increasingly reported worldwide (Kaase et al., 2011; Pfeifer et al., 2011; Berrazeg et al., 2014; Karampatakis et al., 2017; Adams et al., 2020; Ramirez et al., 2020).

The emergence of NDM-type carbapenemases, hampering the efficacy of almost all β-lactams, including carbapenems, is of great medical concern. The main reservoir of NDM-like producers is the Indian subcontinent, the Balkans region, and the Middle East (Dortet et al., 2014; Khan et al., 2017). Since the first description of NDM-1, 29 variants have been reported, mainly in members of the Enterobacterales family, such as *Escherichia coli* and *Klebsiella pneumoniae*, but also in *A. baumannii* (e.g., NDM-1, −2, −3, −4, −5, and −7) and *Acinetobacter lwoffii*[2] (e.g., NDM-14; Elbrolosy et al., 2019).

The aim of the present study was the phenotypic and genotypic characterization of a CRAB isolate harboring $bla_{\text{NDM-6}}$ recovered from a patient in Northern Spain.

MATERIALS AND METHODS

Patient and Bacterial Isolate Data, Species Identification, and Antimicrobial Susceptibility Testing

A 70–74 year-old patient, from Maghreb (Northwest Africa) presented to the Hospital de Basurto (Bilbao, Northern Spain) with dysuria in September 2019. The patient had a positive urine culture with >100.000 CFU/ml of a Gram-negative bacillus and reported a previous hospitalization in his home country due to a prostatectomy. Unfortunately, no further data were available about the country of origin.

Species identification of the isolate AbBAS-1 was performed by MALDI-TOF mass spectrometry (Bruker Daltonics, Madrid, Spain) and biochemically with the Phoenix BD UNMIC/ID-409 Panel (Becton Dickinson, Madrid, Spain). Antimicrobial susceptibility testing was performed using the Phoenix BD NMIC-502 Panel, while susceptibility to colistin was tested using the microdilution UMIC kit (Biocentric, Bandol, France). Susceptibility to tigecycline (Molekula, Newcastle upon Tyne, United Kingdom) was also determined using broth microdilution following CLSI guidelines (CLSI, 2019). Finally, susceptibility to imipenem and meropenem was determined by Etest (bioMérieux, Nürtingen, Germany). Minimal inhibitory concentration (MIC) were interpreted using the resistance breakpoints for *Acinetobacter* spp. from EUCAST (Version 10.0, January 2020, http://www.eucast.org/clinical_breakpoints/). For tigecycline, the EUCAST PK-PD (Non-species related) breakpoint of 0.5 mg/L was used.

Detection of Carbapenemase-Encoding Genes

The presence of the carbapenemase-encoding genes $bla_{\text{OXA-51-like, −23-like, −58-like, −40-like, −143-like, and −235-like}}$ was investigated by PCR (Woodford et al., 2006; Higgins et al., 2010, 2013). MBLs genes were investigated by in-house PCRs targeting the genes: bla_{VIM}, bla_{IMP}, and bla_{NDM}. Positive PCR products were purified by mi-PCR purification kit (Metabion, Planegg, Germany) and allelic variants were determined by Sanger sequencing followed by NCBI BLAST analysis. The presence of an MBL was phenotypically confirmed using the Total Metallo-beta-lactamase Confirm Kit (Rosco Diagnostica A/S, Taastrup, Denmark) and the Phoenix BD NMIC-502 Panel followed by an immunochromatographic assay NG-test Carba 5a (NG Biotech, Guipry, France).

S1-Pulsed-Field Gel Electrophoresis and Southern Blot Hybridization

Bacterial DNA embedded in agarose plugs was digested using 50 units S1-nuclease (Thermo Fisher Scientific, Waltham, MA, United States) per plug slice and followed by pulsed-field gel electrophoresis (PFGE). Samples were run on a CHEF-DR II system (Bio-Rad, Munich, Germany) for 17 h at 6 V/cm and 14°C, while initial and final pulses of 4 and 16 s, respectively, were applied. The Lambda PFG and λ DNA-Mono Cut Mix (New England Biolabs, Frankfurt, Germany) were used as markers. Southern blot hybridization was performed to determine the plasmid/chromosomal location by hybridization with digoxigenin-labeled probes (Roche, Mannheim, Germany). A $bla_{\text{NDM-6}}$ specific probe was generated and the chromosomal location was shown by colocalization with a $bla_{\text{OXA-51-like}}$ probe. Signal detection was performed using CDP-Star® ready-to-use (Roche) chemiluminescent substrate by autoradiography on X-ray film (GE Healthcare, Buckinghamshire, United Kingdom).

Electroporation Experiments

To determine the transferability of $bla_{\text{NDM-like}}$ variants, plasmid DNA isolated from AbBAS-1 using the QIAprep Spin Miniprep Kit (Qiagen, Hilden, Germany) and electroporated into the reference strain *A. baumannii* ATCC 17978. Selection of *A. baumannii* transformants was performed on Luria-Bertani agar (Oxoid, Wesel, Germany) supplemented with ticarcillin (150 mg/L). The presence of $bla_{\text{NDM-like}}$ in the obtained transformants was confirmed by PCR.

Whole Genome Sequencing

Total DNA was extracted using the MagAttract HMW DNA Kit (Qiagen) according to manufacturer's instructions and used for short-read sequencing. Sequencing libraries were prepared

[1]https://www.cdc.gov/drugresistance/pdf/threats-report/2019-ar-threats-report-508.pdf
[2]http://www.bldb.eu/BLDB.php?prot=B1#NDM

using a Nextera XT library prep kit (Illumina GmbH, Munich, Germany) for a 250 bp paired-end sequencing run on an Illumina MiSeq platform. The obtained reads were *de novo* assembled with the Velvet assembler integrated in the Ridom SeqSphere+ v. 7.0.4 software (Ridom GmbH, Münster, Germany).

DNA extraction for long-read sequencing was performed using the Genomic-Tips 100/G kit and Genomic DNA Buffers kit (Qiagen) according to the manufacturer's instructions. Libraries were prepared using the 1D Ligation Sequencing Kit (SQK-LSK109) in combination with Native Barcoding Kit (EXP-NBD104; Oxford Nanopore Technologies, Oxford, United Kingdom) and were loaded onto a R9.4 flow cell (Oxford Nanopore Technologies). The run was performed on a MinION MK1b device. Collection of raw electronic signal data and live base-calling was performed using the MinKNOW software and the Guppy basecaller (Oxford Nanopore Technologies). The long-reads were assembled using ONT assembly and Illumina polishing pipeline (Oxford Nanopore Technologies), performing Canu assembly followed by polishing steps, including pilon and BWA mem mapping using the Illumina reads.[3]

Molecular Typing, Genome Annotation, Analysis and Visualization

Multi-locus sequence typing (MLST) was performed using the Oxford and Pasteur typing schemes[4] to assign the sequence type (ST). Clonal complexes (CCs) were assigned using the BURST function available at pubmlst.org. The $bla_{\text{OXA-51-like}}$ variant combined with the CCs derived from both schemes and core-genome MLST (cgMLST) analysis, using the Ridom SeqSphere+ v. 7.0.4 software, were used to assign the isolate to an IC (Higgins et al., 2017).

The resistome of the bacterial isolate was identified using ResFinder v.3.2.0 (Zankari et al., 2012). Capsular polysaccharide-type (KL-type) and the outer core of the lipooligopolisacharide (OCL-type) were assigned using Kaptive Web (Wick et al., 2018). The motility phenotype was analyzed on 0.5% agarose plates, supplemented with 5 g/l tryptone, 2.5 g/l NaCl, and pH 7.4, inoculated on the surface and incubated overnight at 37°C (Skiebe et al., 2012). Prophage-related sequences were screened using the PHASTER tool and virulence factors using virulence factor database (VFDB; Arndt et al., 2016; Liu et al., 2019). The genome was annotated using Prokka integrated in the Galaxy web platform[5] and partially manually edited. SnapGene and SnapGene Viewer (from Insightful Science; available at snapgene.com) were used to predict open reading frames (ORF) and for genome visualization.

RESULTS AND DISCUSSION

The bacterial isolate AbBAS-1 was identified by MALDI-TOF and WGS as *A. baumannii*. Antimicrobial susceptibility testing revealed that the isolate was resistant to all tested antimicrobial agents except for amikacin (MIC <=4 mg/L), colistin (MIC <=0.5 mg/L), and tigecycline (MIC 0.5 mg/L; **Table 1**). Using phenotypical tests, a halo difference of 10 mm between the meropenem disk and both the dipicolinic acid and EDTA disks was observed, suggesting the presence of a MBL. The UNMIC/ID-409 signaled the presence of a carbapenemase and the NMIC-502 and lateral flow immunochromatography identified it as a class B carbapenemase, while, by lateral flow immunochromatography the MBL was identified as part of the NDM-β-lactamase complex.

Sequencing identified the carbapenemase as $bla_{\text{NDM-6}}$, which differs from $bla_{\text{NDM-1}}$ in one amino acid substitution (A233V). New Delhi Metallo-β-Lactamase-6 (NDM-6) has a similar hydrolyzing activity as NDM-1 and has been mainly reported in members of the Enterobacterales family to date (Williamson et al., 2012; Rahman et al., 2014; Bahramian et al., 2019). NDM-1-like derivative enzymes have been reported in carbapenem resistant Gram-negative organisms from multiple countries worldwide (Berrazeg et al., 2014; Dortet et al., 2014) including European countries, e.g., Germany, Switzerland, Slovenia, France, Belgium, Czech Republic, and very recently also in Southern Spain (Pfeifer et al., 2011; Bonnin et al., 2012; Fernandez-Cuenca et al., 2020). However, in the region of the Basque Country (Northern Spain), no NDM-like-enzymes have been previously reported. Our isolate AbBAS-1 was resistant to all β-lactams tested but also to fluoroquinolones and aminoglycosides, these findings are consistent with other NDM-producing isolates limiting the therapeutic options to amikacin, colistin, and tigecycline (Bonnin et al., 2012) or new promising molecules such as cefiderocol (Delgado-Valverde et al., 2020).

The patient had a radical prostatectomy performed in a North African country, where numerous NDM-positive *A. baumannii* isolates have been reported (Berrazeg et al., 2014; Ramoul et al., 2016; Jaidane et al., 2018; Al-Hassan et al., 2019). Unfortunately, there is a lack of a clinical follow up of the patient, who after empiric treatment with cefixime 400 mg/24 h

TABLE 1 | Antimicrobial susceptibility profile of the AbBAS-1 isolate.

Antimicrobial class	Antimicrobial agent	MIC (mg/L)
β-lactam	Amoxicillin-clavulanic acid*	>32/2
	Ertapenem*	>1
	Imipenem[a]	>32
	Meropenem[a]	>32
Aminoglycoside	Gentamicin	>4
	Tobramycin	>4
	Amikacin	<=4
Fluoroquinolone	Ciprofloxacin	>1
	Levofloxacin	>2
	Norfloxacin*	>2
Polymyxin	Colistin[b]	<=0.5
Tetracycline	Tigecycline*,[b]	0.5
Other	Fosfomycin*	>128
	Nitrofurantoin*	>64
	Trimethoprim-sulfamethoxazole	>4/76

*No breakpoint available.
[a]Tested by E-test.
[b]Tested by broth microdilution method.

[3]https://github.com/nanoporetech/ont-assembly-polish
[4]https://pubmlst.org/abaumannii/
[5]https://usegalaxy.org/

never consulted again the Basque Public Health System (Osakidetza). Because up until now NDM-6 has not been identified in Spain, we speculate that the patient acquired the NDM-6-positive CRAB isolate during his previous hospitalization in Northern Africa.

The AbBAS-1 isolate has been assigned as ST85^{Pas} (Pasteur scheme) and ST957^{Ox} (Oxford scheme) and harbored the $bla_{OXA\text{-}51\text{-}like}$ variant $bla_{OXA\text{-}94}$. Furthermore, AbBAS-1 belonged to the clonal complex CC464^{Pas} and CC1078^{Ox} and could be assigned to the recently described IC9 (Müller et al., 2019). The novel IC9 was previously identified in *A. baumannii* isolates recovered between 2012 and 2016 in Belgium ($bla_{NDM\text{-}1}$-positive), Egypt ($bla_{OXA\text{-}23}$-positive), Italy ($bla_{NDM\text{-}1}$-positive), and Pakistan ($bla_{OXA\text{-}23}$-positive; Müller et al., 2019). ST85 *A. baumannii*, carrying $bla_{OXA\text{-}94}$ and $bla_{NDM\text{-}1}$, recovered from Syrian civil war victims were first reported from Lebanon (Rafei et al., 2014). Furthermore, isolates encoding $bla_{OXA\text{-}94}$ and $bla_{NDM\text{-}1}$ were also reported from Southern Spain, Saudi Arabia, and Tunisia, or harboring $bla_{VIM\text{-}1}$ in Egypt, indicating that the novel IC9 clonal lineage has a widespread distribution and was found repeatedly harboring MBLs (Jaidane et al., 2018; Al-Hassan et al., 2019; Al-Hamad et al., 2020; Fernandez-Cuenca et al., 2020). cgMLST analysis using currently available complete genomes of ST85^{Pas} *A. baumannii* isolates revealed that the AbBAS-1 isolate is closely related (81 alleles difference) to an NDM-1-positive CRAB isolated in Southern Spain in 2017 (**Supplementary Figure 1**).

Attempts to transfer the $bla_{NDM\text{-}6}$ by electroporation experiments were not successful, suggesting that the MBL was encoded on the chromosome. S1-PFGE and Southern blot experiments confirmed that $bla_{NDM\text{-}6}$ was encoded on the chromosome. Using WGS the $bla_{NDM\text{-}6}$ environment could be identified arranged in the following order: IS*Aba14*, *aphA6*, IS*Aba125*, $bla_{NDM\text{-}6}$, ble_{MBL} (resistance to bleomycin), *trpF* (phosphoribosylanthranilate isomerase), *dsbC* (tat twin-arginine translocation pathway signal sequence domain protein), *cutA* (periplasmic divalent cation tolerance protein), and IS*Aba14* (**Figure 1**). By BLASTn, the genetic environment of NMD-6 showed 99% similarity to an ST1089^{Ox} *A. baumannii* isolated in India in 2018 (Acc. No. CP038644), a single locus variant of ST957^{Ox} with $bla_{OXA\text{-}94}$, and which harbored a single copy of NDM-1. Further downstream, a 10,462 bp duplication was identified including a second copy of $bla_{NDM\text{-}6}$ in the following genetic composition: IS*Aba125*, $bla_{NDM\text{-}6}$, ble_{MBL}, *trpF*, *dsbC*, *cutA*, and IS*Aba14* (**Figure 1**). The genetic environment of the second MBL was missing the type VI aminoglycoside phosphotransferase. The IS*Aba125* located directly upstream of both copies of $bla_{NDM\text{-}6}$ could indicate that the two copies of the MBL were the result of duplication mediated through the mobile genetic element IS*Aba125* (IS30 family). IS element members of the family IS*30* are known to transpose by a copy-and-paste mechanism (Szabo et al., 2010). Upstream of the *aphA6* and $bla_{NDM\text{-}6}$ a gene (colored green in **Figure 1**) truncated in three fragments was identified and was identical to an ATP-binding protein from an *A. baumannii* (Acc. No. CP038644.1) with the locus tag E5D09_10165. Particularly, 480 bp of the 5' end of the ATP-binding protein containing the start codon were located upstream of the IS*Aba33*, which is followed directly by the next 44 bp of the ATP-binding protein. The 711 bp of the 3' end were found directly downstream of the second copy of IS*Aba14*. Another copy of the 711 bp of the 3' end was also present 9,7 kb downstream supporting the finding of the duplication of the genetic environment of the $bla_{NDM\text{-}6}$.

The AbBAs-1 isolate harbored in addition to $bla_{NDM\text{-}6}$ the intrinsic, ADC-158-like (with no insertion element upstream), *ant(2'')-Ia*-like, *aph(3')-VI*, *mph(E)*, *msr(E)* antibiotic resistance determinants, while upstream of the $bla_{OXA\text{-}94}$ IS*Aba1* was located. The isolate AbBAS-1 also presents an S81L substitution in DNA gyrase subunit A and S84L substitution in ParC, which are known to be associated with fluoroquinolone resistance. By typing the capsular polysaccharide (K and/or O-antigen), which is a critical determinant of virulence, the AbBAS-1 isolate was assigned as KL77, a KL type previously reported in ST2 and ST10 isolates, and OCL6 the third most common OCL type in *A. baumannii*. In accordance to recent studies that have found K & O-antigen diversity within members belonging to the same clone, capsule typing is a promising epidemiological marker in combination with MLST (Wyres et al., 2020). Of note is the mucoviscous phenotype of the AbBAS-1 colonies when grown on agar plates generating a viscous string >5 mm in length between a colony and a inoculation loop (string test), a phenotype that has been associated with hypervirulent *K. pneumoniae* strains (Fang et al., 2004). In addition, the *A. baumannii* isolate exhibited a nonmotile phenotype. Phage analysis identified in the AbBAS-1 two questionable phage regions both similar to *Acinetobacter* phage YMC/09/02/B1251_ABA_BP (Acc. No. NC_019541.1) and an incomplete phage region similar to *Pseudomonas* phage nickie (Acc. No. NC_042091.1). Virulence factors known to be associated with *A. baumannii* have been identified using VFDB and included genes linked with adherence (*ompA*); biofilm formation (*csuE*, *csuC*, *csuB*, *csuA*, *csuA/B*, *pgaD*, *pgaC*, *pgaB*, and *pgaA*); regulation (*bfmR*, *bfmS*, *abaI*, and *abaR*); phospholipases (*plc*, *plcD*); and iron uptake (*basJ*, *basI*, *basH*, *barB*, *barA*, *basG*, *basF*, *entE*, *basD*, *basC*, *bauB*, *bauE*, *bauC*, *basB*, *basA*, and *bauF*).

In conclusion, to the best of our knowledge, this is the first report of $bla_{NDM\text{-}6}$ in an *A. baumannii* isolate. The CRAB isolate encoded two copies of $bla_{NDM\text{-}6}$ in close proximity with IS*Aba125*. The carbapenemase NDM-6 has been detected in a ST85^{Pas} multidrug-resistant isolate belonging to the recently described IC9. The present study highlights the complexity and diversity of the genetic environment of NDM-1-like enzymes contributing to its dissemination. The emergence of NDM-6 in an *A. baumannii* clinical isolate highlights the need of surveillance studies and exhaustive control to prevent its spread in the clinical setting. The implementation of infection control measures should also be a priority to fight against multidrug-resistant isolates in the nosocomial environment.

DATA AVAILABILITY STATEMENT

The assembled genome generated in this project has been deposited in the NCBI and we are awaiting for processing to include the accession number in the manuscript.

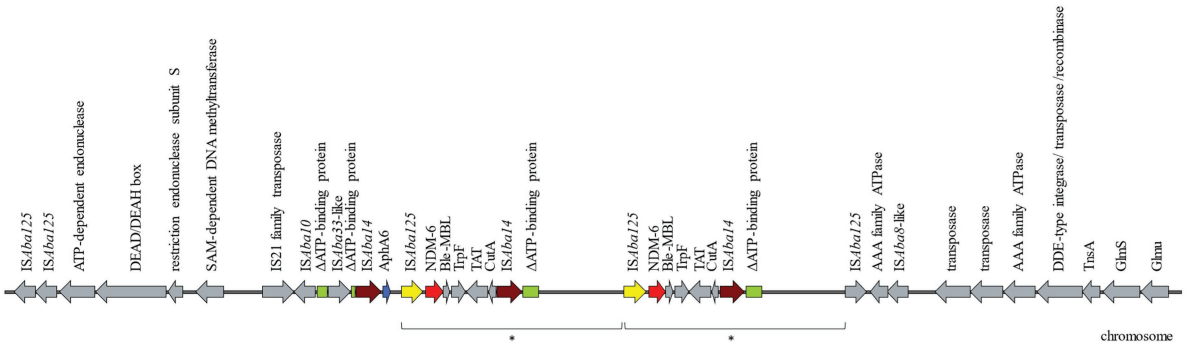

FIGURE 1 | Schematic diagram of the genetic environment of bla_{NDM-6} in the *Acinetobacter baumannii* AbBAS-1 isolate. Arrows indicate the deduced open reading frames (ORFs) and their orientations. The region marked with the asterisk represents a 10,462 bp duplication. Hypothetical proteins are not shown.

ETHICS STATEMENT

Ethical approval for this study was obtained from the clinical research ethics committee of the Hospital Universitario de Basurto-OSI Bilbao Basurto, Northern Spain.

AUTHOR CONTRIBUTIONS

KX, MU-G, PGH, and LG contributed to the design of the experiments. KX, JW, MU-G, and SS-U performed the experiments. KX, JW, HS, PGH, and LG analyzed and interpreted the data. KX, PGH, and LG wrote the manuscript. MU-G, MV-G, and J-LD were responsible for the clinical follow up of the patient, and identification of the isolate and the resistance profile. MU-G also contributed to the preliminary sequence analysis and capsule sequence typing. All authors contributed to the article and approved the submitted version.

FUNDING

SS-U was supported by the University of the Basque Country UPV/EHU (Bilbao, Spain). KX was supported by the German Centre for Infection Research (DZIF), Partner Site Bonn-Cologne, Cologne, Germany.

ACKNOWLEDGMENTS

The authors would like to thank the University of the Basque Country UPV/EHU and Hospital de Basurto for financial support.

SUPPLEMENTARY MATERIAL

The Supplementary Material for this article can be found online at: https://www.frontiersin.org/articles/10.3389/fmicb.2020.589253/full#supplementary-material

Supplementary Figure 1 | Minimum spanning tree generated using Ridom SeqSphere+ for the six ST85Pas *A. baumannii* NDM-positive isolates. Each colored circle represents one individual isolate based on sequence analysis of 2390 cgMLST target genes. Information about the five publicly available isolates: Ab-NDM-1 (Acc. No. NZ_QBBY00000000) recovered in Spain in 2017, AB0964 (available at the https://pubmlst.org under the id 5019) recovered in Singapore, ACMH-6200 (Acc. No. LKMA00000000) recovered in Lebanon in 2012, ACN21 (Acc. No. CP038644) recovered in India in 2018 and MBL_M1 (Acc. No. MWTR00000000) recovered in Tunisia in 2013.

REFERENCES

Adams, M. D., Pasteran, F., Traglia, G. M., Martinez, J., Huang, F., Liu, C., et al. (2020). Distinct mechanisms of dissemination of NDM-1 metallo-beta-lactamase in *Acinetobacter* species in Argentina. *Antimicrob. Agents Chemother.* 64:e00324–20. doi: 10.1128/aac.00324-20

Al-Hamad, A., Pal, T., Leskafi, H., Abbas, H., Hejles, H., Alsubikhy, F., et al. (2020). Molecular characterization of clinical and environmental carbapenem resistant *Acinetobacter baumannii* isolates in a hospital of the eastern region of Saudi Arabia. *J. Infect. Public Health* 13, 632–636. doi: 10.1016/j.jiph.2019.08.013

Al-Hassan, L., Zafer, M. M., and El-Mahalla, H. (2019). Multiple sequence types responsible for healthcare-associated *Acinetobacter baumannii* dissemination in a single Centre in Egypt. *BMC Infect. Dis.* 19:829. doi: 10.1186/s12879-019-4433-1

Arndt, D., Grant, J. R., Marcu, A., Sajed, T., Pon, A., Liang, Y. J., et al. (2016). Phaster: a better, faster version of the phast phage search tool. *Nucleic Acids Res.* 44, W16–W21. doi: 10.1093/nar/gkw387

Bahramian, A., Shariati, A., Azimi, T., Sharahi, J. Y., Bostanghadiri, N., Gachkar, L., et al. (2019). First report of New Delhi metallo-beta-lactamase-6 (NDM-6) among *Klebsiella pneumoniae* ST147 strains isolated from dialysis patients in Iran. *Infect. Genet. Evol.* 69, 142–145. doi: 10.1016/j.meegid.2019.01.030

Berrazeg, M., Diene, S. M., Medjahed, L., Parola, P., Drissi, M., Raoult, D., et al. (2014). New Delhi metallo-beta-lactamase around the world: an eReview using google maps. *Euro Surveill.* 19:20809. doi: 10.2807/1560-7917.es2014.19.20.20809

Bonnin, R. A., Poirel, L., Naas, T., Pirs, M., Seme, K., Schrenzel, J., et al. (2012). Dissemination of New Delhi metallo-ss-lactamase-1-producing *Acinetobacter baumannii* in Europe. *Clin. Microbiol. Infect.* 18, E362–E365. doi: 10.1111/j.1469-0691.2012.03928.x

CLSI (2019). *Performance standards for antimicrobial susceptibility testing. 29th Edn.* Wayne, PA, USA: Clinical and Laboratory Standards Institute.

Delgado-Valverde, M., Conejo, M. D., Serrano, L., Fernandez-Cuenca, F., and Pascual, A. (2020). Activity of cefiderocol against high-risk clones of multidrug-resistant *Enterobacterales*, *Acinetobacter baumannii*, *Pseudomonas aeruginosa*

and *Stenotrophomonas maltophilia*. *J. Antimicrob. Chemother.* 75, 1840–1849. doi: 10.1093/jac/dkaa117

Dortet, L., Poirel, L., and Nordmann, P. (2014). Worldwide dissemination of the NDM-type carbapenemases in gram-negative bacteria. *Biomed Res. Int.* 2014:249856. doi: 10.1155/2014/249856

Elbrolosy, A. M., Labeeb, A. Z., and Hassan, D. M. (2019). New Delhi metallo-beta-lactamase-producing *Acinetobacter* isolates among late-onset VAP patients: multidrug-resistant pathogen and poor outcome. *Infect. Drug Resist.* 12, 373–384. doi: 10.2147/IDR.S186924

Evans, B. A., and Amyes, S. G. B. (2014). OXA beta-lactamases. *Clin. Microbiol. Rev.* 27, 241–263. doi: 10.1128/CMR.00117-13

Fang, C. T., Chuang, Y. P., Shun, C. T., Chang, S. C., and Wang, J. T. (2004). A novel virulence gene in *Klebsiella pneumoniae* strains causing primary liver abscess and septic metastatic complications. *J. Exp. Med.* 199, 697–705. doi: 10.1084/jem.20030857

Fernandez-Cuenca, F., Perez-Palacios, P., Galan-Sanchez, F., Lopez-Cerero, L., Lopez-Hernandez, I., Rojas, R. L., et al. (2020). First identification of Bla(NDM-1) carbapenemase in Bla(OXA-94)-producing *Acinetobacter baumannii* ST85 in Spain. *Enferm. Infecc. Microbiol. Clin.* 38, 11–15. doi: 10.1016/j.eimc.2019.03.008

Higgins, P. G., Dammhayn, C., Hackel, M., and Seifert, H. (2010). Global spread of carbapenem-resistant *Acinetobacter baumannii*. *J. Antimicrob. Chemother.* 65, 233–238. doi: 10.1093/jac/dkp428

Higgins, P. G., Lehmann, M., and Seifert, H. (2010). Inclusion of OXA-143 primers in a multiplex polymerase chain reaction (PCR) for genes encoding prevalent OXA carbapenemases in *Acinetobacter* spp. *Int. J. Antimicrob. Agents* 35:305. doi: 10.1016/j.ijantimicag.2009.10.014

Higgins, P. G., Perez-Llarena, F. J., Zander, E., Fernandez, A., Bou, G., and Seifert, H. (2013). OXA-235, a novel class D beta-lactamase involved in resistance to carbapenems in *Acinetobacter baumannii*. *Antimicrob. Agents Chemother.* 57, 2121–2126. doi: 10.1128/AAC.02413-12

Higgins, P. G., Prior, K., Harmsen, D., and Seifert, H. (2017). Development and evaluation of a core genome multilocus typing scheme for whole-genome sequence-based typing of *Acinetobacter baumannii*. *PLoS One* 12:e0179228. doi: 10.1371/journal.pone.0179228

Jaidane, N., Naas, T., Oueslati, S., Bernabeu, S., Boujaafar, N., Bouallegue, O., et al. (2018). Whole-genome sequencing of NDM-1-producing ST85 *Acinetobacter baumannii* isolates from Tunisia. *Int. J. Antimicrob. Agents* 52, 916–921. doi: 10.1016/j.ijantimicag.2018.05.017

Kaase, M., Nordmann, P., Wichelhaus, T. A., Gatermann, S. G., Bonnin, R. A., and Poirel, L. (2011). NDM-2 carbapenemase in *Acinetobacter baumannii* from Egypt. *J. Antimicrob. Chemother.* 66, 1260–1262. doi: 10.1093/jac/dkr135

Karampatakis, T., Antachopoulos, C., Tsakris, A., and Roilides, E. (2017). Molecular epidemiology of carbapenem-resistant *Acinetobacter baumannii* in Greece: an extended review (2000-2015). *Future Microbiol.* 12, 801–815. doi: 10.2217/fmb-2016-0200

Khan, A. U., Maryam, L., and Zarrilli, R. (2017). Structure, genetics and worldwide spread of New Delhi metallo-beta-lactamase (NDM): a threat to public health. *BMC Microbiol.* 17:101. doi: 10.1186/s12866-017-1012-8

Liu, B., Zheng, D. D., Jin, Q., Chen, L. H., and Yang, J. (2019). VFDB 2019: a comparative pathogenomic platform with an interactive web interface. *Nucleic Acids Res.* 47, D687–D692. doi: 10.1093/nar/gky1080

Müller, C., Stefanik, D., Wille, J., Hackel, M., Higgins, P.G., and Siefert, H. (2019). Molecular epidemiology of carbapenem-resistant *Acinetobacter baumannii* clinical isolates and identification of the novel international clone IC9: results from a worldwide surveillance study (2012–2016). Paper presented at the ECCMID 2019: Proceeding of the 29th European Congress of Clinical Microbiology & Infectious Diseases Amsterdam, Netherlands. April 13–16, 2019.

Peleg, A. Y., Seifert, H., and Paterson, D. L. (2008). *Acinetobacter baumannii*: emergence of a successful pathogen. *Clin. Microbiol. Rev.* 21, 538–582. doi: 10.1128/cmr.00058-07

Pfeifer, Y., Wilharm, G., Zander, E., Wichelhaus, T. A., Gottig, S., Hunfeld, K. P., et al. (2011). Molecular characterization of Bla(NDM-1) in an *Acinetobacter baumannii* strain isolated in Germany in 2007. *J. Antimicrob. Chemother.* 66, 1998–2001. doi: 10.1093/jac/dkr256

Rafei, R., Dabboussi, F., Hamze, M., Eveillard, M., Lemarie, C., Mallat, H., et al. (2014). First report of Bla(NDM-1)-producing *Acinetobacter baumannii* isolated in Lebanon from civilians wounded during the Syrian war. *Int. J. Infect. Dis.* 21, 21–23. doi: 10.1016/j.ijid.2014.01.004

Rahman, M., Shukla, S. K., Prasad, K. N., Ovejero, C. M., Pati, B. K., Tripathi, A., et al. (2014). Prevalence and molecular characterisation of New Delhi metallo-beta-lactamases NDM-1, NDM-5, NDM-6 and NDM-7 in multidrug-resistant Enterobacteriaceae from India. *Int. J. Antimicrob. Agents* 44, 30–37. doi: 10.1016/j.ijantimicag.2014.03.003

Ramirez, M. S., Bonomo, R. A., and Tolmasky, M. E. (2020). Carbapenemases: transforming *Acinetobacter baumannii* into a yet more dangerous menace. *Biomolecules* 10:720. doi: 10.3390/biom10050720

Ramoul, A., Loucif, L., Bakour, S., Amiri, S., Dekhil, M., and Rolain, J. M. (2016). Co-occurrence of Bla(NDM-1) with Bla(OXA-23) or Bla(OXA-58) in clinical multidrug-resistant *Acinetobacter baumannii* isolates in Algeria. *J. Glob. Antimicrob. Resist.* 6, 136–141. doi: 10.1016/j.jgar.2016.05.003

Skiebe, E., de Berardinis, V., Morczinek, P., Kerrinnes, T., Faber, F., Lepka, D., et al. (2012). Surface-associated motility, a common trait of clinical isolates of *Acinetobacter baumannii*, depends on 1,3-diaminopropane. *Int. J. Med. Microbiol.* 302, 117–128. doi: 10.1016/j.ijmm.2012.03.003

Szabo, M., Kiss, J., and Olasz, F. (2010). Functional organization of the inverted repeats of IS30. *J. Bacteriol.* 192, 3414–3423. doi: 10.1128/jb.01382-09

Tal-Jasper, R., Katz, D. E., Amrami, N., Ravid, D., Avivi, D., Zaidenstein, R., et al. (2016). Clinical and epidemiological significance of carbapenem resistance in *Acinetobacter baumannii* infections. *Antimicrob. Agents Chemother.* 60, 3127–3131. doi: 10.1128/aac.02656-15

Tomaschek, F., Higgins, P. G., Stefanik, D., Wisplinghoff, H., and Seifert, H. (2016). Head-to-head comparison of two multi-locus sequence typing (MLST) schemes for characterization of *Acinetobacter baumannii* outbreak and sporadic isolates. *PLoS One* 11:e0153014. doi: 10.1371/journal.pone.0153014

Wick, R. R., Heinz, E., Holt, K. E., and Wyres, K. L. (2018). Kaptive web: user-friendly capsule and lipopolysaccharide serotype prediction for *klebsiella* genomes. *J. Clin. Microbiol.* 56:e00197–18. doi: 10.1128/JCM.00197-18

Williamson, D. A., Sidjabat, H. E., Freeman, J. T., Roberts, S. A., Silvey, A., Woodhouse, R., et al. (2012). Identification and molecular characterisation of New Delhi metallo-beta-lactamase-1 (NDM-1)- and NDM-6-producing Enterobacteriaceae from New Zealand hospitals. *Int. J. Antimicrob. Agents* 39, 529–533. doi: 10.1016/j.ijantimicag.2012.02.017

Woodford, N., Ellington, M. J., Coelho, J. M., Turton, J. F., Ward, M. E., Brown, S., et al. (2006). Multiplex PCR for genes encoding prevalent OXA carbapenemases in *Acinetobacter* spp. *Int. J. Antimicrob. Agents* 27, 351–353. doi: 10.1016/j.ijantimicag.2006.01.004

Wyres, K. L., Cahill, S. M., Holt, K. E., Hall, R. M., and Kenyon, J. J. (2020). Identification of *Acinetobacter baumannii* loci for capsular polysaccharide (KL) and lipooligosaccharide outer core (OCL) synthesis in genome assemblies using curated reference databases compatible with Kaptive. *Microb. Genom.* 6:e000339. doi: 10.1099/mgen.0.000339

Zankari, E., Hasman, H., Cosentino, S., Vestergaard, M., Rasmussen, S., Lund, O., et al. (2012). Identification of acquired antimicrobial resistance genes. *J. Antimicrob. Chemother.* 67, 2640–2644. doi: 10.1093/jac/dks261

Conflict of Interest: The authors declare that the research was conducted in the absence of any commercial or financial relationships that could be construed as a potential conflict of interest.

frontiers in Microbiology

ORIGINAL RESEARCH
published: 13 November 2020
doi: 10.3389/fmicb.2020.588410

Acinetobacter Plasmids: Diversity and Development of Classification Strategies

Sofia Mindlin[1†], Alexey Beletsky[2†], Andrey Rakitin[2], Andrey Mardanov[2] and Mayya Petrova[1]*

[1] Institute of Molecular Genetics of National Research Centre "Kurchatov Institute", Moscow, Russia, [2] Institute of Bioengineering, Research Center of Biotechnology of the Russian Academy of Sciences, Moscow, Russia

OPEN ACCESS

Edited by:
Benjamin Andrew Evans, University of East Anglia, United Kingdom

Reviewed by:
Víctor González, National Autonomous University of Mexico, Mexico
Jesús Navas, University of Cantabria, Spain
Guillermo Daniel Repizo, CONICET Instituto de Biología Molecular y Celular de Rosario (IBR), Argentina

***Correspondence:**
Mayya Petrova
petrova@img.ras.ru

[†] *These authors have contributed equally to this work*

Specialty section:
This article was submitted to Evolutionary and Genomic Microbiology, a section of the journal Frontiers in Microbiology

Received: *28 July 2020*
Accepted: *23 October 2020*
Published: *13 November 2020*

Citation:
Mindlin S, Beletsky A, Rakitin A, Mardanov A and Petrova M (2020) Acinetobacter Plasmids: Diversity and Development of Classification Strategies. Front. Microbiol. 11:588410. doi: 10.3389/fmicb.2020.588410

Bacteria of the genus *Acinetobacter*, with their numerous species common in various habitats, play a significant role as pathogens. Their ability to adapt to different living conditions is largely due to the presence of numerous plasmids containing the necessary adaptive genes. At the same time the diversity of *Acinetobacter* plasmids and their evolutionary dynamics have not been sufficiently studied. Here, we characterized 44 plasmids isolated from five permafrost *Acinetobacter lwoffii* strains, examined their relationship with plasmids of modern *Acinetobacter* strains and identified groups of related plasmids. For this purpose, we have developed a combined approach for classifying all known *Acinetobacter* plasmids. The classification took into account the size of plasmids, the presence and structure of the *rep* and *mob* genes, as well as the structure of their backbone and accessory regions. Based on the analysis, 19 major groups (lineages) of plasmids were identified, of which more than half were small plasmids. The plasmids of each group have common features of the organization of the backbone region with a DNA identity level of at least 80%. In addition, plasmids of the same group have similarities in the organization of accessory regions. We also described a number of plasmids with a unique structure. The presence of plasmids in clinical strains that are closely related to those of environmental permafrost strains provides evidence of the origin of the former from the latter.

Keywords: relaxases, replication initiator proteins, backbone and accessory regions, phylogenetic analysis, adaptation of bacteria

INTRODUCTION

A number of complete bacterial plasmid genomes has increased many times in recent years and continues to grow rapidly (Shintani et al., 2015; Lean and Yeo, 2017; Brovedan et al., 2019, 2020). Against this background, studies of their structure and functioning are noticeably lagging. In particular, not enough attention is paid to the study of the diversity of plasmids and their evolutionary dynamics in environmental bacterial populations.

Bacteria belonging to the genus *Acinetobacter* are a convenient model for such studies, since strains of different species of this genus are widespread and ubiquitous; they play an important role in various ecological niches, including soil, water, associations with various plants and animals,

while many of them are human pathogens (Touchon et al., 2014). An important feature of *Acinetobacter* is also the presence of multiple plasmids in the same strain. In an attempt to study the diversity and prevalence of plasmids in different *Acinetobacter* species, various researchers tried to classify them using approaches based on a comparative analysis of the structure of replication initiator proteins (Bertini et al., 2010; Lean and Yeo, 2017; Cameranesi et al., 2017; Salto et al., 2018; Brovedan et al., 2020) or the structure of mobilization proteins (relaxases; Francia et al., 2004; Garcillán-Barcia et al., 2009; Smillie et al., 2010; Garcillán-Barcia and de la Cruz, 2013; Shintani et al., 2015; Brovedan et al., 2019).

It should be noted that both approaches have their limitations. Some plasmids do not contain known replication initiator proteins while others can contain not one but two or three replication genes or a recombinant replication gene (Bertini et al., 2010; Feng et al., 2016; Thomas et al., 2017; Salto et al., 2018; Salgado-Camargo et al., 2020), which prevents unambiguous identification of plasmids by this criterion. The system designed by Bertini et al. (2010) is rather limited for plasmids of other *Acinetobacter* species (Salto et al., 2018). Therefore, a universal classification system based on the analysis of sequences of replication initiator proteins does not currently exist. On practice, different groups of researchers use different systems to classify plasmids (Salto et al., 2018; Brovedan et al., 2019; Salgado-Camargo et al., 2020).

In comparison with replicases relaxases are less variable (Francia et al., 2004; Smillie et al., 2010; Salto et al., 2018) and their closely related variants are widespread among representatives of various species (Francia et al., 2004; Garcillán-Barcia et al., 2009). However, a number of plasmids do not contain the gene encoding relaxase (*mobA*) and it is necessary to use the analysis of the replication genes in this case.

Thus, one can conclude that there is not and cannot exist a universal system based on the analysis of only one plasmid protein, *rep, mob*, or another. Therefore, it is necessary to develop some new approaches for classification of plasmids.

We have sequenced the genomes of 44 plasmids isolated from environmental *Acinetobacter lwoffii* strains, which allowed to significantly expand the variety of known plasmids of this species. Related plasmids are also found among modern *Acinetobacter* strains. At the same time, an increasing number of strains belonging to different *Acinetobacter* species are isolated in the clinic, many of which contain plasmids with various sets of antibiotic resistance genes. Thus, a modern classification of *Acinetobacter* plasmids is needed for further research of the diversity and evolution of plasmids, as well as for diagnostic purposes.

In this study, we aimed to develop an improved classification system for *Acinetobacter* plasmids, starting from a detailed analysis of the plasmids of ancient *A. lwoffii* strains. By combining different methods for classification of plasmids of various sizes, we propose a "synthetic" approach to classify all known *Acinetobacter* plasmids and test its reliability in comparison with known approaches.

MATERIALS AND METHODS

Bacterial Strains and Growth Conditions

The ancient *A. lwoffii* strains ED23-35, ED45-23, EK30A and VS15 and *A. pseudolwoffii* strain ED9-5a used in this study were previously isolated from 15 thousand to 3 million years old permafrost sediments collected from different regions of Kolyma Lowland (Petrova et al., 2002; Kholodii et al., 2004; Mindlin et al., 2016). The complete list of permafrost *A. lwoffii* plasmids is presented in **Supplementary Table S1**.

Whole-Genome Sequencing and Assembly of Plasmids

Genomic DNA was isolated using the PowerSoil DNA isolation kit (Mo Bio Laboratories Inc., Carlsbad, CA, United States). The sequencing libraries for Illumina sequencing were prepared using the TruSeq nano DNA library prep kit (Illumina, United States) following the manufacturer's instructions. The sequencing of this library on the Illumina MiSeq platform using Miseq Reagent Kit v3 (600 cycles). At least 90-fold sequence coverage was achieved for each genome. Paired overlapped reads were merged into longer reads using FLASH v1.2.11 (Magoč and Salzberg, 2011), and low quality read ends were trimmed using Sickle v.1.33 (option q = 30[1]). Genomic DNA was additionally sequenced on a MinION system (Oxford Nanopore, United Kingdom) using the 1D Genomic DNA by ligation protocol. These long reads were used to assembly the Illumina contigs into longer sequences. Hybrid assembly of Illumina and Nanopore reads was performed using Unicycler v. 0.4.8 (Wick et al., 2017). We identified circular contigs that contained genes for mobilization and/or replication of plasmids.

Bioinformatics Analysis

For the assembly and analysis of plasmid genomes from ancient strains the program UGENE[2] was used. Similarity searches were performed using BLAST on NCBI site (Altschul et al., 1997; Megablast for BlastN and blastp for BlastP) and the resulting alignments were checked manually. Open reading frames (ORFs) were searched using ORF Finder and BLAST software at NCBI. Conserved domains and motifs were identified using the NCBI conserved domain database (CDD; Marchler-Bauer et al., 2011) and the Pfam database (Finn et al., 2009). When annotating new plasmid genomes, we adhered to the recommendations developed by the authors of the review devoted to this problem (Thomas et al., 2017).

Phylogenetic Analysis

For the phylogenetic analysis we analyzed genomes of all set of *Acinetobacter* plasmids from NCBI databases submitted before April 01, 2020. A total of 981 genomes were analyzed, including 44 plasmids from permafrost *A. lwoffii* (**Supplementary Tables S1, S2**). MobQ and RepB proteins were identified using PSI Blast search against pfam03389 and pfam01051 with *e*-value

[1]https://github.com/najoshi/sickle

[2]http://unipro.ru/

TABLE 1 | A primary classification of plasmids from permafrost *Acinetobacter lwoffii* strains.

Large Plasmids (> 40 kb)		Medium Plasmids (12–40 kb)		Small plasmids (2–12 kb)		
Conjugative (III-1)	**Non-conjugative (III-3)**	***mobA-repB* (II-1)**	***repB* (II-3)**	***mobA-repB* (I-1)**	***mobA* (I-2)**	***repB* (I-3)**
2	6	4	3	20	5	3
Total: 8 (18,6%)		Total: 7 (16,3%)		Total: 29 (65,9%)		
Conjugative: 2 (25%)		Mobilizable: 4 (57%)		Mobilizable: 26 (90%)		

1e-8 cutoff. Mob_{HEN} and Mob_P proteins were identified using psiblast search with six iterations and *e*-value 1e-8 cutoff with Mob_{HEN} and Mob_P proteins lists from Garcillán-Barcia et al. (2009) as an input. As a result, *mob* genes were detected in 381 plasmids out of 981 analyzed. A Mob tree was inferred from the alignment of the first 300 amino acids of the N-terminal domain of relaxase proteins; Mob proteins shorter than 200 amino acids were discarded.

Proteins were clustered at 95% identity and 0.9 length reciprocal coverage threshold using blastclust. Proteins representing clusters were aligned using MUSCLE v3.8.31, the alignment was used as an input for maximum likelihood tree construction in PhyML v3.3 with default parameters. Two separate trees for Mob and Rep proteins were constructed and visualized using ggtree v2.2.1 R package.

Classification and Identification of Plasmids Isolated From Permafrost and Modern *Acinetobacter* Strains

Mobilizable plasmids were classified based on the analysis of relaxases using BLAST. As reference sequences, sequences belonging to different families of relaxases described by the developers of the manuals were used (Francia et al., 2004; Garcillán-Barcia et al., 2009). The latest version of the classification system based on the analysis of the relaxases structure was also used (Salto et al., 2018). Non-mobilizable plasmids were classified based on the analysis of replication initiator proteins (Bertini et al., 2010). When forming groups (lineages) of closely related plasmids, the results of a comparative analysis of the structure of their backbone (basic) regions were used. Closely related plasmids from modern *Acinetobacter* strains were identified using BLASTn. Related plasmids from modern Proteobacteria strains were identified using the BLASTp program. Plasmids that not only had the same set of closely related genes in their backbone regions, but also had the same part of the accessory region adjacent to the backbone region, were assigned to the same group. The criteria for forming groups developed by us are described in more detail in the results.

RESULTS

A Primary Classification of *Acinetobacter* Ancient Plasmids

Sequencing of the complete genomes of five strains of the ancient *A. lwoffii* and *A. pseudolwoffii* strains produced complete circular sequences of 44 different plasmids present in these strains (**Supplementary Table S1**). Initially, we analyzed the molecular structure of these plasmids in order to group them by size and by the presence of genes encoding the *mobA* and *repB* proteins (**Table 1** and **Figure 1**). All plasmids were divided into three categories, according to their sizes: large plasmids (more than 40 kb), medium-sized plasmids (12–40 kb) and small plasmids (2–12 kb). Each of these was marked with a Roman numeral depending on the size of the plasmids: I – small; II – medium, III – large. Then the plasmids of each category were divided into three parts, indicated by Arabic numerals: 1 – both mobilization and replication genes are present; 2 – only mobilization genes are present (this variant is found only in small plasmids); 3 – only replication genes are present (**Table 1**).

Thus, based on the size and composition of the backbone region, we divided the ancient *Acinetobacter* plasmids into seven main blocks. It should be mentioned that small plasmids predominate in our collection and that most of them are mobilizable. Four of the seven medium- size plasmids also contained mobilization genes, while two of the eight large plasmids contained conjugative genes (**Table 1**). In total, mobilizable or conjugative plasmids predominate among plasmids originated from permafrost strains (70.5% of all plasmids).

Groups (Lineages) of *Acinetobacter lwoffii* Plasmids Isolated From Permafrost

Further analysis revealed that within each block, distinct groups (lineages) of related plasmids can be distinguished. When identifying groups of related plasmids, several criteria were followed: (i) identification of mobilizable and conjugative plasmids was carried out by comparative analysis of the structure of their relaxases with those of known MobA/MobL families of plasmids; (ii) identification of non-mobilizable plasmids was carried out by comparative analysis of the structure of their replication initiator proteins with those of known groups of *Acinetobacter* plasmids; the presence of two or more replication genes in the same plasmid were taken into account; (iii) the size of the plasmids, as well as the presence and structure of the genes in their accessory region were also taken into account.

As a result, clearly delineated groups of plasmids have been found, which we designated in Latin letters (**Table 2**). Plasmids from a single group possess a common set of genes that make up the backbone region. Furthermore, the similarity of the nucleotide sequences of the backbone regions of representatives of each group is at least 80%. In addition, the plasmids of the

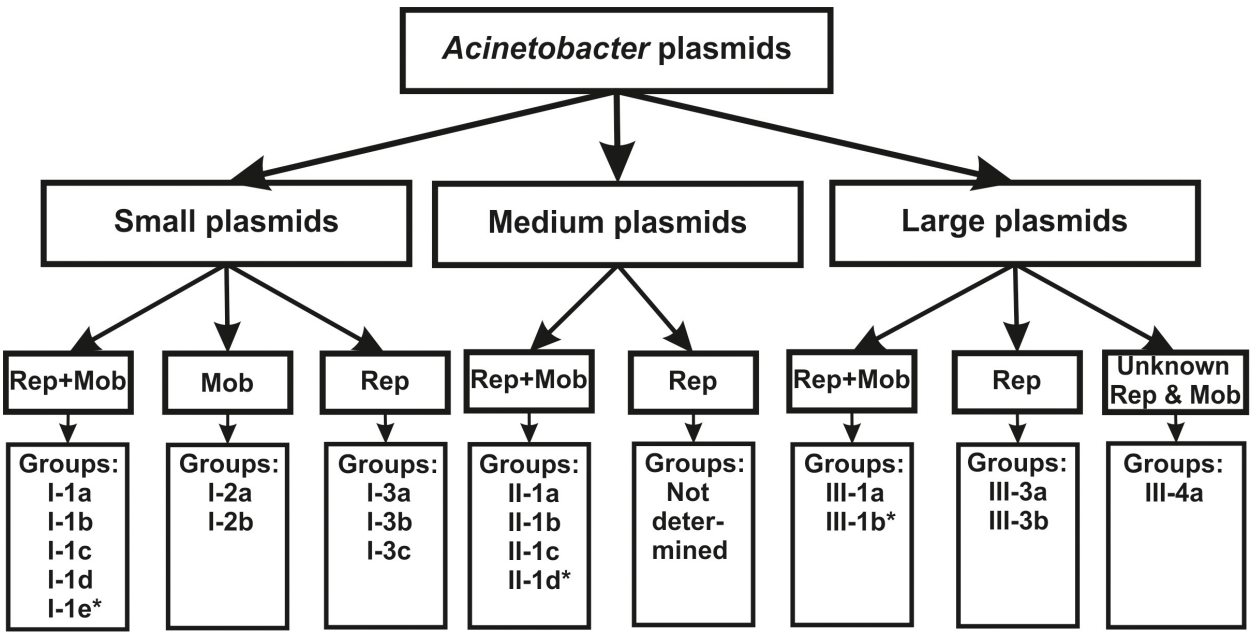

FIGURE 1 | The classification scheme used in the work (see the text for details). * plasmids from this group were found only in modern strains.

same group often have similarities in the organization of the accessory region. Thus, all group I-1a plasmids contain *dif*-modules [a small mobile element surrounded by XerC/XerD recombination sites (Blackwell and Hall, 2017; Mindlin et al., 2019)] with different adaptive genes, while their position in the plasmid genome remain constant. Group I-1b plasmids contain very conserved mobilization genes, while replication genes are characterized by high variability. The plasmids of groups I-1c and I-1d, in addition to belonging to different families, differ in size (**Supplementary Table S3**). The plasmids of groups I-2a and I-2b are united by the absence of replication genes, while differ from each other in other parameters. In particular, their

TABLE 2 | Groups of plasmids revealed in studies of permafrost *Acinetobacter lwoffii* strains.

Group	Reference Plasmid [Accession No]	Structure of the Backbone Region	Family of Plasmids
Small plasmids			
I-1a	pALWED2.6 [CP032121.1]	*mobS-mobA/L-repB*	MOB_{Q2}
I-1b	pALWED1.5 [CP032114.1]	*mobC-mobA/L-repB*	MOB_{Q2}
I-1c	pALWEK1.3 [CP032106.1]	*mobS-mobA/L-repB*	MOB_{Q2}
I-1d	pALWEK1.16 [MT675922]	*mobC-mobA-rep*	MOB_{HEN}
I-2a	pALWED1.7 [CP032116.1]	*traD-mobA/L*	MOB_{Q1}
I-2b	pALWED1.8 [LN873256.1]	*mobC-mobA/L*	MOB_{HEN}
I-3a	pALWEK1.5 [KX426231.1]	*rep-repB*	REP_3 (AR3G8)
I-3b	pALWEK1.14 [MT675921]	*repA*	ND*
I-3c	pALWEK1.15 [MT675925]	*repB*	REP_3 (AR3G1)
Medium plasmids			
II-1a	pALWED3.2 [CP032287.1]	*mobA/L-repB*	MOB_{Q1}
II-1b	pALWED3.5 [KX426230.1]	*mobA/L-repB*	MOB_{Q1}
II-1c	pALWEK1.2 [CP032105]	*mobA/L-repB*	MOB_{Q2}
Large plasmids			
III-1a	pALWED2.2 [CP032117.1]	*trb*-operon-*parA-parB-tra*-operon	MOB_P (P11)
III-3a	pALWED1.2 [CP032112.1]	*parB-parA-repB*	REP_3 (AR3G4)
III-3b	pALWED3.1 [KX528687.1]	*repB-parA*	REP_3 (AR315)
III-4a	pALWED1.1 [KX426227.1]	*rep-parAB-tra*-operon	ND*

**ND, not determined.*

relaxases belong to different families, MOBQ and MOBHEN respectively. At the same time, group I-2a plasmids contain, in addition to the *mobA* gene, the *traD* gene encoding a binding protein (T4CP, coupling protein), which plays in conjugative plasmids a key role in the transfer of single-stranded DNA to a recipient cell (de Paz et al., 2010). As far as we know, the gene *traD* was not previously detected in small plasmids of the MOBQ family.

Large non-conjugative plasmids were divided into two groups based on a comparative analysis of the structure of *repB* genes and the structure of accessory regions (**Supplementary Table S3**). All 5 plasmids of the first group contained a highly conserved backbone region with the replication initiator gene (*repB*) and genes for maintaining plasmid stability (*parA-parB*). At the same time, three plasmids of this group contained a single *repB* gene, while in the other two closely related plasmids (pALWVS1.1 and pALWEK1.1) we found a second *repB* gene with similarity to the *repB* gene of small mobilizable plasmids of group I-1c. Three additional genes related to the small I-1c plasmids, including the *mobA* gene, were found in these two plasmids next to the second *repB* gene, suggesting recombination between these two groups of plasmids. The structure of the plasmid pALWED3.1 was unique, and its replication initiator protein belonged to the AR3G15 group, whereas the Rep protein of the five above-described plasmids belonged to the AR3G1 group, according to classification proposed by Salto et al. (2018).

Phylogenetic Analysis of Relaxases and Replication Initiator Proteins From *Acinetobacter* Plasmids and Their Comparative Analysis

Having found that permafrost plasmids can be divided into groups based on the homology of their nucleotide sequences, we decided to check whether the same groups can be distinguished based on phylogenetic analysis of their relaxases and replication initiator proteins. To this purpose, we constructed phylogenetic trees for the corresponding proteins.

We started this analysis by building a tree of Mob proteins found in permafrost plasmids. It occurred that the groups of plasmids presented in **Table 2** were well separated on the basis of their *mob* gene sequences (data not shown).

We then tried to find out whether it is possible to identify new groups of plasmids in *Acinetobacter* strains by analyzing the phylogenetic tree of relaxases. For this purpose, a new tree was built (**Figure 2**), significantly expanding the previous one by including relaxases of modern *Acinetobacter* strains available in the database (see section "Materials and Methods"). The tree topology generally reflected the phylogenetic relationships of Mob proteins from different families (Garcillán-Barcia et al., 2009). Relaxases of most groups belonged to the MOB_Q family, of two groups – to the MOB_{HEN} family, and one group of large conjugative plasmids contained relaxase from the MOB_P family. As can be seen from **Figure 2**, the majority of modern plasmids belongs to one of the groups revealed among the ancient plasmids. We have found only three groups (I-1e, II-1d, and III-1b), whose members were not found among the ancient plasmids. In these groups the similarity of relaxases also reflected the relationship of the plasmids bearing them.

Recently, Salgado-Camargo et al. (2020) showed that the number of groups (lineages) of plasmids common among strains of *A. baumannii* is 21, with the total number of analyzed plasmids exceeding 170. Thus, the variety of *A. baumannii* plasmids is limited and is apparently associated with their ability to increase the adaptive properties of host bacteria. In our work, we have shown the validity of this conclusion on a much more extensive material, since about 980 plasmids of strains belonging to different species of *Acinetobacter* were analyzed. In total, we identified 19 groups (lineages) of *Acinetobacter* plasmids. Their true number is undoubtedly greater, given the limited use in our work of analysis of plasmid groups not bearing relaxase genes. At the same time, we demonstrated a wide distribution of plasmids from some lineages among various *Acinetobacter* species and even among representatives of other genera (group III-1a).

However, some plasmids are unique and only in some cases have a similarity of less than 80% with representatives of the closest group. Among the ancient plasmids of *A. lwoffii*, we found five such unique plasmids, pALWEK1.9, pALWEK1.13, pALWED1.3, pALWED2.3, and pALWVS1.2 (**Supplementary Table S3**). Perhaps such plasmids have a narrow host range and are spread only among environmental strains and therefore are poorly represented in the database.

Next, we constructed a phylogenetic tree for plasmids containing *rep* genes, including plasmids carrying both *rep* genes and *mob* genes (**Figure 3**). As can be seen, the topology of the resulting tree coincides with that of the previously published phylogenetic analysis (Salto et al., 2018; Walter et al., 2020). In particular, all previously described AR3G groups are clearly represented (**Figure 3**). At the same time, plasmids with similar relaxases and very similar structure may encode Rep proteins belonging to different AR3G groups (see lines on the map shown in different colors). Therefore, one can conclude that there is a lack of coherent evolution of genes encoding proteins involved in the mobilization and replication of plasmids. Moreover, the phylogenetic proximity of mobilization proteins reflects the similarity of the plasmids carrying them, while in the case of replication initiator proteins, such a relationship is often absent.

However, permafrost plasmids without *mob* genes but having related *rep* genes often have a similar structure, i.e., they clearly belong to the same group. Consequently, at least in some cases, *rep* genes can be used to classify plasmids in the absence of *mob* genes. But it should be borne in mind that one clade of Rep can include proteins encoded by non-related plasmids characterized by different structure. Some of these plasmids contain two or even three different *repB* genes. The findings suggest that plasmids are able to exchange by replication genes. For this reason, when classifying plasmids containing *mob*, it is necessary to rely on the analysis of relaxases.

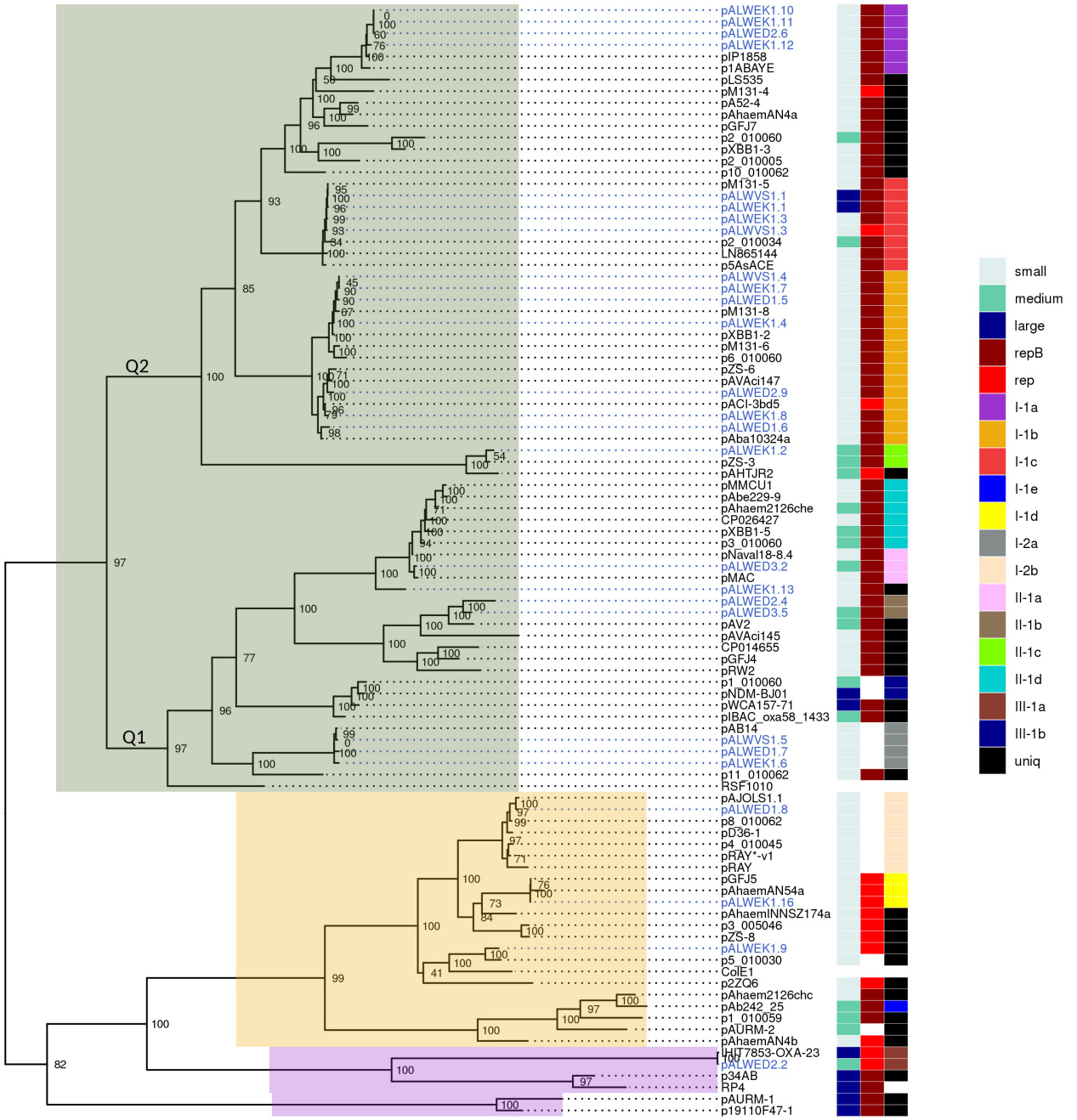

FIGURE 2 | Phylogenetic tree of relaxases from *Acinetobacter* spp. plasmids. ML phylogenetic tree of MobA proteins of all *Acinetobacter* spp. plasmids from databases and from the collection analyzed in this study. Branch support values were calculated using approximate Bayes test. To the right of the tree, three columns show the characteristics of the plasmid encoding this relaxase: size (small, medium, or large), the presence or absence of a replication gene (*repB* or other), and affiliation to a group (with the exception of the reference plasmids RSF1010, ColE1, and RP4). Each of the plasmid groups (lineages) are marked in colors. Ancient plasmids, isolated from permafrost, are marked by blue. Relaxases belonging to the MOB_Q family are highlighted in gray, MOB_{HEN} – pink, and MOB_P – lilac.

Identification of Modern *Acinetobacter* Plasmids Closely Related to Ancient Plasmids of Different Groups

In parallel with the construction of phylogenetic trees for relaxases and replicases we performed the search of plasmids from modern strains closely related to such from permafrost *A. lwoffii* strains. Preliminarily, from each group a single plasmid was selected and used as a reference plasmid when searching relatives among modern plasmids (**Table 2**). In most cases plasmids of the same groups that were found among permafrost strains of *A. lwoffii* were common among modern

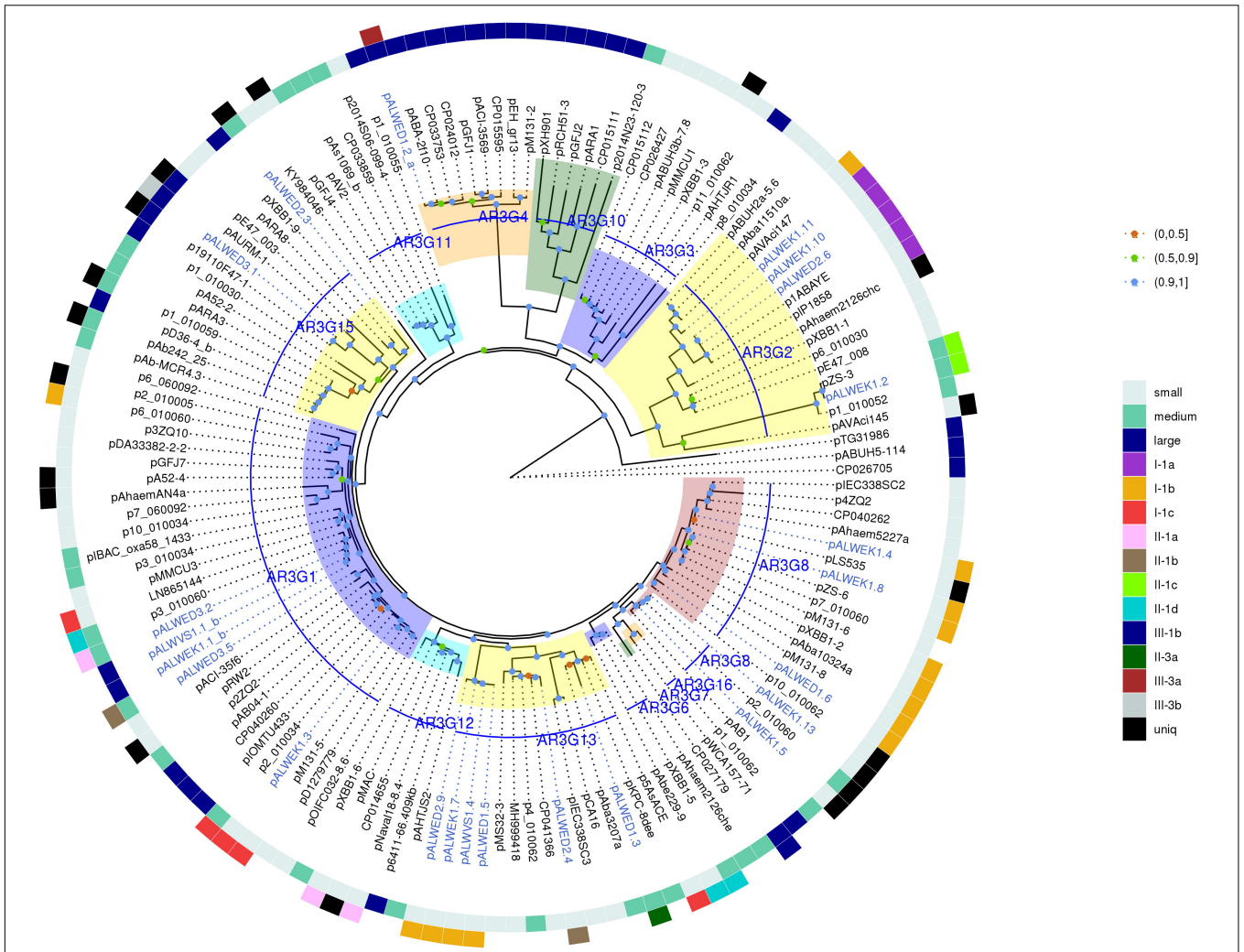

FIGURE 3 | Phylogenetic tree of Rep_3 domain replication initiator proteins from *Acinetobacter* spp. plasmids. ML phylogenetic tree of Rep_3 (Pfam01051) proteins of all *Acinetobacter* spp. plasmids from databases and from the collections analyzed in this study. Proteins were clustered at 95% identity, only a selection of genes from each cluster was used for tree construction. Branch support values were calculated using approximate Bayes test. The characteristics of plasmid encoding this RepB are shown in the two outer circles: size (small, medium, or large), and affiliation to a group. Each of the plasmid groups (lineages) are marked in colors. Ancient plasmids, isolated from permafrost, are marked by blue. Branches corresponding to the different AR3G groups are highlighted in different colors. Bootstrap values are split into three intervals, shown as colored circles: [100, 90] as blue, [90, 50] as green, and [50, 0] as orange.

Acinetobacter strains (**Supplementary Table S3**). The exception was predominantly medium-sized plasmids, especially those that did not contain the *mobA* gene. Perhaps this limits their transfer into the cells of other strains thus explaining the narrow host range of these plasmids. More complex patterns occur in a comparative analysis of permafrost and modern large plasmids. In the case of conjugative plasmids pALWED2.2 (group III-1a) and pALWED1.1 (group III-4a) closely related modern plasmids were discovered by detailed comparative analysis of their structure with that of permafrost plasmids. Plasmids closely related to pALWED2.2 carrying the same conjugative transfer system (Ewers et al., 2016; Silva et al., 2018) contain antibiotic resistance genes (bla_{oxa23} and *strA-strB*) in their accessory region. Modern derivatives of pALWED1.1 were broadly spread among strains of different *Acinetobacter* species but have not been previously identified as conjugative plasmids (see more detailed information presented below).

In the case of non-conjugative plasmids, when identifying related modern plasmids in addition to the comparative analysis of *repB* genes, the structure of *parA* and *parB* genes encoding a plasmid partition system was also taken into account. As a result, it was possible to detect closely related plasmids for plasmids of group III-3a as well as for plasmid pALWED3.1 (group III-3b; **Supplementary Table S3**).

Importantly, the list of modern plasmids contains plasmids originated from strains belonging to different *Acinetobacter* species and isolated from a variety of sources, suggesting horizontal transfer of the most successful (adapted) plasmid variants (**Supplementary Tables S3, S4**).

Data demonstrating the spread of plasmids of group 1-2a among ancient and modern strains of *Acinetobacter*, typical for other groups of plasmids, are presented in **Table 3**. It can be seen that closely related plasmids belonging to the same group are found among the strains of various *Acinetobacter* species inhibiting different ecosystems. It is significant to note that some strains were isolated from environment, while others are clinical strains or sewage dwellers.

The Novel *Acinetobacter* Plasmids

Several groups of plasmid identified in the present work were analyzed in more detail. In particular, plasmids of three groups, one containing large plasmids (III-4a) and two containing small plasmids (I-1a; I-2a) are widely spread among modern *Acinetobacter* strains but have not been described previously.

Group III-4a

Among large plasmids, the most interesting is the extensive group III-4a of conjugative plasmids, since members of the new group differ from previously described conjugative plasmids by the structure of the minimal replicon and the absence of known relaxase and replicase genes. Plasmids from the group III-4a were isolated from strains of various *Acinetobacter* species. We found their prototype plasmid pALWED1.1 among the plasmids of our collection of ancient strains and, based on preliminary studies, revealed its close relationship with plasmids of modern strains. It should be noted that among the modern large conjugative plasmids, there are other variants that are not related to pALWED1.1, but that also do not have known relaxases and replicases (for example, pA297-3 described by Hamidian et al., 2016 and pNDM-BJ01 and related plasmids described by Hu et al., 2012). Perhaps, for such plasmids, the classification can be based on the structure of the *tra* operon.

The Group I-2a of MOB_Q Family

Among the small plasmids, the most interesting are the plasmids of the two groups belonging to MOB_Q family. Group I-2a is the group of the smallest (4–8 kb) plasmids of the MOB_Q family characterized by several distinctive properties: (i) by the absence of the gene *repB*; (ii) by the unique structure of the gene *mobA* which contains only one domain corresponding to the relaxase region of *mobA* from RSF1010; (iii) by the absence of the gene *mobC*; (iv) by the presence of the *traD* gene encoding the coupling conjugational protein located in the plasmid backbone region.

TABLE 3 | Distribution of plasmids belonging to group I-2a among different *Acinetobacter* strains.

Source	*Acinetobacter* Species: Strains	Source
Permafrost	*A.lwoffii:* ED23-35, EK30A	Kolyma, Russia
	A. pseudolwoffii: ED9-5a	Kolyma, Russia
Soil	*A. baumannii:* DS002	India
	A. soli: GFJ2	Thailand
Gold mine	*A. lwoffii:* ZS207	Zloty Stok, Poland
Sewage	*A. wuhouensis:* WCHA60, WCHA62	China
	A. chinensis: WCHAc010005	China
	*A.baumannii:*VB16141	India
Homo sapiens	*A. baumannii:* VB16141, A85	India, Australia
	A. pittii: C54	Australia

Plasmids of this group are extremely widespread among *Acinetobacter* strains, belonging to different species of this genus (**Supplementary Tables S4**, **S5** and **Figure 4**). Some strains contain two (or even three) such plasmids. In particular, we found three strains (*A. lwoffii* EK30A, *A. lwoffii* M2a, and *A. schindleri* HZE33-1) that each contained two plasmids of this group; one strain of *A. lwoffii* ZS207 isolated from Zloty Stok gold mine in Poland contained three plasmids (pZS-4, pZS-7, pZS-9) carrying genes *mobA* and *traD* and belonging to group I-2a.

It should also be noted that the same plasmid, with only a few nucleotide substitutions, could be detected in different *Acinetobacter* strains. So, virtually the same plasmid pALWEK1.6 was found in three different *A. lwoffii* strains: permafrost strain EK30A, the above mentioned strain ZS207 and a strain M2a isolated from a sample of honey in Hungary (Veress et al., 2020). Plasmid pALWVS1.5 was found in two different strains of *A. lwoffii* (VS15 and EK30A) isolated from different permafrost samples at different times. Finally, we found plasmid pVB2486_4 in three different strains of *A. baumannii*. Most likely, that the wide distribution of plasmids belonging to I-2a group can be explained by the presence in their genome of a pair of genes *mobA-traD* that ensure their effective mobilization. A possible effect of these plasmids on bacterial adaptability cannot also be excluded.

Interestingly, we found in the GenBank (whole-genome shotgun contigs) a strain identified by the authors as *Prolinoborus fasciculus* CIP 103579T (family Neisseriaceae) which contained a plasmid almost identical to the reference plasmid pALWED1.7. It seems to us, however, that this fact itself needs a confirmation.

It should be mentioned that accessory regions of different plasmids differed from each other (**Supplementary Table S4** and **Figure 4**). Most of them contain genes that are thought to possess various adaptive functions. Two plasmids isolated from clinical strains of *A. baumannii* contained antibiotic resistance genes (resistance to beta-lactams determined by transposon Tn*2007* and resistance to aminoglycosides). Plasmids isolated from samples of permafrost, antimony deposits, soils, water and honey as well as sewage, contained genes for the metabolism of various amino acids. In some plasmids, accessory genes have not been identified (**Supplementary Table S4**).

The Group I-1a of MOB_Q Family Plasmids

The prototype of this group is the plasmid pALWED2.6 (9,202); CP032121.1) isolated from the permafrost *A. lwoffii* strain ED45-23. The backbone region of pALWED2.6 contains mobilization genes *mobS* and *mobA* as well as the replication initiator gene *repB* and two additional ORFs encoding an SH3 domain protein and an unidentified protein. This region is present in all multiple derivatives of pALWED2.6 which form the I-1a group of plasmids including ancient as well as modern plasmids (**Figure 5**). It should be mentioned that the whole backbone region with both *mobA* and *repB* genes varies only slightly in different plasmids of this group. It can be assumed that unlike to other groups of

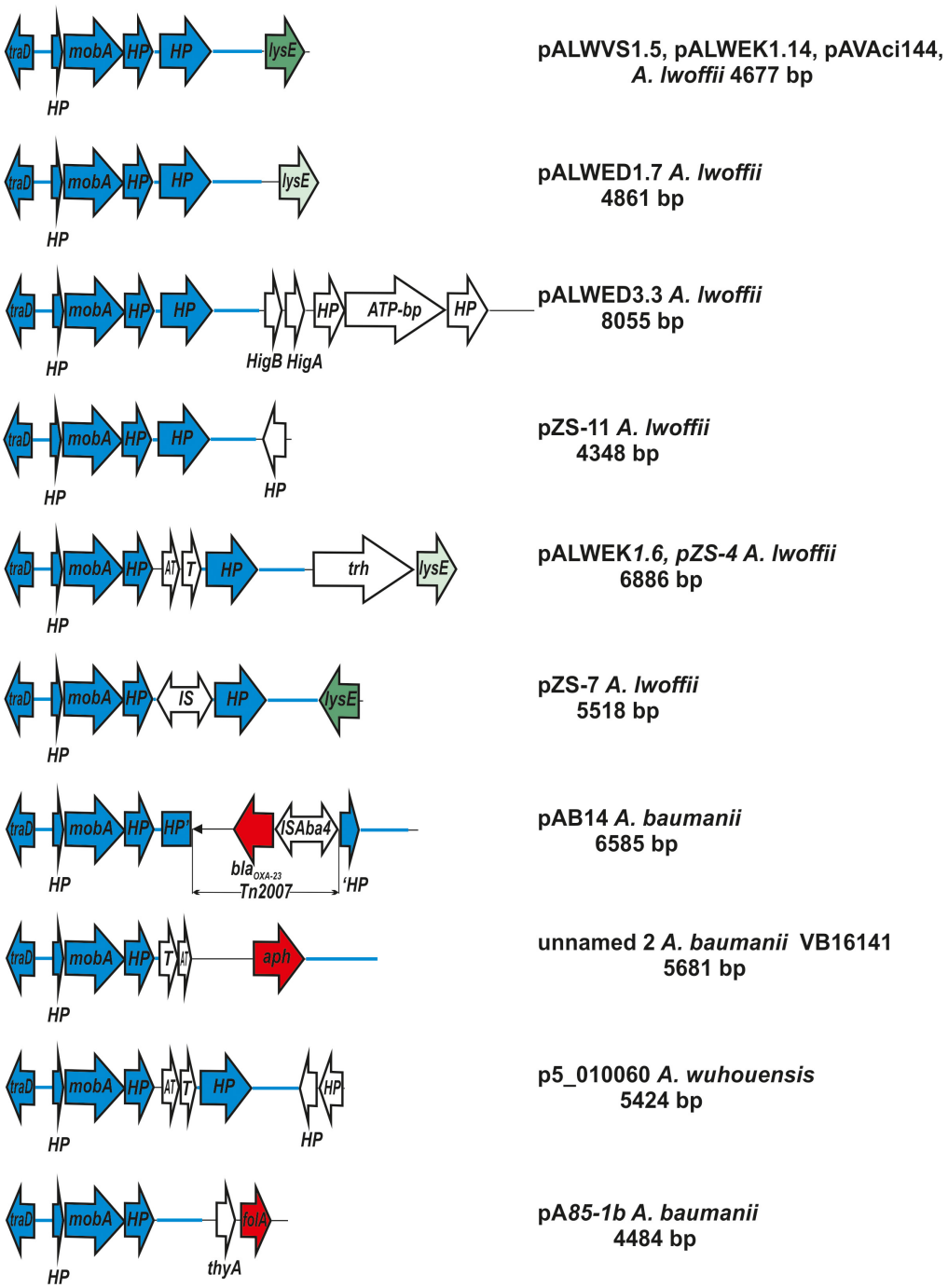

FIGURE 4 | Comparative genetic structures of plasmids belonging to the group I-2a. The locations and polarities of genes and ORFs are shown by arrows; genes and ORFs of the backbone regions – by blue arrows. LysE gene is indicated by green arrow, different shades in different variants. Antibiotic resistance genes: *aph* (resistance to aminoglycosides), bla_{oxa23} (resistance to beta-lactams) and *folA* (trimethoprim resistance) are depicted as a red arrow. The rest genes and ORFs of accessory region are indicated as white arrows. *trh*, gene encoding tryptophan 7-halogenase. Designations of gene products are as follows: HP, hypothetical protein; ATP, ATP-binding protein; HigB, T, toxin; HigA, AT, antitoxin. The picture is drawn to scale.

plasmids, the relaxase and replicase genes of these plasmids evolved together.

The second distinctive feature of the I-1a group of plasmids is the presence of a *dif* module adjacent to the backbone region. While the location of the *dif* modules in different plasmids is the same, these are different modules containing different structural genes (**Figure 5**). In particular, the *dif* module of the plasmid pALWED2.6 contains the *sulP*

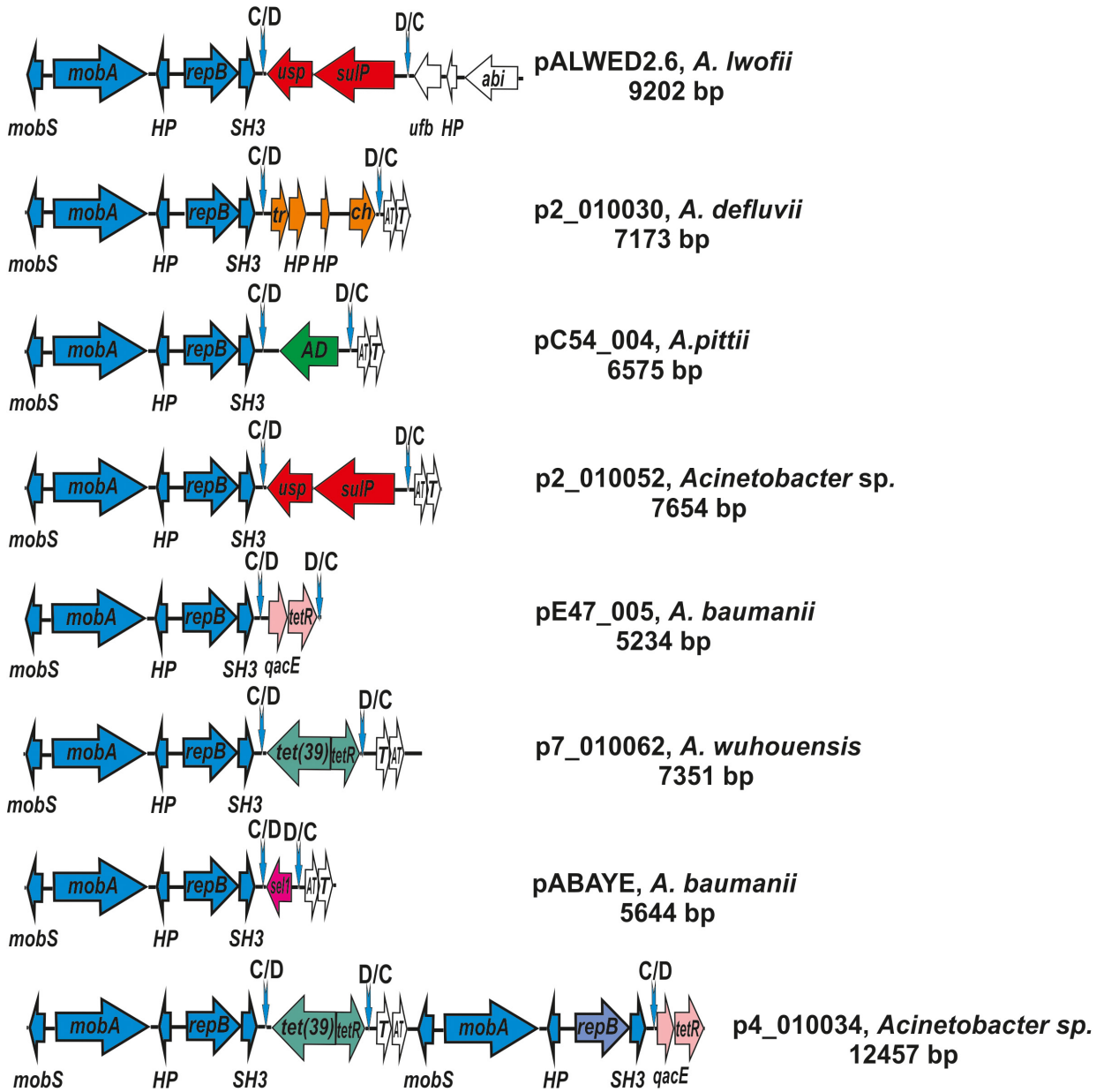

FIGURE 5 | Comparative genetic structures of plasmids belonging to the group I-1a. The locations and polarities of genes and ORFs are shown by arrows; genes and ORFs of the backbone regions – by blue arrows; the components of the *dif* modules – by arrows with different colors; genes and ORFs of accessory regions – by white. Vertical arrows indicate p*dif* sites with the orientation of the subsites shown above. Designations of genes present in *dif* modules are as follows: *usp*, universal stress protein; *sulP*, sulfate permease; *tet*(39), tetracycline resistance; *tet*R, repressor; *sel1*, Sel1-repeat protein. Designations of gene products are as follows: HP, hypothetical protein; Tr, XRE family transcriptional regulator; *ch*, hydrolase; AD, zinc-dependent alcohol dehydrogenase family protein; *qacE*, QacE family quaternary ammonium compound efflux SMR transporter; T, toxin; AT, antitoxin; *tetR*, TetR/AcrR family transcriptional regulator. The picture is drawn to scale.

gene encoding the sulfate permease and the *uspA* gene encoding a universal stress protein. Plasmid p1ABAYE from *A. baumannii* strain contains a *sel1* module encoding a putative virulence factor, and plasmid p7_010062 from *A. wuhouensis* carries a *tet39* module with *tetA39-tetR* genes encoding tetracycline resistance. *Dif*-modules of the remaining plasmids carry some other adaptive genes (**Figure 5**).

It should also be noted that in addition to the small plasmids characteristic of group I-1a, we found three medium-sized plasmids constructed from repeating elements (**Figure 5**).

Two such plasmids (p4_010034; p4_010060) contained backbone regions and two different *dif*-modules each (**Figure 5**). The backbone regions carried the *mobS* and *mobA* mobilization genes, the gene *repB* encoding the replication initiator protein and two additional genes encoding the SH3 domain protein

and the hypothetical protein (**Figure 5**). Interestingly, the first of the backbone regions was almost identical to the corresponding region of small plasmids, while the second region contained identical mobilization genes, but different *repB* genes (77% identity level). The genes encoding toxin-antitoxin system were represented in one copy (**Figure 5**). The largest third plasmid pAcsw19-3 (38391 bp; CP043310.1), found in *A. johnsonii* Acsw19, contained five almost identical copies of the small plasmid, closely related to plasmid p2_010030 [CP029390.2] isolated from *A. defluvii* strain WCHA30. Accordingly, it contained five almost identical copies of the backbone regions, five copies of the genes encoding toxin-antitoxin system, and five *dif*-modules with a gene encoding cysteine hydrolase. The order of the genes in each copy was the same.

Plasmid pIP1858 (KP890934.1) from *A. baumannii* BM2686 strain differs from all other plasmids of the group I-1a. Whereas its backbone region is typical for the group, the accessory region, instead of the *dif* module, contains a complex structure consisting of two different IS elements surrounding three structural genes including an aminoglycoside resistance gene (Yoon et al., 2016). Most likely, the plasmid pIP1858 arose from a typical plasmid of group I-1a as a result of some recombination event(s).

The mechanism that ensures the replacement of *dif* modules located in the plasmids remains unknown. We determined the comparative structure of the plasmid *dif* sites (p*dif*) surrounding various *dif* modules, and found that most of the modern variants differ from the variant found in the ancient plasmid. The greatest variability is found in the central region of the p*dif* sites (dif^{cent}; **Supplementary Figure S1**). It can be assumed that the replacement of *dif* modules can be provided by the site-specific recombination system XerC/XerD (Bloor and Cranenburgh, 2006; Carnoy and Roten, 2009; Castillo et al., 2017; Cameranesi et al., 2018) and may occur in two stages: (1) the old module is excluded from the plasmid, leaving a recombinant p*dif* site in it; (2) a new module is integrated into the plasmid by recombination with the recombinant p*dif* site. A possible alternative mechanism is a recombination through dif sites (Cameranesi et al., 2018).

DISCUSSION

In the present work, we have used a large collection of plasmids from permafrost strains of *A. lwoffii* to analyze the diversity of plasmids of various *Acinetobacter* species and to classify them. The main emphasis was on the analysis of small mobilizable plasmids, based on the structure of the *mobA* genes encoding relaxases. The structure of other genes of the backbone and accessory regions was also taken into account. It was found that: (i) a limited number of plasmid groups are distributed both in the environment and in the clinic; (ii) plasmids of modern *Acinetobacter* strains have their homologs among ancient strains, which allows us to consider the latter as the progenitors of the former; (iii) in the MOB_Q family, new groups of plasmids were identified and characterized; (iv) a novel group of large putative conjugative plasmids was discovered.

Thus, we have confirmed and expanded the conclusions of other authors about the prospects of using a classification system based on the analysis of the structure of relaxases in mobilizable and conjugative plasmids (Francia et al., 2004; Garcillán-Barcia et al., 2009; Garcillán-Barcia and de la Cruz, 2013; Shintani et al., 2015). However, an attempt to use for classification of non-mobilizable plasmids the analysis of the structure of replication initiator proteins was not that successful. In particular, when comparing phylogenetic trees constructed using either MobA or RepB proteins their mismatch was revealed, indicating not coherent evolutionary variability of the *mobA* and *repB* genes (**Figures 2**, **3**). In a number of cases, we also found that plasmids carrying related *repB* genes can be completely different in structure (**Supplementary Table S3**). Furthermore, in two of the eight large plasmids studied, we found two different *repB* genes. Therefore, in the absence of relaxase genes on the plasmid, we recommend to take into account the structure of other genes of the backbone and accessory regions for classification.

In a recently published work (Salgado-Camargo et al., 2020), the authors classified plasmids of only one species, *A. baumannii*, based on the similarity of their Rep proteins and additional regions, excluding Mob proteins. Even in such a limited sample, they were faced with the fact that two groups of similar plasmids may contain different *rep* genes. As can be seen from our study for the entire genus *Acinetobacter*, the classification of plasmids based only on the analysis of replication initiator proteins is associated with significant inaccuracies.

The general structure of the members of each group of plasmids can remain unchanged for thousands of years. At the same time, comparative analysis of the structure of permafrost and modern plasmids from the same group allowed to identify changes in the structure of plasmids with changing living conditions, which confirmed the results of previous studies (Vallenet et al., 2008; Gillings et al., 2008; Brovedan et al., 2019). We showed that the main changes occur in an accessory region of plasmids and do not usually affect the structure of the backbone region. Moreover, in the plasmids of clinical strains, even small ones, we often revealed insertions of antibiotic resistance and virulence genes. Thus, along with medium-size and large plasmids, small plasmids of *Acinetobacter* likely contribute to the acquisition of properties necessary for the adaptation of host bacteria to changing living conditions.

DATA AVAILABILITY STATEMENT

The datasets generated in this study can be found in online repositories. The names of the repository/repositories and accession number(s) can be found below: https://www.ncbi.nlm.nih.gov/genbank/, KX426229.1 CP032117.1 CP032118.1 CP032119.1 CP032120.1 CP032121.1 CP032122.1 CP032123.1 CP032124.1, KX528687.1 CP032287.1 CP032288.1 KX426230.1 CP032290.1 MT675918, KX426227.1 CP032112.1 KX426228.1 CP032113.1 CP032114.1 CP032115.1 CP032116.1 LN873256.1, KX426232.1 MT675923 MT675924 MT319099 MT675926, CP032102.1 CP032105.1 CP032106.1 CP032107.1

KX426231.1 CP032108.1 CP032109.1 CP032110.1 CP032111.1 CP032103.1 CP032104.1 MT675919 MT675920 MT675921 MT675925 MT675922.

AUTHOR CONTRIBUTIONS

MP had the initial idea, which was developed into a project together with SM. AM, AB, AR, and MP conducted the sequencing, assembly of plasmids and genome annotation. SM and MP designed the tables. AB and MP designed the figures. MP, AB, and SM made the analysis of MobA proteins. AB and MP analyzed the RepB proteins. SM, MP, and AM wrote the manuscript. All authors performed the bioinformatic analysis and contributed to manuscript revision, and approved the submitted version.

FUNDING

This study was supported by Center for Genomic Research "Kurchatov Genomic Center" – IMG (Agreement No. 075-15-2019-1664).

ACKNOWLEDGMENTS

The authors are grateful to A. Kulbachinskiy for helpful comments and suggestions and to A. Ermakova for help in assembly of plasmids.

SUPPLEMENTARY MATERIAL

The Supplementary Material for this article can be found online at: https://www.frontiersin.org/articles/10.3389/fmicb.2020.588410/full#supplementary-material

Supplementary Figure 1 | Alignment of the recombination *dif* sites flanking *dif* modules in plasmids of group I-1a.

Supplementary Table 1 | Plasmids from permafrost *Acinetobacter lwoffii* strains.

Supplementary Table 2 | Analyzed *Acinetrobacter* plasmids.

Supplementary Table 3 | Groups of *Acinetobacter* plasmids.

Supplementary Table 4 | Small *Acinetobacter* plasmids belonging to the Group I-2a of MOBQ family.

Supplementary Table 5 | Distribution of MOB_Q plasmids from I-2a group among modern *Acinetobacter* strains (whole genome shotgun contigs).

REFERENCES

Altschul, S. F., Madden, T. L., Schäffer, A. A., Zhang, J., Zhang, Z., Miller, W., et al. (1997). Gapped BLAST and PSI-BLAST: a new generation of protein database search programs. *Nucleic Acids Res.* 25, 3389–3402. doi: 10.1093/nar/25.17.3389

Bertini, A., Poirel, L., Mugnier, P. D., Villa, L., Nordmann, P., and Carattoli, A. (2010). Characterization and PCR-based replicon typing of resistance plasmids in *Acinetobacter baumannii*. *Antimicrob. Agents Chemother.* 54, 4168–4177. doi: 10.1128/AAC.00542-10

Blackwell, G. A., and Hall, R. M. (2017). The tet39 determinant and the msrE-mphE genes in *Acinetobacter* plasmids are each part of discrete modules flanked by inversely oriented pdif (XerC-XerD) sites. *Antimicrob. Agents Chemother.* 61:e780-17. doi: 10.1128/AAC.00780-17

Bloor, A. E., and Cranenburgh, R. M. (2006). An efficient method of selectable marker gene excision by Xer recombination for gene replacement in bacterial chromosomes. *Appl. Environ. Microbiol.* 72, 2520–2525. doi: 10.1128/AEM.72.4.2520-2525.2006

Brovedan, M., Repizo, G. D., Marchiaro, P., Viale, A. M., and Limansky, A. (2019). Characterization of the diverse plasmid pool harbored by the blaNDM-1-containing *Acinetobacter bereziniae* HPC229 clinical strain. *PLoS One* 14:e0220584. doi: 10.1371/journal.pone.0220584

Brovedan, M. A., Cameranesi, M. M., Limansky, A. S., Morán-Barrio, J., Marchiaro, P., and Repizo, G. D. (2020). What do we know about plasmids carried by members of the *Acinetobacter* genus? *World J. Microbiol. Biotechnol.* 36:109. doi: 10.1007/s11274-020-02890-7

Cameranesi, M. M., Limansky, A. S., Morán-Barrio, J., Repizo, G. D., and Viale, A. M. (2017). Three novel *Acinetobacter baumannii* plasmid replicase-homology groups inferred from the analysis of a multidrug-resistant clinical strain isolated in Argentina. *J. Infect. Dis. Epidemiol.* 3:046. doi: 10.23937/2474-3658/1510046

Cameranesi, M. M., Morán-Barrio, J., Limansky, A. S., Repizo, G. D., and Viale, A. M. (2018). Site-Specific recombination at XerC/D sites mediates the formation and resolution of plasmid co-integrates carrying a blaOXA-58 and TnaphA6-resistance module in *Acinetobacter baumannii*. *Front. Microbiol.* 9:66. doi: 10.3389/fmicb.2018.00066

Carnoy, C., and Roten, C. A. (2009). The dif/Xer recombination systems in *proteobacteria*. *PLoS One.* 4:e6531. doi: 10.1371/journal.pone.0006531

Castillo, F., Benmohamed, A., and Szatmari, G. (2017). Xer site specific recombination: double and single recombinase systems. *Front. Microbiol.* 8:453. doi: 10.3389/fmicb.2017.00453

de Paz, H. D., Larrea, D., Zunzunegui, S., Dehio, C., de la Cruz, F., and Llosa, M. (2010). Functional dissection of the conjugative coupling protein TrwB. *J. Bacteriol.* 192, 2655–2669. doi: 10.1128/JB.01692-09

Ewers, C., Klotz, P., Scheufen, S., Leidner, U., Gottig, S., and Semmler, T. (2016). Genome sequence of OXA-23 producing *Acinetobacter baumannii* IHIT7853, a carbapenem-resistant strain from a cat belonging to international clone IC1. *Gut. Pathog.* 8:37. doi: 10.1186/s13099-016-0119-z

Feng, Y., Yang, P., Wang, X., and Zong, Z. (2016). Characterization of *Acinetobacter johnsonii* isolate XBB1 carrying nine plasmids and encoding NDM-1, OXA-58 and PER-1 by genome sequencing. *J. Antimicrob. Chemother.* 71, 71–75. doi: 10.1093/jac/dkv324

Finn, R. D., Mistry, J., Tate, J., Coggill, P., Heger, A., Pollington, J. E., et al. (2009). The Pfam protein families database. *Nucleic Acids Res.* 38, D211–D222. doi: 10.1093/nar/gkp985

Francia, M. V., Varsaki, A., Garcillán-Barcia, M. P., Latorre, A., Drainas, C., and de la Cruz, F. (2004). A classification scheme for mobilization regions of bacterial plasmids. *FEMS Microbiol. Rev.* 28, 79–100. doi: 10.1016/j.femsre.2003.09.001

Garcillán-Barcia, M. P., and de la Cruz, F. (2013). Ordering the bestiary of genetic elements transmissible by conjugation. *Mob. Genet. Elements.* 3:e24263. doi: 10.4161/mge.24263

Garcillán-Barcia, M. P., Francia, M. V., and de la Cruz, F. (2009). The diversity of conjugative relaxases and its application in plasmid classification. *FEMS Microbiol. Rev.* 33, 657–687. doi: 10.1111/j.1574-6976.2009.00168.x

Gillings, M., Boucher, Y., Labbate, M., Holmes, A., Krishnan, S., Holley, M., et al. (2008). The evolution of class 1 integrons and the rise of antibiotic resistance. *J. Bacteriol.* 190, 5095–5100. doi: 10.1128/JB.00152-08

Hamidian, M., Ambrose, S. J., and Hall, R. M. (2016). A large conjugative *Acinetobacter* plasmid carrying the sul2 sulphonamide and strAB streptomycin resistance genes. *Plasmid.* 87-88, 43–50. doi: 10.1016/j.plasmid.2016.09.001

Hu, H., Hu, Y., Pan, Y., Liang, H., Wang, H., Wang, X., et al. (2012). Novel plasmid and its variant harboring both a blaNDM-1 gene and type IV secretion system in clinical isolates of *Acinetobacter lwoffii*. *Antimicrob. Agents Chemother.* 56, 1698–1702. doi: 10.1128/AAC.06199-11

Kholodii, G., Mindlin, S., Gorlenko, Z., Petrova, M., Hobman, J., and Nikiforov, V. (2004). Translocation of transposition-deficient (TndPKLH2-like) transposons in the natural environment: mechanistic insights from the study of adjacent DNA sequences. *Microbiology* 150(Pt 4), 979–992. doi: 10.1099/mic.0.26844-0

Kurakov, A., Mindlin, S., Beletsky, A., Shcherbatova, N., Rakitin, A., Ermakova, A., et al. (2016). The ancient small mobilizable plasmid pALWED1.8 harboring a new variant of the non-cassette streptomycin/spectinomycin resistance gene aadA27. *Plasmid* 8, 36–43. doi: 10.1016/j.plasmid.2016.02.005

Lean, S. S., and Yeo, C. C. (2017). Small, enigmatic plasmids of the nosocomial pathogen, *Acinetobacter baumannii*: good, bad, who knows? *Front Microbiol.* 8:1547. doi: 10.3389/fmicb.2017.01547

Magoč, T., and Salzberg, S. L. (2011). FLASH: fast length adjustment of short reads to improve genome assemblies. *Bioinformatics.* 27, 2957–2963. doi: 10.1093/bioinformatics/btr507

Marchler-Bauer, A., Lu, S., Anderson, J. B., Chitsaz, F., Derbyshire, M. K., DeWeese-Scott, C., et al. (2011). CDD: a conserved domain database for the functional annotation of proteins. *Nucleic Acids Res.* 39, D225–D229. doi: 10.1093/nar/gkq1189

Mindlin, S., Beletsky, A., Mardanov, A., and Petrova, M. (2019). Adaptive dif modules in permafrost strains of *Acinetobacter lwoffii* and their distribution and abundance among present day *Acinetobacter* strains. *Front. Microbiol.* 10:632. doi: 10.3389/fmicb.2019.00632

Mindlin, S., Petrenko, A., Kurakov, A., Beletsky, A., Mardanov, A., and Petrova, M. (2016). Resistance of permafrost and modern *Acinetobacter lwoffii* strains to heavy metals and arsenic revealed by genome analysis. *Biomed. Res. Int.* 2016:3970831. doi: 10.1155/2016/3970831

Petrova, M. A., Mindlin, S. Z., Gorlenko, Z. M., Kaliaeva, E. S., Soina, V. S., and Bogdanova, E. S. (2002). Mercury-resistant bacteria from permafrost sediments and prospects for their use in comparative studies of mercury resistance determinants. *Genetika* 38, 1569–1574.

Salgado-Camargo, A. D., Castro-Jaimes, S., Gutierrez-Rios, R.-M., Lozano, L. F., Altamirano-Pacheco, L., Silva-Sanchez, J., et al. (2020). Structure and evolution of *Acinetobacter baumannii* plasmids. *Front. Microbiol.* 11:1283. doi: 10.3389/fmicb.2020.01283

Salto, I. P., Torres Tejerizo, G., Wibberg, D., Pühler, A., Schlüter, A., and Pistorio, M. (2018). Comparative genomic analysis of *Acinetobacter* spp. plasmids originating from clinical settings and environmental habitats. *Sci. Rep.* 8:7783. doi: 10.1038/s41598-018-26180-3

Shintani, M., Sanchez, Z. K., and Kimbara, K. (2015). Genomics of microbial plasmids: classification and identification based on replication and transfer systems and host taxonomy. *Front. Microbiol.* 6:242. doi: 10.3389/fmicb.2015.00242

Silva, L., Mourao, J., Grosso, F., and Peixe, L. (2018). Uncommon carbapenemase-encoding plasmids in the clinically emergent *Acinetobacter pittii*. *J. Antimicrob. Chemother.* 73, 52–56. doi: 10.1093/jac/dkx364

Smillie, C., Garcillán-Barcia, M. P., Francia, M. V., Rocha, E. P., and de la Cruz, F. (2010). Mobility of plasmids. *Microbiol. Mol. Biol. Rev.* 74, 434–452. doi: 10.1128/MMBR.00020-10

Thomas, C. M., Thomson, N. R., Cerdeño-Tárraga, A. M., Brown, C. J., Top, E. M., and Frost, L. S. (2017). Annotation of plasmid genes. *Plasmid* 91, 61–67. doi: 10.1016/j.plasmid.2017.03.006

Touchon, M., Cury, J., Yoon, E. J., Krizova, L., Cerqueira, G. C., Murphy, C., et al. (2014). The genomic diversification of the whole *Acinetobacter* genus: origins, mechanisms, and consequences. *Genome Biol. Evol.* 6, 2866–2882. doi: 10.1093/gbe/evu225

Vallenet, D., Nordmann, P., Barbe, V., Poirel, L., Mangenot, S., Bataille, E., et al. (2008). Comparative analysis of *Acinetobacters*: three genomes for three lifestyles. *PLoS One* 3:e1805. doi: 10.1371/journal.pone.0001805

Veress, A., Nagy, T., Wilk, T., Kömüves, J., Olasz, F., and Kiss, J. (2020). Abundance of mobile genetic elements in an *Acinetobacter lwoffii* strain isolated from transylvanian honey sample. *Sci. Rep.* 10:2969. doi: 10.1038/s41598-020-59938-9

Walter, T., Klim, J., Jurkowski, M., Gawor, J., Köhling, I., Słodownik, M., et al. (2020). Plasmidome of an environmental *Acinetobacter lwoffii* strain originating from a former gold and arsenic mine. *Plasmid* 110:102505. doi: 10.1016/j.plasmid.2020.102505

Wick, R. R., Judd, L. M., Gorrie, C. L., and Holt, K. E. (2017). Unicycler: resolving bacterial genome assemblies from short and long sequencing reads. *PLoS Comput. Biol.* 13:e1005595. doi: 10.1371/journal.pcbi.1005595

Yoon, E. J., Goussard, S., Nemec, A., Lambert, T., Courvalin, P., and Grillot-Courvalin, C. (2016). Origin in *Acinetobacter gyllenbergii* and dissemination of aminoglycoside-modifying enzyme AAC(6')-Ih. *J. Antimicrob. Chemother.* 71, 601–606. doi: 10.1093/jac/dkv390

Conflict of Interest: The authors declare that the research was conducted in the absence of any commercial or financial relationships that could be construed as a potential conflict of interest.

frontiers in Microbiology

ORIGINAL RESEARCH
published: 13 November 2020
doi: 10.3389/fmicb.2020.587398

Prevalence and Characterization of Carbapenem-Hydrolyzing Class D β-Lactamase-Producing *Acinetobacter* Isolates From Ghana

*Alafate Ayibieke[1], Ayumi Kobayashi[1], Masato Suzuki[2], Wakana Sato[1], Samiratu Mahazu[1,3], Isaac Prah[1,4], Miyuki Mizoguchi[5], Kyoji Moriya[5], Takaya Hayashi[4], Toshihiko Suzuki[6], Shiroh Iwanaga[3], Anthony Ablordey[7] and Ryoichi Saito[1]**

[1] Department of Molecular Microbiology, Tokyo Medical and Dental University, Tokyo, Japan, [2] Antimicrobial Resistance Research Center, National Institute of Infectious Diseases, Tokyo, Japan, [3] Department of Environmental Parasitology, Tokyo Medical and Dental University, Tokyo, Japan, [4] Department of Molecular Virology, Tokyo Medical and Dental University, Tokyo, Japan, [5] Department of Infection Control and Prevention, The University of Tokyo Hospital, Tokyo, Japan, [6] Department of Bacterial Pathogenesis, Tokyo Medical and Dental University, Tokyo, Japan, [7] Department of Bacteriology, Noguchi Memorial Institute for Medical Research, University of Ghana, Accra, Ghana

OPEN ACCESS

Edited by:
Benjamin Andrew Evans,
University of East Anglia,
United Kingdom

Reviewed by:
Andres Felipe Opazo-Capurro,
University of Concepcion, Chile
Branka Bedenić,
University of Zagreb, Croatia

***Correspondence:**
Ryoichi Saito
r-saito.mi@tmd.ac.jp

Specialty section:
This article was submitted to Antimicrobials, Resistance and Chemotherapy, a section of the journal Frontiers in Microbiology

Received: 26 July 2020
Accepted: 15 October 2020
Published: 13 November 2020

Citation:
Ayibieke A, Kobayashi A, Suzuki M, Sato W, Mahazu S, Prah I, Mizoguchi M, Moriya K, Hayashi T, Suzuki T, Iwanaga S, Ablordey A and Saito R (2020) Prevalence and Characterization of Carbapenem-Hydrolyzing Class D β-Lactamase-Producing Acinetobacter Isolates From Ghana. Front. Microbiol. 11:587398. doi: 10.3389/fmicb.2020.587398

Multidrug resistance, especially carbapenem resistance in *Acinetobacter* bacteria is a global healthcare concern. However, available data on the phenotypic and genotypic characteristics of *Acinetobacter* isolates from West Africa, including Ghana is scanty. Our aim was to investigate the antibiotic resistance profile and genotypic characteristics of *Acinetobacter* isolates from Ghana and to characterize carbapenemase producers using whole-genome sequencing (WGS). A total of 36 *Acinetobacter* isolates collected at three hospitals in Ghana between 2016 and 2017 were analyzed. MICs were determined by commercial antibiotic plates. *Acinetobacter baumannii* MLST was determined using the Pasteur scheme. WGS of OXA-carbapenemase producers was performed using short- and long-read sequencing strategies. The resistance rate was highest for trimethoprim/sulfamethoxazole (n = 22; 61%). Six (16.7%) and eight (22.2%) isolates were resistant to ceftazidime and colistin, respectively. Two (5.6%) isolates were resistant and one (2.8%) isolate had intermediate sensitivity to three carbapenems. Fifteen STs were identified in 24 *A. baumannii* isolates including six new STs (ST1467 ∼ ST1472). ST78 was the predominant (n = 6) followed by ST1469 (n = 3). Four carbapenemase-producing *A. baumannii* isolates also were identified. Isogenic ST103 isolates Ab-B004d-c and Ab-D10a-a harbored bla_{OXA-23} within Tn*2007* on identical plasmids, pAb-B004d-c_3, and pAb-D10a-a_3. ST1472 isolate Ab-C102 and ST107 isolate Ab-C63 carried bla_{OXA-58} and $bla_{OXA-420}$, a rare bla_{OXA-58} variant, respectively, within novel genetic contexts. Our results show that *A. baumannii* isolates of diverse and unique genotypes, including OXA-carbapenemase producers, are circulating in Ghana highlighting the need for a wider surveillance of antimicrobial resistance.

Keywords: carbapenem-hydrolyzing class D β-lactamases, carbapenem-resistant *Acinetobacter*, multilocus sequence typing, whole-genome sequencing, *Acinetobacter baumannii*, OXA-type beta-lactamase

INTRODUCTION

Acinetobacter species are important pathogens, responsible for healthcare-related infections. *Acinetobacter baumannii* is the most clinically prevalent species, but the clinical significance of *A. pittii* and *A. nosocomialis* is also increasing (Adams et al., 2008; Chuang et al., 2011; Nemec et al., 2011; Doi et al., 2015). As *Acinetobacter* spp. have intrinsic resistance to several antibiotic classes and can acquire resistance determinants, carbapenems are an optimal treatment option for infections caused by these bacteria. However, carbapenem resistance is rising worldwide, leaving very limited antimicrobial treatment options (Dijkshoorn et al., 2007; Hamidian and Nigro, 2019). Therefore, carbapenem-resistant *Acinetobacter* (CRA) is globally recognized as an urgent threat (World Health Organization, 2017; Centers for Disease Control and Prevention, 2019).

Carbapenem resistance in *Acinetobacter* is mainly caused by the production of carbapenem-hydrolyzing class D β-lactamases (CHDLs) including OXA-23-like, OXA-24-like and OXA-58-like enzymes, or by the production of Ambler class B metallo-β-lactamases (MBLs) such as NDM-, IMP- and VIM-type enzymes (Potron et al., 2015). Until now, only NDM-1-producing *A. baumannii* has been reported in Accra, the capital of Ghana (Codjoe et al., 2019). In *A. baumannii*, overexpression of the intrinsic $bla_{\mathrm{OXA-51}}$-like gene mediated by the insertion sequence IS*Aba1* upstream also confers resistance to carbapenems (Wong et al., 2019). Changes in outer membrane proteins and overexpression of efflux pumps are also associated with carbapenem resistance (Poirel and Nordmann, 2006a; Coyne et al., 2011).

Surveillance of CRA prevalence, associated genotypes, and elucidating the mechanisms underlying resistance are crucial as they enable us to understand how these bacteria disseminate and how best to control their spread. However, due to the poor antimicrobial resistance surveillance in Ghana, data on CRA is limited. Moreover, no data is available yet for CHDL-producing *Acinetobacter* and their genotypic characteristics.

Our aim was to investigate the antibiotic resistance profile and the genotypic characteristics of clinical isolates of *Acinetobacter* spp. collected at three regional hospitals in Ghana. Furthermore, we also characterize OXA-carbapenemase producers using both short- and long-read whole-genome sequencing (WGS).

MATERIALS AND METHODS

Bacterial Isolates and Identification

A total of 36 non-redundant *Acinetobacter* clinical isolates were recovered from different patients at three hospitals in Ghana (Tamale Teaching Hospital, $n = 3$; Cape Coast Teaching Hospital, $n = 2$; and Effia Nkwanta Regional Hospital, $n = 31$) between 2016 and 2017. Specimen types included urine ($n = 12$), sputum ($n = 8$), wound ($n = 3$), high vaginal swabs ($n = 2$), blood ($n = 1$), semen ($n = 1$) and cerebrospinal fluid ($n = 1$). For the remaining six samples, specimen types were not found from the medical records. Microbial identification was performed using the MALDI Biotyper (Bruker Daltonics, Karlsruhe, Germany). *Acinetobacter baumannii* complex (ABC) isolates were further characterized to species level using *gyrB* multiplex PCR method as previously described (Higgins et al., 2010).

Antibiotic Susceptibility Testing

The MICs of 15 antibiotics including meropenem, colistin, and minocycline were determined by broth microdilution using the commercial microplates DP34 and DP35 (Eiken Chemical Co., Tokyo, Japan). Results were interpreted according to the Clinical and Laboratory Standards Institute guideline document M100-S27 (Clinical and Laboratory Standards Institute, 2017).

Screening for Carbapenemase Genes

DNA was extracted using the Cica Geneus™ DNA Extraction reagent (Kanto Chemical Co., Tokyo, Japan) and subsequently screened for common CHDLs such as $bla_{\mathrm{OXA-23}}$-like, $bla_{\mathrm{OXA-24}}$-like, $bla_{\mathrm{OXA-58}}$-like, and $bla_{\mathrm{OXA-235}}$-like, as well as the *A. baumannii* native β-lactamase $bla_{\mathrm{OXA-51}}$-like, using multiplex PCR, as previously described (Woodford et al., 2006; Higgins et al., 2013). Screenings for other carbapenemase genes including $bla_{\mathrm{OXA-48}}$, bla_{NDM}, bla_{KPC}, bla_{IMP}, bla_{VIM}, and bla_{GES} were also conducted for all isolates (Dallenne et al., 2010; Wachino et al., 2011).

Multilocus Sequence Typing

Multilocus sequence typing (MLST) was performed for all confirmed *A. baumannii* isolates using the Pasteur scheme. New allele types and new sequence types (STs) were submitted to PubMLST[1] and assigned new numbers. Genetic relatedness of STs was analyzed and visualized using PHYLOVIZ 2.0 goBURST Full MST analysis (Nascimento et al., 2017).

Whole-Genome Sequencing

Short- and long-read WGS was conducted in four CHDL-producing isolates to determine their complete chromosome and plasmid sequences with high accuracy. DNA was extracted with the NucleoSpin tissue kit (Macherey-Nagel, Düren, Germany) for short-read sequencing; in one of the isolates the DNA library was prepared with the Nextera DNA Flex library prep kit and sequenced with Illumina Miseq (Illumina, San Diego, CA, United States); GIEasy FS PCR-Free DNA Library Prep Set was used for the remaining three isolates and sequenced with MGI DNBSEQ (MGI Tech Co., Shenzhen, China). Nanopore MinION (Oxford Nanopore Technologies, Oxford, United Kingdom) was used for long-read sequencing; DNA was extracted with the MagAttract HMW DNA Kit (Qiagen, Hildon, Germany); multiplexed DNA libraries were prepared for all four isolates using the Native Barcoding Kit EXP-NBD104 and the ligation sequence Kit SQK-LSK109; and sequencing was performed on a single R9.4.1 flow cell. Low-quality reads (MinION $Q < 10$; DNBSEQ $Q < 32$; and MiSeq $Q < 30$) and short reads (MinION length <1,000 bp; DNBSEQ and Miseq length <10 bp) were filtered out.

[1] https://pubmlst.org/abaumannii/

Bioinformatics Analysis

Hybrid *de novo* genome assembly for WGS data was done with Unicycler v0.4.8 and Flye v2.6 using both short and long reads. Sequence annotation was performed using the online system RAST and BLAST searches. Whole-genome SNP typing was done for four CHDL producers using PathoBacTyper[2]. Resfinder v3.2 was used to detect acquired resistance genes (Zankari et al., 2012). Insertion sequences were identified using ISfinder[3]. Plasmid structures and genetic contexts of carbapenemase genes were compared and visualized using Easyfig v2.2.2 (Sullivan et al., 2011).

Phylogenetic Analysis

Forty-five bla_{OXA-58} plasmids and one $bla_{OXA-420}$ plasmid in the repository of PLSDB v.2020_03_04 (Galata et al., 2019), as well as two plasmids from this study (pAbC102_1 and pAbC63_1) were used for phylogenetic analysis. Sequence alignment of plasmids was performed using CLC genomic workbench 20 (CLC bio, Aarhus, Denmark). A maximum parsimony tree with 1,000 bootstrap replicates was generated using MEGA X 10.1 (Kumar et al., 2018).

Accession Numbers

Complete chromosomal and plasmid sequences were deposited in GenBank under Bioproject PRJNA473419.

RESULTS

Phenotypic Characterization of *Acinetobacter* Isolates

Thirty-five out of the 36 isolates belonged to ABC, while the other isolate was identified as *A. haemolyticus*. Among all ABCs, 24 isolates (68.6%) were characterized as *A. baumannii* followed by seven *A. nosocomialis* (20%) and three *A. pittii* (8.6%). The species for the remaining one ABC isolate (identified using MALDI Biotyper) was not determined due to conflicting results from the *gyrB* multiplex PCR; this isolate was negative for the bla_{OXA-51}-like.

Resistance to trimethoprim/sulfamethoxazole was the most prevalent (n = 22; 61%), followed by resistance to piperacillin (n = 14; 38.9%), and tobramycin (n = 13; 36.1%) (**Table 1**). Six (16.7%) isolates were resistant to ceftazidime and eight (22.2%) were resistant to colistin. Two (5.6%) were resistant and one (2.8%) had intermediate susceptibility to three carbapenems. Resistance to amikacin and minocycline was the least frequent (n = 1; 2.8% for each). Resistance to all antibiotics, except for amikacin and colistin, were higher among *A. baumannii* than non-*baumannii Acinetobacter* isolates.

Detection of Carbapenemase Producers

Two *A. baumannii* isolates, Ab-D10a-a and Ab-B004d-c, belonging to ST103, and harboring bla_{OXA-23} were identified. The allelic variant of bla_{OXA-51} was bla_{OXA-70} for both isolates. In addition, *A. baumannii* isolates, Ab-C102A and Ab-C63, belonging to the novel ST1472 and ST107 with bla_{OXA-51} variants of $bla_{OXA-699}$ and bla_{OXA-51} respectively, were also identified and found to harbor CHDLs, bla_{OXA-58} and $bla_{OXA-420}$. All four isolates were collected at the Effia Nkwanta Regional Hospital. Other carbapenemase genes, such as MBL genes were not detected by conventional PCR.

Genetic Diversity of *Acinetobacter baumannii* Isolates

The genetic relatedness of the 24 *A. baumannii* isolates was assessed using the Pasteur MLST scheme. Isolates were assigned into 15 different STs, six of which were novel STs (ST1467, ST1468, ST1469, ST1470, ST1471, and ST1472). Minimum spanning tree analysis revealed that all STs had no genetic relationship with each other (**Figure 1**). ST78 (n = 6; 25%) was the most predominant, followed by the novel ST1467 (n = 3; 12.5%).

Genotypic Characterization of Ab-B004d-c, Ab-D10a-a, and bla_{OXA-23} Genetic Context

Two OXA-23-producing ST103 isolates, Ab-B004d-c, and Ab-D10a-a, were recovered from sputum and cerebrospinal fluid samples of different patients in January 2016 (**Figure 2**). Both isolates were resistant to most antibiotics, including carbapenems, but were fully susceptible to colistin (**Table 2**). Over 4 Gb short-read sequences and about 1.8 Gb long-read sequences were obtained for each isolate after quality filtering (**Supplementary Table 1**). Using *de novo* hybrid assembly, two circular chromosomes with 4,091,477 and 4,100,469 bp were generated for Ab-B004d-c and Ab-D10a-a, respectively (**Supplementary Table 2**). Both isolates were isogenic, differing by only 10 SNPs (**Figure 2**). Four pairs of identical plasmids ranging in size from 2,697–48,239 bp also were generated for both isolates (**Supplementary Table 2**). Ab-D10a-a carried an extra 6,619 bp plasmid (**Supplementary Table 2**). The chromosomes of both isolates carried the aminoglycoside resistance gene *aac*(3)-IIa, the sulphonamide resistance gene *sul*1, the intrinsic β-lactamase gene bla_{OXA-70}, the extended-spectrum β-lactamase (ESBL) gene $bla_{CTX-M-15}$, and the intrinsic AmpC gene $bla_{ADC-203}$. No insertion sequences were detected upstream of bla_{OXA-70} and $bla_{ADC-203}$. The trimethoprim resistance gene *dfr*A1, the aminoglycoside resistance gene *aac*(3)-IId, the tetracycline resistance gene *tet*(39), and macrolide resistance genes *msr*(E) and *mph*(E) were found on two identical plasmids with 48,239 bp (pAb-B004d-c_1 and pAb-D10a-a_1) in both isolates.

The bla_{OXA-23} gene was present on two identical 8,215 bp plasmids (pAb-B004d-c_3 and pAb-D10a-a_3) within Tn*2007*, and flanked upstream by IS*Aba4* and downstream by a truncated ATPase gene (**Figure 3A**). No other resistance genes were detected in these plasmids. Annotation results and BLAST searches for ORFs failed to identify any replication origin protein (Rep) gene in these plasmids. The linearized sequences of pAb-B004d-c_3 and pAb-D10a-a_3 were compared with

[2]http://halst.nhri.org.tw/PathoBacTyper/index.jsp

[3]https://isfinder.biotoul.fr/

TABLE 1 | Antibiotic resistance profile of 36 *Acinetobacter* isolates.

Antibiotic	All isolates (*n* = 36)				*A. baumannii* isolates (*n* = 24)				Non-*baumannii Acinetobacter* isolates (*n* = 12)			
	MIC (μg/ml)			%R[a]	MIC (μg/ml)			%R[a]	MIC (μg/ml)			%R[a]
	Range	MIC_{50}	MIC_{90}		Range	MIC_{50}	MIC_{90}		Range	MIC_{50}	MIC_{90}	
Piperacillin	8 to >64	32	>64	38.9	8 to >64	>64	>64	50	8 to >64	32	>64	16.7
Ampicillin-sulbactam	1/2 to >8/16	1/2	4/8	5.6	1/2 to >8/16	2/4	8/16	8.3	1/2 to 4/8	1/2	2/4	0
Piperacillin-tazobactam	≤4/16 to >4/64	≤4/16	>4/64	22.2	≤4/16 to >4/64	4/32	>4/64	29.2	≤4/16 to >4/64	≤4/16	4/32	8.3
Ceftazidime	2 to >16	4	>16	16.7	4 to >16	4	>16	20.8	2 to >16	4	16	8.3
Cefepime	1 to >16	4	>16	13.9	2 to >16	4	>16	16.7	1 to >16	2	16	8.3
Imipenem	≤0.25 to >8	≤0.25	1	5.6	≤0.25 to >8	≤0.25	4	8.3	≤0.25 to 1	≤0.25	≤0.25	0
Meropenem	≤0.25 to >8	0.5	2	5.6	≤0.25 to >8	0.5	4	8.3	≤0.25 to 2	≤0.25	1	0
Doripenem	≤0.25 to >8	≤0.25	1	5.6	≤0.25 to >8	0.5	4	8.3	≤0.25 to 1	≤0.25	1	0
Gentamycin	0.5 to >8	0.5	>8	33.3	0.5 to >8	>8	>8	50	0.5 to 2	0.5	2	0
Tobramycin	0.5 to >8	1	>8	36.1	0.5 to >8	8	>8	50	0.5 to >8	0.5	2	8.3
Amikacin	≤1 to >32	2	4	2.8	2 to 16	2	4	0	≤1 to >32	2	8	1.3
Minocycline	≤0.25 to >8	0.5	2	2.8	≤0.25 to >8	0.5	4	4.2	≤0.25 to 4	≤0.25	1	0
Colistin	≤2 to 8	≤2	4	22.2	≤2 to 4	≤2	4	12.5	≤2 to >8	≤2	8	41.7
Ciprofloxacin	0.12 to >2	0.5	>2	33.3	0.12 to >2	>2	>2	50	0.12 to 1	0.25	1	0
Levofloxacin	≤1 to >4	≤1	>4	16.7	≤1 to >4	4	>4	25	≤1	≤1	≤1	0
Trimethoprim-sulfamethoxazole	≤19/1 to >38/2	>38/2	>38/2	61.1	≤19/1 to >38/2	>38/2	>38/2	66.7	≤19/1 to >38/2	>38/2	>38/2	50

[a]*Resistant.*

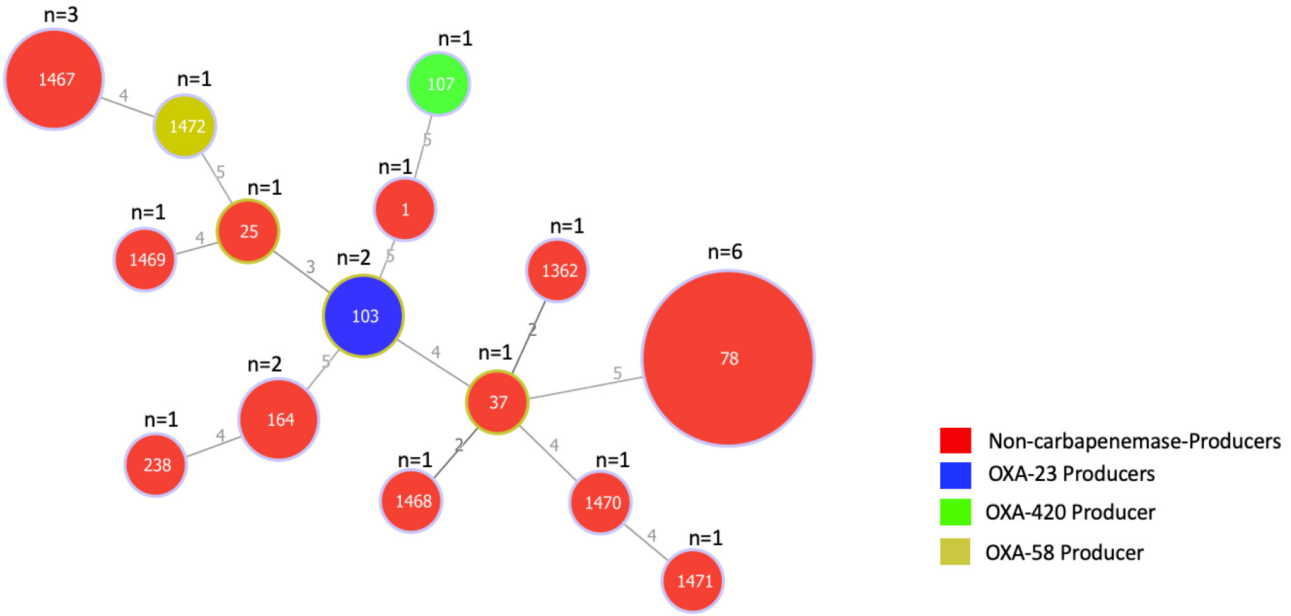

FIGURE 1 | Minimum spanning tree based on the allelic profiles of 15 STs identified in 24 *A. baumannii* isolates. The number of isolates for each ST is shown at the top of each node. Node sizes are proportional to the number of isolates for each ST and numbers on connecting lines indicate the number of locus variants determined by pair-wise comparisons. Colors indicate whether isolates are carbapenemase producers and if so, the type of carbapenemase they produce.

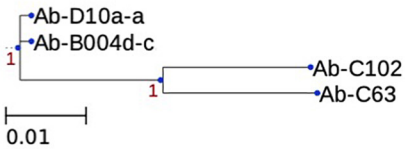

Accession Number	Specimen	Isolation Date	Genome Size (bp)	GC%
CP051869	CSF*	Jan 2016	4,100,469	39.1
CP051875	Sputum	Jan 2016	4,091,477	39.1
CP051862	Blood	Mar 2016	3,763,047	39.2
CP051866	Sputum	Feb 2016	3,873,866	39.0

FIGURE 2 | Whole-genome SNP analysis of chromosomal sequences of four CHDL-producing isolates and their characteristics. Scale bar indicates nucleotide substitutions per site (1 SNP per 100 sites). Confidence levels are shown close to the branches. *CSF, cerebral spinal fluid.

the bla_{OXA-23}-containing region of pAB14 from *A. baumannii* (accession number: EF059914). Results showed that the genetic structure of Tn*2007* was highly identical in pAb-B004d-c_3, pAb-D10a-a_3 and pAB14. In addition, a *higBA* toxin-antitoxin locus was found downstream of Tn*2007*.

Genotypic Characterization of Ab-C102 and bla_{OXA-58} Genetic Context

The OXA-58-producing ST1472 isolate Ab-C102 was recovered from the blood of a patient. Ab-C102 was susceptible to almost all antibiotics but displayed a low meropenem MIC (1 mg/L) (**Table 2**).

Similar to the isolates described before, more than 4 Gb of short-read and near 1 Gb of long-read sequences were obtained by WGS for the isolate Ab-C102, after quality filtering (**Supplementary Table 1**). A circular chromosome with 3,763,047 bp and three circular plasmids with 19,853, 67,097, and 90,089 bp were generated by hybrid *de novo* genome assembly (**Supplementary Table 2**). A novel variant of the intrinsic bla_{OXA-65} gene with three synonymous nucleotide substitutions, and an intrinsic bla_{ADC-32} gene were identified on the chromosome. No insertion sequences were detected upstream of these genes. The carbapenemase gene bla_{OXA-58} along with other resistance genes such as *aph*(6)-Id were identified on a 90,089 bp plasmid (pAb-C102_1; **Table 2**).

This plasmid encodes a RepB family plasmid Rep that share 100% identity with its counterpart in *A. baumannii* WB103 (accession number: AZM37906). Phylogenetic analysis showed that the genetically closest plasmid to pAb-C102_1 was pNDM-1_010045, with which it share 46% query cover and 97.25% identity (**Figure 4**). Interestingly, a BLAST search found that the full plasmid sequence of pAb-C102_1 had the highest homology with the draft WGS data of WB103, sharing 88% of query cover and 99.88% of identity.

The genetic environment of bla_{OXA-58} in pAb-C102_1 was comparable to that in pWA3 (accession number: JQ241791), with a similar genetic structure (**Figure 3B**). In both plasmids, the

TABLE 2 | Genotypic and phenotypic antibiotic resistance profiles of four CHDL-producing *A. baumannii* isolates.

Isolates	CHDL type	Chromosome/ plasmid	Resistance genes	MIC (mg/L)														
				PIPC	S/A	TAZ/PIPC	CAZ	CFPM	IPM	MEPM	DRPM	GM	TOB	AMK	MINO	CL	CPFX	LVFX	ST
Ab-B004d-c	OXA-23	Chromosome	*bla*ADC-66, *bla*OXA-70, *sul*1, *ant*(3″)-IIa, *aac*(3)-IIa and *bla*CTX-M-15	>64	>8/16	>4/64	>16	>16	>8	>8	>8	>8	>8	8	0.5	≤2	>2	>4	>38/2
		Plasmid	*dfr*A1, *mph*(E), *msr*(E), *tet*(39), *aac*(3)-IId and *bla*OXA-23																
Ab-D10a-a	OXA-23	Chromosome	*bla*ADC-66, *bla*OXA-70, *sul*1, *ant*(3″)-IIa, *aac*(3)-IIa and *bla*CTX-M-15	>64	>8/16	>4/64	>16	>16	>8	>8	>8	>8	>8	16	0.5	≤2	>2	>4	>38/2
		Plasmid	*dfr*A1, *mph*(E), *msr*(E), *tet*(39), *aac*(3)-IId and *bla*OXA-23																
Ab-C102	OXA-58	Chromosome	*ant*(3″)-IIa, *bla*OXA-699 and *bla*ADC-32	64	1/2	4/32	8	4	1	1	0.5	0.5	2	2	≤0.25	≤2	0.5	≤1	>38/2
		Plasmid	*aph*(6)-Id, *aph*(3″)-Ib, *sul*2, *aph*(3′)-Ia, *flo*R and *bla*OXA-58																
Ab-C63	OXA-420	Chromosome	*bla*ADC-87, *bla*OXA-51 and *ant*(3″)-IIa	>64	8/16	>4/64	4	8	4	4	4	>8	>8	2	0.5	4	>2	>4	>38/2
		Plasmid	*mph*(E), *msr*(E), *tet*(39), *dfr*A20, *sul*2, *aph*(6)-Id, *aph*(3″)-Ib, *bla*OXA-420, *ant*(2″)-Ia and *aph*(3')-Ia																

Abbreviations: PIPC, piperacillin; S/A, ampicillin-sulbactam; TAZ/PIPC, piperacillin-tazobactam; CAZ, ceftazidime; CFPM, cefepime; IPM, imipenem; MEPM, meropenem; DRPM, doripenem; GM, gentamycin; TOB, tobramycin; AMK, amikacin; MINO, minocycline; CL, colistin, CPFX, ciprofloxacin; LVFX, levofloxacin; ST, trimethoprim-sulfamethoxazole.

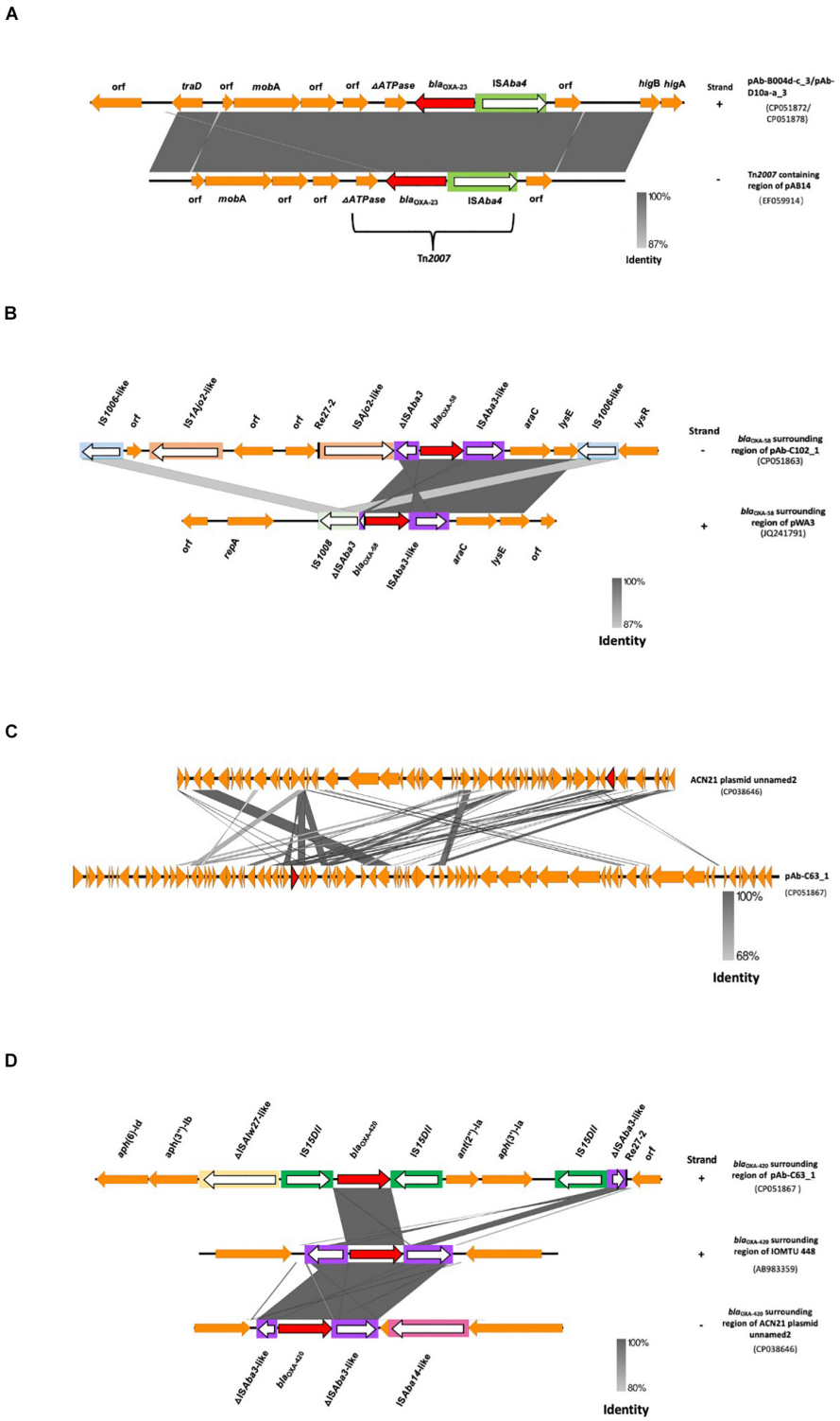

FIGURE 3 | Genetic contexts of CHDLs in *A. baumannii* from Ghana. **(A)** Linearized whole plasmid sequence of bla_{OXA-23}-containing plasmids pAb-B004d-c_3 and pAb-D10a-a_3, compared to the Tn*2007*-containing region of pAB14. **(B)** bla_{OXA-58}-surrounding region of pAb-C102_1 compared with that of pWA3. **(C)** Linearized whole plasmid backbone structure of pAb-C63_1 compared with that of ACN21 plasmid unnamed2. **(D)** $bla_{OXA-420}$-surrounding region of pAb-C102_1 compared with that of IOMTU 448 and ACN21 plasmid unnamed2. Carbapenemase genes are represented by red arrows, and other coding sequences are represented in orange. IS elements are inside rectangular boxes. The direction of transposase genes is indicated by white arrows. Same or highly similar IS elements are depicted in the same colors. Re-27 sequences are represented by vertical black bars. Positive and reverse strands are labeled at the right end of each sequence with the symbols "+" and "–", respectively.

same IS*Aba3*-like-*ara*C1-*lys*E structure was found downstream of bla_{OXA-58} and the same three nucleotide substitutions were present in both IS*Aba3*-like. The IS*Aba3*-like-*ara*C1-*lys*E was followed by one IS*1006*-like copy (one nucleotide substitution compared to IS*1006*) and the *lys*R gene. Upstream of bla_{OXA-58}, a 427 bp truncated form of IS*Aba3* was interrupted by a putative novel IS*Ajo2*-like sequence. This contrasted with pWA3 in which a 121 bp truncated form of IS*Aba3* is interrupted by IS*1008*. A Re27-2 region, which is a p*dif* site targeted by the XerC/XerD-like site-specific recombinases, was found 13 bp upstream of the IS*Ajo2*-like sequence. A second copy of IS*Ajo2*-like and IS*1006*-like (three nucleotide substitutions compared with IS*1006*) was found upstream of the Re27-2 region. Neither a second copy of Re27-2 nor Re27-1 (single nucleotide variant of Re27-2) were found downstream of bla_{OXA-58}.

Genotypic Characterization of Ab-C63 and $bla_{OXA-420}$ Genetic Context

Ab-C63 was an isolate recovered from a sputum sample that belonged to ST107 and produced OXA-420, a rare CHDL of the OXA-58 family. This isolate had intermediate susceptibility to carbapenems and was resistant to aminoglycosides, fluoroquinolones and colistin (**Table 2**).

A 3,873,864 bp circular chromosome and two plasmids with 81,353 and 10,662 bp were generated by hybrid assembly using quality-filtered ∼350 Mb short-read and ∼1.2 Gb long-read sequences (**Supplementary Tables 1** and **2**). The intrinsic β-lactamase genes bla_{ADC-87} and bla_{OXA-51}, as well as the aminoglycoside resistance gene *ant*(3″)-IIa were found on the chromosome. The $bla_{OXA-420}$ gene and other resistance genes such as *mph*(E) were located on a plasmid with 81,353 bp (pAb-C63_1; **Table 2**). This plasmid harbored a novel gene encoding a RepB family plasmid Rep which shared the highest similarity (99.7% identity) with proteins from *Acinetobacter* spp. and *A. brisouii* (accession numbers: WP_004761033, WP_151711075).

Phylogenetic analysis (**Figure 4**) showed pAB-C63_1 to be genetically distinct from the $bla_{OXA-420}$-containing *A. baumannii* ACN21 plasmid unnamed2 (NZ_CP038646), collected in India, but genetically close to the bla_{OXA-58}-containing pAI01 (NZ_CP044019), with which it shares 42% query cover and 95% identity. Plasmid backbone structure comparisons also revealed that pAb-C63_1 had a novel backbone compared with ACN21 plasmid unnamed2 (**Figure 3C**). Moreover, a completely distinct genetic context was found surrounding $bla_{OXA-420}$ in pAbC63_1, in which the gene was flanked by two copies of IS*15DII*, in contrast with ACN21 plasmid unnamed2 and *A. baumannii* strain IOMTU in which $bla_{OXA-420}$ is flanked by IS*Aba3*-like and truncated IS*Aba3*-like elements (**Figure 3D**). In addition, a third copy of IS*15DII* was found downstream, interrupting an IS*Aba3* sequence. The resistance genes *ant*(2″)-Ia and *aph*(3′)-Ia were flanked by the second and third copies of IS*15DII*. The Re27-2 sequence was detected 65 bp downstream of the truncated IS*Aba3*. Moreover, a novel insertion sequence, a ΔIS*Alw27*-like element (coverage = 1268/1282; identities = 1213/1268), was detected upstream of the first copy of IS*15DII*.

DISCUSSION

Carbapenem resistance in *Acinetobacter* spp. is a major health threat worldwide. Most of the studies on CRA in Africa were conducted in Northern or Southern regions (Manenzhe et al., 2015), while the current situation in sub-Saharan Africa may be underestimated given the limited laboratory and surveillance capacity. Here, we showed that *Acinetobacter* species, predominantly *A. baumannii*, are disseminating in Ghanaian healthcare facilities. *A. nosocomialis* and *A. pittii* (previously known as *Acinetobacter* genomics species 13UT and 3, respectively) were also prevalent. The proportion of these species is parallel to those causing nosocomial bloodstream infections in the United States (Wisplinghoff et al., 2012). Conventional identification methods can not distinguish between ABCs, resulting in misidentification of some species as *A. baumannii* (Wisplinghoff et al., 2012). Although, *gyrB* multiplex PCR has been reported as one of the most highly sensitive methods distinguishing species within ABCs (Lee et al., 2014), the conflicting result that we obtained for an ABC isolate using this method has proven the difficulty associated with species identification among ABCs. Multidrug resistance, including to carbapenems, was detected in the *Acinetobacter* isolates. However, carbapenem resistance was less prevalent (5.6%), in our study (primarily conducted in the Western region of Ghana) compared with a prior study conducted in the country's capital, Accra, in which seven out of nine *A. baumannii* isolates from burn wounds were resistant to meropenem (Forson et al., 2017). Higher carbapenem resistance, 51.5 and 10%, have been reported in the West African countries of Nigeria and Sierra Leone, respectively (Nsofor and Chekwube, 2017; Lakoh et al., 2020). Such discrepancy suggests that CRA dissemination varies by region, and may be attributed to the variability in antibiotic choice, infection control, and prevention practices. Moreover, the use of carbapenems in clinical setting in Ghana has been reported as low, and its unavailability as an essential drug on the Ghanaian national health insurance scheme may be associated with low prescription (Labi et al., 2018). We speculate this low carbapenems usage is correlated with low resistance selective pressure which may explain the observed lower carbapenem resistance prevalence in our study. The 22.2% prevalence of colistin resistance among all *Acinetobacter* isolates as well as 12.5% among *A. baumannii* isolates in this study are high in comparison with other countries where the resistance prevalence was mostly at single digit levels for *A. baumannii* (Pormohammad et al., 2020). Such high resistance is alarming especially since colistin has become one of the last-resort antibiotics used for multidrug-resistant gram-negative bacterial infections. The acquired resistance mediated by plasmid originated *mcr* gene resulted in the global spread of the colistin resistance among *Enterobacteriaceae* (Wang et al., 2018; Wise et al., 2018). In *A. baumannii*, colistin resistance is not associated with the *mcr* gene, rather caused by the overexpressed PetN

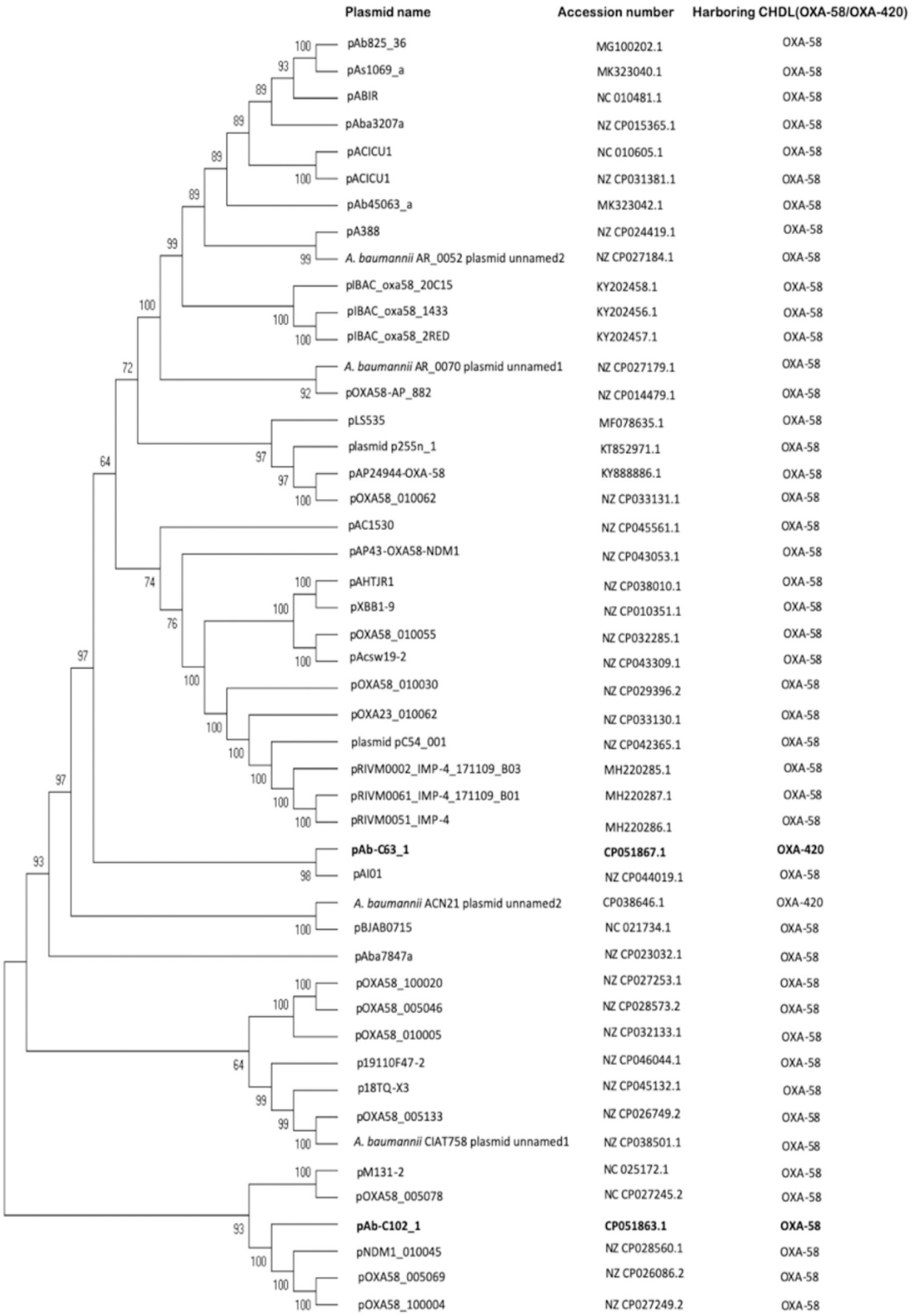

FIGURE 4 | Maximum parsimony tree of OXA-58- and OXA-420-containing plasmids. Two plasmids from the current study (highlighted in bold), 45 OXA-58-producing plasmids and one OXA-420-producing plasmid listed in PLSDB database were included. Bootstrap values are shown at each node.

transferases mediated by two pathways, overexpressed *pmrC* from mutations in *pmrCAB* operon and overexpressed *pmrC* homolog *eptA* from the insertion of IS*Aba1* on the upstream (Trebosc et al., 2019). Further investigation remains warranted to elucidate the resistance mechanisms involved in non-*baumannii Acinetobacter* isolates.

Several global clones (GC) of *A. baumannii* have emerged in the last decades with GC2, represented by ST2, being the most widespread, followed by GC1, represented by ST1. Multidrug resistance and carbapenemase production are mostly associated with the spread of these specific clones (Hamidian and Nigro, 2019). Here, we showed that *A. baumannii* isolates recovered in Ghana have high genetic diversity, associated with 15 STs among which six are novel. The predominant GC2 was absent and only a single isolate belonged to GC1. ST78, also known as the "Italian clone" (Carretto et al., 2011), was the predominant sequence type detected in Ghana. However, neither ST1 nor ST78 isolates were associated with carbapenemase production. The CHDL producers found belong to ST103, ST107 and ST1472; Both of ST103, and ST107 were uncommon, while ST1472 is a novel type. OXA-23 production is the leading carbapenem resistance mechanism in *A. baumannii*, mostly associated with GC2 and GC1 (Hamidian and Nigro, 2019). Although ST103 strains were associated with NDM-2-producing isolates in Egypt, UAE, and Palestine (Kaase et al., 2011; Ghazawi et al., 2012; Sjölander et al., 2014), and an OXA-235-producing strain was reported in Australia (Hamidian et al., 2017), to the best of our knowledge this is the first study to identify ST103 associated with OXA-23 production (isolates Ab-B004d-c and Ab-D10a-a). Based on the occurrence of OXA-58 carbapenemase in several *Acinetobacter* species and in *Proteus mirabilis* (Fu et al., 2014; Feng et al., 2016; Lange et al., 2017; Matos et al., 2019), it has been suggested that horizontal gene transfer rather than clonal spread is the main mechanism of bla_{OXA-58} dissemination. This may also explain the detection of a novel sequence type, ST1472 (isolate Ab-C102). ST107 isolate Ab-C63 carried $bla_{OXA-420}$, a rare variant of bla_{OXA-58} that was first described in *A. baumannii* ST623 and ST32 clinical isolates in Nepal (Shrestha et al., 2015). Ab-C63 was genetically distinct from the Nepalese isolates and other isolates identified in France and Brazil, which had the same ST and produced different CHDLs including OXA-24, OXA-143 and OXA-231 (Jeannot et al., 2014; Rodrigues-Costa et al., 2019).

We identified two isogenic OXA-23 producers, Ab-B004d-c and Ab-D10a-a. These two isolates were recovered from different patients in the same hospital, indicating a possible nosocomial outbreak. The ESBL gene $bla_{CTX-M-15}$ was also found on the chromosome of both isolates. Third-generation cephalosporin resistance in *A. baumannii* results mainly from the production of ESBLs of PER, GES and VEB types, or the overexpression of intrinsic AmpC β-lactamases owing to the upstream insertion of specific sequences such as IS*Aba1* (Hamidian and Hall, 2013; Potron et al., 2015). The ESBL gene $bla_{CTX-M-15}$ is the main mechanism of resistance to third-generation cephalosporins in *Enterobacteriaceae*, but not a common one in *Acinetobacter*. There are only a few report of its occurrence in *A. baumannii* isolates from India, Haiti, and Brazil (Shakil and Khan, 2010; Potron et al., 2011; Zago et al., 2016). Therefore, by detecting $bla_{CTX-M-15}$ in isolates from Ghana, our study provides evidence of its wider spread among *Acinetobacter* species.

The bla_{OXA-23} gene is the most common carbapenemase gene in *A. baumannii* and is usually mobilized by Tn*2006*, Tn*2007*, Tn*2008* (including its variants), Tn*2009*, Tn*6549*, and AbaR4 into the chromosome and plasmids. Tn*2006* is the most abundant of these mobile elements (Hamidian and Nigro, 2019). Tn*2007*, which was identified in plasmids pAb-B004d-c_3 and pAb-D10a-a_3 is relatively uncommon with no plasmids listed on PLSDB and only one in GenBank (pAB14) carrying it. However, its detection has been reported in isolates from Algeria, France, Spain, China, and Tanzania (Corvec et al., 2007; Guerrero-Lozano et al., 2015; Wang et al., 2015; Kumburu et al., 2019). The identification of Tn*2007* in samples from Ghana, within a plasmid that share a high level of sequence identity with pAB14 (identified in Algeria and Tanzania) strongly supports the importance of plasmids in the spread of carbapenemase genes, especially in Africa.

The bla_{OXA-58}-containing plasmid pAb-C102_1 (isolate Ab-C102) share the same Rep as well as the highest query cover and sequence homology with the draft genome of *A. baumannii* WB103, an isolate recovered from hospital wastewaters in Singapore and that also carry bla_{OXA-58} (Chen et al., 2019). It was not possible to compare the genetic structure between the two isolates because WB103 plasmid sequences are not assembled, but the findings suggest that pAb-C102_1 likely derived from a plasmid from WB103.

Diverse genetic environments are described for bla_{OXA-58}. The gene is commonly embedded in structures like IS*Aba2*:IS*Aba3*-bla_{OXA-58}-IS*Aba3* and IS*6* family element-ΔIS*Aba3*-bla_{OXA-58}-IS*Aba3*. Usually, these structures are accompanied downstream by *ara*C1 and *lys*E (Poirel and Nordmann, 2006b; Fu et al., 2014; Cameranesi et al., 2018); the former is involved in bla_{OXA-58} regulation (Fondi et al., 2010). Mobilization and acquisition of bla_{OXA-58} is driven by site-specific recombination at XerC/D-like sites (including mediation by Re27) rather than through its surrounding IS elements, leading to diverse structure arrangements (Poirel and Nordmann, 2006b; Cameranesi et al., 2018). We observed a similar pattern in pAb-C102_1, in which an IS*Aba3* element interrupted by a novel IS*Ajo2*-like sequence was followed by IS*Aba3*-like-*ara*C1-lysE, a structure that commonly surrounds bla_{OXA-58}. In addition, a Re27-2 site was found next to the novel IS*Ajo2*-like element. These results indicate that bla_{OXA-58} was acquired via a similar XerC/D-like site-specific recombination in pAb-C102_1, and that the second copy of the gene created in the process may have been lost. Moreover, different arrangements in insertion sequences upstream of bla_{OXA-58} were associated with its overexpression; compared with IS*Aba3* this resulted in a stronger promoter leading to higher carbapenem resistance levels (Chen et al., 2008, 2010; Fu et al., 2014). It is unclear whether the low carbapenem MIC levels in Ab-C102 is a consequence of IS*Ajo2*-like-ΔIS*Aba3* arrangement and a relatively weak bla_{OXA-58} promoter. Further investigations are needed to clarify this issue.

The gene $bla_{OXA-420}$ has three nucleotide substitutions and a single amino acid substitution compared with bla_{OXA-58}, and was first identified in 16 *A. baumannii* isolates from Nepal (Shrestha et al., 2015). Our BLAST search identified *A. baumannii* strain ACN21, isolated from India, that also carry $bla_{OXA-420}$, indicating that this specific variant is mostly spread in South Asia. To the best of our knowledge this study is the first to detect a $bla_{OXA-420}$-carrying isolate outside of Asia. Isolate Ab-C63 is not genetically related to earlier isolates from Nepal and India. Moreover, the genetic context of $bla_{OXA-420}$ in pAb-C63_1 is novel while those from India and Nepal are similar. The presence of a Re27-2 sequence, commonly associated with bla_{OXA-58} acquisition, near $bla_{OXA-420}$, suggests that this resistance gene also was acquired by XerC/D-mediated site-specific recombination in Ab-C63.

One limitation of our study is the limited sample size. Isolates were collected at three hospitals only, and the number of isolates obtained from two of the hospitals was extremely low. Hence, the results may not reflect the whole situation in Ghana.

In this study, we have demonstrated that the prevalence of carbapenem resistance in Ghana is low and that there is a high level of genetic diversity among clinical isolates of *Acinetobacter*. Furthermore, we characterized, for the first time in Ghana, OXA- 23-, OXA-58- and OXA-420-producing *A. baumannii* isolated belonging to ST103, ST1472 and ST107, respectively. By combining short-read and long-read WGS we revealed that bla_{OXA-23} was within Tn*2007* in two plasmids (pAb-B004d-c_3 and pAb-D10a-a_3) and identified novel genetic structures surrounding bla_{OXA-58} and $bla_{OXA-420}$ (novel plasmids pAb-C102_1 and pAb-C63_1, respectively). Altogether, our results show that genetically diverse and unique *A. baumannii* isolates, including OXA-carbapenemase producers, are circulating in Ghana, measures to strengthen and expand surveillance of antimicrobial resistance worldwide remains essential.

DATA AVAILABILITY STATEMENT

The datasets presented in this study can be found in online repositories. The names of the repository/repositories and accession number(s) can be found in the article/ **Supplementary Material**.

ETHICS STATEMENT

The studies involving human participants were reviewed and approved by the ethics committee of the Faculty of Medicine, Tokyo Medical and Dental University (M2017-208) and the ethics committee of Noguchi Memorial Institute for Medical Research, University of Ghana (FWA 00001824). Written informed consent to participate in this study was provided by the participants' legal guardian/next of kin.

AUTHOR CONTRIBUTIONS

AAy, AAb, and RS conceived and designed the experiments. AAy, AK, MS, WS, SM, IP, MM, and RS performed the experiments. AAy, MS, TH, TS, SI, AAb, and RS analyzed the data. MS, KM, TH, TS, SI, AAb, and RS contributed to reagents, materials, and analysis tools. AAy, MS, AAb, and RS contributed to the writing of the manuscript. All authors contributed to the article and approved the submitted version.

FUNDING

This work was supported by the Japan Agency for Medical Research and Development (AMED, URL: http://www.amed.go.jp/en/) under Grant Numbers JP19fm0108010 (TH, TS, SI, and RS) and JP20fk0108133 (MS). The funder had no role in study design, data collection and analysis, decision to publish, or preparation of the manuscript.

ACKNOWLEDGMENTS

We are grateful for the excellent technical support from the Tamale teaching hospital, Cape Coast teaching hospital and Effia Nkwanta regional hospital.

SUPPLEMENTARY MATERIAL

The Supplementary Material for this article can be found online at: https://www.frontiersin.org/articles/10.3389/fmicb.2020.587398/full#supplementary-material

REFERENCES

Adams, M. D., Goglin, K., Molyneaux, N., Hujer, K. M., Lavender, H., Jamison, J. J., et al. (2008). Comparative genome sequence analysis of multidrug-resistant *Acinetobacter baumannii*. *J. Bacteriol.* 190, 8053–8064.

Cameranesi, M. M., Morán-Barrio, J., Limansky, A. S., Repizo, G. D., and Viale, A. M. (2018). Site-Specific Recombination at XerC/D Sites Mediates the Formation and Resolution of Plasmid Co-integrates Carrying a *bla*OXA-58- and Tn*aphA6*-Resistance Module in *Acinetobacter baumannii*. *Front. Microbiol.* 9:66. doi: 10.3389/fmicb.2018.00066

Carretto, E., Barbarini, D., Dijkshoorn, L., Van Der Reijden, T. J., Brisse, S., Passet, V., et al. (2011). Widespread carbapenem resistant *Acinetobacter baumannii* clones in Italian hospitals revealed by a multicenter study. *Infect. Genet. Evol.* 11, 1319–1326. doi: 10.1016/j.meegid.2011.04.024

Centers for Disease Control and Prevention (2019). *Antibiotic resistance threats in the United States, 2019*. Available online at: https://www.cdc.gov/drugresistance/pdf/threats-report/2019-ar-threats-report-508.pdf [accessed on April 30, 2020]

Chen, H., Gu, X., Ng, C., Haller, L., Rathinam Charles, F., and Gin, K. Y. (2019). Draft genome sequences of a ceftazidime-resistant *Acinetobacter baumannii* donor and a conjugal *Escherichia coli* recipient with acquired resistance. *Microbiol. Resour. Announc.* 8:e00024-19

Chen, T. L., Chang, W. C., Kuo, S. C., Lee, Y. T., Chen, C. P., Siu, L. K., et al. (2010). Contribution of a plasmid-borne *bla*OXA-58 gene with its hybrid promoter provided by IS*1006* and an IS*Aba3*-like element to beta-lactam resistance

in *acinetobacter* genomic species 13TU. *Antimicrob. Agents Chemother.* 54, 3107–3112. doi: 10.1128/aac.00128-10

Chen, T. L., Wu, R. C., Shaio, M. F., Fung, C. P., and Cho, W. L. (2008). Acquisition of a plasmid-borne *bla*OXA-58 gene with an upstream IS*1008* insertion conferring a high level of carbapenem resistance to *Acinetobacter baumannii*. *Antimicrob. Agents Chemother.* 52, 2573–2580. doi: 10.1128/aac.00393-08

Chuang, Y. C., Sheng, W. H., Li, S. Y., Lin, Y. C., Wang, J. T., Chen, Y. C., et al. (2011). Influence of genospecies of *Acinetobacter baumannii* complex on clinical outcomes of patients with acinetobacter bacteremia. *Clin. Infect. Dis.* 52, 352–360. doi: 10.1093/cid/ciq154

Clinical and Laboratory Standards Institute (2017). *Performance Standards for Antimicrobial Susceptibility Testing: Twenty-Seventh Informational Supplement M100-S27*. Wayne, PA: CLSI.

Codjoe, F. S., Brown, C. A., Smith, T. J., Miller, K., and Donkor, E. S. (2019). Genetic relatedness in carbapenem-resistant isolates from clinical specimens in Ghana using ERIC-PCR technique. *PLoS One* 14:e0222168. doi: 10.1371/journal.pone.0222168

Corvec, S., Poirel, L., Naas, T., Drugeon, H., and Nordmann, P. (2007). Genetics and expression of the carbapenem-hydrolyzing oxacillinase gene *bla*OXA-23 in *Acinetobacter baumannii*. *Antimicrob. Agents Chemother.* 51, 1530–1533. doi: 10.1128/aac.01132-06

Coyne, S., Courvalin, P., and Périchon, B. (2011). Efflux-mediated antibiotic resistance in *Acinetobacter* spp. *Antimicrob. Agents Chemother.* 55, 947–953. doi: 10.1128/aac.01388-10

Dallenne, C., Da Costa, A., Decré, D., Favier, C., and Arlet, G. (2010). Development of a set of multiplex PCR assays for the detection of genes encoding important β-lactamases in *Enterobacteriaceae*. *J. Antimicrobial. Chemother.* 65, 490–495. doi: 10.1093/jac/dkp498

Dijkshoorn, L., Nemec, A., and Seifert, H. (2007). An increasing threat in hospitals: multidrug-resistant *Acinetobacter baumannii*. *Nat. Rev. Microbiol.* 5, 939–951. doi: 10.1038/nrmicro1789

Doi, Y., Murray, G. L., and Peleg, A. Y. (2015). *Acinetobacter baumannii*: evolution of antimicrobial resistance-treatment options. *Semin. Respir. Crit. Care Med.* 36, 85–98.

Feng, Y., Yang, P., Wang, X., and Zong, Z. (2016). Characterization of Acinetobacter johnsonii isolate XBB1 carrying nine plasmids and encoding NDM-1. *OXA-58 and PER-1 by genome sequencing. J. Antimicrob. Chemother.* 71, 71–75. doi: 10.1093/jac/dkv324

Fondi, M., Bacci, G., Brilli, M., Papaleo, M. C., Mengoni, A., Vaneechoutte, M., et al. (2010). Exploring the evolutionary dynamics of plasmids: the *Acinetobacter* pan-plasmidome. *BMC Evol. Biol.* 10:59. doi: 10.1186/1471-2148-10-59

Forson, O. A., Ayanka, E., Olu-Taiwo, M., Pappoe-Ashong, P. J., and Ayeh-Kumi, P. J. (2017). Bacterial infections in burn wound patients at a tertiary teaching hospital in Accra. *Ghana. Ann. Burns Fire Dis.* 30, 116–120.

Fu, Y., Jiang, J., Zhou, H., Jiang, Y., Yu, Y., and Zhou, J. (2014). Characterization of a novel plasmid type and various genetic contexts of *bla*OXA-58 in *Acinetobacter* spp. *from multiple cities in China. PLoS One* 9:e84680. doi: 10.1371/journal.pone.0084680

Galata, V., Fehlmann, T., Backes, C., and Keller, A. (2019). PLSDB: a resource of complete bacterial plasmids. *Nucl. Acids Res.* 47, D195–D202.

Ghazawi, A., Sonnevend, A., Bonnin, R. A., Poirel, L., Nordmann, P., Hashmey, R., et al. (2012). NDM-2 carbapenemase-producing *Acinetobacter baumannii* in the United Arab Emirates. *Clin. Microbiol. Infect.* 18, E34–E36.

Guerrero-Lozano, I., Fernández-Cuenca, F., Galán-Sánchez, F., Egea, P., Rodríguez-Iglesias, M., and Pascual, Á (2015). Description of the OXA-23 β-lactamase gene located within Tn*2007* in a clinical isolate of *Acinetobacter baumannii* from Spain. *Microb. Drug Resist* 21, 215–217. doi: 10.1089/mdr.2014.0155

Hamidian, M., and Hall, R. M. (2013). IS*Aba1* targets a specific position upstream of the intrinsic ampC gene of *Acinetobacter baumannii* leading to cephalosporin resistance. *J. Antimicrob. Chemother.* 68, 2682–2683. doi: 10.1093/jac/dkt233

Hamidian, M., and Nigro, S. J. (2019). Emergence, molecular mechanisms and global spread of carbapenem-resistant *Acinetobacter baumannii*. *Microb. Genom.* 5:e000306.

Hamidian, M., Nigro, S. J., Hartstein, R. M., and Hall, R. M. (2017). RCH51, a multiply antibiotic-resistant *Acinetobacter baumannii* ST103IP isolate, carries resistance genes in three plasmids, including a novel potentially conjugative plasmid carrying oxa235 in transposon Tn*6252*. *J. Antimicrob. Chemother.* 72, 1907–1910. doi: 10.1093/jac/dkx069

Higgins, P. G., Lehmann, M., Wisplinghoff, H., and Seifert, H. (2010). *gyrB* multiplex PCR to differentiate between *Acinetobacter calcoaceticus* and *Acinetobacter* genomic species 3. *J. Clin. Microbiol.* 48, 4592–4594.

Higgins, P. G., Pérez-Llarena, F. J., Zander, E., Fernández, A., Bou, G., and Seifert, H. (2013). OXA-235, a novel class D β-lactamase involved in resistance to carbapenems in *Acinetobacter baumannii*. *Antimicrob. Agents Chemother.* 57, 2121–2126. doi: 10.1128/aac.02413-12

Jeannot, K., Diancourt, L., Vaux, S., Thouverez, M., Ribeiro, A., Coignard, B., et al. (2014). Molecular epidemiology of carbapenem non-susceptible *Acinetobacter baumannii* in France. *PLoS One* 9:e115452. doi: 10.1371/journal.pone.0115452

Kaase, M., Nordmann, P., Wichelhaus, T. A., Gatermann, S. G., Bonnin, R. A., and Poirel, L. (2011). NDM-2 carbapenemase in *Acinetobacter baumannii* from Egypt. *J. Antimicrob. Chemother.* 66, 1260–1262. doi: 10.1093/jac/dkr135

Kumar, S., Stecher, G., Li, M., Knyaz, C., and Tamura, K. (2018). MEGA X: Molecular Evolutionary Genetics Analysis across Computing Platforms. *Mol. Biol. Evol.* 35, 1547–1549. doi: 10.1093/molbev/msy096

Kumburu, H. H., Sonda, T., Van Zwetselaar, M., Leekitcharoenphon, P., Lukjancenko, O., Mmbaga, B. T., et al. (2019). Using WGS to identify antibiotic resistance genes and predict antimicrobial resistance phenotypes in MDR *Acinetobacter baumannii* in Tanzania. *J. Antimicrob. Chemother.* 74, 1484–1493. doi: 10.1093/jac/dkz055

Labi, A., Obeng-Nkrumah, N., Nartey, E. T., Bjerrum, S., Adu-Aryee, N. A., Ofori-Adjei, Y. A., et al. (2018). Antibiotic use in a tertiary healthcare facility in Ghana: a point prevalence survey. *Antimicrob. Resist. Infect. Control* 7:15.

Lakoh, S., Li, L., Sevalie, S., Guo, X., Adekanmbi, O., Yang, G., et al. (2020). Antibiotic resistance in patients with clinical features of healthcare-associated infections in an urban tertiary hospital in Sierra Leone: a cross-sectional study. *Antimicrob. Resist. Infect. Control* 9:38.

Lange, F., Pfennigwerth, N., Gerigk, S., Gohlke, F., Oberdorfer, K., Purr, I., et al. (2017). Dissemination of *bla*OXA-58 in *Proteus mirabilis* isolates from Germany. *J. Antimicrob. Chemother.* 72, 1334–1339.

Lee, M. J., Jang, S. J., Li, X. M., Park, G., Kook, J., Kim, M. J., et al. (2014). Comparison of *rpoB* gene sequencing, 16S rRNA gene sequencing, *gyrB* multiplex PCR, and the VITEK2 system for identification of *Acinetobacter* clinical isolates. *Diagn Microbiol. Infect. Dis.* 78, 29–34. doi: 10.1016/j.diagmicrobio.2013.07.013

Manenzhe, R. I., Zar, H. J., Nicol, M. P., and Kaba, M. (2015). The spread of carbapenemase-producing bacteria in Africa: a systematic review. *J. Antimicrob. Chemother.* 70, 23–40. doi: 10.1093/jac/dku356

Matos, A. P., Cayô, R., Almeida, L. G. P., Streling, A. P., Nodari, C. S., Martins, W. M. B. S., et al. (2019). Genetic Characterization of Plasmid-Borne *bla*OXA-58 in Distinct *Acinetobacter* Species. *mSphere* 4:e00376-19.

Nascimento, M., Sousa, A., Ramirez, M., Francisco, A. P., Carriço, J. A., and Vaz, C. (2017). PHYLOViZ 2.0*: providing scalable data integration and visualization for multiple phylogenetic inference methods*. *Bioinformatics* 33, 128–129. doi: 10.1093/bioinformatics/btw582

Nemec, A., Krizova, L., Maixnerova, M., Van Der Reijden, T. J., Deschaght, P., Passet, V., et al. (2011). Genotypic and phenotypic characterization of the *Acinetobacter calcoaceticus-Acinetobacter baumannii* complex with the proposal of *Acinetobacter pittii* sp. *nov.* (*formerly Acinetobacter genomic species* 3) and *Acinetobacter nosocomialis* sp. nov. (formerly *Acinetobacter* genomic species 13TU). *Res. Microbiol.* 162, 393–404. doi: 10.1016/j.resmic.2011.02.006

Nsofor, C. A., and Chekwube, L. O. (2017). High antibiotics resistance observed in *Acinetobacter baumannii* isolated from south east Nigeria. *EC Microbiol.* 8, 266–271.

Poirel, L., and Nordmann, P. (2006a). Carbapenem resistance in *Acinetobacter baumannii*: mechanisms and epidemiology. *Clin. Microbiol. Infect.* 12, 826–836. doi: 10.1111/j.1469-0691.2006.01456.x

Poirel, L., and Nordmann, P. (2006b). Genetic structures at the origin of acquisition and expression of the carbapenem-hydrolyzing oxacillinase gene *bla*OXA-58 in *Acinetobacter baumannii*. *Antimicrob. Agents Chemother.* 50, 1442–1448. doi: 10.1128/aac.50.4.1442-1448.2006

Pormohammad, A., Mehdinejadiani, K., Gholizadeh, P., Nasiri, M. J., Mohtavinejad, N., Dadashi, M., et al. (2020). Global prevalence of colistin resistance in clinical isolates of *Acinetobacter baumannii*: A

systematic review and meta-analysis. *Microb. Pathog.* 139, 103887. doi: 10.1016/j.micpath.2019.103887

Potron, A., Munoz-Price, L. S., Nordmann, P., Cleary, T., and Poirel, L. (2011). Genetic features of CTX-M-15-producing *Acinetobacter baumannii* from Haiti. *Antimicrob. Agents Chemother.* 55, 5946–5948. doi: 10.1128/aac.05124-11

Potron, A., Poirel, L., and Nordmann, P. (2015). Emerging broad-spectrum resistance in *Pseudomonas aeruginosa* and *Acinetobacter baumannii*: Mechanisms and epidemiology. *Int. J. Antimicrob. Agents* 45, 568–585. doi: 10.1016/j.ijantimicag.2015.03.001

Rodrigues-Costa, F., Cayô, R., Matos, A. P., Girardello, R., Martins, W. M. B. S., Carrara-Marroni, F. E., et al. (2019). Temporal evolution of *Acinetobacter baumannii* ST107 clone: conversion of *bla*OXA-143 into *bla*OXA-231 coupled with mobilization of IS*Aba1* upstream *occ*AB1. *Res. Microbiol.* 170, 53–59.

Shakil, S., and Khan, A. U. (2010). Detection of CTX-M-15-producing and carbapenem-resistant *Acinetobacter baumannii* strains from urine from an Indian hospital. *J. Chemother.* 22, 324–327. doi: 10.1179/joc.2010.22.5.324

Shrestha, S., Tada, T., Miyoshi-Akiyama, T., Ohara, H., Shimada, K., Satou, K., et al. (2015). Molecular epidemiology of multidrug-resistant *Acinetobacter baumannii* isolates in a university hospital in Nepal reveals the emergence of a novel epidemic clonal lineage. *Int. J. Antimicrob. Agents* 46, 526–531. doi: 10.1016/j.ijantimicag.2015.07.012

Sjölander, I., Hansen, F., Elmanama, A., Khayyat, R., Abu-Zant, A., Hussein, A., et al. (2014). Detection of NDM-2-producing *Acinetobacter baumannii* and VIM-producing *Pseudomonas aeruginosa* in Palestine. *J. Glob. Antimicrob. Resist.* 2, 93–97. doi: 10.1016/j.jgar.2013.11.002

Sullivan, M. J., Petty, N. K., and Beatson, S. A. (2011). Easyfig: a genome comparison visualizer. *Bioinformatics* 27, 1009–1010. doi: 10.1093/bioinformatics/btr039

Trebosc, V., Gartenmann, S., Tötzl, M., Lucchini, V., Schellhorn, B., Pieren, M., et al. (2019). Dissecting colistin resistance mechanisms in extensively drug-resistant *Acinetobacter baumannii* clinical isolates. *MBio* 10:1083.

Wachino, J., Yoshida, H., Yamane, K., Suzuki, S., Matsui, M., Yamagishi, T., et al. (2011). SMB-1, a novel subclass B3 metallo-beta-lactamase, associated with IS*CR1* and a class 1 integron, from a carbapenem-resistant *Serratia marcescens* clinical isolate. *Antimicrob. Agents Chemother.* 55, 5143–5149. doi: 10.1128/aac.05045-11

Wang, D., Yan, D., Hou, W., Zeng, X., Qi, Y., and Chen, J. (2015). Characterization of bla(OxA-23) gene regions in isolates of *Acinetobacter baumannii*. *J. Microbiol. Immunol. Infect.* 48, 284–290.

Wang, R., van Dorp, L., Shaw, L. P., Bradley, P., Wang, Q., Wang, X., et al. (2018). The global distribution and spread of the mobilized colistin resistance gene *mcr*-1. *Nat. Commun.* 9, 1–9.

Wise, M. G., Estabrook, M. A., Sahm, D. F., Stone, G. G., and Kazmierczak, K. M. (2018). Prevalence of mcr-type genes among colistin-resistant *Enterobacteriaceae* collected in 2014-2016 as part of the INFORM global surveillance program. *PLoS One.* 13:e0195281. doi: 10.1371/journal.pone.0195281

Wisplinghoff, H., Paulus, T., Lugenheim, M., Stefanik, D., Higgins, P. G., Edmond, M. B., et al. (2012). Nosocomial bloodstream infections due to *Acinetobacter baumannii*. *Acinetobacter pittii* and *Acinetobacter nosocomialis* in the United States. *J. Infect.* 64, 282–290. doi: 10.1016/j.jinf.2011.12.008

Wong, M. H., Chan, B. K., Chan, E. W., and Chen, S. (2019). Over-expression of IS*Aba1*-linked intrinsic and exogenously acquired OXA type carbapenem-hydrolyzing-class D-ß-lactamase-encoding genes is key mechanism underlying carbapenem resistance in *Acinetobacter baumannii*. *Front. Microbiol.* 10:2809. doi: 10.3389/fmicb.2019.02809

Woodford, N., Ellington, M. J., Coelho, J. M., Turton, J. F., Ward, M. E., Brown, S., et al. (2006). Multiplex PCR for genes encoding prevalent OXA carbapenemases in *Acinetobacter* spp. *Int. J. Antimicrob. Agents* 27, 351–353. doi: 10.1016/j.ijantimicag.2006.01.004

World Health Organization (2017). *Global priority list of antibiotic-resistant bacteria to guide research, discover, and development of new antibiotics*. Available online at: https://www.who.int/medicines/publications/WHO-PPL-Short_Summary_25Feb-ET_NM_WHO.pdf [accessed on April 30, 2020]

Zago, M. C., Viana, G. F., Ecker, A. B., Nishiyama, S. A., Zarpellon, M. N., Dias, J. R., et al. (2016). First report of CTX-M-15-producing *Acinetobacter baumannii* in Brazil. *J. Hosp. Infect.* 92, 298–299. doi: 10.1016/j.jhin.2015.11.016

Zankari, E., Hasman, H., Cosentino, S., Vestergaard, M., Rasmussen, S., Lund, O., et al. (2012). Identification of acquired antimicrobial resistance genes. *J. Antimicrob. Chemother.* 67, 2640–2644. doi: 10.1093/jac/dks261

Conflict of Interest: The authors declare that the research was conducted in the absence of any commercial or financial relationships that could be construed as a potential conflict of interest.

frontiers in Microbiology

ORIGINAL RESEARCH
published: 30 November 2020
doi: 10.3389/fmicb.2020.584603

Genomic Analysis of Carbapenem-Resistant *Acinetobacter baumannii* Isolates Belonging to Major Endemic Clones in South America

Carolina Silva Nodari[1], Rodrigo Cayô[1,2], Ana Paula Streling[1], Felipe Lei[1], Julia Wille[3,4], Myriam S. Almeida[5], Alexandre Inacio de Paula[6], Antonio Carlos Campos Pignatari[7], Harald Seifert[3,4], Paul G. Higgins[3,4] and Ana Cristina Gales[1,7]*

[1] Universidade Federal de São Paulo (UNIFESP), Laboratório Alerta, Division of Infectious Diseases, Department of Internal Medicine, Escola Paulista de Medicina (EPM), São Paulo, Brazil, [2] Universidade Federal de São Paulo (UNIFESP), Laboratório de Imunologia e Bacteriologia (LIB), Setor de Biologia Molecular, Microbiologia e Imunologia – Departamento de Ciências Biológicas (DCB), Instituto de Ciências Ambientais, Químicas e Farmacêuticas (ICAQF), Diadema, Brazil, [3] Institute for Medical Microbiology, Immunology and Hygiene, University of Cologne, Cologne, Germany, [4] German Center for Infection Research (DZIF), Partner Site Bonn-Cologne, Cologne, Germany, [5] Laboratório de Microbiologia, Hospital Universitário Cassiano Antônio de Moraes, Universidade Federal do Espírito Santo (UFES), Vitória, Brazil, [6] Setor de Microbiologia – Serviço de Análises Clínicas, Hospital do Servidor Público Estadual (IAMSPE), São Paulo, Brazil, [7] Universidade Federal de São Paulo (UNIFESP), Laboratório Especial de Microbiologia Clínica (LEMC), Division of Infectious Diseases, Department of Internal Medicine, Escola Paulista de Medicina (EPM), São Paulo, Brazil

OPEN ACCESS

Edited by:
Ayush Kumar, University of Manitoba, Canada

Reviewed by:
Andres Felipe Opazo-Capurro, University of Concepcion, Chile
Santiago Castillo Ramírez, National Autonomous University of Mexico, Mexico

***Correspondence:**
Carolina Silva Nodari
carol.nodari@gmail.com

Specialty section:
This article was submitted to Antimicrobials, Resistance and Chemotherapy, a section of the journal Frontiers in Microbiology

Received: *17 July 2020*
Accepted: *04 November 2020*
Published: *30 November 2020*

Citation:
Nodari CS, Cayô R, Streling AP, Lei F, Wille J, Almeida MS, de Paula AI, Pignatari ACC, Seifert H, Higgins PG and Gales AC (2020) Genomic Analysis of Carbapenem-Resistant Acinetobacter baumannii Isolates Belonging to Major Endemic Clones in South America. Front. Microbiol. 11:584603. doi: 10.3389/fmicb.2020.584603

Carbapenem-resistant *Acinetobacter baumannii* (CRAB) are emerging worldwide. In South America, clinical isolates presenting such a phenotype usually do not belong to the globally distributed international clone 2 (IC2). The majority of these isolates are also resistant to multiple other antimicrobials and are often designated extremely drug-resistant (XDR). The aim of this study was to characterize the resistance mechanisms presented by 18 carbapenem-resistant *A. baumannii* isolates from five different Brazilian hospitals. Species identification was determined by *rpoB* sequencing, and antimicrobial susceptibility was determined by broth microdilution. Isolates were submitted to whole genome sequencing using Illumina platform and genetic similarity was determined by PFGE, MLST, and cgMLST. Genome analysis was used to identify intrinsic and acquired resistance determinants, including mutations in the AdeRSABC efflux system and in outer membrane proteins (OMPs). All isolates were identified as *A. baumannii* and grouped into 4 pulsotypes by PFGE, which belonged to clonal complexes (CC) $15^{Pas}/103^{Ox}$ (n = 4) and $79^{Pas}/113^{Ox}$ (n = 14), corresponding to IC4 and IC5, respectively. High MIC values to carbapenems, broad-spectrum cephalosporins, amikacin, and ciprofloxacin were observed in all isolates, while MICs of ampicillin/sulbactam, gentamicin, and tigecycline varied among the isolates. Minocycline was the most active antimicrobial agent tested. Moreover, 12 isolates (66.7%) were considered resistant to polymyxins. Besides intrinsic OXA-51 and ADC variants, all isolates harbored an acquired carbapenem-hydrolyzing class D β-lactamase (CHDL) encoding gene, either bla_{OXA-23} or bla_{OXA-72}. A diversity of

aminoglycoside modifying enzymes and resistance determinants to other antimicrobial classes were found, as well as mutations in *gyrA* and *parC*. Non-synonymous mutations have also been identified in the AdeRSABC efflux system and in most OMPs, but they were considered natural polymorphisms. Moreover, resistance to polymyxins among isolates belonging to IC5 were associated to non-synonymous mutations in *pmrB*, but no known polymyxin resistance mechanism was identified in isolates belonging to IC4. In conclusion, *A. baumannii* clinical isolates belonging to South America's major clones present a myriad of antimicrobial resistance determinants. Special attention should be paid to natural polymorphisms observed in each clonal lineage, especially regarding non-synonymous mutations in constitutive genes associated with distinct resistance phenotypes.

Keywords: Brazil, IC4, IC5, CHDL, outer membrane proteins, polymyxin resistance, nosocomial infection, two component systems

INTRODUCTION

Acinetobacter baumannii is a major nosocomial pathogen causing serious infections (Antunes et al., 2014). In Brazil, it is the fourth most frequent pathogen recovered from central catheter-associated bloodstream infections (BSI) in adult intensive care units (ICU), with carbapenem resistance rates as high as 79% (Agência Nacional de Vigilância Sanitária [ANVISA], 2020). Carbapenem resistance in *A. baumannii* is mainly caused by horizontal transfer of carbapenem-hydrolyzing class D β-lactamases (CHDL) encoding genes, particularly in worldwide epidemic clones (Higgins et al., 2010).

Most carbapenem-resistant isolates also harbor resistance determinants to other antimicrobial classes, such as aminoglycosides and fluoroquinolones. Additionally, resistance to polymyxins has been sporadically reported among some carbapenem-resistant endemic clones (Qureshi et al., 2015), and these isolates are often classified as XDR or pan-drug resistant (PDR) (Nowak et al., 2017). Carbapenem-resistant *A. baumannii* (CRAB) isolates usually belong to the worldwide disseminated international clone 2 (IC2) (Hamidian and Nigro, 2019) and carbapenem-resistance rates vary between 40 and 80% (Kuo et al., 2012; Chmielarczyk et al., 2016). In Latin America, the frequency of XDR *A. baumannii* has increased from 17 to 86.6% between 1997 and 2016 (Gales et al., 2019).

Interestingly, CRAB isolates in South America are not associated with IC2. In Brazil, as well as Argentina, Chile, and Paraguay, the major carbapenemase-producing clones belong to clonal complexes (CCs) 15 and 79, which correspond to IC4 and IC5, respectively (Higgins et al., 2010; Chagas et al., 2014; Cardoso et al., 2016; Rodríguez et al., 2016; Opazo-Capurro et al., 2019). Despite the variety of studies focusing on the genetic context of carbapenemase encoding genes (Chagas et al., 2017; Romanin et al., 2019), comprehensive studies on the genetic basis of XDR phenotype among isolates representing these important ICs are still missing (Graña-Miraglia et al., 2020). Herein, we explored the molecular determinants associated with resistance toward multiple drugs among *A. baumannii* clinical isolates belonging to the major South American clonal lineages recovered in distinct Brazilian hospitals.

MATERIALS AND METHODS

Bacterial Strains and Antimicrobial Susceptibility Testing

A total of 18 *Acinetobacter* spp. clinical isolates were included in study. They were recovered in five tertiary hospitals located in two Brazilian states between April 2012 and October 2017. Isolates were identified to the species level by *rpoB* sequencing as previously described (La Scola et al., 2006). Minimal Inhibitory Concentrations (MICs) for amikacin, ceftazidime, ciprofloxacin, colistin, cefepime, gentamicin, imipenem, meropenem, minocycline, polymyxin B, and tigecycline (Sigma-Aldrich, St. Louis, United States) were determined by cation-adjusted broth microdilution and interpreted according to Brazilian Committee on Antimicrobial Susceptibility Testing (BrCAST/EUCAST) guidelines[1], when clinical breakpoints for *Acinetobacter* spp. were available. Ampicillin/sulbactam MICs were determined following the guidelines established by BrCAST/EUCAST for Enterobacteriales.

Whole Genome Sequencing (WGS) and Draft Genome Analysis

All the isolates were subjected to WGS using an Illumina MiSeq sequencer (Illumina Inc., CA, United States) (Higgins et al., 2017), and genomes were assembled with the program Velvet as part of the SeqSphere v.7.0.4 software (Ridom GmbH, Münster, Germany) as described previously (Higgins et al., 2017). To determine differences in specific ORFs in each draft genome sequence, the genome assemblies were aligned to the *A. baumannii* reference strain ACICU and compared to nucleotide and protein sequences of *A. baumannii* ATCC 19606 (accession number NZ_KL810966.1) and ATCC 17978 (accession number NZ_CP018664.1).

Molecular Typing

Clonal relatedness of *A. baumannii* isolates was determined by pulsed-field gel electrophoresis (PFGE) using *Apa*I restriction

[1]http://brcast.org.br/

enzyme (New England BioLabs, Ipswich, MA, United States) and fingerprints were analyzed with previously described criteria (Seifert et al., 2005). WGS data were also used to characterize the isolates by core genome multilocus sequence typing (cgMLST), as previously published (Higgins et al., 2017) and to determine the sequence types (STs) using PubMLST[2].

Resistome Analysis

Intrinsic and acquired resistance determinants were screened using ResFinder, version 3.2[3] and manually curated using Artemis. The presence of insertion sequences upstream of β-lactamase encoding genes was also screened using ISfinder[4]. Non-synonymous mutations in *gyrA* and *parC* were detected comparing the genome sequences with reference *A. baumannii* strain ATCC 19606. Moreover, amino acid substitutions in polymyxin resistance associated systems LpxACD and PmrAB were detected as described by Gerson et al. (2020). This approach was also used to identify potential amino acid substitutions associated with antimicrobial resistance in the efflux pumps system AdeABC, its regulator AdeRS, and in outer membrane proteins (OMPs) CarO, OmpA, OmpW, Omp33-36, and OccAB1. Additionally, the relative expression of *pmrAB* was determined by qRT-PCR using specific primers previously described (Girardello et al., 2017). Assays were performed in triplicate and expression was compared to that of *A. baumannii* ATCC 19606, using *rpoB* as a normalizing gene (Hornsey et al., 2010).

RESULTS

A. baumannii Clinical Isolates Belonged to South America's Most Prevalent Clones

All isolates were identified as *A. baumannii* and were mainly recovered from blood cultures (n = 9) followed by lower respiratory tract cultures (n = 6) (**Table 1**). According to PFGE, they were grouped into four distinct pulsotypes, which were included in different STs belonging to Institute Pasteur scheme (Pas) CC79 and CC15, and corresponded to the Oxford scheme (Ox) CC113 and CC103, respectively (**Table 1** and **Supplementary Figure 1**). Interestingly, the ST distribution following the Oxford scheme presented a better correlation to the results observed with PFGE, since ST227, ST233, ST236, and the novel ST2141 were strongly associated with PFGE clusters 1, 2, 4, and 3, respectively (**Supplementary Figure 1**). Moreover, cgMLST delineated the isolates into four transmission clusters and seven singletons (**Figure 1** and **Supplementary Figure 1**). According to MLST analysis, all CRAB clinical isolates were grouped into two major South American clones, namely IC4 ($CC15^{Pas}$/$CC103^{Ox}$; n = 4) and IC5 ($CC79^{Pas}$/$CC113^{Ox}$; n = 14). It should also be noted that every CC was found over time and in distinct hospitals, confirming the wide spread of those STs in Brazil.

Most *A. baumannii* Were Highly Resistant to Diverse Antimicrobials

All isolates were resistant to a broad range of antimicrobial agents (**Table 1**). High MICs were observed in most isolates for ampicillin/sulbactam (MIC range, ≤0.5–>256/4 μg/mL), ceftazidime (MIC range, 8–>128 μg/mL), cefepime (32–>256 μg/mL), imipenem (64–>256 μg/mL), meropenem (32–256 μg/mL), amikacin (16–512 μg/mL), and ciprofloxacin (32–>64 μg/mL). Additionally, 66 and 72% of the isolates were resistant to gentamicin (≤0.5–>128 μg/mL) and both polymyxins (polymyxin B and colistin; ≤0.25–>128 μg/mL), respectively. On the other hand, MICs values for tigecycline ranged from 0.5 to 16 μg/mL. Only minocycline showed consistent activity against all *A. baumannii* isolates (MICs, ≤0.25–2 μg/mL; **Table 1**). Interestingly, polymyxin B presented a higher *in vitro* activity compared to colistin against polymyxin-resistant isolates, since colistin MICs were at least two-fold dilutions higher than polymyxin B. In contrast, polymyxin B and colistin MICs did not differ among polymyxin-susceptible isolates.

A Variety of Intrinsic and Acquired β-Lactamases Were Found in CRAB Isolates, Including Novel Variants of bla_{ADC}

As expected, all *A. baumannii* isolates harbored intrinsic chromosome encoded $bla_{OXA-51-like}$ genes. Moreover, each variant was correlated to an IC, being bla_{OXA-65} (n = 14; IC5, $CC79^{Pas}$) the most frequently identified (**Figure 2** and **Supplementary Table 1**). The insertion sequence (IS) IS*Aba1* was found upstream of those genes in one and five isolates belonging to IC4 and IC5, respectively. All isolates harbored novel variants of bla_{ADC} flanked upstream by IS*Aba1*, namely $bla_{ADC-181}$ (n = 4), $bla_{ADC-182}$ (n = 13), and $bla_{ADC-183}$ (n = 1), and were associated with $ST15^{Pas}$, $ST79^{Pas}$, and $ST730^{Pas}$, respectively. The acquired CHDL encoding genes bla_{OXA-23} and bla_{OXA-72} were found in 13 (72.2%) and five (27.8%) *A. baumannii* isolates, respectively. The bla_{OXA-23} gene was also flanked upstream by IS*Aba1* in all isolates included in the study. Interestingly, bla_{OXA-72} was only detected in isolates belonging to IC5 (**Figure 2** and **Supplementary Table 1**). Furthermore, the narrow-spectrum β-lactamase encoding gene bla_{TEM-1} was also found in 83.3% of isolates (n = 15). No other β-lactamase encoding gene was detected among these isolates.

Each IC Was Associated With Distinct Resistance Determinants

The reduced susceptibility to amikacin observed in all isolates was associated with the presence of the aminoglycoside modifying enzyme (AME) *aph(3′)-VIa* (**Figure 2** and **Supplementary Table 1**). Additionally, the isolates belonging to IC5 also harbored the phosphotransferase encoding genes *strA* and *strB*, as well as the nucleotidyltransferase encoding gene *aadA1*. Moreover,

[2]https://pubmlst.org/abaumannii/

[3]https://cge.cbs.dtu.dk/services/ResFinder/

[4]https://isfinder.biotoul.fr/blast.php

TABLE 1 | Clinical and epidemiological data and antimicrobial susceptibility profile of *A. baumannii* clinical isolates included in the study.

Isolate	Hospital	State	Collection Date	Clinical Sample	PFGE	ST (Pas/Ox)	MIC (μ g/mL)[a]											
							SAM[b]	CAZ[b]	FEP[b]	IPM	MEM	GEN	AMK	CIP	MIN[b]	TGC[b]	PMB[c]	CST[c]
52944	A	SP	Apr/13/2012	Blood	1A	79/233	>256/4	>128	128	128	256	8	512	>64	2	16	64	128
61317	B	SP	Apr/11/2014	Urine	1B	79/227	256/4	>128	128	64	64	>128	256	>64	0.5	8	64	>128
61979	B	SP	May/29/2014	Tracheal aspirate	1B	79/227	128/4	>128	128	64	64	>128	128	>64	0.5	8	64	>128
63231	B	SP	Aug/30/2014	Blood	1C	79/227	>256/4	>128	64	128	256	>128	64	>64	≤0.25	0.5	1	1
63485	B	SP	Sep/14/2014	Blood	1C	79/227	>256/4	>128	64	128	128	>128	64	>64	≤0.25	0.5	1	1
66116	B	SP	Mar/25/2015	Tracheal aspirate	2A	79/233	≤0.5/4	>128	128	128	128	4	64	>64	≤0.25	4	16	64
67098	B	SP	May/25/2015	Blood	2B	79/233	>256/4	>128	32	128	256	8	64	>64	0.5	0.5	1	1
67510	B	SP	Jun/22/2015	Tracheal aspirate	1B	79/227	256/4	>128	256	64	64	>128	128	>64	0.5	8	64	>128
67745	B	SP	Jul/14/2015	Blood	2C	79/233	>256/4	>128	128	128	256	16	64	>64	0.5	1	1	1
20189365	C	SP	Jun/03/2017	Tracheal aspirate	2D	79/233	≤0.5/4	>128	64	128	64	4	128	>64	1	8	4	16
20216722	B	SP	Jun/09/2017	Tracheal aspirate	2D	79/233	≤0.5/4	>128	128	256	256	8	128	>64	0.5	4	8	16
182122	D	SP	Jun/19/2017	CSF	3	15/2141	≤0.5/4	8	64	128	32	≤0.5	16	>64	0.5	16	32	>128
71838	B	SP	Jul/05/2017	Blood	4A	15/236	>256/4	>128	64	128	128	2	32	32	≤0.25	0.5	≤0.25	≤0.25
206182	D	SP	Jul/10/2017	Ascitic fluid	2E	730/227	256/4	128	>256	>256	256	>128	256	>64	1	16	8	16
71813	B	SP	Jul/14/2017	Blood	4B	15/236	>256/4	>128	128	256	256	4	64	>64	≤0.25	0.5	≤0.25	≤0.25
278860	D	SP	Sep/11/2017	Blood	2F	79/233	>256/4	>128	>256	>256	128	4	128	>64	1	8	64	>128
300736	D	SP	Sep/28/2017	BAL	2F	79/233	>256/4	>128	>256	>256	128	16	128	>64	1	16	16	64
10042	E	ES	Oct/06/2017	Catheter blood	4C	15/236	>256/4	>128	128	64	128	>128	64	>64	0.5	4	64	>128

AMK, amikacin; BAL, bronchoalveolar lavage; CAZ, ceftazidime; CIP, ciprofloxacin; CSF, cerebrospinal fluid; CST, colistin; ES, Espírito Santo; FEP, cefepime; GEN, gentamicin; IPM, imipenem; MEM, meropenem; MIC, minimal inhibitory concentration; MIN, minocycline; Ox, Oxford scheme; Pas, Pasteur scheme; PFGE, pulsed field gel electrophoresis; PMB, polymyxin B; SAM, ampicillin/sulbactam; SP, São Paulo; ST, sequence type; TGC, tigecycline. [a]*In vitro susceptibility according to BrCAST/EUCAST clinical breakpoints are highlighted in the gray boxes.* [b]*Clinical breakpoints not established by BrCAST/EUCAST.* [c]*BrCAST provided breakpoints for both polymyxins, while EUCAST provided only for colistin.*

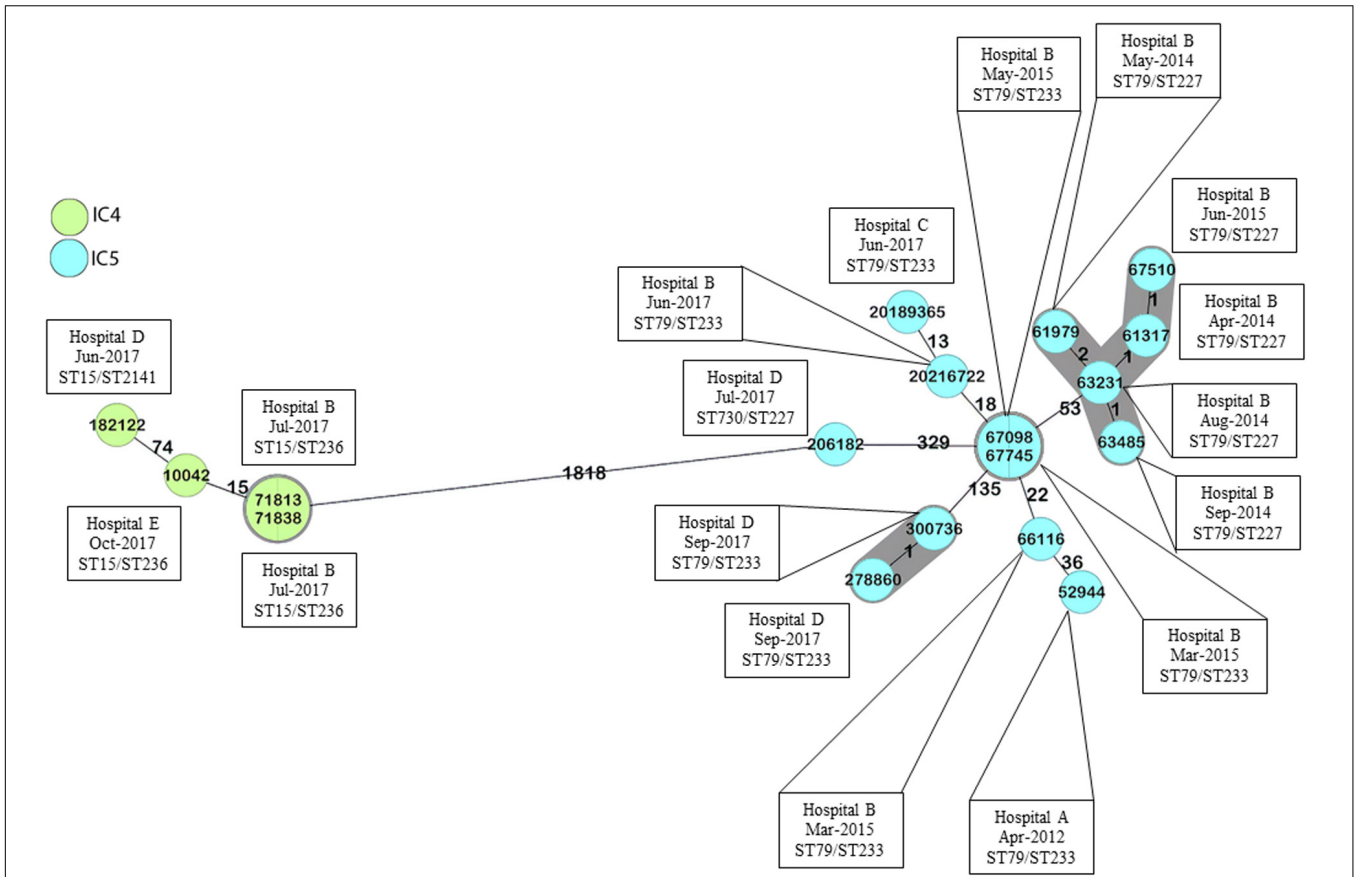

FIGURE 1 | Minimum spanning tree of *A. baumannii* clinical isolates, according to cgMLST. Numbers between isolates indicate the allele differences identified among the 2,390 alleles that belong to *A. baumannii* core genome, ignoring missing values. Colors indicate isolates belonging to the same international clones. Gray zones indicate isolates belonging to the same cluster, and isolate numbers in the same circle were considered identical. Cluster distance threshold: 9. Minimum spanning tree built using Ridom SeqSphere+.

one IC5 genetic cluster produced an acetyltransferase belonging to the AAC(6′)-Ib family, which explains the high gentamicin resistance levels observed in such isolates (>128 μg/mL). On the other hand, only one isolate belonging to IC4 harbored an acetyltransferase encoding gene, *aac(3)-IIa*, and no additional AME was observed in IC4 isolates (**Figure 2** and **Supplementary Table 1**). The arsenal of acquired resistance determinants observed in IC5 also included *sul2*, *dfrA1*, and *floR*-like genes, which promote reduced susceptibility to sulfamethoxazole, trimethoprim, and chloramphenicol, respectively (**Figure 2** and **Supplementary Table 1**). Additionally, the ST79^{Pas} isolates 67098, 67745, and 20216722 harbored the macrolide resistance determinants *mph(E)* and *msr(E)*, which were also found in the ST15^{Pas} isolates 71813 and 71838. Finally, the isolate 206182 harbored both *sul1* and *sul2*.

Resistance to Fluoroquinolones and Polymyxins Was Associated With Point Mutations in Constitutive Genes

The high ciprofloxacin MICs observed in all the isolates can be explained by the simultaneous presence of Ser_{83}Leu and Ser_{80}Leu amino acid substitutions in the quinolone resistance determinant region (QRDR) of *gyrA* and *parC*, respectively (**Supplementary Table 1**). Additionally, point mutations were observed in *pmrAB* in most polymyxin-resistant isolates belonging to IC5 (**Table 2**). However, the presence of such mutations was not always associated with overexpression of that two-component system (TCS) (**Supplementary Figure 2**). Interestingly, IS*Aba125* was observed within *pmrA* in two polymyxin-susceptible *A. baumannii* isolates belonging to ST79^{Pas}, which might have disrupted the function of this transcriptional regulator (**Supplementary Table 1**). In fact, these isolates presented a reduced expression of *pmrA*, as assessed by qRT-PCR (**Supplementary Figure 2**). It was also worth noting that some mutations observed in IC5 were present in both polymyxin-resistant and -susceptible isolates and were considered natural polymorphisms associated with this IC, including a duplication of ten amino acids in PmrB observed in some isolates (**Supplementary Table 1**). A high number of polymorphisms was also observed in isolates belonging to IC4 (**Figure 3**). However, none of them was exclusively found in polymyxin-resistant isolates, suggesting that such substitutions were not associated with polymyxin resistance in IC4, and might explain the absence

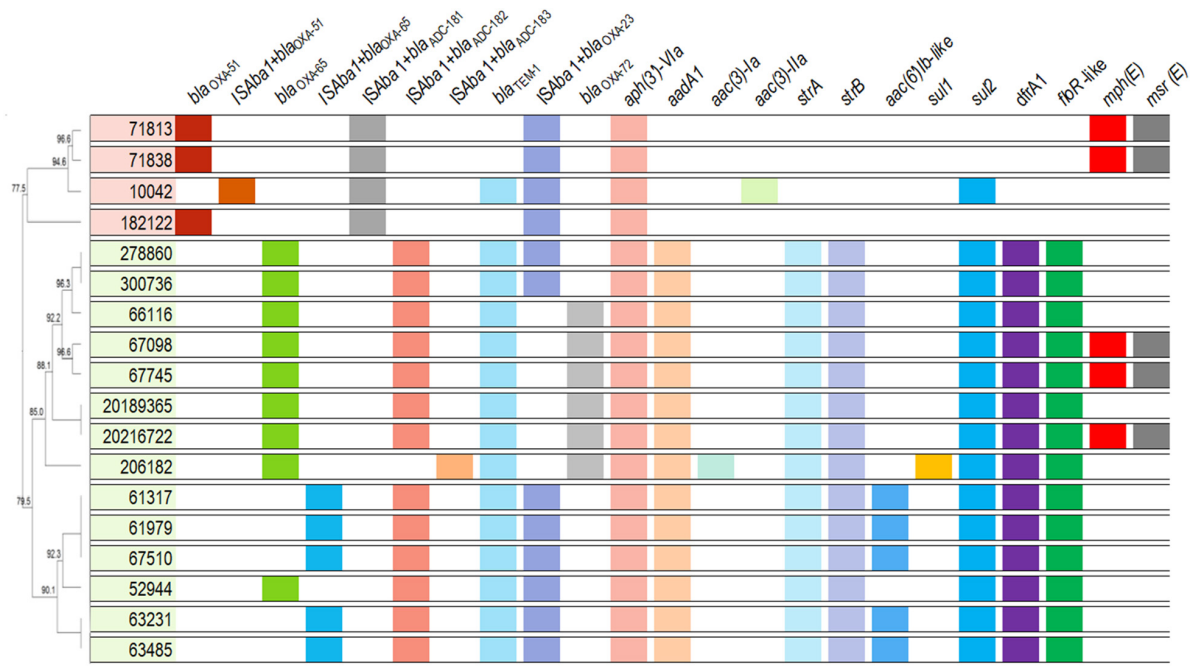

FIGURE 2 | Overview of the acquired antimicrobial resistance determinants and intrinsic β-lactamases encoding genes observed in *A. baumannii* clinical isolates. Isolates belonging to distinct CCs are indicated by different colors. Dendrogram was generated using UPGMA method with BioNumerics, version 7.5, based on ApaI-PFGE results.

of *pmrAB* overexpression among those isolates (**Supplementary Table 1** and **Supplementary Figure 2**).

The substitutions observed in LpxD in all isolates were also considered to be natural polymorphisms, as they were strictly related to the genetic background of the isolates rather than their resistance phenotype (**Supplementary Table 1**). While only isolates belonging to IC5 harbored the *pmrC* homolog *eptA*, no *mcr* genes were detected among the 18 *A. baumannii* isolates evaluated. In fact, no known polymyxin resistance mechanism was identified among those isolates belonging to IC4, suggesting that novel mechanisms might be responsible for the high polymyxins MICs (ranging from 32 to >128 μg/mL) observed in isolates 182122 and 10042 (**Table 1**).

OMPs and AdeA Protein Sequences Were Distinct in Each Endemic Clone

Genes encoding OMPs also presented clone-associated alleles. As shown in **Table 3**, the allelic variation of *ompA* included non-synonymous mutations specific for each CC. This was also observed in CarO, where isolates belonging to IC5 presented protein sequences identical to the one observed in the *A. baumannii* reference strain ATCC 19606, while those belonging to IC4 presented more than 60 amino acid substitutions (73.1% identity; **Figure 4** and **Supplementary Table 1**). In contrast, the OprD-like protein OccAb1 was identical in both ICs, even though three amino acid substitutions were observed compared to the reference strain (**Table 3**). No amino acid substitutions were observed in OmpW and Omp33-36.

Even though the protein sequences of AdeB were conserved in *A. baumannii* clinical isolates belonging to both IC4 and IC5 and identical to the *A. baumannii* reference strain ATCC 19606, *adeA* presented distinct alleles in each IC. While this gene was identified as wild type in isolates belonging to IC5, two amino acid substitutions were identified in all IC4 isolates, namely $Ala_{368}Leu$ and $Thr_{386}Asn$ (**Supplementary Table 1**). Moreover, proteins belonging to the TCS AdeRS also presented distinct sequences in each CC, which differ from ATCC 19606 (**Figure 5**). It should be noted that some amino acid substitutions were observed in both IC4 and IC5 isolates, such as $Val_{136}Ala$ and $Leu_{142}Ile$ in AdeR, and $Ala_{153}Thr$, $Leu_{214}Phe$, $Ser_{263}Ala$, $Ala_{280}Ser$, and $Asp_{281}Gln$ in AdeS.

DISCUSSION

The worldwide spread of multidrug-resistant (MDR) *A. baumannii* clones is considered a public health concern. The World Health Organization considers research and surveillance of emerging resistance phenotypes as one of the strategic goals of their Global Action Plan on Antimicrobial Resistance (WHO, 2015). Over the years, the evolution of successful *A. baumannii* clones allowed them to acquire an increasing number of resistance determinants, not only via mobile genetic elements, but also through mutations in constitutive genes (Antunes et al., 2014). In the present study we demonstrated that this genetic plasticity is also responsible for resistance to several antimicrobials among South American *A. baumannii* major clones.

TABLE 2 | Amino acid substitutions and relative expression of TCS PmrAB in polymyxin-resistant *A. baumannii* clinical isolates belonging to IC5.

Isolate	ST (Pas/Ox)	PmrA		PmrB	
		Amino acid substitution[a]	Relative expression[b]	Amino acid substitution[a]	Relative expression[b]
52944	79/233	ND	2.37	ND	2.17
61317	79/227	ND	4.45	ND	6.61
61979	79/227	ND	9.16	ND	8.43
66116	79/233	ND	−3.36	$Tyr_{149}Phe$, $Gln_{240}Glu$	−5.81
67510	79/227	ND	3.64	ND	5.37
20189365	79/233	$Asp_{10}Val$	−2.9	$Gly_{414}Arg$	1.13
20216722	79/233	ND	2.67	$Arg_{263}Cys$	−4.17
206182	730/227	ND	1.15	$Ser_{14}Ala$	−4.08
278860	79/233	ND	2.58	$Thr_{187}Phe$, $Leu_{272}Phe$	1.99
300736	79/233	ND	5.52	$Thr_{187}Phe$, $Leu_{272}Phe$	3.11

ND, not detected; Ox, Oxford scheme; Pas, Pasteur scheme; ST, sequence type. [a]Amino acid substitutions were identified based on the comparison with polymyxin-susceptible isolates belonging to IC5. [b]Relative expression of pmrAB is expressed in terms of fold change, compared to transcriptional levels observed in A. baumannii ATCC 19606.

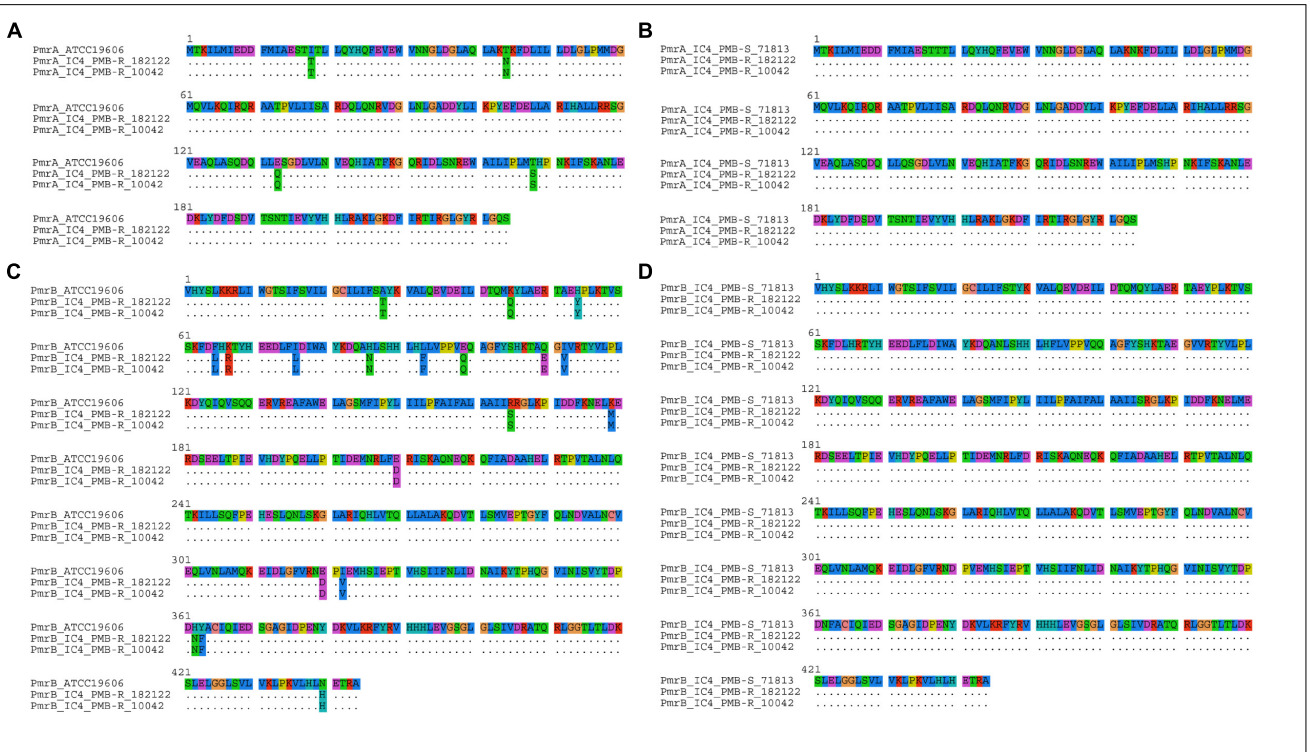

FIGURE 3 | Alignment of PmrA **(A,B)** and PmrB **(C,D)** protein sequences observed in polymyxin-resistant *A. baumannii* clinical isolates 182122 and 10042 belonging to IC4, compared to *A. baumannii* reference strain ATCC 19606 **(A,C)** or to the polymyxin-susceptible IC4 *A. baumannii* isolate 71813 **(B,D)**.

The importance of *A. baumannii* clinical isolates belonging to IC4 and IC5 in South America has been previously demonstrated (Cieslinski et al., 2013; Stietz et al., 2013; Rodríguez et al., 2016; Opazo-Capurro et al., 2019; Müller et al., 2019). The higher frequency of those clones was also observed in different regions in Brazil and has been associated with an XDR phenotype (Royer et al., 2018; Pagano et al., 2019; Tavares et al., 2019). Interestingly, despite their wide distribution through time and space, the IC4 and IC5 clinical isolates included in this study remained highly genetically related, as determined using both PFGE and cgMLST. Vasconcelos et al. (2015) have also identified highly similar *A. baumannii* clinical isolates causing BSI in distinct Brazilian medical centers by REP-PCR, and the most frequent clones described also belonged to IC4 and IC5. Even though most isolates belonging to the same pulsotype were not grouped in the same cluster according to cgMLST, the number of allele differences between those isolates were usually lower than the ones observed between isolates that were not considered genetically related according to PFGE. It should be noted, however, that the cgMLST cluster distance threshold was

TABLE 3 | Amino acid substitutions observed in OMPs in *A. baumannii* clinical isolates.

Isolate	OmpA[a]	OmpW[a]	OccAb1[a]	Omp33-36[a]
52944	Gly_{52}Ser, Thr_{144}Asn	WT	Ile_{121}Leu, Leu_{293}Ile, Arg_{445}His	WT
61317	Gly_{52}Ser, Thr_{144}Asn	WT	Ile_{121}Leu, Leu_{293}Ile, Arg_{445}His	WT
61979	Gly_{52}Ser, Thr_{144}Asn	WT	Ile_{121}Leu, Leu_{293}Ile, Arg_{445}His	WT
63231	Gly_{52}Ser, Thr_{144}Asn	WT	Ile_{121}Leu, Leu_{293}Ile, Arg_{445}His	WT
63485	Gly_{52}Ser, Thr_{144}Asn	WT	Ile_{121}Leu, Leu_{293}Ile, Arg_{445}His	WT
66116	Gly_{52}Ser, Thr_{144}Asn	WT	Ile_{121}Leu, Leu_{293}Ile, Arg_{445}His	WT
67098	Gly_{52}Ser, Thr_{144}Asn	WT	Ile_{121}Leu, Leu_{293}Ile, Arg_{445}His	WT
67510	Gly_{52}Ser, Thr_{144}Asn	WT	Ile_{121}Leu, Leu_{293}Ile, Arg_{445}His	WT
67745	Gly_{52}Ser, Thr_{144}Asn	WT	Ile_{121}Leu, Leu_{293}Ile, Arg_{445}His	WT
20189365	Gly_{52}Ser, Thr_{144}Asn	WT	Ile_{121}Leu, Leu_{293}Ile, Arg_{445}His	WT
20216722	Gly_{52}Ser, Thr_{144}Asn	WT	Ile_{121}Leu, Leu_{293}Ile, Arg_{445}His	WT
182122	Gly_{52}Ala	WT	Ile_{121}Leu, Leu_{293}Ile, Arg_{445}His	WT
71838	Gly_{52}Ala	WT	Ile_{121}Leu, Leu_{293}Ile, Arg_{445}His	WT
206182	Gly_{52}Ser, Thr_{144}Asn	WT	Ile_{121}Leu, Leu_{293}Ile, Arg_{445}His	WT
71813	Gly_{52}Ala	WT	Ile_{121}Leu, Leu_{293}Ile, Arg_{445}His	WT
278860	Gly_{52}Ser, Thr_{144}Asn	WT	Ile_{121}Leu, Leu_{293}Ile, Arg_{445}His	WT
300736	Gly_{52}Ser, Thr_{144}Asn	WT	Ile_{121}Leu, Leu_{293}Ile, Arg_{445}His	WT
10042	Gly_{52}Ala	WT	Ile_{121}Leu, Leu_{293}Ile, Arg_{445}His	WT

OMP, outer membrane protein; WT, wild type. [a]*Amino acid substitutions are based on sequences of reference strain A. baumannii ATCC 19606.*

FIGURE 4 | Alignment of CarO protein sequences observed in *A. baumannii* clinical isolates belonging to IC4, compared to *A. baumannii* reference strain ATCC 19606.

established based on the allele differences and designed for the investigation of *A. baumannii* transmission clusters or outbreaks (Higgins et al., 2017). These values should be interpreted with caution when evaluating isolates broadly distributed over time and space. In the current study, some isolates were separated in time by several years, and by a distance of over 1000 km. Moreover, it should be noted that isolates belonging to the same ST not always form monophyletic groups based on cgMLST, as previously reported (Castillo-Ramírez and Graña-Miraglia, 2019; Gaiarsa et al., 2019). Additionally, the differences observed in isolates belonging to $ST227^{Ox}$ and $ST233^{Ox}$ (both part of $ST79^{Pas}$) might be associated with recombination events in the vicinities of the *gpi* allele, as described by Hamouda et al. (2010).

The variety of intrinsic β-lactamase encoding genes was also related to the clonal groups each isolate was assigned to. As expected, all isolates belonging to IC5 harbored bla_{OXA-65}, while bla_{OXA-51} was present in all isolates belonging to IC4, as previously described (Zander et al., 2012). However, the presence of the IS*Aba1* upstream the bla_{OXA-51}-like genes was associated to specific pulsotypes within each IC, namely 1B and 1C from IC5, and 3 from IC4. It should be noted that the low frequency of IS*Aba1*-bla_{OXA-51}-like structure among Brazilian isolates, especially in bla_{OXA-23}-producing strains, was previously reported (Pagano et al., 2013). On the other hand, this IS was observed upstream of bla_{ADC}-like genes in all isolates and could have been responsible for the high third-generation

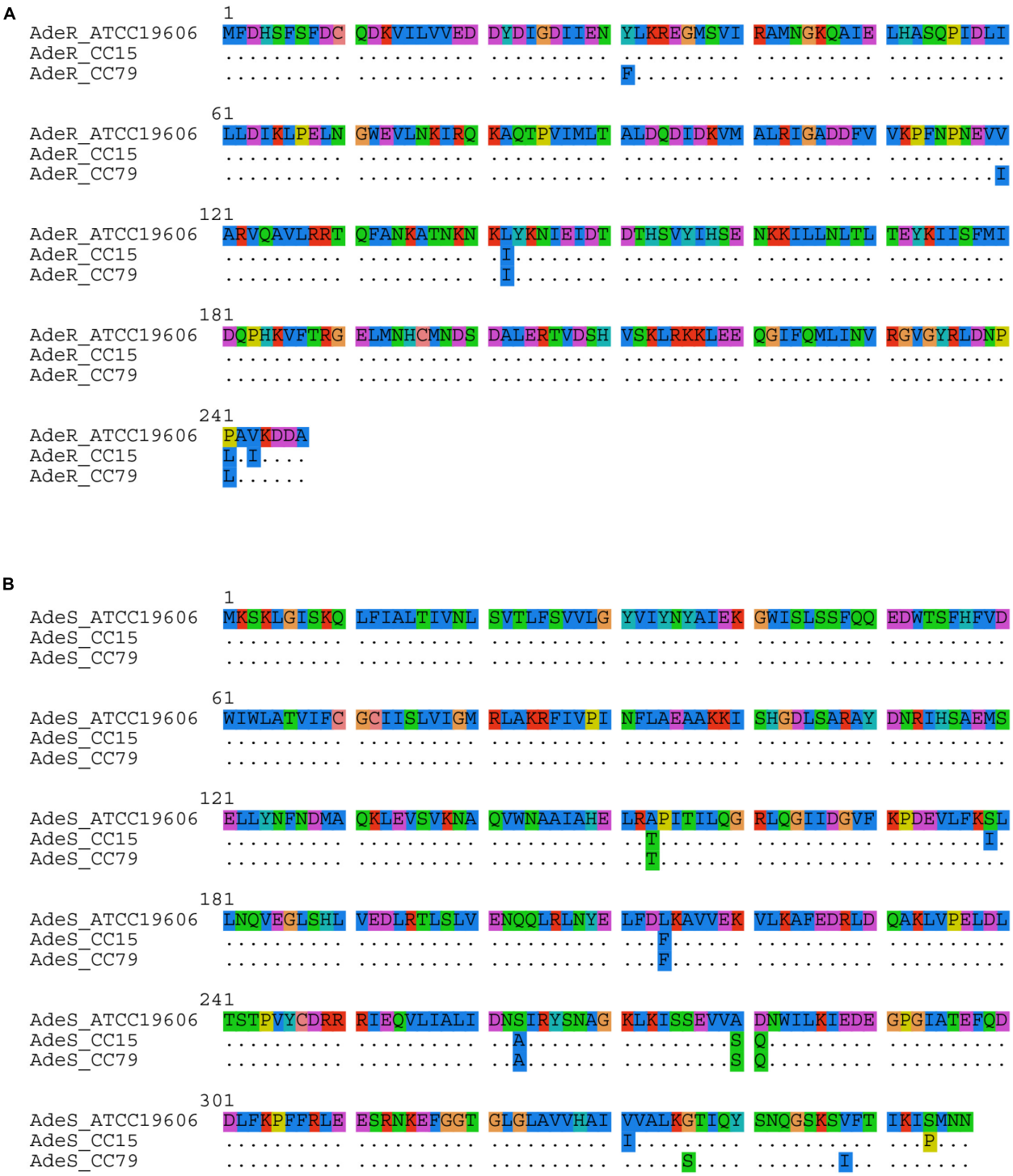

FIGURE 5 | Alignment of **(A)** AdeR and **(B)** AdeS protein sequences observed in *A. baumannii* clinical isolates belonging to IC4 and IC5, compared to *A. baumannii* reference strain ATCC 19606.

cephalosporin MIC values observed (Cardoso et al., 2016). It is worth noting that each novel ADC variant was identified in a different ST, even though it is not yet clear if the presence of specific ADCs in *A. baumannii* isolates can also be linked to an IC, as demonstrated for bla_{OXA-51} (Rodríguez-Martínez et al., 2010; Karah et al., 2017).

Although the intrinsic OXA-51 and ADC variants were closely related to each IC included in the study, the acquired CHDL

encoding gene bla_{OXA-23} was observed in both ICs, as expected. OXA-23 remains the most frequent carbapenem resistance determinant among *A. baumannii* worldwide (Hamidian and Nigro, 2019), and is highly frequent in IC4 and IC5, as previously described (Rodríguez et al., 2016). On the other hand, the production of OXA-72 was restricted to *A. baumannii* clinical isolates belonging $CC79^{Pas}$/$CC113^{Ox}$. Previous studies have demonstrated the emergence of this CHDL not only within $ST79^{Pas}$, but also within its single locus variant (SLV) ST730, in different Brazilian states (Vasconcelos et al., 2015; de Azevedo et al., 2019), as well as among carbapenem-resistant *A. baumannii* belonging to $ST15^{Pas}$ (Pagano et al., 2017), but such wide distribution of bla_{OXA-72} was not observed among our isolates.

Overall, isolates belonging to IC5 presented a broader spectrum of acquired antimicrobial resistance determinants compared to IC4. The presence of the AME encoding genes *aadA1*, *strA* and *strB*, as well as *dfrA1*, has been previously associated to class 2 integrons in IC5 in different Latin American countries (Martins et al., 2015; Ramírez et al., 2015; Pagano et al., 2019; Romanin et al., 2019). Moreover, bla_{TEM-1} was more frequent in this IC and might have contributed to the high ampicillin-sulbactam MICs observed, especially among OXA-23-producing isolates, as previously described (Krizova et al., 2013; Cardoso et al., 2016). Interestingly, all IC4 and IC5 bla_{TEM-1}-producing isolates also carried *sul2*, suggesting that both antimicrobial resistance determinants could be located in the same mobile genetic element, as previously reported (Hammad et al., 2019).

Despite the differences observed between the major South American *A. baumannii* clones, the high amikacin resistance levels observed in all isolates was associated with the presence of *aph(3′)-VIa*. The Aph(3′)-VIa AME was first described in *A. baumannii* and its activity spectrum includes amikacin (Ramírez and Tolmasky, 2010). Previous studies have also described the high frequency of this AME among *A. baumannii* clinical isolates worldwide, including in Brazil (Aghazadeh et al., 2013; Polotto et al., 2019). Other studies have also highlighted that gentamicin resistance was associated with distinct acetyltransferases, as observed among our isolates, and have suggested that a combination of AMEs could be responsible for that phenotype, as observed in our isolate 206182 (Ballaben et al., 2018). Additionally, Matos et al. (2019) described the presence of *aac(3)-IIa* and bla_{TEM-1} in a plasmid of an *A. baumannii* $ST15^{Pas}$ clinical isolate, as observed in our 10042 isolate, which also belonged to the same ST. Interestingly, that plasmid also harbored the CHDL encoding gene bla_{OXA-58} (Matos et al., 2019), which was not observed in our isolate.

Despite the critical role that acquired resistance determinants play in the acquisition and maintenance of MDR among *A. baumannii* clones, mutations in constitutive genes can also cause high resistance levels to important antimicrobial agents. Holt et al. (2016) have previously suggested that the presence of mutations in *gyrA* and *parC* was one of the features leading to the epidemiological success of IC1, however, this lineage is now rarely found and yet fluoroquinolone resistance remains high. In fact, the combination of Ser_{83}Leu and Ser_{80}Leu in GyrA and ParC, respectively, was additive (Vila et al., 1997), leading to high ciprofloxacin MICs, as observed among our isolates.

Mutations in the constitutive *pmrAB* genes seemed to be responsible for reduced susceptibility to polymyxins among IC5 isolates. The majority of amino acid substitutions were observed in PmrB and, to the best of our knowledge, most of them have not been described elsewhere. In fact, amino acid substitutions in the histidine kinase of this TCS seem to play an important role in reduced susceptibility to polymyxin in *A. baumannii*, since a high number of non-synonymous mutations in *pmrB* among colistin-resistant isolates was previously highlighted (Olaitan et al., 2014; Poirel et al., 2017; Gerson et al., 2020). The Ser_{119}Thr substitution in PmrA, observed in all isolates belonging to IC5, has been previously associated with polymyxin resistance (Arroyo et al., 2011), including in Brazilian isolates (Leite et al., 2019). However, this substitution was also observed among polymyxin-susceptible isolates, suggesting that it might have just a limited role in this phenotype. Moreover, it should be noted that most substitutions described in our study were considered natural polymorphisms associated with distinct clonal linages. These substitutions were also not associated with the higher *in vitro* activity of polymyxin B, compared to colistin, observed among polymyxin-resistant isolates. Such variation might be related to recombination events, as described for other *Acinetobacter* species (Kim and Ko, 2015). It has been previously suggested that polymyxin B and colistin MIC values may be distinct among *A. baumannii* clinical isolates, but the MIC variations were always ± one-fold dilution, and colistin MICs were not consistently higher than polymyxin B (Gales et al., 2001). To test this hypothesis, a larger number of isolates should be evaluated to confirm the distinct activities of both polymyxins among *A. baumannii* isolates presenting reduced susceptibility to those antimicrobial agents.

Gerson et al. (2020) have recently demonstrated that the identification of PmrCAB amino acid substitutions with potential roles in polymyxin resistance should be carried out in isogenic isolates to eliminate natural polymorphisms between lineages. However, the authors have mainly explored that feature among IC2 isolates. We have demonstrated that this is also true for South American major clones, especially among IC4 isolates, where a high number of *pmrAB* mutations was observed but none of them was unique to polymyxin-resistant isolates. This is also valid for the *lpxACD* operon, which has previously been associated with polymyxin resistance in *A. baumannii* (Moffatt et al., 2010). Some of the amino acid substitutions observed in LpxD have been previously described in polymyxin-susceptible and -resistant isolates (Oikonomou et al., 2015), corroborating our findings and confirming they were natural polymorphisms. Additionally, the absence of *eptA* among IC4 belonging isolates observed in our study has been previously described (Gerson et al., 2019) and highlights the presence of unknown polymyxin resistance mechanisms among $CC15^{Pas}$/$CC103^{Oxf}$ *A. baumannii* clinical isolates.

The reduced susceptibility to tigecycline observed among some *A. baumannii* isolates suggested that the AdeABC efflux system might have been overexpressed, considering that this glycylcycline is a substrate for this system (Lashinsky et al., 2017). The TCS AdeRS regulates its expression and amino

acid substitutions in those proteins have been associated with higher tigecycline MICs (Ruzin et al., 2007; Gerson et al., 2018). Although a high number of amino acid substitutions was observed in AdeRS in the isolates included in this study, they did not seem to have influenced tigecycline MICs, since isolates with the same pattern of mutations presented MICs ranging from 0.5 to 16 μg/mL. In fact, the substitution patterns were identical within each IC, suggesting that they were only natural polymorphisms. Therefore, the activity of other efflux systems, such as AdeIJK, might have been responsible for tigecycline MIC variations observed in our study, as previously reported (Damier-Piolle et al., 2008).

The great variety of resistance determinants observed among the isolates in this study might have masked the role of OMPs in our isolates. The high number of amino substitutions observed, especially in CarO, complicates the identification of mutations with a potential role in antimicrobial resistance. Additionally, the fact that the observed mutation patterns were identical in all isolates belonging to the same lineage suggests that they were polymorphisms associated with the evolution of different clonal lineages. Interestingly, Zhu et al. (2019) have previously highlighted the high variability of CarO protein sequences among *A. baumannii* isolates, including the presence of small insertions and deletions, as observed among ST15^{Pas} isolates. Moreover, Mussi et al. (2011) have demonstrated that such diversity could be associated with horizontal gene transfer and assertive recombination. Further studies are required to determine the contribution of this variability to antimicrobial resistance.

In summary, we demonstrated that a diversity of antimicrobial resistance determinants was present in the major South American *A. baumannii* clones. We have also provided evidence that attention should be payed to natural polymorphisms when comparing isolates with distinct phenotypes and genetic background, since most constitutive genes associated with antimicrobial resistance presented amino acid substitutions that did not play a role in reduced antimicrobial susceptibility. In addition, the contribution of high frequency of polymorphisms in hot spot genes among endemic clones must be evaluated with caution. Additionally, we suggested that unknown polymyxin resistance mechanisms might be present in *A. baumannii* isolates belonging to IC4. The resistance phenotype exhibited by endemic *A. baumannii* clones was very worrisome and should be carefully studied, considering that the molecular mechanisms involved seem to be, to some extent, lineage-specific.

IMPORTANCE

Carbapenem-resistant *Acinetobacter baumannii* (CRAB) have emerged worldwide due to the dissemination of successful clones. Even though international clone 2 (IC2) is the most prevalent in many countries, in Latin America CRAB isolates often belong to IC4 and IC5. The majority of CRAB isolates are also resistant to multiple other antimicrobials and have been classified as extremely drug-resistant (XDR). However, data exploring the molecular mechanisms involved in this phenotype among IC4 and IC5 are still scarce. In this study we presented a comprehensive analysis of genome sequencing data from Brazilian *A. baumannii* belonging to these important clones. We demonstrated that a combination of intrinsic and acquired resistance determinants was responsible for the resistance to several antimicrobial agents among Brazilian endemic clones. We also suggested that an unknown mechanism was responsible for the emergence of polymyxin resistance among IC4 clinical isolates. Finally, we highlighted the importance of comparing isolates with similar genetic background when evaluating mutations in constitutive genes, including efflux systems and outer membrane protein encoding genes.

ACCESSION NUMBERS

All raw reads generated were submitted to the Sequencing Read Archive (https://www.ncbi.nlm.nih.gov/sra/) of the National Center for Biotechnology Information (NCBI) under the BioProject number PRJNA632943. The sequences of the novel $bla_{ADC-181}$, $bla_{ADC-182}$, and $bla_{ADC-183}$ genes were deposited in NCBI β-lactamases database under the accession numbers MK248721, MK248722, and MK248723, respectively.

DATA AVAILABILITY STATEMENT

The datasets presented in this study can be found in online repositories. The names of the repository/repositories and accession number(s) can be found below: https://www.ncbi.nlm.nih.gov/, PRJNA632943; https://www.ncbi.nlm.nih.gov/, MK248721; https://www.ncbi.nlm.nih.gov/, MK248722; https://www.ncbi.nlm.nih.gov/, MK248723.

ETHICS STATEMENT

Ethical approval for this study was obtained from Research Ethics Committee from Federal University of São Paulo – UNIFESP/São Paulo Hospital (Process number: CEP N 4665141216).

AUTHOR CONTRIBUTIONS

CN, RC, PH, HS, and AG contributed to the study conception and design. RC and PH supervised the assays. MA, AIdP, and ACCP provided the strains and clinical data. CN, AS, FL, and JW performed the data collection and analysis. CN wrote the first draft of the manuscript and it was edited by RC. PH, HS, and AG reviewed the final draft of manuscript. All authors read and approved the final version of manuscript.

FUNDING

We are grateful to Coordenação de Aperfeiçoamento de Pessoal de Nível Superior (CAPES) for providing PDSE grants to CN (Process number: 88881.187573/2018-01) and

AS and to the National Council for Science and Technological Development (CNPq) for providing grants to FL and AG (Process number: 312066/2019).

ACKNOWLEDGMENTS

We would like to thank Cecília G. Carvalhaes and Thaís Guimarães for providing some of clinical isolates evaluated in this study, and to Larissa Akie Natsumeda and Karen de Castro Bauab for their excellent technical support. This work was presented in part as a Poster (P1109) at the 28th European Congress of Clinical Microbiology and Infectious Diseases (ECCMID) in Madrid, Spain, 2018.

SUPPLEMENTARY MATERIAL

The Supplementary Material for this article can be found online at: https://www.frontiersin.org/articles/10.3389/fmicb.2020.584603/full#supplementary-material

REFERENCES

Agência Nacional de Vigilância Sanitária [ANVISA] (2020). *Boletim Segurança do Paciente e Qualidade em Serviços de Saúde n° 18: Avaliação dos indicadores nacionais das Infecções Relacionadas à Assistência à Saúde (IRAS) e Resistência microbiana do ano de 2018*. Brasília: ANVISA.

Aghazadeh, M., Rezaee, M. A., Nahaei, M. R., Mahdian, R., Pajand, O., Saffari, F., et al. (2013). Dissemination of aminoglycoside-modifying enzymes and 16S rRNA methylases among *Acinetobacter baumannii* and *Pseudomonas aeruginosa* isolates. *Microb. Drug Resist.* 9, 282–288. doi: 10.1089/mdr.2012.0223

Antunes, L. C., Visca, P., and Towner, K. J. (2014). *Acinetobacter baumannii*: evolution of a global pathogen. *Pathog. Dis.* 71, 292–301. doi: 10.1111/2049-632X.12125

Arroyo, L. A., Herrera, C. M., Fernandez, L., Hankins, J. V., Trent, M. S., and Hancock, R. E. (2011). The *pmrCAB* operon mediates polymyxin resistance in *Acinetobacter baumannii* ATCC 17978 and clinical isolates through phosphoethanolamine modification of lipid A. *Antimicrob. Agents Chemother.* 55, 3743–3751. doi: 10.1128/AAC.00256-11

Ballaben, A. S., Andrade, L. N., Galetti, R., Ferreira, J. C., McElheny, C. L., Mettus, R. T., et al. (2018). Diversity of high-level aminoglycoside resistance mechanisms among Gram-negative nosocomial pathogens in Brazil. *Antimicrob. Agents Chemother.* 62:e01550-18. doi: 10.1128/AAC.01550-18

Cardoso, J. P., Cayô, R., Girardello, R., and Gales, A. C. (2016). Diversity of mechanisms conferring resistance to β-lactams among OXA-23-producing *Acinetobacter baumannii* clones. *Diagn. Microbiol. Infect. Dis.* 85, 90–97. doi: 10.1016/j.diagmicrobio.2016.01.018

Castillo-Ramírez, S., and Graña-Miraglia, L. (2019). Inaccurate multilocus sequence typing of *Acinetobacter baumannii*. *Emerg. Infect. Dis.* 25, 186–187. doi: 10.3201/eid2501.180374

Chagas, T. P., Carvalho, K. R., de Oliveira Santos, I. C., Carvalho-Assef, A. P., and Asensi, M. D. (2014). Characterization of carbapenem-resistant *Acinetobacter baumannii* in Brazil (2008-2011): countrywide spread of OXA-23-producing clones (CC15 and CC79). *Diagn. Microbiol. Infect. Dis.* 79, 468–472. doi: 10.1016/j.diagmicrobio.2014.03.006

Chagas, T. P. G., Tavares, E., Oliveira, T. R., D'Alincourt Carvalho-Assef, A. P., Albano, R. M., and Asensi, M. D. (2017). Carbapenem-resistant *Acinetobacter pittii* strain harboring bla(OXA-72) from Brazil. *Diagn. Microbiol. Infect. Dis.* 88, 93–94. doi: 10.1016/j.diagmicrobio.2017.01.022

Chmielarczyk, A., Pilarczyk-Żurek, M., Kamińska, W., Pobiega, M., Romaniszyn, D., Ziółkowski, G., et al. (2016). Molecular Epidemiology and drug resistance of *Acinetobacter baumannii* isolated from hospitals in Southern Poland: ICU as a risk factor for XDR strains. *Microb. Drug Resist.* 22, 328–335. doi: 10.1089/mdr.2015.0224

Cieslinski, J. M., Arend, L., Tuon, F. F., Silva, E. P., Ekermann, R. G., Dalla-Costa, L. M., et al. (2013). Molecular epidemiology characterization of OXA-23 carbapenemase-producing *Acinetobacter baumannii* isolated from 8 Brazilian hospitals using repetitive sequence-based PCR. *Diagn. Microbiol. Infect. Dis.* 77, 337–340. doi: 10.1016/j.diagmicrobio.2013.07.018

Damier-Piolle, L., Magnet, S., Brémont, S., Lambert, T., and Courvalin, P. (2008). AdeIJK, a resistance-nodulation-cell division pump effluxing multiple antibiotics in *Acinetobacter baumannii*. *Antimicrob. Agents Chemother.* 52, 557–562. doi: 10.1128/AAC.00732-07

de Azevedo, F. K. S. F., Dutra, V., Nakazato, L., Mello, C. M., Pepato, M. A., de Sousa, A. T. H. I., et al. (2019). Molecular epidemiology of multidrug-resistant *Acinetobacter baumannii* infection in two hospitals in Central Brazil: the role of ST730 and ST162 in clinical outcomes. *J. Med. Microbiol.* 68, 31–40. doi: 10.1099/jmm.0.000853

Gaiarsa, S., Batisti Biffignandi, G., Esposito, E. P., Castelli, M., Jolley, K. A., Brisse, S., et al. (2019). Comparative analysis of the two *Acinetobacter baumannii* multilocus sequence typing (MLST) schemes. *Front. Microbiol.* 10:930. doi: 10.3389/fmicb.2019.00930

Gales, A. C., Reis, A. O., and Jones, R. N. (2001). Contemporary assessment of antimicrobial susceptibility testing methods for polymyxin B and colistin: review of available interpretative criteria and quality control guidelines. *J. Clin. Microbiol.* 39, 183–190. doi: 10.1128/JCM.39.1.183-190.2001

Gales, A. C., Seifert, H., Gur, D., Castanheira, M., Jones, R. N., and Sader, H. S. (2019). Antimicrobial susceptibility of *Acinetobacter calcoaceticus-Acinetobacter baumannii* complex and *Stenotrophomonas maltophilia* clinical isolates: results from the SENTRY antimicrobial surveillance program (1997-2016). *Open Forum Infect. Dis.* 6(Suppl. 1), S34–S46. doi: 10.1093/ofid/ofy293

Gerson, S., Betts, J. W., Lucaßen, K., Nodari, C. S., Wille, J., Josten, M., et al. (2019). Investigation of novel PmrB and EptA mutations in isogenic *Acinetobacter baumannii* isolates associated with colistin resistance and increased virulence *in vivo*. *Antimicrob. Agents Chemother.* 63:e01586-18. doi: 10.1128/AAC.01586-18

Gerson, S., Lucaßen, K., Wille, J., Nodari, C. S., Stefanik, D., Nowak, J., et al. (2020). Diversity of amino acid substitutions in PmrCAB associated with colistin resistance in clinical *Acinetobacter baumannii* isolates. *Int. J. Antimicrob. Agents* 55:105862. doi: 10.1016/j.ijantimicag.2019.105862

Gerson, S., Nowak, J., Zander, E., Ertel, J., Wen, Y., Krut, O., et al. (2018). Diversity of mutations in regulatory genes of resistance-nodulation-cell division efflux pumps in association with tigecycline resistance in *Acinetobacter baumannii*. *J. Antimicrob. Chemother.* 73, 1501–1508. doi: 10.1093/jac/dky083

Girardello, R., Visconde, M., Cayô, R., Figueiredo, R. C., Mori, M. A., Lincopan, N., et al. (2017). Diversity of polymyxin resistance mechanisms among *Acinetobacter baumannii* clinical isolates. *Diagn. Microbiol. Infect. Dis.* 87, 37–44. doi: 10.1016/j.diagmicrobio.2016.10.011

Graña-Miraglia, L., Evans, B. A., López-Jácome, L. E., Hernández-Durán, M., Colín-Castro, C. A., Volkow-Fernández, P., et al. (2020). Origin of OXA-23 Variant OXA-239 from a recently emerged lineage of *Acinetobacter baumannii* international clone V. *mSphere* 5, e801–e819. doi: 10.1128/mSphere.00801-19

Hamidian, M., and Nigro, S. J. (2019). Emergence, molecular mechanisms and global spread of carbapenem-resistant *Acinetobacter baumannii*. *Microb. Genom.* 5:e000306. doi: 10.1099/mgen.0.000306

Hammad, A. M., Hoffmann, M., Gonzalez-Escalona, N., Abbas, N. H., Yao, K., Koenig, S., et al. (2019). Genomic features of colistin resistant *Escherichia coli* ST69 strain harboring mcr-1 on IncHI2 plasmid from raw milk cheese in Egypt. *Infect. Genet. Evol.* 73, 126–131. doi: 10.1016/j.meegid.2019.04.021

Hamouda, A., Evans, B. A., Towner, K. J., and Amyes, S. G. (2010). Characterization of epidemiologically unrelated *Acinetobacter baumannii* isolates from four continents by use of multilocus sequence typing, pulsed-field gel electrophoresis, and sequence-based typing of bla(OXA-51-like) genes. *J. Clin. Microbiol.* 48, 2476–2483. doi: 10.1128/JCM.02431-09

Higgins, P. G., Dammhayn, C., Hackel, M., and Seifert, H. (2010). Global spread of carbapenem-resistant *Acinetobacter baumannii*. *J. Antimicrob. Chemother.* 65, 233–238. doi: 10.1093/jac/dkp428

Higgins, P. G., Prior, K., Harmsen, D., and Seifert, H. (2017). Development and evaluation of a core genome multilocus typing scheme for whole-genome sequence-based typing of *Acinetobacter baumannii*. *PLoS One* 12:e0179228. doi: 10.1371/journal.pone.0179228

Holt, K., Kenyon, J. J., Hamidian, M., Schultz, M. B., Pickard, D. J., Dougan, G., et al. (2016). Five decades of genome evolution in the globally distributed, extensively antibiotic-resistant *Acinetobacter baumannii* global clone 1. *Microb. Genom.* 2:e000052. doi: 10.1099/mgen.0.000052

Hornsey, M., Ellington, M. J., Doumith, M., Thomas, C. P., Gordon, N. C., Wareham, D. W., et al. (2010). AdeABC-mediated efflux and tigecycline MICs for epidemic clones of *Acinetobacter baumannii*. *J. Antimicrob. Chemother.* 65, 1589–1593. doi: 10.1093/jac/dkq218

Karah, N., Jolley, K. A., Hall, R. M., and Uhlin, B. E. (2017). Database for the *ampC* alleles in *Acinetobacter baumannii*. *PLoS One* 12:e0176695. doi: 10.1371/journal.pone.0176695

Kim, D. H., and Ko, K. S. (2015). A distinct alleles and genetic recombination of *pmrCAB* operon in species of *Acinetobacter baumannii* complex isolates. *Diagn. Microbiol. Infect. Dis.* 82, 183–188. doi: 10.1016/j.diagmicrobio.2015.03.021

Krizova, L., Poirel, L., Nordmann, P., and Nemec, A. (2013). TEM-1 β-lactamase as a source of resistance to sulbactam in clinical strains of *Acinetobacter baumannii*. *J. Antimicrob. Chemother.* 68, 2786–2791. doi: 10.1093/jac/dkt275

Kuo, S. C., Chang, S. C., Wang, H. Y., Lai, J. F., Chen, P. C., Shiau, Y. R., et al. (2012). Emergence of extensively drug-resistant *Acinetobacter baumannii* complex over 10 years: nationwide data from the Taiwan Surveillance of Antimicrobial Resistance (TSAR) program. *BMC Infect. Dis.* 12:200. doi: 10.1186/1471-2334-12-200

La Scola, B., Gundi, V. A., Khamis, A., and Raoult, D. (2006). Sequencing of the *rpoB* gene and flanking spacers for molecular identification of *Acinetobacter* species. *J. Clin. Microbiol.* 44, 827–832. doi: 10.1128/JCM.44.3.827-832.2006

Lashinsky, J. N., Henig, O., Pogue, J. M., and Kaye, K. S. (2017). Minocycline for the treatment of multidrug and extensively drug-resistant *A. baumannii*: a review. *Infect. Dis. Ther.* 6, 199–211. doi: 10.1007/s40121-017-0153-2

Leite, G. C., Stabler, R. A., Neves, P., Perdigão Neto, L. V., Ruedas Martins, R. C., Rizek, C., et al. (2019). Genetic and virulence characterization of colistin-resistant and colistin-sensitive *A. baumannii* clinical isolates. *Diagn. Microbiol. Infect. Dis.* 95, 99–101. doi: 10.1016/j.diagmicrobio.2019.04.013

Martins, N., Picão, R. C., Adams-Sapper, S., Riley, L. W., and Moreira, B. M. (2015). Association of class 1 and 2 integrons with multidrug-resistant *Acinetobacter baumannii* international clones and *Acinetobacter nosocomialis* isolates. *Antimicrob. Agents Chemother.* 59, 698–701. doi: 10.1128/AAC.02415-14

Matos, A. P., Cayô, R., Almeida, L. G. P., Streling, A. P., Nodari, C. S., Martins, W. M. B. S., et al. (2019). Genetic characterization of plasmid-borne *bla*OXA-58 in distinct *Acinetobacter* species. *mSphere* 4:e000376-19. doi: 10.1128/mSphere.00376-19

Moffatt, J. H., Harper, M., Harrison, P., Hale, J. D., Vinogradov, E., Seemann, T., et al. (2010). Colistin resistance in *Acinetobacter baumannii* is mediated by complete loss of lipopolysaccharide production. *Antimicrob. Agents Chemother.* 54, 4971–4977. doi: 10.1128/AAC.00834-10

Müller, C., Stefanik, D., Wille, J., Hackel, M., Higgins, P. G., and Seifert, H. (2019). "Molecular epidemiology of carbapenem-resistant *Acinetobacter baumannii* clinical isolates and identification of the novel international clone IC9: results from a worldwide surveillance study (2012 - 2016)," in *Proceedings of the Abstract Book of the 29th European Congress of Clinical Microbiology and Infectious Diseases, P0947*, Amsterdam.

Mussi, M. A., Limansky, A. S., Relling, V., Ravasi, P., Arakaki, A., Actis, L. A., et al. (2011). Horizontal gene transfer and assortative recombination within the *Acinetobacter baumannii* clinical population provide genetic diversity at the single *carO* gene, encoding a major outer membrane protein channel. *J. Bacteriol.* 193, 4736–4748. doi: 10.1128/JB.01533-10

Nowak, J., Zander, E., Stefanik, D., Higgins, P. G., Roca, I., Vila, J., et al. (2017). High incidence of pandrug-resistant *Acinetobacter baumannii* isolates collected from patients with ventilator-associated pneumonia in Greece, Italy and Spain as part of the MagicBullet clinical trial. *J. Antimicrob. Chemother.* 72, 3277–3282. doi: 10.1093/jac/dkx322

Oikonomou, O., Sarrou, S., Papagiannitsis, C. C., Georgiadou, S., Mantzarlis, K., Zakynthinos, E., et al. (2015). Rapid dissemination of colistin and carbapenem resistant *Acinetobacter baumannii* in Central Greece: mechanisms of resistance, molecular identification and epidemiological data. *BMC Infect. Dis.* 15:559. doi: 10.1186/s12879-015-1297-x

Olaitan, A. O., Morand, S., and Rolain, J. M. (2014). Mechanisms of polymyxin resistance: acquired and intrinsic resistance in bacteria. *Front. Microbiol.* 5:643. doi: 10.3389/fmicb.2014.00643

Opazo-Capurro, A., San Martín, I., Quezada-Aguiluz, M., Morales-León, F., Domínguez-Yévenes, M., Lima, C. A., et al. (2019). Evolutionary dynamics of carbapenem-resistant *Acinetobacter baumannii* circulating in Chilean hospitals. *Infect. Genet. Evol.* 73, 93–97. doi: 10.1016/j.meegid.2019.04.022

Pagano, M., Martins, A. F., Machado, A. B., Barin, J., and Barth, A. L. (2013). Carbapenem-susceptible *Acinetobacter baumannii* carrying the ISAba1 upstream *bla*OXA-51-like gene in Porto Alegre, southern Brazil. *Epidemiol. Infect.* 141, 330–333. doi: 10.1017/S095026881200074X

Pagano, M., Nunes, L. S., Niada, M., Barth, A. L., and Martins, A. F. (2019). Comparative analysis of carbapenem-resistant *Acinetobacter baumannii* sequence types in Southern Brazil: from the first outbreak (2007-2008) to the endemic period (2013-2014). *Microb. Drug Resist.* 25, 538–542. doi: 10.1089/mdr.2018.0262

Pagano, M., Rocha, L., Sampaio, J. L., Martins, A. F., and Barth, A. L. (2017). Emergence of OXA-72-producing *Acinetobacter baumannii* belonging to high-risk clones (CC15 and CC79) in different Brazilian States. *Infect. Control. Hosp. Epidemiol.* 38, 252–254. doi: 10.1017/ice.2016.287

Poirel, L., Jayol, A., and Nordmann, P. (2017). Polymyxins: antibacterial activity, susceptibility testing, and resistance mechanisms encoded by plasmids or chromosomes. *Clin. Microbiol. Rev.* 30, 557–596. doi: 10.1128/CMR.00064-16

Polotto, M., Casella, T., Tolentino, F. M., Mataruco, M. M., Porto, N. K. M., Binhardi, M. F. B., et al. (2019). Investigation of carbapenemases and aminoglycoside modifying enzymes of *Acinetobacter baumannii* isolates recovered from patients admitted to intensive care units in a tertiary-care hospital in Brazil. *Rev. Soc. Bras. Med. Trop.* 53:e20190044. doi: 10.1590/0037-8682-0094-2019

Qureshi, Z. A., Hittle, L. E., O'Hara, J. A., Rivera, J. I., Syed, A., Shields, R. K., et al. (2015). Colistin-resistant *Acinetobacter baumannii*: beyond carbapenem resistance. *Clin. Infect. Dis.* 60, 1295–1303. doi: 10.1093/cid/civ048

Ramírez, M. S., Montaña, S., Cassini, M., and Centrón, D. (2015). Preferential carriage of class 2 integrons in *Acinetobacter baumannii* CC113 and novel singletons. *Epidemiol. Infect.* 143, 3118–3121. doi: 10.1017/S0950268815000060

Ramírez, M. S., and Tolmasky, M. E. (2010). Aminoglycoside modifying enzymes. *Drug Resist. Updat.* 13, 151–171. doi: 10.1016/j.drup.2010.08.003

Rodríguez, C. H., Balderrama Yarhui, N., Nastro, M., Nuñez Quezada, T., Castro Cañarte, G., Magne Ventura, R., et al. (2016). Molecular epidemiology of carbapenem-resistant *Acinetobacter baumannii* in South America. *J. Med. Microbiol.* 65, 1088–1091. doi: 10.1099/jmm.0.000328

Rodríguez-Martínez, J. M., Poirel, L., and Nordmann, P. (2010). Genetic and functional variability of AmpC-type β-lactamases from *Acinetobacter baumannii*. *Antimicrob. Agents Chemother.* 54, 4930–4933. doi: 10.1128/AAC.00427-10

Romanin, P., Palermo, R. L., Cavalini, J. F., Fávaro, L. D. S., De Paula-Petroli, S. B., Fernandes, E. V., et al. (2019). Multidrug- and extensively drug-resistant *Acinetobacter baumannii* in a tertiary hospital from Brazil: the importance of carbapenemase encoding genes and epidemic clonal complexes in a 10-year study. *Microb. Drug Resist.* 25, 1365–1373. doi: 10.1089/mdr.2019.0002

Royer, S., de Campos, P. A., Araújo, B. F., Ferreira, M. L., Gonçalves, I. R., Batistão, D. W. D. F., et al. (2018). Molecular characterization and clonal dynamics of nosocomial *bla*OXA-23 producing XDR *Acinetobacter baumannii*. *PLoS One* 13:e0198643. doi: 10.1371/journal.pone.0198643

Ruzin, A., Keeney, D., and Bradford, P. A. (2007). AdeABC multidrug efflux pump is associated with decreased susceptibility to tigecycline in *Acinetobacter calcoaceticus-Acinetobacter baumannii* complex. *J. Antimicrob. Chemother.* 59, 1001–1004. doi: 10.1093/jac/dkm058

Seifert, H., Dolzani, L., Bressan, R., van der Reijden, T., van Strijen, B., Stefanik, D., et al. (2005). Standardization and interlaboratory reproducibility assessment of pulsed-field gel electrophoresis-generated fingerprints of *Acinetobacter*

baumannii. *J. Clin. Microbiol.* 43, 4328–4335. doi: 10.1128/JCM.43.9.4328-4335.2005

Stietz, M. S., Ramírez, M. S., Vilacoba, E., Merkier, A. K., Limansky, A. S., Centrón, D., et al. (2013). *Acinetobacter baumannii* extensively drug resistant lineages in Buenos Aires hospitals differ from the international clones I-III. *Infect. Genet. Evol.* 14, 294–301. doi: 10.1016/j.meegid.2012.12.020

Tavares, L. C. B., de Vasconcellos, F. M., de Sousa, W. V., Rocchetti, T. T., Mondelli, A. L., Ferreira, A. M., et al. (2019). Emergence and persistence of high-risk clones among MDR and XDR *A. baumannii* at a Brazilian teaching hospital. *Front. Microbiol.* 9:2898. doi: 10.3389/fmicb.2018.02898

Vasconcelos, A. T., Barth, A. L., Zavascki, A. P., Gales, A. C., Levin, A. S., Lucarevschi, B. R., et al. (2015). The changing epidemiology of *Acinetobacter* spp. producing OXA carbapenemases causing bloodstream infections in Brazil: a BrasNet report. *Diagn. Microbiol. Infect. Dis.* 83, 382–385. doi: 10.1016/j.diagmicrobio.2015.08.006

Vila, J., Ruiz, J., Goñi, P., and Jimenez de Anta, T. (1997). Quinolone-resistance mutations in the topoisomerase IV *parC* gene of *Acinetobacter baumannii*. *J. Antimicrob. Chemother.* 39, 757–762. doi: 10.1093/jac/39.6.757

WHO (2015). *Global Action Plan on Antimicrobial Resistance*. Geneva: WHO.

Zander, E., Nemec, A., Seifert, H., and Higgins, P. G. (2012). Association between β-lactamase-encoding bla(OXA-51) variants and DiversiLab rep-PCR-based typing of *Acinetobacter baumannii* isolates. *J. Clin. Microbiol.* 50, 1900–1904. doi: 10.1128/JCM.06462-11

Zhu, L. J., Chen, X. Y., and Hou, P. F. (2019). Mutation of CarO participates in drug resistance in imipenem-resistant *Acinetobacter baumannii*. *J. Clin. Lab. Anal.* 33:e22976. doi: 10.1002/jcla.22976

Conflict of Interest: AG has recently received research funding and/or consultation fees from Bayer, Cristália, InfectoPharm, Eurofarma, MSD, Pfizer and Zambon.

The remaining authors declare that the research was conducted in the absence of any commercial or financial relationships that could be construed as a potential conflict of interest.

frontiers in Microbiology

ORIGINAL RESEARCH
published: 02 December 2020
doi: 10.3389/fmicb.2020.605952

A Novel Family of *Acinetobacter* Mega-Plasmids Are Disseminating Multi-Drug Resistance Across the Globe While Acquiring Location-Specific Accessory Genes

Timothy M. Ghaly[1], Ian T. Paulsen[2,3], Ammara Sajjad[1], Sasha G. Tetu[2,3] and Michael R. Gillings[1,3]*

[1]*Department of Biological Sciences, Macquarie University, Sydney, NSW, Australia,* [2]*Department of Molecular Sciences, Macquarie University, Sydney, NSW, Australia,* [3]*ARC Centre of Excellence in Synthetic Biology, Macquarie University, Sydney, NSW, Australia*

OPEN ACCESS

Edited by:
Santiago Castillo Ramírez, National Autonomous University of Mexico, Mexico

Reviewed by:
Xiaoting Hua, Zhejiang University, China
Olga Maria Perez-Carrascal, Université de Montréal, Canada

***Correspondence:**
Timothy M. Ghaly
timothy.ghaly@mq.edu.au

Specialty section:
This article was submitted to Evolutionary and Genomic Microbiology, a section of the journal Frontiers in Microbiology

Received: *14 September 2020*
Accepted: *10 November 2020*
Published: *02 December 2020*

Citation:
Ghaly TM, Paulsen IT, Sajjad A, Tetu SG and Gillings MR (2020) A Novel Family of Acinetobacter Mega-Plasmids Are Disseminating Multi-Drug Resistance Across the Globe While Acquiring Location-Specific Accessory Genes. Front. Microbiol. 11:605952. doi: 10.3389/fmicb.2020.605952

Acinetobacter species are emerging as major nosocomial pathogens, aided by their ability to acquire resistance to all classes of antibiotics. A key factor leading to their multi-drug resistance phenotypes is the acquisition of a wide variety of mobile genetic elements, particularly large conjugative plasmids. Here, we characterize a family of 21 multi-drug resistance mega-plasmids in 11 different *Acinetobacter* species isolated from various locations across the globe. The plasmid family exhibits a highly dynamic and diverse accessory genome, including 221 antibiotic resistance genes (ARGs) that confer resistance to 13 classes of antibiotics. We show that plasmids isolated within the same geographic region are often evolutionarily divergent members of this family based on their core-genome, yet they exhibit a more similar accessory genome. Individual plasmids, therefore, can disseminate to different locations around the globe, where they then appear to acquire diverse sets of accessory genes from their local surroundings. Further, we show that plasmids from several geographic regions were enriched with location-specific functional traits. Together, our findings show that these mega-plasmids can transmit across species boundaries, have the capacity for global dissemination, can accumulate a diverse suite of location-specific accessory genes, and can confer multi-drug resistance phenotypes of significant concern for human health. We therefore highlight this previously undescribed plasmid family as a serious threat to healthcare systems worldwide. These findings also add to the growing concern that mega-plasmids are key disseminators of antibiotic resistance and require global surveillance.

Keywords: multi-drug resistance, pathogens, mobile genetic elements, nosocomial infections, plasmid pangenome

INTRODUCTION

Acinetobacter is a diverse genus of bacteria that commonly occur in soil and water, and in association with animals and plants (Fondi et al., 2010). Several species are emerging as major nosocomial pathogens (Almasaudi, 2018). In particular, *Acinetobacter baumannii*, *Acinetobacter nosocomialis*, *Acinetobacter pitti*, *Acinetobacter ursingii*, *Acinetobacter haemolyticus*, and *Acinetobacter calcoaceticus* are now a serious threat to human health (Antunes et al., 2014; Chusri et al., 2014; Weber et al., 2016; Castro-Jaimes et al., 2020; Rivera-Izquierdo et al., 2020). Clinical isolates are often characterized by their multi-drug resistance, with some isolates being resistant to all classes of antibiotics (Göttig et al., 2014). One of the key features leading to their multi-drug resistance is the acquisition of a wide variety of mobile DNA elements (Fournier et al., 2006; Hamidian et al., 2014, 2016; Lean and Yeo, 2017). In particular, *Acinetobacter* strains are known to harbor a strikingly diverse pool of plasmids (Fournier et al., 2006; Fondi et al., 2010; Merino et al., 2010; Lean and Yeo, 2017; Salto et al., 2018).

The evolutionary and ecological dynamics of *Acinetobacter* plasmids are particularly interesting as their host species can colonize a wide variety of environments and display diverse metabolic activities, even among closely related strains (Hawkey and Munday, 2004; Bach and Gutnick, 2006; Albarracín et al., 2012; Garcia-Garcera et al., 2017). Such variety in niche adaptation is largely driven by the open pangenome of their plasmids (Fondi et al., 2010). Plasmids, in general, can rapidly diversify through a series of recombinatorial and transpositional events that generate novel mosaic elements (Stokes and Gillings, 2011). These mosaic elements are characterized by a nested structure of diverse mobile elements, including transposons and "clinical" forms of integrons (Ghaly et al., 2017; Gillings, 2017), each of which are prolific at acquiring diverse antibiotic resistance genes (ARGs; Babakhani and Oloomi, 2018; Ghaly et al., 2020). Humans, largely through the use of various selective agents, such as heavy metals, disinfectants, and antibiotics, are increasing the frequency of such occurrences (Gillings and Stokes, 2012; Gillings et al., 2018). The same selective agents also upregulate the horizontal transmission mechanisms of these mosaic elements, leading to the widespread dissemination of their genetic cargo (Beaber et al., 2004; Schreiber et al., 2013; Ghaly and Gillings, 2018). In clinical settings, this has led to the emergence of multi-drug resistant pathogens that are well adapted to a nosocomial lifestyle.

An extensive range of resistance genes in *Acinetobacter* are plasmid-borne (Cerezales et al., 2020). In particular, large plasmids of more than 100 kb, referred to as mega-plasmids, are known to carry arrays of multiple resistance genes (Hamidian et al., 2016; Nigro and Hall, 2017). Mega-plasmids, in general, are characterized by their mosaic structure and carry genetic regions that originate from various ancestral sources (Pesesky et al., 2019). Recently, a family of mega-plasmids has been identified as a major disseminator of multi-drug resistance among *Pseudomonas* species (Cazares et al., 2020). These mega-plasmids carried large arrays of complex and dynamic resistance regions, suggesting that they play a key role in the spread of resistance.

Global surveillance of such mega-plasmids using a whole-genome sequencing approach has been highlighted as a top priority for public health management (Cazares et al., 2020). However, fully sequencing these mega-plasmids with short-read data remains difficult as they contain long repeat regions (Arredondo-Alonso et al., 2017). Long-read sequencing, however, allows these mega-plasmids to be fully resolved (Botelho et al., 2019). The accuracy of assemblies can be improved by combining short-read and long-read sequencing approaches.

Here, we use a combination of PacBio long-read and Illumina short-read sequencing to fully assemble four multi-resistance mega-plasmids resident in both clinical and environmental *Acinetobacter* strains. We collected an additional 17 publicly available complete plasmid sequences within this family, isolated from various locations across the world. This previously undescribed mega-plasmid family, found in 11 different *Acinetobacter* species so far, shares a tight core-genome, yet varies extensively in its accessory genome. By characterizing its pangenome, we show that this plasmid family can rapidly disperse around the globe, where it subsequently accumulates a diverse suite of niche-adaptive accessory genes.

MATERIALS AND METHODS

Sampling, DNA Extraction, and Sequencing

The novel plasmids described in this study were recovered from *Acinetobacter* species. Three were isolated from *Acinetobacter* strains inhabiting the digestive tracts of wild-caught prawns, harvested from the Australian east coast (pR4WN-1BD1, pR4WN-12CE1, and pR4WN-E10B), and one from an ICU patient at Westmead Hospital, Sydney, Australia (pWM98B). The method by which each *Acinetobacter* host was isolated from the wild-caught prawns (Gillings et al., 2009; Sajjad et al., 2011) and the Westmead Hospital patient (Valenzuela et al., 2007) have been previously described. These bacterial isolates were of interest because they showed sequence similarity in the genomic landscape flanking a previously described class 1 integron (Gillings et al., 2009). To investigate this further, DNA was extracted from pure cultures using a standard phenol:chloroform protocol (Sambrook and Russell, 2006). Whole genome *de novo* sequencing was performed using both long-read and 100 bp paired-end sequencing on the PacBio® *RS* and the Illumina® HiSeq 2500 systems, respectively. Sequencing was carried out at the Macrogen Sequencing Facility (Seoul, South Korea).

Plasmid Assembly and Polishing

PacBio long-reads were assembled with Flye v2.7.1 (Kolmogorov et al., 2019) with three iterations of Flye's in-built polisher (parameters: –plasmids -i 3). The Flye assemblies were then further polished with the HiSeq paired-end reads using Pilon v1.23 (Walker et al., 2014). Polishing with Pilon

first involved mapping all paired-end reads to the PacBio assemblies using BWA v0.7.12-r1039 (Li and Durbin, 2009). The BWA mapping was then used by Pilon to polish the assemblies. Several rounds of polishing (3–4 iterations) were implemented until no further changes were made to the previous round. Polished contigs were then identified to be circular using Circlator v1.5.5 (Hunt et al., 2015), which outputs a linearized version of each circular contig (parameters: all -- assembler canu). Circularized contigs were then re-polished with the paired-end reads using Pilon. All assemblies required a further two rounds of Pilon polishing until no changes were made to the previous round.

Taxonomic Labeling and Collecting Related Plasmids

Contigs representing the complete chromosome from each assembly were assigned a taxonomy by best BLASTn match using BLAST v2.7.1 (Madden, 2013) against all complete bacterial genomes in RefSeq (downloaded: June 25, 2020). Taxonomic identification was then confirmed with Kraken v1.0 (Wood and Salzberg, 2014; parameters: -- threads 24).

From each of the four samples, a complete sequence was also assembled for the plasmid carrying the integron of interest. Sequence coverage statistics for each of these were generating by mapping sequence reads to each plasmid assembly using Minimap2 v2.17-r941 (Li, 2018) with the parameters (-ax map-pb) and (-ax sr) for PacBio and Illumina mapping, respectively. Sequence coverage details were then extracted from each read mapping using BEDTools v2.27.1 (Quinlan and Hall, 2010; parameters: genomeCoveragBed).

To identify all related plasmids that had previously been sequenced and submitted to NCBI, each plasmid was used to query the complete nr/nt database as of June 26, 2020[1] using BLASTn. All plasmids that were considered related had a BLAST query cover greater than 64% and a percent identity greater than 98.5%. This resulted in an additional 17 plasmids for inclusion in the detailed analyses below (GenBank accessions: CP010351, CP029396, CP032285, CP033130, CP033531, CP033569, CP038010, CP042365, CP042557, CP043053, CP043309, CP048828, KX426227, MH220285 – MH220287, and MK134375). Plasmid alignment visualizations were generated using Chromatiblock v0.4.2 (Sullivan and van Bakel, 2019) and AliTV v1.0.6 (Ankenbrand et al., 2017).

To determine to which Rep family the plasmids belonged, we identified replication initiation proteins by annotation with InterProScan v5.44-79.0 (Jones et al., 2014; parameters: -goterms) and by BLASTP alignments with representative Rep proteins from every known *Acinetobacter* Rep family (available as **Supplementary Figure S2** from Salgado-Camargo et al., 2020).

Plasmid Pan- and Core-Genome Analyses

Gene and protein sequences for all 21 plasmids were predicted using Prokka v1.13 (parameters: -- kingdom Bacteria). Plasmid pan- and core-genome analyses were carried out using Perl scripts available in the GET_HOMOLOGUES v20092018 software package (Contreras-Moreira and Vinuesa, 2013; Vinuesa and Contreras-Moreira, 2015). For the plasmid pan-genome, this involved generating two pangenome matrices based on the COGtriangles (Kristensen et al., 2010) and OMCL (Li et al., 2003) clustering algorithms using the get_homologues.pl script. The parameters (-X -c -n 8 -t 0 -A -G) and (-X -c -n 8 -t 0 -A -G -M) were implemented, respectively. Based on the intersection of the two sets of clustered sequences, a consensus pangenome matrix was obtained using the compare_clusters.pl script (parameters: -m -T). The identified plasmid core-genome was based on the intersection of the BDBH, COGtriangles, and OMCL clustering algorithms using the get_homologues.pl script with parameters (-t 21 -e), (-G t0), and (-M -t 0), respectively.

The plasmid pangenome was divided into four occupancy classes. The core-genome was made up of the "soft core" (Kaas et al., 2012), which consisted of the genes found in >95% of plasmids, and the "core," which contained genes found in all plasmids. The accessory genome was made up of the "cloud" (Wolf et al., 2012), which contained the rare genes found in only one to two plasmids, and the "shell" (Wolf et al., 2012), which comprised the remaining, moderately conserved genes.

The primary Perl script, get_homologues.pl with the above parameters, also estimated the minimum core-genome size for this family of plasmids. The estimate was based on 10 random samples of the 21 plasmids with a fitted curve following the function proposed by Tettelin et al. (2005).

To generate a maximum-likelihood tree that clustered plasmids based on the presence and absence of all accessory genes in the pangenome, the pangenome matrix, reduced to a binary format, was used. The tree was generated using IQ-TREE v1.6.12 (Nguyen et al., 2015; Hoang et al., 2018) with 1,000 bootstrap replicates (parameters: -alrt 1000 -bb 1000). The resulting tree was annotated with FigTree v.1.4.3 (Rambaut, 2017) with midpoint root.

Phylogenetic Analysis

The evolutionary relationship between plasmids was inferred from the plasmid core-genome. Appropriate phylogenetic loci were identified using the GET_PHYLOMARKERS software package (Vinuesa et al., 2018) with default parameters. The GET_PHYLOMARKERS uses the single-copy plasmid core-genome clusters identified by GET_HOMOLOGUES and removes recombinant sequences as well as loci that produce outlier phylogenies. This resulted in eight high-quality phylogenetic markers. These included genes that encode a TraX conjugative transfer protein, an integrase, three membrane-associated proteins, and three hypothetical proteins of unknown functions. The nucleotide sequences were concatenated and aligned using MAFFT v7.271 (Katoh and Standley, 2013; paramters: -localpair -maxiterate 1000). The best-fit substitution model to suit the alignment was determined using ModelFinder (Kalyaanamoorthy et al., 2017), and a maximum-likelihood tree was generated using IQ-TREE

[1]http://www.ncbi.nlm.nih.gov/BLAST/

v1.6.12 (Nguyen et al., 2015; Hoang et al., 2018) with 1,000 bootstrap replicates (parameters: -m MFP -alrt 1000 -bb 1000). The resulting tree was annotated with FigTree v.1.4.3 (Rambaut, 2017) with midpoint root.

To test whether plasmids have transmitted horizontally across species boundaries, a co-phylogeny was generated to compare host cell and plasmid phylogenies. We used a whole-genome-based phylogeny of the host chromosomes using the GET_PHYLOMARKERS software package (Vinuesa et al., 2018) as described above. Five of the plasmids retrieved from GenBank did not have a corresponding host chromosome sequence publicly available and were thus excluded from the co-phylogenetic analysis. A co-phylogeny comparing the plasmids and their respective host strains was produced using the R package phytools v0.7-47 (Revell, 2012), which rotates the nodes of both trees to optimize congruence between the tips.

Tree topologies were quantitatively compared using a normalized PH85 tree topological distance (nPH85; Geoghegan et al., 2017). This was used to compare the two plasmid trees based on their core and accessory genomes, respectively, as well as to compare the plasmid and host co-phylogenies. The nPH85 distance quantifies the number of bipartitions that are not shared between the two trees. This is done by randomizing the tip labels for one of the trees, and calculating the PH85 for each replicate to generate a null distribution of the tree topology distance. The nPH85 metric ranges from 0, for identical trees, to 1 for trees that have no clades in common. We calculated nPH85 using the R package NELSI v0.2 (Ho et al., 2015) with 1,000 randomizations, which is shown to be robust even for very large trees (Geoghegan et al., 2017).

Gene Ontology Enrichment Analysis

A gene ontology (GO) enrichment analysis was done to investigate what functional traits were prevalent among the plasmids from each geographic region. To do this, all proteins encoded by the plasmid pangenome were annotated based on the terms from the GO database (Ashburner et al., 2000; The Gene Ontology Consortium, 2019) using InterProScan v5.44-79.0 (Jones et al., 2014; parameters: -goterms). Proteins from plasmids in each geographic region were tested for GO terms that were significantly enriched relative to the complete plasmid pangenome using WEGO v2.0 (Ye et al., 2018).

Screening for Antibiotic, Biocide and Metal Resistance Genes, and IS Elements

Antibiotic resistance genes were detected using ABRicate v0.8 (Seemann, 2018) using default parameters. To determine which ARGs were part of integron gene cassettes, IntegronFinder v1.5.1 (Cury et al., 2016) was used (parameters: -local_max -func_annot). We used CARD (Alcock et al., 2020) to confirm the class of antibiotic to which each gene conferred resistance. To screen for metal and biocide resistance genes, the complete manually-curated BactMet2 database (Pal et al., 2014) was used. All proteins were aligned against the BacMet2 database using DIAMOND v0.8.33.95 (Buchfink et al., 2015) with a cut-off alignment criteria of e-value 1×10^{-5}, 80% similarity, and 90% subject cover length (parameters: --evalue 0.00005 --id 80 --subject-cover 90 --max-target-seqs 1).

Sequence Data Availability

The complete sequences of the four novel plasmids described here are available in GenBank as accessions MT742180 – MT742183. The complete chromosome sequences of their respective hosts are also available in GenBank as accessions CP059078 – CP059081.

RESULTS AND DISCUSSION

Plasmid Family and Host Species

Using a combination of PacBio and Illumina sequencing, we generated complete assemblies of four novel mega-plasmids, all of which were recovered from *Acinetobacter* species. Each plasmid had a PacBio sequence coverage > 300x and an Illumina sequence coverage > 500x, except for pWM98B (46x Illumina coverage). Three of these (pR4WN-1BD1, pR4WN-12 CE1, and pR4WN-E10B) were isolated from the digestive tracts of wild-caught prawns and one (pWM98B) from an ICU patient. Another 17 related *Acinetobacter* plasmids were identified in the GenBank database, isolated from various locations across the world and were included in all subsequent analyses. The 21 mega-plasmids were ranged from 250 to 400 kb in size and were harbored by 11 different *Acinetobacter* species (see **Supplementary Table S1** for more detailed plasmid information and taxonomy of host bacteria).

We have identified four of the 21 plasmids (pXBB1-9, pAHTJR1, p34AB, and pOXA23_010062) to be part of the Rep-3 superfamily group, based on their replication initiation (Rep) protein. Intriguingly, no Rep protein could be identified in any of the other plasmids, suggesting that it is not needed for successful replication. Similarly, other *Acinetobacter* plasmids, notably pRAY-type plasmids, have no known Rep protein (Hamidian et al., 2012; Lean and Yeo, 2017). It has been proposed that these *rep*-lacking *Acinetobacter* plasmids may use their host machinery for DNA melting and primase activity during plasmid replication, as is the case in ColE1-type plasmids (Lean and Yeo, 2017). It is possible that these mega-plasmids have acquired this replication strategy and subsequently lost their *rep* gene.

Plasmid Pan- and Core-Genome Analyses

The plasmid pangenome, comprising 1,303 homologous gene clusters, was divided into four occupancy classes (see the section "Methods" for definitions), where the "core" and "soft core" classes make up the core-genome and the "shell"

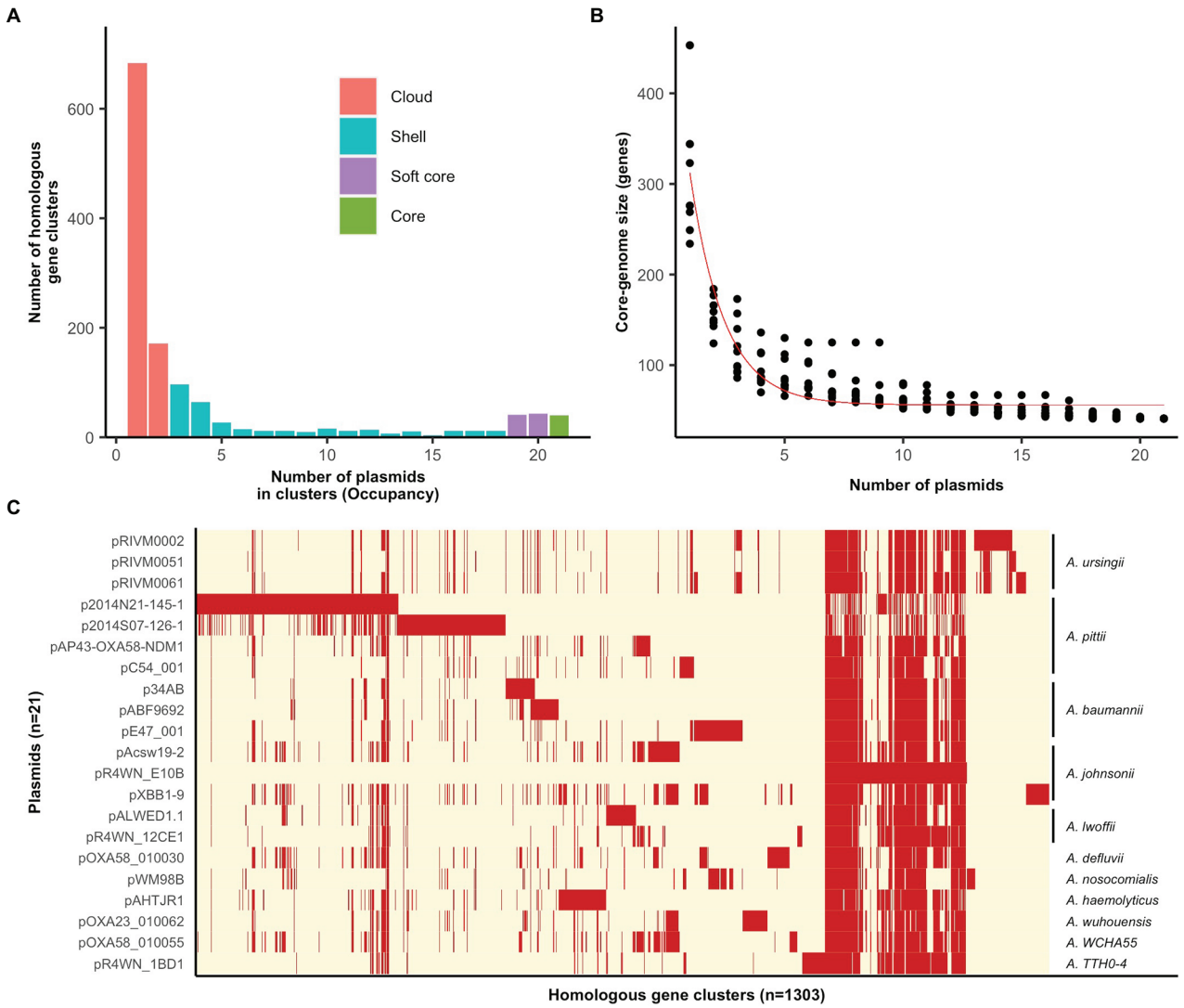

FIGURE 1 | Pan- and core-genomic analyses of the mega-plasmid family. **(A)** The plasmid pangenome can be divided into occupancy classes based on the number of plasmids contributing to each homologous gene cluster. The majority of genes belong to the accessory genome, constituting the cloud and shell classes. **(B)** The estimate of the coregenome size (genes) for this plasmid family was generated from 10 random samples of the 21 plasmids. The fitted curve follows the function proposed by Tettelin et al. (2005). **(C)** A pangenome matrix showing the presence (red) and absence (cream) of genes among the plasmids. The *Acinetobacter* species in which each plasmid was resident in are annotated on the right. Plasmids share a tight core-genome, yet, vary extensively in their accessory genomes.

and "cloud" classes make up the accessory genome (**Figure 1A**). The vast majority of genes carried by this plasmid family are accessory genes (**Figures 1A,C**), with a minimum set of 40 genes comprising the plasmid core-genome (**Figures 1B,C**). Individual plasmids carried 95–340 accessory genes each (**Supplementary Table S1**). It is thus evident that these mega-plasmids have the capacity to accumulate large and diverse sets of accessory genes that drives their diversification.

The plasmids consist of a number of core conserved genomic blocks separated by highly variable regions (**Figure 2A**). In particular, there are two "hotspots" of considerable genomic variability, labeled as "Hotspot 1" and "Hotspot 2" (**Figures 2A,B**). Hotspots 1 and 2 ranged from 7,000–140,000 bp and 15,000–90,000 bp in length, respectively. Alignments of the two hotspots showed a significant number of insertions, deletions, and large-scale rearrangements (**Figure 2B**; **Supplementary Figures S1**, **S2**). We speculate that these highly dynamic regions represent locations were genomic complexity can arise without interfering with core genes or regulatory networks. Interestingly, ARGs were overrepresented in Hotspot 2. This region, which on average constitutes less than 20% of each plasmid, contains greater than 65% of all ARGs (**Supplementary Figures S1**, **S2**).

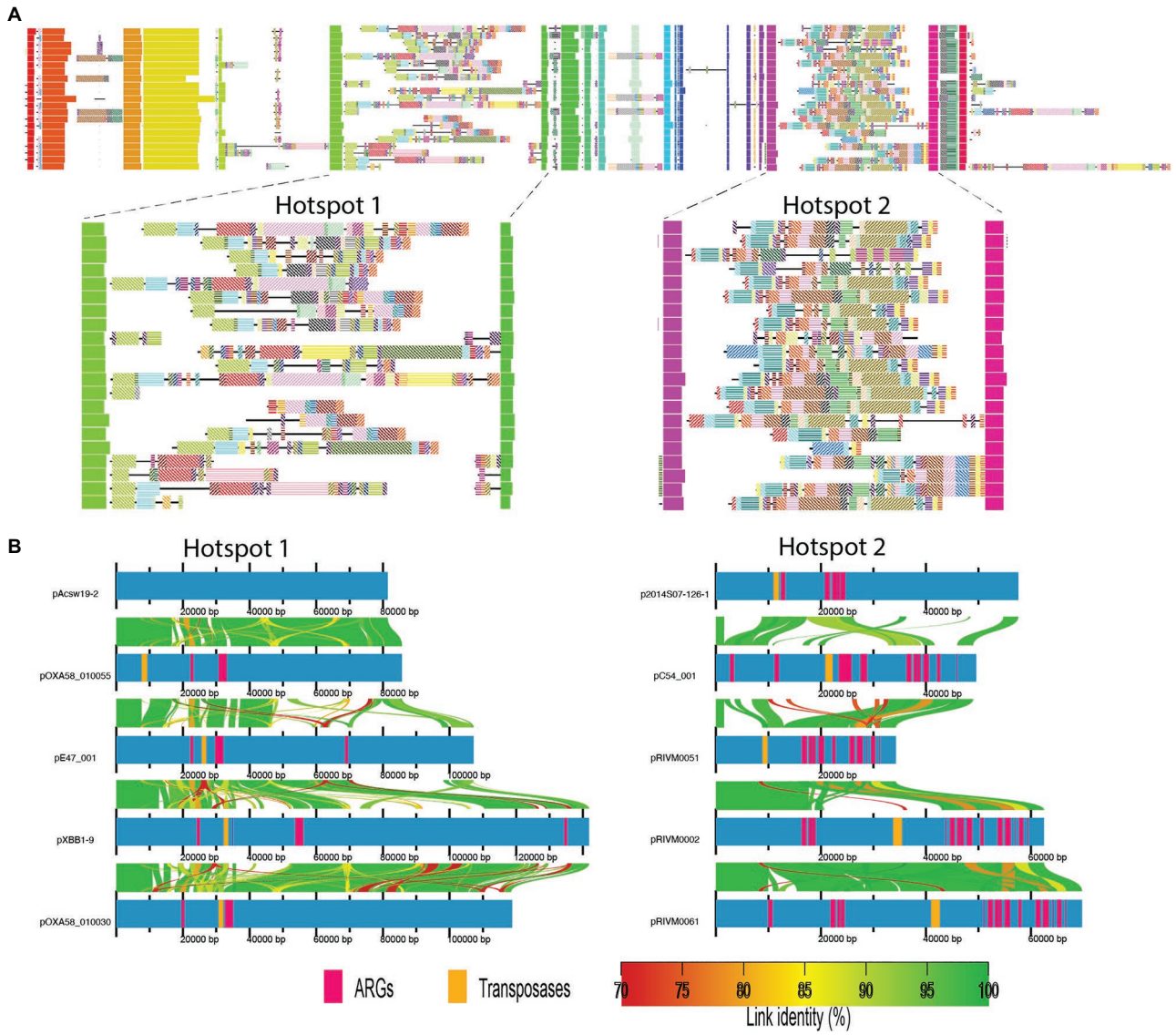

FIGURE 2 | Alignment of the mega-plasmid family. **(A)** A global alignment view of the complete plasmid sequences in this family. Each row represents a single plasmid. Core genomic blocks are visualized as vertically aligned solid rectangles that are colored according to their position in the genome. Non-core blocks are visualized as patterned rectangles. Sequences unique to a single plasmid are depicted as solid black lines. Note that, there are two "hotspots" of considerable genomic variability, labeled as "Hotspot 1" and "Hotspot2." **(B)** A local alignment view of each hotspot region from five example plasmids. Homologous regions are shown by links that are colored according to their percent nucleotide identity. Locations of antibiotic resistance genes (ARGs) and transposases are annotated on each plasmid. Interestingly, Hotspot 2, on average, constitutes less than 20% of each plasmid, yet contains greater than 65% of all ARGs among these plasmids. Note that, these hotspots have undergone a significant amount of insertions, deletions, and rearrangements. To view the alignments of all 21 plasmids for hotspots 1 and 2, see **Supplementary Figures S1, S2**, respectively.

Plasmid Phylogeny

The evolutionary relationship between plasmids was inferred from the plasmid core-genome using a maximum-likelihood method (**Figure 3**). In addition, plasmids were clustered based on the presence and absence of all 1,262 accessory genes, also using a maximum-likelihood method (**Figure 3**). Here, we show that plasmid phylogeny based on core genes does not cluster well according to geographic region. However, based on the presence and absence of all accessory genes, the plasmids do cluster according to their isolation location. Quantitative comparison between the two tree topologies was measured using an nPH85 metric (Geoghegan et al., 2017). The nPH85 metric ranges from 0, for identical trees, to 1, for trees that have no clade bipartitions in common. The accessory and core-genome tree comparison returned an nPH85 value of 0.84, indicating a high-level of incongruence.

Together, these data show that plasmids from the same geographic region are not necessarily evolutionarily closely

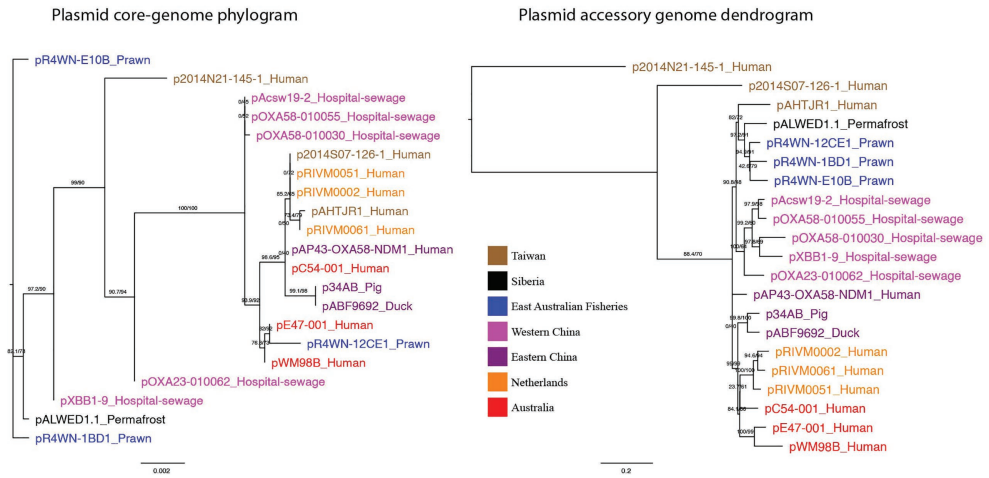

FIGURE 3 | Plasmid core-genome phylogram and accessory genome dendrogram. (left) A maximum-likelihood tree showing the inferred plasmid phylogeny based on the plasmid core-genome and (right) a maximum-likelihood tree based on the presence and absence of all 1,262 accessory genes in the plasmid pangenome. Branch labels signify SH-aLRT support (%)/bootstrap support (%). Plasmids are named in the format of "plasmid-ID"_"Isolation-source" and are colored based on the geographic region from which they were sampled. Together, the two trees show that plasmids from the same geographic region are not necessarily evolutionarily closely related, yet they exhibit a more similar accessory genome.

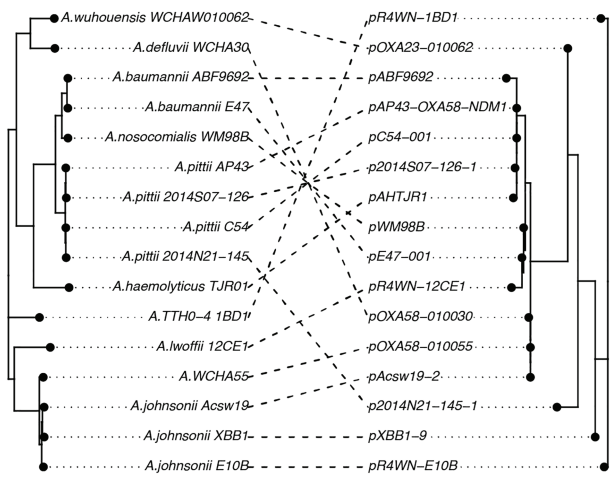

FIGURE 4 | A co-phylogeny linking the host strain (left) and plasmid (right) phylogenies. Connections link host strains with their resident plasmid. Nodes have been rotated to maximize congruency between the two trees. Host phylogeny was inferred from the host core genomes using a maximum-likelihood method. The inferred plasmid phylogeny was based on the plasmid core-genome also using a maximum-likelihood approach. The high level of incongruence between the phylogenies (nPH85 = 1.0) indicates that cross-species transmission is highly prevalent among this family of plasmids.

related, yet they exhibit a more similar accessory genome. This strongly indicates that (a) the plasmids can rapidly disseminate across the globe, given that closely related sister plasmids can be isolated from different parts of the world, and (b) these plasmids preferentially acquire their repertoire of accessory genes from their local environment.

In contrast, the pBT2436-like mega-plasmid family that is driving the dissemination of multi-drug resistance in *Pseudomonas* (Cazares et al., 2020), exhibit similar topologies in their core and accessory genome trees, both of which cluster according to geographic location. This suggests that the *Acinetobacter* mega-plasmids described here have a comparatively greater capacity for global transmission and local acquisition of accessory genes.

Further, we show that the topologies of plasmid and host phylogenetic trees are highly incongruent (nPH85 = 1.0; **Figure 4**). The host and plasmid phylogenies thus share no clade bipartitions in common. Such co-phylogenetic analyses can be used to distinguish between a history of host-plasmid co-divergence (co-phylogenetic congruence) and cross-species transmission (co-phylogenetic incongruence). Our findings provide evidence that cross-species horizontal transmission among *Acinetobacter* species is highly prevalent for this plasmid family.

Location-Specific Enrichment of Functional Traits

Since the accessory genomes of the plasmids cluster according to geographic region (**Figure 3**), we investigated whether there were any functional traits that were prevalent among the plasmids from each region. For this, we annotated proteins based on terms from the GO database. We found that plasmids from four of the seven regions had GO terms that were significantly enriched relative to the plasmid pangenome (Chi-squared tests, $p < 0.05$; **Figure 5**).

From these results, we can infer the broad-scale selection pressures within each region. For example, plasmids from Western China were largely enriched with genes involved in detoxification, metabolism, and cyclic compound binding (**Figure 5**). We speculate that these are traits that might be selected in environments of greater pollution. This is particularly significant

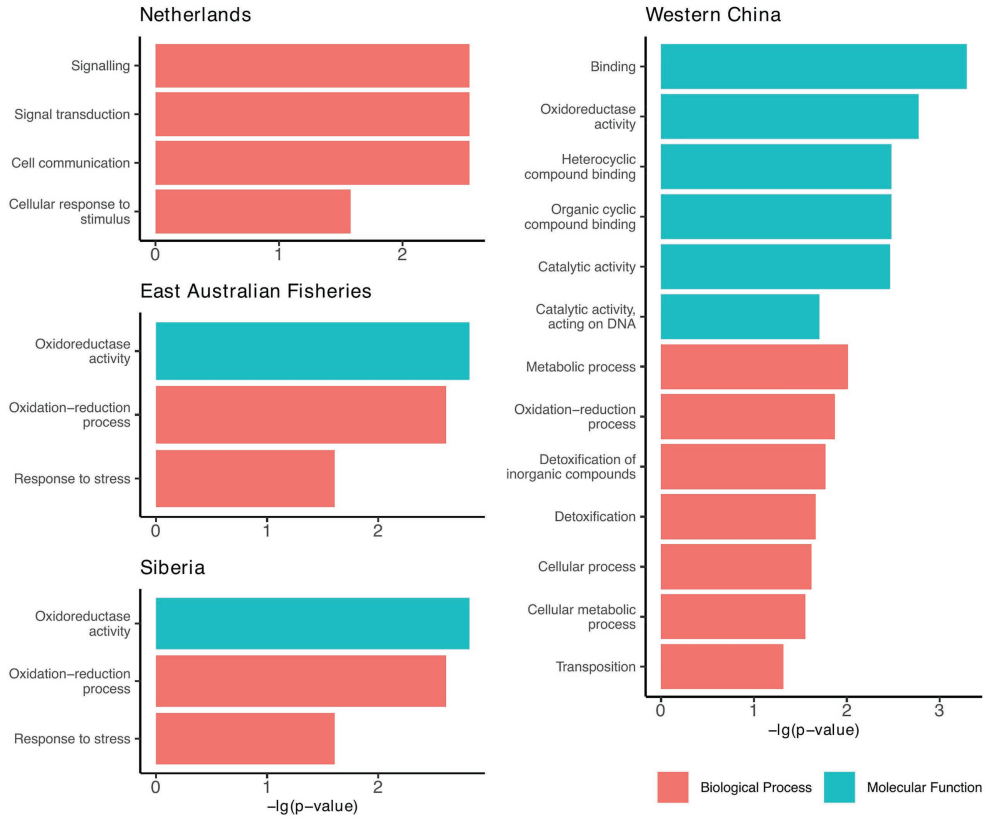

FIGURE 5 | Geographic regions that had plasmids enriched with functional traits relative to the plasmid pangenome. Functions are based on the gene ontology (GO) database and include only those that were significantly enriched compared to the plasmid pangenome (Chi-squared tests, $p < 0.05$).

as the Western China plasmids are polyphyletic (**Figure 3**), but they share common accessory traits, presumably a result of co-evolution by acquiring accessory genes from the local environment.

Genetic Cargo of Clinical Relevance

Collectively, the 21 plasmids carried 221 ARGs. All plasmids carried between 3 and 24 ARGs each, except for the plasmid isolated from Siberia (pALWED1.1), which only had one (tetracycline resistance). Together, the 221 genes encoded 35 different proteins known to confer resistance to 13 classes of antibiotics (**Figure 6**, full list of all ARGs in **Supplementary Table S2**). Of these, 31% (n = 67) were part of gene cassettes associated with class 1 integrons. In total, there were 20 class 1 integrons found in 14 of the plasmids. Consequently, class 1 integrons play a significant role in the accumulation of antibiotic resistance determinants in this plasmid family.

In particular, several of the class 1 integrons were associated with the same flanking miniature inverted-repeat transposable elements (MITEs; **Figure 7**). MITEs are non-autonomous mobile elements that transpose *via* molecular machinery provided *in trans* (Delihas, 2008). Fifteen of the 21 plasmids carried an identical pair of MITEs, each sharing the same insertion site (**Figure 7A**). Of these, 13 of the MITE pairs were flanking at least one class 1 integron carrying multiple ARG cassettes. Collectively, the MITEs were associated with 15 different ARGs, two virulence factors, and three biocide/metal resistance genes. There were eight unique MITE variants that we grouped into five different MITE "types" based on their cargo of resistance genes (**Figure 7B**). Interestingly, the same MITE type often occurred in multiple plasmid lineages and could also be present on plasmids from different geographic regions (**Figure 7B**). This suggests that the MITE-resistance region is highly dynamic and transmissible. Indeed, the same MITE-integron complex has also been detected within a clinical *A. baumannii* strain isolated from a human urine sample in Portugal (Domingues et al., 2011). The Portuguese MITE structure, however, was inserted into a different genomic context, further suggesting its high potential for transmission among *Acinetobacter* strains.

In addition, the plasmids carried 108 genes conferring resistance to bacterial biocides and heavy metals. Together, these genes confer resistance to six heavy metals (Hg, Cu, Au, Cr, Ni, and Co) and nine classes of biocides (acridines, azines, xanthenes, organosulfates, organomercury compounds, quaternary ammonium compounds, biguanides, diamindines, and paraquats). All of the detected metal/biocide resistance

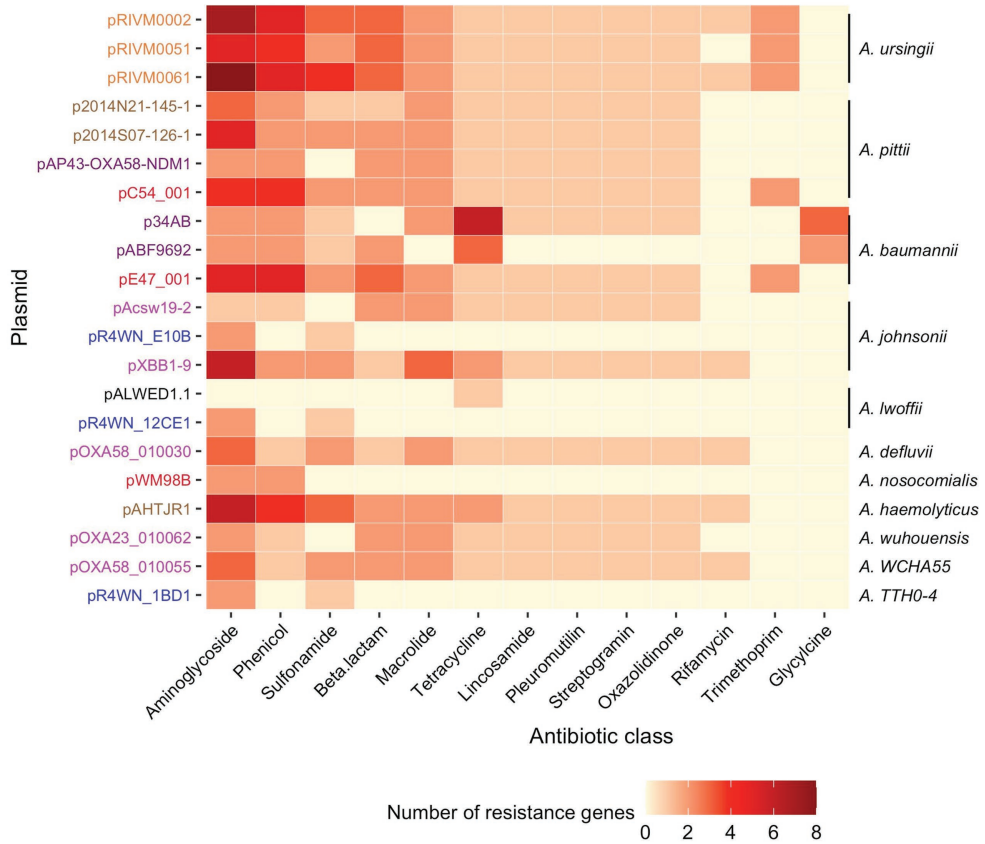

FIGURE 6 | Diversity and abundance of ARGs. The number of resistance genes (color scale bar) is shown for each plasmid (rows). Plasmid names are colored according to the geographic region from which they were sampled, as described in **Figure 3**. The *Acinetobacter* species in which each plasmid was resident in are annotated on the right. Resistance genes are grouped according to the class of antibiotic that they are known to confer resistance to.

genes are part of efflux systems. For a full list of all biocide and metal resistance genes, see **Supplementary Table S3**.

CONCLUSION

The *Acinetobacter* mega-plasmids characterized here appear to be highly proficient in acquiring niche-adaptive accessory genes. Thus, the significant collection of ARGs observed within many of these is likely a selective response to exposure to one or more antibiotics. This is of serious concern, as global antibiotic usage continues to increase, particularly for antibiotics of "last-resort" (Klein et al., 2018). As an often-overlooked consequence of this, antibiotics are polluting the environment, radiating from areas of human populations and agricultural areas (Kümmerer, 2001; Campagnolo et al., 2002). Indeed, environmental concentrations of antibiotics are now often observed within the range of biological and evolutionary significance (Chow et al., 2021). Such intense and ubiquitous antibiotic selection surrounding dense human populations is likely driving the accumulation of diverse ARGs by these plasmids across the globe. Further, it is likely that each plasmid can accrue different suites of resistance genes, reflecting the specific conditions and selection pressures in their particular local environment. Thus, our findings highlight this plasmid family as a serious threat to successful bacterial infection control and human health, particularly for nosocomial infections. These findings also add to the growing concern that mega-plasmids are key disseminators of antibiotic resistance and require wide-spread surveillance (Cazares et al., 2020).

We have characterized a family of multi-drug resistance *Acinetobacter* mega-plasmids. We present evidence that these plasmids are highly transmissible, have the capacity for dispersing at a global-scale, can accumulate a vast cargo of niche-adaptive accessory genes, and can confer multi-drug resistance phenotypes of significant concern for human health. These findings add to a growing idea in the literature that points to the importance of viewing the antibiotic resistance crisis from a mobile element-centred outlook as opposed to a host cell-centric point of view (Lopatkin et al., 2017; Stevenson et al., 2017; Ghaly and Gillings, 2018; Pinilla-Redondo et al., 2018). Thus, expanding our therapeutic focus to consider ways of interfering with the transmission of mobile DNAs may

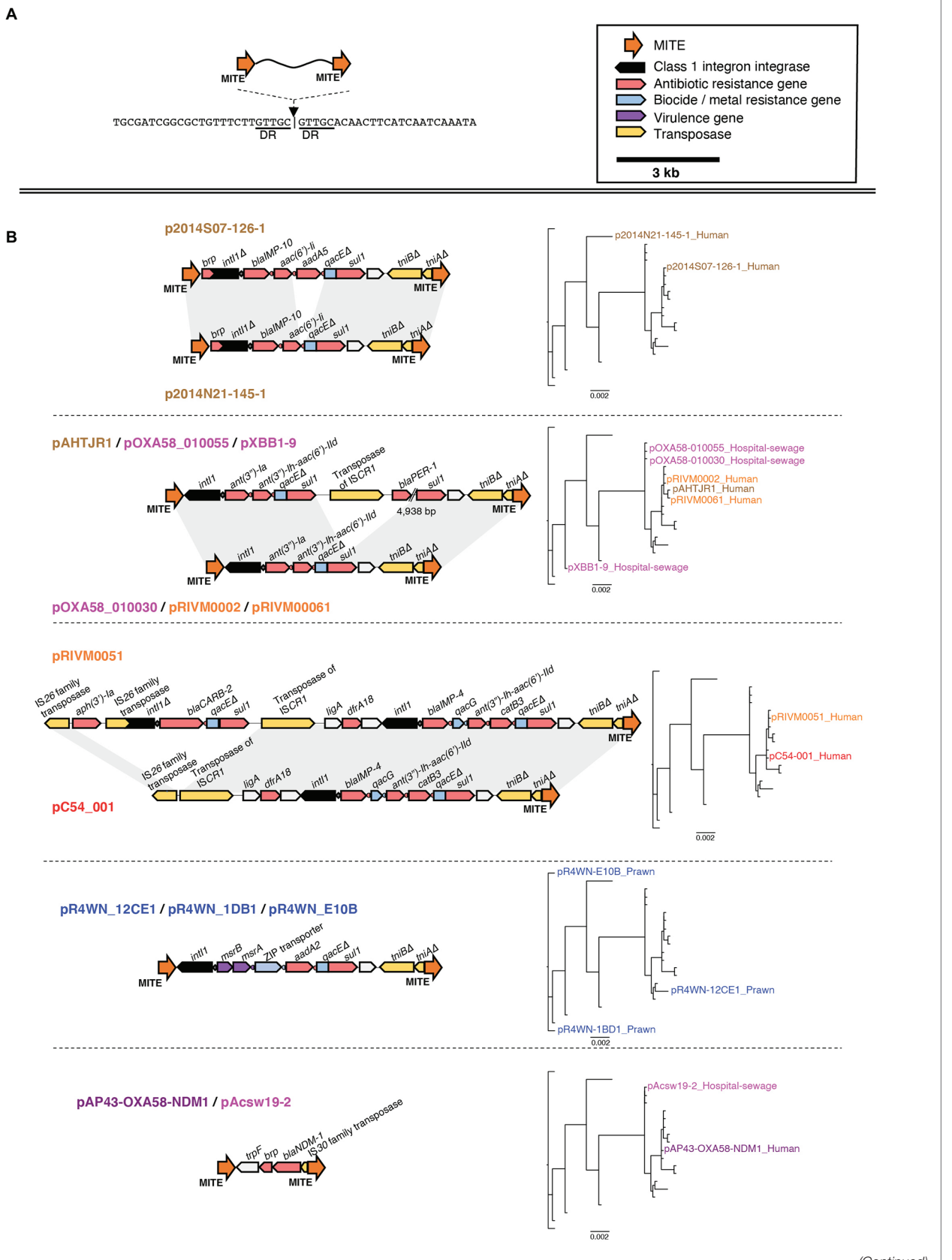
A
MITE
MITE
TGCGATCGGCGCTGTTTCTTGTTGC GTTGCACAACTTCATCAATCAAATA
DR DR
MITE
Class 1 integron integrase
Antibiotic resistance gene
Biocide / metal resistance gene
Virulence gene
Transposase
3 kb
B
p2014S07-126-1
brp intI1Δ blaIMP-10 aac(6')-Ii aadA5 qacEΔ sul1 tniBΔ tniAΔ
MITE
MITE
p2014N21-145-1
p2014N21-145-1_Human
p2014S07-126-1_Human
0.002
pAHTJR1 / pOXA58_010055 / pXBB1-9
intI1 ant(3'')-Ia ant(3'')-Ih-aac(6')-Ild qacEΔ sul1 Transposase of ISCR1 blaPER-1 sul1 tniBΔ tniAΔ
4,938 bp
MITE
MITE
pOXA58-010055_Hospital-sewage
pOXA58-010030_Hospital-sewage
pRIVM0002_Human
pAHTJR1_Human
pRIVM0061_Human
pXBB1-9_Hospital-sewage
0.002
pOXA58_010030 / pRIVM0002 / pRIVM00061
pRIVM0051
IS26 family transposase aph(3')-Ia IS26 family transposase intI1Δ blaCARB-2 qacEΔ sul1 Transposase of ISCR1 ligA dfrA18 intI1 blaIMP-4 qacG ant(3'')-Ih-aac(6')-Ild catB3 qacEΔ sul1 tniBΔ tniAΔ
MITE
pC54_001
IS26 family transposase Transposase of ISCR1 ligA dfrA18 intI1 blaIMP-4 qacG ant(3'')-Ih-aac(6')-Ild catB3 qacEΔ sul1 tniBΔ tniAΔ
MITE
pRIVM0051_Human
pC54-001_Human
0.002
pR4WN_12CE1 / pR4WN_1DB1 / pR4WN_E10B
intI1 msrB msrA ZIP transporter aacA2 qacEΔ sul1 tniBΔ tniAΔ
MITE
MITE
pR4WN-E10B_Prawn
pR4WN-12CE1_Prawn
pR4WN-1BD1_Prawn
0.002
pAP43-OXA58-NDM1 / pAcsw19-2
trpF brp blaNDM-1 IS30 family transposase
MITE
MITE
pAcsw19-2_Hospital-sewage
pAP43-OXA58-NDM1_Human
0.002

(Continued)

FIGURE 7 | Genetic map of the miniature inverted-repeated transposable element (MITE)-integron complex present among 15 of the 21 plasmids. The insertion site of the MITEs is shown in **(A)**. The structure of each MITE variant is shown in **(B)** and is grouped according to MITE "type." The plasmids that carry each MITE variant are listed above/below each genetic map. Plasmid names are colored according to the geographic region from which they were sampled, as described in **Figure 3**. Directional blocks represent genes, while orange arrows represent MITEs as annotated in the top right corner of the figure. All maps are drawn to scale. To the right of each MITE type is the inferred plasmid core-genome phylogeny, highlighting each plasmid that carries the corresponding MITE type. Note that, the same MITE type often occurred in multiple plasmid lineages and could also be present on plasmids from different geographic regions. This suggests that this MITE-resistance region is highly dynamic and transmissible.

be provide an additional, fruitful means of combating the spread of antibiotic resistance (Ghaly and Gillings, 2018).

DATA AVAILABILITY STATEMENT

The datasets presented in this study can be found in online repositories. The names of the repository/repositories and accession number(s) can be found in the article/**Supplementary Material**.

AUTHOR CONTRIBUTIONS

TG contributed to sample processing and collection, contributed to the conception and design of analyses, performed the analyses, wrote the original draft of manuscript, and contributed to the final editing of manuscript. IP contributed to the conception and design of analyses and contributed to the final editing of manuscript. AS contributed to sample processing and collection and contributed to the final editing of manuscript. ST contributed to the conception and design of analyses and contributed to the final editing of manuscript. MG contributed to sample processing and collection, contributed to the conception and design of analyses, performed funding acquisition, and contributed to the final editing of manuscript. All authors contributed to the article and approved the submitted version.

FUNDING

This work was funded by Australian Research Council Discovery Grants DP0877196 and DP130103839.

ACKNOWLEDGMENTS

We thank Jon Iredell for the *Acinetobacter nosocomialis* WM98B isolate. TG would like to thank Mary and Saoirse Ghaly for loving support.

SUPPLEMENTARY MATERIAL

The Supplementary Material for this article can be found online at: https://www.frontiersin.org/articles/10.3389/fmicb.2020.605952/full#supplementary-material

REFERENCES

Albarracín, V. H., Pathak, G. P., Douki, T., Cadet, J., Borsarelli, C. D., Gärtner, W., et al. (2012). Extremophilic *Acinetobacter* strains from high-altitude lakes in Argentinean Puna: remarkable UV-B resistance and efficient DNA damage repair. *Orig. Life Evol. Biosph.* 42, 201–221. doi: 10.1007/s11084-012-9276-3

Alcock, B. P., Raphenya, A. R., Lau, T. T., Tsang, K. K., Bouchard, M., Edalatmand, A., et al. (2020). CARD 2020: antibiotic resistome surveillance with the comprehensive antibiotic resistance database. *Nucleic Acids Res.* 48, D517–D525. doi: 10.1093/nar/gkz935

Almasaudi, S. B. (2018). *Acinetobacter* spp. as nosocomial pathogens: epidemiology and resistance features. *Saudi J. Biol. Sci.* 25, 586–596. doi: 10.1016/j.sjbs.2016.02.009

Ankenbrand, M. J., Hohlfeld, S., Hackl, T., and Förster, F. (2017). AliTV—interactive visualization of whole genome comparisons. *PeerJ Comput. Sci.* 3:e116. doi: 10.7717/peerj-cs.116

Antunes, L., Visca, P., and Towner, K. J. (2014). *Acinetobacter baumannii*: evolution of a global pathogen. *Pathog. Dis.* 71, 292–301. doi: 10.1111/2049-632X.12125

Arredondo-Alonso, S., Willems, R. J., van Schaik, W., and Schürch, A. C. (2017). On the (im)possibility of reconstructing plasmids from whole-genome short-read sequencing data. *Microb Genom.* 3:e000128. doi: 10.1099/mgen.0.000128

Ashburner, M., Ball, C. A., Blake, J. A., Botstein, D., Butler, H., Cherry, J. M., et al. (2000). Gene ontology: tool for the unification of biology. *Nat. Genet.* 25, 25–29. doi: 10.1038/75556

Babakhani, S., and Oloomi, M. (2018). Transposons: the agents of antibiotic resistance in bacteria. *J. Basic Microbiol.* 58, 905–917. doi: 10.1002/jobm.201800204

Bach, H., and Gutnick, D. L. (2006). Novel polysaccharide—protein-based amphipathic formulations. *Appl. Microbiol. Biotechnol.* 71, 34–38. doi: 10.1007/s00253-005-0149-9

Beaber, J. W., Hochhut, B., and Waldor, M. K. (2004). SOS response promotes horizontal dissemination of antibiotic resistance genes. *Nature* 427, 72–74. doi: 10.1038/nature02241

Botelho, J., Lood, C., Partridge, S. R., van Noort, V., Lavigne, R., Grosso, F., et al. (2019). Combining sequencing approaches to fully resolve a carbapenemase-encoding megaplasmid in a *Pseudomonas shirazica* clinical strain. *Emerg. Microbes Infect.* 8, 1186–1194. doi: 10.1080/22221751.2019.1648182

Buchfink, B., Xie, C., and Huson, D. H. (2015). Fast and sensitive protein alignment using DIAMOND. *Nat. Methods* 12, 59–60. doi: 10.1038/nmeth.3176

Campagnolo, E. R., Johnson, K. R., Karpati, A., Rubin, C. S., Kolpin, D. W., Meyer, M. T., et al. (2002). Antimicrobial residues in animal waste and water resources proximal to large-scale swine and poultry feeding operations. *Sci. Total Environ.* 299, 89–95. doi: 10.1016/s0048-9697(02)00233-4

Castro-Jaimes, S., Bello-López, E., Velázquez-Acosta, C., Volkow-Fernández, P., Lozano-Zarain, P., Castillo Ramírez, S., et al. (2020). Chromosome architecture and gene content of the emergent pathogen *Acinetobacter haemolyticus*. *Front. Microbiol.* 11:926. doi: 10.3389/fmicb.2020.00926

Cazares, A., Moore, M. P., Hall, J. P., Wright, L. L., Grimes, M., Emond-Rhéault, J. -G., et al. (2020). A megaplasmid family driving dissemination of multidrug resistance in *Pseudomonas*. *Nat. Commun.* 11:1370. doi: 10.1038/s41467-020-15081-7

Cerezales, M., Xanthopoulou, K., Wille, J., Krut, O., Seifert, H., Gallego, L., et al. (2020). Mobile genetic elements harboring antibiotic resistance determinants in *Acinetobacter baumannii* isolates from Bolivia. *Front. Microbiol.* 11:919. doi: 10.3389/fmicb.2020.00919

Chow, L. K., Ghaly, T. M., and Gillings, M. R. (2021). A survey of sub-inhibitory concentrations of antibiotics in the environment. *J. Environ. Sci.* 99, 21–27. doi: 10.1016/j.jes.2020.05.030

Chusri, S., Chongsuvivatwong, V., Rivera, J. I., Silpapojakul, K., Singkhamanan, K., McNeil, E., et al. (2014). Clinical outcomes of hospital-acquired infection with *Acinetobacter nosocomialis* and *Acinetobacter pittii*. *Antimicrob. Agents Chemother.* 58, 4172–4179. doi: 10.1128/AAC.02992-14

Contreras-Moreira, B., and Vinuesa, P. (2013). GET_HOMOLOGUES, a versatile software package for scalable and robust microbial pangenome analysis. *Appl. Environ. Microbiol.* 79, 7696–7701. doi: 10.1128/AEM.02411-13

Cury, J., Jové, T., Touchon, M., Néron, B., and Rocha, E. P. (2016). Identification and analysis of integrons and cassette arrays in bacterial genomes. *Nucleic Acids Res.* 44, 4539–4550. doi: 10.1093/nar/gkw319

Delihas, N. (2008). Small mobile sequences in bacteria display diverse structure/function motifs. *Mol. Microbiol.* 67, 475–481. doi: 10.1111/j.1365-2958.2007.06068.x

Domingues, S., Nielsen, K. M., and da Silva, G. J. (2011). The blaIMP-5-carrying integron in a clinical *Acinetobacter baumannii* strain is flanked by miniature inverted-repeat transposable elements (MITEs). *J. Antimicrob. Chemother.* 66, 2667–2668. doi: 10.1093/jac/dkr327

Fondi, M., Bacci, G., Brilli, M., Papaleo, M. C., Mengoni, A., Vaneechoutte, M., et al. (2010). Exploring the evolutionary dynamics of plasmids: the *Acinetobacter* pan-plasmidome. *BMC Evol. Biol.* 10:59. doi: 10.1186/1471-2148-10-59

Fournier, P. -E., Vallenet, D., Barbe, V., Audic, S., Ogata, H., Poirel, L., et al. (2006). Comparative genomics of multidrug resistance in *Acinetobacter baumannii*. *PLoS Genet.* 2:e7. doi: 10.1371/journal.pgen.0020007

Garcia-Garcera, M., Touchon, M., Brisse, S., and Rocha, E. P. (2017). Metagenomic assessment of the interplay between the environment and the genetic diversification of *Acinetobacter*. *Environ. Microbiol.* 19, 5010–5024. doi: 10.1111/1462-2920.13949

Geoghegan, J. L., Duchêne, S., and Holmes, E. C. (2017). Comparative analysis estimates the relative frequencies of co-divergence and cross-species transmission within viral families. *PLoS Pathog.* 13:e1006215. doi: 10.1371/journal.ppat.1006215

Ghaly, T. M., Chow, L., Asher, A. J., Waldron, L. S., and Gillings, M. R. (2017). Evolution of class 1 integrons: mobilization and dispersal via food-borne bacteria. *PLoS One* 12:e0179169. doi: 10.1371/journal.pone.0179169

Ghaly, T. M., Geoghegan, J. L., Tetu, S. G., and Gillings, M. R. (2020). The peril and promise of integrons: beyond antibiotic resistance. *Trends Microbiol.* 28, 455–464. doi: 10.1016/j.tim.2019.12.002

Ghaly, T. M., and Gillings, M. R. (2018). Mobile DNAs as ecologically and evolutionarily independent units of life. *Trends Microbiol.* 26, 904–912. doi: 10.1016/j.tim.2018.05.008

Gillings, M. R. (2017). Class 1 integrons as invasive species. *Curr. Opin. Microbiol.* 38, 10–15. doi: 10.1016/j.mib.2017.03.002

Gillings, M. R., Labbate, M., Sajjad, A., Giguère, N. J., Holley, M. P., and Stokes, H. (2009). Mobilization of a Tn*402*-like class 1 integron with a novel cassette array via flanking miniature inverted-repeat transposable element-like structures. *Appl. Environ. Microbiol.* 75, 6002–6004. doi: 10.1128/AEM.01033-09

Gillings, M. R., and Stokes, H. (2012). Are humans increasing bacterial evolvability? Trends Ecol. *Evolution* 27, 346–352. doi: 10.1016/j.tree.2012.02.006

Gillings, M., Westoby, M., and Ghaly, T. (2018). Pollutants that replicate: xenogenetic DNAs. *Trends Microbiol.* 26, 975–977. doi: 10.1016/j.tim.2018.08.003

Göttig, S., Gruber, T. M., Higgins, P. G., Wachsmuth, M., Seifert, H., and Kempf, V. A. (2014). Detection of pan drug-resistant *Acinetobacter baumannii* in Germany. *J. Antimicrob. Chemother.* 69, 2578–2579. doi: 10.1093/jac/dku170

Hamidian, M., Ambrose, S. J., and Hall, R. M. (2016). A large conjugative *Acinetobacter baumannii* plasmid carrying the *sul2* sulphonamide and *strAB* streptomycin resistance genes. *Plasmid* 87, 43–50. doi: 10.1016/j.plasmid.2016.09.001

Hamidian, M., Holt, K. E., Pickard, D., Dougan, G., and Hall, R. M. (2014). A GC1 *Acinetobacter baumannii* isolate carrying AbaR3 and the aminoglycoside resistance transposon TnaphA6 in a conjugative plasmid. *J. Antimicrob. Chemother.* 69, 955–958. doi: 10.1093/jac/dkt454

Hamidian, M., Nigro, S. J., and Hall, R. M. (2012). Variants of the gentamicin and tobramycin resistance plasmid pRAY are widely distributed in *Acinetobacter*. *J. Antimicrob. Chemother.* 67, 2833–2836. doi: 10.1093/jac/dks318

Hawkey, P. M., and Munday, C. J. (2004). Multiple resistance in gram-negative bacteria. *Rev. Med. Microbiol.* 15, 51–61. doi: 10.1097/01.revmedmi.00001 31427.13353.7f

Ho, S. Y., Duchêne, S., and Duchêne, D. (2015). Simulating and detecting autocorrelation of molecular evolutionary rates among lineages. *Mol. Ecol. Resour.* 15, 688–696. doi: 10.1111/1755-0998.12320

Hoang, D. T., Chernomor, O., von Haeseler, A., Minh, B. Q., and Vinh, L. S. (2018). UFBoot2: improving the ultrafast bootstrap approximation. *Mol. Biol. Evol.* 35, 518–522. doi: 10.1093/molbev/msx281

Hunt, M., De Silva, N., Otto, T. D., Parkhill, J., Keane, J. A., and Harris, S. R. (2015). Circlator: automated circularization of genome assemblies using long sequencing reads. *Genome Biol.* 16:294. doi: 10.1186/s13059-015-0849-0

Jones, P., Binns, D., Chang, H. -Y., Fraser, M., Li, W., McAnulla, C., et al. (2014). InterProScan 5: genome-scale protein function classification. *Bioinformatics* 30, 1236–1240. doi: 10.1093/bioinformatics/btu031

Kaas, R. S., Friis, C., Ussery, D. W., and Aarestrup, F. M. (2012). Estimating variation within the genes and inferring the phylogeny of 186 sequenced diverse *Escherichia coli* genomes. *BMC Genomics* 13:577. doi: 10.1186/1471-2164-13-577

Kalyaanamoorthy, S., Minh, B. Q., Wong, T. K., von Haeseler, A., and Jermiin, L. S. (2017). ModelFinder: fast model selection for accurate phylogenetic estimates. *Nat. Methods* 14, 587–589. doi: 10.1038/nmeth.4285

Katoh, K., and Standley, D. M. (2013). MAFFT multiple sequence alignment software version 7: improvements in performance and usability. *Mol. Biol. Evol.* 30, 772–780. doi: 10.1093/molbev/mst010

Klein, E. Y., van Boeckel, T. P., Martinez, E. M., Pant, S., Gandra, S., Levin, S. A., et al. (2018). Global increase and geographic convergence in antibiotic consumption between 2000 and 2015. *Proc. Natl. Acad. Sci.* 115, E3463–E3470. doi: 10.1073/pnas.1717295115

Kolmogorov, M., Yuan, J., Lin, Y., and Pevzner, P. A. (2019). Assembly of long, error-prone reads using repeat graphs. *Nat. Biotechnol.* 37, 540–546. doi: 10.1038/s41587-019-0072-8

Kristensen, D. M., Kannan, L., Coleman, M. K., Wolf, Y. I., Sorokin, A., Koonin, E. V., et al. (2010). A low-polynomial algorithm for assembling clusters of orthologous groups from intergenomic symmetric best matches. *Bioinformatics* 26, 1481–1487. doi: 10.1093/bioinformatics/btq229

Kümmerer, K. (2001). Drugs in the environment: emission of drugs, diagnostic aids and disinfectants into wastewater by hospitals in relation to other sources—a review. *Chemosphere* 45, 957–969. doi: 10.1016/S0045-6535(01)00144-8

Lean, S. S., and Yeo, C. C. (2017). Small, enigmatic plasmids of the nosocomial pathogen, *Acinetobacter baumannii*: good, bad, who knows? *Front. Microbiol.* 8:1547. doi: 10.3389/fmicb.2017.01547

Li, H. (2018). Minimap2: pairwise alignment for nucleotide sequences. *Bioinformatics* 34, 3094–3100. doi: 10.1093/bioinformatics/bty191

Li, H., and Durbin, R. (2009). Fast and accurate short read alignment with burrows-wheeler transform. *Bioinformatics* 25, 1754–1760. doi: 10.1093/bioinformatics/btp324

Li, L., Stoeckert, C. J., and Roos, D. S. (2003). OrthoMCL: identification of ortholog groups for eukaryotic genomes. *Genome Res.* 13, 2178–2189. doi: 10.1101/gr.1224503

Lopatkin, A. J., Meredith, H. R., Srimani, J. K., Pfeiffer, C., Durrett, R., and You, L. (2017). Persistence and reversal of plasmid-mediated antibiotic resistance. *Nat. Commun.* 8:1689. doi: 10.1038/s41467-017-01532-1

Madden, T. (2013). "The BLAST sequence analysis tool" in *The NCBI handbook [internet]. 2nd Edn.* eds. J. Beck, D. Benson, J. Coleman, M. Hoeppner, M. Johnson, and D. Maglott, et al. (Bethesda, MD, USA: National Center for Biotechnology Information (US)).

Merino, M., Acosta, J., Poza, M., Sanz, F., Beceiro, A., Chaves, F., et al. (2010). OXA-24 carbapenemase gene flanked by XerC/XerD-like recombination sites in different plasmids from different *Acinetobacter* species isolated during a nosocomial outbreak. *Antimicrob. Agents Chemother.* 54, 2724–2727. doi: 10.1128/AAC.01674-09

Nguyen, L. -T., Schmidt, H. A., von Haeseler, A., and Minh, B. Q. (2015). IQ-TREE: a fast and effective stochastic algorithm for estimating maximum-likelihood phylogenies. *Mol. Biol. Evol.* 32, 268–274. doi: 10.1093/molbev/msu300

Nigro, S. J., and Hall, R. M. (2017). A large plasmid, pD46-4, carrying a complex resistance region in an extensively antibiotic-resistant ST25

Acinetobacter baumannii. *J. Antimicrob. Chemother.* 72, 3496–3498. doi: 10.1093/jac/dkx287

Pal, C., Bengtsson-Palme, J., Rensing, C., Kristiansson, E., and Larsson, D. J. (2014). BacMet: antibacterial biocide and metal resistance genes database. *Nucleic Acids Res.* 42, D737–D743. doi: 10.1093/nar/gkt1252

Pesesky, M. W., Tilley, R., and Beck, D. A. (2019). Mosaic plasmids are abundant and unevenly distributed across prokaryotic taxa. *Plasmid* 102, 10–18. doi: 10.1016/j.plasmid.2019.02.003

Pinilla-Redondo, R., Cyriaque, V., Jacquiod, S., Sørensen, S. J., and Riber, L. (2018). Monitoring plasmid-mediated horizontal gene transfer in microbiomes: recent advances and future perspectives. *Plasmid* 99, 56–67. doi: 10.1016/j.plasmid.2018.08.002

Quinlan, A. R., and Hall, I. M. (2010). BEDTools: a flexible suite of utilities for comparing genomic features. *Bioinformatics* 26, 841–842. doi: 10.1093/bioinformatics/btq033

Rambaut, A. (2017). FigTree-version 1.4.3, a graphical viewer of phylogenetic trees. Available at: http://tree.bio.ed.ac.uk/software/figtree (Accessed October 5, 2016).

Revell, L. J. (2012). Phytools: an R package for phylogenetic comparative biology (and other things). *Methods Ecol. Evol.* 3, 217–223. doi: 10.1111/j.2041-210x.2011.00169.x

Rivera-Izquierdo, M., Valero-Ubierna, C., and Masso-Guijarro, P. (2020). Nosocomial bacteraemia caused by *Acinetobacter ursingii* in neonatology critical care unit in Spain: a rising challenge. *Pediatr. Infect. Dis. J.* 39, e28–e29. doi: 10.1097/INF.0000000000002562

Sajjad, A., Holley, M. P., Labbate, M., Stokes, H., and Gillings, M. R. (2011). Preclinical class 1 integron with a complete Tn402-like transposition module. *Appl. Environ. Microbiol.* 77, 335–337. doi: 10.1128/AEM.02142-10

Salgado-Camargo, A. D., Castro-Jaimes, S., Gutierrez-Rios, R. -M., Lozano, L. F., Altamirano-Pacheco, L., Silva-Sanchez, J., et al. (2020). Structure and evolution of *Acinetobacter baumannii* plasmids. *Front. Microbiol.* 11:1283. doi: 10.3389/fmicb.2020.01283

Salto, I. P., Tejerizo, G. T., Wibberg, D., Pühler, A., Schlüter, A., and Pistorio, M. (2018). Comparative genomic analysis of *Acinetobacter* spp. plasmids originating from clinical settings and environmental habitats. *Sci. Rep.* 8:7783. doi: 10.1038/s41598-018-26180-3

Sambrook, J., and Russell, D. W. (2006). Purification of nucleic acids by extraction with phenol:chloroform. *Cold Spring Harb Protoc.* 2006:pdb.prot4455. doi: 10.1101/pdb.prot4455

Schreiber, F., Szekat, C., Josten, M., Sahl, H. -G., and Bierbaum, G. (2013). Antibiotic-induced autoactivation of IS*256* in *Staphylococcus aureus*. *Antimicrob. Agents Chemother.* 57, 6381–6384. doi: 10.1128/AAC.01585-13

Seemann, T. (2018). ABRicate: mass screening of contigs for antimicrobial and virulence genes. Department of Microbiology and Immunology, The University of Melbourne, Melbourne, Australia. Available at: https://github.com/tseemann/abricate (Accessed October 5, 2016).

Stevenson, C., Hall, J. P. J., Harrison, E., Wood, A., and Brockhurst, M. A. (2017). Gene mobility promotes the spread of resistance in bacterial populations. *ISME J.* 11, 1930–1932. doi: 10.1038/ismej.2017.42

Stokes, H. W., and Gillings, M. R. (2011). Gene flow, mobile genetic elements and the recruitment of antibiotic resistance genes into gram-negative pathogens. *FEMS Microbiol. Rev.* 35, 790–819. doi: 10.1111/j.1574-6976.2011.00273.x

Sullivan, M. J., and van Bakel, H. (2019). Chromatiblock: scalable whole-genome visualization of structural differences in prokaryotes. bioRxiv [Preprint]. doi: 10.1101/800920

Tettelin, H., Masignani, V., Cieslewicz, M. J., Donati, C., Medini, D., Ward, N. L., et al. (2005). Genome analysis of multiple pathogenic isolates of *Streptococcus agalactiae*: implications for the microbial "pan-genome." *Proc. Natl. Acad. Sci.* 102, 13950–13955. doi: 10.1073/pnas.0506758102

The Gene Ontology Consortium (2019). The gene ontology resource: 20 years and still GOing strong. *Nucleic Acids Res.* 47, D330–D338. doi: 10.1093/nar/gky1055

Valenzuela, J. K., Thomas, L., Partridge, S. R., Van Der Reijden, T., Dijkshoorn, L., and Iredell, J. (2007). Horizontal gene transfer in a polyclonal outbreak of carbapenem-resistant *Acinetobacter baumannii*. *J. Clin. Microbiol.* 45, 453–460. doi: 10.1128/JCM.01971-06

Vinuesa, P., and Contreras-Moreira, B. (2015). "Robust identification of orthologues and paralogues for microbial pan-genomics using GET_HOMOLOGUES: a case study of pIncA/C plasmids" in *Bacterial pangenomics: Methods and protocols (methods in molecular biology)*. eds. A. Mengoni, M. Galardini and M. Fondi (New York, USA: Springer Nature), 203–232.

Vinuesa, P., Ochoa-Sánchez, L. E., and Contreras-Moreira, B. (2018). GET_PHYLOMARKERS, a software package to select optimal orthologous clusters for phylogenomics and inferring pan-genome phylogenies, used for a critical geno-taxonomic revision of the genus *Stenotrophomonas*. *Front. Microbiol.* 9:771. doi: 10.3389/fmicb.2018.00771

Walker, B. J., Abeel, T., Shea, T., Priest, M., Abouelliel, A., Sakthikumar, S., et al. (2014). Pilon: an integrated tool for comprehensive microbial variant detection and genome assembly improvement. *PLoS One* 9:e112963. doi: 10.1371/journal.pone.0112963

Weber, B. S., Harding, C. M., and Feldman, M. F. (2016). Pathogenic *Acinetobacter*: from the cell surface to infinity and beyond. *J. Bacteriol.* 198, 880–887. doi: 10.1128/JB.00906-15

Wolf, Y. I., Makarova, K. S., Yutin, N., and Koonin, E. V. (2012). Updated clusters of orthologous genes for Archaea: a complex ancestor of the Archaea and the byways of horizontal gene transfer. *Biol. Direct* 7:46. doi: 10.1186/1745-6150-7-46

Wood, D. E., and Salzberg, S. L. (2014). Kraken: ultrafast metagenomic sequence classification using exact alignments. *Genome Biol.* 15:R46. doi: 10.1186/gb-2014-15-3-r46

Ye, J., Zhang, Y., Cui, H., Liu, J., Wu, Y., Cheng, Y., et al. (2018). WEGO 2.0: a web tool for analyzing and plotting GO annotations, 2018 update. *Nucleic Acids Res.* 46, W71–W75. doi: 10.1093/nar/gky400

Conflict of Interest: The authors declare that the research was conducted in the absence of any commercial or financial relationships that could be construed as a potential conflict of interest.

frontiers in Microbiology

ORIGINAL RESEARCH
published: 16 February 2021
doi: 10.3389/fmicb.2020.610109

Impact of an Intervention to Control Imipenem-Resistant *Acinetobacter baumannii* and Its Resistance Mechanisms: An 8-Year Survey

Lida Chen[1,2†], Pinghai Tan[3†], Jianming Zeng[4,5], Xuegao Yu[1], Yimei Cai[1], Kang Liao[1], Penghao Guo[1], Yili Chen[1], Zongwen Wu[1], Pinghua Qu[4,5], Renxin Cai[4,5], Cha Chen[4,5] and Bin Huang[1]**

[1] Department of Laboratory Medicine, The First Affiliated Hospital, Sun Yat-sen University, Guangzhou, China, [2] Department of Blood Transfusion, China-Japan Friendship Hospital, Beijing, China, [3] Department of Hematology, Zhujiang Hospital, Southern Medical University, Guangzhou, China, [4] Department of Laboratory Medicine, The Second Affiliated Hospital, Guangzhou University of Chinese Medicine, Guangzhou, China, [5] Department of Laboratory Medicine, Guangdong Provincial Hospital of Chinese Medicine, Guangzhou, China

OPEN ACCESS

Edited by:
Santiago Castillo Ramírez, National Autonomous University of Mexico, Mexico

Reviewed by:
Jesus Silva-Sanchez, National Institute of Public Health, Mexico
Rayane Rafei, Lebanese University, Lebanon

***Correspondence:**
Cha Chen
chencha906@163.com
Bin Huang
huangb3@mail.sysu.edu.cn

† These authors have contributed equally to this work

Specialty section:
This article was submitted to Antimicrobials, Resistance and Chemotherapy, a section of the journal Frontiers in Microbiology

Received: 25 September 2020
Accepted: 24 December 2020
Published: 16 February 2021

Citation:
Chen L, Tan P, Zeng J, Yu X, Cai Y, Liao K, Guo P, Chen Y, Wu Z, Qu P, Cai R, Chen C and Huang B (2021) Impact of an Intervention to Control Imipenem-Resistant Acinetobacter baumannii and Its Resistance Mechanisms: An 8-Year Survey. Front. Microbiol. 11:610109. doi: 10.3389/fmicb.2020.610109

Background: This study aimed to examine the impact of an intervention carried out in 2011 to combat multi-drug resistance and outbreaks of imipenem-resistant *Acinetobacter baumannii* (IRAB), and to explore its resistance mechanism.

Methods: A total of 2572 isolates of *A. baumannii*, including 1673 IRAB isolates, were collected between 2007 and 2014. An intervention was implemented to control *A. baumannii* resistance and outbreaks. Antimicrobial susceptibility was tested by calculating minimal inhibitory concentrations (MICs), and outbreaks were typed using pulsed-field gel electrophoresis (PFGE). Resistance mechanisms were explored by polymerase chain reaction (PCR) and whole genome sequencing (WGS).

Results: Following the intervention in 2011, the resistance rates of *A. baumannii* to almost all tested antibiotics decreased, from 85.3 to 72.6% for imipenem, 100 to 80.8% for ceftriaxone, and 45.0 to 6.9% for tigecycline. The intervention resulted in a decrease in the number (seven to five), duration (8–3 months), and departments (five to three) affected by outbreaks; no outbreaks occurred in 2011. After the intervention, only bla_{AMPC} (76.47 to 100%) and bla_{TEM-1} (75.74 to 96.92%) increased ($P < 0.0001$); whereas bla_{GES-1} (32.35 to 3.07%), bla_{PER-1} (21.32 to 1.54%), bla_{OXA-58} (60.29 to 1.54%), *carO* (37.50 to 7.69%), and *adeB* (9.56 to 3.08%) decreased ($P < 0.0001$). Interestingly, the frequency of class B β-lactamase genes decreased from 91.18% (bla_{SPM-1}) and 61.03% (bla_{IMP-1}) to 0%, while that of class D bla_{OXA-23} increased to 96.92% ($P < 0.0001$). WGS showed that the major PFGE types causing outbreaks each year (type 01, 11, 18, 23, 26, and 31) carried the same resistance genes (bla_{KPC-1}, bla_{ADC-25}, bla_{OXA-66}, and *adeABC*), AdeR-S mutations (G186V and A136V), and a partially blocked porin channel CarO. Meanwhile, plasmids harboring bla_{OXA-23} were found after the intervention.

Conclusion: The intervention was highly effective in reducing multi-drug resistance of *A. baumannii* and IRAB outbreaks in the long term. The resistance mechanisms of IRAB may involve genes encoding β-lactamases, efflux pump overexpression, outer membrane porin blockade, and plasmids; in particular, clonal spread of bla_{OXA-23} was the major cause of outbreaks. Similar interventions may also help reduce bacterial resistance rates and outbreaks in other hospitals.

Keywords: intervention, *Acinetobacter baumannii*, antibiotic resistance, outbreak, mechanism

BACKGROUND

Acinetobacter baumannii is a life-threatening hospital pathogen, causing severe morbidity and mortality, particularly in intensive care units (ICUs) (Jain et al., 2019). Its rate of carbapenem resistance is surprisingly high (Singkham-In and Chatsuwan, 2018), and carbapenem-resistant strains of *A. baumannii*, especially imipenem-resistant *A. baumannii* (IRAB), have caused hospital outbreaks worldwide (Vauchel et al., 2019). To the best of our knowledge, many *A. baumannii* resistance studies have only reported the severity of IRAB resistance, such as mortality and outbreaks (Venditti et al., 2019; Wang et al., 2020). A few measures have been proposed in China (Yu et al., 2019); however, their impact was rarely monitored for a long period.

Hence, the aim of this study was to examine the efficacy of an intervention applied for the prevention and control of IRAB resistance and outbreaks. To discover changes before and after the intervention, we conducted an 8-year continuous survey of IRAB strains with respect to antibiotic resistance, outbreaks, detection of resistance genes, porin channels, and efflux pumps from 2007 to 2014 in a Chinese tertiary hospital.

We believe that similar interventions can help control infections and outbreaks in other hospitals as well, even for other pathogenic bacteria.

MATERIALS AND METHODS

Isolation and Identification of Bacterial Strains

A total of 2572 non-repetitive *A. baumannii* strains, including 1673 IRAB strains, were recovered from samples collected from patients treated in different departments of The First Affiliated Hospital of Sun Yat-sen University, Guangzhou, China between January 2007 and December 2014, and identified using a Vitek2 compact automatic microbiological analysis system with GN colorimetric identification cards (bioMérieux, Marcy l'Etoile, France). These 2572 *A. baumannii* strains were tested for antibiotic resistance; among them, 201 IRAB strains were randomly selected by stratified random sampling method. Of these 201 IRAB strains, the first isolated from different patients each month were randomly selected, and among them a total of 25–26 strains were selected each year (2007–2014). This stratified random sampling method ensured that each IRAB strain had the same probability to be selected, and enabled to monitor statistically the major trends of occurrence of all isolates, reflected by those of the 201 IRAB strains.

These 201 IRAB strains were subjected to pulsed-field gel electrophoresis (PFGE), outbreak analyses, and PCR-based detection of resistance genes. Using whole genome sequencing (WGS), six major PFGE types of outbreak IRAB strains and two control imipenem-sensitive *A. baumannii* (ISAB) strains were sequenced. This study was approved by the Clinical Research and Ethics Committee of The First Affiliated Hospital of Sun Yat-sen University [2019(483)].

Antimicrobial Susceptibility Testing

Susceptibility testing was performed using AST-GN and AST-GN13 cards on the Vitek2 compact system (bioMérieux, Marcy l'Etoile, France). The microbroth dilution method was used in accordance with the standards published by the Clinical and Laboratory Standards Institute (CLSI). The test agents included imipenem, meropenem, gentamicin, tobramycin, ampicillin/sulbactam, piperacillin/tazobactam, levofloxacin, ciprofloxacin, cefepime, ceftazidime, ceftriaxone, sulfamethoxazole, furantoin, and tigecycline. Based on CLSI clinical breakpoints, isolates were designated as IRAB if imipenem MICs $\geq$ 8 μg/mL (2018; CLSI Document M100-S28). Quality control for susceptibility testing was performed with *Pseudomonas aeruginosa* ATCC 27853, *Staphylococcus aureus* ATCC 29213, and *Escherichia coli* ATCC 25922, which were purchased from the National Clinical Laboratory Center.

Pulsed-Field Gel Electrophoresis (PFGE)

The standard protocol of CDC PulseNet[1] used to subtype *Salmonella* was used for bacterial DNA preparation for PFGE. Agarose plugs containing DNA were digested with 10 U of the restriction enzyme *Apa*I (TaKaRa, Ipswich, MA, United States) for 4 h. Electrophoresis was performed with a 1% SeaKem Gold® agarose gel (Lonza, Basel, Switzerland) in 0.5 × TBE buffer (45 mM Tris, 45 mM boric acid, 1 mM EDTA, pH 8.3) using CHEF Mapper® XA (Bio-Rad Laboratories, Hercules, CA, United States) and alternating pulses at 120°, 6 V/cm, and 5–20 s for 18 h. Genomic DNA of standard *Salmonella* H9812 from the Centers for Disease Control and Prevention was digested with 50 U of *Xba*I and used as a molecular size marker. The interpretation of band patterning was performed according to the criteria of Tenover et al. (1995).

[1] http://www.cdc.gov/pulsenet/

PCR for Identification of Drug Resistance Genes

Bacterial DNA was extracted from *A. baumannii* isolates by boiling at 100°C for 10 min. PCR was performed for antibiotic resistance-related genes using TaKaRa Ex Taq (Takara Bio Inc., Otsu, Japan) in a 50 μL reaction mixture containing 5 μL 10×buffer, 4 μL of a dNTPs mixture (2.5 mM), 0.25 μL Taq polymerase (5 U/μL), 1 μL forward primer (20 μM), 1 μL reverse primer (20 μM), 1 μL DNA template (20 ng/μL), and nuclease-free water. The PCR cycle consisted of denaturation at 93°C for 2 min, followed by 35cycles of 60 s at 93°C, annealing for 60 s at 55°C, and extension at 72°C for 60 s, with a final extension at 72°C for 10 min. An agarose gel (1%) was used to resolve and detect the PCR products. The primer sequences used for amplification of drug resistance genes are shown in **Table 1**.

Whole Genome Sequencing (WGS) and Assembly Based Analysis

Genomic DNA was extracted directly from six IRAB isolates of the major outbreak PFGE types and two ISAB isolates as control strains using the MiniBEST kit (Takara Bio Inc.). DNA libraries were prepared using QIAseq FX DNA Library Kits (QIAGEN, Hilden, Germany) and sequenced on an Illumina NextSeq 500 platform (Illumina, San Diego, CA, United States). Paired reads were assembled using SPAdes 3.13.0, and the resulting contigs were annotated in the Prokka website[2]. Assembled contigs were analyzed using the Pasteur Multilocus Sequence Typing (MLST) scheme[3] and SnapGene 4.3.8.1. SWISS-MODEL[4] was used for protein modeling.

Intervention Strategies

We applied a comprehensive intervention to reduce *A. baumannii* resistance rates and IRAB outbreaks in 2011. The intervention focused of five aspects: health-care workers, patients, antibiotic use, medical equipment, and environmental protection. The details of the measures are shown in **Figure 1** and summarized as follows:

(1) Health-care workers: The hospital personnel received lectures on a regular basis about hand hygiene, standardized sample delivery, reasonable use of antibiotics, and dedicated care for infected patients, and routine culture of bacteria isolated from the hands of doctors and nurses every 2 weeks.
(2) Patients: Patients infected or colonized by outbreak bacteria were isolated. In addition, an enhanced personal hygiene, by washing hands, towels, fruits, toothbrushes, etc., and the disposal of waste at specific locations were deemed essential for the containment of *A. baumannii* transmission.
(3) Antibiotic use: Antimicrobials were used more effectively to prevent spread of harmful bacteria and outbreaks, through regular monitoring of antibiotic resistance and adjustment of the hospital antibiotics list every few

[2]http://www.vicbioinformatics.com/software.prokka.shtml

[3]www.genomicepidemiology.org

[4]https://swissmodel.expasy.org

TABLE 1 | Primer sequences for the amplification of drug resistance genes by PCR.

Genes		Primer sequences		Products (bp)
β-Lactamases				
Class A				
	TEM-1	F:5′-AGGAAGAGTATGATTCAACA-3′	R:5′-CTCGTCGTTTGGTATGGC-3′	535
	SHV-1	F:5′-TGCGCAAGCTGCTGACCAGC-3′	R:5′-TTAGCGTTGCCAGTGCTCG A-3′	305
	GES-1	F:5′-ATGCGCTTCATTCACGCAC-3′	R:5′-CTATTTGTCCGTGCTCAGG-3′	864
	PER-1	F:5′-AGTCAGCGGCTTAGATA-3′	R:5′-CGTATGAAAAGGACAATC-3′	978
Class B				
	IMP-1	F:5′-CGGCCGCAGGAGAGGCTTT-3′	R:5′-AACCAGTTTTGCCTTACCAT-3′	587
	VIM-1	F:5′-ATTCCGGTCGGAGAGGTCCG-3′	R:5′-GAGCAAGTCTAGACCGCCCG-3′	633
	SPM-1	F:5′-CCTACAATCTAACGGCGACC-3′	R:5′-TCGCCGTGTCCAGGTATAAC-3′	349
	AIM-1	F:5′-CTCGGTTTCAGGCCGGAGGA-3′	R:5′-GGGTGACCAGGATGTCGCAGT-3′	478
	GIM-1	F:5′-ATTACTTGTAGCGTTGCC-3′	R:5′-CTCTATAAGCCCATTTCC-3′	418
	NDM-1	F:5′-GGCGGAATGGCTCATCACGA-3′	R:5′-CGCAACACAGCCTGACTTTC-3′	287
Class C				
	AMPC	F:5′-GCCTGGTAAGTATTGGAAAG-3′	R:5′-CCGAAACGGTTAGTTGAGCC-3′	696
	DHA-1	F:5′-GCTGCCACTGCTGATAGAA-3′	R:5′-GTTGCCGTCTCCGTAAAG-3′	331
Class D				
	OXA-23	F:5′-GATGTGTCATAGTATTCGTCG-3′	R:5′-TCACAACAACTAAAAGCACTG-3′	1067
	OXA-24	F:5′-GTACTAATCAAAGTTGTGAA-3′	R:5′-TTCCCCTAACATGAATTTGT-3′	800
	OXA-40	F:5′-GATGAAGCTCAAACACAGGGTG-3′	R:5′ -TTTCCATTAGCTTGCTCCACC-3′	587
	OXA-58	F:5′-AAGTATTGGGGCTTGTGCTG-3′	R:5′-CCCCTCTGCGCTCTACATAC-3′	599
Porin channel	*carO*	F:5′-TATGGATCCTACCAAGCTGAAGT TGGTGGTCG-3′	R:5′-TATGAATTCTTAGAAGCGGTATG CTGCACGAAC-3′	642
Efflux pump	*adeB*	F:5′-GGATTATGGCGACAGAAGGA-3′	R:5′-AATACTGCCGCCAATACCAG-3′	702

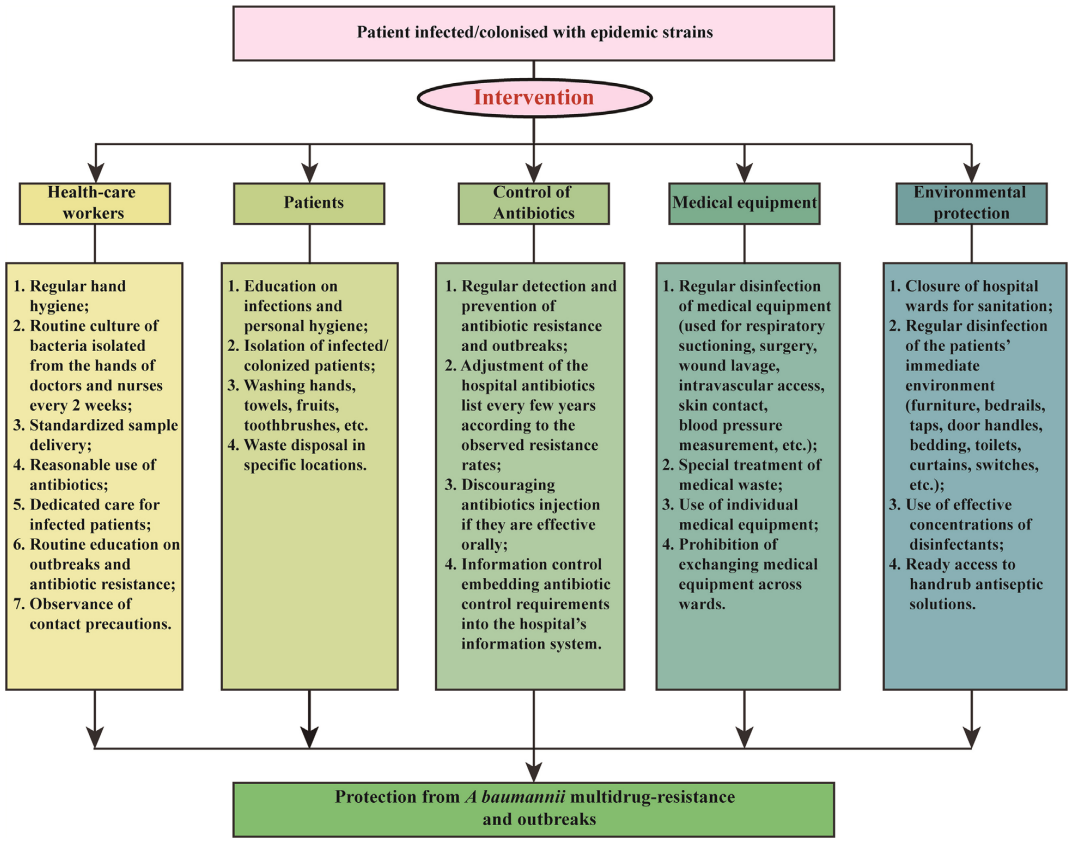

FIGURE 1 | Multicomponent intervention to control *A. baumannii* resistance rates and imipenem-resistant *A. baumannii* outbreaks.

years according to the observed resistance rates. For example, before the intervention the antibiotics in use were imipenem, meropenem, gentamicin, tobramycin, ampicillin/sulbactam, piperacillin/tazobactam, levofloxacin, ciprofloxacin, cefepime, ceftazidime, ceftriaxone, sulfamethoxazole, and furantoin; however, during the intervention of 2011, meropenem was removed from the hospital antibiotic list due to a rapidly increasing resistance rate, while tigecycline were added to the list. In addition, the injection of antibiotics was avoided if these were effective orally. Finally, an information control system embedding antibiotic control requirements into the hospital's information system was also applied.

(4) Medical equipment: Special attention was paid to the regular disinfection of medical equipment, such as that used for respiratory suctioning, wound lavage, intravascular access, surgery, skin contact, blood pressure measurement, etc., with 75% ethyl alcohol on a daily basis. Additionally, the use of individual medical equipment and prohibition of exchanging medical equipment across wards also contributed to the control of *A. baumannii* outbreaks.

(5) Environmental protection: Hospital wards were carefully closed for sanitation and effective disinfection of the patients' immediate environment, including furniture, bedrails, taps, door handles, bedding, toilets, curtains, switches, etc. Moreover, ready access to handrub antiseptic solutions increased the compliance to hand hygiene as well.

Statistical Analysis

Continuous variables are presented as means ± standard deviation (SD); categorical variables are shown as numbers and percentages. For continuous variables, comparisons between groups were analyzed by Mann–Whitney test or Student's *t*-test. For categorical variables, comparisons between groups were analyzed by χ^2 test. SPSS 19.0 (SPSS Inc., Chicago, IL, United States) was used for data analysis. Results displaying $P < 0.05$ were considered statistically significant. The flow chart of the current research methods are shown in **Figure 2**.

RESULTS

Reduction in Antimicrobial Resistance Rates After Intervention

The findings of the antibiotic susceptibility testing for all 2572 *A. baumannii* isolates are shown in **Table 2**. From 2007 to 2010, a total of 811 *A. baumannii* strains were recovered. The rates of resistance to various antibiotics increased every year (**Figure 3A** and **Table 2**). Specifically, the resistance rates increased rapidly

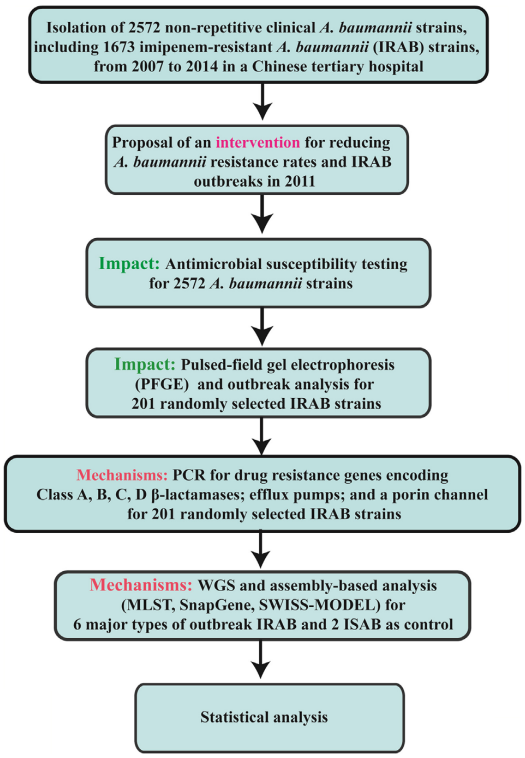

FIGURE 2 | Flow chart of the current research methods.

from 13.8 to 57.2% for imipenem, from 11.0 to 53.1% for meropenem, and from 21.4 to 51.8% for piperacillin/tazobactam. In 2011, *A. baumannii* had the highest resistance rate to imipenem, reaching 85.3%; this trend was also observed for other antibiotics. Interestingly, after reaching its peak in 2011, with the implementation of the intervention in June 2011 (**Figure 1**), the rates of *A. baumannii* resistance to various antibiotics decreased every year (**Figure 3A**). Due to the rapidly increasing resistance rate, meropenem was removed from the hospital antibiotics list in 2011, while tigecycline were added to the list after the intervention. From 2011 to 2014, a total of 1761 *A. baumannii* strains were isolated for which the rate of imipenem resistance dropped from 85.3 to 72.6%, that of levofloxacin resistance from 74.9 to 42.5%, that of ceftazidime resistance from 85.4 to 51.0%, that of ceftriaxone resistance from 100.0 to 80.8%, and that of tigecycline resistance from 45.0 to 6.9%. Thus, the resistance rates of *A. baumannii* to almost all the antibiotics in use were reduced after the intervention. The results of antibiotic susceptibility testing for IRAB are shown in **Table 2**. Unlike *A. baumannii*, the resistance rates of IRAB hardly changed from 2007 to 2014 (**Figure 3B** and **Table 2**). A total of 1673 IRAB isolates were resistant to most antibiotics.

Pulsed-Field Gel Electrophoresis and Outbreak Analysis From 2007 to 2014

Analysis of 201 IRAB strains by PFGE showed that there were seven outbreaks from January 2007 to December 2010 before intervention (**Figure 4**). Three outbreaks of type 01 occurred between January and December 2008, with a total of 13 cases in the medical ICU (MICU). In 2009 there were three outbreaks: an outbreak of type 06 in the respiratory and neurology departments involving a total of seven cases between April and December; an outbreak of type 11 in the neurology ICU (NICU) and neurology departments with 10 cases from April to December; and an outbreak of type 15 in the surgical ICU (SICU) with three cases from July to September. Furthermore, an outbreak of type 18 involving three cases occurred in MICU from July to September 2010. Almost all outbreak strains (98%) were isolated from sputum specimens. However, after the intervention was applied in 2011 (**Figure 1**), only five outbreaks were observed from January 2011 to December 2014 (**Figure 4**). Of these five outbreaks, four cases of type 23 outbreak occurred in the NICU and SICU from July to December 2012, seven cases of type 23 outbreak occurred in the MICU and NICU from April to June 2013, four cases of type 26 outbreak occurred in the MICU from July to December 2012 and three cases from January to March 2014; finally, three cases of type 31 outbreak occurred from October to December 2013 in the MICU and NICU. In summary, after the intervention, the frequency of IRAB outbreaks, the duration of each outbreak, and the number of outbreak strains decreased notably; in addition, there was no outbreak in 2011, and the major PFGE types of outbreak strains before and after the intervention were also different.

Distribution of Genes Encoding β-Lactamases, Porin Channels, and Efflux Pumps

The distribution of genes encoding β-lactamases, porin channels, and efflux pumps in 201 randomly selected IRAB strains is shown in **Table 3**. Screening of resistance genes showed that before the intervention, from 2007 to 2010, the most prevalent β-lactamase-coding resistance gene was bla_{AMPC} (76.47%) of class C, followed by bla_{TEM-1} (75.74%) of class A. Moreover, the IRAB isolates were found to harbor bla_{IMP-1} (61.03%), bla_{VIM-1} (40.44%), bla_{SPM-1} (91.18%), bla_{AIM-1} (43.38%), bla_{GIM-1} (14.71%), and bla_{NDM-1} (1.47%). However, the prevalence of the resistance genes from the 2011–2014 periods changed after the intervention. Among the IRAB strains, the prevalence of bla_{TEM-1} (96.92%), bla_{AMPC} (100.00%), and bla_{OXA-23} (96.92%) had significantly increased ($P < 0.001$). Notably, the prevalence of the bla_{OXA-23} gene had significantly increased from 23.53% to 96.92% ($P < 0.001$), whereas that of bla_{GES-1} (3.07%), bla_{PER-1} (1.54%) of class A, bla_{DHA} (1.54%) of class C, bla_{OXA-58} (1.54%) of class D, and *carO* (7.69%) had significantly decreased ($P < 0.0001$). In addition, the prevalence of class B genes, such as bla_{SPM-1}, bla_{IMP-1}, bla_{VIM-1}, bla_{AIM-1}, and bla_{GIM-1}, decreased to negligible levels ($P < 0.0001$).

Whole Genome Sequencing (WGS) and Assembly Based Analysis

Whole genome sequencing was used to detect the major outbreak PFGE types (**Figure 4**) of IRAB strains before the intervention (SQ001-type 01, SQ002-type 11, and

TABLE 2 | Antibiotic resistance rates of 2572 *A. baumannii* stains including 1673 IRAB stains from 2007 to 2014.

Antibiotics agents	2007		2008		2009		2010		2011		2012		2013		2014	
	AB (145) R (%)	IRAB (20) R (%)	AB (200) R (%)	IRAB (43) R (%)	AB (244) R (%)	IRAB (108) R (%)	AB (222) R (%)	IRAB (127) R (%)	AB (407) R (%)	IRAB (347) R (%)	AB (447) R (%)	IRAB (352) R (%)	AB (422) R (%)	IRAB (324) R (%)	AB (485) R (%)	IRAB (352) R (%)
Carbapenems																
Imipenem	13.8	100	21.5	100	44.3	100	57.2	100	85.3	100	78.7	100	76.8	100	72.6	100
Meropenem	11.0	60	28.8	83.9	48.7	96.2	53.1	100	88.5	100	–	–	–	–	–	–
Aminoglycosides																
Gentamicin	75.9	91.3	77.5	95.5	77.0	95.9	70.3	88.4	84.0	97.1	78.3	95.7	70.9	90.4	69.3	94.3
Tobramycin	54.5	56.5	64.5	75.8	57.8	69.4	67.6	86.2	81.8	94.2	69.8	87.5	65.5	88.9	66.3	90.3
β-lactam antibiotics / enzyme inhibitors																
Ampicillin/sulbactam	60.3	92.3	61.7	85.7	71.0	89.9	72.1	89.9	81.8	94.8	75.9	98.1	55.6	93.7	51.6	98.7
Piperacillin/tazobactam	21.4	69.6	22.5	58.5	39.3	66.1	51.8	79.0	79.9	85.8	77.6	98.9	73.7	96.3	69.7	97.2
Quinolones																
Levofloxacin	50.3	82.6	69.8	86.4	66.0	86.8	71.2	90.6	74.9	86.2	54.4	86.5	39.8	89.4	42.5	88.0
Ciprofloxacin	73.8	100	80.0	93.9	79.1	98.3	78.4	97.1	86.7	98.6	80.3	98.9	77.0	97.8	74.6	100
Cephalosporins																
Cefepime	40.0	69.6	43.2	54.5	65.2	79.3	61.3	79.0	81.3	94.2	79.0	98.3	76.4	97.5	72.6	99.1
Ceftazidime	73.1	95.7	77.9	98.5	77.5	99.2	77.5	97.1	85.4	98.6	77.9	99.2	58.5	96.2	51.0	100
Ceftriaxone	73.8	95.7	80.9	97.0	77.9	99.2	80.6	100	100	98.6	97.2	98.3	89.8	98.8	80.8	100
Sulfonamides																
Sulfamethoxazole	75.2	100	82.4	98.5	78.7	97.5	78.4	97.8	86.0	97.1	65.8	97.6	60.2	98.0	60.8	98.1
Nitrofurans																
Furantoin	100	100	100	100	100	100	99.5	100	100	100	94.0	100	86.3	100	79.6	100
Tetracyclines																
Tigecycline	–	–	–	–	–	–	–	–	–	–	45.0	51.7	16.6	19.2	6.9	7.6

R(%), antibiotic resistance rates (%); AB, A. baumannii; IRAB was included in AB in the same year.

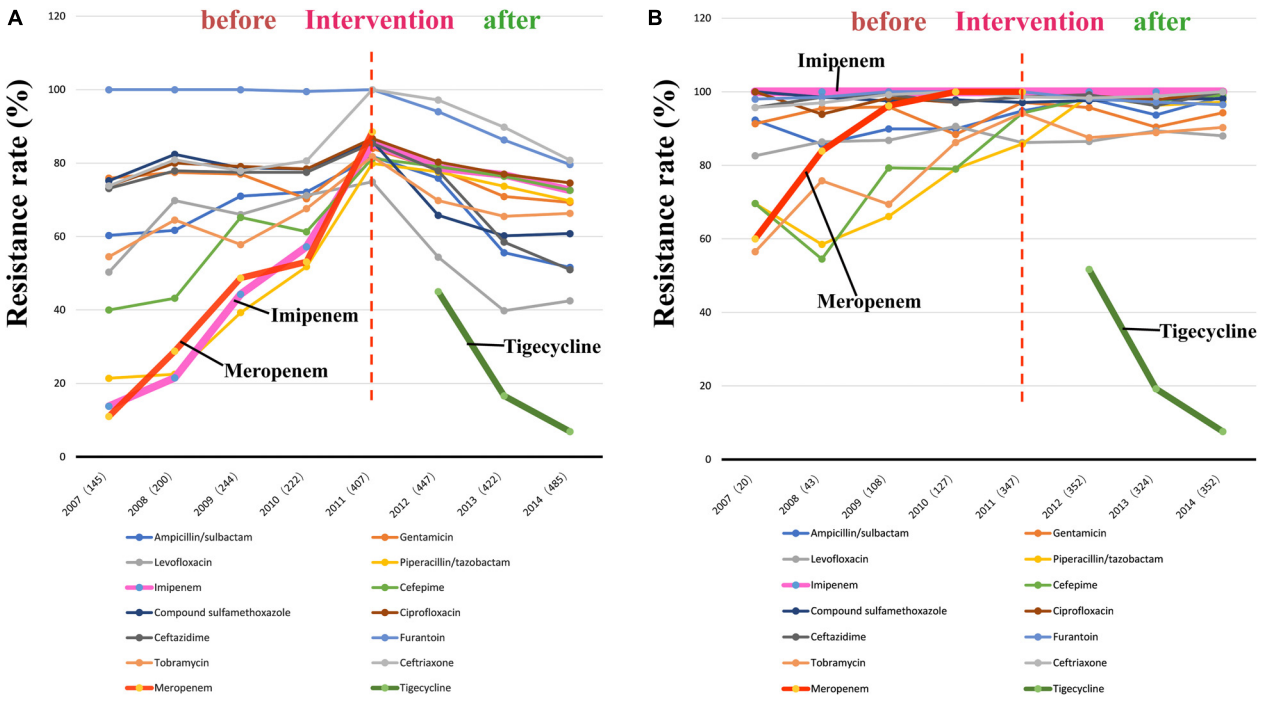

FIGURE 3 | Changes in antibiotic resistance rates during 8 years spanningfrom before to after the intervention. **(A)** Antibiotic resistance rates of 2572 ***A. baumannii*** stains from 2007 to 2014; **(B)** Antibiotic resistance rates of 1673 **IRAB** stains from 2007 to 2014.

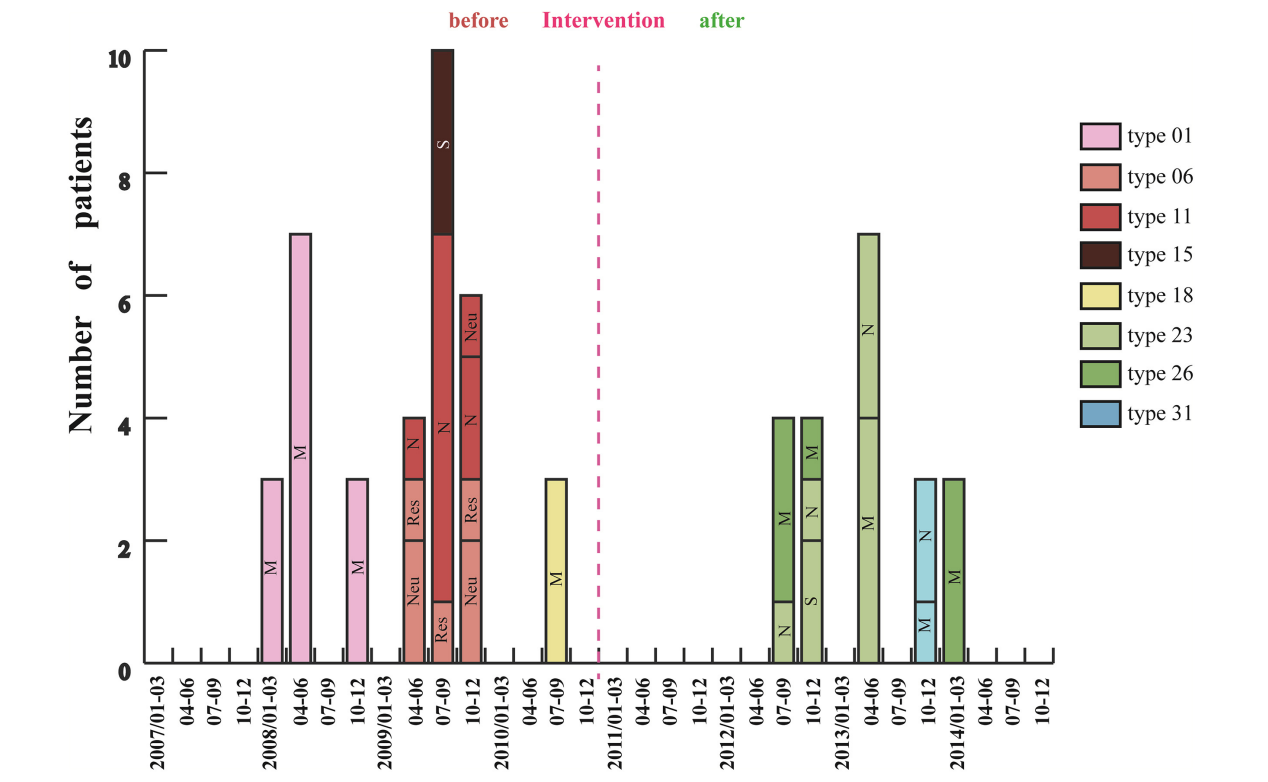

FIGURE 4 | Changes in IRAB outbreaks across 8 years before and after the intervention. Each vertical bar represents an outbreak. M: MICU, Medical Intensive Care Unit; S: SICU, Surgical Intensive Care Unit; N: NICU, Neurology Intensive Care Unit; Neu, Neurology department; and Res, Respiratory department.

TABLE 3 | Distribution of resistance genes in 201 IRAB isolates from 2007 to 2014.

Genes	2007–2010 IRAB (*n* = 136) Prevalence rate (%) before the intervention	2011-2014 IRAB (*n* = 65) Prevalence rate (%) after the intervention	χ^2	*P*-value
β-lactamases Class A				
bla_{TEM-1}	75.74 (103/136)	96.92 (63/65)	13.729	<0.0001
bla_{SHV-1}	1.47 (2/136)	0 (0/65)	0.965	1.000
bla_{GES-1}	32.35 (44/136)	3.07 (2/65)	21.359	<0.0001
bla_{PER-1}	21.32 (29/136)	1.54 (1/65)	13.558	<0.0001
Class B				
bla_{IMP-1}	61.03 (83/136)	0 (0/65)	67.572	<0.0001
bla_{VIM-1}	40.44 (55/136)	0 (0/65)	36.189	<0.0001
bla_{SPM-1}	91.18 (124/136)	0 (0/65)	154.704	<0.0001
bla_{AIM-1}	43.38 (59/136)	0 (0/65)	39.915	<0.0001
bla_{GIM-1}	14.71 (20/136)	0 (0/65)	10.615	<0.0001
bla_{NDM-1}	1.47 (2/136)	0 (0/65)	0.965	1.000
Class C				
bla_{AMPC}	76.47 (104/136)	100 (65/65)	0.965	<0.0001
bla_{DHA-1}	19.85 (27/136)	1.54 (1/65)	12.304	<0.0001
Class D				
bla_{OXA-23}	23.53 (32/136)	96.92 (63/65)	95.046	<0.0001
bla_{OXA-24}	2.21 (3/136)	0 (0/65)	1.456	0.552
bla_{OXA-40}	0.74 (1/136)	0 (0/65)	0.480	1.000
bla_{OXA-58}	60.29 (82/136)	1.54 (1/65)	62.631	<0.0001
Porin channel				
carO	37.5 (51/136)	7.69 (5/65)	19.442	<0.0001
Effux pump				
adeB	9.56 (13/136)	3.08 (2/65)	1.819	0.151

SQ003-type 18), after the intervention (SQ081-type 31, SQ092-type 23, and SQ093-type 26), and the control strains SQ082-ISAB (S) and SQ080-ISAB (MDR) to analyze the resistance mechanisms of IRAB. The control strain SQ082-ISAB (S) was sensitive to all antibiotics. SQ080-ISAB (MDR-AB) and SQ081-IRAB belonged to the same PFGE type 31; SQ080 was resistant to multi-antibiotics, but sensitive to imipenem, while SQ081 was resistant to both multi-antibiotics and imipenem.

The study of the virulence mechanism of outbreak strains by WGS revealed that these differed before and after the intervention (**Table 4**). For instance, the bla_{OXA-23} gene, coding for a class D β-lactamase, was present in IRAB (SQ081-type 31, SQ092-type 23, and SQ093-type 26) isolated after the intervention, but not in those IRAB isolates (SQ001-type 01, SQ002-type 11, and SQ003-type 18) that had been collected before the intervention. Second, the six IRAB isolates collected before (SQ001-type 01, SQ002-type 11, and SQ003-type 18) and after (SQ081-type 31, SQ092-type 23, and SQ093-type 26) the intervention showed some similarities in multiple drug resistance mechanisms, differing from ISAB (S) (SQ082): ① The six IRAB isolates were all ST2 by MLST analysis, while ISAB (S) (SQ082) was ST218; ② Compared to ISAB (S) (SQ082), these IRAB carried a wide variety of antibiotic enzymes: their β-lactamase genes included bla_{KPC-1} in class A, bla_{ADC-25} in class C, and bla_{OXA-66} in class D; ③ Unlike ISAB(S) (SQ082), these IRAB displayed genes encoding aminoglycoside-modifying enzymes including *ant(3′)*, *ant(3′′)*, and *aph;* ④ Among efflux pumps, although the *adeABC* operon could be detected in IRAB, *adeC* could not be detected in ISAB(S) (SQ082). AdeR carried a A136V mutation, and AdeS a G186V mutation in IRAB, but AdeR-S showed no mutations in ISAB(S). IRAB also presented the genes *msrE* and *tetA*, encoding efflux pumps, while ISAB(S) (SQ082) did not; ⑤ With respect to the outer membrane porin permeability of antibiotics, the amino acid sequence of the CarO of IRAB (SQ001-type 01, SQ002-type 11, SQ003-type 18, SQ081-type 31, SQ092-type 23, and SQ093-type 26) matched that of the sequence under NCBI accession number WP_004714722.1, while that of ISAB(S) (SQ082) matched the sequence of the NCBI accession number WP_ 000866519.1. The SWISS-MODEL for CarO shows that the upper part of ATCC 19606 (**Figure 5A**) consists of a large channel formed by 14 β-sheets, while that of IRAB is formed by 8 β-sheets, leading to partial blockade of the channel (**Figure 5B**). The similarity between the CarO of IRAB and the CarO template 4fuv.1.A was 100% (**Figure 5B**), whereas the similarity between the CarO of ISAB (S) (SQ082) and the template 4fuv.1.A was only 75.93%; ⑥ Plasmid analysis revealed that the plasmid carried by IRAB (SQ081-type 31, SQ092-type 23, and SQ093-type 26) was similar to the plasmid pAC29b (NCBI registration number CP008851). The comparison of plasmids and contigs using the SnapGene software revealed that the IRAB plasmid covered the full length of bla_{OXA-23} on

plasmid pAC29b, which contained the bla_{OXA-23} gene, indicating that bla_{OXA-23} was present on the plasmid of IRAB after the intervention (**Figure 5C**).

Potential Resistance Mechanism of IRAB Before and After the Intervention

The following multi-drug resistance mechanisms were observed in IRAB isolates before and after the intervention. First, common mechanisms included (1) the partial blockade of the CarO porin channel, which reduced the antibiotic permeability of IRAB (**Table 3** and **Figure 5B**); (2) the possible overexpression of the efflux pump AdeABC, owing to AdeR-S mutations (**Tables 3**, **4**), which enhanced the antibiotic efflux capacity of IRAB; (3) the presence of enzymes residing in the periplasmic space, such as β-lactamases (encoded by bla_{TEM-1}, bla_{TEM-4}, bla_{GES-1}, and bla_{PER-1} in class A; bla_{AMPC}, bla_{DHA}, and bla_{ADC-25} in class C; and bla_{OXA-66} in class D) (**Tables 3**, **4**) and aminoglycoside-modifying enzymes [encoded by *ant(3′)*, *ant(3′′)*, *aph*] (**Table 4**) which can degrade various antibiotics in IRAB. Second, WGS highlighted the occurrence of different mechanisms before and after intervention: in particular, among the enzymes residing in the periplasmic space, the types of β-lactamases changed, as bla_{OXA-23} in class D was only detected on the bacterial plasmid after the intervention (**Table 4**). Therefore, the plasmids harboring bla_{OXA-23} may be the major cause of IRAB outbreak after the intervention (**Table 4** and **Figures 4**, **5C**). The multi-drug resistance mechanisms of IRAB after the intervention are shown in **Figure 6**.

Imipenem-resistant *Acinetobacter baumannii* contains an outer membrane, periplasmic space, cytoplasmic membrane, cytoplasm, chromosome, and plasmids. Antibiotics must cross the outer membrane through porin channels (outer membrane proteins such as CarO) to reach the periplasmic space and then bind to the final targets of penicillin-binding proteins located at the level of the cytoplasmic membrane. Antibiotics can be degraded by enzymes (e.g., β-Lactamases of Class A, B, C, and D), and can also be actively expelled from the bacterial structure through efflux pumps (e.g., AdeABC and AdeR-S).

Impact of the Intervention

The intervention triggered many positive effects, that we describe as follows: ① the resistance rates of *A. baumannii* decreased after the intervention; ② the intervention resulted in a decrease in the number and duration of outbreaks, as well as in the number of departments affected by of outbreaks; ③ the frequency of most resistance genes decreased after the intervention; ④ the resistance mechanisms characterizing IRAB both before and after the intervention included porin channel blockade, efflux pump overexpression, and chromosomes harboring resistance genes and various enzymes; conversely, the frequent genes encoding β-lactamases passed from genes encoding class B β-lactamases to bla_{OXA-23} after the intervention.

DISCUSSION

This Study Proposed a Systemic Intervention to Control *A. baumannii* Resistance and IRAB Outbreaks

Imipenem-resistant *Acinetobacter baumannii* is the most important group of bacteria associated with hospital-acquired infections and outbreaks worldwide (Xie et al., 2018). Several control measures have been applied against IRAB (Birgand et al., 2015, 2016), and some articles display various degrees of severity and prevalence of IRAB over many years (Du et al., 2019; Park et al., 2019). However, few studies similar to the present study have been published. In the present study, we proposed a systemic control intervention and also investigated the changes in severity and prevalence of resistance mechanisms of IRAB for a long time (8 years). The aim of this study was to characterize the impact of an intervention to control resistance and outbreaks of IRAB and to explore its resistance mechanisms through an 8-year survey. We hope that our results can help hospitals in other countries to prevent and control *A. baumannii* resistance and IRAB outbreaks.

The Intervention Reduced the Antibiotic Resistance Rate of *A. baumannii* and the Occurrence Rate of IRAB

Before the intervention, the drug resistance rate of *A. baumannii* increased every year, and the resistance rate for imipenem increased from 13.8% to 85.3%. During the intervention in 2011, meropenem was removed from the hospital antibiotics list due to a rapid growth of resistance rate, while tigecycline were added. After the intervention, the resistance rates of *A. baumannii* to various antibiotics decreased significantly every year. However, IRAB isolates were almost completely resistant to other antibiotics, and the resistance rates of IRAB to other antibiotics did not change significantly during the 8 years of the survey, which suggests that the intervention could effectively prevent and control the resistance rates of *A. baumannii* to various antibiotics and to imipenem, but had limited effect on *A. baumannii* that is already resistant to imipenem (IRAB). This could be due to the complex resistance mechanisms characterizing IRAB reported by Lee et al. (2017); indeed, once *A. baumannii* becomes IRAB, it might be difficult to reduce the drug resistance rates due to the emergence of complex resistance mechanisms to many antibiotics.

The Intervention Reduced the Frequency, Duration, and Isolate Number of IRAB Outbreaks

Pulsed-field gel electrophoresis analysis showed that the frequency of IRAB outbreaks before the intervention was 2–3 times per year, which decreased to almost once a year after the intervention. The duration of the IRAB outbreak was shortened from 8 to 3 months. The outbreaks occurred in the MICU,

TABLE 4 | Whole genome sequencing for major outbreak types before and after the intervention.

Strains	**Control**		**Before**			**After**		
	SQ082	**SQ080**	**SQ001**	**SQ002**	**SQ003**	**SQ081**	**SQ092**	**SQ093**
Resistance	ISAB(S)	ISAB(MDR)	IRAB	IRAB	IRAB	IRAB	IRAB	IRAB
Accession No.	JADQAD 000000000	JADPZY 000000000	JADQAA 000000000	JADPZZ 000000000	JADQAG 000000000	JADQAC 000000000	JADQAE 000000000	JADQAF 000000000
PFGE	Type 35	Type 31	Type 01	Type 11	Type 18	Type 31	Type 23	Type 26
MLST	218	2	2	2	2	2	2	2
β-Lactamases								
Class A	bla_{TEM-4}	bla_{TEM-4}	bla_{TEM-4}	bla_{TEM-4}	bla_{TEM-4}	bla_{TEM-4}	bla_{TEM-4}	bla_{TEM-4}
	$bla_{TEM-104}$	$bla_{TEM-104}$	–	–	–	–	–	–
	$bla_{TEM-143}$	$bla_{TEM-143}$	–	–	–	–	–	–
	–	–	**bla_{KPC-}**	**bla_{KPC-1}**	**bla_{KPC-1}**	**bla_{KPC-1}**	–	–
Class B	–	–	–	–	–	–	–	–
Class C	bla_{ADC-80}	**bla_{ADC-25}**	**bla_{ADC-25}**	**bla_{ADC-25}**	**bla_{ADC-25}**	**bla_{ADC-25}**	**bla_{ADC-25}**	**bla_{ADC-25}**
Class D	–	–	–	–	–	**bla_{OXA-23}**	**bla_{OXA-23}**	**bla_{OXA-23}**
	–	**bla_{OXA-66}**	**bla_{OXA-66}**	**bla_{OXA-66}**	**bla_{OXA-66}**	**bla_{OXA-66}**	**bla_{OXA-66}**	**bla_{OXA-66}**
Aminoglycoside	*AAC(3)*	*AAC(3)*	*AAC(3)*	*AAC(3)*	*AAC(3)*	*AAC(3)*	–	–
modifying	*AAC(6′)-Ib8*	*AAC(6′)-Ib8*	*AAC(6′)-Ib8*	–	–	*AAC(6′)-Ib8*	–	–
enzymes	*AddA*	*AddA*	*AddA*	–	–	*AddA*	–	
	ANT	*ANT*	*ANT*	*ANT*	*ANT*	*ANT*	–	–
	–	**aph**	**aph**	**aph**	**aph**	**aph**	**aph**	
	–	–	–	**ant(3′)**	**ant(3′)**	–	**ant(3′)**	**ant(3′)**
Efflux pumps								
adeABC	*adeAB*	*adeABC*	*adeABC*	*adeABC*	*adeABC*	*adeABC*	*adeABC*	*adeABC*
adeFGH	+	+	+	+	+	+	+	+
adeIJK	+	+	+	+	+	+	+	+
AdeR mutation	–	A136V	A136V	A136V	A136V	A136V	A136V	A136V
AdeS mutation	–	G186V	G186V	G186V	G186V	G186V	G186V	G186V
others	*abeM*	*abeM*	*abeM*	*abeM*	*abeM*	*abeM*	*abeM*	*abeM*
	abeS	*abeS*	*abeS*	*abeS*	*abeS*	*abeS*	*abeS*	*abeS*
	emrA	–	–	–	–	*emrA*	–	–
	emrB	–	–	–	–	–	–	–
	–	*msrE*	*msrE*	–	*msrE*	–	*msrE*	*msrE*
	–	*tet(A)*	*tet(A)*	–	*tet(A)*	*tet(A)*	*tet(A)*	*tet(A)*
porin								
CarO (NCBI)	+	+	+	+	+	+	+	+
	WP_ 000866519.1	WP_ 004714722.1	WP_ 004714722.1	WP_ 004714722.1	WP_ 004714722.1	WP_ 004714722.1	WP_ 004714722.1	WP_ 004714722.1

The accession numbers of JAD. . .originate from database https://www.ncbi.nlm.nih.gov/assembly/, and the accession numbers of WP_. . .originate from database https://www.ncbi.nlm.nih.gov/protein/.

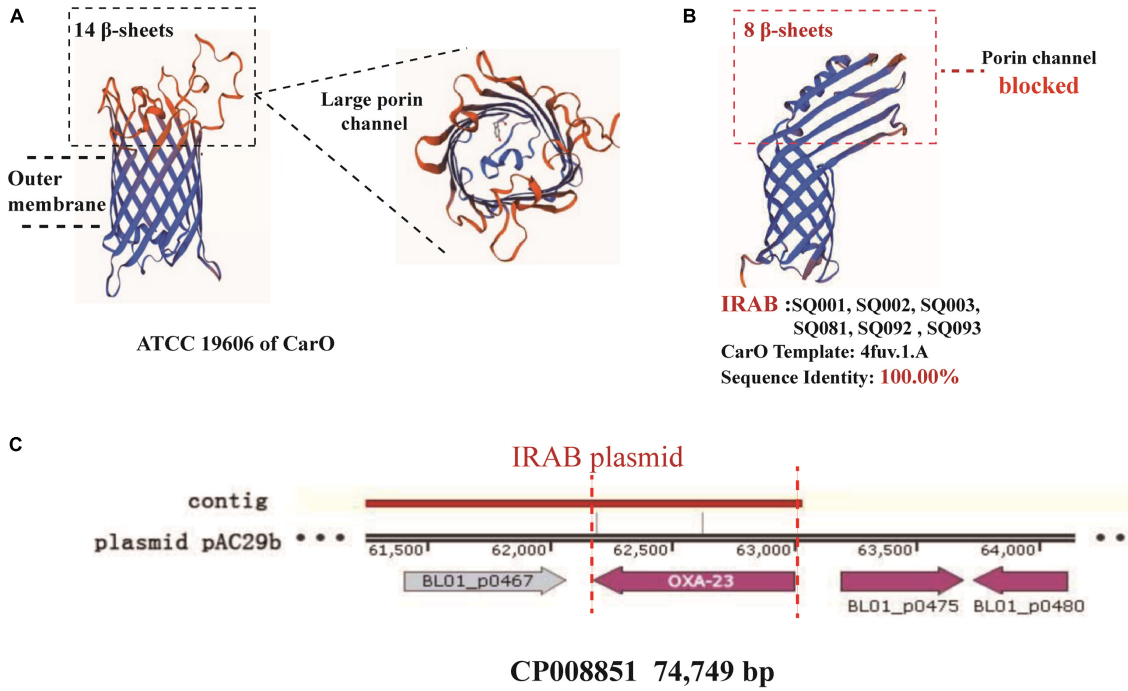

FIGURE 5 | SWISS-model for porin permeability to imipenem and plasmid harboring bla_{OXA-23} in IRAB isolates. **(A)** 3D model for CarO of ATCC 19606 with 14 β-sheets, which form a large porin channel for imipenem to pass through; **(B)** 3D model for CarO of IRAB with 8 β-sheets, which block the porin channel to hinder the passage of imipenem; the sequence identity with the template 4fuv.1.A was 100%; **(C)** plasmid harboring bla_{OXA-23} in IRAB isolates.

SICU, NICU, and respiratory and neurology departments before the intervention, but only in the MICU, SICU, and NICU after the intervention. Daniel et al. (2019) reported that MICU, SICU, and NICU were the key departments of IRAB outbreaks, consistent with our findings. The number of IRAB strains per outbreak was reduced from 11 to 3 isolates. Notably, there was no outbreak in 2011, the first year after implementing the intervention, which could be attributed to the replacements in the hospital antibiotic list and other control measures in the intervention. However, new IRAB strains that were resistant to new antibiotics and selection pressures caused new outbreaks after 2011. Therefore, regular replacement of antibiotics to prevent the emergence of new IRAB strains is also a key feature of this intervention.

PCR-Based Mechanistic Studies Showed That Changing Antibiotics in the Intervention May Lead to Changes in IRAB Resistance Mechanisms

Imipenem-resistant *Acinetobacter baumannii* resistance was the result of a combination of multiple resistance mechanisms. PCR analysis showed that genes encoding β-lactamases, such as bla_{AMPC} and bla_{TEM-1}were the major resistance genes of IRAB before and after the intervention. Before the intervention, bla_{SPM-1} and bla_{IMP-1} in class B were detected at a frequency of 91.18 and 61.03%, respectively, while bla_{OXA-23} in class D accounted for only 23.53%. However, after the intervention, the frequency of genes in class B decreased to 0.00%, but that of bla_{OXA-23} of class D increased to 96.92%, suggesting that there was clonal spread (or horizontal spread) of bla_{OXA-23} after 2011. Harboring the bla_{OXA-23} gene may have been one of the main resistance mechanisms of IRAB from 2011 to 2014. In the intervention, meropenem was replaced with tigecycline. Kulengowski et al. (2019) reported that bla_{VIM-1} of class B was related to meropenem resistance, while Savari et al. (2017) reported that bla_{OXA-23} and overexpression of the AdeABC efflux pump were associated with tigecycline resistance. Therefore, the significant differences in frequency between class B genes and bla_{OXA-23} before and after the intervention may be due to the replacement of antibiotics, which changed the selection pressure of *A. baumannii*, leading to changes in the drug resistance mechanism. The gene *adeB* encoding an efflux pump and the gene *carO* encoding a porin channel were also analyzed before and after the intervention. Therefore, multiple drug resistance mechanisms mediated widespread IRAB resistance.

WGS-Based Mechanistic Analysis Confirmed That IRAB Has a Combination of Resistance Mechanisms, and That Plasmids Harboring bla_{OXA-23} May Lead to New Outbreaks After the Intervention

Whole genome sequencing showed that IRAB had multiple drug resistance mechanisms compared to ISAB (S) (SQ080): (1) There

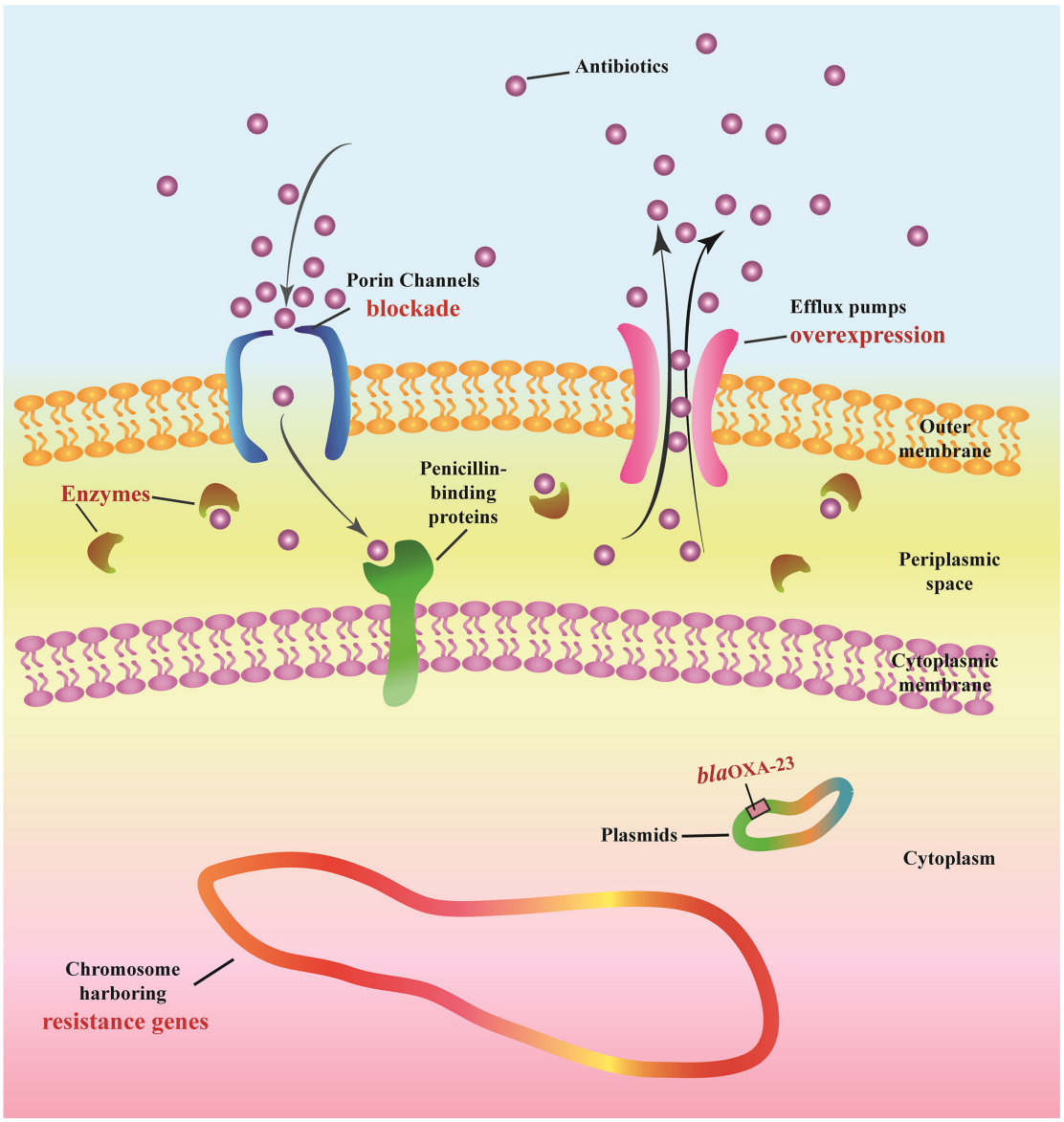

FIGURE 6 | Potential mechanisms of antimicrobial resistance in IRAB.

are many types of enzymes for modification of antibiotics, such as β-lactamases and aminoglycoside-modifying enzymes. First, the production of β-lactamases is a major antibiotic resistance mechanism in *A. baumannii*; these enzymes inactivate β-lactam, and comprise four molecular classes: A, B, C, and D (Sawa et al., 2020). In this study, unlike ISAB (S)(SQ082), IRAB contained bla_{KPC-1} of class A, bla_{ADC-25} of class C, and bla_{OXA-23}, and bla_{OXA-66} of class D. Class A β-lactamases degrade early generation cephalosporins (Sawa et al., 2020); class C β-lactamases can confer resistance to cephamycins (cefoxitin and cefotetan), penicillins, and cephalosporins (Uddin et al., 2018); class D β-lactamases, also called OXAs (oxacillinases), hydrolyze oxacillin, and the presence of carbapenem-hydrolyzing class D β-lactamases is a major carbapenem resistance mechanism in *A. baumannii* (Stewart et al., 2019). Unlike the serine-dependent β-lactamases (classes A, C, and D), class B β-lactamases are metallo-β-lactamases that require zinc or another heavy metal for catalysis (Amin et al., 2019). However, genes of class B were not detected in IRAB or ISAB, indicating that class B β-lactamases did not cause IRAB resistance. Second, aminoglycoside-modifying enzymes are classified into acetyltransferases, adenyltransferases, and phosphotransferases (Sheikhalizadeh et al., 2017). In the present study, IRAB had *ant(3′)*, *ant(3″)*, and *aph* genes, which conferred resistance to aminoglycosides. (2) Efflux pumps are associated with resistance against many different classes of antibiotics, such as imipenem and tigecycline, in *A. baumannii* (Knight et al., 2018). AdeABC is associated with aminoglycoside resistance and with decreasing susceptibility to tigecycline and

fluoroquinolone antibiotics (Yoon et al., 2013). The *adeABC* gene was detected in IRAB, but *adeC* was not detected in ISAB, suggesting that efflux pumps of IRAB are more effective than those of ISAB. Notably, mutations in the AdeR-S two-component system lead to the overexpression of AdeABC (Yang et al., 2019). In IRAB, AdeR had a G186V mutation, and AdeS had an A136V mutation, but AdeR-S of ISAB had no mutation, suggesting overexpression of efflux pumps that are more effective than those of ISAB for antibiotic efflux. (3) To investigate the porin channel mechanism, the 3D structure of CarO was modeled using the SWISS-MODEL software. Compared to the structure of CarO from the standard strain ATCC 19606, it was found that the upper part of CarO from ATCC 19606 was a large channel formed by 14 β-sheets, while the upper part of CarO from IRAB in this study was only a small channel formed by 8 β-sheets; such change in the tertiary structure of the IRAB CarO suggested that the porin channel was partly blocked. In addition, the structure of CarO from IRAB elaborated in this study was 100% identical to that of the template 4fuv.1.A in SWISS-MODEL, representing a CarO channel with low permeability to imipenem. Zhu et al. (2019) reported that a partial blockade of the CarO porin channel can reduce the penetration of antibiotics into bacteria, leading to drug resistance, consistent with the results of this study. (4) Plasmid mechanistic analysis revealed that bla_{OXA-23} was present on the plasmid of IRAB after the intervention, and WGS showed that bla_{OXA-23} transmitted drug resistance through the plasmid and became the major reason for IRAB prevalence and outbreak after the intervention. Xiong et al. (2015) reported that changes in drug resistance mechanisms of bacteria may be due to different environmental selection pressure; therefore, with our intervention we might have induced a modification of the prevalent drug resistance mechanisms through a variety of control measures and adjustment of antibiotics use. For example, during the intervention meropenem, showing a fast-growing resistance rate, was discontinued while tigecycline was adopted. Such changes in environmental selection pressure may have reduced the prevalence of class B β-lactamases; consequently, bla_{OXA-23} began to spread and became the main epidemic factor after the intervention. This phenomenon could also explain why the outbreak did not occur throughout 2011 after applying the intervention, but started in July 2012: indeed, *A. baumannii* may have adapted, and major strains harboring the plasmid bearing bla_{OXA-23} may have been selected under the new environmental pressure throughout 2011. Therefore, the resistance to new antibiotics must be regularly monitored, and these should be replaced to prevent the emergence of new resistant strains in each new round of intervention. The present study demonstrated that strengthening the management of health-care workers, patients, medical equipment, and environmental protection is an effective measure against IRAB outbreaks. In addition, modifying the antibiotics list of the hospital according to the results of drug sensitivity is also an effective measure against IRAB resistance, for example by removing ampicillin, furantoin, and ceftriaxone to exhibit high resistance rates, and adding ceftazidime/avibactam (CZA). In fact, Norelle et al. (2018) reported that CZA exerted good inhibitory effects on bacteria carrying bla_{OXA-23}.

CONCLUSION

In this study we proposed and applied a systemic intervention to control the antibiotic resistance of *A. baumannii* and the outbreak of IRAB, which included five aspects: health-care workers, patients, antibiotic use, medical equipment, and environmental protection. An 8-year survey has proven the effectiveness of the intervention, which led to a significant reduction in resistance rates; a decrease in the number, duration, and number of departments affected by outbreaks; and a reduced frequency of most resistance genes. The resistance mechanisms of IRAB include porin channel blockade, efflux pump overexpression, various enzymes, chromosomes harboring resistance genes, and bla_{OXA-23} on plasmids, which was the major reason for outbreaks after the intervention. As part of our intervention strategy, new rounds of interventions should be taken every few years to prevent the emergence of new resistant strains. We hope that this intervention strategy can help other countries and regions control the resistance of *A. baumannii* and outbreaks of IRAB.

DATA AVAILABILITY STATEMENT

The original contributions presented in the study are included in the article/supplementary material, further inquiries can be directed to the corresponding author/s.

ETHICS STATEMENT

This study was approved by the Clinical Research and Ethics Committee of The First Affiliated Hospital of Sun Yat-sen University [2019(483)].

AUTHOR CONTRIBUTIONS

LC, PT, JZ, XY, YC, KL, PG, YC, ZW, PQ, and RC conducted the experiments. LC wrote the manuscript. CC and BH edited the manuscript. All the authors contributed to the article and approved the submitted version.

FUNDING

This work was supported in part by the National Natural Science Foundation of China (grants 81772249, 81672081, and 81871703).

ACKNOWLEDGMENTS

We thank Professor Liang Chen from the Hackensack Meridian School of Medicine for his valuable guidance on sequencing data analysis.

REFERENCES

Amin, M., Navidifar, T., Saleh, S. F., and Goodarzi, H. (2019). Association of the genes encoding metallo-beta-lactamase with the presence of integrons among multidrug-resistant clinical isolates of *Acinetobacter baumannii*. *Infect. Drng Resist.* 12, 1171–1180. doi: 10.2147/idr.s196575

Birgand, G., Johansson, A., Szilagyi, E., and Lucet, J. C. (2015). Overcoming the obstacles of implementing infection prevention and control guidelines. *Clin. Microbiol. Infect.* 21, 1067–1071. doi: 10.1016/j.cmi.2015.09.005

Birgand, G., Moore, L., Bourigault, C., Vella, V., Lepelletier, D., Holmes, A. H., et al. (2016). Measures to eradicate multidrug-resistant organism outbreaks: how much do they cost? *Clin. Microbiol. Infect.* 22, 161–162.

Daniel, M., Benoît, V., Marlène, S., Pascal, C., Michelle, T., Xavier, B., et al. (2019). Fourier-transform infrared spectroscopy can quickly type gram-negative bacilli responsible for hospital outbreaks. *Front. Microbiol.* 26:1440. doi: 10.3389/fmicb.2019.01440

Du, X., Xu, X., Yao, J., Deng, K., Chen, S., Shen, Z., et al. (2019). Predictors of mortality in patients infected with carbapenem-resistant *Acinetobacter baumannii*: a systematic review and meta-analysis. *Am. J. Infect. Control* 47, 1140–1145. doi: 10.1016/j.ajic.2019.03.003

Jain, M., Sharma, A., Sen, M. K., Rani, V., Gaind, R., and Suri, J. C. (2019). Phenotypic and molecular characterization of *Acinetobacter baumannii* isolates causing lower respiratory infections among ICU patients. *Microb. Pathog.* 128, 75–81. doi: 10.1016/j.micpath.2018.12.023

Knight, D. B., Rudin, S. D., Bonomo, R. A., and Rather, P. N. (2018). *Acinetobacter nosocomialis*: defining the role of efflux pumps in resistance to antimicrobial therapy, surface motility, and biofilm formation. *Front. Microbiol.* 9:1902. doi: 10.3389/fmicb.2018.01902

Kulengowski, B., Clark, J. A., and Burgess, D. S. (2019). Killing activity of meropenem in combination with amikacin against VIM- or KPC-producing Enterobacteriaceae that are susceptible, intermediate, or resistant to amikacin. *Diagn. Microbiol. Infect. Dis.* 93, 372–375. doi: 10.1016/j.diagmicrobio.2018.10.020

Lee, C. R., Lee, J. H., Park, M., Park, K. S., Bae, I. K., Kim, Y. B., et al. (2017). Biology of *Acinetobacter baumannii*: pathogenesis, antibiotic resistance mechanisms, and prospective treatment options. *Front. Cell. Infect. Microbiol.* 7:55. doi: 10.3389/fcimb.2017.00055

Norelle, L. S., Sarah, L. B., and Benjamin, P. H. (2018). Ceftazidime/avibactam susceptibility by three different susceptibility testing methods in carbapenemase-producing Gram-negative bacteria from Australia. *J. Antimicrob. Agents* 52, 82–85. doi: 10.1016/j.ijantimicag.2018.02.017

Park, J. J., Seo, Y. B., Choi, Y. K., Kym, D., and Lee, J. (2019). Changes in the prevalence of causative pathogens isolated from severe burn patients from 2012 to 2017. *Burns* 46, 695–701. doi: 10.1016/j.burns.2019.09.008

Savari, M., Ekrami, A., Shoja, S., and Bahador, A. (2017). Plasmid borne Carbapenem-Hydrolyzing Class D beta-Lactamases (CHDLs) and AdeABC efflux pump conferring carbapenem-tigecycline resistance among *Acinetobacter baumannii* isolates harboring TnAbaRs. *Microb. Pathog.* 104, 310–317. doi: 10.1016/j.micpath.2017.01.045

Sawa, T., Kooguchi, K., and Moriyama, K. (2020). Molecular diversity of extended-spectrum beta-lactamases and carbapenemases, and antimicrobial resistance. *J. Intensive Care* 8:13.

Sheikhalizadeh, V., Hasani, A., Ahangarzadeh, R. M., Rahmati-Yamchi, M., Hasani, A., Ghotaslou, R., et al. (2017). Comprehensive study to investigate the role of various aminoglycoside resistance mechanisms in clinical isolates of *Acinetobacter baumannii*. *J. Infect. Chemother.* 23, 74–79. doi: 10.1016/j.jiac.2016.09.012

Singkham-In, U., and Chatsuwan, T. (2018). In vitro activities of carbapenems in combination with amikacin, colistin, or fosfomycin against carbapenem-resistant *Acinetobacter baumannii* clinical isolates. *Diagn. Microbiol. Infect. Dis.* 91, 169–174. doi: 10.1016/j.diagmicrobio.2018.01.008

Stewart, N. K., Smith, C. A., Antunes, N. T., Toth, M., and Vakulenko, S. B. (2019). Role of the hydrophobic bridge in the carbapenemase activity of class D beta-lactamases. *Antimicrob. Agents Chemother.* 63:e02191-18.

Tenover, F. C., Arbeit, R. D., Goering, R. V., Mickelsen, P. A., Murray, B. E., Persing, D. H., et al. (1995). Interpreting chromosomal DNA restriction patterns produced by pulsed-field gel electrophoresis: criteria for bacterial strain typing. *J. Clin. Microbiol.* 33, 2233–2239. doi: 10.1128/jcm.33.9.2233-2239.1995

Uddin, F., McHugh, T. D., Roulston, K., Platt, G., Khan, T. A., and Sohail, M. (2018). Detection of carbapenemases, AmpC and ESBL genes in *Acinetobacter* isolates from ICUs by DNA microarray. *J. Microbiol. Methods* 155, 19–23. doi: 10.1016/j.mimet.2018.11.004

Vauchel, T., Pirracchio, R., Chaussard, M., Lafaurie, M., Rouveau, M., Rousseau, C., et al. (2019). Impact of an *Acinetobacter baumannii* outbreak on kidney events in a burn unit: a targeted machine learning analysis. *Am. J. Infect. Control* 47, 435–438. doi: 10.1016/j.ajic.2018.09.010

Venditti, C., Vulcano, A., D'Arezzo, S., Gruber, C., Selleri, M., Antonini, M., et al. (2019). Epidemiological investigation of an *Acinetobacter baumannii* outbreak using core genome multilocus sequence typing. *J. Glob. Antimicrob. Resist.* 17, 245–249. doi: 10.1016/j.jgar.2018.11.027

Wang, Y. C., Ku, W. W., Yang, Y. S., Kao, C. C., Kang, F. Y., Kuo, S. C., et al. (2020). Is polymicrobial bacteremia an independent risk factor for mortality in *Acinetobacter baumannii* bacteremia? *J. Clin. Med.* 9:153. doi: 10.3390/jcm9010153

Xie, R. Q., Zhang, X. H. D., Zhao, Q., Peng, B., and Zheng, J. (2018). Analysis of global prevalence of antibiotic resistance in *Acinetobacter baumannii* infections disclosed a faster increase in OECD countries. *Emerg. Microbes Infect.* 7:31.

Xiong, W. G., Sun, Y. X., Ding, X. Y., Wang, M. Z., and Zeng, Z. L. (2015). Selective pressure of antibiotics on ARGs and bacterial communities in manure-polluted freshwater-sediment microcosms. *Front. Microbiol.* 11:194. doi: 10.3389/fmicb.2015.00194

Yang, Y. S., Chen, H. Y., Hsu, W. J., Chou, Y. C., Perng, C. L., Shang, H. S., et al. (2019). Overexpression of AdeABC efflux pump associated with tigecycline resistance in clinical *Acinetobacter nosocomialis* isolates. *Clin. Microbiol. Infect.* 25, 511–512.

Yoon, E. J., Courvalin, P., and Grillot-Courvalin, C. (2013). RND-type efflux pumps in multidrug-resistant clinical isolates of *Acinetobacter baumannii*: major role for AdeABC overexpression and AdeR-S mutations. *Antimicrob. Agents Chemother.* 57, 2989–2995. doi: 10.1128/aac.02556-12

Yu, X., Wang, R., Peng, W., Huang, H., Liu, G., Yang, Q., et al. (2019). Incidence, distribution and clinical relevance of microbial contamination of preservation solution in deceased kidney transplant recipients: a retrospective cohort study from China. *Clin. Microbiol. Infect.* 25, 595–600. doi: 10.1016/j.cmi.2018.12.040

Zhu, L. J., Chen, X. Y., and Hou, P. F. (2019). Mutation of CarO participates in drug resistance in imipenem-resistant *Acinetobacter baumannii*. *J. Clin. Lab. Anal.* 33:e22976.

Conflict of Interest: The authors declare that the research was conducted in the absence of any commercial or financial relationships that could be construed as a potential conflict of interest.

frontiers in Microbiology

ORIGINAL RESEARCH
published: 11 March 2021
doi: 10.3389/fmicb.2021.602724

Overexpression of Efflux Pumps, Mutations in the Pumps' Regulators, Chromosomal Mutations, and AAC(6′)-Ib-cr Are Associated With Fluoroquinolone Resistance in Diverse Sequence Types of Neonatal Septicaemic *Acinetobacter baumannii*: A 7-Year Single Center Study

Subhasree Roy[1], Somdatta Chatterjee[1†], Amrita Bhattacharjee[1], Pinaki Chattopadhyay[2], Bijan Saha[2], Shanta Dutta[1] and Sulagna Basu[1]*

[1] Division of Bacteriology, Indian Council of Medical Research (ICMR)-National Institute of Cholera and Enteric Diseases, Kolkata, India, [2] Department of Neonatology, Institute of Post-Graduate Medical Education and Research, Kolkata, India

This study investigates susceptibility toward three fluoroquinolones (ciprofloxacin, levofloxacin, moxifloxacin), multiple fluoroquinolone-resistance mechanisms, and epidemiological relationship of neonatal septicaemic *Acinetobacter baumannii*. Previous studies on fluoroquinolone resistance in *A. baumannii* focused primarily on ciprofloxacin susceptibility and assessed a particular mechanism of resistance; a more holistic approach was taken here. Epidemiological relationship was evaluated by Multi Locus Sequence Typing. Minimum Inhibitory Concentrations of fluoroquinolones was determined with and without efflux pump inhibitors. Overexpression of efflux pumps, resistance-nodulation-cell-division (RND)-type, and multidrug and toxic compound extrusion (MATE)-type efflux pumps were evaluated by reverse transcriptase-qPCR. Mutations within regulatory proteins (AdeRS, AdeN, and AdeL) of RND-pumps were examined. Chromosomal mutations, presence of *qnr* and *aac(6′)-Ib-cr* were investigated. *A. baumannii* were highly diverse as 24 sequence-types with seven novel STs (ST-1440/ST-1441/ST-1481/ST-1482/ST-1483/ST-1484/ST-1486) were identified among 47 *A. baumannii.* High resistance to ciprofloxacin (96%), levofloxacin (92%), and particularly moxifloxacin (90%) was observed, with multiple mechanisms being active. Resistance to 4th generation fluoroquinolone (moxifloxacin) in neonatal isolates is worrisome. Mutations within GyrA (S83L) and ParC (S80L) were detected in more than 90% of fluoroquinolone-resistant *A. baumannii* (FQRAB) spread across 10 different clonal complexes

Edited by:
Rustam Aminov, University of Aberdeen, United Kingdom

Reviewed by:
Bela Kocsis, Semmelweis University, Hungary
Benjamin Andrew Evans, University of East Anglia, United Kingdom

***Correspondence:**
Sulagna Basu
basus.niced@gov.in; supabasu@yahoo.co.in

†Present address:
Somdatta Chatterjee, Environmental Health and Disease Laboratory, Department of Environmental Health Sciences, University of South Carolina, Columbia, SC, United States

Specialty section:
This article was submitted to Antimicrobials, Resistance and Chemotherapy, a section of the journal Frontiers in Microbiology

Received: *04 September 2020*
Accepted: *21 January 2021*
Published: *11 March 2021*

Citation:
Roy S, Chatterjee S, Bhattacharjee A, Chattopadhyay P, Saha B, Dutta S and Basu S (2021) Overexpression of Efflux Pumps, Mutations in the Pumps' Regulators, Chromosomal Mutations, and AAC(6′)-Ib-cr Are Associated With Fluoroquinolone Resistance in Diverse Sequence Types of Neonatal Septicaemic Acinetobacter baumannii: A 7-Year Single Center Study. Front. Microbiol. 12:602724. doi: 10.3389/fmicb.2021.602724

(CC1/CC2/CC10/CC25/CC32/CC126/CC149/CC216/CC218/CC513). Efflux-based FQ resistance was found in 65% of FQRAB with ≥2 different active pumps in 38% of strains. Overexpression of *adeB* was highest (2.2−34-folds) followed by *adeJ*, *adeG*, and *abeM*. Amino acid changes in the regulators (AdeRS/AdeN/AdeL) either as single or multiple substitutions substantiated the overexpression of the pumps. Diverse mutations within AdeRS were detected among different CCs whereas mutations within AdeN linked to CC10 and CC32. Chromosomal mutations and active efflux pumps were detected simultaneously among 64% of FQRAB. Presence of *aac(6′)-Ib-cr* was also high (74% of FQRAB) but *qnrS* were absent. As most FQRABs had chromosomal mutations, this was considered predominant, however, isolates where pumps were also active had higher MIC values, establishing the critical role of the efflux pumps. The high variability of FQ susceptibility among FQRAB, possessing the same set of mutations in *gyrA*, *parC,* and efflux pump regulators, was also noted. This reveals the complexity of interpreting the interplay of multiple resistance mechanisms in *A. baumannii*.

Keywords: *A. baumannii*, neonatal sepsis, sequence types, ciprofloxacin/levofloxacin/moxifloxacin, RND pumps, AdeRS/AdeL/AdeN, *gyrA*/*parC*, India

INTRODUCTION

Acinetobacter baumannii remains in the forefront as a nosocomial pathogen, causing infections and outbreaks in adults and neonates (Qu et al., 2016; Hujer et al., 2017; Gramatniece et al., 2019). Studies from our laboratory have shown the clinical significance of *A. baumannii* infection and colonization among neonates (Roy et al., 2010; Chatterjee et al., 2016). The ability to survive under unfavorable conditions and the propensity to acquire resistance determinants has made infections with this pathogen difficult to treat in intensive care units (Asif et al., 2018).

In comparison to broad-spectrum cephalosporins and aminoglycosides, fluoroquinolones (FQs) are more active in reduction of infections caused by a wide range of Gram-positive and Gram-negative pathogenic bacteria including *A. baumannii.* However, a high rate of resistance to FQs was also detected (Lopes and Amyes, 2013; Ardebili et al., 2015). WHO indicated these antibiotics as the highest priority agents among the Critically Important Antimicrobials for Human Medicine (World Health Organization, 2019).

There are now four generations of quinolone/fluoroquinolone antibiotics in clinical use, among which, the most commonly prescribed FQs in current medical practice are ciprofloxacin, levofloxacin, and moxifloxacin (Redgrave et al., 2014). All FQs target DNA gyrase and topoisomerase IV, involved in the process of DNA replication, with varying efficiency in different bacteria. However, subsequent studies found that in a given bacterial species, different fluoroquinolones have been shown to have different primary targets. The issue of quinolone targeting is still a matter of debate, and the relative contributions of gyrase vs. topoisomerase IV to quinolone action need to be evaluated on a species-by-species and drug-by-drug basis (Ferrara, 2007; Aldred et al., 2014). Chromosomal mutations in the quinolone resistance determining regions (QRDRs) of DNA gyrase subunit A (*gyrA*) or topoisomerase IV subunit C (*parC*) is a well-recognized mechanism of FQ resistance in *A. baumannii* (Redgrave et al., 2014). Another important mechanism is overexpression of efflux pumps (Redgrave et al., 2014). To date, three RND-family (resistance nodulation division) pumps AdeABC, AdeIJK, AdeFGH, and one MATE-family (multidrug and toxic compound extrusion) pump AbeM have been reported to be associated with efflux of FQs in *A. baumannii* (Marchand et al., 2004; Su et al., 2005; Damier-Piolle et al., 2008; Coyne et al., 2010). Efflux pump genes are chromosomally encoded and controlled by regulators. AdeRS, a two-component regulatory system regulates the expression of AdeABC pump. Expression level of AdeFGH is controlled by a LysR-type transcription regulator AdeL whereas AdeN, a TetR-like transcription regulator, represses expression of AdeIJK. In addition, plasmid-mediated quinolone resistance determinants (PMQRs) such as *qnr* have been identified in *A. baumannii,* though infrequently (Touati et al., 2008; Jiang et al., 2014; Yang et al., 2015). Another PMQR, *aac(6′)-Ib-cr* is a variant of an aminoglycoside acetyltransferase that contains two specific point mutations, Trp102Arg and Asp179Tyr. This enzyme modifies only ciprofloxacin and norfloxacin by N-acetylation at the amino nitrogen on its piperazinyl substituent. These two mutations are required for quinolone acetylating activity. Acetylation of fluoroquinolones by AAC(6′)-Ib-cr decrease drug activity and provides low-level resistance to fluoroquinolones (Aldred et al., 2014; Rodríguez-Martínez et al., 2016).

The rate of antimicrobial resistance in India is high. The consumption of FQs is higher in India in comparison to cephalosporins and macrolides (Laxminarayan and Chaudhury, 2016; Farooqui et al., 2018). Empirical treatment for neonatal sepsis, recommended in current WHO guidelines is intravenous ampicillin (or penicillin) plus gentamicin for 7 days. Fluoroquinolones could be an option as second line for sepsis or severe infection due to MDR bacteria. Though the use of this antibiotic is restricted in the pediatric population due to its potential toxicity, judicial and appropriate use of this class of drug can be a choice for the treatment of sepsis among neonates (Fuchs et al., 2016). A thorough evaluation of

the susceptibility of these pathogens toward different classes of FQs and the resistance mechanisms would thus make this study clinically relevant.

To date, majority of the studies on fluoroquinolone resistance in *A. baumannii* focused on only ciprofloxacin resistance and studied either chromosomal mutations (Spence and Towner, 2003; Hujer et al., 2009; Park et al., 2011; Liu et al., 2012; Ardebili et al., 2015) or AdeABC pump (Park et al., 2011; Lopes and Amyes, 2013; Ardebili et al., 2014). It is necessary to study the susceptibility of higher generation FQs such as moxifloxacin among diverse sequence types of *A. baumannii* in comparison to all known clinically important older fluoroquinolones over time and correlate the contribution of all possible mechanisms simultaneously in a single isolate. Till now, none of the previous studies have delineated all these mechanisms simultaneously. To fill this gap in knowledge, this study aims to evaluate (i) susceptibility pattern of the three most clinically important FQs (ciprofloxacin, levofloxacin, and moxifloxacin) in neonatal septicaemic *A. baumannii*, (ii) prevalence of different sequence types (STs) among neonatal septicaemic *A. baumannii* in a single center, (iii) role of the chromosomal mutations (*gyrA* and *parC* genes) in FQ resistance, (iv) role of RND and MATE-family efflux pumps in FQ resistance, (v) association of mutations found within regulators of RND pumps with overexpression of efflux pumps, and (vi) role of PMQRs in FQ resistance.

MATERIALS AND METHODS

Bacterial Isolates and Multi Locus Sequence Typing (MLST)

A total of 47 *A. baumannii* were collected by standard procedure from blood of septicaemic neonates admitted to the NICU (Neonatal Intensive Care Unit) of IPGMER hospital, Kolkata, India during 2009–2015. Identification of *A. baumannii* isolates was initially confirmed by the VITEK 2 compact system (BioMérieux, Marcy l'Etoile, France).

Identification of *A. baumannii* was further confirmed by Multi Locus Sequence Typing using the MLST Pasteur Scheme[1] which uses internal fragments of the seven housekeeping genes (*cnp60*, *fusA*, *gltA*, *pyrG*, *recA*, *rplB,* and *rpoB*). Global optimal eBURST (goeBURST) analysis was performed using the software goeBURST 1.2.1 version available on the website to assign the STs into respective clonal complexes (goeburst.phyloviz.net) and were defined as single locus (SLVs), double loci variants (DLVs), and triple loci variants (TLVs).

Determination of Susceptibility to FQs

MIC (Minimum Inhibitory Concentration) of FQs was determined using broth microdilution method and resistance was interpreted according to EUCAST breakpoints (European Committee on Antimicrobial Susceptibility Testing) for *Acinetobacter* spp. (ciprofloxacin: resistant > 1 mg/L and levofloxacin: resistant > 1 mg/L) (Rules, 2018). The breakpoint of moxifloxacin was not available for *Acinetobacter* spp. in EUCAST. As breakpoints of resistance for ciprofloxacin and levofloxacin in Enterobacteriaceae (ciprofloxacin: resistant > 0.5 mg/L and levofloxacin: resistant > 1 mg/L) were quite comparable to *Acinetobacter* in EUCAST, thus the moxifloxacin resistance breakpoint for Enterobacteriaceae (resistant > 0.25 mg/L) in EUCAST was used for *A. baumannii*. The MIC_{90} values over time for all FQs were also calculated.

Susceptibility towards other antimicrobials like ceftazidime (resistant ≥ 32 mg/L), cefepime (resistant ≥ 32 mg/L), meropenem (resistant ≥ 8 mg/L), imipenem (resistant ≥ 8 mg/L), amikacin (resistant > 64 mg/L), and minocycline (resistant ≥ 16 mg/L) was determined by VITEK 2 compact system and interpreted according to CLSI (Clinical and Laboratory Standards Institute) breakpoints (Clinical and Laboratory Standards Institute [CLSI], 2019). MIC of colistin was determined by broth microdilution method and interpreted according to CLSI breakpoints (resistant ≥ 4 mg/L).

Genotypic Characterization of the FQ-Resistant Strains

The QRDRs of the *gyrA* and *parC* genes were PCR amplified and subsequently sequenced (Valentine et al., 2008; Hujer et al., 2009). *A. baumannii* ATCC 17978 was used as reference for sequence comparison. The 5′- and 3′-nucleotide positions of the primers used to amplify the full QRDR region of *gyrA* and *parC*, the annealing temperatures and respective product sizes are mentioned in **Supplementary Table S1**. RND-family efflux pump genes (*adeB, adeJ, adeG*) and MATE-family efflux pump gene (*abeM*) were screened by PCR and PMQR determinants (*qnrA*, *qnrB,* and *qnrS*) were also checked (Cattoir et al., 2007; Rumbo et al., 2013). *aac(6′)-Ib* was amplified with primers known to amplify all known *aac(6′)-Ib* variants (Park et al., 2006). Specific bands were digested with BtscI (New England Biolabs, MA) to identify *aac(6′)-Ib-cr* responsible for ciprofloxacin resistance (Park et al., 2006).

Responsiveness of the Strains to Efflux Pump Inhibitors

To understand the extent of involvement of efflux pumps in the FQ resistance phenotype, susceptibility to FQs in the presence of two efflux pump inhibitors (EPI), namely phenylalanine arginine β-naphthylamide (PAβN; Sigma) and 1-(1-naphtylmethyl)-piperazine (NMP; Sigma) at 50 mg/L was tested (Pannek et al., 2006; Blanchard et al., 2014). A significant inhibition was defined as a 4-fold or greater reduction of MIC in the presence of efflux pump inhibitors (Pannek et al., 2006). Previous studies of *A. baumannii* also showed the use of PAβN and NMP at 50 mg/L or even higher (100 mg/L) concentration to establish efflux mediated resistance (Pannek et al., 2006; Valentine et al., 2008; Blanchard et al., 2014). To rule out any bactericidal activity of the inhibitors (PAβN and NMP) at the concentrations used in the study (50 mg/L), MIC value for the two inhibitors was determined in the absence of antibiotics for half of the isolates chosen randomly amongst those showing reduction of FQ MIC in presence of inhibitors.

[1] https://pubmlst.org/abaumannii/

Reverse Transcriptase Quantitative PCR (RT-qPCR)

Strains which showed ≥ 4-fold reduction of MIC for FQs were considered for overexpression study of RND-family pump genes (*adeB*, *adeJ*, *adeG*) and MATE-family pump gene (*abeM*) by RT-qPCR. The expression of pump genes was normalized to the housekeeping gene (16S rRNA).

Total RNA was initially extracted from 1 ml (about 10^8 cells/ml) of mid-logarithmic bacterial cultures using Nucleospin RNA isolation kit (Nucleospin, Macherey-Nagel, Düren). Contaminating DNA was removed by RNase-free DNase I (New England Biolabs, United States). The concentrations and purity of RNA were quantified with a spectrophotometer at 260 and 280 nm (260/280 ratio of > 1.8). Reverse transcription was performed with 2 μg of RNA according to manufacturer's instructions using the high-capacity cDNA reverse transcription kit (Applied Biosystems, Warrington, United Kingdom).

Quantification of the expression of the target genes was performed with Power SYBR Green PCR Master Mix (Applied Biosystems) using the StepOne Plus Real-Time PCR System and software (Applied Biosystems, United States) according to the manufacturer's instructions. Oligonucleotide primer sequences used for pump genes and 16S rRNA is shown in **Supplementary Table S1**. After a 10 min activation of the modified Taq polymerase at 95°C, 40 cycles of 30 s at 95°C, 45 s at 55°C or 58°C and 1 min at 60°C were performed. Data were acquired at 60°C. The relative gene expression (ΔCT) for pump genes transcripts was calculated against that for the 16S rRNA gene (ΔCT of test gene = *CT* of test gene- *CT* of 16S), and the $\triangle\triangle CT$ was calculated against that for the ciprofloxacin-susceptible strain, *A. baumannii* ATCC 19606 (expression = 1), which served as the control. Relative expression level of pump genes was calculated by the $2^{-\Delta\Delta\ CT}$ method. An effect on gene expression was considered significant when the corresponding ratios were > 2.0.

Nucleotide Sequencing of Pump Regulatory Elements

The regulatory components of AdeABC pump (AdeR and AdeS) were investigated for strains overexpressing *adeB* gene (≥2-fold in real time analysis). PCR and sequencing of *adeS* gene were carried out according to Rumbo et al. (2013). AdeR, AdeN (regulator of AdeIJK pump), and AdeL (regulator of AdeFGH pump) were sequenced with the primers designed in this study using Primer Premier 5.0 software (**Supplementary Table S1**).

RESULTS AND DISCUSSION

MLST Profiles of *A. baumannii*

Analysis of Sequence Types (STs) of the 47 *A. baumannii* isolates identified 24 different STs among which seventeen were previously described STs (ST-1, ST-2, ST-7, ST-10, ST-25, ST-32, ST-149, ST-526, ST-575, ST-622, ST-623, ST-625, ST-767, ST-902, ST-905, ST-976, ST-1406). Seven novel STs (ST-1440, ST-1441, ST-1481, ST-1482, ST-1483, ST-1484, ST-1486) were identified and deposited in the MLST database (see text footnote 1). The predominant ST in this study was ST-149 ($n = 6$, 13%). ST profiles of the 47 clinical isolates of *A. baumannii* are summarized in **Table 1**.

goeBURST analysis showed that all 47 *A. baumannii* isolates were highly diverse. Isolates were clustered into 10 clonal complexes, **CC1** (ST-1, ST-7, ST-623 and ST-902); **CC2** (ST-2 and ST-526); **CC10** (ST-10, ST-575, ST-1406 and ST-1483); **CC25** (ST-25); **CC32** (ST-32 and ST-905); **CC149** (ST-149, ST-622 and ST-1482); **CC216** (ST767); **CC218** (ST-1440); **CC513** (ST-625); **CC126** (ST-1441). Four STs (ST976, ST1481, ST1484, and ST1486) were found to be singletons since they did not share any homology with the known STs in the data base (**Table 1** and **Figure 1**). Among these singletons, ST-1484 and ST-1486 were novel STs.

Susceptibility of the Organisms

Ninety-six percent, 92%, and 90% of *A. baumannii* were resistant to ciprofloxacin, levofloxacin, and moxifloxacin, respectively. The majority of isolates (98%) showed high resistance to ciprofloxacin (MIC ≥ 32 mg/L). On the other hand, 80 and 70% of the strains showed MIC of ≥ 8 mg/L for levofloxacin and moxifloxacin, respectively. Only two strains (A_126, A_135) were susceptible to all three FQs tested (**Table 1**). The strains were highly resistant not only to ciprofloxacin and levofloxacin, but also to 4th generation FQ, moxifloxacin, which is contrary to previous reports (Heinemann et al., 2000; Spence and Towner, 2003; Liu et al., 2012). This indicates that even the higher generation FQ, such as moxifloxacin is not active against *A. baumannii*. This is probably a rare finding in case of neonatal septicaemic *A. baumannii*. The high FQ resistance among *A. baumannii* may be due to excessive use or exploitation of these agents worldwide for different therapeutic purposes or the presence of multiple mechanisms that have been found to be functional in *A. baumannii*. Since most of the *A. baumannii* were resistant to ciprofloxacin (96%), levofloxacin (92%), and moxifloxacin (90%), thus susceptibility of the organisms toward FQs was not associated with a particular ST-type or clonal complex.

The overall (2009—2015) MIC_{90} values for the different FQs were as follows: ciprofloxacin, 256 mg/L; levofloxacin, 64 mg/L; and moxifloxacin, 32 mg/L, respectively. Comparison of MIC_{90} values for FQs also indicated that though levofloxacin or moxifloxacin MIC in each year was ≥ 4-fold lower in comparison to the MIC of ciprofloxacin but 90% of the strains in each year were resistant to these three FQs (**Figure 2**). This again indicated that most of the septicemic *A. baumannii* were highly resistant to older and newer clinically important FQs.

Besides fluoroquinolone resistance, organisms showed resistance to other antimicrobials such as ceftazidime (81%), cefepime (81%), meropenem (77%), imipenem (79%), aztreonam (94%), amikacin (66%) and colistin (9%). No resistance was detected for minocycline.

TABLE 1 | Multilocus Sequence typing (MLST), Clonal Complexes (CC), chromosomal mutations, presence of AAC(6′)-Ib-cr, and Minimum Inhibitory Concentration (MIC) values of ciprofloxacin (CIP), levofloxacin (LVX), and moxifloxacin (MOXI) with or without the presence of efflux pump inhibitors (EPI) (NMP and PAβN) in neonatal septicaemic *Acinetobacter baumannii* (*n* = 47).

Strain number/ MLST/clonal complex	Amino acid substitutions within QRDR	Silent mutations	PMQR	MIC in absence and presence of EPIs			Fold change in MIC in presence of EPI		
	GyrA/ ParC	GyrA and ParC	AAC(6′)-Ib-cr	CIP alone/ CIP+NMP/CIP+PAβN	LVX alone/ LVX+NMP/LVX+PAβN	MOXI alone/ MOXI+NMP/MOXI+PAβN	CIP+NMP/ CIP+PAβ N	LVX+NMP/ LVX+PAβ N	MOXI+NMP/ MOXI+PAβ N
A_112/ST-32/CC32	S83L/E84K	Ala193, Pro201 and Leu31, Gly107, Pro109, Lys113, Ala123, Lys124, Ser126, Ala159 Val174, Ala177	+	256/32/256	64/32/32	8/1/4	**8-fold/**NFC	2-fold/2-fold	**8-fold/**2-fold
A_113/ST-32/CC32	S83L/E84K	Ala193 and Leu31, Gly107, Pro109, Lys113, Ala123,Ala159,Val174, Ala177	+	64/16/64	4/4/4	4/4/4	**4-fold/**NFC	NFC/NFC	NFC/NFC
A_115/ST-1441/CC126	NM/S80L	Gly114, Ala117,Ala172, Ala193,Pro201 and Ala22, Leu31,Ala48, Gly107,Pro109, Lys113,Ala123, Ala159,Val174	+	32/16/32	2/2/2	2/2/2	2-fold/NFC	NFC/NFC	NFC/NFC
A_117/ST-10/CC10	S83L/S80L	Ala193 and Ala22, Leu31,Ala48, Gly107,Pro109, Lys113,Ala123, Ala159,Val174	-	256/64/256	8/2/4	2/1/2	**4-fold/**NFC	**4-fold/**2-fold	2-fold/NFC
A_118/ST-1486/Singleton	S83L/NM	Ala193 and Leu31, Gly107, Pro109, Lys113, Ala123, Iso155, Ala159, Leu166,Thre169, Thre170, Iso172, Ala177	-	8/4/4	0.25/ND/ND	0.125/ND/ND	2-fold/2-fold	ND/ND	ND/ND
A_120/ST-25/CC25	S83L/S80L	Nil and Leu31, Ala48,Ser108, Asp110,Ser114, Ala123,Ala159, Val174	+	32/32/32	4/4/4	2/2/2	NFC/NFC	NFC/NFC	NFC/NFC
A_123/ST-622/CC149	S83L/S80L	Ala172, Ala193 and Leu31, Tyr95, Pro98, Leu99, Iso100, Gly102, Gly107, Pro109 Lys113, Ala123,Ala159, Val174	+	32/32/32	16/16/8	8/4/8	NFC/NFC	NFC/2-fold	2-fold/NFC
A_124/ST-1440/CC218	NM/NM	Gly114, Ala117,Ala193 and Leu31, Ala85, Tyr87, Ala123,Ala159, Leu165,Val174	+	256/64/256	0.25/ND/ND	0.125/ND/ND	**64-fold/**NFC	ND/ND	ND/ND
A_125/ST-2/CC2	S83L/S80L	Pro160, Ala193,Ala196 and Leu31, Ala48,Gly107, Pro109,Ala123, Ala159, Val174	+	32/16/32	8/8/8	4/0.125/4	2-fold/NFC	NFC/NFC	**32-fold/**NFC
A_126/ST-767/CC216	NM/NM	Gly114, Ala117, Ala193 and Leu31, Ala48,Lys61, Iso100, Ala159, Val174	-	0.25/ND/ND	0.25/ND/ND	0.25/ND/ND	ND/ND	ND/ND	ND/ND
A_130/ST-575/CC10	S83L/S80L	Ala193, Ala196 and Leu31, Asp36, Gly107, Pro109, Lys113, Ala123, Iso155, Thre156, Ala159, Leu166, Thre169 Thre170, Iso172, Ala177	-	32/8/16	8/8/8	8/1/2	**4-fold/**2-fold	NFC/NFC	**8-fold/4-fold**
A_131/ST-902/CC1	S83L/S80L	Ala193, Pro201 and Ala22, Leu31,Ala48, Gly107,Pro109, Lys113,Ala123, Ala159,Val174	+	64/0.5/32	4/4/4	4/0.25/4	**128-fold/** 2-fold	NFC/NFC	**16-fold/**NFC
A_132/ST-10/CC10	S83L, E87Q/S80L	Ala193 and Ala22, Leu31,Ala48, Gly107,Pro109, Lys113,Ala123, Ala159,Val174	-	512/64/128	64/32/32	16/0.25/8	**4-fold/**2-fold	2-fold/2-fold	**64-fold/**NFC
A_133/ST-1406/CC10	S83L/S80L	Ala193 and Leu31, Gly107, Pro109, Lys113, Ala123, Iso155, Thre156, Ala159, Leu166, Thre169, Thre170, Iso172, Ala177	+	32/16/16	8/8/4	8/4/4	2-fold/2-fold	NFC/2-fold	NFC/NFC
A_134/ST-1482/CC149	S83L/S80L	Ala193, Pro201 and Ala22, Leu31,Ala48, Gly107,Pro109, Lys113,Ala123, Ala159,Val174	+	256/256/256	32/16/16	32/16/16	NFC/NFC	2-fold/2-fold	2-fold/NFC
A_135/ST-1481/Singleton	NM/NM	Gly114, Ala117, Iso168, Ala172 And Leu31, Pro98, Leu99, Gly107, Ala123, Gly139, Ala159, Val174	-	1/1/1	1/1/1	0.0625/ND/ ND	NFC/NFC	NFC/NFC	ND/ND
A_136/ST-149/CC149	S83L/S80L	Ala172, Ala193 and Ala22, Leu31,Ala48, Gly107,Pro109, Lys113,Ala123, Ala159,Val174	-	256/64/64	32/4/16	8/0.125/4	**4-fold/4-fold**	**8-fold/**2-fold	**64-fold/**2-fold
A_138/ST-905/CC32	S83L/S80L	Ala193, Pro201 and Ala22, Leu31,Ala48, Gly107, Lys113, Ala123,Ala159,Val174	-	64/16/32	8/2/4	4/4/4	**4-fold/**2-fold	**4-fold/**2-fold	NFC/NFC
A_141/ST-149/CC149	S83L/S80L	Ala172, Ala193 and Ala22, Leu31,Ala48, Gly107, Ala123, Ala159	-	128/64/128	64/32/32	32/16/16	2-fold/NFC	2-fold/2-fold	2-fold/NFC
A_145/ST-149/CC149	S83L/S80L	Ala193, Ala196, Pro201 and Ala22, Leu31,Ala48, Gly107,Pro109, Lys113,Ala123, Ala159,Val174	-	256/256/128	64/16/32	32/0.5/16	NFC/2-fold	**4-fold/**2-fold	**64-fold/**NFC
A_146/ST-1406/CC10	S83L/S80L	Ala172, Ala193 and Leu31, Tyr95, Arg96, Pro98, Iso100, Gly107, Pro109, Lys113, Ala123, Gly139, Ala159, Val174	+	64/16/32	16/8/8	8/0.125/2	**4-fold/**2-fold	2-fold/2-fold	**64-fold/4-fold**
A_147/ST-1482/CC149	S83L/S80L	Ala172, Ala193 and Ala22, Leu31,Ala48,Gly107, Ala123,Ala159	+	256/256/256	64/32/32	16/16/16	NFC/NFC	2-fold/2-fold	NFC/NFC

(Continued)

TABLE 1 | Continued

Strain number/ MLST/clonal complex	Amino acid substitutions within QRDR	Silent mutations	PMQR	MIC in absence and presence of EPIs			Fold change in MIC in presence of EPI		
	GyrA/ ParC	GyrA and ParC	AAC(6′)-Ib-cr	CIP alone/ CIP+NMP/CIP+PAβN	LVX alone/ LVX+NMP/LVX+PAβN	MOXI alone/ MOXI+NMP/MOXI+PAβN	CIP+NMP/ CIP+PAβ N	LVX+NMP/ LVX+PAβ N	MOXI+NMP/ MOXI+PAβ N
A_149/ST-149/CC149	S83L/S80L	Ala172, Ala193, Pro201 and Ala22, Leu31,Ala48, Gly107,Pro109, Lys113,Ala123, Ala159,Val174	+	256/32/64	64/16/32	16/4/8	**8-fold/4-fold**	**4-fold/**2-fold	**4-fold/**2-fold
A_150/ST-10/CC10	S83L/S80L	Ala193, Pro201 and Leu31,Gly107,Pro109,Lys113,Ala123,Iso155, Thre156,Ala159 Leu166,Thre169,Ala177	+	32/16/32	8/4/4	8/1/4	2-fold/NFC	2-fold/2-fold	**8-fold/**2-fold
A_151/ ST-623/CC1	S83L/S80L	Ala193, Pro201 and Ala22, Leu31,Ala48, Gly107, Lys113, Ala123,Ala159,Val174,Tyr209	+	32/16/32	8/4/4	8/8/8	2-fold/NFC	2-fold/2-fold	NFC/NFC
A_152/ST-623/CC1	S83L/S80L	Ala193 and Ala22, Leu31,Ala48, Gly107, Lys113, Ala123,Ala159,Val174	+	64/4/64	8/2/8	8/4/4	**16-fold/**NFC	**4-fold/**NFC	2-fold/2-fold
A_153/ST-623/CC1	S83L/S80L	Ala193, Pro201 and Ala22, Ala48,Gly107, Pro109,Lys113, Ala123,Ala159, Ala207	+	64/4/64	8/4/4	4/0.125/4	**16-fold/**NFC	2-fold/2-fold	**32-fold/**NFC
A_155/ST-10/CC10	S83L/S80L	Ala193, Pro201 and Leu31, Asp36, Gly107, Pro109, Lys113, Ala159, Leu166, Thre169, Thre170, Gly175	-	128/32/128	64/8/32	32/16/16	**4-fold/**NFC	**8-fold/**2-fold	2-fold/2-fold
A_158/ST-1483/CC10	S83L/S80L	Ala193 and Ala22, Leu31,Ala48, Gly107, Lys113, Ala123,Ala159,Val174	+	512/64/32	128/32/32	16/16/16	**8-fold/ 16-fold**	**4-fold/4-fold**	NFC/NFC
A_159/ST-1483/CC10	S83L/S80L	Ala193 and Leu31, Gly107,Lys113, Ala123, Iso155, Ala159 Leu166, Thre169,Thre170, Iso172, Ala177	+	512/128/256	128/32/64	32/8/8	**4-fold/**2-fold	**4-fold/**2-fold	**4-fold/4-fold**
A_160/ST-1/CC1	S83L/S80L	Ala193, Pro201 and Leu31, Tyr95, Pro98, Iso100, Aspg105, Asp111, Thre121, Gly137, Ala159, Val188, Val189, Ala194	+	128/4/128	32/16/32	16/16/16	**32-fold/**NFC	2-fold/NFC	NFC/NFC
A_161/ST-149/CC149	S83L/S80L	Gly170, Ala172 and Ala22, Leu31, Met49, Ser108, Asp110, Pro112, Ser114, Leu125, Val174	+	256/64/128	64/32/32	32/32/32	**4-fold/**2-fold	2-fold/2-fold	NFC/NFC
A_162/ST-140CC10	S83L/S80L	Ala193, Pro201 and Leu31, Gly107, Pro109, Phe115, Ala123, Iso155,Aspg167, Ala177	+	64/32/32	32/2/32	8/0.25/2	2-fold/2-fold	**16-fold/**NFC	**32-fold/4-fold**
A_163/ST-575/CC10	S83L/S80L	Ala193, Pro201 and Ala22, Leu31,Ala48, Gly107, Pro109, Lys113, Ala123,Ala159, Val174	+	64/16/32	8/8/4	4/0.125/2	**4-fold/**2-fold	NFC/2-fold	**32-fold/**2-fold
A_166/ST-625/CC513	S83L/S80L	Ala117, Thre128, Pro201 and Ala22, Leu31,Ala48, Gly107, Pro109, Lys113, Ala123,Ala159, Val174	+	64/32/64	8/4/8	8/0.25/8	2-fold/NFC	2-fold/NFC	**32-fold/**NFC
A_167/ST-2/CC2	S83L/S80L	Ala193, Pro201 and Ala22, Leu31,Ala48, Gly107, Pro109, Lys113, Ala123,Ala159, Val174	-	64/64/64	16/8/8	8/0.25/8	NFC/NFC	2-fold/2-fold	**32-fold/**NFC
A_168/ST-149/CC149	S83L/S80L	Ala172, Ala193 and Ala22, Leu31,Ala48, Gly107, Pro109, Lys113, Ala123,Ala159, Val174	-	256/256/256	32/32/32	16/16/16	NFC/NFC	NFC/NFC	NFC/NFC
A_169/ST-976/Singleton	S83L/S80L	Pro201 and Ala22, Leu31,Ala48, Gly107, Pro109, Lys113, Ala123,Ala159, Val174	+	128/128/128	4/4/4	0.5/0.5/0.5	NFC/NFC	NFC/NFC	NFC/NFC
A_170/ST-2/CC2	S83L/S80L	Ala193, Pro201 And Ala22, Leu31,Ala48, Gly107, Pro109, Lys113, Ala123,Ala159, Val174	+	256/128/128	16/16/8	16/16/16	2-fold/2-fold	NFC/2-fold	NFC/NFC
A_171/ST-976/Singleton	S83L/S80L	Pro201 and Leu31, Ala48, Gly107, Phe115, Ala123, Ala159, Val174	+	32/16/64	4/4/4	2/2/2	2-fold/NFC	NFC/NFC	NFC/NFC
A_172/ST-526/CC2	S83L/S80L	Ala193 and Leu31, Ala48, Gly107, Phe115, Ala123, Ala159, Val174	+	64/16/64	16/16/16	16/0.125/8	**4-fold/**NFC	NFC/NFC	**128-fold/** 2-fold
A_173/ST-526/CC2	S83L/S80L	Ala193, Pro201 and Ala22, Leu31,Ala48, Gly107, Pro109, Lys113, Ala123,Ala159, Val174	-	64/64/64	16/16/16	16/0.125/8	NFC/NFC	NFC/NFC	**128-fold/** 2-fold
A_176/ST-25/CC25	S83L/S80L	Ala193, Pro201 and Leu31, Ala48, Gly107, Phe115, Ala123, Ala159, Val174	+	64/32/64	4/4/4	4/4/4	2-fold/NFC	NFC/NFC	NFC/NFC
A_177/ST-1484/Singleton	S83L/S80L	Nil and Leu31, Ala48, Lys61, Iso100, Ala159, Val174	+	64/4/8	4/4/4	4/4/4	**16-fold/8-fold**	NFC/NFC	NFC/NFC
A_178/ST-622/CC149	S83L/S80L	Leu165, Ala193 and Ala22, Leu31,Ala48, Gly107, Pro109, Lys113, Ala123,Ala159, Val174	+	64/32/64	8/8/8	8/8/8	2-fold/NFC	NFC/NFC	NFC/NFC
A_179/ST-7/CC1	S83L/S80L	Ala172, Ala193 and Ala22, Leu31,Ala48, Gly107, Pro109, Lys113, Ala123,Ala159, Val174	+	64/32/64	8/2/4	8/4/8	2-fold/NFC	**4-fold/**2-fold	2-fold/NFC
A_180/ST-976/Singleton	S83L/S80L	Pro201 and Leu31, Ala48, Gly107, Phe115, Ala123, Ala159	+	32/32/32	4/4/4	2/2/2	NFC/NFC	NFC/NFC	NFC/NFC

NM=No mutation detected within QRDR of GyrA or ParC, ND = FQ MIC change in presence of efflux pump inhibitors were not determined for FQ susceptible A. baumannii isolates and written as ND, NFC = No fold change, FQ-resistant A. baumannii isolates which showed ≥4-fold MIC decrease in presence of efflux pump inhibitors were marked as bold and the strain number, sequence types, clonal complexes of these isolates were also indicated as bold.

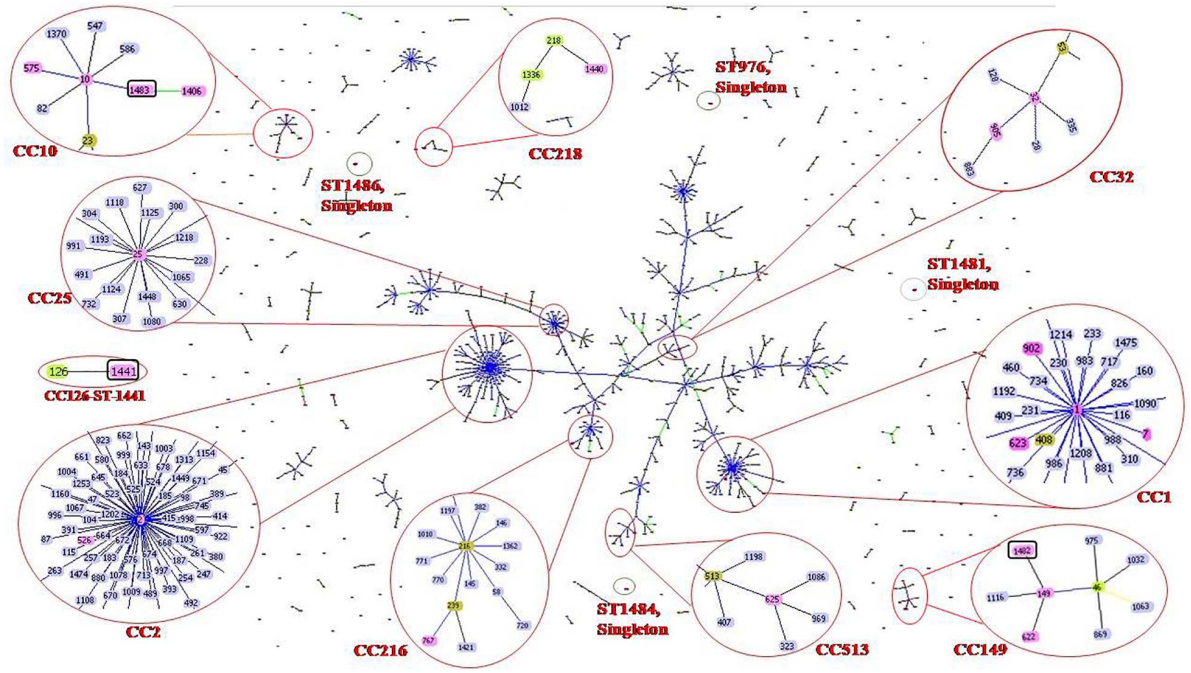

FIGURE 1 | Sequence types (STs) of neonatal septicaemic *Acinetobacter baumannii*. STs of 47 *A. baumannii* are shown in the context of all of the 1507 STs (as per Pasteur analysis) present in the global MLST database (http://www.pasteur.fr/mlst; as of July 2020). The scheme is constructed using the Global optimal eBURST (goeBURST) analysis. The Clonal Complexes (CCs) and STs observed in the present study are enlarged and circled with red color. STs from MLST data base are highlighted with light blue color, the STs identified in the study are highlighted with pink color, founder STs in each CC is highlighted with light green color although few STs (ST-1, ST-2, ST-10, ST-25, ST-32, ST-149) which are identified in this study and also the founder STs, are highlighted with pink. Seven novel STs are identified in the study among which three are related to known CCs, highlighted with pink color and circled with black color. Rest of the novel STs found as singletons is indicated as red dot, circled by black color. Single locus variants (SLVs) of the founder STs in a particular CC are linked by blue or black solid lines (SLV at two different loci for two different STs) and Double locus variants (DLV) are linked by green color solid lines. Numbers of all clonal complexes (CCs) to which the STs were identified in the study are classified.

Mutations Within QRDR of GyrA and ParC

The major mutations that were identified in this study were S83L (93%) and S80L (96%) within the QRDRs of GyrA and ParC in FQ-resistant *A. baumannii* (FQRAB) (**Table 1**). Though the information is not new, however, it collaborates with other earlier studies and underscores the importance of chromosomal mutations in FQ resistance. Mutations in the QRDRs of both GyrA/ParC alter the three-dimensional structure of the target protein. Alteration of the target protein structure reduces the affinity of quinolones for the enzyme-DNA complex (Hooper and Jacoby, 2015; Kivata et al., 2019). In this study, no amino acid sequence changes were observed at the other "hot spots" (Gly-81, and Ala-84) within the GyrA as reported previously (Valentine et al., 2008). Consistent with the literature (Vila, 2002), the FQRAB (98%, 44/45) which possessed both *gyrA* and *parC* mutations, had a ciprofloxacin MIC $\geq$ 32 mg/L. Isolate A_132 with ciprofloxacin MIC 512 mg/L, possessed more than one mutation (S83L and E87Q) within GyrA and also possessed S80L within ParC. On the other hand, isolate A_118 showed only S83L conversion within GyrA but no mutation within ParC and had a MIC of CIP 8 mg/L. This isolate was susceptible to levofloxacin and moxifloxacin. Similarly, another isolate A_115 with ciprofloxacin MIC 32 mg/L, showed only S80L conversion within ParC but no mutation within GyrA. This isolate was resistant to levofloxacin and moxifloxacin (MIC 2 mg/L) (**Table 1**). This indicated that a single *gyrA* mutation is sufficient to cause clinically significant levels of ciprofloxacin resistance (Maleki et al., 2014; Ardebili et al., 2015) but mutation within *parC* gene or more than one mutation within *gyrA* is necessary for high-level ciprofloxacin resistance in *A. baumannii* as reported previously (Vila, 2002; Spence and Towner, 2003). Moreover, S80L mutation within ParC is also necessary for levofloxacin and moxifloxacin resistance (Spence and Towner, 2003).

Two other FQRAB (A_112 and A_113) had E84K mutation within ParC instead of S80L. These mutations (E87Q and E84K) had previously been reported to be associated with FQ resistance in *A. baumannii* (Valentine et al., 2008; Park et al., 2011). Alteration of Glu-84 to Lys within ParC implies that replacement of acidic amino acid with basic amino acid at position 84 may change the structural arrangement of the active site of ParC and its contact with surrounding amino acids which in turn make FQs incapable to bind to the enzyme. Several other mutations within GyrA (Gly81Val, Ala84Pro, Gly81Cys, Gly81Asp, Ser97Thr) and ParC (Lys59Gln, Gly78Cys, Ser80Trp, ser80Tyr, Ala85Pro), associated with FQ resistance in FQRAB,

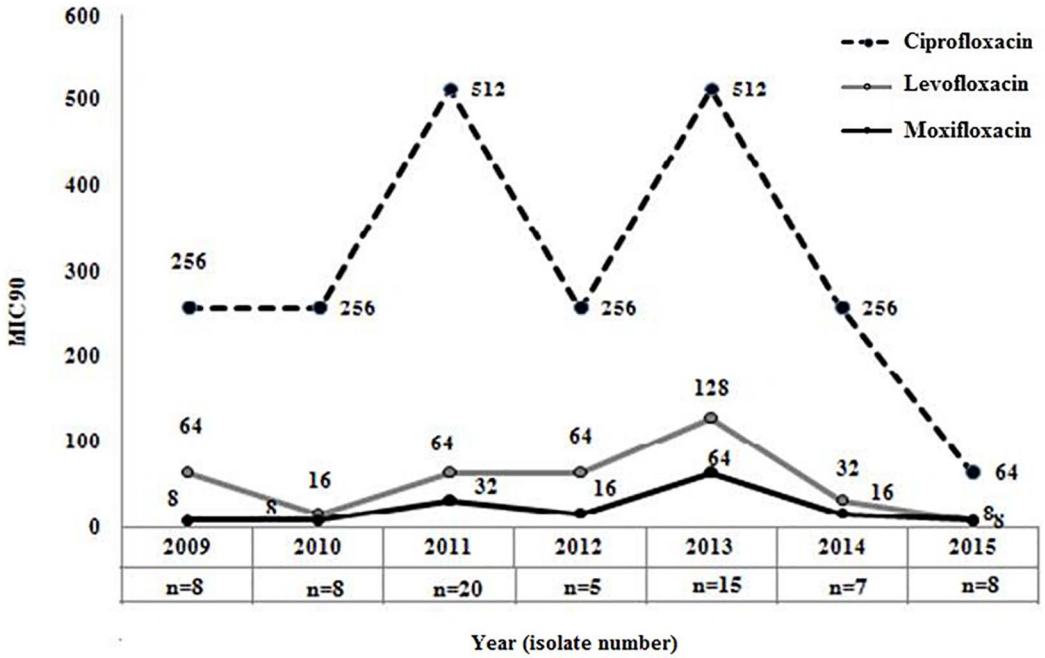

FIGURE 2 | Distribution of MIC_{90} for three clinically important fluoroquinolones among *Acinetobacter baumannii*. MIC_{90} of ciprofloxacin (2nd generation), levofloxacin (2nd generation), and moxifloxacin (4th generation) was determined by broth microdilution method among all septicaemic *A. baumannii* (*n* = 47) isolated during 2009–2015.

were reported by other studies but such mutations were not detected in any of the study isolates (Hamouda and Amyes, 2004; Chiu et al., 2010; Park et al., 2011; Hongbo et al., 2013; Ardebili et al., 2015). Isolate A_124 showed high MIC for ciprofloxacin (256 mg/L) but had no mutations within ParC or GyrA. This isolate showed overexpression of AdeB efflux pump. Since both mutations within GyrA (S83L) and ParC (S80L) were observed in diverse STs, thus chromosomal mutations responsible for FQ resistance were not associated with any particular ST or clonal complex, rather detected among 10 clonal complexes found in this study. Silent mutations within *gyrA* and *parC* were also observed (**Table 1**). In the case of *parC*, all isolates possessed more than seven different silent mutations. The numbers of silent mutations within *parC* gene was higher than *gyrA* gene (47 vs. 12) as also observed in previous studies (Sun et al., 2015). The function of these mutations is still unknown.

Prevalence of PMQRs

Among the PMQRs investigated in this study, only *aac(6′)-Ib-cr* was detected in 74% of ciprofloxacin-resistant *A. baumannii* (**Table 1**). None of the *A. baumannii* showed the presence of *qnr* genes. It has previously been reported that strains possessing this enzyme remain susceptible as acetylation of FQ with AAC(6′)-Ib-cr reduces drug activity and confers a low level of FQ resistance (Rodríguez-Martínez et al., 2016). But this enzyme may create an environment which facilitates topoisomerase mutations (Frasson et al., 2011). In this study, AAC(6′)-Ib-cr-possessing FQRAB isolates also possessed chromosomal mutations and/or showed overexpression of efflux pumps (discussed below). Thus, isolates are highly resistant to FQs.

Effects of EPIs on FQ Resistance

None of the isolates showed the bactericidal effect of EPIs at a concentration of 50 mg/L. This confirms that the reduction of MIC for FQs in presence of EPIs was due to the presence of efflux pumps. Reduction in MIC with NMP was observed for ciprofloxacin (4−128-folds), levofloxacin (4−16-fold), and moxifloxacin (4−128-fold) among 48, 25, and 44% of FQRAB, respectively. On the other hand, PAβN also decreased the MIC of FQs to some extent [ciprofloxacin (4−16-folds) in 11% of FQRAB, levofloxacin (4-fold) in 2% of FQRAB, moxifloxacin (4-fold) in 12% of FQRAB]. Of the two EPIs used, NMP was more active in reduction of FQ MIC than PAβN. This result is in agreement with a previous report suggesting that activities of these two compounds were dissimilar (Pannek et al., 2006). This is consistent with the view that different antibiotics may have different binding sites on the pump with which the EPI (here NMP or PAβN) might interact in a variable manner (Elkins and Nikaido, 2002).

Overall, 63% (*n* = 29) of FQRAB showed reduction of MICs (4−128-fold) for FQs in presence of EPIs and 37% of the FQRAB were not affected by EPIs, establishing the fact that FQ resistance is not solely due to the participation of efflux pumps in some of the strains (**Table 1**). The strains which showed participation of efflux pumps in FQ resistance belonged predominantly to CC1 (5 out of 6 isolates), CC2 (4 out of 5 isolates), CC10 (10 out of 11 isolates), and CC32 (all 3 isolates of this group). Very few

isolates belonging to CC149 (4 out of 10 isolates), CC218 (n = 1), and CC513 (n = 1) also showed participation of efflux pumps in presence of EPI (**Table 2**).

Overexpression of Efflux Pumps

In this study, four different efflux pump genes were investigated for each isolate and such simultaneous assessment of multiple pumps had not been carried out before. Earlier studies reported overexpression of either one pump (AdeABC) or two pumps together (AdeABC, AeIJK) (Chiu et al., 2010; Park et al., 2011; Lopes and Amyes, 2013; Ardebili et al., 2014). Overexpression of *adeB* gene was detected among 70% (21/30) of *A. baumannii* strains which showed ≥4-fold decrease in MICs for FQs in presence of EPIs. This was followed by *adeJ* (53%, n = 16), *abeM* (30%, n = 9), and *adeG* (23%, n = 7) (**Table 2**). Significantly higher numbers of *A. baumannii* showed overexpression of *adeB* in comparison to *adeG* (Fisher's exact test; p = 0.0041) and *adeM* (Fisher's exact test; p = 0.0006). However, no statistically significant differences were found between the numbers of strains overexpressing *adeB* and *adeJ* (Fisher's exact test; p = 0.1872). However, the relative expression level of *adeB* was highest (2.2−34-fold) among all pumps tested. The other target efflux pump genes *adeJ*, *adeG*, and *abeM* showed expression levels between 2.1−10.7-fold, 2−17.4-fold, and 2−25-fold, respectively (**Table 2**). This indicated that though the involvement of *adeB* was highest in FQ resistance, overexpression of other pumps cannot be neglected. Since AdeIJK pump is intrinsic to *A. baumannii,* thus it was detected among large numbers of strains but in comparison to *adeB*, the relative fold change of *adeJ* was low supporting the fact that overexpression of AdeIJK is toxic to *A. baumannii* (Damier-Piolle et al., 2008). In three out of 30 isolates (A_117, A_150, and A_159), *adeB* could not be amplified. On the other hand, in five out of 30 isolates (A_130, A_132, A_152, A_153, and A_177), overexpression of AdeABC was not detected. In these five isolates, either AdeRS could not be detected or mutations were absent within AdeRS. It has previously been reported that the loss of *adeRS* or *adeB* could significantly modify the transcriptional level of AdeABC efflux pump of *A. baumannii* resulting in a decreased expression of *adeABC* (Richmond et al., 2016). In these isolates, an association of overexpression of other pumps (*adeJ* or *adeG* or *abeM*) with elevated FQ MICs is thus likely (**Table 2**). One isolate (A_160) did not show overexpression of any of the efflux pumps studied here in spite of FQ MIC decrement in presence of EPI indicating involvement of other efflux pumps as five uncharacterized RND pumps have been reported in *A. baumannii* (Nowak et al., 2015). In this study, ≥ 2 different pumps were overexpressed simultaneously among 38% of FQRAB (17/45).

Correlation Between Fluoroquinolone MIC and Different Resistance Mechanisms

An attempt was made to correlate the FQ MIC values with the three different resistance mechanisms studied here: chromosomal mutations, over expression of efflux pumps, and presence of *aac(6′)-Ib-cr*.

Presence of these three mechanisms simultaneously was detected among 33% of FQRAB and the FQ MIC for three drugs was as follows: ciprofloxacin MIC (64−512) mg/L, levofloxacin MIC (4−128) mg/L, and moxifloxacin MIC (4−64) mg/L. FQRAB (30%) that did not express efflux pumps but where the other two mechanisms were detected exhibited ciprofloxacin MIC (32−256) mg/L, levofloxacin MIC (2−64) mg/L, and moxifloxacin MIC (0.5−32) mg/L. Decreased FQ MIC (≥2-fold) in these strains clearly indicated the role of efflux pumps in FQ resistance. However, 13% of FQRAB did not possess AAC(6′)-Ib-cr, but showed chromosomal mutations along with overexpression of pumps and had ciprofloxacin MIC (64−512 mg/L). AAC(6′)-Ib-cr can reduce the activity of ciprofloxacin by acetylation but was not able to acetylate moxifloxacin and levofloxacin (Robicsek et al., 2006). The ciprofloxacin MIC in the study isolates with or without AAC(6′)-Ib-cr could not be assessed as the other two mechanisms were also present. Mutations only in GyrA and ParC were detected in 7% of strains without the involvement of efflux pumps and *aac(6′)-Ib-cr*. These isolates showed ≥8-fold lower FQ MIC as follows: ciprofloxacin MIC (8−256) mg/L, levofloxacin MIC (0.25−64) mg/L, moxifloxacin MIC (0.125−32) mg/L (**Supplementary Table S2**).

When three mechanisms work together in isolates, it is difficult to delineate the contribution of each mechanism. However, the study showed that both chromosomal mutations and efflux pumps are important as the absence of pumps is reflected in the lower MIC values. Strains with all three mechanisms showed high FQ MIC.

Analysis of Regulators of RND Family Efflux Pumps

To further assess the mechanism of *adeB, adeJ,* and *adeG* overexpression, the protein sequences of the respective pump regulators AdeRS, AdeN, and adeL were studied. These sequences were compared with the four *A. baumannii* reference strains (*A. baumannii* AYE, ATCC 17978, ATCC 19606, and *A. baumannii* ACICU) in order to exclude polymorphisms.

The AdeABC efflux pump is controlled by the AdeRS two-component regulatory system (Yoon et al., 2013). AdeS is the sensor histidine kinase (HK) that autophosphorylates at an internal histidine. The phosphate group is then transferred to an aspartate residue of the cytoplasmic response regulator which acts as a transcriptional activator (AdeR). Phosphorylated AdeR binds to an intercistronic space (ICS), located between the promoter and coding sequences of adeABC. This binding prevents the transcription of adeABC mRNA. Thus, binding of AdeR to ICS control the expression of AdeABC operon (Chang et al., 2016).

In AdeR, four different amino acid substitutions (F132S, I175L, L227I, and I228V) were detected (**Table 3**). The substitutions were present either as single substitution or in combinations. None of these substitutions were detected in the reference strains. The substitution F132S (n = 1) was located in the signal receiver domain of AdeR. Mutation in this domain may change the interactions between the

TABLE 2 | Expression levels (fold change) of RND-family (AdeB, AdeJ, AdeG) and MATE-family efflux pumps (AbeM) detected by reverse transcriptase quantitative PCR (RT-qPCR) in *Acinetobacter baumannii* that showed reduction of MIC for fluoroquinolones in presence of efflux pump inhibitors.

Strain No	MLST/Clonal complex	*adeB* fold change	*adeJ* fold change	*adeG* fold change	*abeM* fold change
A_112	ST-32/CC32	**3.6**	**2.1**	1.2	0.2
A_113	ST032/CC32	**3.7**	**4.1**	1.1	**2**
A_117	ST-10/CC10	ND	**2.1**	**5.6**	ND
A_124	ST-1440/CC218	**3.03**	ND	ND	0.29
A_125	ST-2/CC2	**7.0**	**2.8**	**7.7**	**2.69**
A_130	ST-575/CC10	0.06	**2.9**	0.14	0.6
A_131	ST-902/CC1	**34**	**2**	0.73	1.4
A_132	ST-10/CC10	0.044	**3.5**	1.3	**4.47**
A_136	ST-149/CC149	**5**	ND	ND	0.7
A_138	ST-905/CC32	**8.65**	**3.1**	0.8	**2.0**
A_145	ST-149/CC149	**12.7**	0.7	0.6	0.8
A_146	ST-1406/CC10	**3**	0.1	ND	0.1
A_149	ST-149/CC149	**2.2**	0.2	0.7	0.4
A_150	ST-10/CC10	ND	**3.79**	ND	0.49
A_152	ST-623CC1	1.5	1.2	0.4	**5.9**
A_153	ST-623/CC1	1.1	0.5	**13.9**	**7.5**
A_155	ST-10/CC10	**5.4**	**3.1**	0.3	0.5
A_158	ST-1483/CC10	**22**	1.5	**2.5**	1.1
A_159	ST-1483/CC10	ND	**2.4**	ND	1.2
A_160	ST-1/CC1	0.1	ND	ND	0.12
A_161	ST-149/CC149	**21.5**	0.1	0.8	0.9
A_162	ST-1406/CC10	**17.5**	**2.8**	0.03	0.2
A_163	ST-575/CC10	**20**	**2.8**	0.007	0.6
A_166	ST-625/CC513	**11.0**	**10.7**	**3.2**	1.05
A_167	ST-2/CC2	**25.3**	**2.5**	**2.8**	1.7
A_172	ST-526/CC2	**9.8**	0.5	1.8	**4**
A_173	ST-526/CC2	**18.35**	**10.64**	**17.4**	1.097
A_177	ST-1484 (singleton)	0.021	0.757	0.383	**25**
A-179	ST-7/CC1	**15.0**	0.6	0.25	1.1

RND, Resistance Nodulation Division family; MATE, Multidrug and Toxin Extrusion family; MIC, Minimum Inhibitory Concentration; ND, No Detection. The relative gene expression (ΔCT) for pump genes transcripts was calculated against that for the 16S rRNA gene, [ΔCT of test gene= CT of test gene − CT of 16S] and the ΔΔCT was calculated against that for the ciprofloxacin-susceptible strain, A. baumannii ATCC 19606 (expression = 1), which served as the control. Relative expression levels of pump genes were calculated by the $2^{-\Delta\Delta CT}$ method. Expression level of pump gene which was ≥2-fold higher in comparison to the control strain A. baumannii ATCC 19606 (expression = 1), indicated as bold and considered as overexpression of the pump.

AdeS and AdeR and prevent the subsequent binding to intercistronic space (ICS) leading to AdeABC overexpression (Yoon et al., 2013). Furthermore, substitutions I175L (n = 2), L227I (n = 2), and I228V (n = 1), located in the effector domain again prevent the binding of AdeR to ICS and cause overexpression of AdeABC which subsequently leads to FQ resistance (**Table 3**). Two substitutions of AdeR (I120 and A136V) were detected in most of the AdeABC-overexpressing strains (11/21). These two substitutions were considered as silent polymorphisms as they were also detected in the reference strain *A. baumannii* ACICU (**Supplementary Table S3**; Gerson et al., 2018).

Six different amino acid substitutions (E121K, G186V, S188F, V255I, I257V, L322F) were detected in AdeS (**Table 3**). None of these substitutions were detected in the reference strains. Of these substitutions, G186V (n = 9) was located in the α-helix of the DHp domain and has previously been reported (**Table 3**). Mutation in this domain could prevent the phosphotransfer to AdeR. Thus, inability of AdeR to bind to the ICS region leads to lack of control over the expression of AdeABC efflux pump, leading to FQ resistance (Yoon et al., 2013; Sun et al., 2016). Substitutions E121K (n = 2) and S188F (n = 6) were located in the HAMP domain and C-terminal end of the DHp domain of histidine kinase, respectively. Amino acid substitutions in the HAMP domain of AdeS protein disrupt transmembrane signal transduction and have been suggested to be associated with constitutive phenotypes and overexpression of AdeABC effux pump (Yoon et al., 2013). In addition, substitutions V255I (n = 6), I257V (n = 1), and L322F (n = 2) were located in the catalytic domain. Mutations in this domain could affect ATP binding leading to prevention of autophosphorylation of AdeS which simultaneously prevent the phosphotransfer to AdeR. Thus, AdeR does not bind to the ICS region, leading to

TABLE 3 | Amino acids substitutions in AdeRS two component system in fluoroquinolone-resistant *Acinetobacter baumannii* isolates overexpressing AdeABC efflux pump.

		Amino acid at the indicated position*									
		AdeS (360 aa)						**AdeR (247 aa)**			
Different mutational patterns in AdeRS (No. of isolates in each pattern)	**Isolate numbers (MLST/CC)**	**HAMP (82–138)**	**DHp (138–246)**		**CA (246–360)**			**REC (1–140)**	**Output domain (141–247)**		
		121	186	188	255	257	322	132	175	227	228
		E	G	S	V	I	L	F	I	L	I
Type 1 (*n* = 1)	A_112 (ST-32/CC32)				I				L	I	
Type 2 (*n* = 1)	A_113 (ST-32/CC32)			F						I	
Type 3 (*n* = 1)	A_124 (ST-1440/CC218)		V								V
Type 4 (*n* = 1)	A_138 (ST-905/CC32)		V		I				L		
Type 5 (*n* = 1)	A_166 (ST-625/CC513)					V		S			
Type 6 (*n* = 1)	A_146 (ST-1406/CC10)	K							No amino acid substitutions		
Type 7 (*n* = 2)	A_136 (ST-149/CC149), A_149 (ST_149/CC149)			F	I				No amino acid substitutions		
Type 8 (*n* = 7)	A_125 (ST-2/CC2), A_162 (ST-1406/CC10), A_163 (ST-575/CC10), A_167 (ST-2/CC2), A_172 (ST-526/CC2), A_173 (ST-526/CC2), A_179 (ST-7/CC1)		V						No amino acid substitutions		
Type 9 (*n* = 1)	A_161 (ST-149/CC149)				I				No amino acid substitutions		
Type 10 (*n* = 2)	A_131 (ST-902/CC1), A_158 (ST-1483/CC10)			F	I				No amino acid substitutions		
Type 11 (*n* = 1)	A_145 (ST-149/CC149)			F	I		F		No amino acid substitutions		
Type 12 (*n* = 1)	A_155 (ST-10/CC10)	K					F		No amino acid substitutions		

aa, amino acids; CA, catalytic and ATP-binding domain; DHp, dimerization and histidine-containing phosphotransfer domain; HAMP, histidine kinase, adenylylcyclase, methyl-accepting protein, and phosphatase linker domain; REC, receiver domain; CC, Clonal Complex.

** The AdeR and AdeS amino acid sequences of A. baumannii ACICU, A. baumannii AYE, ATCC 17978, and ATCC 19606 were used as reference strains for comparison. Amino acid substitutions are indicated using the one-letter code.*

hyperexpression of AdeABC efflux pump (**Table 3**; Yoon et al., 2013). Several common polymorphisms within AdeS (V27I, V32I, A94V, L172P, F214L, D227H, N268H, S280A, Q281D, Q299R, Y303F, I331V, and Q339K) were also detected in the reference strains and in some study isolates not overexpressing AdeABC (**Supplementary Table S3**). These changes were considered to be silent polymorphisms and not associated with overexpression of the pump and were excluded (Yoon et al., 2013). In this study, mutations within AdeR and AdeS were not found to be associated with any particular clonal complex but were rather found within diverse STs belonging to different clonal complexes (CC1, CC2, CC10, CC32, CC149, CC218, CC513) (**Table 3**).

In AdeN (regulator of AdeIJK), amino acid substitutions K15E (*n* = 1), P16T (*n* = 2), Q17P (*n* = 1), L26S (*n* = 1), F64I (*n* = 4), and M174T (*n* = 3) were detected in different combinations among 12 isolates while in AdeL (regulator of AdeFGH), substitutions L34F (*n* = 1), I50F (*n* = 2), L38V (*n* = 1), T46D (*n* = 1), and D107V (*n* = 2) were detected in different combinations within three isolates. These amino acid substitutions seemed to be associated with FQ resistance as these mutations were not present in the reference strains (**Table 4**). Premature stop codons had been detected in two isolates at codon position 13 and 175 within the protein sequence of AdeN. Amino acid substitutions within AdeN were predominantly detected among *A. baumannii* belonging to clonal complex CC10 and CC32 whereas amino acid substitutions within AdeL detected in only three isolates belonged to CC1, CC2, and CC10 (**Table 4**). Few of the isolates (*n* = 4, **Table 4**) showed overexpression of AdeIJK and AdeFGH but did not possess any mutations within AdeN and AdeL regulators, respectively. Furthermore, disruption of *adeRS* or *adeN* by insertion of IS elements and nucleotide deletions or insertion within the regulators were not evident in any of the study isolates as had been reported previously (Park et al., 2011; Gerson et al., 2018). The amino acid substitutions detected in the three regulators, has not been

TABLE 4 | Amino acid substitutions in AdeN and AdeL in fluoroquinolone-resistant *Acinetobacter baumannii* (FQRAB) overexpressing AdeIJK and AdeFGH efflux pumps, respectively.

RND-family efflux pumps	Regulators of the respective pumps	No of FQRAB overexpressing the efflux pumps	Mutations within the regulators (No of FQRAB with overexpression of the pump and possessed the changes)	Isolate numbers (MLST/CC)
AdeJ	AdeN	16	K15E (*n* = 1)	A_167 (ST-2/CC2)
			P16T, Q17P (*n* = 1)	A_112 (ST-32/CC32)
			P16T (*n* = 1)	A_113 (ST-32/CC32)
			L26S, F64I (*n* = 1)	A_159 (ST-1483/CC10)
			F64I (*n* = 3)	A_117 (ST-10/CC10), A_150 (ST-10/CC10) A_155 (ST-10/CC10)
			M174T (*n* = 3)	A_130 (ST-575/CC10), A_162 (ST-1406/CC10), A-163 (ST-575/CC10)
			Stop codon at codon numbers 13 and 175 (*n* = 2)	A_132 (ST-10/CC10), A_138 (ST-905/CC32)
			No amino acids substitution (*n* = 4)	A_125 (ST-2/CC2), A_131 (ST-902/CC1), A_166 (ST-625/CC513), A_173 (ST-526/CC2)
AdeG	AdeL	7	I50F (*n* = 1)	A_125 (ST-2/CC2)
			L34F, I50F, D107V (*n* = 1)	A_153 (ST-623/CC1)
			L38V, T46D, D107V (*n* = 1)	A_158 (ST-1483/CC10)
			No mutations detected (*n* = 4)	A_117 (ST-10/CC10), A_166 (ST-625/CC513), A_167 (ST-2/CC2), A_173 (ST-526/CC2)

described previously, future studies should be carried out to know the role of these mutations and their association with FQ resistance phenotype.

CONCLUSION

FQ-resistance has been studied earlier by several authors highlighting different mechanisms simultaneously in gram-negative organisms (Oethinger et al., 2000; Ge et al., 2005; Lopes and Amyes, 2013). However, none of these studies analyzed the cumulative effect of multiple mechanisms of FQ resistance among diverse STs of neonatal septicemic *A. baumannii*. Moreover, as the testing of newer FQs continues, there is no comprehensive data regarding the resistance to higher generation FQs such as moxifloxacin available from India in spite of high antimicrobial resistance. This is most concerning as 90% of *A. baumannii* isolated from neonates in this study were resistant to moxifloxacin.

This study showed the diversity of the strains in this NICU during the study period as 24 different STs were detected among 47 *A. baumannii* with seven novel sequence types: ST-1440, ST-1441, ST-1481, ST-1482, ST-1483, ST-1484, and ST-1486. Our approach also revealed chromosomal mutations [both GyrA (S83L) and ParC (S80L)] were the predominant mechanism associated with FQ resistance as it was detected in > 90% of FQRAB analyzed. Previous studies have reported several other mutations associated with FQ resistance within GyrA and ParC of FQRAB which were not evident in this study. The second important mechanism associated with FQ resistance was overexpression of efflux pumps. Earlier studies reported overexpression of either one pump (AdeABC) or simultaneous overexpression of two pumps together (AdeABC, AeIJK). In this study, four different efflux pumps were investigated for each isolate and such simultaneous assessment of multiple pumps had not been carried out before. Simultaneous overexpression of ≥2 different pumps was detected among 38% of *A. baumannii*. Though the m-RNA transcription level of *adeB* was highest but other pumps were also found to be associated with FQ resistance. In this study, lower MIC of FQ (≥8-folds) was detected among the FQRAB which showed only chromosomal mutations in comparison to the strains where both chromosomal mutations and overexpression of efflux pumps were detected simultaneously. This indicated the importance of efflux pumps in FQ resistance. Among the PMQRs investigated in this study, only AAC(6′)-Ib-cr was detected in a substantial proportion of FQRAB. Though, presence of this enzyme confers lower level of resistance to ciprofloxacin but they facilitate the generation of GyrA/ParC mutations. In this study, AAC(6′)-Ib-cr-possessing FQRAB also had chromosomal mutations and/or showed overexpression of efflux pumps, exhibiting high resistance to FQs. Overall, presence of chromosomal mutations was evident among all 10 clonal groups (CC1, CC2, CC10, CC25, CC32, CC126, CC149, CC216, CC218, and CC513) detected in this study. On the other hand, participation of efflux pumps was predominantly detected among the isolates belonging to CC1, CC2, CC10, and CC32. In contrast to earlier studies which reported disruption of *adeRS* or *adeN* by insertion of IS elements, nucleotide deletions or insertion within the pump regulators, this study revealed amino acid substitutions in the regulatory proteins of RND-pumps. It shows that *A. baumannii* isolated from different geographical locations exhibit differences

in mutational patterns in the regulators. Mutations within AdeRS detected among different STs belonged to different clonal complexes and were not associated to a particular clonal complex. On the other hand, mutations within AdeN predominantly belonged to CC10 and CC32.

Interpretation of susceptibility patterns by studying the cumulative effect of various mechanisms is not an easy task. This study noted high variability of FQ susceptibility among FQRAB in spite of possessing the same set of resistance mutations in GyrA, ParC, and, efflux pump regulators. This variability might be due to other factors such as the reduction in outer membrane porin diffusion channels, or mutations in genes encoding regulatory proteins of the porin genes or mutations in efflux pump structural genes or involvement of other efflux pumps or even mutations in *gyrB*/*parE* that were not analyzed in this study (Hamouda and Amyes, 2006; Hooper and Jacoby, 2015). Further, the study showed that antibiotic resistance is dynamic, and changes geographically. An understanding of susceptibility patterns of MDR *A. baumannii* toward higher generation fluoroquinolones such as moxifloxacin in developing countries is important to optimize therapeutic strategies accordingly.

DATA AVAILABILITY STATEMENT

The raw data supporting the conclusions of this article will be made available by the authors, without undue reservation.

ETHICS STATEMENT

The study protocol was carefully reviewed and approved by the Institutional Ethics Committee of the ICMR-National Institute of Cholera and Enteric Diseases (Indian Council of Medical Research) (No. A-1/2016-IEC, dated 3rd May 2016). Individual informed consent was not required as the study was carried out on *Acinetobacter baumannii* strains archived at ICMR-NICED. These strains were isolated from neonates during the course of routine diagnosis of sepsis and did not pose any additional risks to the patients.

AUTHOR CONTRIBUTIONS

SR, SC, and AB performed the experiments. SR participated in experimental design, manuscript writing, and interpretation of data. PC and BS helped in acquisition of clinical strains. SD helped in drafting of manuscript. SB conceived the study, participated in data analysis, oversaw the project, and was involved in manuscript writing. All authors contributed to the article and approved the submitted version.

FUNDING

The study was supported by the ICMR (Indian Council of Medical Research) intramural funding. SR was a recipient of the Senior Research Associateship (Scientist' Pool No: 9022A) from CSIR, SC, and AB was recipient of the Senior Research Fellowship from ICMR.

ACKNOWLEDGMENTS

We are thankful to Sabine Schuster for providing the control *A. baumannii* ATCC19606. We also extend our thanks to Mr. Subhadeep De for his laboratory assistance and to the staff of the Department of Neonatology, IPGMER Hospital for caring the neonates included in the study. We also thank curators of MLST data base for assigning the novel sequence types.

SUPPLEMENTARY MATERIAL

The Supplementary Material for this article can be found online at: https://www.frontiersin.org/articles/10.3389/fmicb.2021.602724/full#supplementary-material

REFERENCES

Aldred, K. J., Kerns, R. J., and Osheroff, N. (2014). Mechanism of quinolone action and resistance. *Biochemistry* 53, 1565–1574. doi: 10.1021/bi5000564

Ardebili, A., Lari, A. R., Beheshti, M., and Lari, E. R. (2015). Association between mutations in gyrA and parC genes of *Acinetobacter baumannii* clinical isolates and ciprofloxacin resistance. *Iran. J. Basic Med. Sci.* 18, 623–626.

Ardebili, A., Lari, A. R., and Talebi, M. (2014). Correlation of ciprofloxacin resistance with the AdeABC efflux system in *Acinetobacter baumannii* clinical isolates. *Ann. Lab. Med.* 34, 433–438. doi: 10.3343/alm.2014.34.6.433

Asif, M., Alvi, I. A., and Ur Rehman, S. (2018). Insight into *acinetobacter baumannii*: pathogenesis, global resistance, mechanisms of resistance, treatment options, and alternative modalities. *Infect. Drug Resist.* 11, 1249–1260. doi: 10.2147/IDR.S166750

Blanchard, C., Barnett, P., Perlmutter, J., and Dunman, P. M. (2014). Identification of *Acinetobacter baumannii* serum-associated antibiotic efflux pump inhibitors. *Antimicrob. Agents Chemother.* 58, 6360–6370. doi: 10.1128/AAC.03535-14

Cattoir, V., Poirel, L., Rotimi, V., Soussy, C. J., and Nordmann, P. (2007). Multiplex PCR for detection of plasmid-mediated quinolone resistance qnr genes in ESBL-producing enterobacterial isolates. *J. Antimicrob. Chemother.* 60, 394–397. doi: 10.1093/jac/dkm204

Chang, T. Y., Huang, B. J., Sun, J. R., Perng, C. L., Chan, M. C., Yu, C. P., et al. (2016). AdeR protein regulates adeABC expression by binding to a direct-repeat motif in the intercistronic spacer. *Microbiol. Res.* 183, 60–67. doi: 10.1016/j.micres.2015.11.010

Chatterjee, S., Datta, S., Roy, S., Ramanan, L., Saha, A., Viswanathan, R., et al. (2016). Carbapenem resistance in *Acinetobacter baumannii* and other acinetobacter spp. causing neonatal sepsis: focus on NDM-1 and its linkage to ISAba125. *Front. Microbiol.* 7:1126. doi: 10.3389/fmicb.2016.01126

Chiu, C. H., Lee, H. Y., Tseng, L. Y., Chen, C. L., Chia, J. H., Su, L. H., et al. (2010). Mechanisms of resistance to ciprofloxacin, ampicillin/sulbactam and imipenem in *Acinetobacter baumannii* clinical isolates in Taiwan. *Int. J. Antimicrob. Agents.* 35, 382–386. doi: 10.1016/j.ijantimicag.2009.12.009

Clinical and Laboratory Standards Institute [CLSI] (2019). *Performance Standards for Antimicrobial Susceptibility Testing: Eighteenth Informational Supplement M100*, 29th Edn. Wayne, PA: CLSI.

Coyne, S., Rosenfeld, N., Lambert, T., Courvalin, P., and Périchon, B. (2010). Overexpression of resistance-nodulation-cell division pump AdeFGH

confers multidrug resistance in *Acinetobacter baumannii*. *Antimicrob. Agents Chemother.* 54, 4389–4393. doi: 10.1128/AAC.00155-10

Damier-Piolle, L., Magnet, S., Brémont, S., Lambert, T., and Courvalin, P. (2008). AdeIJK, a resistance-nodulation-cell division pump effluxing multiple antibiotics in *Acinetobacter baumannii*. *Antimicrob. Agents Chemother.* 52, 557–562. doi: 10.1128/AAC.00732-07

Elkins, C. A., and Nikaido, H. (2002). Substrate specificity of the RND-type multidrug efflux pumps AcrB and AcrD of. *J. Bacteriol.* 184, 6490–6498. doi: 10.1128/JB.184.23.6490

Farooqui, H. H., Selvaraj, S., Mehta, A., and Heymann, D. L. (2018). Community level antibiotic utilization in India and its comparison vis-à-vis European countries: evidence from pharmaceutical sales data. *PLoS One* 13:e0204805. doi: 10.1371/journal.pone.0204805

Ferrara, A. M. (2007). A brief review of moxifloxacin in the treatment of elderly patients with community-acquired pneumonia (CAP). *Clin. Interv. Aging* 2, 179–187.

Frasson, I., Cavallaro, A., Bergo, C., Richter, S. N., and Palù, G. (2011). Prevalence of aac(6')-Ib-cr plasmid-mediated and chromosome-encoded fluoroquinolone resistance in *Enterobacteriaceae* in Italy. *Gut. Pathog.* 3:12.

Fuchs, A., Bielicki, J., Mathur, S., Sharland, M., Anker, J. N., Shah, B. A., et al. (2016). *Antibiotic Use for Sepsis in Neonates and Children: 2016 Evidence Update*. Geneva: WHO.

Ge, B., McDermot, T. P. F., White, D. G., and Meng, J. (2005). Role of efflux pumps and topoisomerase mutations in fluoroquinolone resistance in *Campylobacter jejuni* and Campylobacter coli. *Antimicrob. Agents Chemother.* 49, 3347–3354.

Gerson, S., Nowak, J., Zander, E., Ertel, J., Wen, Y., Krut, O., et al. (2018). Diversity of mutations in regulatory genes of resistance-nodulationcell division efflux pumps in association with tigecycline resistance in *Acinetobacter baumannii*. *J. Antimicrob.Chemother.* 73, 1501–1508. doi: 10.1093/jac/dky083

Gramatniece, A., Silamikelis, I., Zahare, I.E, Urtans, V., Zahare, I., Dimina, E., et al. (2019). Control of *Acinetobacter baumannii* outbreak in the neonatal intensive care unit in latvia : whole-genome sequencing powered investigation and closure of the ward. 8:84.

Hamouda, A., and Amyes, S. G. (2004). Novel gyrA and parC point mutations in two strains of *Acinetobacter baumannii* resistant to ciprofloxacin. *J. Antimicrob. Chemother.* 54, 695–696. doi: 10.1093/jac/dkh368

Hamouda, A., and Amyes, S. G. (2006). Development of highly ciprofloxacin-resistant laboratory mutants of Acinetobacterbaumannii lacking topoisomerase IV gene mutations. *J. Antimicrob. Chemother.* 57, 155–156. doi: 10.1093/jac/dki397

Heinemann, B., Wisplinghoff, H., Edmond, M., and Seifert, H. (2000). Comparative activities of ciprofloxacin, clinafloxacin, gatifloxacin, gemifloxacin, levofloxacin, moxifloxacin, and trovafloxacin against epidemiologically defined *Acinetobacter baumannii* strains. *Antimicrob. Agents Chemother.* 44, 2211–2213. doi: 10.1128/AAC.44.8.2211-2213.2000

Hongbo, L., Zhen, S., Xu, X., and Shengqi, L. (2013). Mutations in the quinolone resistance determining region in isogenic mutant *Acinetobacter baumannii* strains. *AJMR* 7, 3559–3562. doi: 10.5897/AJMR2013.5932

Hooper, D. C., and Jacoby, G. A. (2015). Mechanisms of drug resistance: quinolone resistance. *Ann. N. Y. Acad. Sci.* 1354, 12–31. doi: 10.1111/nyas.12830

Hujer, A. M., Higgins, P. G., Rudin, S. D., Buser, G. L., Marshall, S. H., Xanthopoulou, K., et al. (2017). Nosocomial outbreak of extensively drug-resistant *Acinetobacter baumannii* isolates containing bla OXA-237 carried on a plasmid. *Antimicrob. Agents Chemother.* 61:e797-17. doi: 10.1128/aac.00797-17

Hujer, K. M., Hujer, A. M., Endimiani, A., Thomson, J. M., Adams, M. D., Goglin, K., et al. (2009). Rapid determination of quinolone resistance in *Acinetobacter* spp. *J. Clin. Microbiol.* 47, 1436–1442. doi: 10.1128/JCM.02380-08

Jiang, X., Yu, T., Jiang, X., Zhang, W., Zhang, L., and Ma, J. (2014). Emergence of plasmid-mediated quinolone resistance genes in clinical isolates of *Acinetobacter baumannii* and *Pseudomonas aeruginosa* in Henan, China. *Diagn. Microbiol. Infect. Dis.* 79, 381–383. doi: 10.1016/j.diagmicrobio.2014.03.025

Kivata, M. W., Mbuchi, M., Eyase, F. L., Bulimo, W. D., Kyanya, C. K., and Oundo, V. (2019). gyrA and parC mutations in fluoroquinolone-resistant *Neisseria gonorrhoeae* isolates from Kenya. *BMC Microbiol.* 19:76. doi: 10.1186/s12866-019-1439-1

Laxminarayan, R., and Chaudhury, R. R. (2016). Antibiotic resistance in india: drivers and opportunities for action. *PLoS Med.* 13:e1001974. doi: 10.1371/journal.pmed.1001974

Liu, Y. H., Kuo, S. C., Lee, Y. T., Chang, I. C. Y., Yang, S. P., Chen, T. L., et al. (2012). Amino acid substitutions of quinolone resistance determining regions in GyrA and ParC associated with quinolone resistance in *Acinetobacter baumannii* and *Acinetobacter* genomic species 13TU. *J. Microbiol. Immunol. Infect.* 45, 108–112.

Lopes, B. S., and Amyes, S. G. B. (2013). Insertion sequence disruption of adeR and ciprofloxacin resistance caused by efflux pumps and gyrA and parC mutations in *Acinetobacter baumannii*. *Int. J. Antimicrob. Agents* 41, 117–121. doi: 10.1016/j.ijantimicag.2012.08.012

Maleki, M. H., Azizi Jalilian, F., Kkayat, H., Mohamadi, M., Pourahmad, F., Asadollahi, K. H., et al. (2014). Detection of highly ciprofloxacin resistance. *MAEDICA* 9, 162–167.

Marchand, I., Marchand, I., Damier-piolle, L., Damier-piolle, L., Courvalin, P., Courvalin, P., et al. (2004). Expression of the RND-type Ef ux Pump AdeABC in *Acinetobacter baumannii* is regulated by the AdeRS two-component system. *Society* 48, 3298–3304. doi: 10.1128/AAC.48.9.3298

Nowak, J., Seifert, H., and Higgins, P. G. (2015). Prevalence of eight resistance-nodulation-division efflux pump genes in epidemiologically characterized *Acinetobacter baumannii* of worldwide origin. *J. Med. Microbiol.* 64, 630–635. doi: 10.1099/jmm.0.000069

Oethinger, M., Kern, W. V., Jellen-Ritter, A. S., McMurry, L. M., and Levy, S. B. (2000). Ineffectiveness of topoisomerase mutations in mediating clinically significant fluoroquinolone resistance in *Escherichia coli* in the absence of the AcrAB efflux pump. *Antimicrob. Agents Chemother.* 44, 10–13.

Pannek, S., Higgins, P. G., Steinke, P., Jonas, D., Akova, M., Bohnert, J. A., et al. (2006). Multidrug efflux inhibition in *Acinetobacter baumannii*: comparison between 1-(1-naphthylmethyl)-piperazine and phenyl-arginine-β-naphthylamide. *J. Antimicrob. Chemother.* 57, 970–974. doi: 10.1093/jac/dkl081

Park, C. H., Robicsek, A., Jacoby, G. A., Sahm, D., and Hooper, D. C. (2006). Prevalence in the United States of aac(6′)-Ib-cr encoding a ciprofloxacin-modifying enzyme. *Antimicrob. Agents Chemother.* 50, 3953–3955. doi: 10.1128/AAC.00915-06

Park, S., Lee, K. M., Yoo, Y. S., Yoo, J. S., Il Yoo, J., Kim, H. S., et al. (2011). Alterations of gyrA, gyrB, and parC and Activity of efflux pump in fluoroquinolone-resistant *Acinetobacter baumannii*. *Osong Public Heal. Res. Perspect.* 2, 164–170. doi: 10.1016/j.phrp.2011.11.040

Qu, J., Du, Y., Yu, R., and Lü, X. (2016). The first outbreak caused by *Acinetobacter baumannii* ST208 and ST195 in China. *Biomed Res. Int.* 2016:9254907. doi: 10.1155/2016/9254907

Redgrave, L. S., Sutton, S. B., Webber, M. A., and Piddock, L. J. V. (2014). Fluoroquinolone resistance: mechanisms, impact on bacteria, and role in evolutionary success. *Trends Microbiol.* 22, 438–445. doi: 10.1016/j.tim.2014.04.007

Richmond, G. E., Evans, L. P., Anderson, M. J., Wand, M. E., Bonney, L. C., Ivens, A., et al. (2016). Regulates genes required for multidrug efflux, biofilm formation, and virulence in a strain-specific manner. *MBio* 7:e430-16. doi: 10.1128/mBio.00430-16

Robicsek, A., Strahilevitz, J., Jacoby, G. A., Macielag, M., Abbanat, D., Chi, H. P., et al. (2006). Fluoroquinolone-modifying enzyme: a new adaptation of a common aminoglycoside acetyltransferase. *Nat. Med.* 12, 83–88. doi: 10.1038/nm1347

Rodríguez-Martínez, J. M., Machuca, J., Cano, M. E., Calvo, J., Martínez-Martínez, L., and Pascual, A. (2016). Plasmid-mediated quinolone resistance: two decades on. *Drug Resist. Updat.* 29, 13–29. doi: 10.1016/j.drup.2016.09.001

Roy, S., Viswanathan, R., Singh, A., Das, P., and Basu, S. (2010). Gut colonization by multidrug-resistant and carbapenem-resistant *Acinetobacter baumannii* in neonates. *Eur. J. Clin. Microbiol. Infect. Dis.* 29, 1495–1500. doi: 10.1007/s10096-010-1030-z

Rules, E. (2018). *The European Committee on Antimicrobial Susceptibility Testing. Breakpoint tables for interpretation of MICs and zone Version 9.0*.

Rumbo, C., Gato, E., López, M., Ruiz De Alegría, C., Fernández-Cuenca, F., Martínez-Martínez, L., et al. (2013). Contribution of efflux pumps, porins, and β-lactamases to multidrug resistance in clinical isolates of *Acinetobacter baumannii*. *Antimicrob. Agents Chemother.* 57, 5247–5257. doi: 10.1128/AAC.00730-13

Spence, R. P., and Towner, K. J. (2003). Frequencies and mechanisms of resistance to moxifloxacin in nosocomial isolates of *Acinetobacter baumannii*. *J. Antimicrob. Chemother.* 52, 687–690. doi: 10.1093/jac/dkg424

Su, X., Su, X., Chen, J., Chen, J., Mizushima, T., Mizushima, T., et al. (2005). AbeM, an H+-coupled *Acinetobacter baumannii* multidrug efflux pump belonging to the MATE family of transporters. *Society* 49, 4362–4364. doi: 10.1128/AAC.49.10.4362

Sun, C., Hao, J., Dou, M., and Gong, Y. (2015). Mutant prevention concentrations of levofloxacin, pazufloxacin and ciprofloxacin for *A. baumannii* and mutations in gyrA and parC genes. *J. Antibiot.* 68, 313–317. doi: 10.1038/ja.2014.150

Sun, J. R., Jeng, W. Y., Perng, C. L., Yang, Y. S., Soo, P. C., Chiang, Y., et al. (2016). Single amino acid substitution Gly186Val in AdeS restores tigecycline susceptibility of *Acinetobacter baumannii*. *J. Antimicrob. Chemother.* 71, 1488–1492. doi: 10.1093/jac/dkw002

Touati, A., Brasme, L., Benallaoua, S., Gharout, A., Madoux, J., and De Champs, C. (2008). First report of qnrB-producing *Enterobacter cloacae* and qnrA-producing *Acinetobacter baumannii* recovered from Algerian hospitals. *Diagn. Microbiol. Infect. Dis.* 60, 287–290. doi: 10.1016/j.diagmicrobio.2007.10.002

Valentine, S. C., Contreras, D., Tan, S., Real, L. J., Chu, S., and Xu, H. H. (2008). Phenotypic and molecular characterization of *Acinetobacter baumannii* clinical isolates from nosocomial outbreaks in Los Angeles County, California. *J. Clin. Microbiol.* 46, 2499–2507. doi: 10.1128/JCM.00367-08

Vila, J. (2002). Activity of clinafloxacin, compared with six other quinolones, against *Acinetobacter baumannii* clinical isolates. *J. Antimicrob. Chemother.* 49, 471–477. doi: 10.1093/jac/49.3.471

World Health Organization. (2019). *World Health Organization Model List of Essential Medicines, 21st List, 2019*. Geneva: World Health Organization.

Yang, H., Hu, L., Liu, Y., Ye, Y., and Li, J. (2015). Detection of the plasmid-mediated quinolone resistance determinants in clinical isolates of *Acinetobacter baumannii* in China. *J. Chemother.* 28, 443–445. doi: 10.1179/1973947815y.0000000017

Yoon, E.-J., Courvalin, P., and Grillot-Courvalin, C. (2013). RND-Type efflux pumps in multidrug-resistant clinical isolates of *Acinetobacter baumannii*: major role for AdeABC overexpression and AdeRS mutations. *Antimicrob. Agents Chemother.* 57, 2989–2995. doi: 10.1128/aac.02556-12

Conflict of Interest: The authors declare that the research was conducted in the absence of any commercial or financial relationships that could be construed as a potential conflict of interest.

Advantages of publishing in Frontiers

OPEN ACCESS
Articles are free to read for greatest visibility and readership

FAST PUBLICATION
Around 90 days from submission to decision

HIGH QUALITY PEER-REVIEW
Rigorous, collaborative, and constructive peer-review

TRANSPARENT PEER-REVIEW
Editors and reviewers acknowledged by name on published articles

Frontiers
Avenue du Tribunal-Fédéral 34
1005 Lausanne | Switzerland

Visit us: www.frontiersin.org
Contact us: frontiersin.org/about/contact

REPRODUCIBILITY OF RESEARCH
Support open data and methods to enhance research reproducibility

DIGITAL PUBLISHING
Articles designed for optimal readership across devices

FOLLOW US
@frontiersin

IMPACT METRICS
Advanced article metrics track visibility across digital media

EXTENSIVE PROMOTION
Marketing and promotion of impactful research

LOOP RESEARCH NETWORK
Our network increases your article's readership